Frog skin host-defence peptides and their synthetic analogues with therapeutic potential for type 2 diabetes

A thesis presented for the degree of

Doctor of Philosophy

In the

School of Biomedical Sciences

Faculty of Life and Health Sciences

Vishal Vishwanath Vidya Musale B.Sc., M.Sc.

February 2019

Dedication

I dedicate my thesis to my family, teachers and friends

CONTENTS

ACKNOWLEDMENTS

I would like to thank my supervisors; Dr Yasser Abdel-Wahab, Prof Peter Flatt and Prof Michael Conlon for giving me the opportunity to join as a PhD researcher in the Diabetes Research Group. I am particularly grateful for their valuable guidance, encouragement and excellent supervision. I also thank to all the staff members and PhD students within the DRG group for their support and advice.

I am grateful for Ulster University for supporting my PhD study through the award of a Vice-Chancellors Research Scholarships and for providing world-class research facilities. This research was partly funded by a project grant from Diabetes UK.

I express my sincere thanks to my family (Aai, Papa, Appa, Princu, Nidhu, Vinay, Shweta) for all love and moral support. I am grateful to Nandu bhau for guiding me through tough times.

Summary

Amphibian skin secretions are a rich source of biomolecules (peptides, alkaloids and biogenic amines) which play a significant role in protecting the host from predators and microbial attack. Peptides from frog skin secretions have shown antimicrobial activity against a wide range of microorganisms. Also, these peptides have been shown to possess anticancer, immunomodulatory and insulinotropic activities. In this thesis, peptides from skin secretions of frogs belonging to the family of Alytidae, Hylidae, Pipidae, and Ranidae were examined for insulinotropic and antidiabetic activities.

Frenatin 2D and its synthetic analogues from *Discoglossus sardus*, [A14K] and [S4K] analogues of PGLa-AM1 and CPF-AM1 respectively from *Xenopus amieti*, temporin peptides from *Rana temporaria* and esculentin-1 from *Rana esculenta* demonstrated concentration-dependent insulinotropic activities in rat clonal pancreatic beta cells (BRIN-BD11) and human-derived pancreatic beta cells (1.1B4). Insulinotropic activities of the esculentin-1 peptides were associated with an increase in membrane potential and intracellular calcium, whereas frenatin 2D and temporin peptides had no effect on these parameters. In BRIN-BD11 cells, frenatin 2D peptides produced a significant increase in cAMP production and its insulin-releasing activity was abolished in PKA downregulated cells. In addition to their insulinotropic activities, these peptides protected BRIN-BD11 cells against cytokine-induced apoptosis as well as stimulated proliferation of beta-cell. Frenatin 2D and its synthetic analogues [D1W] and [G7W], temporin G and esculentin (1-21)1c improved blood glucose and increased insulin concentration in lean mice.

In genetically obese-diabetic mice (*db/db*), frenatin 2D, [A14K] PGLa-AM1 and [S4K] CPF-AM1 improved blood glucose, insulin sensitivity, insulin secretory responses of islets to glucose and established insulin secretagogues, lipid profile and both kidney and

liver function. The gradual demise of beta cells and a decrease of circulating insulin in *db/db* mice was delayed significantly by these peptides. Also, genes involved in both insulin signalling and secretion were improved.

In conclusion, this thesis highlights the potential of frog skin peptides belonging to the family of Alytidae, Hylidae, Pipidae and Ranidae for further development into therapeutic agents for type 2 diabetes.

ABBREVIATIONS

ABCC	ATP binding cassette subfamily C member 8
ADP	Adenosine diphosphate
AGIs	Alpha-glucosidase inhibitors
AKT1	Protein Kinase B
ANOVA	Analysis of variance
ATP	Adenosine triphosphate
AUC	Area under the curve
B2RP	Brevinin-2 related peptide
BMC	Bone mineral content
BMD	Bone mineral density
BSA	Bovine serum albumin
bw	Body weight
$CaCl_2.2H_2O$	Calcium chloride dihydrate
CACNA1C	Calcium voltage-gated channel subunit alpha1 C
cAMP	Cyclic adenosine monophosphate
CCK	Cholecystokinin
cDNA	Complementary DNA
CH_2Cl_2	Dichloromethane
cm	Centimetre

CO_2	Carbon dioxide
CoA	Coenzyme A
CPF	Caerulein precursor fragment
cpm	Counts per minutes
CPT-1	Carnitine palmitoyltransferase 1
Da	Dalton
DAG	Diacylglycerol
DAPI	4' 6-diamidino-2-phenylindole
DCC	Dextran-coated charcoal
DIDS	4 4-diisothiocyanostilbene-2 2-disulfonic acid
DM	Diabetes mellitus
DMEM	Dulbecco's Modified Eagle's medium
DPP-4	Dipeptidyl peptidase 4
DUK	Diabetes United Kingdom
DXA	Dual-energy X-ray absorptiometry
EDTA	Ethylenediamine tetraacetic acid
EGTA	Ethylene glycol-bis-N N N'N'-tetraacetic acid
ELISA	Enzyme-linked immunosorbent assay
ER	Endoplasmic reticulum
ES-MS	Electrospray mass spectrometry

FBS	Foetal bovine serum
FFA	Free fatty acids
FLIPR	Fluorescent Imaging Plate Reader
g	Gram
GCK	Glucokinase
GCG	Pro glucagon
GIP	Glucose-dependent insulinotropic peptide
GLP-1	Glucagon-like peptide 1
GLUT2	Glucose transporter 2
GLUT4	Glucose transporter 4
GRP	Gastrin-releasing peptide
GTT	Glucose tolerance test
HBSS	Hanks balanced salt solution
HCl	Hydrochloric acid
HDL	High-density lipoprotein
HEPES	4-(2-hydroxyethyl)-1-piperazineethanesulfonic acid
HLA	Human leukocyte antigen
HOMA-IR	Homeostatic model assessment of insulin resistance
HPLC	High-performance liquid chromatography
IAPP	Islet amyloid polypeptide

IBMX	1-methyl-3-(2-methylpropyl)-7H-purine-2 6-dione
IDF	International Diabetes Federation
IFNγ	Interferon-gamma
IGT	Impaired glucose tolerance
IL-1β	Interleukin 1 beta
INS	Insulin gene
INSR	Insulin receptor
InsP3	Inositol 1, 4, 5-triphosphate
i.p	Intraperitoneal
IPGTT	Intraperitoneal glucose tolerance test
IRS1	Insulin receptor substrate 1
IRS2	Insulin receptor substrate 2
IUCN	International Union for Conservation of Nature
KCl	Potassium chloride
KCNJ11	Potassium inwardly-rectifying channel subfamily J member 11
kg	Kilogram
KH_2PO_4	Potassium dihydrogen orthophosphate
KRBB	Kreb's ringer bicarbonate buffer
kV	Kilovolt
L	Litre

LDH	Lactate dehydrogenase
LDL	Low-density lipoprotein
m/z	Mass per charge
MALDI-TOF MS	Matrix-assisted laser desorption/ionization mass spectrometry
mCi	Millicurie
mg	Milligram
$MgSO_4$	Magnesium sulphate
MHC	Major Histocompatibility Complex
min	Minute
ml	Millilitre
mM	Millimolar
mmol	Millimole
MW	Molecular weight
N	Normal
Na_2HPO_4	Disodium hydrogen orthophosphate
NaCl	Sodium chloride
NAD	Nicotinamide adenine dinucleotide
NADH	Nicotinamide adenine dinucleotide reduced
$NaHCO_3$	Sodium bicarbonate
$Na^{125}I$	Sodium iodide

NaOH	Sodium hydroxide
NEFAs	Non-esterified fatty acids
ng	Nanogram
NHS	National Health Service
nm	Nanometer
nmol	Nanomole
nM	Nanomolar
OD	Optical density
O_2	Oxygen
OGTT	Oral glucose tolerance test
PBS	Phosphate buffer saline
PC	Prohormone convertase
PDK1	3-phosphinositide dependent protein kinase 1
PDX-1	Pancreatic and duodenal homeobox 1
PGLa	Peptide glycine leucine amide
PMA	Phorbol 12-myristate 13-acetate
PI3KCA	Phosphoinositide-3-kinase catalytic alpha polypeptide
PKA	Protein kinase A
PKB	Protein kinase B
PKC	Protein kinase C

PLC	Phospholipase C
pM	Picomolar
PP	Pancreatic polypeptide
PPARγ	Peroxisome proliferator-activated receptor γ
PTB 1	Protein phosphatase 1B
PtdInsP2	Phosphatidylinositol 4 5-bisphosphate
RFU	Relative fluorescence unit
RIA	Radioimmunoassay
RLU	Relative light units
ROS	Reactive oxygen species
rpm	Revolutions per minute
RPMI	Roswell Park Memorial Institute
SEM	Standard error of mean
SGLT2	Sodium-glucose transporter 2
SLC2A4	Glucose transporter 4
SLC2A2	Glucose transporter 2
STAT1	Signal transducer and activator of transcription 1, isoform 1
STZ	Streptozotocin
SUR1	Sulphonylurea receptor 1
T1DM	Type 1 diabetes mellitus

T2DM	Type 2 diabetes mellitus
TCA	Tricarboxylic acid cycle
TEA	Triethanolamine
TFA	Trifluoroacetic acid
TNF α	Tumour necrosis factor α
TUNEL	Terminal deoxynucleotidyl transferase dUTP nick end labeling
TZDs	Thiazolidinediones
UDP	Uridine diphosphate
UK	United Kingdom
UKPDS	United Kingdom Prospective Diabetes Study
USA	United States of America
USD	U.S. Dollars
µg	Microgram
µl	Microlitre
µM	Micromolar
V	Volts
v/v	Volume/volume
VDCC	Voltage dependent calcium channel
VLDL	Very low-density lipoprotein
WHO	World Health Organization

w/v	Weight per volume
XPF	Xenopsin precursor fragment

List of amino acids and their abbreviations

Amino Acid	3-Letter	1-Letter	Side-chain polarity	Side-chain charge (pH 7.4)
Alanine	Ala	A	Nonpolar	Neutral
Arginine	Arg	R	Polar	Positive
Asparagine	Asn	N	Polar	Neutral
Aspartic acid	Asp	D	Polar	Negative
Cysteine	Cys	C	Nonpolar	Neutral
Glutamic acid	Glu	E	Polar	Negative
Glutamine	Gln	Q	Polar	Neutral
Glycine	Gly	G	Nonpolar	Neutral
Histidine	His	H	Polar	Positive
Isoleucine	Ile	I	Nonpolar	Neutral
Leucine	Leu	L	Nonpolar	Neutral
Lysine	Lys	K	Polar	Positive
Methionine	Met	M	Nonpolar	Neutral
Phenylalanine	Phe	F	Nonpolar	Neutral
Proline	Pro	P	Nonpolar	Neutral
Serine	Ser	S	Polar	Neutral
Threonine	Thr	T	Polar	Neutral
Tryptophan	Trp	W	Nonpolar	Neutral
Tyrosine	Try	Y	Polar	Neutral
Valine	Val	V	Nonpolar	Neutral

PUBLICATIONS ARISING FROM THE THESIS

Full-Length Scientific Papers

1. Vishal Musale, Laure Guilhaudis, Yasser H.A. Abdel-Wahab, Peter R. Flatt, J. Michael Conlon (2018) Insulinotropic activity of the host-defense peptide frenatin 2D: Conformational, structure-function and mechanistic studies. *Biochimie*; 156, 12-21 (Chapter 4).

2. Vishal Musale, Maria Luisa Mangoni, Yasser H.A. Abdel-Wahab, Peter R. Flatt, J. Michael Conlon (2018) Insulinotropic, glucose-lowering, and beta-cell anti-apoptotic actions of peptides related to esculentin-1a(1-21).NH_2. *Amino Acids*, 50:723-734 (Chapter 3).

3. Vishal Musale, Bruno Casciaro, Maria Luisa Mangoni, Yasser H.A. Abdel-Wahab, Peter R. Flatt, J. Michael Conlon (2018) Assessment of the potential of temporin peptides from the frog *Rana temporaria* (Ranidae) as anti-diabetic agents. *Journal of Peptide Science*, doi: 10.1002/psc.3065 (Chapter 3).

4. J. Michael Conlon, Vishal Musale, Samir Attoub, Maria Luisa Mangoni, Jérôme Leprince, Laurent Coquet, Thierry Jouenn, Yasser H. A. Abdel-Wahab, Peter R. Flatt and Andrea C. Rinaldi (2017) Cytotoxic peptides with insulin-releasing activities from skin secretions of the Italian stream frog *Rana italica* (Ranidae). *Journal of Peptide Science*, 23: 769–776.

Refereed Conference Abstracts

YHA Abdel-Wahab, V Musale, BO Owolabi, RC Moffett, OO Ojo, JM Conlon and PR Flatt (2018). [S4K] CPF-AM1- Mechanisms underlying beneficial actions on pancreatic beta cells *in vitro* and high fat diet induced obesity-diabetes *in vivo*, Diabetic Medicine, 35 (Supplement 1) : 69 (Chapter 6).

YHA Abdel-Wahab, V Musale, BO Owolabi, RC Moffett, JM Conlon and PR Flatt (2017). [A14K] PGLa-AM1- Mechanisms underlying beneficial actions on pancreatic beta cells *in vitro* and high fat diet induced obesity-diabetes *in vivo*, Diabetic Medicine, 44 (Supplement 1) : 64-65 (Chapter 5).

Musale V, Owolabi BO, Conlon JM, Flatt PR, Abdel-Wahab YHA (2016). *In vitro* insulinotropic activities of frenatin peptides in rat clonal pancreatic beta cell line. Irish journal of Medical Science, 185 (Supplement 7) : 379 (Chapter 4).

YHA Abdel-Wahab, V Musale, JM Conlon, and PR Flatt (2019). Beneficial effects of frenatin 2D peptide from *Discoglossus sardus* on pancreatic beta cell function and glucose homeostasis in db/db mice, Diabetic Medicine, in press (Chapter 4).

DECLARATION

"I hereby declare that for two years from the date, on which the thesis is deposited in the library of the Ulster University, the thesis shall remain confidential with access or copying prohibited. Following expiry of this period, I permit the Librarian of the University to allow the thesis to be copied in whole or in part without reference to me on the understanding that such authority applies to the provision of single copies made for study purposes or for inclusion within the stock of another library. This restriction does not apply to British Library Service (which, subject to the expiry of the period of confidentiality, is permitted to copy the thesis on demand for loan or sale under the terms of a separate agreement) nor to the copying or publication of the title and abstract of the thesis.

IT IS A CONDITION OF USE OF THIS DISSERTATION THAT ANYONE WHO CONSULTS IT MUST RECOGNISE THAT THE COPYRIGHT RESTS WITH THE AUTHOR AND THAT NO QUOTATION FROM THE DISSERTATION AND NO INFORMATION DERIVED FROM IT MAY BE PUBLISHED UNLESS THE SOURCE IS PROPERLY ACKNOWLEDGED"

Chapter 1

General Introduction

1.1 Diabetes mellitus

Diabetes mellitus is a group of metabolic diseases characterised by high blood glucose level (hyperglycaemia). In diabetes, blood glucose level escalates either due to pancreatic beta cell dysfunction or inability of the body to respond to available insulin or both. Diabetes and its related complications can be managed and delayed by making lifestyle changes (such as healthy diet, regular exercise) and using appropriate pharmacological interventions.

As a result of the global rise in the rate of prevalence, mortality and morbidity together with increasing costs of treatment, diabetes has become one of the most significant healthcare problems. Rapid urbanisation, excessive calorie intake and increasingly sedentary lifestyle have resulted in a diabetes epidemic (Basu *et al.*, 2013). According to the International Diabetes Federation (IDF) report, in 2017 more than 425 million people were affected by diabetes globally. This figure could rise to 629 million in 2045 if no urgent actions are taken to improve diabetes outcome. In the UK alone, the diabetes population has increased from 1.8 million to 3.7 million in last two decade, according to a recent analysis by Diabetes UK. Due to the exponential rise in the prevalence of diabetes, healthcare expenditure globally has reached USD 727 billion per/annum. Despite spending such a considerable amount, there is still a large proportion of the worldwide diabetes population with no access to antidiabetic drugs, particularly in developing nations (IDF, 2017).

1.1.1 History of diabetes

The following scheme summarizes the history of diabetes and the manufacturing of first human insulin.

1500 BC Characteristic similar to diabetes mellitus were described by ancient Hindu and Egyptians scholar.

⇩

250 BC Apollonius of Memphis coined term *Diabetes*.

⇩

450-500AD Ancient Indian Scholar Sushruta called it *Madhumeha* (honey urine).

⇩ Sushruta (Physician) and Charaka (Surgeon), the early pioneers of treating diabetes, identified two types of diabetes (now known by type1 and type 2 diabetes).

980-1037 Persian physician Avicenna, not only observed abnormal appetite and diabetic gangrene but also used plants seeds (lupin, fenugreek, zedoary) for treatment.

⇩

1776 Matthew Dobson confirmed that diabetes patient has excess sugar in urine and blood.

⇩

1798 British Surgeon-General John Rollo coined the term *mellitus* (Latin, 'sweet like honey' or sweet urine).

⇩

1857 Claude Bernard established the role of the liver in diabetes

⇩

1869 Paul Langerhans, observed clusters of cells scattered all over pancreas

⇩

1889 Joseph von Mering and Oskar Minkowski discovered the role of the pancreas in diabetes.

⇩

1916 Sir Edward Albert Sharpey-Schafer coined the word "insulin".

⇩

1919 Dr Frederick Allen, introduced starvation treatment to manage diabetes

⇩

1923 Dr Fredrick Banting and Prof John James Rickard Macleod received Nobel Prize for the discovery of insulin.

⇩

1936 British Scientist Sir Harold Percival (Harry) Himsworth, in his work, distinguished two main types of diabetes.

⇩

1959 British biochemist Frederick Sanger received Nobel Prize for his work on the structure of human insulin.

⇩

1978 David Goeddel produced synthetic "human" insulin using recombinant DNA technology

The data in the above scheme is adapted from Ahmed, 2003, Das & Shah *et al.,* 2011, Lakhtakia, 2013, Vecchio *et al.,* 2018.

1.1.2 Classification of Diabetes Mellitus

Diabetes is classified mainly into two main types:

A) Type1 diabetes mellitus (T1DM).

B) Type 2 diabetes mellitus (T2DM).

1.1.2.1 Type 1 diabetes mellitus (T1DM)

In T1DM, insulin-producing pancreatic beta cells are challenged by the body's immune system resulting in insulin deficiency (Maahs *et al.,* 2012). Such individuals depend on external insulin source to maintain healthy blood sugar levels. It is a severe and permanent condition that can be developed at any stage of life, but more frequently

occurs in children (Frese & Sandholzer, 2013). For these reasons, T1DM was also called "insulin-dependent diabetes" or "juvenile-onset diabetes. T1DM can be managed by proper insulin treatment, regular monitoring of blood sugar and maintaining a healthy lifestyle. According to the International Diabetes Federation, in 2017 about 1 million children and adolescent (below age 20) were projected to have T1DM. In some parts of the world such as Europe, North America and Caribbean was recorded with the highest number of T1DM patient (below age 20). In high-income countries, the prevalence of T1DM was estimated between 7-12% of the total diabetes population (WHO, 2016).

The cause of T1DM is not entirely understood, but it has been suggested that the genetic and environmental factors may activate an immune system that destroys beta cells population (Atkinson & Eisenbarth, 2001, Patterson *et al.*, 2014). The polymorphism in Human leukocyte antigen (HLA) genes located on chromosome 6p21 that encodes major histocompatibility complex, is considered as one of the main inherited factors that may contribute to T1DM. Mainly, the HLA alleles DR4-DQ8 & DR3-DQ2 account for 40-50% of heritable risk (Hirschhorn, 2003). It has also been proposed that environmental factors including toxins and virus may trigger this gene to produce antibodies that attack beta cells (You & Henneberg, 2016). Auto-antibodies to islet cells, insulin, glutamate decarboxylase, tyrosine phosphatase (IA-2a and IA-2b) and zinc transporter 8 (ZnT8) have been reported that facilitate the destruction of pancreatic beta cells (Daneman, 2006, American Diabetes Association, 2015).

1.1.2.2 Type 2 diabetes mellitus (T2DM)

In T2DM, pancreatic beta cells fail to meet body requirement for insulin or the body loses its efficiency to utilise available insulin or both, resulting in hyperglycaemia.

This type is most prevalent among adults and accounts for 90% of the total diabetes population. T2DM is also seen occurring in children and young adults. This is mainly due to rapid urbanisation, the rising level of obesity, high energy intake and physical inactivity (Basu *et al.*, 2013). According to the International Diabetes Federation (IDF), in 2015, more than 400 million people were affected by T2DM, and this figure will rise to 629 million by 2045. The incidence of T2DM population has been high, particularly in developing nations, which account for 80% of global diabetes population. T2DM can be managed by adopting a healthy lifestyle (healthy diet and physical exercise) and by taking appropriate medical treatment such as (metformin, sulphonylureas, thiazolidinediones, acarbose, GLP-1 agonists, DPP-4 inhibitors, SGLT2 inhibitors or insulin). If affected individuals did not receive appropriate treatment, they are at high risk of developing complications associated with diabetes such as microvascular (nephropathy, neuropathy, and retinopathy) and macrovascular complications (cardiovascular diseases) (Van Dieren & Beulens, 2010).

T2DM is a complex disease and has multiple factors contributing to its development. Among these, genetic predisposition and environmental factors are the important ones, which interacts to cause T2DM. Genetic factors have a major influence on susceptibility to develop T2DM, which is supported by studies in monozygotic twins and certain ethnic groups (Rimoin, 1969, Poulsen *et al.*, 1999). Further studies identified multiple genetic variants that increase the risk of T2DM (McCarthy, 2010). A study conducted by Grant *et al*., 2006, identified variants in transcription factor 7-like 2 (TCF7L2) gene in Iceland individuals with T2DM. A similar finding was replicated in T2DM individuals from various ethnic groups (Cauchi *et al.*, 2007). Some examples of genes associated with T2DM risk are: *INS* (insulin), *IRS1* (insulin receptor substrate 1), *PPARγ* (peroxisome proliferator-activated receptor gamma),

KCNJ11 (potassium inwardly rectifying channel, subfamily J, member 11), ABCC8 (ATP-binding cassette transporter sub-family C member 8), SLC30A8 (solute carrier family 30 member 8), PCSK1 (proprotein convertase subtilisin/kexin type 1), KCNQ1 (potassium voltage-gated channel subfamily Q member 1) (McCarthy, 2010, Wen *et al.,* 2012, Grarup *et al.,* 2014). Environmental factors such as excess body fat, overweight, obesity, high energy intake and physical inactivity, increase the risk of T2DM (Forouzanfar *et al.,* 2015). Beyond these factors, differences in the gut flora and also socioeconomic status could play a role in the development of T2DM (Moreno-Indias *et al.,* 2014).

1.2 Pancreas

The pancreas is an elongated organ, about 14-20 cm long, that lies horizontally in the upper abdomen behind the peritoneum. It is divided into four main parts head, neck, body and tail. The pancreas has two main components, exocrine pancreas and endocrine pancreas. Exocrine pancreas accounts for 98% of the pancreatic mass and is composed of acinar and ductal epithelial cells which produce digestive enzymes such as amylase, lipases and protease. These digestive enzymes travel through pancreatic duct into the duodenum where they digest macromolecules. Endocrine pancreas (2% of pancreatic mass) is composed of alpha (α) beta (β), delta (δ), epsilon (ε) and pancreatic polypeptide (PP) cells which produce important hormones glucagon, insulin, somatostatin, ghrelin and pancreatic polypeptide respectively (Longnecker, 2014). These hormones are released into the bloodstream to regulate metabolic function. The endocrine cells are present in the form of clusters surrounded by acinar cells, and these clusters are called islets of Langerhans.

1.2.1 Islets of Langerhans

In 1869, Paul Langerhans was first to observe clusters of cells scattered all over pancreas. The French pathologist and histologist Laguesse proposed that secretion from these cluster of cells could play a key role in digestion and decided to name these cells after the name of Langerhans in 1893. The function of the pancreas in diabetes first was established by Von Mering and Minkowski in 1889. They observed a rise in blood glucose level in dogs after surgical removal of the pancreas (Xavier *et al.*, 2018). In 1921, Frederick Banting and Charles Best discovered insulin and showed that insulin produced by pancreas reduces blood glucose level. Frederick Banting further collaborated with John Macleod for the clinical development of insulin. In 1923, Frederick Banting along with John Macleod were awarded Nobel Prize in the field of Medicine. Since then, the focus has been directed towards islet biology (Xavier *et al.*, 2018).

In humans, it is estimated that pancreas has about 1million islets (Ionescu-Tirgoviste *et al.*, 2015). The average size of islets varies between 50-250 μM in diameter. Alpha (α), beta (β), delta (δ) and pancreatic polypeptide (PP) cells are the four major cells that constitute the islets of Langerhans (Figure 1). ε-cells are also present in islets but present in few numbers. The composition of these cells, as well as the structure of islet, vary between and within species (Kim *et al.*, 2009). Human islets are composed of 52-74% insulin producing β-cells, ~20% glucagon-producing α-cells, ~5% somatostatin-producing δ-cells, 1-2% pancreatic polypeptide-producing PP cells and very few ghrelin-producing ε-cells (Powers and Stein, 2012). In humans, these cells are populated randomly throughout the islet, whereas in rodents insulin-producing beta cells occupy the core of the islet surrounded by other endocrine cells (Kim *et al.*,

2009, Steiner *et al.*, 2010, Xavier *et al.*, 2018). In addition to these cells, islet also contains other cells such as immune cells, vascular cells and neural elements.

Insulin and glucagon produced by beta and alpha cells respectively have opposite effects on blood glucose. These hormones are released in response to a change in blood glucose. Insulin not only mediates glucose uptake but also promote synthesis of glycogen, fats and proteins and inhibit hepatic glucose production. Glucagon, on the other hand, increases blood glucose by increasing hepatic glucose production and regulating the breakdown of glycogen and fats. Somatostatin expressed by delta cells inhibits the release of insulin, glucagon and pancreatic polypeptide (Kailey *et al.*, 2012). Ghrelin acts directly on the delta cell and promotes the release of somatostatin (Adriaenssens *et al.*, 2016). Pancreatic polypeptide cells (also called F cells), majorly found in the head region of a pancreas release pancreatic polypeptide that reduces appetite and has also shown to inhibit glucagon release at low glucose (Tan & Bloom, 2013). Ghrelin produced by epsilon cells has been identified to inhibit insulin secretion during fasting (Broglio *et al.*, 2013). Moreover, ghrelin has been proposed for its role in beta cell function and survival (Andralojc *et al.* 2009). In both T1DM and T2DM, not only islet architecture is disrupted but also communication between islet cells type (Brereton *et al.*, 2015).

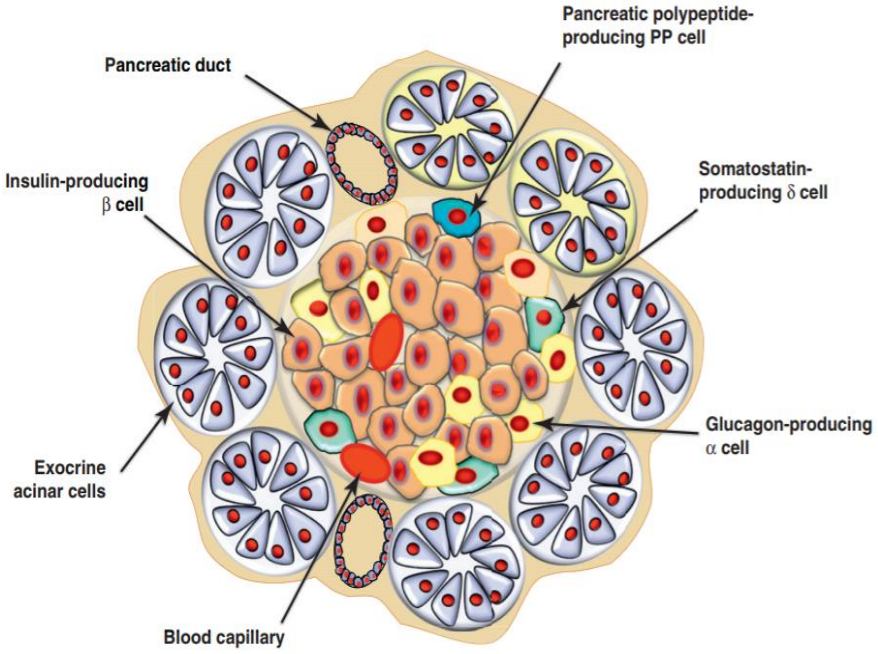

Figure 1: Schematic representation of islet (Adapted from Efrat and Russ, 2012)

1.2.2 Insulin synthesis

Insulin hormone, which regulates carbohydrates, protein and fats metabolism, is synthesised in a significant quantity by beta cells of islets of Langerhans. The synthesised insulin contains 51 amino acids in two polypeptide chains [Chain A (21 amino acids) and chain B (30 amino acids)] (Figure 2) and has a molecular weight of 5.8KDa. The two polypeptide chains (A chain and B chain) are linked by two disulphide bonds at position A7-B7 and A20-B19, and an additional disulphide bond is found at position A6-A11 within A the chain (Chang *et al.*, 2003, van Lierop *et al.*, 2017).

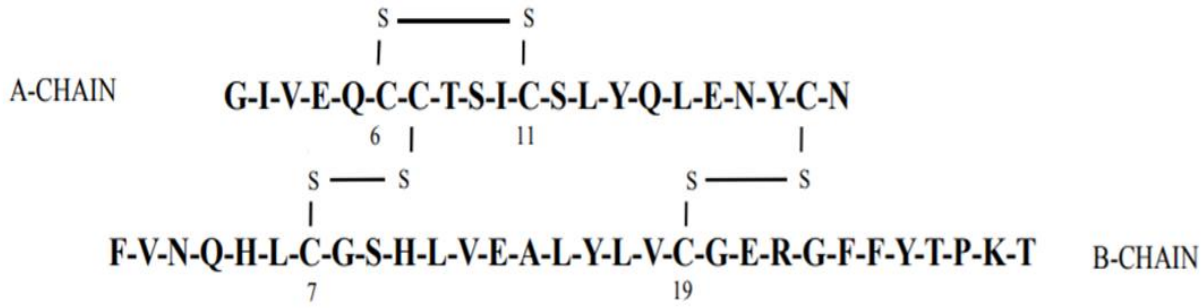

Figure 2: Primary structure of insulin (Adapted from Belgi *et al.*, 2011)

The *insulin* gene present on chromosome 11 in beta cells of the pancreas encodes insulin precursor known as preproinsulin. Preproinsulin contains 110 amino acids in four polypeptide chain (A chain, B chain, signal peptide and C-peptide). The signal recognition particles (SRP), a cytosolic ribonucleoprotein facilitate transportation of synthesised preproinsulin by interacting with hydrophobic N-terminal signal peptide into the endoplasmic reticulum lumen (Wolin & Walter, 1993). On translocation, the signal peptide is cleaved from preproinsulin by a signal peptidase to produce proinsulin. In the endoplasmic reticulum lumen, chaperone proteins assist rapid folding of proinsulin and formation of three disulphide bonds. The three-dimensional structure of proinsulin is further translocated to the Golgi complex, where proinsulin is believed to form hexamers around Zn^{+2} ions (Haataja *et al.*, 2013, Liu *et al.*, 2014). Proinsulin is further processed by prohormone convertase (PC1 and PC2) and carboxypeptidase E in secretory granules to yield insulin and C-peptide (Davidson, 2004). The schematic representation of insulin biosynthesis is shown in Figure 3.

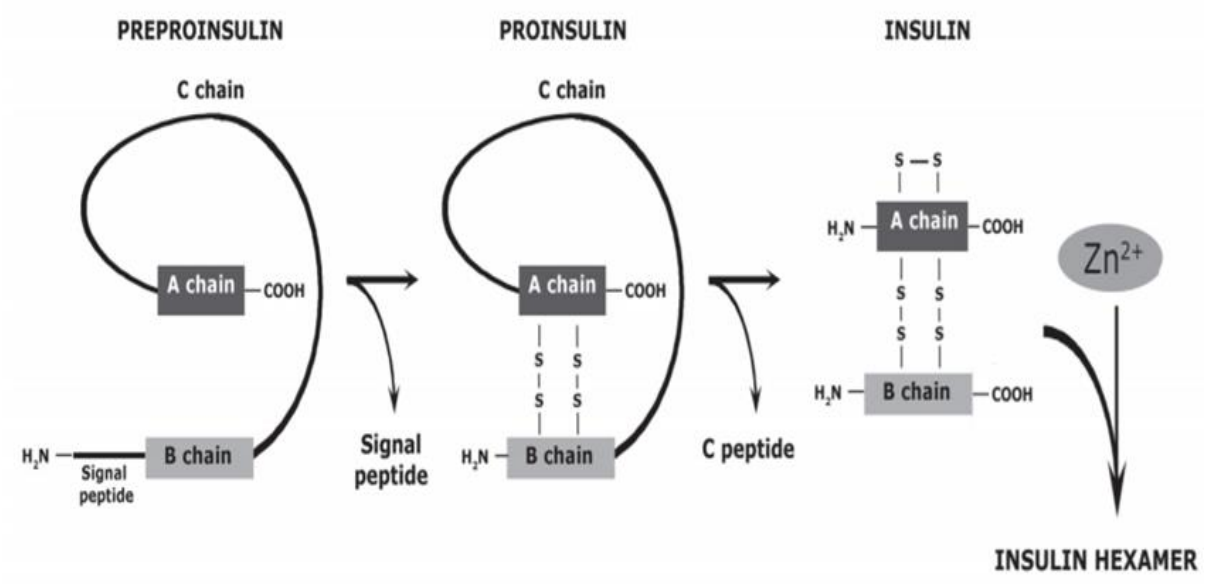

Figure 3: Insulin biosynthesis (Adapted from Skelin *et al.*, 2010)

1.2.3 Biology of insulin secretion

Insulin secretion from beta cells is initiated by the sequential activation of multiple metabolic pathways. The macronutrients like glucose, proteins and fatty acids play a vital role in the release of insulin from pancreatic beta cells. A study conducted by Chang *et al.*, 1978 has shown that the amount of insulin release by beta cells in response to oral glucose is more significant than protein and fatty acids when taken in the same amount. Glucose is taken up by beta cell by facilitated diffusion through GLUT2 transporter protein (GLUT1 in humans) and metabolised to pyruvate in the cytoplasm by glycolytic enzymes. Pyruvate is further transported to mitochondria and oxidised to acetyl CoA by pyruvate dehydrogenase enzyme. Acetyl CoA enters the kerbs cycle and produces a reduced electron carrier (NADH & $FADH_2$), which further undergoes oxidative phosphorylation to generate ATP. The depolarization of the cell membrane occurs when the generated ATP block the potassium channel followed by the opening of voltage-dependent calcium channel. This event leads to the elevation

of intracellular Ca^{2+}, which subsequently triggers insulin release from secretory granules by exocytosis (Rorsman & Aschcroft, 2018). The intermediate of Krebs cycle like NADPH, malonyl-CoA, and glutamate have been reported to further amplify the insulin secretion from beta cells (Maechler & Wollheim, 2009). The schematic representation of insulin secretion is shown in Figure 4.

Previous studies have confirmed that some amino acids also stimulate insulin release from beta cells. Amino acids including alanine, asparagine, tryptophan and glycine stimulate insulin release in the presence of glucose by membrane depolarization (Newsholme *et al.,* 2006, Newsholme & Krause, 2012). Glutamine demonstrated insulinotropic effects only in combination with leucine (Dixon *et al.,* 2003). Amino acids like alanine and glutamine elevate blood glucose level by stimulating the release of glucagon. This elevated glucose, in turn, triggers insulin secretion.

GLP-1 (glucagon-like peptide) and GIP (glucose-dependent insulinotropic polypeptide) are incretin hormones produced by intestinal tract in response to food intake. These hormones act directly on pancreatic beta cells by binding to their receptors and subsequently activating adenylate cyclase enzyme that elevates the concentration of cAMP generated from ATP. In turn, cAMP activates protein kinase A (PKA) and type 2 ryanodine receptor (RY2) protein, which promotes insulin release via increasing intracellular Ca^{2+} concentration. Activated protein kinase A also influences insulin synthesis by preventing degradation of insulin mRNA gene by transporting phosphorylated polypyrimidine tract binding protein (PTBP-1) to the nucleus (Knoch *et al.,* 2006).

Previous studies have demonstrated that free fatty acids also promote insulin secretion from beta cells (Haber *et al.,* 2003). At low glucose concentrations, free fatty acids are used as a source of energy by pancreatic islets. Free fatty acids are converted to

long-chain acyl CoA by acyl CoA synthase. Long-chain acyl CoA is further oxidised by the mitochondrial enzyme carnitine palmitoyl transferase 1 (CPT-1) to generate energy and to release insulin. However, high glucose concentrations, due to inactivation of CPT-1 activity, long chain acyl CoA accumulate which induce insulin release by increasing intracellular Ca^{2+} concentration (Newsholme & Krause, 2012). Hormones like acetylcholine and cholecystokinin stimulate insulin release by activation of phospholipase C. Phospholipase C is ubiquitous, membrane-associated enzyme, which on activation cleaves phospholipid phosphatidylinositol 4,5-bisphosphate (PIP_2) to inositol 1,4,5-trisphosphate (IP_3) and diacylglycerol (DAG). IP_3 promotes insulin release by mobilising intracellular Ca^{2+} and DAG by activating protein kinase C (PKC) (Berridge *et al.*, 2003). Other hormones like estrogen potentiate insulin release by K_{ATP} channel-dependent pathway (Nadal *et al.*, 1998).

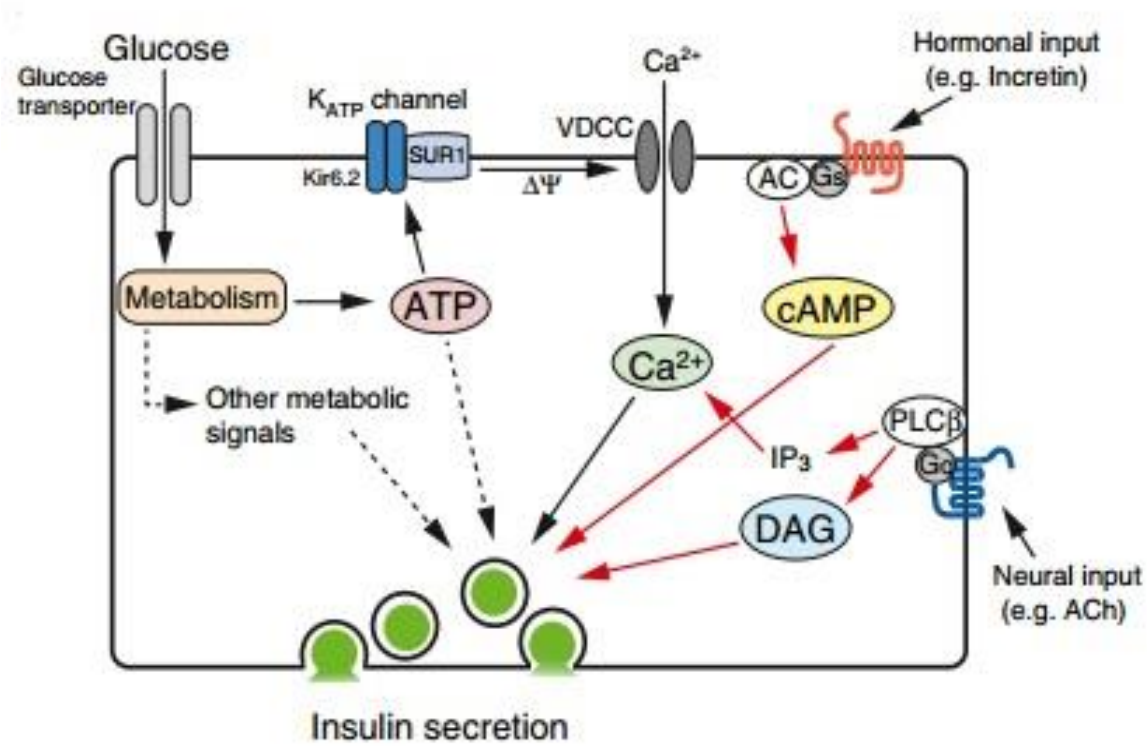

Figure 4: Schematic representation of insulin secretion (Adapted from Seino 2012)

1.2.4 Insulin action

Insulin hormone, synthesised and released by pancreatic beta cells, initiate its action by binding to its transmembrane receptor present on target cells (Kido *et al.,* 2001, De Meyts *et al.,* 2013). Insulin receptor belongs to the receptor tyrosine kinase family, consisting of two α subunit (insulin binding domains) and two β subunits (signal transduction domains) (Menting *et al.,* 2013). The extracellular alpha subunit undergoes conformational changes on interaction with insulin. These conformational changes in alpha subunit allow binding of ATP to intracellular beta subunit which activates tyrosine kinase. On activation of tyrosine kinase, beta subunit undergoes autophosphorylation, which further propagates phosphorylation of other endogenous substrate or other insulin signalling molecules such as insulin receptor substrate (IRS), phosphatidylinositol 3 kinase (PI(3)K), protein kinase A (PKA), Protein kinase B (PKB) and mitogen-activated protein (MAP) kinase. These activated signalling molecules in turn directly or indirectly regulate metabolic functions (Saltiel & Kahn *et al.,* 2001). The schematic representation of insulin action is shown in Figure 5.

Insulin mediates glucose uptake in skeletal muscles, liver and adipose tissue by recruiting GLUT4 transporter protein from cytoplasm to the cell surface, which regulate the entry of glucose inside cells (Huang & Michael, 2007, Bogan *et al.,* 2012, Atkinson *et al.,* 2013). At an elevated concentration of glucose, insulin promotes storage of glucose in the form of glycogen in liver and muscles cells by upregulating key enzyme involved in glycogenesis pathway such as glycogen synthase (Samuel & Shulman, 2012). Activated PI(3)K and Akt increase the activity of glycogen synthase by restricting the activity of glycogen synthase kinase by phosphorylation. After entering the cells, glucose is converted to glucose 6 phosphate by cytosolic hexokinase enzyme. Glucose 6 phosphate is further metabolised to UDP glucose by

phosphoglucomutase and glucose 1-phosphate uridylyltransferase. By the action of glycogen synthase, UDP glucose is converted to glycogen (Bouskila *et al.,* 2008).

Insulin also limits the production and release of glucose from the liver by inhibiting the expression of enzymes of gluconeogenesis and glycogenolysis pathways (Ramnanan *et al.,* 2010). Transcription of the genes encoding for phosphoenolpyruvate carboxylase, fructose 1,6 bisphosphates and glucose 6 phosphatases gene transcription is reduced, while transcription of glycolytic and lipogenic enzymes is increased by insulin (Hall *et al.,* 2007).

In adipocytes, insulin promotes the synthesis of lipids from glucose by activation of fatty acid synthase and acetyl-CoA carboxylase enzymes (Saltiel & Kahn *et al.,* 2001, Samuel & Shulman, 2012). Insulin also inhibits the degradation of lipid by limiting the activity of lipase enzyme by dephosphorylation (Zimmermann *et al.,* 2009, Lass *et al.,* 2011). These effects of insulin decrease the flow of free fatty acids to the liver, thus reducing gluconeogenesis, ketogenesis, as well as the production of very low-density lipoproteins (VLDL) (Keller *et al.,* 1988, Fukao *et al.,* 2004). Insulin also stimulates protein synthesis by facilitating the transport of amino acids and regulating the translation of mRNA (Hyde *et al.,* 2002, Proud, 2006, Drummond *et al.,* 2010). In addition, insulin has paracrine effects on other hormone-producing cells of pancreatic islets. Insulin decreases the release of glucagon by directly acting on alpha cells, which in turn augments the metabolic effects of insulin (Briant *et al.,* 2016).

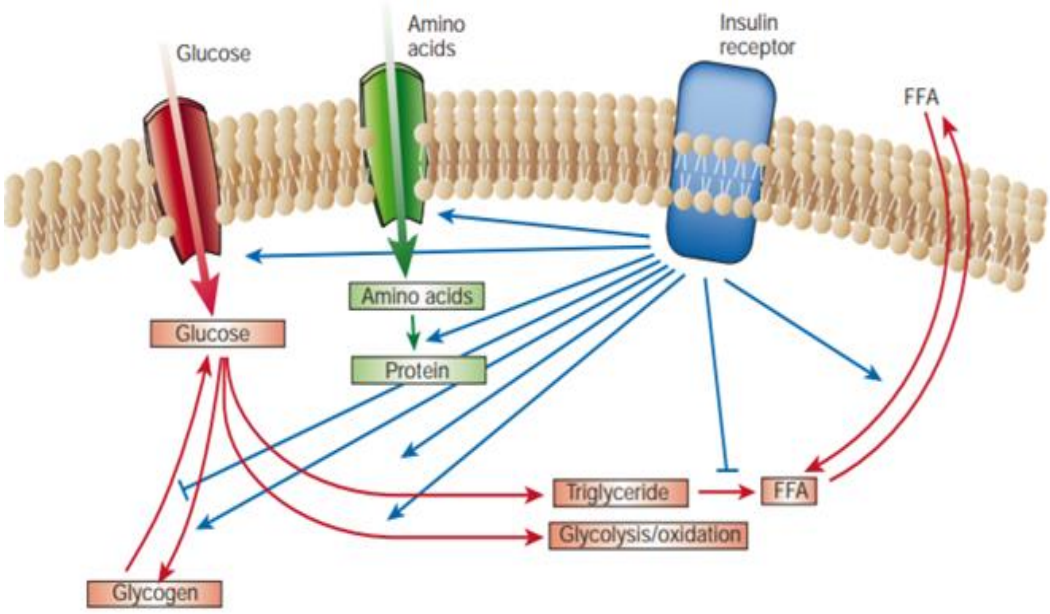

Figure 5: Schematic representation of insulin action (Adapted from Saltiel & Kahn 2001)

1.3 Beta-cell dysfunction

Insulin hormone, produced by the beta cells of the pancreas, perform an important function in maintaining the blood glucose level within a normal physiological range. In healthy individuals, when the insulin resistance occurs, the beta cell population is increased to compensate for the insulin demand and maintain normal glycemia. However, when the beta cells fail to compensate for increased insulin demand, it results in a rise of blood glucose and free fatty acids which further induces structural and functional changes contributing to beta cell dysfunction, followed by beta cell death (Tan *et al.*, 2013). The schematic representation of islet beta cell dysfunction is shown in Figure 6.

Several studies have highlighted the detrimental effects of high blood glucose on pancreatic beta cells function, and the process is termed as glucotoxicity. This includes

impaired insulin release in response to intravenous glucose and non-glucose secretagogues, a decrease in intracellular storage of insulin due to beta cell exhaustion and a decrease in insulin production due to damage of cellular components by increased ROS level (Robertson & Harmon, 2003, Cernea & Dobreanu, 2013). Hyperglycaemia is also believed to be an important factor that contributes to beta cell dedifferentiation by altering important transcription factor FOXO1, where beta cells lose their identity and functions and get converted to other endocrine cells. (Talchai *et al.,* 2012, Taylor *et al.,* 2013, Puri *et al.,* 2013, Guo *et al.,* 2013, Wang *et al.,* 2014). Studies have also reported adverse effects of elevated free fatty acids on beta-cell function, and the process is termed as lipotoxicity. Impaired glucose-stimulated insulin release and decreased insulin production was observed in pancreatic beta cells after chronic exposure to free fatty acids. It promotes beta cell loss by increasing expression of cytokines (such as TNFα and IL-2) and by activating ER stress by diminishing ER calcium store (DeFronzo, 2004, Cernea & Dobreanu, 2013, Sharma & Alonso, 2014) Islet amyloid polypeptide (IAPP, or amylin) secreted together with insulin by pancreatic beta cells, maintain glucose homeostasis by delaying gastric emptying and promoting satiety. Recent studies have reported that deposited islet amyloid polypeptide (IAPP) has cytotoxic properties which contribute to β-cell dysfunction and death (Akter *et al.,* 2016).

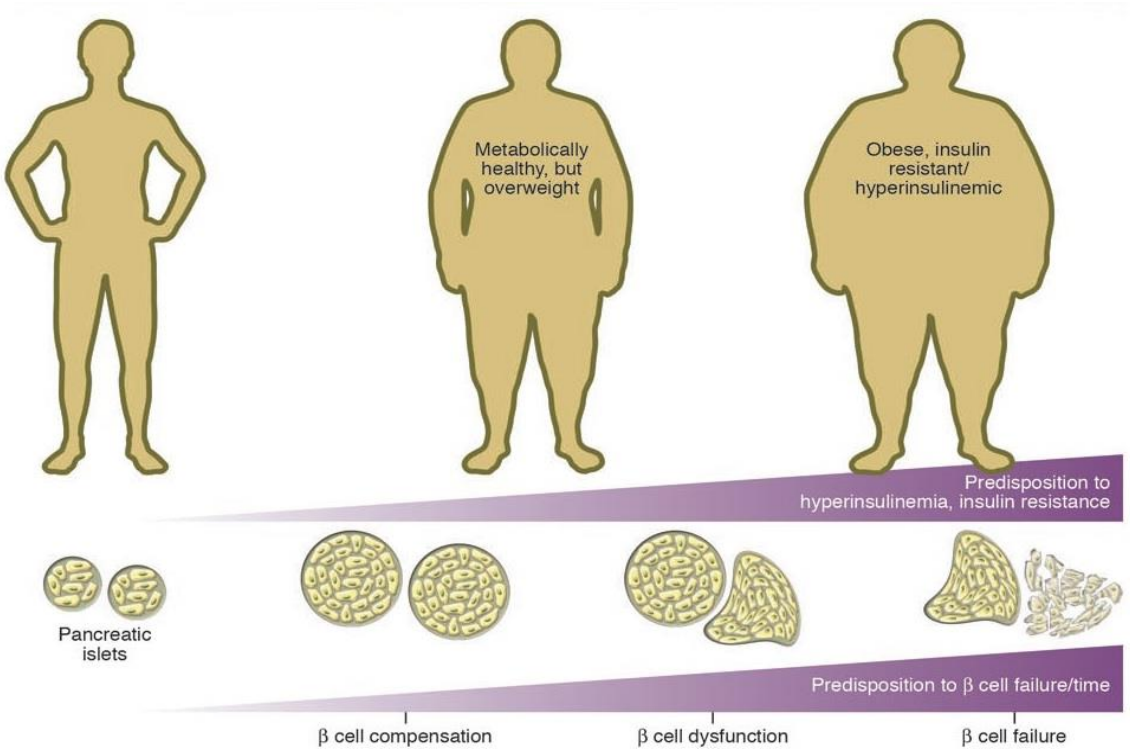

Figure 6: Schematic representation of islet beta cell dysfunction (Adapted from Prentki *et al.,* 2006)

1.4 Insulin resistance

Insulin resistance is when the body fails to use insulin effectively or respond weakly to available insulin, resulting in hyperglycaemia (American Diabetes Association, 2010). As the insulin resistance progresses, pancreatic beta cells increase the production of insulin to compensate insulin demand, further contributing to hyperinsulinemia. The prevalence of insulin resistance among obese individuals is well documented, and these individuals are at high risk of developing T2DM. In addition, insulin resistance also occurs in old age, pregnant women and sometimes individuals at puberty (Buchanan *et al.,* 1990, Sonagra *et al.,* 2014). In obese individuals, it is believed that the accumulation of fat in the abdominal area influences the early development of insulin resistance. These fats are less sensitive to the

antilipolytic effects of insulin and results in an increase in the level of non-esterified fatty acids (NEFA) in the blood. Studies conducted by Roden *et al.,* 1997, observed the development of insulin resistance and impaired glucose tolerance with rising plasma NEFA levels in humans. In obese and diabetic individuals, a decrease in insulin sensitivity was observed with rising NEFA level (Zeirath *et al.,* 1998). NEFA enters the cells and undergoes oxidation to produce diacylglycerol, fatty acyl CoA and ceramides metabolites. These metabolites further activate serine/threonine kinase cascade, which phosphorylates serine/threonine residue of insulin receptor substrate-1 (IRS1) and insulin receptor substrate-2 (IRS-2). In their phosphorylated form, IRS1 and IRS2 fail to activate other molecules of insulin signalling and this results in loss of glucose entry in the cells. An alternative mechanism involves an increase in acetyl CoA/CoA and NADH/NAD^+ ratio after fatty acid oxidation that leads to inactivation of pyruvate dehydrogenase enzyme and accumulation of citrate which subsequently inactivate glycolytic enzymes including phosphofructokinase and hexokinase enzyme. Inactivation of glycolytic enzymes results in the accumulation of glucose inside cells thereby affecting glucose uptake (Randle *et al.,* 1963, Shulman, 2000). Proinflammatory cytokines such as tumour necrosis factor-α (TNF-α), interleukin-6 (IL-6) release from adipose tissue also play a vital role in the development of insulin resistance by diminishing insulin signalling events (Kahn *et al.,* 2006, Tangvarasittichai *et al.,* 2016).

1.5 Current Therapies for Diabetes

1.5.1 Lifestyle modification

The progression of T2DM can be prevented or delayed by following a healthy lifestyle (Miller *et al.,* 2014). Studies have demonstrated that following a healthy diet, regular

exercise and weight management can help to keep blood glucose under control (Chong *et al.,* 2017). A study conducted by Tuomileho *et al.,* 2001, has shown that regular physical exercise helps to maintain a healthy blood glucose level and reduces the risk of secondary complications in people with T2DM. The risk of onset of T2DM in patients with impaired glucose tolerance was significantly reduced by following a strict diet which is low in saturated and total fat and rich in carbohydrate and dietary fibre (Liu *et al.,* 2015). Knowler *et al.,* 2002, reported that lifestyle intervention is more effective than metformin in treating T2DM.

1.5.2 Metformin

The oral glucose-lowering agent Metformin, derived from plant *Galega officinalis,* was first reported by Dr Jean Sterne and his colleagues in 1950 (Rojas *et al.,* 2013). After the UK Prospective Diabetes Study (UKPDS) in 1998, metformin was used as first-line treatment for T2DM. Also, according to clinical practice guidelines by the American Diabetes Association (2015), metformin was recommended as an initial treatment for managing T2DM. Traditionally, metformin is believed to control blood glucose level by suppressing gluconeogenesis and glycogenolysis pathways in the liver (Rena *et al.,* 2017). Recent studies have also shown that metformin treatment also controls blood sugar level by improving 1) insulin sensitivity, 2) lipid metabolism and 3) islet insulin secretory responses (Kashi *et al.,* 2016, Kocer *et al.,* 2014). Further studies have also shown that metformin could also lower the risk of cardiovascular diseases associated with diabetes (Holman *et al.,* 2008). At the molecular level, metformin has shown to demonstrate its effects via both AMP-activated protein kinase (AMPK)-dependent and an independent mechanism (Rena *et al.,* 2017). Metformin

treatment can cause side effects such as abdominal pain, lactic acidosis and diarrhoea (Kalantar-Zadeh *et al.*, 2013, DeFronzo *et al.*, 2016).

1.5.3 Insulin

The discovery of Insulin by Dr Fredrick Bathing and his colleagues in 1921, was one of the important breakthroughs in the history of medicine. In T1DM patients, the pancreas does not produce insulin due to the destruction of beta cells. Such patients have to take insulin from external source multiple times a day to maintain near-normal blood sugar levels. Also, in T2DM as the diseases progress, the pancreas does not produce enough insulin due to loss of beta cell mass and function. In such circumstances, oral antidiabetic agents become therapeutically ineffective for the treatment. Eventually, many patients with T2DM will depend on external insulin to improve hyperglycaemia and complications associated with diabetes (Home *et al.*, 2014). Insulin demonstrates its glucose-lowering effects a) by recruiting GLUT4 transporter protein to the plasma membrane, b) stimulating synthesis of glycogen, fatty acid and triacylglycerol c) inhibiting gluconeogenesis and glycogenolysis (Dimitriadis *et al.*, 2011). Currently, several types of insulin are available such as rapid-acting, short-acting, mixed, intermediate-acting and long-acting insulin. Hypoglycaemia and weight gain are the main side effects associated with insulin treatment (Nansel *et al.*, 2013, Boucher-Berry1 *et al.*, 2016).

1.5.4 Amylin

Amylin is a 37-amino acid peptide that is synthesised by pancreatic beta cells and co-secreted with insulin. Amylin controls blood glucose by several mechanisms including suppressing postprandial glucagon secretion, reducing hepatic glucose production and

food intake and by slowing down gastric emptying. Pramlintide, a synthetic version of amylin, controls blood glucose by a similar mechanism. Additionally, pramlintide has been shown to improve lipid metabolism in both T1DM and T2DM (Hoogwerf *et al.,* 2008). Nausea is commonly observed in pramlintide treated patient. Other side effects such as anorexia and hypoglycaemia were also reported (Nogid and Pam, 2006).

1.5.5 Thiazolidinedione (glitazones)

Thiazolidinediones (TZD) are oral hypoglycemic agents and were first approved for the treatment of T2DM in 1966 by the Food and Drug Administration (FDA) (Kendall, 2006). TZDs control blood glucose by improving insulin action in the muscle, liver and adipose tissue, thus, allowing insulin produced pancreas to work effectively (Davidson *et al.,* 2017). TZDs demonstrate its efficacy by targeting peroxisome proliferator-activated receptor γ (PPARγ), which in turn activates genes involved in glucose and lipid metabolism. The expression of proinflammatory cytokines which contribute to insulin resistance was significantly downregulated by TZD treatment. Pioglitazone is the only thiazolidinedione, currently available for the treatment. Troglitazone followed by rosiglitazone, were withdrawn from the market because of its toxic effects (Jaeschke, 2007, Hemmeryckx *et al.,* 2013). TZD is prescribed for the treatment of T2DM patient if other oral antidiabetic agents (e.g. metformin and sulfonylureas) fail to lower blood glucose level. Side effects of TZD may include weight gain, liver failure, heart problems and bone fractures (Rizos *et al.,* 2009)

1.5.6 Sulfonylureas

Sulfonylureas and their hypoglycemic effects were first reported in 1942 by Janbon and his colleagues. Sulfonylureas class of drugs (e.g., tolbutamide, gliclazide, glibenclamide) increase plasma insulin concentration by stimulating the release of insulin from beta cells of the pancreas by K_{ATP} channel-dependent pathway (Sola *et al.,* 2013). Sulfonylureas act directly on beta cells by binding to the sulfonylurea receptor (SUR-1) present on the cell membrane. In treated patients, a decrease in blood HbA1C level and improvement of secondary complications were observed (Nathan *et al.,* 2009). These drugs demonstrate insulinotropic effects in a glucose-independent manner. As a result, treated patients run a high risk of hypoglycaemia, and which is augmented in patients with kidney diseases (Dalem *et al.,* 2013). The potency of sulfonylureas depends on beta cell function. Hence this drug is only effective or should be recommended only at an early stage of T2DM (Kalra *et al.,* 2016). Side effects including cardiovascular diseases, weight gain and beta-cell dysfunction were noticed in sulfonylureas treatment (Thulé & Umpierrez, 2014, Maedler *et al.,* 2015, Kalra *et al.,* 2016).

1.5.7 Meglitinides

Meglitinides are short-acting insulin secretagogues, which control blood glucose by increasing plasma insulin levels. This class of drug induces its effects by blocking K_{ATP} channels in beta cells resulting in an increase in Ca^{2+} influx and insulin secretion. Meglitinides such as repaglinide and nateglinide were approved by the FDA in 1997 and 2000 respectively for the treatment of T2DM (Stein *et al.,* 2013). In several clinical studies, a decrease in blood HbA1C was observed in repaglinide-treated patients. However, this class of drugs is, like sulfonylureas, associated with the risk of hypoglycaemia (Wu *et al.,* 2018).

1.5.8 Alpha-glucosidase inhibitors (AGIs)

Alpha-glucosidase inhibitors like acarbose, miglitol and voglibose are oral antidiabetic agents. This class of drugs demonstrates glucose lowering effects by suppressing the activity of the alpha-glucosidase enzyme, which subsequently delays the digestion of carbohydrate to glucose (He *et al.,* 2014). Moreover, AGI treatment has shown to improve body weight, lipid metabolism and blood pressure (Hanefeld & Schaper, 2008). Beneficial effects of AGIs were observed on cardiovascular events in treated diabetes patients. However, this class of drugs demonstrated poor glycaemic control compared to metformin and sulfonylureas and caused gastrointestinal complaints (Standl and Schnell, 2012).

1.5.9 GLP-1 analogues and DPP-4 inhibitors

Glucagon-like peptide-1 (GLP-1) and GIP are incretin hormones, synthesised by enteroendocrine cells in the intestine and released following food intake. Studies have shown that GLP-1 maintains glucose homeostasis through several mechanisms: 1) stimulated release of insulin from beta cells in a glucose-dependent manner, 2) delayed gastric emptying, 3) decreased energy intake and 4) reduced postprandial glucagon level (Tasyurek *et al.*, 2014). Furthermore, GLP-1 has been shown to improve beta cell proliferation, survival, and beta cell mass by inhibiting apoptosis (Lee *et al.*, 2016). GLP-1 has a short half-life (less than 2 min) and is degraded by dipeptidyl peptidase-IV (DPP-IV). Because of this, the clinical efficacy of native GLP-1 is limited (Manandhar & Ahn, 2014). Research overcame this limitation by developing two pharmacological approaches: 1) synthesising GLP-1 analogues with improved half-life and 2) suppressing activity of DPP4 enzyme to improve endogenous GLP-1 level (Chon & Gauiter, 2016).

To date, six GLP-1 analogues including exenatide, liraglutide, albiglutide, dulaglutide, lixisenatide and semaglutide are in used for the treatment of T2DM. According to guidelines of the National Institute for Health and Care Excellence, this class of drugs is considered for the treatment in combination with metformin and sulfonylureas. The risk of hypoglycaemia associated with this class of drugs is limited, as their insulin-releasing effects are glucose dependent. Moreover, improvement in glycaemic response, a decrease in glucagon release, reduction in energy intake and weight loss were observed with GLP-1 analogues treatment (Lepsen *et al.*, 2015). Nausea, vomiting and gastrointestinal problems were the main side effects associated with this class of drugs (Bettge *et al.*, 2017).

DPP-4 inhibitors (gliptins) are oral antidiabetic agents that increase the level of the endogenous GLP-1 level (2-3 fold) by suppressing the activity of DPP-4 enzyme. To date, five DPP4 inhibitors including sitagliptin, vildagliptin, saxagliptin, alogliptin, linagliptin are in clinical use. DPP4 inhibitors can be used as monotherapy in patients who may not be able to take metformin due to renal dysfunction or in combination with other oral antidiabetic agents such as metformin and sulfonylureas for the management of T2DM (Dicker, 2011). Unlike some of the other oral antidiabetic drugs, DDP-4 inhibitors have low hypoglycaemia risk profile and are weight neutral (Aschner *et al.*, 2006, Malmgren & Ahrén, 2015). A headache, nasopharyngitis, upper respiratory tract infection, urinary tract infection was most common adverse reaction observed in a treated patient (Amori *et al.*, 2007, Yazbeck *et al.*, 2007, Richter *et al.*, 2008).

1.5.10 SGLT2 Inhibitors

SGLT2 inhibitors are a new class of oral glucose-lowering agents for the treatment of T2DM (Karla, 2014). SGLT2 inhibitors target sodium-dependent glucose co-transporter 2 (SGLT-2) proteins, which are exclusively expressed on proximal tubule of the nephron in the kidney. SGLT2 inhibitors, lower blood glucose through suppressing glucose reabsorption by blocking SGLT-2 transporter proteins (Lee *et al.,* 2007, Hummel *et al.,* 2011). Dapagliflozin and canagliflozin are two popular SGLT2 inhibitor drugs that have been approved by the regulatory agency for the treatment of T2DM. In SGLT-2 inhibitor treatment, reduction in glycated haemoglobin, body weight and blood pressure were observed in patients. Recent studies have issued warning that SGLT2 inhibitors treatment could increase the risk of diabetic ketoacidosis, pancreatitis and bone fracture (FDA, 2015, Chowdhary *et al.,* 2015, Fadini *et al.,* 2017, Hsia *et al.,* 2017). Other side effects associated with SGLT-2 inhibitor are urinary tract infection and polyurea (Geerlings *et al.,* 2014).

1.5.11 Bariatric surgery for the treatment of diabetes

Research studies have confirmed the beneficial effects of weight loss surgery (bariatric surgeries) in patients with gross obesity and T2DM (Kassem *et al.,* 2017). Bariatric surgery has been shown to improve glucose homeostasis through several mechanisms including increasing insulin secretion, insulin sensitivity, satiation and weight loss (Cummings and Cohen, 2016, Rubino *et al.,* 2016). Additionally, bariatric surgery has resulted in a dramatic reduction in cardiovascular diseases risk. According to NICE guidelines, a patient is considered for bariatric surgery assessment if BMI ranges between 30.0-34.9. For BMI above 50, bariatric surgery is recommended as a treatment option. The four main bariatric procedures are: 1) Vertical sleeve gastrectomy (VSG), 2) Laparoscopic adjustable gastric banding (LAGB), 3)

Laparoscopic Roux-en-Y gastric bypass surgery (RYGB), 4) Biliopancreatic Diversion (BPD). These procedures are mainly classified into restrictive (decrease gastric capacity) or malabsorptive (decrease absorptive capacity). RYGB is the most popular restrictive and malabsorptive procedure, which had shown an 88% diabetes remission rate and 50-84% reduction in CV risk. However, despite these beneficial effects, bariatric surgeries are associated with high cost and complications such as abdominal pain and nutritional deficiencies (Abdeen and le Roux, 2016)

1.5.12 New medications for diabetes

In the last 12 years, several new drugs, including oral and injectables, were approved by the European Medicines agency for the treatment of diabetes (Figure: 7).

Oral drugs include:

- **Xigduo:** Xigduo from AstraZeneca contains metformin (biguanides) and dapagliflozin (SGLT2 inhibitors).
- **Qtern**: Qtern form AstraZeneca is a combination of dapagliflozin and saxagliptin.
- **Segluromet:** Steglujan from Merck Sharp & Dohme B.V is a combination of ertugliflozin and metformin hydrochloride
- **Steglujan:** Steglujan from Merck Sharp & Dohme B.V, combined ertugliflozin with sitagliptin.

Injectable drugs include:

- **Soliqua: Soliqua** from Sanofi contain long-acting insulin glargine and lixisenatide.
- **Ozempic:** Ozempic from Novo Nordisk is a GLP-1 receptor agonist

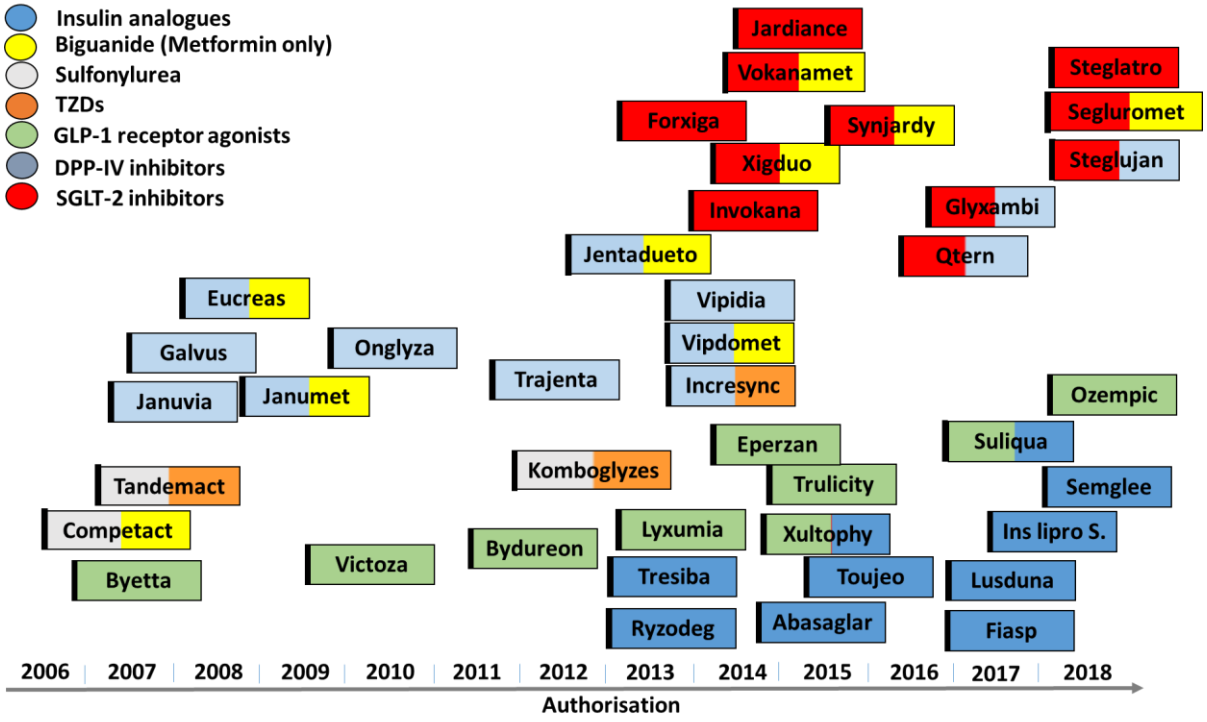

Figure 7: Antidiabetic drugs approved by European Medicines Agencies since 2006, (Adapted from Blind *et al.*, 2018).

1.6 New treatments

According to the IDF, diabetes is one of the leading health problems affecting 8.8% of the global population, of whom about 80% live in low and middle-income nations. The cost for the treatment has reached USD 727 billion per annum and is expected to rise dramatically due to the growing diabetes population particularly in developing nations (IDF, 2017). Although many classes of glucose-lowering drugs are available, none of them has shown the ability to achieve long-term glycaemic control, prevent secondary complications and restore pancreatic beta cell function. Moreover, these drugs are often given in combination to bring down blood glucose, which makes the treated patient susceptible to more side effects associated with drugs. Further, the increasing cost of the treatment is imposing a heavy financial burden on the world

economy. Therefore, the search for new alternative therapies that are cost-effective and can overcome the limitations of existing drugs are required.

1.7 Amphibian Skin secretions

The name Amphibian was first coined by Linnaeus, to introduce to that class of vertebrates which is in-between fish and reptiles. In 1931, Nobel referred to amphibians as cold-blooded vertebrates that live in the aquatic and terrestrial environment. Amphibians are grouped in 3 classes Anura, Urodeles and Gymnophions.

The skin of amphibians is a complex organ rich in glands which play an essential role in the amphibian survival under different environmental conditions. The primary roles of amphibian skin include respiration, water regulation, defence, temperature control, reproduction and excretion. It consists of two main glands, mucus and granular glands, which are connected to the skin surface by secretory ductus (Wells, 2007). Mucus glands produce mucopolysaccharides that keep the skin moist, smooth, prevent loss of water, protect skin from mechanical damage and trap the pathogens. Granular glands (also known as poison glands) are present below the skin surface across the body, secrete chemical compounds that play a crucial role in host defence against microbial and fungal infection, as well as against predators. The secretions of granular glands, which are controlled by sympathetic nerves, are rich in peptides, bufotoxins (steroids), alkaloids, amines and bufogenines, and released during stress/injuries (Clark *et al.*, 1997).

In many ancient cultures, skin secretions of amphibians were used in the preparation of medicine for the treatment of diseases. Secretions of dried toad skin were used in Chinese traditional medicine for the treatment of arthritis. Chan Su, prepared from

skin glands of Chinese toad, is Chinese traditional medicine, was used for the treatment of heart diseases, leukaemia, rhinosinusitis and other diseases (Gomes *et al.*, 2007).

In early 1970, research work by scientist Vittorio Erspamer and his colleagues identified several peptides in the skin secretions of amphibians (listed below).

Sr no	Peptide	Amphibian	Year
1	Bradykinin	*Phyllomedusae* and *Ranae* species	1962
2	Caerulein	*Hyla caerulea*	1966
3	Bombesin	*Bombina bombina* *Bombina variegata*	1971

These peptides were found to be identical to mammalian peptides and hormones found in the gastrointestinal and central nervous system. For example, Caerulein isolated from frog *Litoria caerulea,* which has been shown to stimulate secretion of insulin, glucagon and calcitonin, was homologues of cholecystokinin and gastrin, and bombesin from genus bombina was found similar to gastrin-releasing peptides (GRP), which act on smooth muscles of gut (Pukala *et al.,* 2006, Ohki-Hamazaki *et al.,* 2005). After these discoveries, the search for amphibian skin peptides has gained momentum (Wang *et al.,* 2009). The isolation and characterization of magainins from South African clawed frog *Xenopus levis,* is considered as a significant finding, which has resulted in the isolation of several other bioactive peptides from skin secretions of frogs/amphibian (Clarke 1997, Rinaldi, 2002). Isolated magainins demonstrated low or moderate potency against both gram-positive (*Streptococcus, Staphylococcus*) and gram-negative (*Escherichia, Pseudomonas, Acinetobacter* and *Helicobacter*) bacteria. As well they displayed low haemolytic activity against human erythrocytes (Zasloff, 1987). Several recent studies have also revealed that magainin-2 peptides exhibit bactericidal activities by forming pores in lipid membranes (Imura *et al.,* 2008, Tamba

et al., 2010). The biological activity of amphibian skin peptides is not only confined to antimicrobial activity. Research has confirmed the presence of bufalin, and other antineoplastic and immunostimulatory agents in Chan Su medicine (Bhuiyan *et al.,* 2003, Shimizu & Inoue, 2004, Ko *et al.,* 2005). Recent studies have also reported a wide range of biological activities of amphibian/frog skin peptides (Gomes *et al.,* 2007, Conlon *et al.,* 2012a, Conlon & Mechkarska, 2014).

Earlier, methanolic extraction method was used to separate peptides from sun-dried amphibian skins (Tyler *et al.,* 1992). This method involves the killing of frogs, sun drying of skin and grinding of dried skin. Due to these multiple steps, the methanolic extraction method is more prone to contamination with foreign substances and peptide degradation. Hence using this method to isolate pure peptide is not considered desirable. In another method of extraction, frog skin is homogenised in sodium acetate containing protease inhibitors. However, this method is time-consuming and not feasible economically. The use of mild electric stimulation and injection of norepinephrine are considered as a most effective and non-harmful method for the isolation of pure compounds from skin secretions (Conlon *et al.,* 2007a, Zahid *et al.,* 2011).

1.7.1 Biological properties of amphibian skin peptides

Peptides found in skin secretions of frogs vary in size from 8 to 63 amino acid residues. Sequence analysis revealed that these peptides do not have a conserved domain connected with their biological properties. However, these peptides are rich in positively charged amino acids including lysine, arginine and histidine and contain nearly 40-70% of hydrophobic amino acids. Due to the presence of multiple positive amino acids, these peptides carry positive charge between +2 and +6 at pH 7. In

aqueous solution, these peptides do not have any stable secondary structure, but in the vicinity of a phospholipid, bilayer peptides tend to form amphipathic alpha helix structure (Conlon & Mechkarska, 2014).

Zasloff and his colleagues were first to report the antibacterial activity of peptides found in skin secretions of frogs (Andrade, 2015). Magainins peptides isolated from *Xenopus levis* demonstrated antimicrobial activity against both gram-positive and gram-negative bacteria. Subsequently, other antimicrobial peptides were isolated from *X.levis* and termed peptide glycine-leucine amide (PGLa), caerulein precursor fragment (CPF) and xenopsin precursor fragment (XPF) (Gibson *et al.,* 1986, Soravia *et al.,* 1988, Conlon & Mechkarska, 2014). Orthologues of these peptides were found in several species of frogs belonging to genus *Xenopus*. Both PGLa-AM1 and CPF-AM1 from *X. amieti,* demonstrated broad-spectrum bactericidal activity against *Escherichia coli* and *Staphylococcus aureus.* Also, frog skin peptides showed activity against microorganisms that are resistance to currently available antibiotics. PGLa has an inhibitory effect against amphotericin B-resistant *Candida albicans,* and fluconazole-resistant *Candida glabrata* isolate (Helmerhorst *et al.,* 1999). CPF-AM1 displayed an inhibitory effect against the colistin-resistant strain of (clinical isolates of multidrug-resistant) *Acinetobacter baumannii* (Conlon Mechkarska, 2014). Temporin-Dra from *Rana draytonii,* and Frenatin 2.1S and Frenatin 2.2S from *Sphaenorhynchus lacteus* were effective against methicillin-resistant strains of Staphylococcus aureus (MRSA) (Conlon *et al.,* 2011, 2014b).

In addition to antimicrobial activity, frog skin peptides also showed cytotoxic potency against a variety of tumour cell lines. Ascaphin-8 from *Ascaphus truei,* Peptide XT7 from *Silurana tropicalis* and Dermaseptin L1 and Phylloseptin L1 from *Agalychnis lemur,* showed cytotoxicity against hepatocarcinoma HepG2 cells (Conlon *et al.,*

2007b, Conlon *et al.,* 2008). Esculentin-2CHa from *Lithobates chiricahuensis* and Hymenochirin 1B from *Hymenochirus boettgeri* were active against lung adenocarcinoma (Attoub *et al.,* 2013a, b). Magainin-2 from *Xenopus laevis* demonstrated tumoricidal activity against lung cancer cell line, bladder cancer cell line and hematopoietic cell line (Cruciani *et al.,* 1991, Ohsaki *et al.,* 1992, Lehmann *et al.,* 2006). Temporin-1CEa from Chinese brown frog *Rana chensinensis* and Hymenochirin 1B from *Hymenochirus boettgeri,* displayed cytotoxic activity against a human breast cancer cell line (Wang *et al.,* 2013, Attoub *et al.,* 2013a). Dermaptin B2 & B3 from *Phyllomedusa bicolor* demonstrated both cytotoxic and angiostatic properties against prostatic adenocarcinoma PC3 cells (Van Zoggel *et al.,* 2012).

Recent studies have shown antiviral activities of several frog skin peptide. Magainin-1 and -2 from *Xenopus levis*, Dermaseptins S1–S5 from *Phyllomedusa sauvagei* and Brevinin-1 from *Pelophylax porosus* were effective inhibitors against herpes simplex virus type 1 (HSV-1) and herpes simplex virus type 2 (HSV-2) (Matanic *et al.,* 2004, Belaid *et al.,*2002, Bergaoui *et al.,* 2013). PGLa-AM1 and CPF-AM1 from *Xenopus amieti* showed antiviral properties against HSV-1, Caerin 1.1, 1.9, and maculatin 1.1 from Australian tree frogs demonstrated antiviral activity against HIV infection (VanCompernolle *et al.,* 2005).

Frog skin peptides have also been shown to possess immunomodulatory activities. The synthetic analogues of ascaphin-8, temporin-Dra, XT-7 and hymenochirin-1B peptides enhanced the release proinflammatory cytokines while demonstrating antimicrobial activity, suggesting a possible role in protection from inflammation (Pantic *et al.,* 2017b). Frenatin 2.1S from *Sphaenorhynchus lacteus* displayed antimicrobial activity by promoting immune cells including NK (Natural Killer cells),

NKT (Natural Killer T cells) and macrophages (Waldhauer & Steinle, 2008, Vivier *et al.,* 2008).

1.7.2 Insulin-releasing peptides from skin secretion of frogs

The search for antidiabetic peptides from animal sources has gained momentum after the approval of exenatide, isolated from the venom of *Heloderma suspectum*, for the treatment of T2DM. The peptides found in skin secretions of frogs, which were initially characterised based on antimicrobial activity showed the ability to demonstrate insulin-releasing activity. Studies conducted in our laboratory have identified insulin releasing peptides derived from skin secretion of frogs belonging to Ranidae, Hylidae, Dicroglossidae, Leptodactylidae, Bombinatoridae & Pipidae families (Table 1.1). The isolated frog skin peptides demonstrated insulin release *in vitro* using rat clonal pancreatic beta cells (BRIN-BD11 cells), human-derived pancreatic beta cells (1.1B4), primary islet cells and *in vivo* in lean and high fat fed mice.

Marenah *et al.*, 2004b, demonstrated insulin-releasing activity of skin secretion of frog *Rana palustri*. The isolated active compound, which demonstrated concentration-dependent insulin release, exhibited 48% identity with brevinin-1, an antimicrobial peptide found in the skin secretion of various Rana species. Hence the peptide was named as brevinin-1. Subsequently, novel insulin releasing peptide (24 amino acid) was isolated from skin secretion of *Rana pipiens*. This peptide showed 100% homology to pipinin-1, which was initially characterised as an antimicrobial peptide (Marenah *et al.*, 2005). Similarly, four insulinotropic peptides were isolated from skin secretions of *Rana saharica* that were identical to antimicrobial esculentin-1, esculentin-1B brevinin-1E and brevinin-2EC (Marenah *et al.,* 2006).

Antimicrobial peptides belonging to the temporin family have also demonstrated insulin-releasing activity. Temporin-Oe, Temporin -Vb, Temporin -DRb, and Temporin -TGb isolated from *Rana ornativentris, Lithobates virgatipes, Rana draytonii* and *Rana tagoi* respectively, stimulated dose-dependent insulin release from BRIN-BD11 cells without affecting cell viability. Temporin-Oe was potent and displayed a 2.6-fold increase in insulin release compared to control (Abdel-Wahab *et al.,* 2007). Seven peptides isolated from norepinephrine stimulated skin secretions of the *Lithobates catesbeianus,* potentiated insulin release from BRIN-BD11 cells with no release of LDH enzyme (Mechkarska *et al.,* 2011).

Peptides belonging to the Phylloseptin family also produced significant insulinotropic effects. Phylloseptin-L2 (a 15 amino acid peptide) from *H. lemur* stimulated insulin release from BRIN-BD11 cells by K_{ATP} channel-independent pathway (Abdel-Wahab *et al.,* 2008b). Furthermore, this peptide also improved glucose tolerance in healthy mice by increasing insulin concentrations. Peptides with insulin releasing properties were also identified in the skin secretions of frogs belong to the subfamily Phyllomedusinae. RK-13 peptide from skin secretions of *A. calcarifer* stimulated insulin release in a dose-dependent manner from BRIN-BD11 cells without affecting cell viability. Early mechanistic studies revealed that peptide might stimulate insulin release cells by activation of protein kinase A (PKA) pathway (Abdel-Wahab *et al.,* 2005).

A recent study has described insulinotropic effects of Tigerinin-1R peptide (RVCSAIPLPICH.NH_2) found in the skin secretions of frog *Hoplobatrachus rugulosus* (formerly known by *Rana rugulosa*). The insulinotropic effects of the peptide were not associated with the release of LDH enzyme, suggesting the integrity of the plasma membrane. The maximum response produced by tigerinin-1R was

greater than that produced by GLP-1 and GIP under the same experimental condition. Like KCl and alanine, tigerinin-1R depolarised BRIN-BD11 beta cells and increased intracellular Ca^{2+}. This study also revealed that C- terminal amidation is essential for good insulinotropic potency. Acute administration of Tigernin-1R significantly enhanced insulin release and improved glycaemic response in high-fat-fed mice (Ojo *et al.*, 2015b).

More recently, Owolabi *et al.*, 2015 reported the dose-dependent insulin-releasing effects of Hymenochirin-1B, isolated from *Hymenochirus boettgeri,* in BRIN-BD11 and isolated mouse islets. Preliminary mechanistic studies revealed that peptide might stimulate insulin release by PKA pathway. In high-fat-fed mice Hymenochirin-1B, significantly improved glycaemic control with a concomitant increase in insulin release after acute administration.

1.7.3 Frog species studied in this thesis

1.7.3.1 *Discoglossus sardus*

Discoglossus sardus, also known as Tyrrhenian painted frog, is a medium-sized frog (up to 75 mm in length) that belong to the family *Alytiade*. Their population is scattered on Mediterranean islands but predominantly found on the island of Sardinia and Corsica. They are naturally found in a wide range of aquatic and terrestrial habitats. Unlike other frog skin peptides, the peptides found in the norepinephrine-stimulated skin secretions of *D. sardus* did not exhibit antimicrobial or haemolytic activity. The peptidomic analysis of the norepinephrine-stimulated skin secretions revealed the presence of peptides that showed structural similarity to frenatin 2 peptides found in the skin secretions of Australian frog *Litoria infrafrenata.* Henceforth, isolated peptides were termed as frenatin 2D, and frenatin 2D.1 Frenatin

2D predominately displayed immunostimulatory activities as demonstrated by enhancing the production of proinflammatory cytokines (TNF-α, IL-1β) by stimulating macrophages. Also, frenatin 2D has been shown to increase the production of IL-12 in LPS-stimulated and unstimulated macrophages (Lin & Karin, 2008, Conlon *et al.,* 2013).

1.7.3.2 *Sphaenorhynchus lacteus*

Sphaenorhynchus lacteus (also referred as Orinoco Lime Treefrog), belonging to the family *Hylidae,* is found in the Amazon basin of South America and on the islands of Trinidad and Tobago (Frost, 2014). In norepinephrine-stimulated granular glands secretions of this frog species, three host defence peptides were found identical to frenatin 2. Hence these peptides were named as frenatin 2.1S, frenatin 2.2S and frenatin 2.3S. The former two are rich in glycine/leucine amino acids and α-amidation at C-terminal, while later lacks a α-amidation at C-terminus. Unlike frenatin 2D, frenatin 2.1S and frenatin 2.2S exhibited antimicrobial activity against gram-positive bacteria including *methicillin-resistant Staphylococcus aureus* (MRSA) and *Staphylococcus epidermidis*. Also, both of these peptides demonstrated immunostimulatory activity (Conlon *et al.,* 2014b, Pantic *et al.,* 2017a).

1.7.3.3 *Xenopus amieti*

Xenopus amieti (also known by Volcano clawed frog), belongs to family *Pipidae* is majorly populated in volcanic highland areas of western Cameroon. Their skin secretions are an abundant source of peptides with antimicrobial and cytotoxicity properties. Nine peptides identified in norepinephrine-stimulated skin secretions of *X. amieti*, demonstrated differential antimicrobial activity against *Staphylococcus aureus*

and *Escherichia coli*. These peptides shared a high degree of structural similarity with peptides (magainin, PGLa, CPF, XPF) isolated from *X. laevis* and *Silurana* (formerly Xenopus) *tropicalis* (Conlona *et al.*, 2010).

A PGLa-AM1 peptide isolated from *X. amieti,* demonstrated broad-spectrum bactericidal activity against *Escherichia coli* and *Staphylococcus aureus,* and potent growth-inhibitory activity against colistin resistant *Acinetobacter baumannii,* with low haemolytic activity (Conlon & Mechkarska 2014). Also, PGLa-AM1 stimulated the release of GLP-1 from GLUTag cells (Ojo *et al.*, 2013a). In a recent study, PGLa-AM1 produced a dose-dependent stimulation of insulin release from rat clonal pancreatic beta cells (BRIN-BD11 cells) without the release of lactate dehydrogenase enzyme (LDH) indicating lack of cytotoxicity at concentrations up to 3μM. Its cationic analogues [A14K] & [A20K], containing L-lysine substitution at 14^{th} and 20^{th} position respectively, demonstrated superior insulinotropic potency than parent peptide in BRIN-BD11 cells, and primary mouse islets. Acute administration of [A14K] & [A20K] improved glucose tolerance and increased plasma insulin level both in healthy lean and high fat-fed mice (Owolabi *et al.*, 2017).

Like PGLa-AM1, CPF-AM1 (isolated from *Xenopus amieti*) exhibited antimicrobial activity against *Escherichia coli*, *Staphylococcus aureus* and clinical isolates of *Acinetobacter baumannii* combined with moderate haemolytic activity. It also significantly stimulated release GLP-1 from GLUTag cells (Conlon Mechkarska, 2014, Ojo *et al.*, 2013a). In recent studies, CPF-AM1 showed concentration-dependent insulinotropic effects in BRIN-BD11 cells (Ojo *et al.*, 2012). Its four cationic analogues produced by substitution of amino acids at the 4^{th} and 14^{th} position with either L lysine or L arginine demonstrated significant insulinotropic effects without causing beta cell cytotoxicity. The [S4K] analogue was the most potent, producing

greater stimulatory response both in BRIN-BD11 and isolate mouse islets than the parent peptide. Also, in acute *in vivo* studies, the [S4K] analogue appeared to be more potent than the native peptide at improving glucose tolerance and increasing plasma insulin level in high fat fed mice (unpublished data).

1.7.3.4 *Rana temporaria*

Rana temporaria also referred to as the European common frog, belongs to the family Ranidae. Their population is scattered in Great Britain, Europe and north-west Asia. They are naturally found near mountain lakes. *Rana temporaria* is one of the two amphibian species that inhabit regions north of the Arctic Circle (Ludwiga *et al.*, 2015). Temporin peptides were first isolated from skin secretions of *R.temporaria* (Slmmaco *et al.,* 1996). Subsequently, peptides showing structural similarity to temporins were identified in other frogs' species of both American and Eurasian origin (Rinaldi *et al.,* 2013). The members of temporin family have demonstrated activity against both gram-positive and gram-negative bacteria (Wade *et al.,* 2000, Mangoni *et al.,* 2013. Temporin A and Temporin B have shown potent growth-inhibitory activity against multidrug-resistant clinical isolates of *Staphylococcus aureus,* without affecting infected cells (Grazia *et al.,* 2014). In addition, a few members of temporin family including Temporin-1Vb, -1Oe, -1DRb, and -1TGb demonstrated insulin-releasing activity without cell cytotoxicity (Abdel Wahab *et al.,* 2007).

1.7.3.5 *Rana esculenta*

Rana esculenta is a hybrid of *Pelophylax lessonae* (Pool frog) & *Pelophylax ridibundus* (marsh frog) (Conlon, 2008)**.** Peptides from the skin secretions of these hybrid frogs mainly belong to brevinine 1, brevinine 2, esculentin 1 & esculentin 2

peptide family. Esculentin 1 was first isolated from the skin secretions of this frog and subsequently identified in other frog species. Esculentin 1 is one of the largest antimicrobial peptides comprised of 46 amino acids. It has demonstrated potent inhibitory activity against *Pseudomonas aeruginosa*, *Candida albicans* and *Saccharomyces cerevisiae* (Simmaco *et al.,* 1994, Islas-Rodrìguez *et al.,* 2009, Kang *et al.,* 2010). The antibacterial activity of the N-terminal 1–18 amino acids of esculentin-1 was found similar to that of the intact peptide, suggesting that N terminal region is important for antimicrobial activity (Mangoni *et al.,* 2003).

1.7.4 Peptide Analogues

The therapeutic potential of bioactive peptides isolated from natural sources (plants, animals or humans) is often challenged by poor oral availability, short/reduced metabolic stability, rapid degradation by digestive enzymes, lack of selective binding (interaction with nonspecific receptors), rapid renal clearance, risk of immunogenic effects and cytotoxicity (Lau and Dunn, 2018). The progress in peptide synthesis technology made it possible for the researchers to minimise these shortcomings by design and synthesising the analogues of the peptide with enhanced pharmaceutical properties. Several structure-activity relationship studies of host defence peptides helped to understand the importance of cationicity, hydrophobicity, amphipathicity, helicity and angle subtended by charged residue on biological activities of peptides. Based on this knowledge, several cytotoxic peptides with lower antimicrobial potency from skin secretion of frogs were modified to produce promising antimicrobial agents through the design and synthesis of their analogues (Conlon and Mechkarska, 2014). Analogues of frog skin peptides magainins, CPF peptides and hymenochirin-1B peptide have shown strong antimicrobial potency against multidrug-resistant

microorganism, with reduced haemolytic activity (Zasloff *et al.,* 1998, Cuervo *et al.,* 1988, Conlon *et al.*, 2008, Mechkarska *et al.,* 2013). For example, a synthetic analogue of Hymenochirin-1B, [E6k, D9k] hymenochirin-1B, was designed to exhibit increased cationicity while maintaining amphipathicity, by substituting Glu^{6} and Asp^{9} by D-Lysine, which produced high potency against multidrug resistant clinical isolate and low haemolytic activity (Mechkarska *et al.,* 2013).

Using a similar approach, insulin-releasing peptides were transformed into analogues which displayed potent insulinotropic activities both *in vitro* and *in vivo*. The insulin releasing potency of Pseudin-2 from paradoxical frog *Pseudis paradoxa* was enhanced by designing an analogue with increased cationicity. The analogue designed by substituting $Leu^{18} \rightarrow$ Lys, produced a 215% increase in insulin release at 10^{-6} M concentration in BRIN-BD11 cells, with no adverse effect on the integrity of plasma membrane (Abdel-Wahab *et al.,* 2008a). Structure-activity study of alyteserin-2a (ILGKLLSTAAGLLSNLa), by Ojo *et al.,* 2013b, demonstrated that cationic analogues containing L-lysine and D-lysine substitution show greater insulinotropic potency than the native peptide at 3 µM concentration. Acute administration of [G11k] alyteserin-2a (75 nmol/ kg body weight), resulted in a significant increase in insulin release and improved blood glucose in high fat fed mice. Structure-activity studies of Hymenochirin-1B (isolated from *Hymenochryus begiottri*) demonstrated that [P5K] and [D9k] analogues, nontoxic up to 3 µM concentration, produced maximum rate of insulin release than native from isolated mouse islets, and also improved glycaemic response with a concomitant increase in insulin secretion in high fat fed mice. Treatment of high fat fed mice for 28 days with [P5K] hymenochirin–1B, (75 nmol/kg body weight) significantly decreased blood glucose which was associated with enhanced insulin secretion. Molecular studies confirmed that genes involved in insulin

signalling (muscles) and secretion (isolated islets) were improved significantly in treated mice (Owolabi *et al.*, 2015).

The improvement in the insulinotropic activity of peptide analogue containing tryptophan substitution was also observed (Srinivasan *et al.*, 2015). The recent study demonstrated that Trp^{10} substituted analogue of tigerinin-1R, produced greater insulinotropic potency both in BRIN-BD11 cells and primary isolated islet, in comparison with native peptide. Furthermore, twice daily intraperitoneal administration of Trp^{10} Tigerinin-1R (75 nmol/kg bw) in high-fat-diet-induced diabetic mice for 28 days, improved insulin sensitivity, islet insulin secretory responses, and glycaemic control (Srinivasan *et al.*, 2015). In another study, the insulinotropic activity of the frog skin peptide was enhanced by designing analogues containing fatty acid moiety. Vasu *et al.*, 2017 designed stable analogues of esculentin-2CHa(1–30) peptide by covalently attaching fatty acid (l-octanoate) to Lys at 15^{th} position. In comparison with native peptide, [Lys15-octanoate]-esculentin-2Cha (1–30) exhibited resistance to degradation by plasma peptidases and demonstrated potent insulin-releasing effects in BRIN-BD11, 1.1B4 and primary mouse islets. Treatment of high fat fed mice with [Lys15-octanoate]-esculentin-2Cha (1–30) for 28 days, produced significant improvements in glucose tolerance, insulin sensitivity and decreased HbA1C level similar to exendin-4 treated mice.

1.8 Objectives and Aims

1.8.1 General Objectives

The primary objectives of this thesis were to characterise the bioactive peptides with insulinotropic and antidiabetic properties from skin secretions of selected frog species (listed in Table 1.2) and to assess the metabolic effects and potential role in

transdifferentiation of glucagon producing alpha cells to insulin producing beta cells of substituted analogue of PGLa-AM1 and CPF-AM1, from skin secretions of *Xenopus amieti* (Family: Pipidae), in different mice models of diabetes.

1.8.2 Aims

1.8.2.1 *In vitro* studies

- Synthesis of frog skin bioactive peptides and designing synthetic analogues of these peptides with enhanced insulinotropic activity.
- Confirmation of purity & identity of peptides using reverse-phase high-performance liquid chromatography (HPLC) & Matrix Assisted Laser Desorption Ionisation-Time of Flight (MALDI-TOF) respectively.
- Assessment of acute concentration-dependent insulin-releasing effects of peptides in rat clonal beta cells (BRIN-BD11), human clonal beta cells (1.1B4) and isolated mouse islets, and cell cytotoxicity studies by lactate dehydrogenase assay.
- Preliminary studies to delineate mechanism of insulinotropic action of peptides by assessing their effects on membrane potential and intracellular calcium, cAMP production, insulin release in the presence of known insulin secretagogues and calcium-free buffer, as well as in PKA/PKC downregulated cells.
- Assessing the effects of active peptides on apoptosis and cell proliferation in BRIN-BD11 cells, and glucose uptake using C2C12 muscle cells.
- Investigation of metabolic stability of active peptide in mouse plasma.

1.8.2.2 *In vivo* studies

- Investigation of acute *in vivo* effects of the active peptide on glucose tolerance, plasma insulin and food intake in lean mice to identify most promising peptide that can be used as templet for further modifications.
- Evaluating the metabolic effects of long-term (28 days) administration of active peptides on energy intake, body weight, water intake, blood glucose, plasma insulin, blood HbA1C, glucose tolerance, insulin sensitivity, fat composition, liver and kidney functions, plasma lipid profile, islet morphology and genes involved in glucose homeostasis in diabetic mice model (*db/db* mice).
- Investigating the effects of [A14K] PGLa-AM1 and [S4K] CPF-AM1 peptides on the regeneration of insulin-producing beta cells through and transdifferentiation of glucagon-producing alpha cells using GluCre-ROSA26EYFP mice.

Table 1.1 List of amphibian skin peptides with insulinotropic activities from families Pipidae, Leptodactylidae, Hylidae, Ranidae, Bombinatoridae and Dicroglossidae

Species	Family	Peptide	Primary structure
Xenopus borealis	Pipida	Caerulein-B1	<EQDY(SO3)GTGWMDF[a]
Xenopus amieti	Pipidae	Xenopsin	<EGKRPWIL
Xenopus amieti	Pipidae	Xenopsin-AM2	<EGRRPWIL
Xenopus amieti	Pipidae	CPF-AM1	GLGSVLGKALKIGANLL[a]
Xenopus amieti	Pipidae	PGLa-AM1	GMASKAGSVLGKVAKVALKAAL[a]
Leptodactylus laticeps	Leptodactylidae	Ocellatin-L2	GVVDILKGAAKDLAGHLATKVMDKL[a]
Agalychnis lemur	Hylidae	Phylloseptin L2	FLSLIPHVISALSSL[a]
Agalychnis litodryas	Hylidae	Dermaseptin-L11	AVWKDFLKNIGKAAGKAVLNSVTDMVNE
Pseudis paradoxa	Hylidae	Pseudin-2	GLNALKKVFQGIHEAIKLINNHVQ
Rana ornativentris	Ranidae	Temporin-Oe	ILPLLGNLLNGLL[a]
Lithobates catesbeianus	Ranidae	Ranatuerin-2CBd	GFLDIIKNLGKTFAGHMLDKIRCTIGTCPPSP
Lithobates catesbeianus	Ranidae	Brevinin-1CBb	FLPFIARLAAKVFPSIICSVTKKC
Lithobates septentrionalis	Ranidae	Brevinin-2-related peptide	GIWDTIKSMGKVFAGKILQNL[a]
Rana pipiens	Ranidae	Brevinin-1Pa	FLPIIAGVAAKVFPKIFCAISKKC
Rana palustris	Ranidae	Palustrin-1C	ALSILRGLEKLAKMGIALTNCKATKKC
Bombina variegata	Bombinatoridae	Bombesin	<EQRLGNQWAVGHLM[a]
Bombina variegata	Bombinatoridae	Bombesin-related peptide	<EQRLGHQWAVGHLM[a]
Bombina variegata	IN-21	Bombesin-related peptide	IYNAICPCKHCNKCKPGLLAN
Hoplobatrachus rugulosus	Dicroglossidae	Tigerinin-1R	RVCSAIPLPICH$_a$

Adapted from Ojo (2013). a = C-terminal α amidation.

Table 1.2: List of selected frog species and peptide studied in this thesis

Sr no	Frog species	Family	Peptide
1	*Discoglossus sardus*	Alytidae	▪ Frenatin 2D
2	*Sphaenorhynchus lacteus*	Hylidae	▪ Frenatin 2.1S ▪ Frenatin 2.2S ▪ Frenatin 2.3S
3	*Rana temporaria*	Ranidae	▪ Temporin A ▪ Temporin B ▪ Temporin C ▪ Temporin E ▪ Temporin F ▪ Temporin G ▪ Temporin H ▪ Temporin K
4	*Rana esculenta*	Ranidae	• Esculentin-1a(1-21) • Esculentin-1a(1-14) • Esculentin-1a(9-21) • Esculentin-1b(1-18)

Chapter 2

Materials and Methods

2.1 Materials

The chemical reagents, assay kits and peptides used in experiments and their supplier are listed in the appendices.

2.2 Peptides from skin secretions of frogs

Peptides from skin secretions of frog *Discoglossus sardus, Sphaenorhynchus lacteus, Rana temporaria* and *Rana esculenta* were kindly provided in pure form by Professor J.M. Conlon. Synthetic peptides were supplied in crude as well as in >95% pure form by SynPeptide Co Ltd. (China). The procedure from the collection of skin secretions to structural characterisation of peptides is as follows:

Collection of skin secretion from Norepinephrine (injected/immersed) stimulated frogs

⇩

Partial purification of secretions using Sep-Pak C18 cartridges

⇩

Investigating insulinotropic activity of each fraction in BRIN-BD11 cells

⇩

Separation of peptide components from desired fractions using reversed-phase HPLC on C18 columns

⇩

Investigating insulinotropic activity of each purified peptide components in BRIN-BD11 cells

⇩

Structural characterisation of the purified peptide by sequencing and mass spectrometry

⇩

Synthesis of peptide and analogues

⇩

Insulin-releasing studies *In vivo* and *In vitro*

2.2.1 Reverse-phase high-performance liquid chromatography (RP-HPLC)

2.2.1.1 Purification of peptides

Synthetic peptides supplied in crude form by SynPeptide Co Ltd. (China), were purified using Reverse phase-HPLC (Thermo Fisher Scientific Inc. Waltham, Massachusetts, USA). The representative image of Reversed-phase HPLC is shown in Figure 2.5. The crude peptide (5 mg) was dissolved in 1 ml of 0.1% (v/v) TFA/water and injected into Vydac 218TP1022 (C-18) reversed-phase HPLC column at the flow rate of 6 ml/min. Acetonitrile/water/TFA (70:29.9:0.1 v/v/v) concentration in the eluting solvent was increased to 30% over 10 min and to 70% over a period of 60 min. The absorbance was set at 214 nm to detect peptide. The selected peaks were collected in 15 ml centrifuge tubes and subjected to vacuum concentrator SPD2010 (Integrated SpeedVac Systems, MA, USA) to remove acetonitrile. The purity of purified peptide and also those peptides that received in >95% pure form, was determined by Luna 5u C8 250x4.6mm column using a gradient from 0 to 100% acetonitrile over 28 min, and MALDI-TOF MS.

2.2.2 Determination of molecular mass of peptides by matrix-assisted laser desorption ionisation time of flight mass spectrometry (MALDI-TOF MS)

The molecular mass of purified peptide was determined using an analytical device Voyager-DE Bio spectrometry Workstation (PerSeptive Biosystems, Framingham, MA, USA). First, the instrument was calibrated with a peptide of known molecular mass in the range of 2000-4000 Da. After calibration, peptide sample (1.5 µl) was mixed with equal

volume of matrix solution [prepared by dissolving 10 mg of α-Cyano-4-hydroxycinnamic acid in 1 ml of acetonitrile/ethanol (1/1 ratio)] and placed on 100-well stainless-steel plate. After complete drying of the samples, the MALDI plate was injected into a Voyager DE-PRO instrument, which calculates the molecular mass of peptide as a mass-to-charge (m/z) ratio. The experimental molecular mass of peptide obtained was compared with the theoretical mass of the peptide.

2.3 Cell Culture

2.3.1 Culturing of insulin-secreting cell lines (BRIN-BD11 and 1.1 B4 cells)

BRIN-BD11 and 1.1B4 cells are insulin-secreting cell lines, the former was produced by electrofusion of RINm5f cells with New England Deaconess Hospital rat pancreatic islet cells (McClenaghan *et al.,* 1996). The latter was generated by electrofusion of primary culture of human beta cells with PANC-1, a human pancreatic ductal carcinoma cell line (McCluskey 2011). These cell lines were stored in liquid nitrogen, in the cryogenic vials ($1x10^6$ cells/vial) containing freezing medium (10% DMSO, 10% RPMI-1640 medium and 80% foetal bovine serum). For culturing of cells, cryovial was taken out from liquid nitrogen and immediately kept in the icebox. After thawing, the cell suspension was transferred to 15 ml of centrifuge tube and pre-warmed warm media RPMI-1640 media (10 ml) containing foetal bovine serum 10% (v/v) (FBS) and 1% (v/v) antibiotics – penicillin (100 U/ml) and streptomycin (0.1 mg/l), was slowly added to avoid osmotic shock to cells. The tube was then centrifugation at 900 rpm for 5 min; the supernatant was discarded and fresh 10 ml pre-warmed RPMI-1640 (supplemented like previously described) media was added. Cells were homogenously distributed by pipetting and transferred to a sterile tissue culture flask (75 cm^2, Nunc, Roskilde, Denmark). Additional 15 ml of pre-warmed

RPMI-1640 media was added. The flask was then kept in a CO_2 incubator at 37°C, 5% CO_2 and 95% air (LEEC secure CO_2 incubator, LEEC, Nottingham) until 80% confluent with cells. These cells attach to the surface of the flask and grow as a monolayer with epithelioid characteristics. For subculturing, media was discarded from the flask and cells were washed with HBSS solution (1X concentration). Monolayer formed cells were detached by incubating with 3 ml of trypsin (0.25% (w/v) containing 1 mM EDTA) at 37°C for 3 min. After 3 min incubation, pre-warmed RPMI-1640 medium (10 ml) was added (FBS in media inhibit the action of trypsin), and the cell suspension was centrifuged at 900 rpm for 5 min. The supernatant was discarded, and 30 ml of RPMI-1640 medium was added to cell pellets. Cell population in 100 µl of cell suspension was determined by mixing with an equal volume of trypan blue dye (0.4%). The viable cells (unstained and bright) were counted using Neubauer haemocytometer under a microscope (magnification 10X). Cells were maintained by transferring 1 ml of cell suspension back to the flask with an additional 25 ml of pre-warmed RPMI-1640 medium and incubated in a CO_2 incubator at 37°C for further experiments. The image of BRIN-BD11 cells growing in culture media is shown in Figure 2.4 (A).

2.3.2 Culturing and differentiation of a skeletal muscle cell line (C2C12 cells)

The skeletal muscle cell line (C2C12 cells) obtained from the Sigma-Aldrich (Catalogue number: 91031101-1VL) were maintained in growth media [D-MEM (Dulbecco's modified Eagle's medium: high glucose (4500 mg/L) + glutamine, no sodium pyruvate) supplemented with 20% FBS and 1% Pen/Strip] at 37°C with 95% air and 5% CO_2 incubator until they reached 50–60% confluence. Differentiation was induced by replacing growth media with differentiation medium [D-MEM

(Dulbecco's modified Eagle's medium: high glucose + glutamine, no sodium pyruvate) supplemented with 2% donor equine serum and 1% Pen/Strip] (Balasubramanian *et al.,* 2014). Differentiation media was changed every 24 hrs up to 3 days. Before experiments, differentiated cells were serum starved for 12 hrs.

2.4 *In vitro* insulin-release studies

2.4.1 Insulin release studies using BRIN-BD11 and 1.1B4 cells

2.4.1.1 Acute *in vitro* insulin releasing studies in BRIN-BD11 and 1.1B4 cells

Acute insulin-releasing effects of frog skin peptides were assessed according to the method described by Owolabi *et al.,* 2017. After harvesting and counting (as described in Section 2.3.1), cells were seeded at a density of 150,000 cells/well in 24 well plates (Nunc, Roskilde, Denmark) and incubated for 18 hr in a CO_2 incubator at 37°C to form a monolayer. Following 18 hr incubation, culture media was replaced by 1 ml of preincubation buffer i.e. Krebs–Ringer bicarbonate buffer (KRBB- 115 mmol/l NaCl, 4.7 mmol/l KCl, 1.2 mmol/l $MgSO_4$ $7H_2O$,, 1.28 mmol/l $CaCl_2$ $2H_2O$, 1.2 mmol/l KH_2PO_4, 20 mmol/l HEPES and 25 mmol/l $NaHCO_3$, containing 0.5% (w/v) BSA, pH 7.4) supplemented with 1.1 mM glucose. After 40 min, preincubation buffer was replaced by 1 ml of test peptides (ranging concentration from $3x10^{-6}$ to 10^{-12} M) insulin secretagogues prepared in KRBB buffer [supplemented with glucose (5.6 mmol/l or 16.7 mmol/l)], and plates were incubated at 37°C for 20 min. After incubation, a test solution (950 µl) was transferred to LP4 tubes and stored at -20°C to measure insulin concentration using radioimmunoassay (RIA) (described in Section 2.4.3).

2.4.1.2 Acute insulin release studies in the presence of modulators of insulin release

The mechanism of insulinotropic action of frog skin peptides was determined by using known modulators of insulin release (Srinivasan *et al.*, 2013). In the presence or absence of frog skin peptides, BRIN-BD11 cells were incubated with either insulin modulators such as verapamil (50 µM, block calcium channel), diazoxide (300 µM, open ATP sensitive potassium channel), IBMX (200 µM, increase activity of adenylate cyclase), tolbutamide (200 µM, block ATP sensitive potassium channel) or DIDS (0.66 Mm, block chloride channel) prepared in KRB buffer supplemented with 5.6 mM glucose. In another set of experiments, BRIN-BD11 cells were incubated with KCl (30 mM) prepared in KRB buffer supplemented with 16.7 mM glucose in the presence or absence of frog skin peptides. The procedure to perform the acute test is detailed in Section 2.4.1.1.

2.4.1.3 Acute insulin release studies in the absence of extracellular calcium

Effects of extracellular calcium on the insulinotropic activity of the peptide was investigated by incubating BRIN-BD11 cells with calcium-free KRB buffer [115 mM NaCl, 4.7 mM KCl, 1.28 mM $CaCl_2$, 1.2 mM $MgSO_4$, 1.2 mM KH_2PO_4, 20 mM HEPES, 25 mM $NaHCO_3$, 0.1 mM EGTA and 0.1% BSA (pH 7.4)] (Srinivasan *et al.*, 2013). First, cells were preincubated for 40 min at 37°C with calcium-free KRB buffer supplemented with 1.1 mM glucose. After 40 min, the preincubation buffer was replaced by 1 ml of calcium-free KRB buffer supplement with 5.6 mM glucose in the presence or absence of frog skin peptides and incubated for 20 min at 37°C. The experimental protocol is detailed in Section 2.4.1.1.

2.4.2 Insulin-release studies in primary islet cells isolated from the mouse

2.4.2.1 Isolation of pancreatic islets

Islets were isolated from mice (NIH Swiss or C57 or *db/db* mice) pancreatic tissue by collagenase digestion method adapted from Lacy and Kostianovsky (1967). Hank's Balanced Salt Solution (HBSS) was freshly prepared by dissolving 8 g/l NaCl, 0.4 g/l KCl, 0.14 g/l $CaCl_2$, 0.1 g/l $MgSO_4.7H_2O$, 0.1 g/l $MgCl_2.6H2O$, 0.06 g/l $Na_2HPO_4.H_2O$, 0.006 g/l, KH_2PO_4, 1 g/l glucose, 0.02 g/l phenol red, 0.35 g/l $NaHCO_3$ in distilled water. Wash buffer and collagenase solution were prepared by dissolving BSA (0.1%) and collagenase (1.4 mg/ml) in stock HBSS buffer, respectively, and kept in the icebox for further use. After the above preparations, mice were sacrificed by cervical dislocation methods by following procedure approved by the U.K. Animals (Scientific Procedures) Act 1986. The abdominal cavity of mice was opened with scissors, and pancreatic tissue was dissected from the spleen and bile duct. The dissected pancreas was kept in a collagenase solution (5 ml/pancreas) and chopped with scissors. To accelerate tissue digestion process tubes were placed in a water bath for 8-9 min at 37°C followed by intermediate shaking. After incubation, cold wash buffer was added to slow down the activity of collagenase, this prevents tissue from over digestion, and preserved viability of islet cells. Further, tubes were centrifuged at 1200 rpm for 2 min; the supernatant was discarded, and a fresh wash buffer was added. This washing process was repeated twice, at the third washing step solution was filtered using a strainer to separate undigested tissue. Wash buffer was added to the filtrate and centrifuged again for 2 min at 1200 rpm. The supernatant was discarded, and pre-warmed RPMI-1640 media supplemented with 10% BSA, 1% penicillin/streptomycin was added to the cell pellet. By pipetting, the cell pellet was homogenously distributed in media and transferred to a petri dish, which was further kept in 5% CO_2 incubator (Laboratory technical engineering, Nottingham, UK) at 37°C. The islets obtained were used to study the acute effects of peptides/insulin

secretagogues on insulin release within 72 hr of their isolation. The image of islet cells growing in culture media is shown in Figure 2.4 (B).

2.4.2.2 Acute insulin release studies from isolated mouse islets

Islets isolated from mice pancreatic tissue (described in Section 2.4.2.1) were used to investigate the acute effects of frog skin peptides and insulin secretagogues on insulin release. After 48 hr culturing of cells in RPMI-1640 media, fifteen islets were picked from Petri dish and transferred to a 1.5 ml Eppendorf tube. After the transfer of cells, tubes were centrifuged (1200 rpm for 5 min) to remove excess of media, followed by 1 hr preincubation of cells with 500 µl of KRBB buffer containing 1.4 Mm glucose at 37°C. After preincubation, tubes were centrifuged (1200 rpm for 5 min) and cells were test incubated for 1 h at 37°C with peptides (10^{-6} M and 10^{-8} M) and insulin secretagogues prepared in KRBB buffer supplemented with 16.7 mM glucose. After 1 hr of incubation, the tubes were centrifuged, the supernatant was aliquoted in LP3 tubes and stored at -20°C to measure insulin by dextran-coated charcoal radioimmunoassay as described in Section 2.4.4.

2.4.2.3 Terminal islet studies

The long-term effects of peptide administration on beta cell function were investigated in an animal model of diabetes (*db/db*). Following 28 days of treatment with peptide, pancreases were excised from sacrificed *db/db* mice and islets were isolated as described in Section 2.4.2.1. The isolated islets were incubated with insulin secretagogues such as alanine (10 mM), arginine (10 mM), KCl (10 mM), GLP-1 (1µM) and GIP (1µM), to test insulin secretory response (experimental procedure described in Section 2.4.2.2).

2.4.2.4 Measurement of total insulin content of islets

Total insulin content of islet was measured using the acid ethanol method as described by Otani *et al.,* 2003. After performing islet acute insulin release studies, test solutions were retrieved, and islet cells were incubated with 500 µl of acid-ethanol solution (1.5% HCl, 75% ethanol and 23.5% H_2O), overnight at 4°C. On the following day, samples/tubes were centrifuged at 1200 rpm for 2 min at 4°C, and the supernatant was aliquoted in LP3 tubes. Tubes were stored at -20°C for measuring insulin concentration by radioimmunoassay (described in Section 2.4.4).

2.4.3 Iodination of insulin

The method of iodination was first developed by Fraker and Speck in 1978. Iodination of bovine insulin was performed in RIA (radioimmunoassay) suite at Ulster University, as per the procedure established by Diabetes Research Group (DRG). In this experiment, iodogen (1,3,4,6-tetrachloro-3α,6α-diphenyl glycoluril) was used to catalyse iodination of bovine insulin. The iodogen solution was prepared fresh, by dissolving 2 mg of iodogen in 10 ml of dichloromethane. After preparation, 200 µl aliquot of iodogen solution was dispensed in a series of clear bottom 1.5 ml Eppendorf tubes. Tubes were kept in a water bath for 5 min at 37°C to allow the solvent to evaporate and to form a uniform coating of iodogen. Insulin solution which was prepared by dissolving 1 mg of bovine insulin in 1 ml of 10 mM HCl, was further diluted to 125 µg/ml (1:8) in 500 mM phosphate buffer (pH 7). The reaction mixture was prepared by adding 20 µl of bovine insulin (125 µg/ml) and 5 µl of sodium iodide ($Na^{125}I$ 100 mCi/ml stock, Perkin Elmer, Cambridge, UK) to iodogen tubes. All additions were performed inside the standard laboratory chemical fume hood in RIA suite. After additions, iodogen tubes were kept in the icebox for 15 min with gentle

agitation by tapping with fingers every 3-4 min. The reaction mixture was transferred to clean 1.5 ml Eppendorf tubes, and 500 µl of 50 mM sodium phosphate buffer was added to stop the reaction. From the reaction mixture, iodinated ^{125}I - bovine insulin was separated from unbound Sodium iodide ($Na^{125}I$) by Vydac C-8 (4.6 x 250 mm) analytical reverse phase HPLC column (LKB Bromma, Sweden), operated at a flow rate of 1 ml/min. In the elution solvent, the concentration of organic modifier (acetonitrile) was increased from 0 to 56% over a period of 50 min and from 56% to 70% over a period of 10 min. During 67 min HPLC run, fractions were collected into LP5 tubes by fraction collector (Frac-100, LKB) which was set at 1-min intervals. HPLC profile of iodinated bovine insulin is shown in Figure 2.1. The radioactivity of each fraction was measured by running 5 µl sample from each on Wizard™ 1470 automatic gamma counter (Perkin Elmer, USA). Selected fractions were diluted with equal volume working RIA buffer and proceed for the binding test using different antibody dilutions (1:25,000, 1:35,000,1:45,000). Desired fractions were pooled together and stored at 4°C.

2.4.4 Insulin radioimmunoassay (RIA)

Dextran-coated charcoal radioimmunoassay (RIA) developed by Flatt and Bailey (1981), was used to measure insulin concentration in acute test and plasma samples. This assay was performed using a stock buffer for RIA contain disodium hydrogen orthophosphate (40 mM), thimerosal (0.2 g/l) and NaCl (0.3% (w/v). The pH of the stock RIA buffer was adjusted to 7.4 by adding sodium dihydrogen orthophosphate (40 mM). Working RIA buffer was prepared by dissolving bovine serum albumin (BSA) 0.5% (w/v) to stock RIA buffer. After preparation of buffer, insulin standards, ranging concentration from 20 ng/ml to 0.039 ng/ml were made by serial diluting rat

insulin (stock: 40 ng/ml) in working RIA buffer. Guinea pig anti-porcine antibody dilution was prepared from 1:25000 to 1:45000 in working RIA buffer to obtain 40% binding. Radiolabelled insulin (^{125}I-insulin) was made up in assay buffer to achieve ~10,000 counts per minute (CPM) /100 µl of assay buffer. Insulin standards and unknown samples (200 µl) were aliquoted in triplicates and duplicates respectively in LP3 tubes. 100 µl each of guinea pig anti-porcine antibody and ^{125}I-insulin was added to standard (triplicates), unknown samples (duplicates) tubes and control tube (200 µl of assay buffer). The tube for total count contains the only 100 µl of the label, while the nonspecific binding tube, contains 300 µl of assay buffer and 100 µl of the ^{125}I-insulin. After all additions, tubes were incubated at 4°C for 48 hr. Stock dextran-coated charcoal (DCC) was made up by suspending 5 gm of dextran T 70 and 50 gm charcoal in 40 mM sodium phosphate buffer (1 litre). Stock DCC was further diluted with assay buffer (1:5) to make working DCC and stirrer for 30 min before use. After 48 hr incubation, 1 ml of working DCC was added to the reaction mixture tubes (except tube for the total count) and incubated for 20 min at 4°C. The tubes were then centrifuged (Model J-6B centrifuge, Beckman Instruments Inc., UK) at 2500 rpm for 20 min, the supernatant was discarded, and radioactivity of the pellet (which contain free radiolabelled insulin) was recorded by gamma counter (Perkin Elmer Wallac Wizard 1470 Automatic Gamma Counter). The gamma counter used a spline-curve fitting algorithm to determine insulin concentration against the known values of standard insulin.

2.5 Cytotoxicity studies

Lactate dehydrogenase (LDH) assay was performed to determine the cytotoxic effects of frog skin peptides. LDH is a cytosolic enzyme when the cell membrane is

compromised or damaged, this enzyme is released into extracellular space. LDH enzyme was measured using the CytoTox 96® non-radioactive cytotoxicity kit (Promega, UK), following the protocol provided in the kit. The test was performed in 96 well plates. Acute test samples (50 µl) were mixed with an equal volume of light-sensitive substrate mixture. The plate was covered with foil and incubated at room temperature for 30 min followed by addition of 50 µl of stop solution to stop the reaction. The chemical compound tetrazolium salt present in substrate mixture, get converted to red coloured formazan product in the presence of LDH. The change is colour was analysed by measuring absorbance at 490 nm, using VersaMax™ Microplate Reader (Molecular Device).

2.6 Effects of peptides on beta cell membrane potential

Change in membrane potential in peptide-treated BRIN-BD11 cells was determined using FLIPR membrane potential assay kit and Flex Station scanning fluorimeter (Molecular assay devices, USA), as previously described by Mathews *et al*., 2006. The assay kit was provided with a fluorescent dye (anionic and lipophilic by nature), which can move across the cell membrane, and emit a fluorescent signal on the increase in membrane potential. BRIN-BD11 cells were seeded at a density of 10000 cells/well in 96 well microplates (Costar, Roskilde, Denmark) and incubated overnight at 37°C in 5% CO_2 incubator. After overnight incubation, FLIPR membrane potential dye and test peptides (5X concentration) were prepared in fresh KRB buffer (supplemented with 5.6 mM glucose). Culture media was discarded and cells were incubated with 100 µl of KRB buffer (supplemented with 5.6 mM glucose) for 10 min at 37°C and subsequently with 100 µl of FLIPR membrane potential dye (prepared in KRB buffer) for 60 min. Following settings were made in flex station to measure the

change in membrane potential: 1) Excitation and the emission wavelength was set to 530 nm and 565 nm respectively. 2) The interval between each reading: 1.52 seconds. 3) Transfer of test solution to the reading plate was set to 50 µl. The test solution was added 20 sec after the start of data acquisition at a rate of ~62 µl/sec. After incubation with dye, the plate was subjected to flex station, and fluorescent signals were recorded. Membrane depolarising agent KCl (30 mM) was used as positive control.

2.7 Effects of peptides on intracellular Ca^{2+}

The assay protocol for measuring intracellular calcium in peptide treated BRIN-BD11 cells is very similar to that used for measuring the change in membrane potential (described in Section 2.6). The experiment was performed using intracellular Ca^{2+} assay kit and KRBB buffer supplemented with 500 µmol/l probenecid, 1.28 mM $CaCl_2$ and 10nM $NaHCO_3$. The assay kit consists of calcium indicators dye which emits a fluorescent signal on binding to intracellular Ca^{2+} only. The probenecid in assay buffer improves intracellular retention of the dye. Alanine (10 mM) was used as positive control and peptide concentration used is mentioned in corresponding chapters. Also, the settings in flux station for measuring intracellular Ca^{2+} is the same as that set for measuring membrane potential except excitation and the emission wavelength, which is set to 485 nm and 525 nm respectively

2.8 Effects of peptide on adenosine 3'5'-cyclic monophosphate (cAMP) level

The cAMP level in peptide treated BRIN-BD11 cells was determined as previously described by Owolabi *et al.,* 2015. BRIN-BD11 cells were seeded in 24-well plate at a density of 200000 cells per well and cultured for 18 hr at 37°C. After preincubation with KRB buffer as described in Section 2.4.1.1, cells were treated with test solutions

for 20 min, which was prepared in KRB buffer supplemented with glucose (5.6 mM) and 3-isobutyl-1-methylxanthine (200 µM). After 20 min incubation, the supernatant was aliquoted in LP4 tubes for measuring insulin concentration by radioimmunoassay (described in Section 2.4.4). Cells were lysed by adding 200 µl of lysis buffer (provided in the cAMP assay kit) and stored at -70°C in 1.5 ml Eppendorf tubes. The cAMP was measured in cell lysate by following the instruction provided in the cAMP assay kit (R&D system parameter, Abingdon, UK). The standard curve for the cAMP assay is shown in Figure 2.3.

2.9 Effects of downregulation of protein kinase A (PKA) or protein kinase C (PKC) pathway on the insulinotropic activity of frog skin peptides

Forskolin (25 µM, Sigma-Aldrich, UK) and phorbol 12-myristate 13-acetate (PMA 10 nM, Sigma-Aldrich, UK) stimulate insulin release by activation of PKA and PKC pathway respectively. However, after the overnight incubation of BRIN-BD11 cells with forskolin or PMA or both, downregulation of PKA or PKC or both were observed respectively (Owolabi *et al*., 2015). Either or both of these pathways were down-regulated to investigate the mechanism of insulinotropic actions of peptides. To perform this experiment BRIN-BD11 cells were seeded in 24 well plates at a density of 15000 cells/well and incubated with either forskolin or PMA or both for 18 hr at 37°C in an atmosphere of 5% CO_2 and 95% air. After incubation media was discarded and cell were treated with preincubation buffer for 40 min followed by 20 min incubation with test solutions as described in Section 2.4.1.1. GLP-1 (10 nM), CCK8 (10 nM), Forskolin (25 µM), PMA (10 nM) and forskolin (25 µM) + PMA (10 nM) were used as controls in experiments.

2.10 Effects of peptides on cytokine-induced apoptosis and proliferation in BRIN-BD11 cells

The ability of frog skin peptides to protect cells against cytokine-induced DNA damage was analysed by using *In situ* Cell Death Detection Kit (Roche Diagnostics, Burgess Hill, UK) following the manufacturer's instructions. BRIN-BD11 cells were harvested from the flask and counted using hemocytometer as described in Section 2.3.1. BRIN-BD11 cells were seeded at a density of 4 x 10^4 cells on sterilised glass coverslips in 12 well plates for 18 h at 37°C with or without cytokine mixture, in the presence or absence of peptide/GLP-1 (1 µM). Cytokine mixture contained 200 U/ml tumour-necrosis factor-α, 20 U/ml interferon-γ and 100 U/ml interleukin-1β. All the treatment conditions were prepared in RPMI-1640 media. Following incubation, media was decanted, and the cells were washed with 0.9% phosphate-buffered saline (PBS) and fixed using 4% paraformaldehyde (Sigma Aldrich). After fixing, the permeability of cells was improved by treatment with 0.1 M sodium citrate buffer (pH 6.0) at 94°C for 20 min in a water bath. The plates were removed from the water bath and allowed to cool for 20 min at room temperature. Sodium citrate buffer was decanted and cells were incubated with TUNEL reaction mixture (50 µl/well) for 1 hr at 37°C. Following incubation, the TUNEL reaction mixture was decanted, and the cells were washed with phosphate buffer solution (PBS) thrice for 5 min. A small drop of mounting media (prepared by mixing equal volume glycerol and PBS) was put on the slide. With the help of forceps, the coverslip was removed carefully from the well and placed cell-side down onto mountant. Two coverslips were mounted on a single glass slide. Slides were viewed using a fluorescent microscope with 488 nm filter (Olympus System Microscope, model BX51; Southend-on-Sea, UK) and photographed by a DP70 camera adapter system.

The positive effect of the peptide on β-cell proliferation was investigated by using Ki-67 primary antibody (Abcam, Cambridge, UK). BRIN-BD11 cells were seeded as outlined above in 12 well plates containing sterilised coverslip and incubated with either peptide (1 µM) or GLP-1 (1 µM) for 18 hr at 37°C. As mentioned above after incubation, cells were fixed and permeabilised by using 4% paraformaldehyde and 0.1 M sodium citrate buffer (pH 6.0), respectively. To avoid nonspecific antibody binding cells were treated with 300 µl of 1.1% BSA for 30 min, followed by treatment with rabbit anti-Ki-67 primary antibody for 2 hr at 37°C. After treatment with primary antibody, cells were washed thrice with PBS for 5 min and subsequently treated with Alexa Fluor 594 secondary antibody, which stains proliferating cells in red (Abcam. Cambridge, UK). As described above, two coverslips were mounted on a single glass slide. Approximately 150 cells per replicate were analysed, and proliferation frequency was expressed as % of total cells analysed.

2.11 Effects of peptides on glucose uptake in C2C12

Acute effects of frog skin peptides on glucose uptake in C2C12 cells were examined using Cell-Based assay kit (Cayman Chemicals), which is supplied with fluorescent glucose (2-NDBG) that emit a fluorescent signal at 485 nm. After attaining 50-60% confluent, C2C12 cells were harvested from the flask and counted as described in Section 2.3.1. C2C12 cells were then seeded into 96-well clear bottom plates at a density of 5×10^4 cells/well and maintained in growth media followed by differentiation media and serum-free media as described in Section 2.3.2**.** Peptides (1 µM) were tested both in the presence and absence of insulin (10^{-6} M). Test solutions were prepared in DMEM-No glucose media supplemented with 2-NDBG (150 µg/ml). Serum-starved media was replaced by 100 µl of test solutions, and the plates were

incubated for 30 min at 37°C with 95% air and 5% CO_2 incubator. After incubation plate was centrifuged for 5 min at 400 rpm at RT and supernatant was discarded. The assay buffer (200 µl) was added to each well and plates were again centrifuged. After centrifugation supernatant was discarded and 100 µl of assay buffer was added to each well and plates were subjected to flex station to record fluorescent signals. In the experiment, apigenin (50 µM) was used as negative control and insulin (10^{-6} M) as a positive control.

2.12 Assessment of plasma degradation of the peptide

The stability of peptide in plasma was investigated by following the procedure described by Ojo *et al.,* 2015. Briefly, 100 µg of test peptide was incubated with 10 µl of mouse plasma and 395 µl of 50 mM triethanolamine-HCl (pH 7.8) and kept on a shaker at 37°C. The reaction was stopped by adding 10% trifluoroacetic acid (TFA) at 0 min and 4 hr. The samples stopped at time point 0 and 4 hr were run separately on reverse phase HPLC column equilibrated with 0.1% TFA at the flow rate of 1 ml/min, to separated degraded and intact peptide. The collected peaks were subjected to the bioanalytical device MALDI-TOF, to determine molecular weight as described in Section 2.2.2.

2.13 *In vivo* studies

In vivo insulin-releasing activity of frog skin peptides were studied using normal mice (NIH swiss TO mice) and diabetic mice (*db/db* mice). All the animals were handled by following the guidelines according to the U.K. Animals (Scientific Procedures) Act 1986.

2.13.1 Animal models

2.13.1.1 NIH Swiss mice

Male NIH Swiss mice (6-8 weeks) were purchased from Envigo, Huntingdon, UK. After arrival of mice to Ulster University's Behavioural and Biomedical Research Unit (BBRU), they were housed individually with access to water and standard laboratory chow (10% fat, 30% protein, 60% carbohydrate; percentage of total energy 12.99 KJ/g; Trouw Nutrition, Cheshire, UK) in air-conditioned room (22 ± 2°C) and with a 12:12-h light-dark cycle. Mice were kept for 1-week acclimation period before the start of the experiment. For acute feeding studies, mice were trained to have a time-restricted 3-hour feeding at a specific time (10 am to 1 pm) every day.

2.13.1.2 Diabetic (*db/db*) mice

Diabetic mice (*db/db*, BKS.Cg-+Leprdb/+Leprdb/OlaHsd) and normal littermates (BKS.Cg-(Lean)/OlaHsd) were purchased from Envigo, Huntingdon, UK**.** As the name suggests, *db/db* mice show symptoms of diabetes like polyurea, hyperglycaemia, hyperinsulinemia and obesity, and hence were used to investigate the antidiabetic potential of peptides. This mouse model which was first described in 1966 by Hummel *et al*., were derived from an autosomal recessive mutation in the leptin receptor gene located on chromosome 4. Gly to Thr mutation in the leptin receptor gene results in the production of a non-functional Ob-R protein (an isoform of the leptin receptor), which lead to severe metabolic changes as mentioned above. The *db/db* mice exhibit hyperglycemia within 4-8 week after birth (Yang *et al.,* 2015).

The procedure described in Section 2.13.1.1 were followed after the arrival of animals at Ulster University's Behavioural and Biomedical Research Unit (BBRU). Prior to initiation of the treatment, blood glucose and body weight of mice were measured and

grouped accordingly to ensure that no statistical difference is observed in these parameters between the groups.

2.13.1.3 GluCre-ROSA26EYFP mouse model

Glu-CreROSA26EYFP is a transgenic mouse model developed by crossing ROSA26-EYFP and glucagon-Cre mice (Quoix *et al.*, 2007). These mice express the yellow fluorescent protein (EYFP) in pancreatic islet alpha cells. Before commencement of studies, male animals were housed individually with access to water and standard laboratory chow (10% fat, 30% protein, 60% carbohydrate; percentage of total energy 12.99 KJ/g; Trouw Nutrition, Cheshire, UK). Tamoxifen (~32 mg/kg bw) was given to all non-fasted mice intraperitoneally to induce the expression of the yellow fluorescent protein. After tamoxifen dose, animals were monitored five days for any adverse effects. On 5^{th} day onwards, animals were given a low dose of streptozotocin (50 mg/kg bw) injection for the five consecutive days. Before injecting streptozotocin (STZ), animals were fasted overnight for 12 hr, and STZ was prepared fresh in citrate buffer, pH 4.5 on each occasion. Animals were monitored for 10 consecative days for hyperglycemia and body weight. Once diabetes was established, animals were grouped with matching average body weights and blood glucose prior to initiation of treatment.

2.13.2 Glucose tolerance test (intraperitoneal and oral)

Acute *in vivo* effects of the peptides on blood glucose and plasma insulin concentration was investigated by intraperitoneal administration of glucose alone (18 mmol/kg bw) or in combination with test peptides (25/50/75 nmol/kg bw) or GLP-1 (25 nmol/kg bw) to overnight fasted lean mice. Blood glucose was collected into heparinised

microcentrifuge tubes (Sarstedt, Germany) by tail bleeding at time points 0, 15, 30, 60 and 90 min.

Following 28 days of treatment with peptides, IPGTT and OGTT were performed in *db/db* mice. Glucose alone (18 mmol/kg bw) was administered intraperitoneally or orally to overnight fasted *db/db* mice and blood was collected by tail bleeding at time points 0, 15, 30 and 60 min. The collected blood was further analysed for glucose and insulin concentration (Section 2.13.5).

2.13.3 Insulin sensitivity test

Insulin sensitivity test was performed at the end of the treatment period. The body weight of *db/db* mice was measured and the insulin dose (50 U/kg bw) was administered accordingly. Blood glucose was measured prior to (t=0) and after intraperitoneal administration of bovine insulin at time points 15, 30 and 60 min. The improvement in insulin resistance was also determined by the homeostatic model assessment (HOMA). Blood was collected from 18 hr fasted *db/db* mice and analysed for glucose (Section 2.13.5) and insulin concentration (Section 2.13.6). The measured glucose and insulin concentration were used in the homeostatic model assessment (HOMA) formula to calculate insulin resistance:

HOMA-IR = fasting plasma glucose x fasting plasma insulin/22.5

2.13.4 Acute feeding studies (trained animals)

Anti-obesity effects of the peptides were investigated by performing feeding studies in fasted (21 hours) NIH Swiss male mice that were housed individually. These mice had been trained to feed at 10 am to 1 pm for 3 hr each day. After intraperitoneal administration with either saline or test peptide (75 nmol/kg bw), mice were given the

known amount of food (i.e. pre-weighed), and food weight was measured at timepoint 0, 30, 60, 90, 120, 150 and 180 min.

2.13.5 Measurement of blood and plasma glucose, and plasma insulin concentrations

The glucose concentration in blood (collected by tail bleeding) was measured in whole blood using Ascenacia Counter Blood Glucose Meter (Bayer, Newbury, UK). Blood was also collected in fluoride micro-centrifuge tubes (Sarstedt, Numbrecht, Germany) and centrifuged at 13000 rpm for 3 min at 4°C to separate plasma. Plasma was transferred to 0.5 ml fresh eppendorf tubes and stored at -20°C to perform biochemical tests. Plasma glucose was also sometimes measured by the GOD-PAP method (GL 364, Randox Laboratories Ltd., UK). First, the working reagent was prepared by mixing buffer with GOD-PAP reagent (provided in the kit). The test was performed in 96 well plates. Blood sample (2.5 µl) was mixed with freshly prepared working reagent (250 µl) and incubated for 10 min at RT. After incubation, the plate was subjected to VersaMax™ Microplate Reader (Molecular Devices, US) and absorbance was measured at 505 nm. A standard curve for glucose by GOD-PAP reagent is shown in Figure 2.2. Briefly, glucose oxidase enzyme converts glucose in plasma to gluconic acid and hydrogen peroxide (H_2O_2). In the presence of peroxidase, hydrogen peroxide (H_2O_2) react with 4-aminophenazone and phenol to form a red-violet quinonimine dye. The amount of dye produced is directly proportional to glucose concentration in the sample. The intensity of colour was measured at 505 nm. For measuring plasma insulin, plasma samples were diluted with working RIA buffer (1:10 dilution) and measured for insulin concentration by radioimmunoassay as described in Section 2.4.4.

2.13.6 Assessment of long-term (28 days) *in vivo* effects of the peptide in *db/db* mice

Grouped male *db/db* mice received twice daily intraperitoneal injection of saline or peptide (75 nmol/kg bw) for 28 consecutive days. The dose of peptide was selected based on preliminary studies. Before commencement of treatment, mice were acclimatised to handling and injection by injecting twice daily with saline for 3 days. After the initiation of the treatment, body weight, food intake, water intake and blood glucose (once every 3 days) were monitored, and blood was collected by tail bleeding and analysed for insulin concentration by RIA (Section 2.13.6). After the end of the treatment period, terminal blood was collected, and animals were sacrificed by cervical dislocation and tissues were excised for further studies.

2.13.7 Assessment of long-term (11 days) *in vivo* effects of the peptide in GluCre-ROSA26EYFP mice

For 11 consecutive days, GluCre mice received twice daily intraperitoneal injections of saline or test peptide (75 nmol/kg bw). During the treatment period every 3 days interval, non-fasting blood glucose, body weight, food intake and water intake were recorded. Blood samples collected at the start and end of the experiment were analysed for insulin concentration using RIA, as described previously in section 2.13.6. After the treatment, animals were sacrificed by cervical dislocation, and pancreatic tissues were excised and processed for histological staining as described in Sections 2.14 and 2.14.1.

2.13.8 Assessment of body fat composition by DXA scanning

Effects of chronic treatment of peptide on bone mineral density (BMD), bone mineral composition (BMC), bone area and body fat composition (lean body mass and % of body fat) in *db/db* mice were assessed using Dual-energy X-ray absorptiometry (DXA) PIXImus densitometer (Lunar Corp, Madison, Wisconsin). DXA measure these parameters by producing two different energy levels, 40 and 70 keV photons, which passes through only soft tissue (Rothney *et al.*, 2009). DXA instrument was calibrated using a phantom mouse supplied by the manufacturer, and mice were sacrificed and positioned on a specimen tray for scanning. The data generated by densitometer for tissue and bone were analysed separately by Lunar Software version 2.0. The representative image of DXA PIXImus densitometer is shown in Figure 2.6.

2.13.9 HbA1c measurement

After long-term treatment of peptides for 28 days, the HbA1c levels were measured in *db/db* mice using A1cNow^{+} kits (PTS diagnostics, IN, USA) by following the manufacturer's instructions.

2.13.10 Tissue excision

After chronic treatment with peptides, terminal blood was collected, and mice were sacrificed by cervical dislocation. The abdominal cavity of mice was opened with scissors to dissect tissues (pancreas, adipose tissue, skeletal muscle, intestine and liver). Dissected tissues were covered in aluminium foil, labelled and snapped frozen in liquid nitrogen. Samples were then stored at -70°C to measure hormone content and to study the expression of key genes involved in glucose homeostasis. In addition, pancreatic tissue was processed for histological staining as described in Sections 2.14 and 2.14.1.

2.13.11 Pancreatic insulin content

Insulin content in the pancreas of saline and peptide-treated mice was measured by acid ethanol method. The pancreas was weighed and homogenised in 5 ml of freshly made acid ethanol using a VWR VDI 12 handheld homogenizer (VWR, UK). Tubes then centrifuged for 20 min at 5000 rpm, and the supernatant was transferred to a 15 ml tube. 10 ml of tris base (pH 7) was added to supernatant and tubes were kept in speed wax overnight until the solution evaporates. The powder obtained was dissolved in 2 ml Tris base (pH 7) and stored at -20°C. 5 µl of the pancreatic extract was aliquoted in LP3 tubes and diluted to 200 µl using working RIA buffer and measured for insulin by radioimmunoassay (described in Section 2.4.4).

2.13.12 Effects of the peptide on lipid profile, liver and kidney function, and amylase activity

Plasma retrieved from terminal blood as described in the Section 2.13.5, was measured for total cholesterol, HDL cholesterol, and plasma triglycerides, creatinine, alanine transaminase (ALT), aspartate transaminase (AST), alkaline phosphatase (ALP) level and amylase activity by following the procedure described in assay kits from suppliers. LDL cholesterol was determined by the de Cordova equation: 3/4 (total cholesterol - HDL-c).

2.14 Immunohistochemistry

Pancreatic tissues were excised from treated and untreated animals and fixed in 4% paraformaldehyde at 4°C for 48 h. Pancreatic tissues were processed using an automated tissue processor (Leica TP1020, Leica Microsystems, Nussloch, Germany). Tissues were embedded in paraffin wax and sectioned with a microtome (Shandon

finesse 325, Thermo Scientific, UK) to produce 7 μm thick sections. The section at an interval of 10 sections was placed on the same Polysine slide (Thermo Scientific, UK) and allowed to dry overnight on a hotplate (Thermo Scientific).

2.14.1 Immunohistochemical staining for analysis of islet morphology

The sections of processed pancreatic tissue were stained for insulin and glucagon as described previously by Vasu *et al.,* 2014. First, sections were dewaxed and rehydrated using xylene (Sigma Aldrich, Dorset, UK) and an ethanol solution (100% for 5 min, 95% for 5 min and 80% for 5 min), respectively. The sections were then incubated in sodium citrate buffer (10mM sodium citrate, 0.05% Tween 20, pH 6.0) at 94°C for 20 min for the retrieval of antigen. To prevent nonspecific binding, sections were blocked using 2% BSA for 30 min. Three different types of double staining were performed depending on experiments: A) insulin-glucagon staining, B) insulin-GFP staining, C) glucagon-GFP staining. Slides were incubated with primary antibody [mouse anti-insulin antibody (1:400; Abcam, ab6995) for insulin, guinea-pig anti-glucagon antibody (PCA2/4, 1:50; raised in-house) for glucagon and rabbit anti-GFP (1/400) for GFP] overnight at 4 °C. After overnight incubation with primary antibody, sections were washed twice with phosphate buffer solution (PBS) and incubated with secondary antibody (Alexa Fluor 488 goat anti-mouse-1/400, 594 goat anti-guinea pig-1/400 and 594 rabbit anti-GFP-1/400) for 45 min at 37°C. After treatment with secondary antibody, slides were washed with PBS, and nuclear staining was performed by incubating slides with 4',6-diamidino-2-phenylindole (DAPI) stain for 15 min at 37°C. Following nuclear staining, the slide was washed with PBS and mounted using the anti-fade mounting medium. The slides were then viewed using a fluorescent microscope (Olympus System Microscope BX51, Olympus instruments,

UK), using a FITC filter (488 nm) and TRITC filter (594 nm). The images were captured using a DP70 camera adapter system as described by Vasu *et al.*, 2013. Using Cell^F imaging software (Olympus System Microscope BX51, Olympus instruments, UK) islet number, islet area, beta cell area, alpha cell area and islet size distribution were measured. The representative image of the fluorescent microscope is shown in Figure 2.7.

2.15 Gene expression studies

2.15.1 RNA extraction

RNA was isolated from the skeletal muscle tissue and islet cells of the treated and untreated animal using TriPure Isolation reagent (Roche, UK). 50-100 gm of tissue was added to 1 ml of tripure reagent in Biju tubes and homogenised using VWR VDI 12 handheld homogeniser (VWR, UK). The homogenate was kept at room temperature for 5 min to dissolve the nucleoprotein complex. Chloroform (0.2 ml) was added to the homogenate, shaken vigorously for 15 sec and incubated for 10 min at 20°C. The homogenate was transferred to the 1.5 ml centrifuge tubes, and tubes were centrifuged at 12000 rpm for 15 min at 4°C. Chloroform separates RNA, DNA and protein into aqueous, interphase and organic phase respectively. The aqueous phase (containing RNA) was transferred to RNase free tubes. After the addition of isopropanol (0.5 ml), tubes were mixed by inversion and incubated for 10 min at 20°C followed by centrifugation at 12000 rpm for 15 min at 4°C. Isopropanol precipitates RNA, hence after centrifugation supernatant was discarded. The pellet obtained was washed with 75% ethanol (1 ml) made in diethylpyrocarbonate (DEPC) treated water followed by centrifugation at 7500 rpm for 5 min. After centrifugation supernatant was discarded and pellets were air dried and resuspended in DEPC treated water (30

µl). RNA concentration in the samples was measured by Nanodrop (absorbance at 260 nm) and stored at -20°C for cDNA synthesis.

2.15.2 cDNA synthesis

RNA isolated from skeletal muscle tissue and islet cells was converted to cDNA using SuperScript II reverse transcriptase (Invitrogen, Life Technologies, UK) following the manufacturer's instruction. Using Nanodrop, the concentration of RNA in the sample was calculated, and 3 µg of RNA was converted to cDNA using a three-step reaction in a thermocycler (G-STORM, UK). For the first step, reaction volume was prepared in RNase free tube by adding 1 µl of the Oligodt (Invitrogen, Life Technologies), a sample containing 3 µg of RNA and the volume was adjusted to 12 µl by adding the appropriate volume of RNase free water. In thermocycler tubes were heated at 70°C for 10 min. In the second step, tubes were incubated at 42°C for 2 min after adding 4 µl of 5 X First strand buffer, 2 µl of 0.1 M of DTT (Invitrogen, Life Technologies) and 1 µl of 10 mM dNTP to the reaction volume. Finally, in the third step, SuperScript II RT (1 µl) was added, and tubes were incubated at 42°C for 50 min followed by 70°C for 15. After completion of the third step, tubes were stored at -20°C until needed for PCR.

2.15.3 Gene amplification

Amplification of genes was carried out using real-time polymerase chain reaction Bio-Rad MJ Mini personal Thermal cycler (Bio-Rad Laboratories, UK). The reaction mixture (10.5 µl) for PCR was prepared in 8 well PCR tube strips by adding the following components:

1	Quantifast SYBR green PCR mix	4.5 µl
2	Forward primers	1 µl
3	Reverse primers	1 µl
4	c-DNA	3 µl
5	RNase free water	1 µl

(Forward and reverse primers are listed in Table 1 and 2)

After preparation of the reaction mixture, PCR condition was set as follows:

- Initial denaturation at 95°C for 5 min
- A 40 cycle of cDNA amplification.
- Final denaturation at 95°C for 30 Sec
- Annealing temperature at 58°C for 30 sec
- Final extension at 72°C for 30 sec (SYBR Green fluorescence was read after each cycle for amplification curve).

Genes studied for the expression and the primer used are listed in table 1. All the genes were normalised to β-actin (Actb) expression and analysed using the $^{\Delta\Delta}$Ct method.

2.16 Statistical Analysis

The experimental data were analysed using GraphPad Prism (Version 3). Acute *in vitro* insulin secretion studies for test peptides with 8 technical replicates and acute and long-term *in vivo* studies with 6 and 8 biological replictaes respectively, were performed. Values were expressed as mean ± SEM for a given number of replicates (n). Data were compared using unpaired Students t-test (non-parametric), with two-tailed P values and 95% confidence interval) and one-way ANOVA followed by

student Newman-Keuls post hoc test. Using the trapezoidal rule with baseline subtraction, the area under curve was calculated from data obtained. Group of datasets were considered to be significantly different if $P<0.05$.

Table 1: List of the primers and their sequence for gene expression studies in islets

Sr no	Gene	Common name	Forward Primer sequence	Reverse Primer sequence
1	*Ins1*	Mus musculus insulin 1	AAG CTG GTG GGC ATC CAG TA	GAC AAA AGC CTG GGT GGG TT
2	*Slc2α2*	Glucose transporter 2	GAA GAA GAG TGG TTC GGC CC	CGC ACA CCG AGG AAG GAA TC
3	*Gck*	Glucokinase, Transcript variant 1	AGG CCC TGA CAG GAG ACA TC	GCC TCT AGA CGG ACT CAG CA
4	*Abcc8*	ATP-binding cassette, sub-family C (CFTR/MRP), member 8	TGA AGC GCA TCC ACA CAC TC	ATC TTC TGT CCT GGG GCG AT
5	*Kcnj11*	Potassium inwardly-rectifying channel, subfamily J, member 11 (Transcript variant 1)	TGG GTT GGG GGC TCA GTA AG	ACC TCT AGG CTG GTA TGC CC
6	*Cacna1c*	Calcium channel,voltage-dependent, L-type, alpha 1C subunit	ACA TGC TTT TCA CCG GCC TC	GCT CCC AAT GAC GAT GAG GAA G
7	*Glp1r*	Glucagon-1 like peptide receptor	GCT GAG GGT CTC TGG CTA CA	GGG ACA GGA GCT GTT CCT CA
8	*Gipr*	Gastric inhibitory polypeptide receptor	TGC CCC GAC TAC CGA CTA AG	GCC TTC AAC CTG TTC CTC CG
9	*Pdx1*	Pancreatic and duodenal homeobox 1	CCT AGG CGT CGC ACA AGA AG	TCG CTT GGC ATC AGA AGC AG
10	*Gcg*	Proglucagon gene	GCC ACC AGG GAC TTC ATC AAC	CAA GTG ACT GGC ACG AGA TGT
11	*Stat1*	Signal transducer and activator of transcription 1, isoform 1	CAT CCC GCA GAG AGA ACG C	GGT GCA GGT TCG GGA TTC AA

Table 2: List of the primers and their sequence for gene expression studies in skeletal muscle tissue.

Sr no	Gene	Common name	Forward Primer sequence	Reverse Primer sequence
1	*Irs1*	Insulin receptors substrate	AGG ACC TCA CGT CTT CCT CTT	TTC CGG TGT CAC AGT GCT TTC
2	*Insr*	Insulin receptor	GCA GGA AAT GGC TCC TGG AC	GGG GTC CAA TGA TAA TTT TGG CAA T
3	*Ptb1*	Protein phosphatase 1B	TCG CCT GCG CAT TTG TAC TC	TGA GTT TTC CAG TGC CCC AAA
4	*Pdk1*	3-phosphoinositide dependent protein kinase 1	TGG GTC CAG TGG ATA AGC GAA	CCG GTA ATT ACA TCG TGT GGA CAA
5	*Pik3Ca*	Phosphatidylinositol 3-Kinase, catalytic, alpha polypeptide	ACA GAG ACA GAG CAC GAT CCA	TCC ACG TGC TGT GAG GTT TC
6	*Akt1*	Protein kinase B alpha	GCC GCC TGA TCA AGT TCT CC	CAG CGC ATC CGA GAA ACA AAA C
7	*Slc2α4*	Glucose transporter 4 (Glut4)	ACT AGA TCC CGG AGA GCC TGG	TGG AAA CCC GAC GGC ATC TT

Figures 2.1 HPLC Separation of iodinated bovine insulin

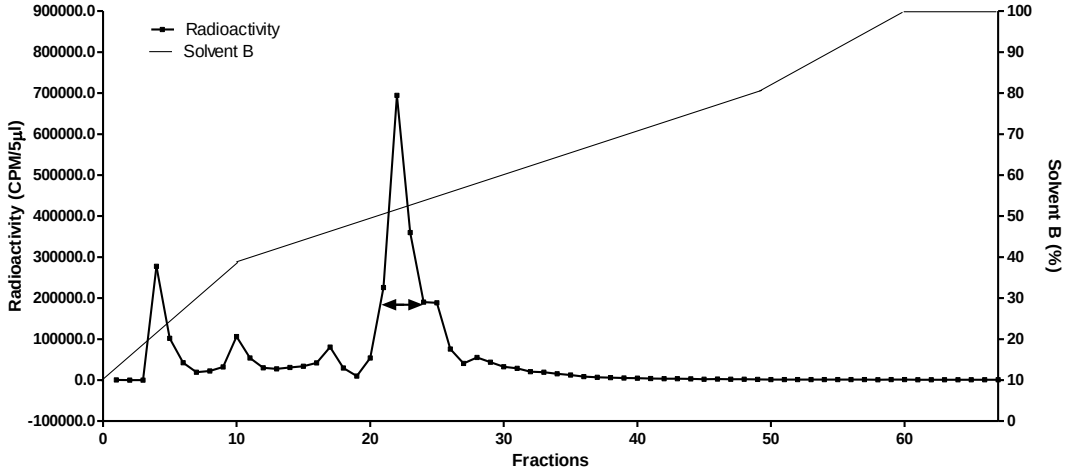

Iodinated ^{125}I - bovine insulin was purified from the reaction mixture by reversed-phase HPLC, operated at a flow rate of 1 ml/min. All fractions were collected using an automated fraction collector. Radioactivity of each fraction was determined by running 5 µl sample from each on Wizard™ 1470 automatic gamma counter (Perkin Elmer, USA), gamma counter. Fractions collected between 5-7 min (Peak A) contain unbound Sodium iodide ($Na^{125}I$), and hence it was disposed off. Whereas the fraction between 21-26 min (Peak B) contained iodinated insulin which was selected to perform antibody binding test.

Figure 2.2 Standard curve for glucose analysis by GOD-PAP reagent

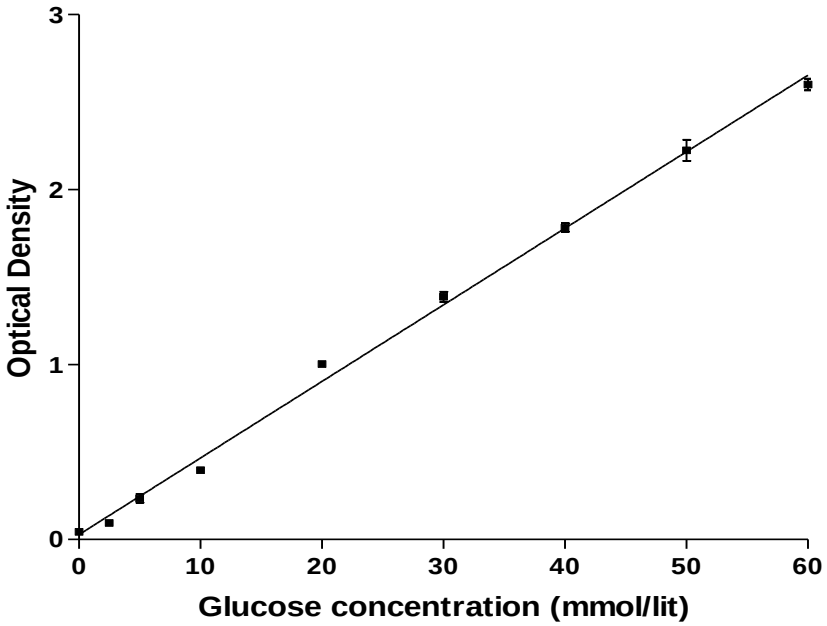

Standard curve of glucose was prepared over a concentration range of 0-60 mmol/lit. O.D. was measured at 505 nm.

Figure 2.3 A typical standard curve for cAMP assay

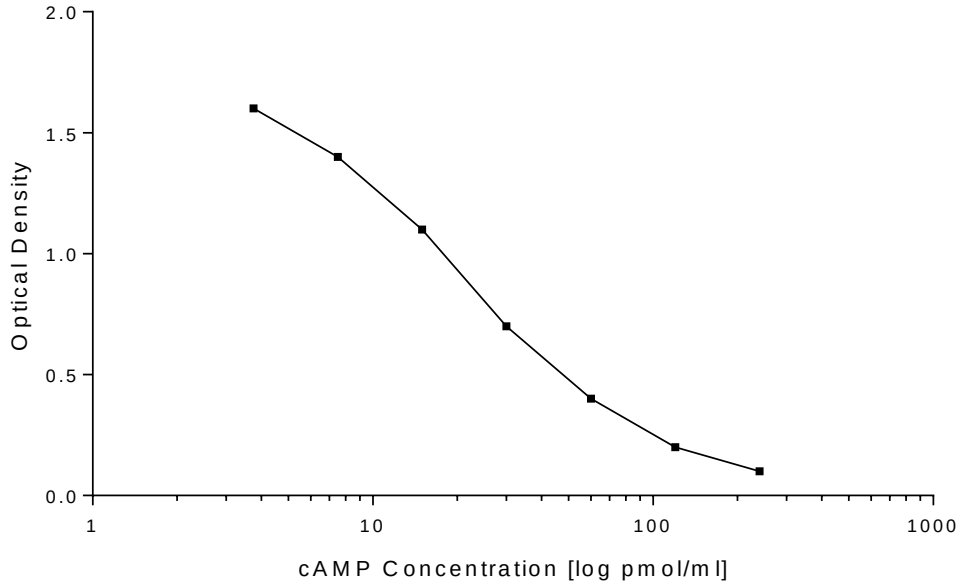

A standard curve of stock solution (provided in kit) was prepared over a concentration range of 240-3.75 pmol/ml. O.D. was measured at 450 and 540 nm.

Figures 2.4 BRIN-BD11 Cells (A) and Islet cells (B) growing in culture

A)

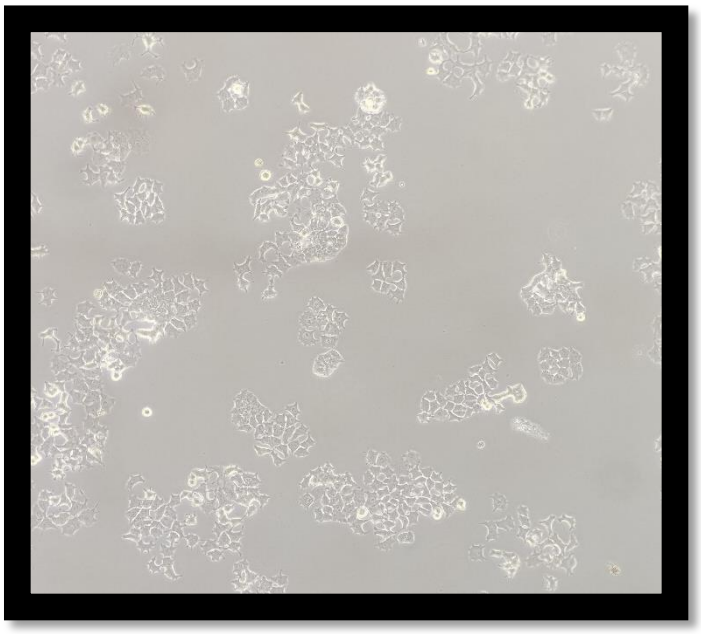

B)

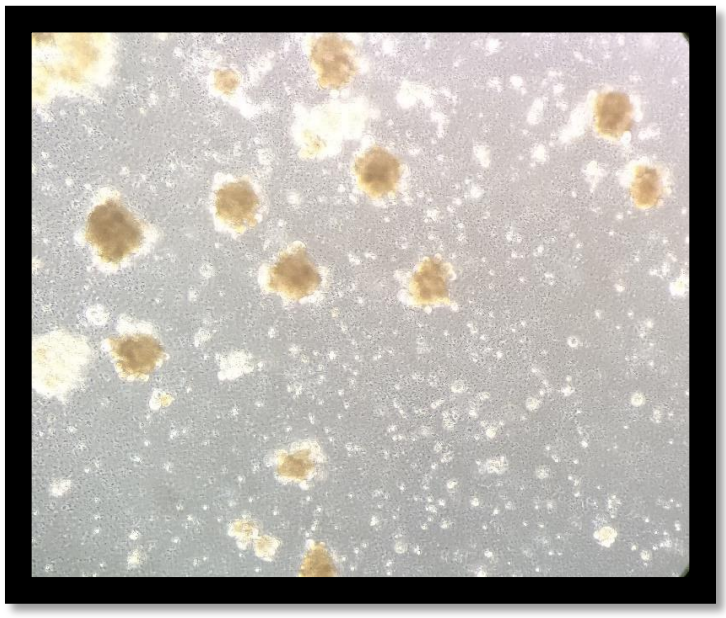

Figure 2.5 Reversed-phase HPLC

Figure 2.6 Dual-energy X-ray Absorptiometry (DXA) PIXImus densitometer

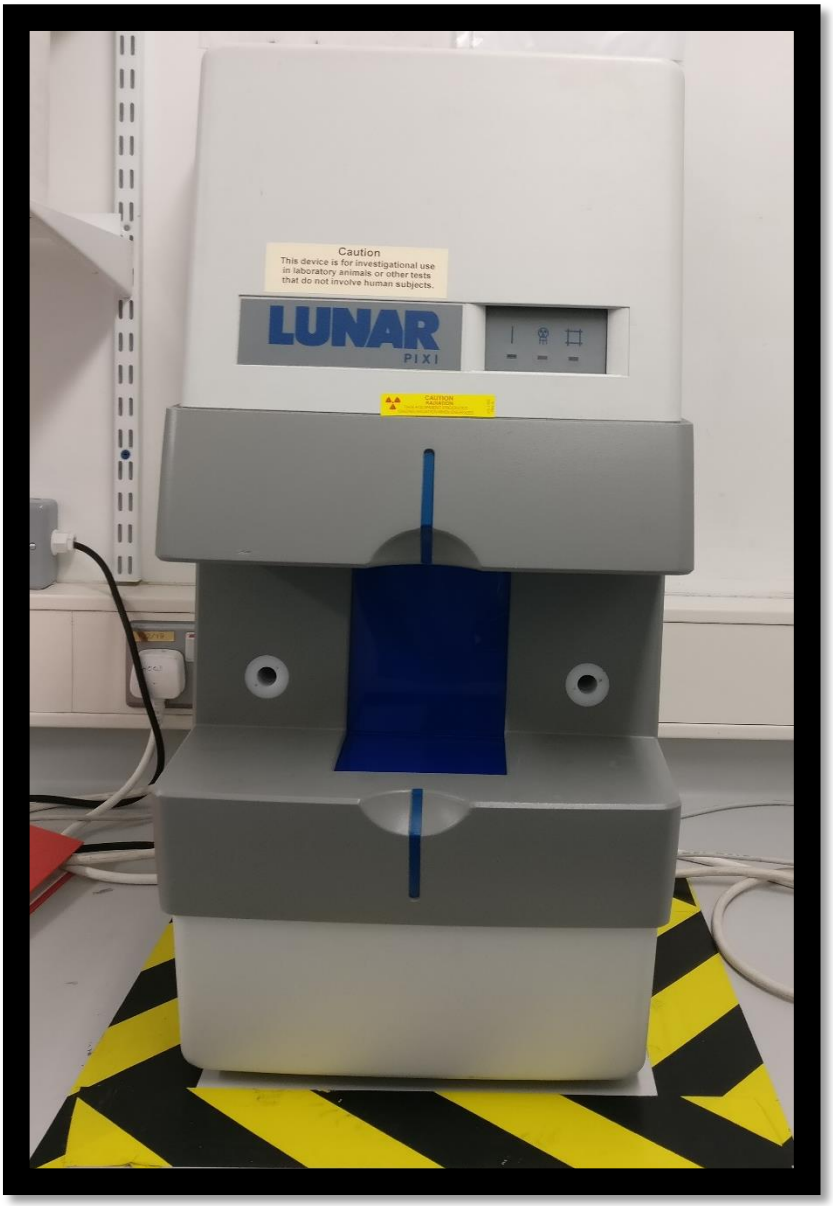

Figure 2.7 Fluorescent microscope (Olympus System Microscope BX51, Olympus instruments, UK).

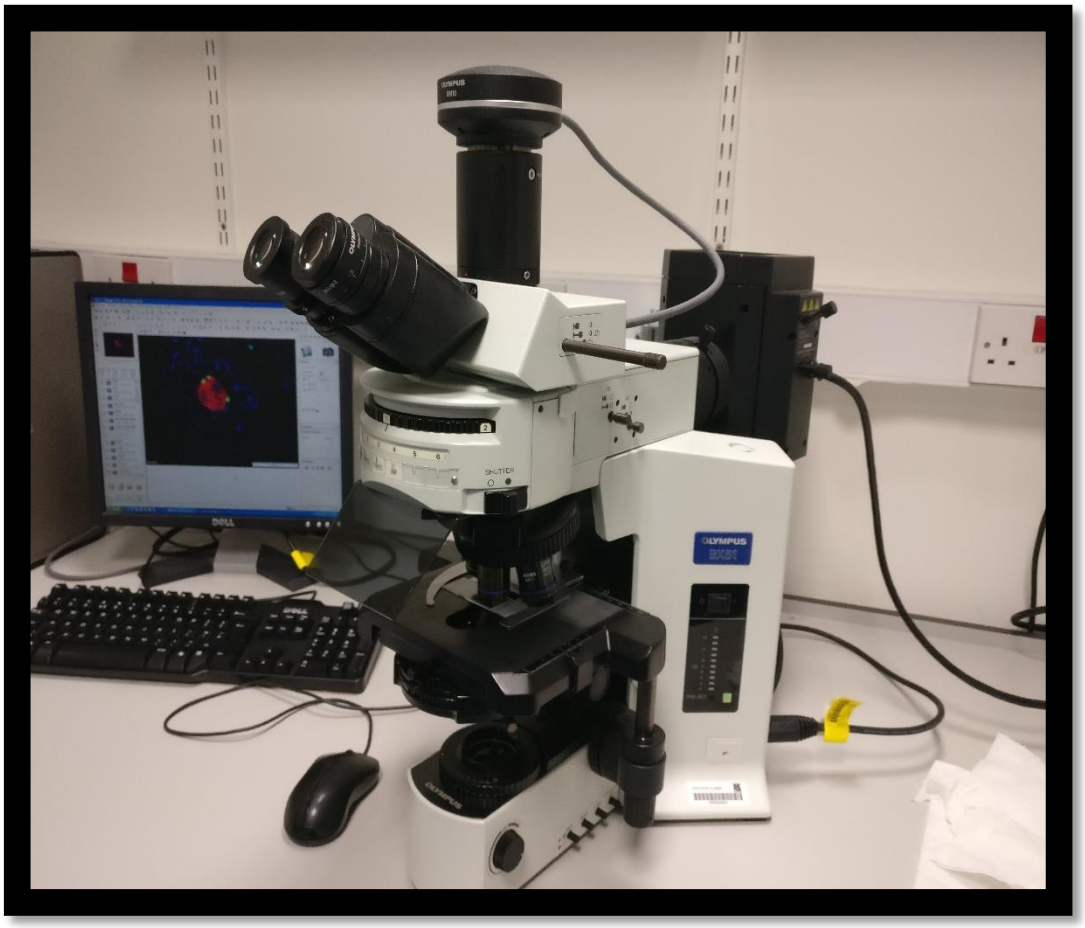

Chapter 3

Insulinotropic, glucose-lowering and beta-cell anti-apoptotic actions of temporin and esculentin peptides from skin secretions of frogs belonging to family of Ranidae

3.1 Summary

The present Chapter evaluated whether temporin and esculentin-1 peptides, identified in skin secretion of frog *Rana temporaria* and *Rana esculenta,* respectively, could represent a template for the design of new types of drugs for use in T2DM therapy. Temporin A, temporin F, and temporin G, and Esculentin-1a (1-21).NH_2, esculentin-1b(1-18).NH_2, and esculentin-1a(1-14).NH_2 evoked concentration-dependent stimulation of insulin release from BRIN-BD11 rat clonal β-cells, 1.1B4 human-derived pancreatic β-cells and isolated mouse islets with no cytotoxicity at concentrations up to 3 μM. In contrast, temporin B, C, E, and analog [D-Lys^{14}, D-Ser^{17}] esculentin-1a (1-21).NH_2 (esculentin (1-21)-1c) were less potent and, temporin H, K and esculentin-1a(9-21) were inactive. The data indicate that cationicity, hydrophobicity, and the angle subtended by the charged residues in the temporin, and helicity in the esculentin-1 peptides are important determinants for *in vitro* insulinotropic activity. The mechanism of insulinotropic action of esculentin-1 peptides involved membrane depolarization and an increase in intracellular Ca^{2+} concentrations, whereas temporin peptides had no effect on these parameters. Temporin A, temporin F, esculentin-1a (1-21) NH_2 and esculentin (1-21)-1c (1 μM) protected BRIN-BD11 cells against cytokine-induced apoptosis to a similar extent as GLP-1 (1 μM). In contrast, the protective effects of esculentin-1b (1-18).NH_2 and esculentin-1a (1-14).NH_2 were comparably less, whereas temporin G failed to show any effect. Temporin A, temporin F and esculentin (1-21)-1c (1 μM) also augmented proliferation of the cells to a similar extent as GLP-1. In contrast proliferative effect of esculentin-1a (1-21)NH_2 was less significant, while temporin G, esculentin-1b (1-18).NH_2, and esculentin-1a (1-14).NH_2 failed to show any positive effects. Intraperitoneal injection of either temporin G or esculentin (1-21)-1c together with an intraperitoneal glucose load (18 mmol/kg bw) in NIH Swiss mice improved glucose tolerance with a

concomitant increase in insulin secretion. Whereas temporin A, temporin F, esculentin-1a (1-21).NH_2, esculentin-1b (1-18).NH_2 and esculentin-1a (1-14) administration was without significant effect on plasma glucose levels.

3.2 Introduction

The global rise in the prevalence of Type 2 diabetes mellitus (T2DM) has mandated a search for new therapeutic options for treating patients with the disease (Ríos *et al.*, 2015). After the discovery of insulin therapy, scientists have shown immense interest in exploring peptides with antidiabetic properties from natural sources. Many frog-skin peptides that were first identified on the basis of their ability to inhibit the growth of bacteria and regulate cytokine production have subsequently been shown to evoke insulin release from clonal β-cells *in vitro* and lower blood glucose concentrations in mouse models of T2DM (Conlon *et al.*, 2014a. 2018).

Temporin and esculentin-1 peptides were identified in frogs belonging to the extensive family Ranidae of both Eurasian and N. American (Conlon *et al.*, 2009, Xu & Lai, 2015). The genes encoding a family of such peptides were identified in a cDNA library from the skin of the European common frog *Rana temporaria* (Simmaco *et al.*, 1996) and *Rana esculenta* (Simmaco *et al.*, 1994). Temporins are small (8 - 17 amino acid residues), C-terminally α-amidated peptides, while esculentin-1 peptide is relatively large size, containing a cystine-bridged, cyclic domain rendering them difficult to synthesize. These peptides are best known for their ability to inhibit the growth of the microorganism (Ponti *et al.*, 1999, Mangoni *et al.*, 2016). The N-terminal fragments of the esculentin-1 peptide, esculentin-1b (1-18) (Mangoni *et al.*, 2003, Marcellini *et al.*, 2009, Maisetta *et al.*, 2009, Luca *et al.*, 2014) and esculentin-1a (1-21) (Luca *et al.*, 2014, Mangoni *et al.*, 2015) also retain the full antimicrobial activity of the intact peptides and showed reduced cytotoxic

activity against eukaryotic cells. The certain members of the temporin family have been shown to display chemoattractive (Chen *et al.*, 2004, Di Grazia *et al.*, 2014) anti-inflammatory (Capparelli 2009), and vasorelaxant and antitumour activity (Kim *et al.*, 2000). Recent studies have shown that the truncated forms of the esculentin-1 peptide and the C-terminally α-amidated esculentin-1a (1-21).NH_2 play a significant role in promoting wound healing and in treating *Pseudomonas aeruginosa* infections in patients with cystic fibrosis (Cappiello *et al.*, 2016) and keratitis (Kolar *et al.*, 2015, Casciaro *et al.*, 2017) as well as clinical mastitis caused by bacteria in dairy cows (Islas-Rodrìguez *et al.*, 2009). The therapeutic effects of esculentin-1a (1-21).NH_2 were augmented by incorporation of D-amino acids at positions 11^{th} and 14^{th} position and the resulting analogue, termed Esc(1-21)-1c), showed greater stability in serum, reduced cytotoxicity towards mammalian cells, increased activity against the biofilm form of *P. aeruginosa*, and increased ability to promote migration of lung epithelial cells (Di Grazia *et al.*, 2015, Loffredo *et al.*, 2017).

Preliminary studies have shown that temporins from *Rana ornativentris* and *Lithobates virgatipes* and *Lithobates catesbeianus* (Abdel-Wahab *et al.*, 2007, Mechkarska *et al.*, 2011) and, esculentin 1a and esculentin 1b peptides isolated from *Rana saharica* (Marenah *et al.*, 2006), demonstrated insulinotropic activity in glucose-responsive rat clonal β-cells BRIN-BD11. The present study aimed to investigate the insulin-releasing ability of a series of temporins and synthetic N-terminal fragments of esculentin-1a and -1b peptides *in vitro* using established rat and human clonal β-cell lines and freshly prepared mouse pancreatic islets. Effects of these peptides on glucose tolerance and insulin release *in vivo* also were investigated in overnight fasted lean mice (NIH Swiss mice). It has recently been shown that the frog skin-derived peptide PGLa-AM1 also protects against cytokine-induced DNA damage as well as promotes β-cell proliferation

(Owolabi *et al.*, 2017). Consequently, the effects of the temporin and esculentin-1 peptides on these parameters were also investigated using BRIN-BD11 cells.

3.3 Materials and Methods

3.3.1 Reagents

All reagents used in this study are listed in Chapter 2, Section 2.1.

3.3.2 Peptides

The purity and identity of peptides were confirmed by reversed-phase HPLC (Chapter 2, Section 2.2.1.1) and MALDI-TOF mass spectrometry (Chapter 2, Section 2.2.2) respectively. The primary structures, calculated isoelectric points (pI), and Grand Average of Hydropathy (GRAVY), calculated using the hydrophobicity scale of Kyte and Doolittle. The secondary structures of esculentin-1 peptides were predicted using the AGADIR program.

3.3.3 Acute *in vitro* insulin release studies using BRIN-BD11 and 1.1B4 cells

The culturing of rat clonal pancreatic β-cells (BRIN-BD11) and human-derived pancreatic β-cells (1.1B4) is described in detail in Chapter 2, Section 2.3.1. The acute insulin-releasing effects of temporin and esculentin-1 peptides (3×10^{-6} - 10^{-12} M; n = 8) were performed by incubating with cells for 20 min at 37°C using KRB buffer supplemented with 5.6 mM glucose. The procedure for measuring acute releasing effects of peptides is described in Chapter 2 Section 2.4.1.1. Control incubations were carried out by incubating cells with human GLP-1 (10 nM) and alanine (10 mM). After incubation, the cell supernatant was collected for measuring insulin (Chapter 2, Section 2.4.4) and LDH concentration (Chapter 2, Section 2.5).

3.3.4 Cytotoxicity assay

The cytotoxic effects of peptides (3 x 10^{-6} - 10^{-12} M; n = 4) on BRIN-BD11 cells were measured using a CytoTox 96 non-radioactive cytotoxicity assay kit, as previously described in Chapter 2, Section 2.5.

3.3.5 Insulin release studies using isolated mouse islets

The procedure for pancreatic islets isolation from an adult, male National Institutes of Health (NIH) Swiss mice (Harlan Ltd, Bicester, UK) is outlined in Chapter 2 Section 2.4.2.1. After isolation, islets were cultured for 48 hr under the same conditions as used for BRIN-BD11 and 1.1B4 cells. The experimental procedure for measuring the acute effects of peptides on the rate of insulin release has been described in Chapter 2, Section 2.4.2.2. After incubating islets with peptides (10^{-8} and 10^{-6} M) made in KRB buffer supplemented with 16.7 mM glucose, for 1 hr at 37°C, the supernatant was removed and measured for insulin by radioimmunoassay as outlined in Chapter 2, Section 2.4.4. The islet cells were then subjected to acid ethanol treatment for measuring total insulin content as previously described in Chapter 2, Section 2.4.2.4. GLP-1 (10 nM) and alanine (10 mM) were used as a positive control in the experiment.

3.3.6 Effect of temporin and esculentin-1 peptides on membrane potential and intracellular calcium ($[Ca^{2+}]i$) concentrations

Effects of the temporin and esculentin-1-derived peptides (1 µM) on membrane potential and intracellular Ca^{2+} concentrations in BRIN-BD11 cells were investigated using membrane potential and intracellular Ca^{2+}assay kits (Molecular Devices, Sunnyvale, CA, USA). The experimental procedure is described in detail in Chapter 2, Section 2.6 and 2.7. BRIN-BD11 cells were incubated with peptides (10^{-6} M) at 37°C in 5.6 mM glucose

for 5 min, and information was acquired using a Flex Station scanning fluorimeter (Molecular Devices). Control incubation: 5.6 mM glucose only, Positive control for membrane potential: 5.6 mM glucose plus 30 mM KCl and Positive control for intracellular calcium: 5.6 mM glucose plus 10 mM alanine were also carried out.

3.3.7 Effects of the temporin and esculentin-1 peptides on cytokine-induced apoptosis in BRIN-BD11 cells

The protective effects of temporin and esculentin-1 peptides against cytokine-induced DNA damage was investigated by exposing BRIN-BD11 cells (seeded at a density of 5 x 10^4 cells per well) for 18 hr at 37°C to cytokine mixture (200 U/ml tumour-necrosis factor-a, 20 U/ml interferon-g, and 100 U/ml interleukin-1b) in the presence and absence of peptides (10^{-6} M). GLP-1 (10^{-6} M) was used as a positive control. The experimental procedure is outlined in Chapter 2, Section 2.10. Cells were washed with phosphate-buffered saline (PBS) and fixed immediately using 4 % paraformaldehyde. After fixation, cells were permeabilised by treatment with 0.1 M sodium citrate buffer, pH 6.0 at 94°C for 20 min and then incubated with TUNEL reaction mixture1 hr at 37°C. After incubation, cells were washed again with PBS and slides were viewed using a fluorescent microscope with 488 nm filter (Olympus System Microscope, model BX51; Southend-on-Sea, UK).

3.3.8 Effects of the temporin and esculentin-1 peptides on proliferation in BRIN-BD11 cells

The positive effect of temporin and esculentin-1 peptides on β-cell proliferation was investigated by using Ki-67 primary antibody (Abcam, Cambridge, UK). BRIN-BD11 cells were incubated with 1 µM of test peptide for 18 hr at 37°C as previously described

in Chapter 2, Section 2.10. GLP-1 (10^{-6} M) was used as a positive control. After immediate fixing and permeabilization, cells were subjected to treatment with rabbit anti-Ki-67 primary antibody and subsequently with Alexa Fluor 594 secondary antibody, which stains proliferating cells in red. Approximately 150 cells per replicate were analysed.

3.3.9 Acute *in vivo* insulin release studies

All animal experiments were carried out by the UK Animals (Scientific Procedures) Act 1986 and EU Directive 2010/63EU for animal experiments and approved by Ulster University Animal Ethics Review Committee. All necessary precaution steps were taken to protect the animal from any potential suffering. Healthy adult (8 weeks old) NIH Swiss mice (Harlan Ltd, Bicester, UK), were housed separately and maintained in an air-conditioned room (22 ± 2°C) with a 12-h light: 12- h dark cycle. The procedure for investigating acute *in vivo* effects of the peptide on glucose and insulin concentration is described in Chapter 2, Section 2.13.2. Overnight fasted were injected intraperitoneally with glucose alone (18 mmol/kg bw) or together with the test peptide (75 nmol/ bw). GLP-1 (25 nmol/kg bw) was used as positive control. Blood samples were collected by tail bleeding, before and after peptide injection at time point 15, 30 and 60 min. Blood glucose was measured using an Ascencia Contour Blood Glucose Meter and plasma insulin by radioimmunoassay (Chapter 2, Section 2.13.5).

3.3.10 Statistical Analysis

Experimental data were analysed using GraphPad PRISM (Version 3). Results were expressed as means ± SEM and data compared using unpaired Student's t-test (nonparametric, with two-tailed P values and 95% confidence interval) and one-way

ANOVA with Bonferroni post-hoc test wherever applicable. Group of datasets were considered to be significantly different if $P<0.05$.

3.4 Results

3.4.1 Peptides

Temporin and esculentin-1petides were supplied in pure form (>95%) by Prof Michael Conlon. The purity peptides were confirmed using reverse phase HPLC (Figure 3.1-3.4). The molecular weight of peptides confirmed by MALDI- TOF (Figure 3.5-3.8). The primary structures of the peptides investigated in this study, their molecular charge at pH 7, Grand Average of Hydropathy (GRAVY), calculated using the hydrophobicity scale of Kyte and Doolittle, and predicted secondary structures of esculentin-1, determined using AGADIR program, are shown in Table 3.3 and 3.4.

3.4.2 Effects of temporin and esculentin-1 peptides on insulin release from BRIN BD11 and 1.1B4 cells

As expected, alanine (10 mM) and GLP-1 (10 nM) produced a significant ($P<0.001$) increase (approximately 2.5 - 7 folds) in the rate of insulin release on incubation with BRIN-BD11 cells compared with the rate in the presence of glucose alone. The insulin-releasing effects of temporin and esculentin-1a peptides are summarised in Table 3.5 & 3.6 respectively. The experimental data shows that, among temporin peptides, temporin A, F, and G were the most potent with a threshold concentration of 0.1 nM and produced >2-fold increase in the rate of insulin release at a concentration of 3 µM (Figure 3.9). A similar increase in the rate of insulin release was also produced by esculentin-1a (1-21).NH_2, esculentin-1a (1-14).NH_2 and esculentin-1b (1-18).NH_2 at 3 µM concentration on incubation with BRIN-BD11 cells. The stimulatory effects of these active esculentin-

1a peptides were observed up to 1 nM concentration (Figure 3.11). There was no statistical difference in the responses produced by analogue esculentin (1-21)-1c and the other active esculentin-1a peptides at 3 µM concentration, however, the stimulatory response was observed up to 10 nM concentration. Neither temporin nor esculentin-1 peptides produced a significant increase in the rate of release of the cytosolic enzyme LDH from BRIN-BD11 cells, at concentrations up to and including 3 µM (Figure 3.10 & 3.12), suggesting that integrity of plasma membrane is intact. In the presence of DMSO (100%), significant increase ($P<0.001$) in LDH release was observed.

The insulin-releasing effects of active temporin and esculentin-1 peptides were also reflected in a glucose-responsive 1.1B4 cell line (Figure 3.13 & 3.14). Temporin G on incubation with 1.1B4 cells produced a significant ($P<0.05$) increase in the rate of insulin release at concentrations $\geq$ 0.1 nM. On the other hand, the threshold concentration for temporin A and F was 1 nM. The response produced by temporin G at 3 µM concentration was comparable to that produced by 10 nM GLP-1. Esculentin-1a (1-21).NH_2, esculentin-1a(1-14).NH_2 and esculentin-1b (1-18).NH_2 demonstrated increase in the rate of insulin release up 0.1 nM concentration. Whereas, the threshold concentration of analogue esculentin (1-21)-1C was 10-fold less compared to other active esculentin-1a peptides. Similar to temporin G, the response produced by 3 µM esculentin-1a (1-21).NH_2 was comparable to that produced by 10 nM GLP-1.

3.4.3 Effects of temporin and esculentin-1 peptides on insulin release from isolated mouse islets

Incubation of active temporins (temporins A, F & G) and esculentin-1 [esculentin-1a (1-21).NH_2, Esc(1-21)-1c, esculentin-1b (1-18).NH_2 & esculentin-1a (1-14).NH_2] peptides (10 nM and 1 µM) peptides with isolated islets from NIH Swiss mice produced a

significant ($P<0.05$ - $P<0.001$) and dose-dependent increase in the rate of insulin release compared with the rate in the presence of 16.7 mM glucose alone (Figure 3.15 & 3.16). However, the magnitude of increase in insulin release by active temporin and esculentin-1 peptides was less than that demonstrated by the same concentration of GLP-1.

3.4.4 Effects of temporin and esculentin-1 peptides on membrane depolarization and intracellular calcium ($[Ca^{2+}]i$) in BRIN-BD11 cells

Incubation of cells with insulin secretagogues, 30 mM KCl and alanine (10 mM) produced an immediate and sustained increase in membrane potential (Figure 3.17 & 3.19) and intracellular calcium respectively (Figure 3.18 & 3.20). In contrast, 1 µM of active temporin peptides (temporin A, F & G) which were added 20 sec after start of data acquisition at a rate of ~62 µl/sec, produced no significant effects on membrane depolarization (Figure 3.17) and $[Ca^{2+}]i$ (Figure 3.18) compared with 5.6 mM glucose only. On the other hand, 1 µM of esculentin-1a (1-21).NH_2, esculentin-1b (1-18).NH_2 and esculentin-1a (1-14).NH_2 produced significant increases in both membrane potential (Figure 3.19) and $[Ca^{2+}]i$ (Figure 3.20) compared with control (5.6 mM glucose alone). However, in case of analogue esculentin (1-21)-1c, on incubation with cells did not lead to a significant increase in both membrane potential and $[Ca^{2+}]i$ compared to control.

3.4.5 Effects of temporin and esculentin-1 peptides on cytokine-induced apoptosis and proliferation in BRIN-BD11 cells

As shown in Figure 3.21, treatment of BRIN-BD11 cells with 1 µM concentration of temporin A and F, and GLP-1 alone, had no significant effect on the number of cells displaying DNA damage. In agreement, the number of apoptotic cells increased significantly ($P<0.001$) by 3-fold on incubation with proinflammatory cytokines mixture.

However, when the BRIN-BD11 cells co-incubated with temporin A and the cytokine mixture, the number of apoptotic cells was reduced significantly ($P<0.01$) by 37%. The corresponding value for temporin F was 42% ($P<0.001$). The degree of protection provided by temporin A and temporin F were comparable to that provided by the same concentration of concentration of GLP-1 (40%; $P <0.01$). On the other hand, temporin G failed to provide any protection to cell against cytokine mixture. In similar fashion, treatment of BRIN-BD11 cells with temporin A and temporin F (1 µM) resulted significant ($P<0.01$, $P<0.001$) increased in proliferating cells by 49% and 80% respectively, which were comparable to that produced by 1 µM GLP-1 (65 % increase; $P<0.01$). In temporin G treated cells, no significant effects on cell proliferation was observed (Figure 3.22).

As shown in Figure 3.23, no adverse effects were observed in BRIN-BD11 cells treated with active esculentin-1 peptides. The number of cells exhibiting DNA damage was comparable to control. However, all active esculentin-1 peptides have shown to protect BRIN-BD11 cells against cytokine-induced DNA damage. The degree of protection provided by esculentin-1a (1-21).NH_2 and esculentin (1-21)-1c were comparable to that provided by the same concentration of GLP-1 (39%; $P<0.01$). Esculentin-1b (1-18).NH_2 and esculentin-1a (1-14).NH_2, also protected cells against cytokines but the effect was comparatively less than GLP-1. Similarly, incubation of cells with esculentin-1a (1-21).NH_2 and esculentin (1-21)-1c peptides resulted in significant ($P<0.01$) increase in the number of the proliferating cells (Figure 3.24). The increase produced by esculentin (1-21)-1c was comparable to that produced by the same concentration of GLP-1. In the case of esculentin-1b (1-18).NH_2 and esculentin-1a (1-14).NH_2, no effects on proliferating cells were observed.

3.4.6 Effects of temporin and esculentin-1 peptides on glucose tolerance and insulin concentrations in mice

No adverse effects were observed in the animals following intraperitoneal injection of the temporin and esculentin-1 peptides. Blood glucose concentrations in lean NIH Swiss mice receiving glucose plus temporin G (75 nmol/kg bw) or esculentin (1-21)-1c (75 nmol/kg bw) were significantly ($P<0.05$, $P<0.01$) lower at 15 min and 30 min after injection compared with animals receiving glucose only (Figure 3.25A & 3.27A). Similarly, the overall response of blood glucose (area under the curve) over 60 min was significantly ($P<0.05$) decreased after administration of the temporin G or esculentin (1-21)-1c (Figure 3.25 B & 3.27B). These glucose-lowering effects of peptides were associated with a significant increase in plasma insulin concentration. Plasma insulin concentrations were significantly ($P<0.05$) higher at 15 min after glucose administration in animals receiving temporin G or esculentin (1-21)-1c compared with animals receiving glucose only (Figure 3.25 C & 3.27C) and the integrated response i.e. total amount of insulin released over 60 min was significantly greater ($P<0.05$) (Figure 3.25 D & 3.27D). In contrast, no significant effects on blood glucose were observed at any time point after co-injection of temporin A, temporin F, esculentin-1a (1-21), esculentin-1b (1-18).NH_2 and esculentin-1a (1-14) with glucose compared to injection of glucose only (Figure 3.26 & 3.28).

3.5 Discussion

This study has identified temporins (Temporin A, B, F and G) and peptides derived from the N-terminal domain of the host-defence peptides esculentin-1a and -1b [esculentin-1a (1-21).NH_2, esculentin-1b (1-18).NH_2 and esculentin-1a (1-14).NH_2] that stimulated the release of insulin from rodent and human clonal β-cells and isolated mouse islets at low concentrations without apparent toxicity.

Although the factors that influence the antimicrobial and cytotoxic activities of small peptides are reasonably well understood (Conlon *et al.*, 2007a, Grieco *et al.*, 2011, Mojsoska &, Jenssen 2015, Ramesh *et al.*, 2016), the structural determinants of insulin-releasing activity are largely unknown. Among temporin peptides, temporin A and G with a calculated pI of 10.06 and temporin F with a calculated pI of 8.86 were the most potent with a threshold concentration of 10^{-9} M (Table 3.5). On the other hand, temporin B peptide also produced a significant increase in the rate of insulin release at 10^{-9} M but the maximum effects of the peptide was appreciably less than that of temporin A, F, and G. The significant, albeit weak insulin-releasing activity of anionic peptides, temporin C and E with a threshold concentration of 10^{-7} M, demonstrates that a net positive charge at physiological pH is not a mandatory requirement. Similarly, cationicity is not the only parameter influencing this activity as temporin H and K with a calculated pI of 8.86 lacked insulin-releasing actions at concentrations up to and including 3 x 10^{-6} M. This suggests that peptide hydrophobicity is also an important determinant of activity as these peptides were appreciably more hydrophilic than the other temporins. Despite having the same isoelectric point and similar hydrophobicities, temporin B peptide displayed reduced insulinotropic activity compared with temporin F. In a cationic, amphipathic α-helical peptide, the polar angle (Φ) subtended by the positively charged amino acids is an important determinant of antimicrobial and hemolytic activity (Dathe *et al.*, 2004). In the case of temporin-1DRa analogues, increasing the polar angle to 180^{o} by appropriate substitutions by L-lysine produced inactive components (Conlon *et al.*, 2007a). As shown in Fig. 3.29, the angle subtended by the positive charge on the α-amino group of the N-terminal residue and the positive charge on the ε-amino group of the lysine residue is 180^{o} for temporin B and 120^{o} for temporin F. This could be the reason for the reduced insulin-releasing activity of temporin B compared with temporin F.

The present study has provided evidence that the degree of helicity is of particular importance is determining the insulin-releasing activity of the esculentin-1 peptides. Consistent with secondary structure predictions using the AGADIR algorithm (Kyte, & Doolittle, 1982) (Table 3.4), circular dichroism (Grazia *et al.,* 2015) and NMR (Ghosh *et al.,* 2016) studies have shown that esculentin-1a (1-21).NH_2 possess a random coil structure in aqueous solution but adopts a predominantly α-helical conformation in the environment of lysophosphatidylcholine and lipopolysaccharide micelles. A similar investigation of the preferred conformation of esculentin-1b (1-18).NH_2 has demonstrated that the N-terminal domain of this peptide (Phe3 -Leu11) adopts a stable α-helical structure in the membrane-mimetic solvent 50% trifluoroethanol-water while the more hydrophobic C-terminal portion is unstructured (Manzo *et al.,* 2012). The presence of helix-destabilizing D-amino acid residues in esculentin (1-21)-1c means that the α-helical domain is confined to the N-terminal region of the peptide (Muller *et al.,* 2005). While the cationicity and hydrophobicity of the diastereomer are the same as the native peptide, this reduction in helicity results in a decrease in the *in vitro* insulinotropic activity. Similarly, the molecular charge of esculentin-1a (1-14).NH_2 and esculentin-1a (9-21) are the same, and their hydrophobicities are very similar, but the AGADIR programme predicts that the former peptide has the propensity to adopt a stable α-helical conformation whereas the latter is unstructured in solution. In consequence, esculentin-1a (1-14).NH_2 is equipotent and equally effective as esculentin-1a (1-21).NH_2 in stimulating insulin release whereas esculentin-1a (9-21) is inactive (Table 3.6).

Insulin secretion from pancreatic beta cells is regulated by the K_{ATP} channel-dependent and K_{ATP} channel-independent pathway (Henquin, 2000, 2004). In the former pathway, ATP molecule generated from glucose metabolism depolarize the cell by blocking the ATP-sensitive potassium channel. As a result, calcium ion influx through the opening of

voltage-dependent channels, which induce the beta cell to release insulin. Previous studies have reported that naturally occurring frog skin-derived peptides such as alyteserin-2a (Ojo *et al.* 2013b), tigerinin-1R (Ojo *et al.* 2011), and CPF-6 (Srinivasan *et al.* 2013) stimulate insulin release by depolarising membrane of BRIN-BD11 cells with a significant increase in intracellular Ca^{2+}, suggesting that these peptides operate via the K_{ATP} channel-dependent pathway. In common with these peptides, incubation of BRIN-BD11 cells with esculentin-1 peptides resulted in a significant increase in membrane potential and intracellular calcium. In contrast, hymenochirin 1B (Owolabi *et al.*, 2015), phylloseptin-L2 (Abdel-Wahab *et al.*, 2008b) pseudin-2 (Abdel-Wahab *et al.*, 2008a) peptide did not affect these parameters when incubated with BRIN-BD11 cells under the same condition. Consistent with these, incubation of temporin A, F and G with BRIN-BD11 cells did not have any effects on either membrane depolarization or intracellular calcium suggesting that the insulinotropic action of peptides is mediated via a calcium-independent pathway.

The progression of type 2 diabetes is linked to the loss of beta cell mass as well as beta cell function, which may contribute to impaired insulin secretion (Cantley & Ashcroft, 2015, Arden, 2018). In this regard, we further investigated the proliferative and anti-apoptotic effects of active temporin and esculentin-1 peptides. Consistent with previous reports (Yabe *et al.*, 2011, Lee *et al.*, 2014), GLP-1 protected the beta cell against cytokines induced apoptosis as well as significantly improved proliferation of beta cells. The present study has shown that the proliferative activity of temporin A and temporin F, and esculentin (1-21)-1c was comparable to that of GLP-1. Furthermore, these peptides, including esculentin-1a (1-21) were equally effective as GLP-1 in protecting the beta cell against cytokines induced apoptosis. On the other hand, temporin G, esculentin-1a (1-14) and esculentin-1b (1-18) peptides failed to show any positive effect of beta cell

proliferation. However, the latter two peptides showed weakly, but significant protective effects against cytokines induced beta-cell apoptosis cells.

After demonstrating positive effects on insulin release in BRIN-BD11, 1.1B4 and primary islet cells, active temporin and esculentin-1 peptides were further investigated for their effects on glucose tolerance in lean mice. Temporin A, temporin F, esculentin-1a (1-21), esculentin (1-14) and esculentin (1-18) despite their high insulinotropic potency *in vitro*, failed to lower blood glucose when administered interpretationally to overnight fasted mice. The reason for the loss of activity could be rapid degradation or clearance of these peptides from the circulation. Therefore, it is necessary to design long-acting analogues if these peptides are to find application as incretins in T2DM therapy. The D-amino acid substituted analogue esculentin (1-21)-1c, although a less potent insulin secretagogue *in vitro*, has been shown to possess increased stability in serum (Grazia *et al.,* 2015). Administration of this peptide to mice under the same conditions significantly improved glucose tolerance and increased circulating insulin concentrations. Analogues of the frog skin-derived peptide esculentin-2Cha (1-30) containing D-amino acids have also been designed that exhibit increased resistance to degradation by serum peptidases and consequently show improved glucose-lowering properties in insulin-resistant high fat fed mice compared with the unsubstituted peptide (Vasu *et al.,* 2017). It is well established that individuals with T2DM are more prone to microbial infections than healthy subjects (Muller *et al.,* 2005). Esculentin (1-21)-1c displays potent broad-spectrum antimicrobial activity (Grazia *et al.,* 2015, Loffredo *et al.,* 2017) so that regular injections of the peptide as a part of a therapeutic strategy may have a prophylactic effect on preventing infection as well as promoting glucose homeostasis in these patients. Temporin G (75 nmol/kg bw) also significantly stimulated insulin release and lowered blood glucose concentrations *in*

vivo when administered to mice, however, the effects were less than that produced by GLP-1 (25 nmol/kg bw).

In conclusion, the study has shown the insulinotropic activity of temporin and esculentin-1 peptides and its analogue esculentin (1-21)-1c as well as their positive effects on beta cell proliferation and survival. These peptides could represent a template for the design of new types of drugs for use in T2DM therapy. Further studies are warranted to develop longer-acting forms of peptides for assessment in appropriate animal models of T2DM, such as the insulin-resistant, glucose-intolerant, high fat fed mouse.

Table 3.1 Amino acid sequence of temporin and esculentin-1 peptides

Sr. No	Peptide	Sequence
1	Temporin A	FLPLIGRVLSGIL-NH_2
2	Temporin B	LLPIVGNLLKSLL-NH_2
3	Temporin C	LLPILGNLLNGL-NH_2
4	Temporin E	VLPIIGNLLLNS-NH_2
5	Temporin F	FLPLIGKVLSGIL-NH_2
6	Temporin G	FFPVIGRILNGIL-NH_2
7	Temporin H	LSPNLLKSLL-NH_2
8	Temporin K	LLPNLLKSLL-NH_2
9	Esculentin-1a (1-21)	GlFSKLAGKKlKNLLlSGLKG-NH_2
10	Esculentin (1-21)-1C	GIFSKLAGKKlKN***L***LlSGLKG-NH_2
11	Esculentin-1a (1-14)	GlFSKLAGKKlKNL
12	Esculentin-1a (9-21)	KKlKNLLlSGLKG
13	Esculentin-1b (1-18)	GlFSKLAGKKLKNLLlSG-NH_2

Table 3.2 Reverse phase HPLC, retention time and MALDI-TO MS

Sr. No	Peptide	Molecular weight Da (Theoretical)	Molecular weight Da (Experimental)	Retention time (min)
1	Temporin A	1397	1397.4	28.4
2	Temporin B	1392	1392.7	28.2
3	Temporin C	1362	1362.2	27.5
4	Temporin E	1378	1377.9	27.1
5	Temporin F	1369	1368.9	28.7
6	Temporin G	1458	1458.1	27.3
7	Temporin H	1113	1113.2	25.1
8	Temporin K	1123	1122.7	28.7
9	Esculentin-1a (1-21)	2184	2183.3	26.4
10	Esculentin (1-21)-1C	2184	2184.1	26.3
11	Esculentin-1a (1-14)	1516	1516.2	26.8
12	Esculentin-1a (9-21)	1411	1412	26.2
13	Esculentin-1b (1-18)	1886	1886.1	26.6

Table 3.3 Primary structure and physicochemical properties of the temporin peptides used in this study

Peptide	Primary structure	Calc. pI	GRAVY
Temporin A	FLPLIGRVLSGIL.NH_2	10.06	1.81
Temporin B	LLPIVGNLLKSLL.NH_2	8.86	1.64
Temporin C	LLPILGNLLNGLL.NH_2	5.28	1.67
Temporin E	VLPIIGNLLLNSL.NH_2	5.28	1.55
Temporin F	FLPLIGKVLSGIL.NH_2	8.86	1.85
Temporin G	FFPVIGRILNGIL.NH_2	10.06	1.58
Temporin H	LSP***NLLKSLL.NH_2	8.86	0.84
Temporin K	LLP***NLLKSLL.NH_2	8.86	1.30

Calc.pI refers to calculated isoelectric point and GRAVY represents Grand Average of Hydropathy determined using the hydrophobicity scales of Kyte and Doolittle.

Table 3.4 Primary structure and physicochemical properties of the esculentin-1 peptides used in this study

Peptide	Primary structure	Charge	GRAVY	Helical Domain
Esc-1a(1-21)	GIFSKLAGKKIKNLLISGLKG[a]	+6	0.34	5-14
Esc-1a(1-21-1C	GIFSKLAGKKIKNlLIsGLKG[a]	+6	0.34	ND
Esc-1a(1-14)	GIFSKLAGKKIKNL[a]	+4	0.04	5-11
Esc-1a(9-21)	KKIKNLLISGLKG	+4	-0.02	Nonhelical
Esc-1b(1-18)	GIFSKLAGKKLKNLLISG[a]	+5	0.38	5-14

[a] denotes C-terminal α-amidation. Charge refers to the net charge at pH 7.0 and GRAVY represents Grand Average of Hydropathy determined using the hydrophobicity scales of Kyte and Doolittle. Secondary structure (extent of the helical domain) was predicted using the AGADIR algorithm. ND not determined.

Table 3.5 Effects of temporin peptides on the rate of insulin release from BRIN-BD11 and 1.1B4 clonal β-cells

	BRIN-BD11		1.1B4	
Peptide	**Threshold Conc.(M)**	**Insulin release at 3 µM Conc. ng/10^6 cells/20min**	**Threshold Conc.(M)**	**Insulin release at 3 µM Conc. ng/10^6 cells/20min**
None	NA	0.73 ± 0.08	NA	0.09 ± 0.01
Temporin A	10^{-9}	1.92 ± 0.20***	10^{-9}*	0.18 ± 0.01
Temporin B	10^{-9}	1.25 ± 0.07***	10^{-8}*	ND
Temporin C	10^{-7}	1.11 ± 0.12**	10^{-7}*	ND
Temporin E	10^{-7}	1.10 ± 0.08**	10^{-7}*	ND
Temporin F	10^{-9}	1.85 ± 0.20***	10^{-9}**	0.17 ± 0.01
Temporin G	10^{-9}	1.73 ± 0.17***	10^{-10}*	0.21 ± 0.01
Temporin H	NA	No effect	ND	ND
Temporin K	NA	No effect	ND	ND

Threshold concentration refers to the minimum concentration of peptide producing a significant increase in the rate of insulin release compared with the rate in the presence of glucose only. Max, effect refers to the rate of insulin release in the presence of 3 µM peptide. NA: not applicable; ND: not determined. *P<0.05, **P<0.01, ***P<0.001 vs 5.6 mM glucose alone.

Table 3.6 Effects of the esculentin-1 peptides on the rate of insulin release from BRIN-BD11 and 1.1B4 clonal β-cells

	BRIN-BD11		1.1B4	
Peptide	**Threshold Conc. (M)**	**Insulin release at 3 µM Conc ng/10^6 cells/20min**	**Threshold Conc. (M)**	**Insulin release at 3 µM Conc ng/10^6 cells/20min**
None	NA	1.29 ± 0.08	NA	0.04 ± 0.01
Esculentin-1a(1-21)[a]	10^{-9}*	2.53 ± 0.05***	10^{-10}*	0.07 ± 0.01***
Esculentin (1-21)- 1C	10^{-8}*	2.63 ± 0.12***	10^{-9}*	0.07 ± 0.01***
Esculentin-1a (1-14)[a]	10^{-9}*	2.67 ± 0.03***	10^{-10}*	0.07 ± 0.01***
Esculentin-1a (9-21)	NA	1.29 ± 0.08	ND	ND
Esculentin-1b (1-18)[a]	10^{-9}**	2.81 ± 0.08***	10^{-9}**	0.07 ± 0.01***

Threshold concentration refers to the minimum concentration of peptide producing a significant increase in the rate of insulin release compared with the rate in the presence of glucose only. Max. effect refers to the rate of insulin release in the presence of 3 µM peptide. NA: not applicable; ND: not determined. *P<0.05, **P<0.01, ***P<0.001 vs 5.6 mM glucose alone.

Figure 3.1 Representative reverse-phase HPLC profile of temporin peptides

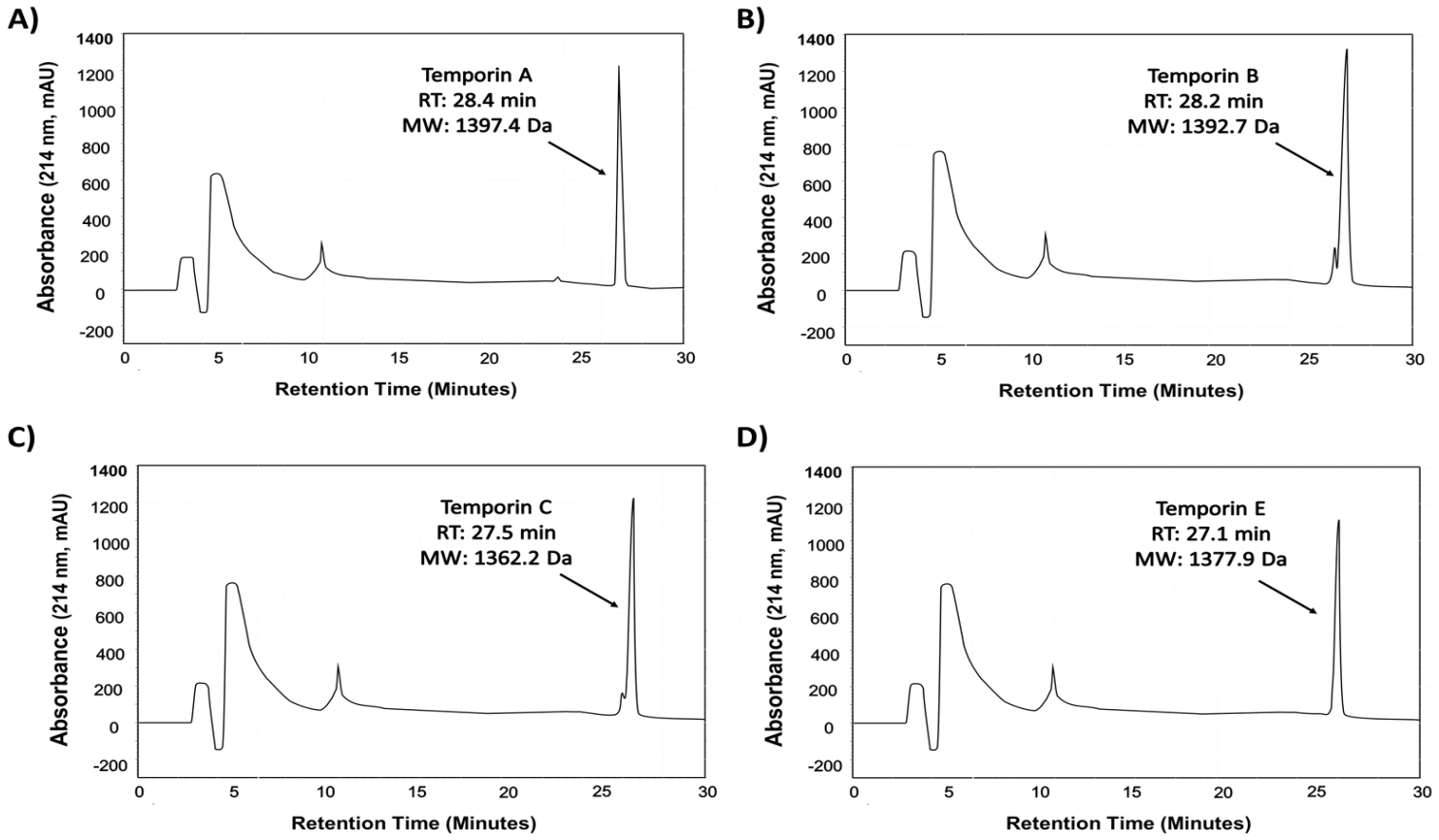

C-8 analytical column was used to obtain a profile using a gradient from 0 to 100 % acetonitrile over 28 min.

Figure 3.2 Representative reverse-phase HPLC profile of temporin peptides

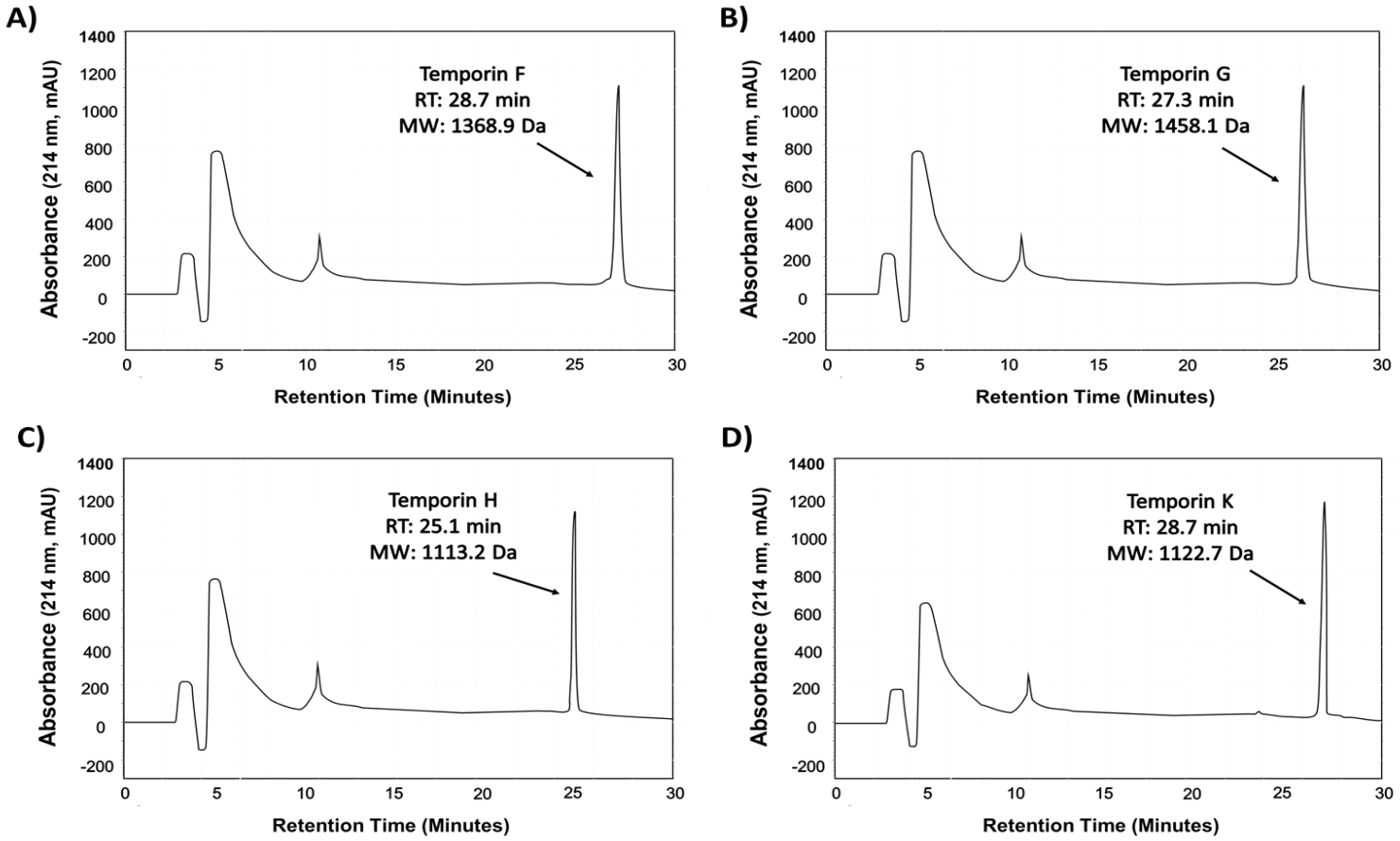

C-8 analytical column was used to obtain a profile using a gradient from 0 to 100 % acetonitrile over 28 min.

Figure 3.3 Representative reverse-phase HPLC profile of esculentin-1 peptides

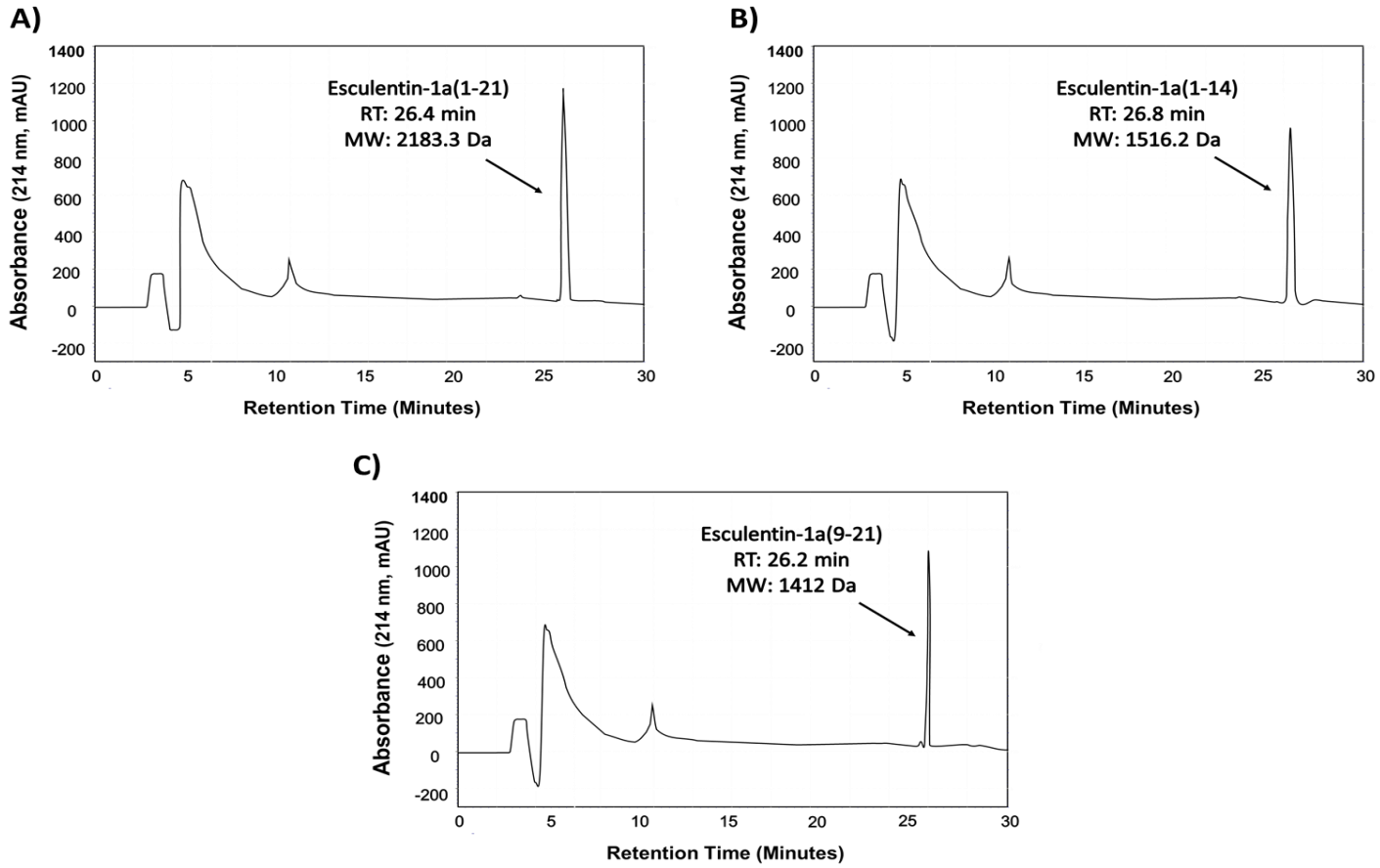

C-8 analytical column was used to obtain a profile using a gradient from 0 to 100 % acetonitrile over 28 min.

Figure 3.4 Representative reverse-phase HPLC profile of esculentin-1 peptides

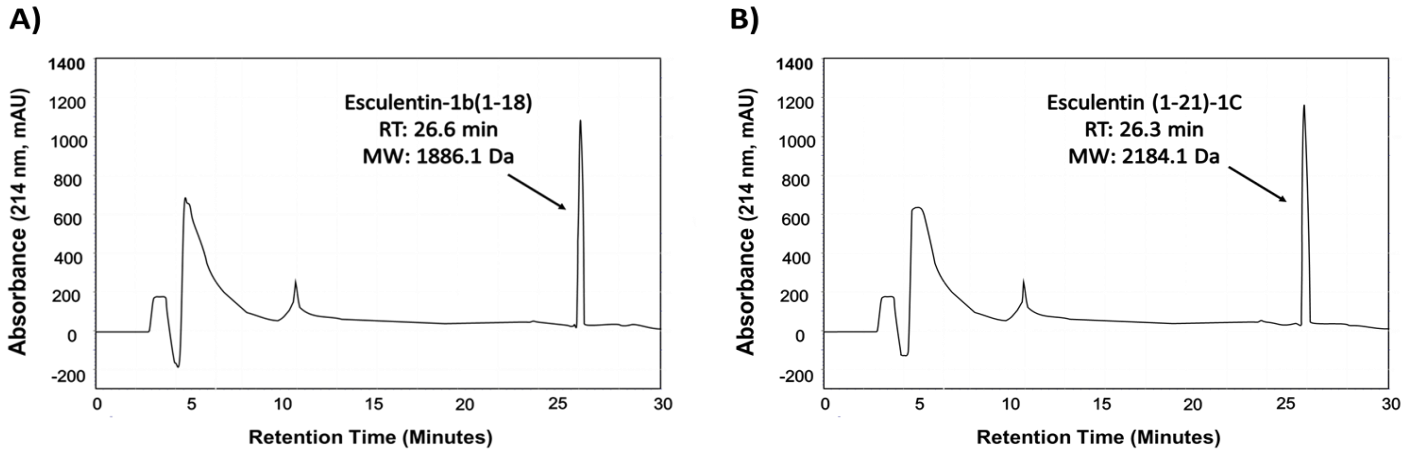

C-8 analytical column was used to obtain a profile using a gradient from 0 to 100 % acetonitrile over 28 min.

Figure 3.5 Representative MALDI-TOF spectra of temporin peptides

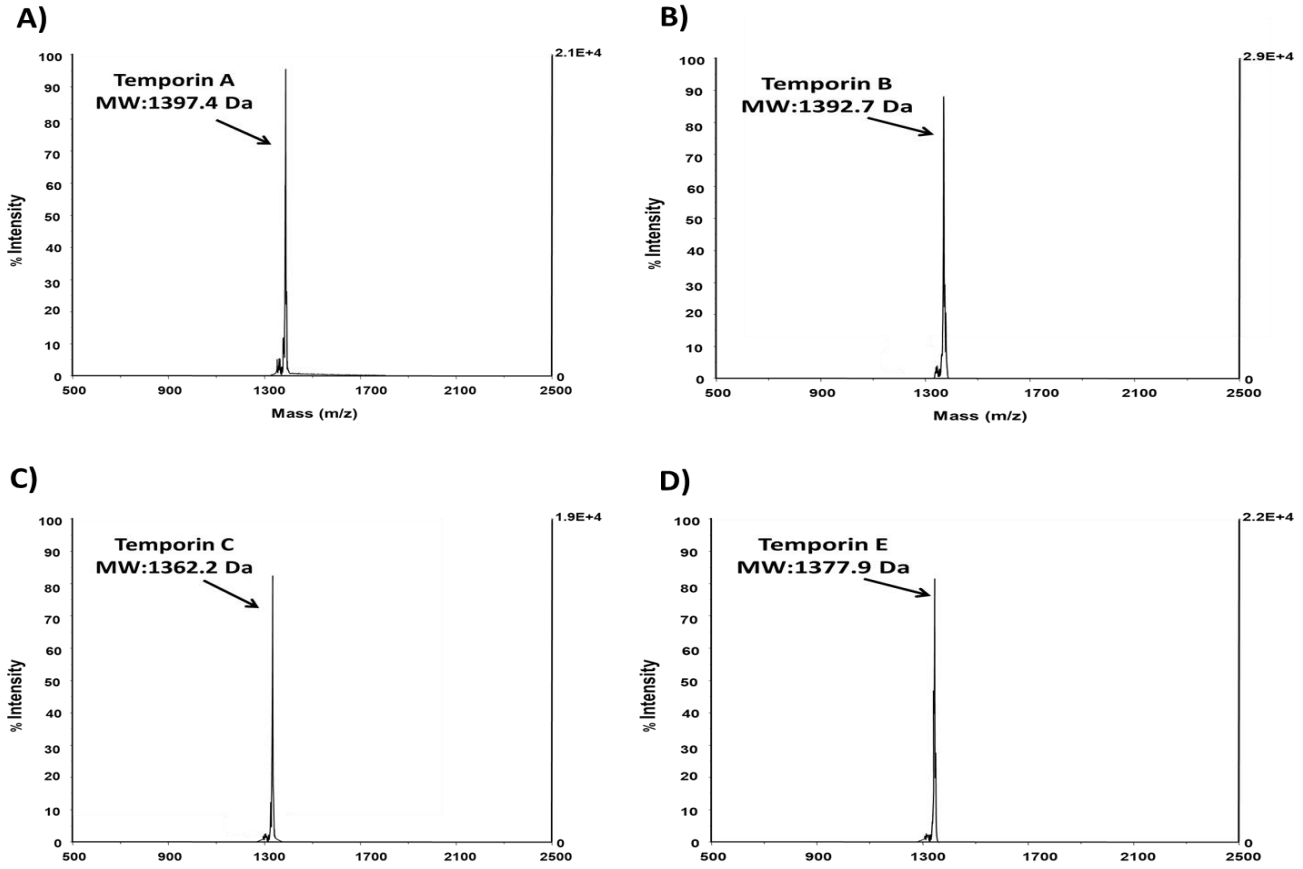

Matrix α-cyano cinnamic acid (1.5 µl) was mixed with purified peptide (1.5 µl) and left to dry on the MALDI plate. After drying, MALDI plate was applied to Voyager DE Bio spectrometry workstation. The mass-to-charge ratio versus peak intensity was recorded.

Figure 3.6 Representative MALDI-TOF spectra of temporin peptides

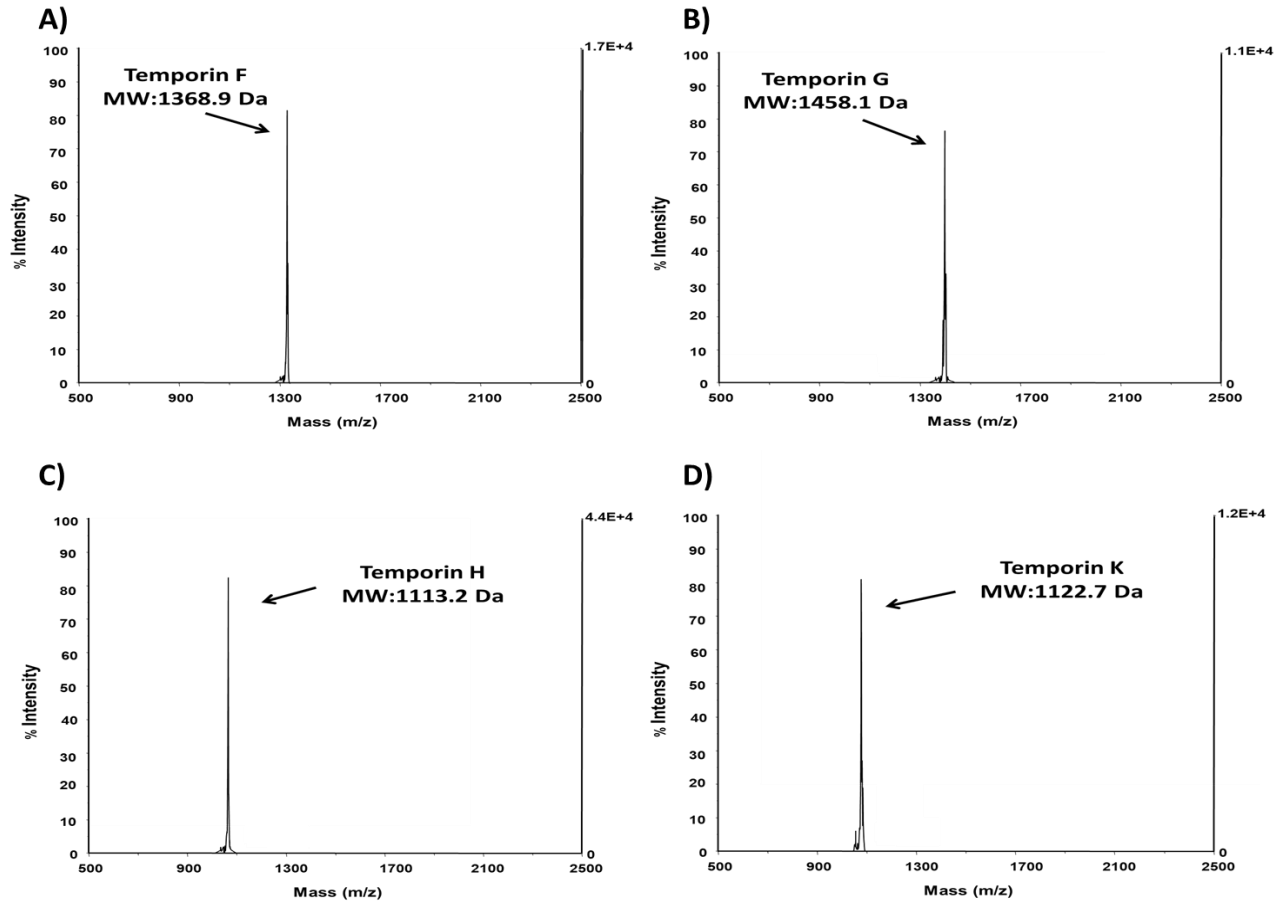

Matrix α-cyano cinnamic acid (1.5 µl) was mixed with purified peptide (1.5 µl) and left to dry on the MALDI plate. After drying, MALDI plate was applied to Voyager DE Bio spectrometry workstation. The mass-to-charge ratio versus peak intensity was recorded.

Figure 3.7 Representative MALDI-TOF spectra of esculentin-1 peptides

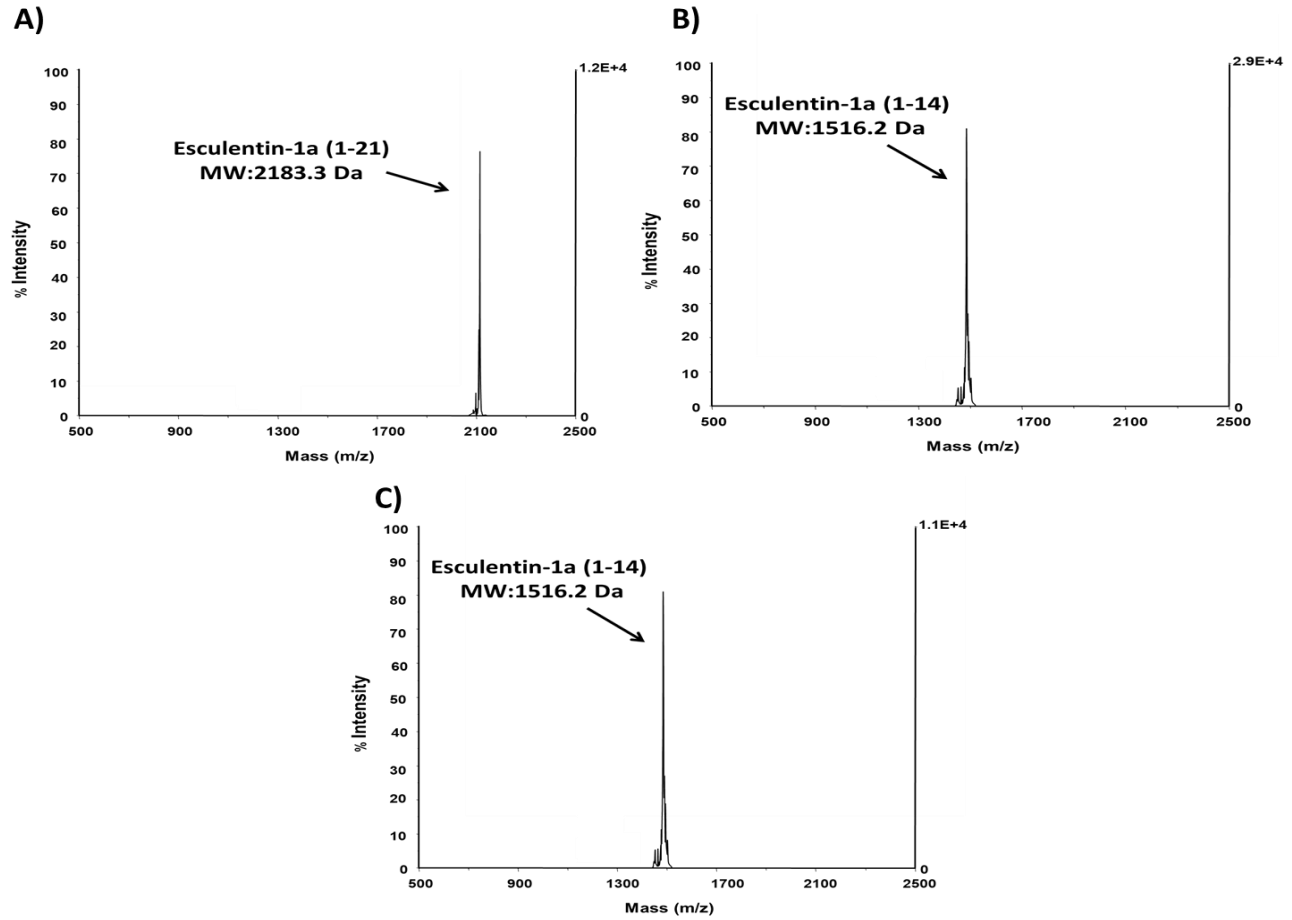

Matrix α-cyano cinnamic acid (1.5 µl) was mixed with purified peptide (1.5 µl) and left to dry on the MALDI plate. After drying, MALDI plate was applied to Voyager DE Bio spectrometry workstation. The mass-to-charge ratio versus peak intensity was recorded.

Figure 3.8 Representative MALDI-TOF spectra of esculentin-1 peptides

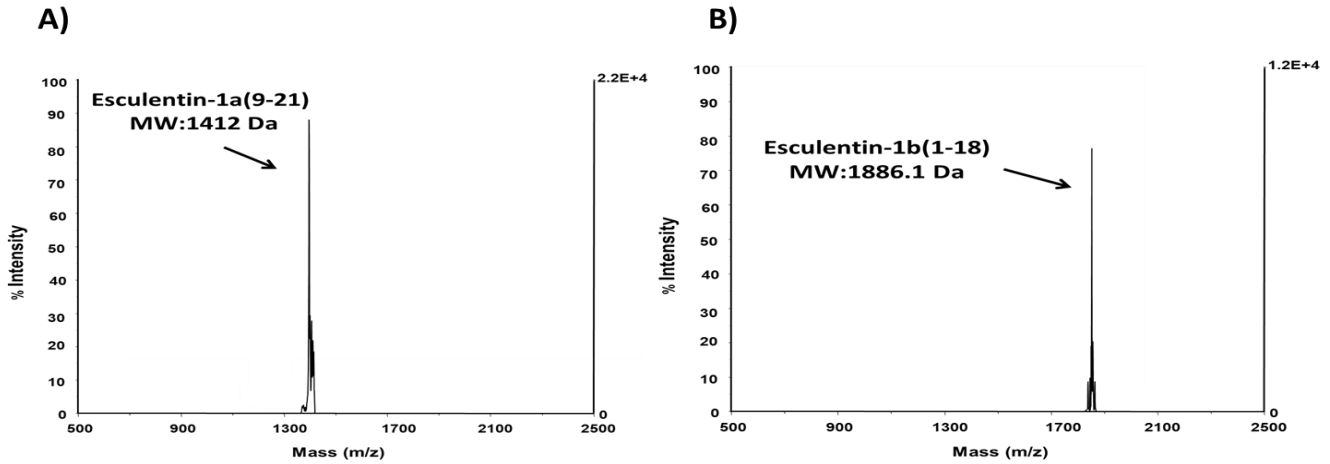

Matrix α-cyano cinnamic acid (1.5 µl) was mixed with purified peptide (1.5 µl) and left to dry on the MALDI plate. After drying, MALDI plate was applied to Voyager DE Bio spectrometry workstation. The mass-to-charge ratio versus peak intensity was recorded.

Figure 3.9 Effects of temporin peptides on insulin release from BRIN-BD11 rat clonal β-cells.

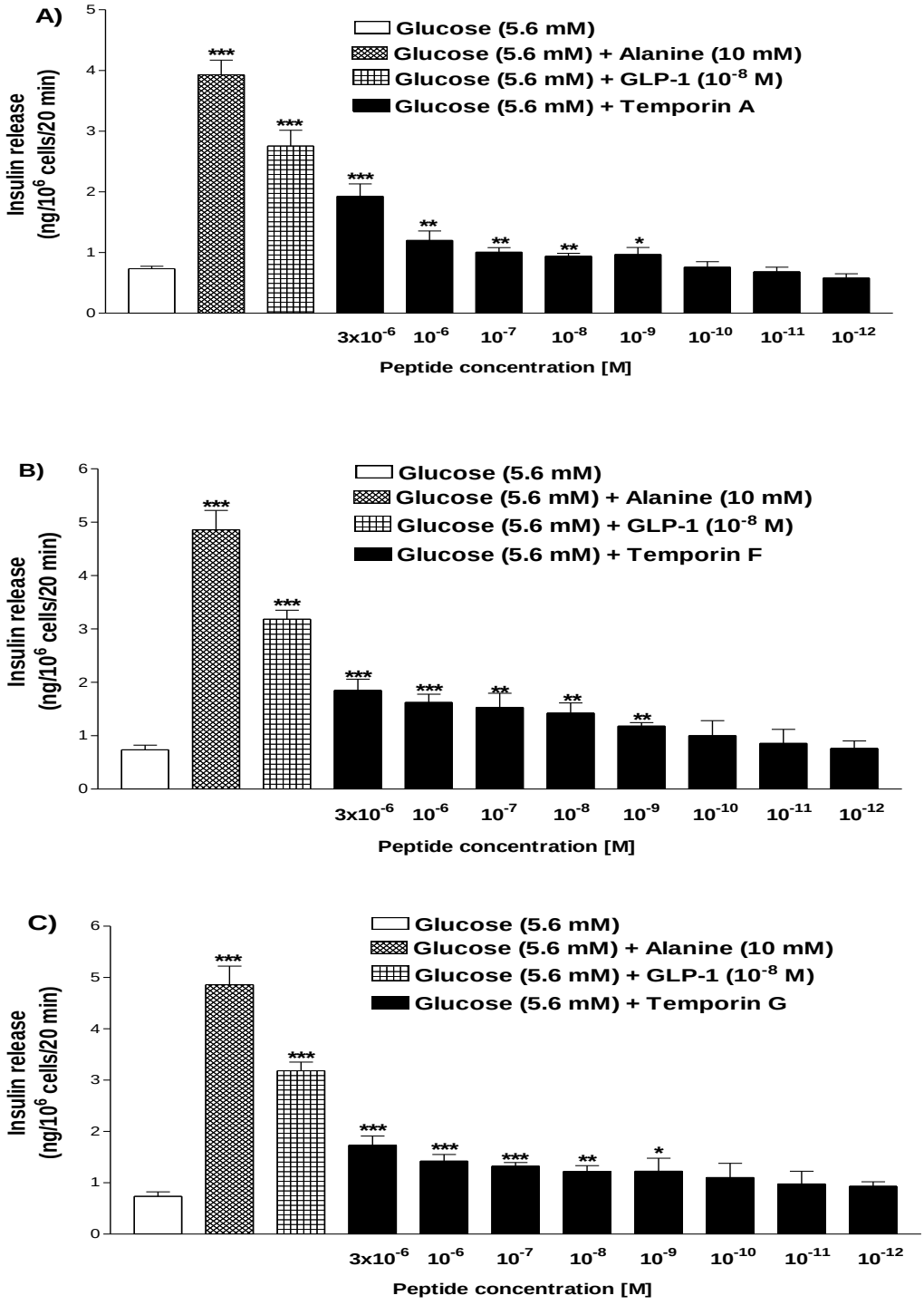

Effects of A) Temporin A, B) Temporin F and C) Temporin G on insulin release from BRIN-BD11 rat clonal β-cells. Values are mean ± SEM for n = 8. *P<0.05, **P<0.01, and ***P<0.001 compared to 5.6 mM glucose alone.

Figure 3.10 Effects of temporin peptides on LDH release from BRIN-BD11 rat clonal β-cells

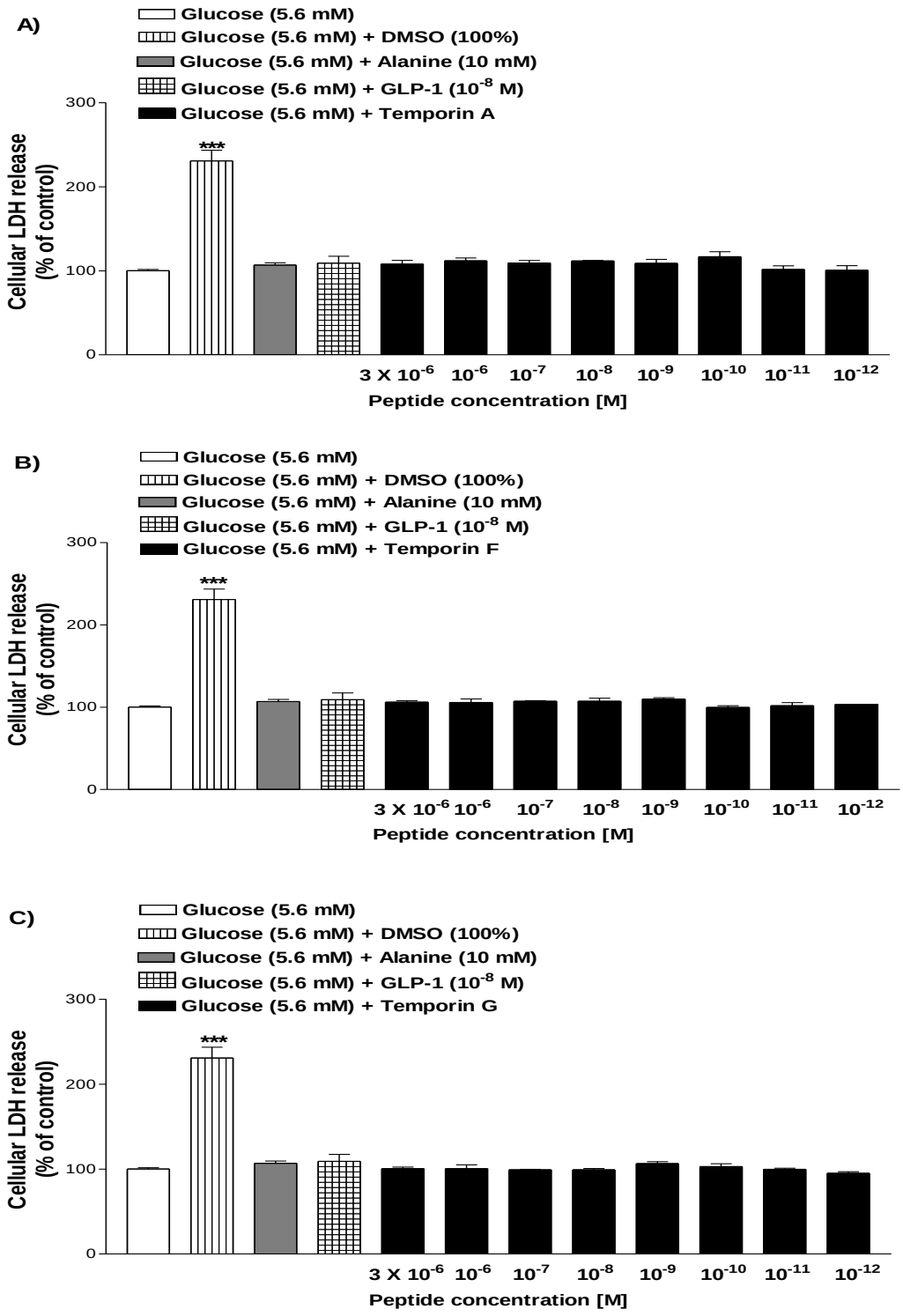

Effects of A) Temporin A, B) Temporin F, and C) Temporin G on LDH release from BRIN-BD11 rat clonal β-cells. DMSO (100%) was used as positive control. Values are Mean ± SEM with n=4 for LDH.

Figure 3.11 Effects of esculentin-1 peptides on insulin release from BRIN-BD11 rat clonal β-cells

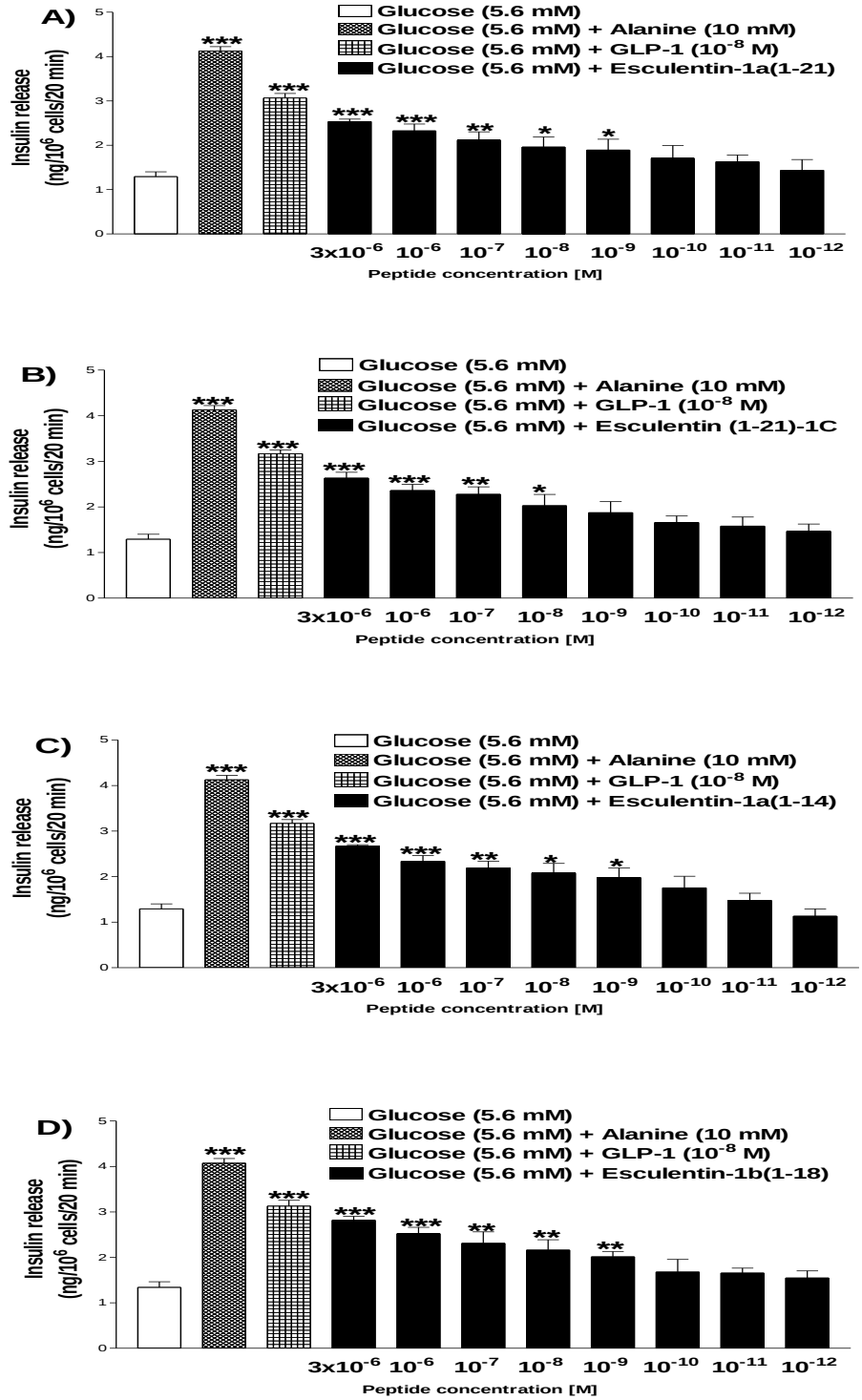

Effects of A) Esculentin-1a (1-21), B) Esculentin (1-21)-1C, C) Esculentin-1a (1-14) and D) Esculentin-1b (1-18) on insulin release from BRIN-BD11 rat clonal β-cells. Values are mean ± SEM for n = 8. *P<0.05, **P<0.01, and ***P<0.001 compared to 5.6 mM glucose alone.

Figure 3.12 Effects of esculentin-1 peptides on LDH release from BRIN-BD11 rat clonal β-cells

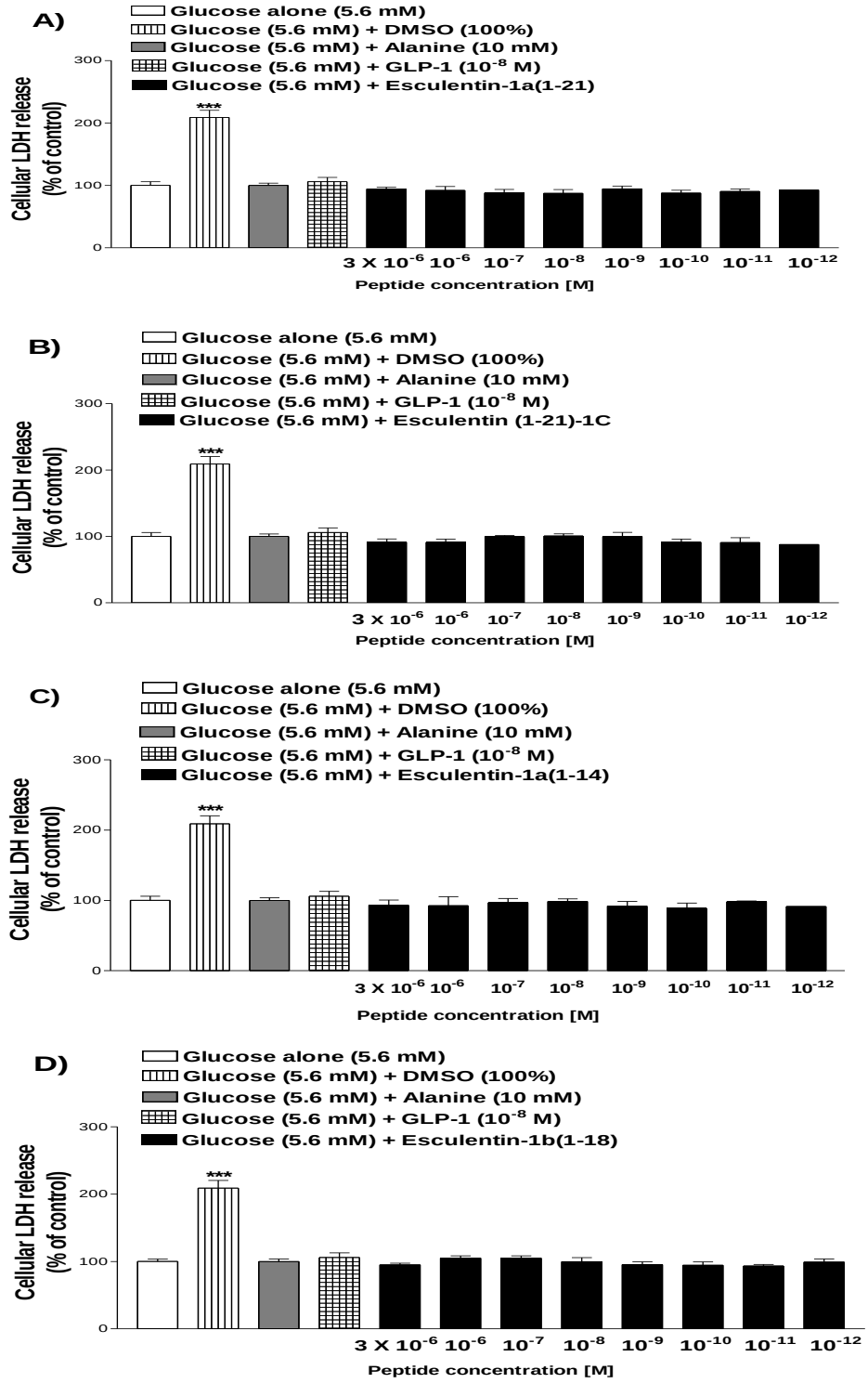

Effects of A) Esculentin-1a (1-21), B) Esculentin (1-21)-1C, C) Esculentin-1a (1-14) and D) Esculentin-1b (1-18) on LDH release from BRIN-BD11 rat clonal β-cells. DMSO (100%) was used as positive control. Values are Mean ± SEM with n=4 for LDH.

Figure 3.13 Effects of temporin peptides on insulin release from 1.1B4 human clonal β-cells

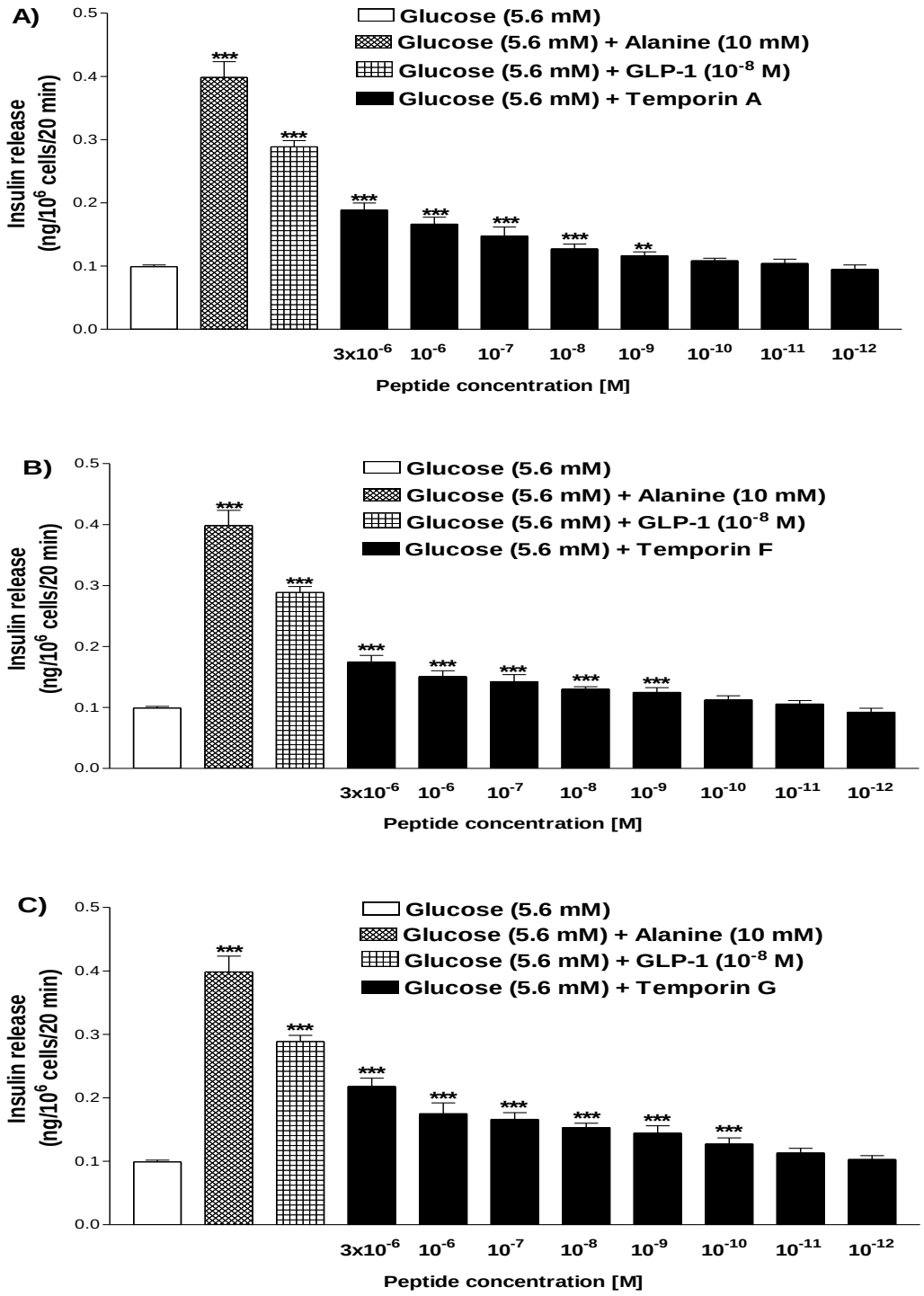

Effects of A) Temporin A, B) Temporin F, and C) Temporin G on insulin release from 1.1B4 human clonal β-cells. Values are mean ± SEM for n = 8. **P<0.01 and ***P<0.001 compared to 5.6 mM glucose alone.

Figure 3.14 Effects of esculentin-1 peptides on insulin release from 1.1B4 human clonal β-cells

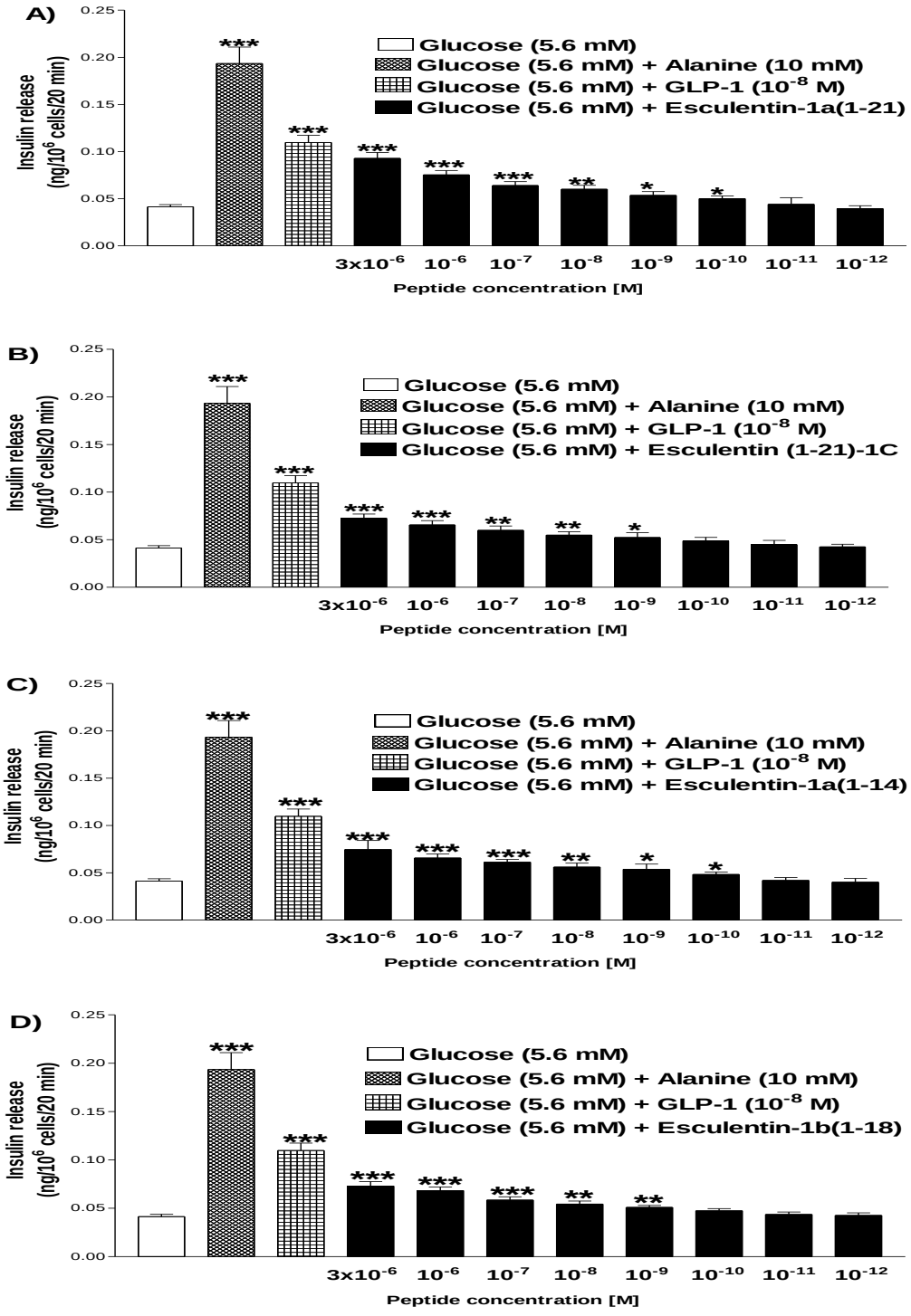

Effects of A) Esculentin-1a (1-21), B) Esculentin (1-21)-1C, C) Esculentin-1a (1-14) and D) Esculentin-1b (1-18) on insulin release from 1.1B4 human clonal β-cells. Values are mean ± SEM for n = 8. *P<0.05, **P<0.01, and ***P<0.001 compared to 5.6 mM glucose alone.

Figure 3.15 Effects of temporin peptides on insulin release from release from isolated mouse islets

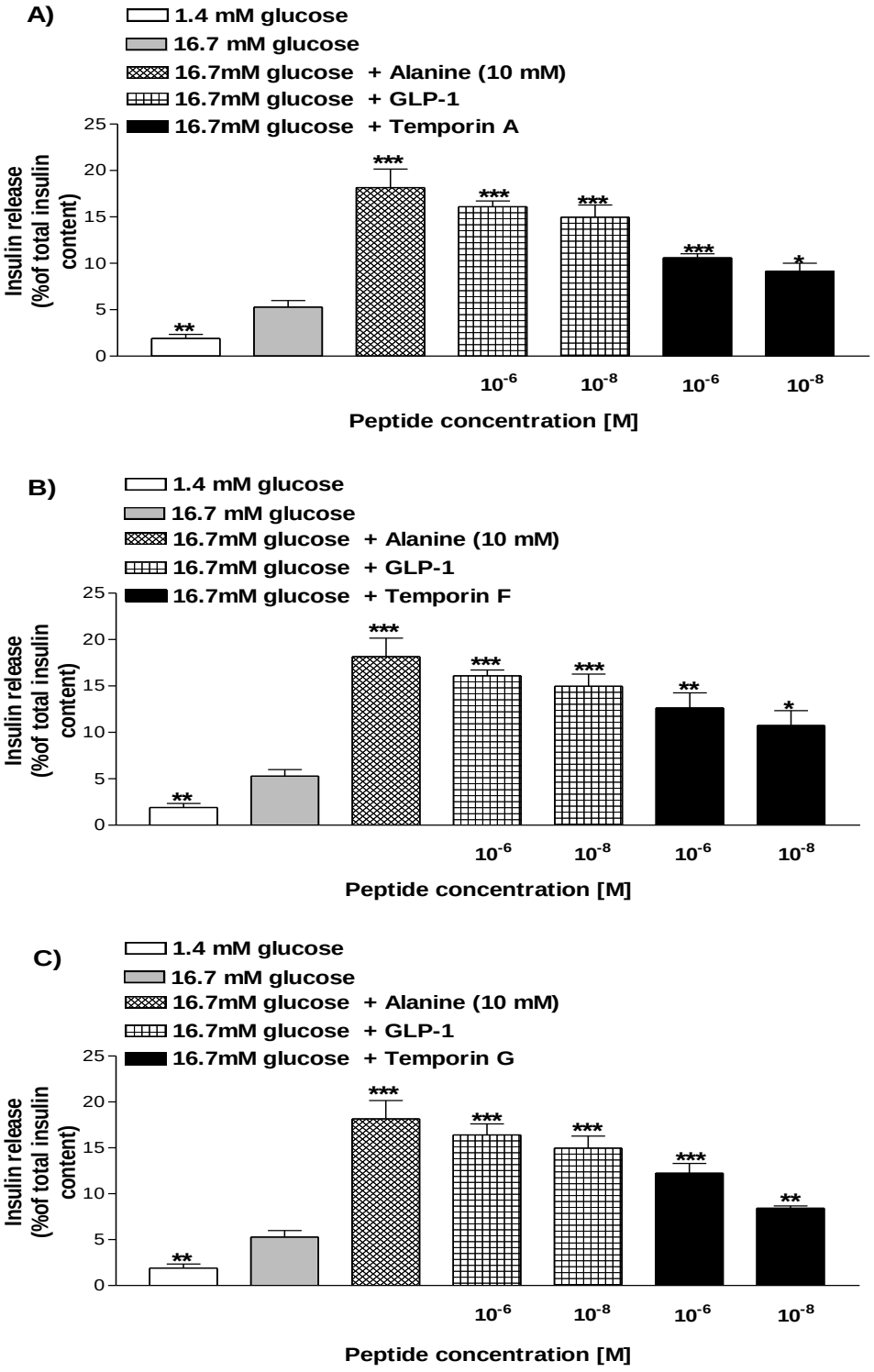

Effects of A) Temporin A, B) Temporin F, and C) Temporin G on insulin release from isolated mouse islets. Values are mean ± SEM for n = 8. *P<0.05, **P<0.01, and ***P<0.001 compared to 5.6 mM glucose alone.

Figure 3.16 Effects of esculentin-1 peptides on insulin release from release from isolated mouse islets

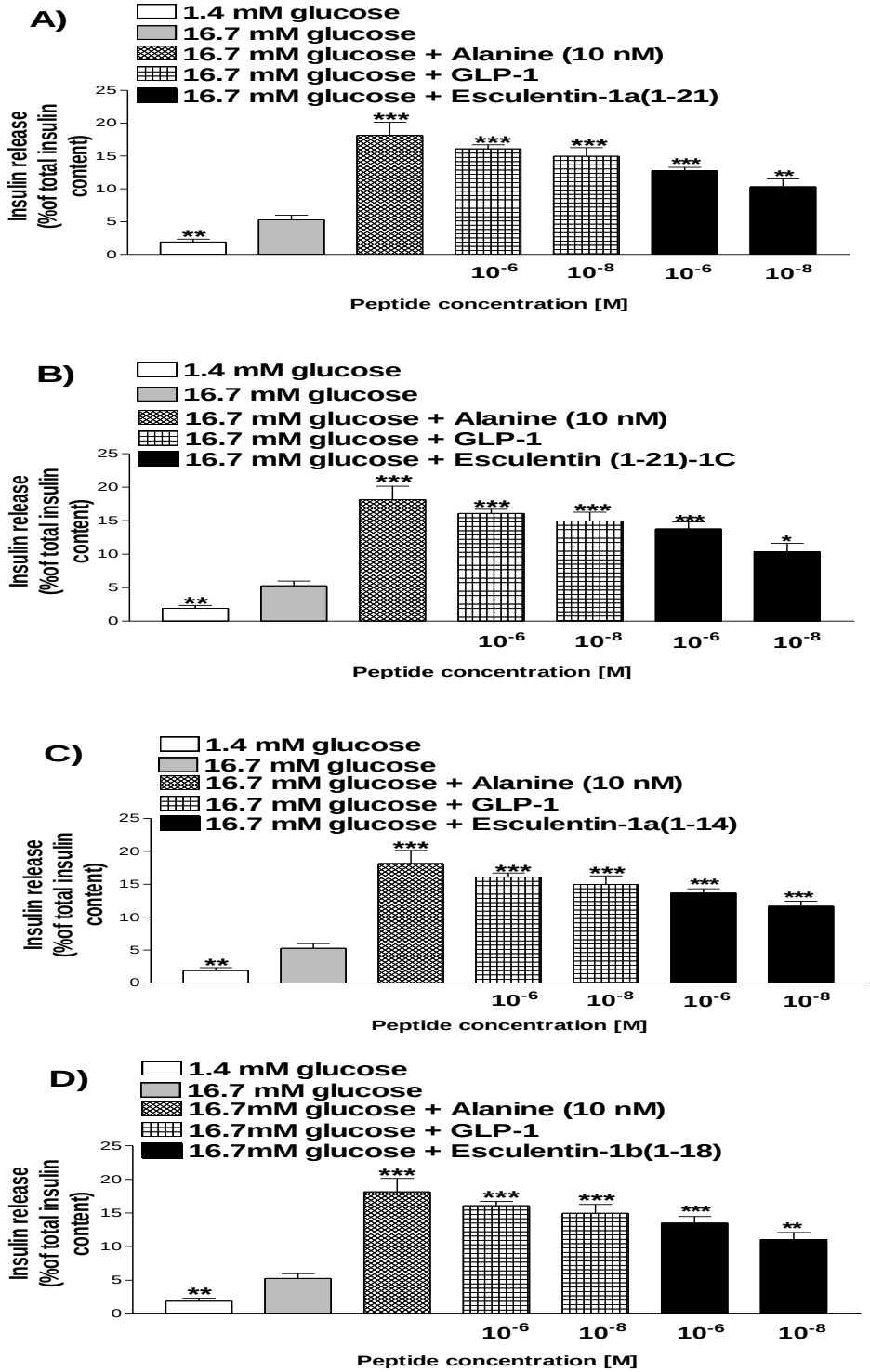

Effects of A) Esculentin-1a (1-21), B) Esculentin (1-21)-1C , C) Esculentin-1a (1-14) and D) Esculentin-1b (1-18) on insulin release from isolated mouse islets. Values are mean ± SEM for n = 8. *P<0.05, **P<0.01 and ***P<0.001 compared to 5.6 mM glucose alone.

Figure 3.17 Effects of temporin peptides on membrane potential in BRIN-BD11 cells expressed as a line graph (A, C, E) and area under the curve (B, D, F)

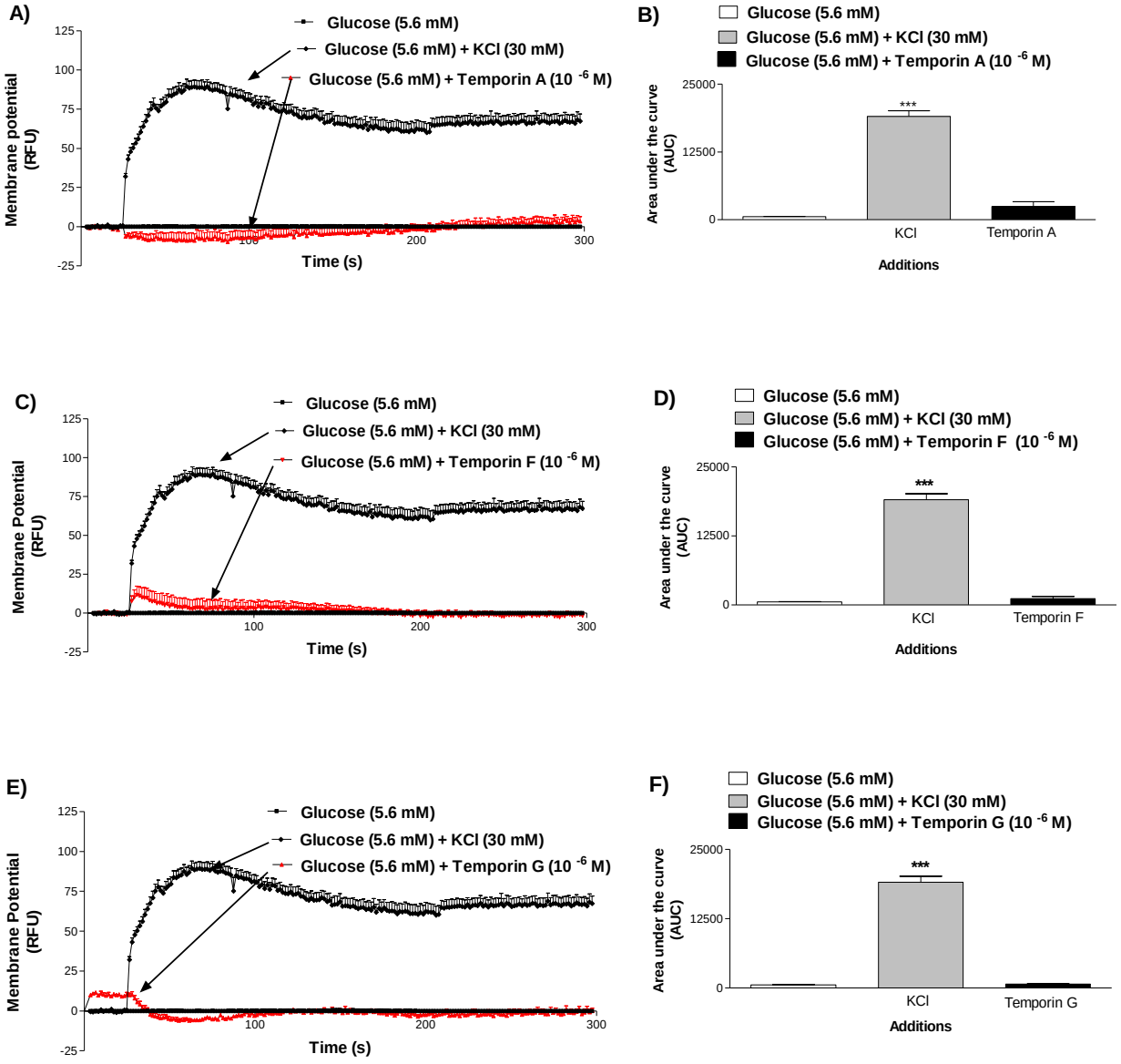

Effects of Temporin A, Temporin F and Temporin G on membrane potential in BRIN-BD11 cells expressed as relative fluorescence units, RFU as a function of time (A, C, E) and the integrated response (area under the curve) (B, D, F) for respective peptide. Peptides were added 20 sec after start of data acquisition at a rate of ~62 µl/sec. Values are mean ± SEM (n = 6). ***P<0.001 compared with 5.6 mM glucose alone.

Figure 3.18 Effects of temporin peptides on intracellular calcium in BRIN-BD11 cells (A, C, E) and area under the curve (B, D, F)

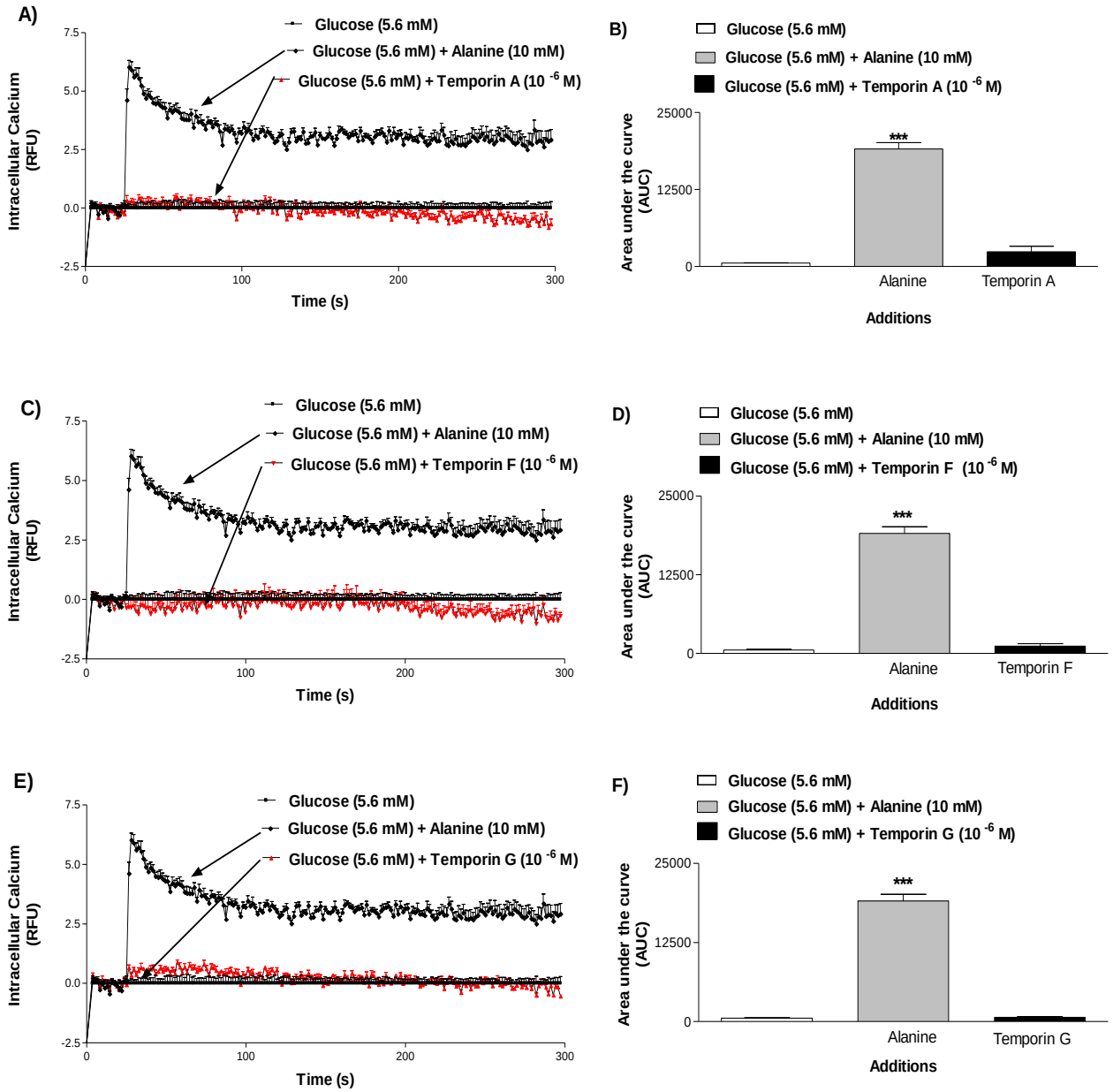

Effects of Temporin A, Temporin F and Temporin G on intracellular calcium in BRIN-BD11 cells expressed as relative fluorescence units, RFU as a function of time (A, C, E) and the integrated response (area under the curve) (B, D, F) for respective peptide. Peptides were added 20 sec after start of data acquisition at a rate of ~62 µl/sec. Values are mean ± SEM (n = 6). ***P<0.001 compared with 5.6 mM glucose alone.

Figure 3.19 Effects of esculentin-1 peptides on membrane potential in BRIN-BD11 cells expressed as a line graph (A, C, E, G) and area under the curve (B, D, F, H)

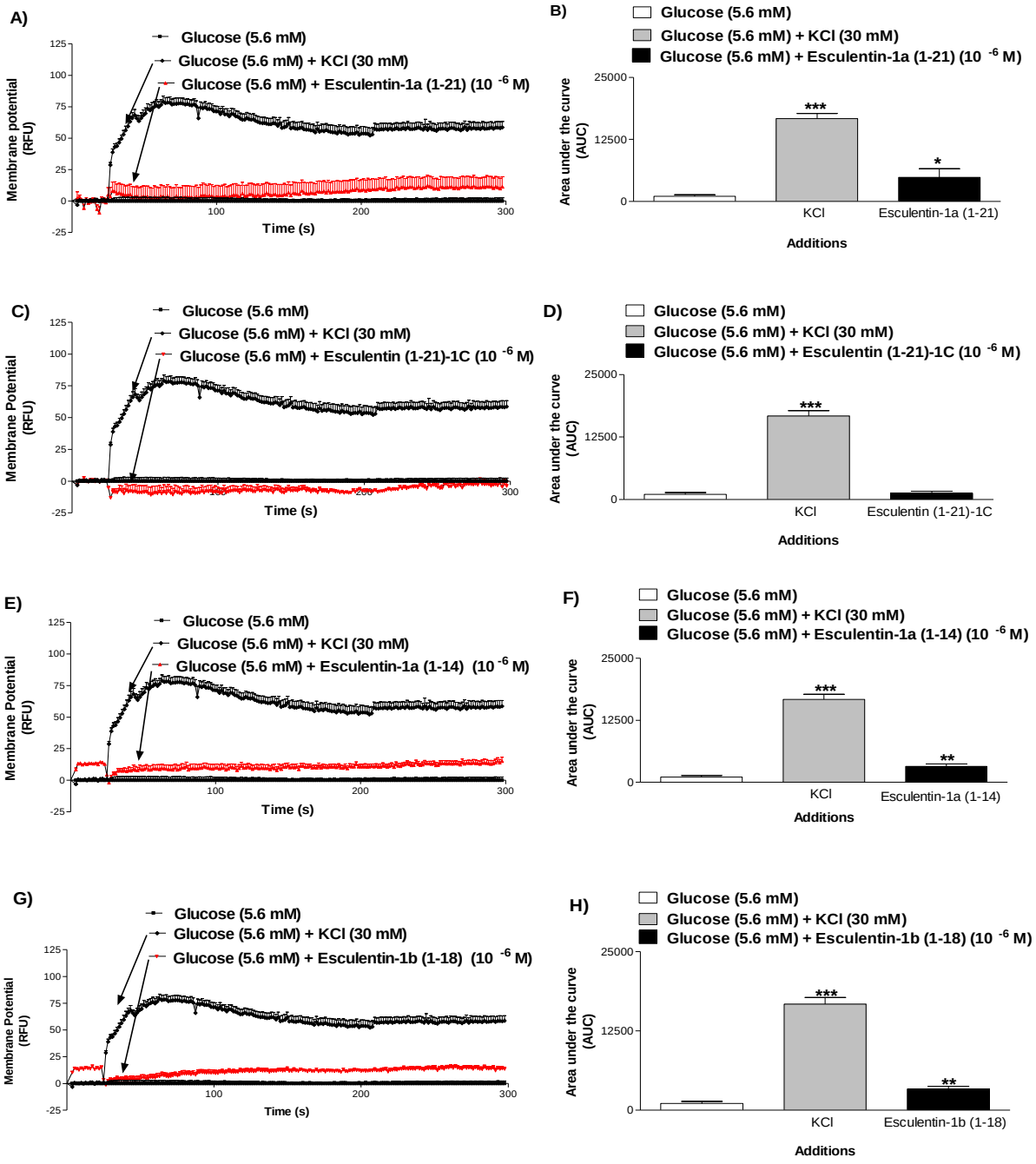

Effects of Esculentin-1a (1-21), Esculentin (1-21)-1C, Esculentin-1a (1-14) and Esculentin-1b (1-18) on membrane potential in BRIN-BD11 cells expressed as relative fluorescence units, RFU as a function of time (A, C, E, G) and the integrated response (area under the curve) (B, D, F, H) for respective peptide. Peptides were added 20 sec after start of data acquisition at a rate of ~62 µl/sec. Values are mean ± SEM (n = 6). *P<0.05, **P<0.01 and ***P<0.001 compared with 5.6 mM glucose alone.

Figure 3.20 Effects of esculentin-1 peptides on intracellular Ca^{2+} in BRIN-BD11 cells expressed as line graph (A, C, E, G) and area under the curve (B, D, F, H)

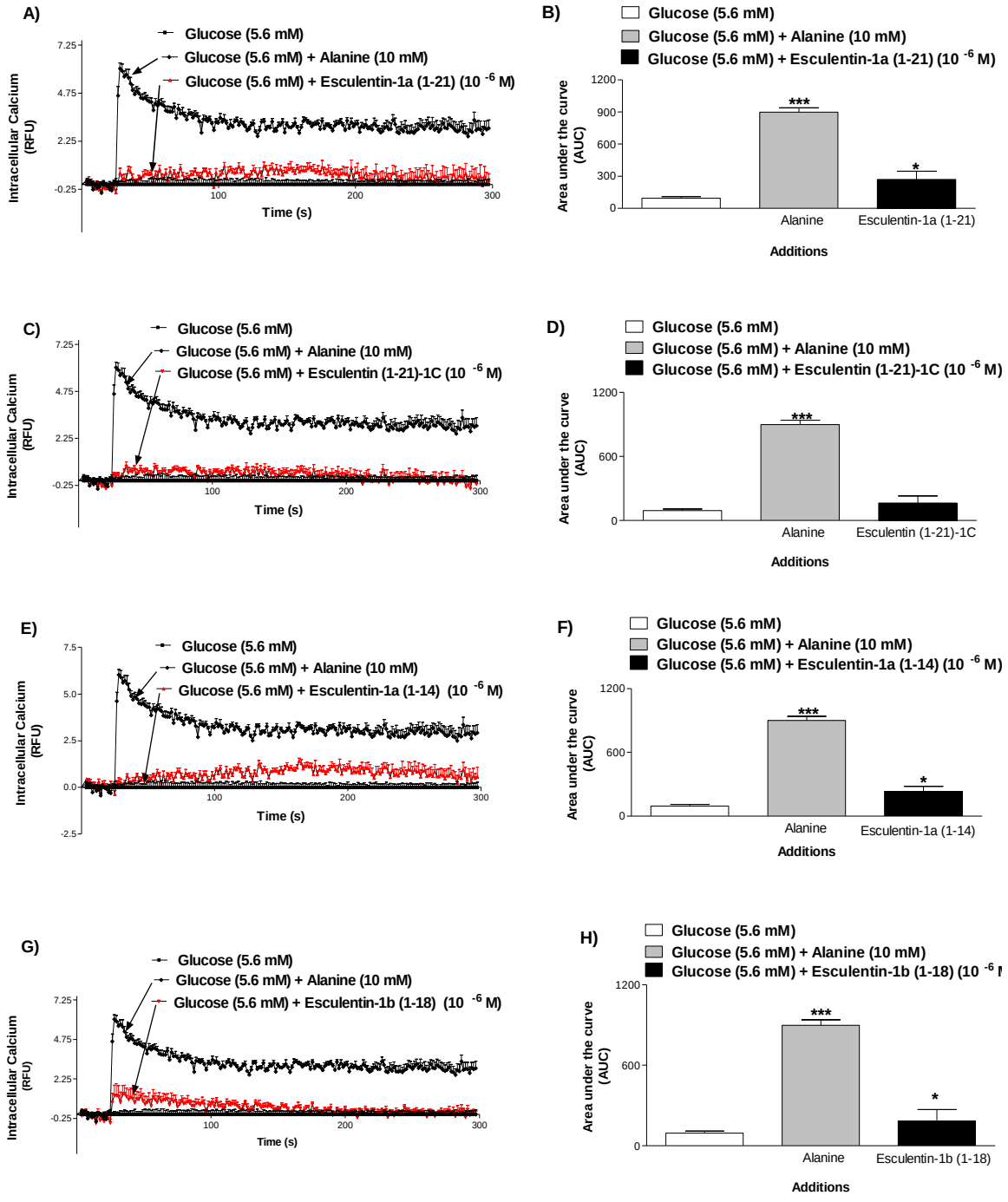

Effects of Esculentin-1a (1-21), Esculentin (1-21)-1C, Esculentin-1a (1-14) and Esculentin-1b (1-18) on intracellular calcium in BRIN-BD11 cells expressed as relative fluorescence units, RFU as a function of time (A, C, E, G) and the integrated response (area under the curve) (B, D, F, H) for respective peptide. Peptides were added 20 sec after start of data acquisition at a rate of ~62 µl/sec. Values are mean ± SEM (n = 6). *P<0.05 and ***P<0.001 compared with 5.6 mM glucose alone.

Figure 3.21 Effect of temporin peptides on cytokine-induced apoptosis in BRIN-BD11 cells

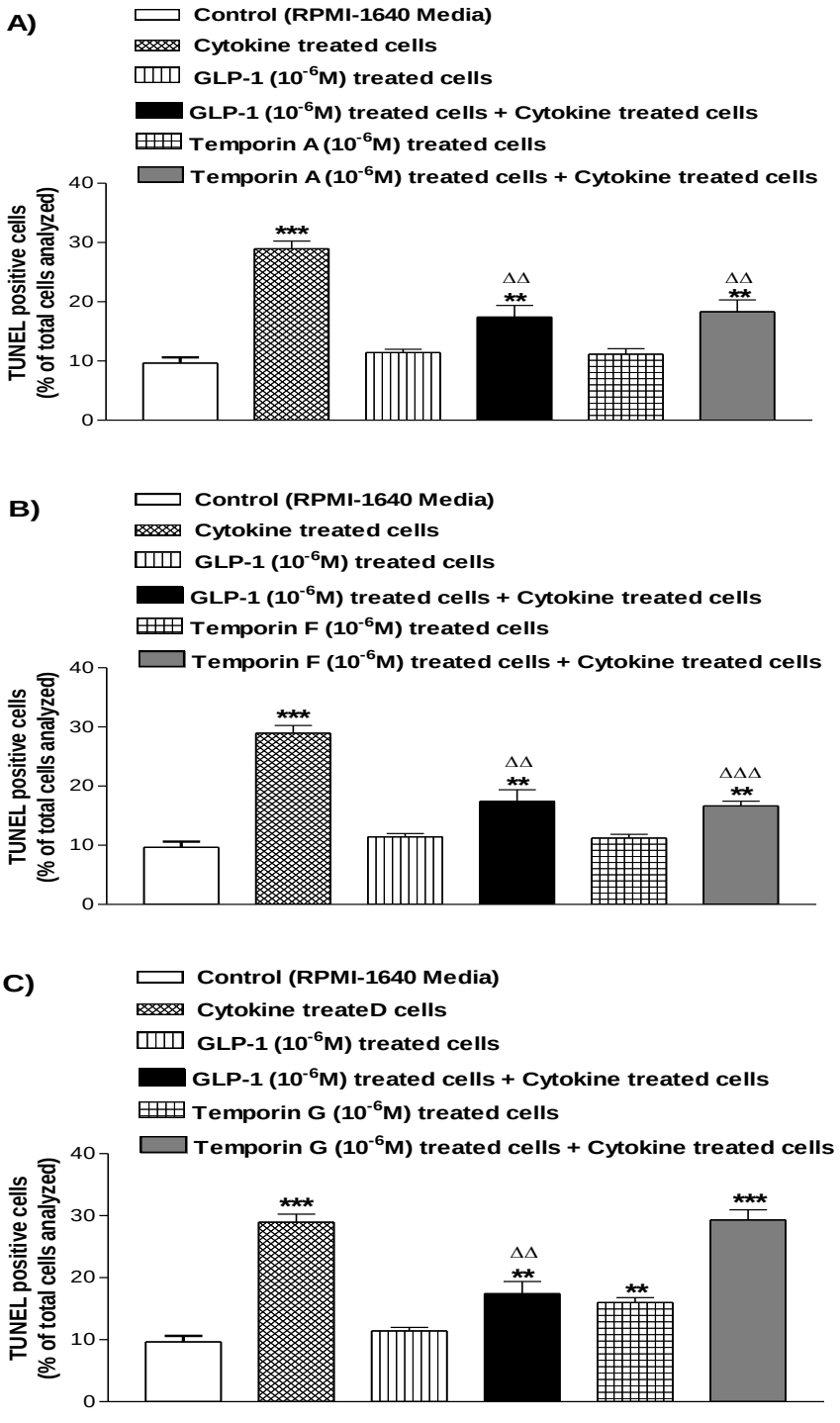

Effects of 1 µM A) Temporin A, B) Temporin F and C) Temporin G on apoptosis in BRIN-BD11 cells compared with 1 µM GLP-1. Values are mean ± SEM for n=3. **P<0.01 and ***P<0.001 compared with incubation in culture medium alone, $^{\Delta\Delta}$P<0.01 and $^{\Delta\Delta\Delta}$P<0.001 compared with incubation in the cytokine-containing medium.

Figure 3.22 Effect of temporin peptides on proliferation in BRIN-BD11 cells

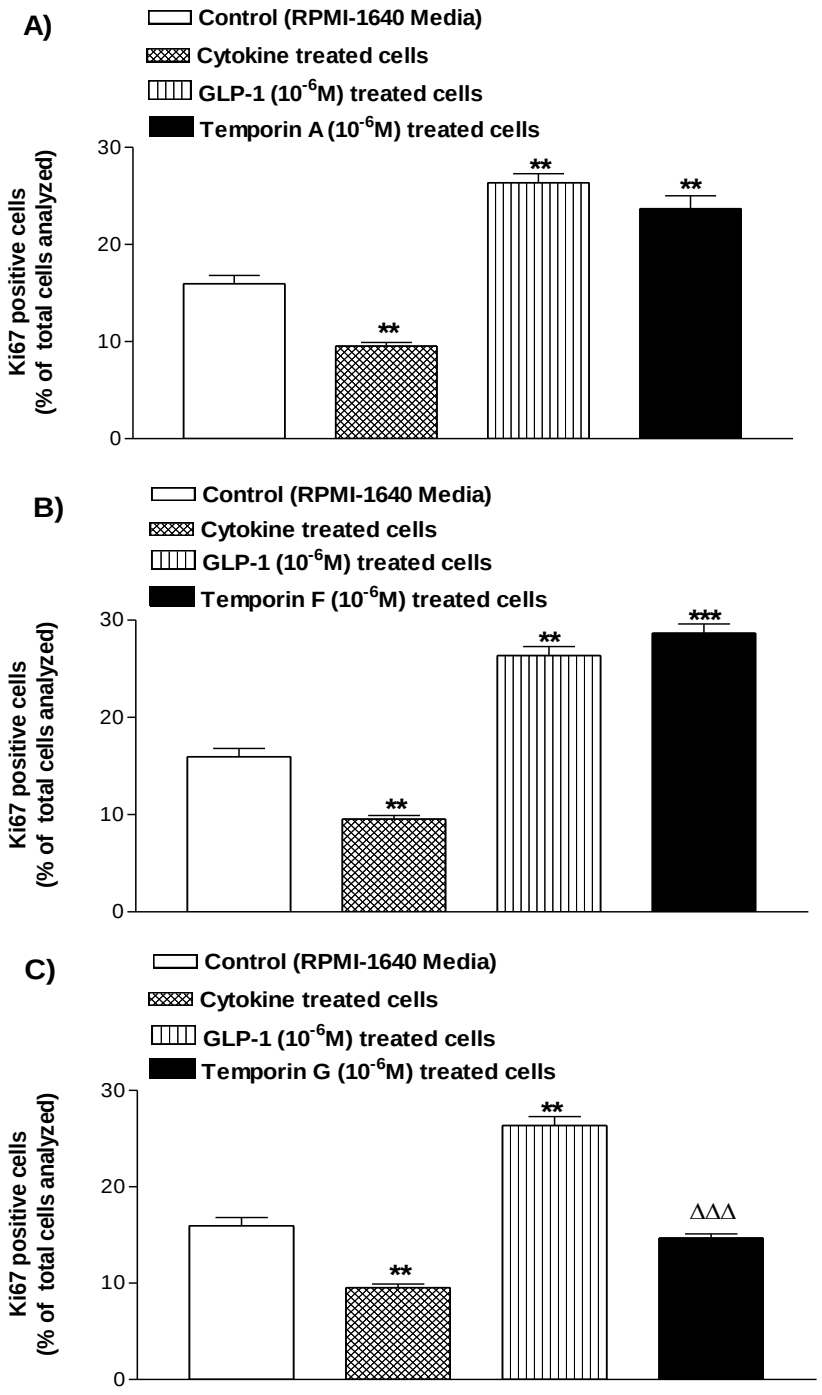

Effects of 1 µM A) Temporin A, B) Temporin F and C) Temporin G on proliferation in BRIN-BD11 cells compared with 1 µM GLP-1. Values are mean ± SEM Values are mean ± SEM for n=3. **P<0.01, ***P<0.001 compared with incubation in culture medium alone, $^{\Delta\Delta\Delta}$P<0.001 compared to GLP-1 treated cells.

Figure 3.23 Effect of esculentin-1 peptides on cytokine-induced apoptosis in BRIN-BD11 cells

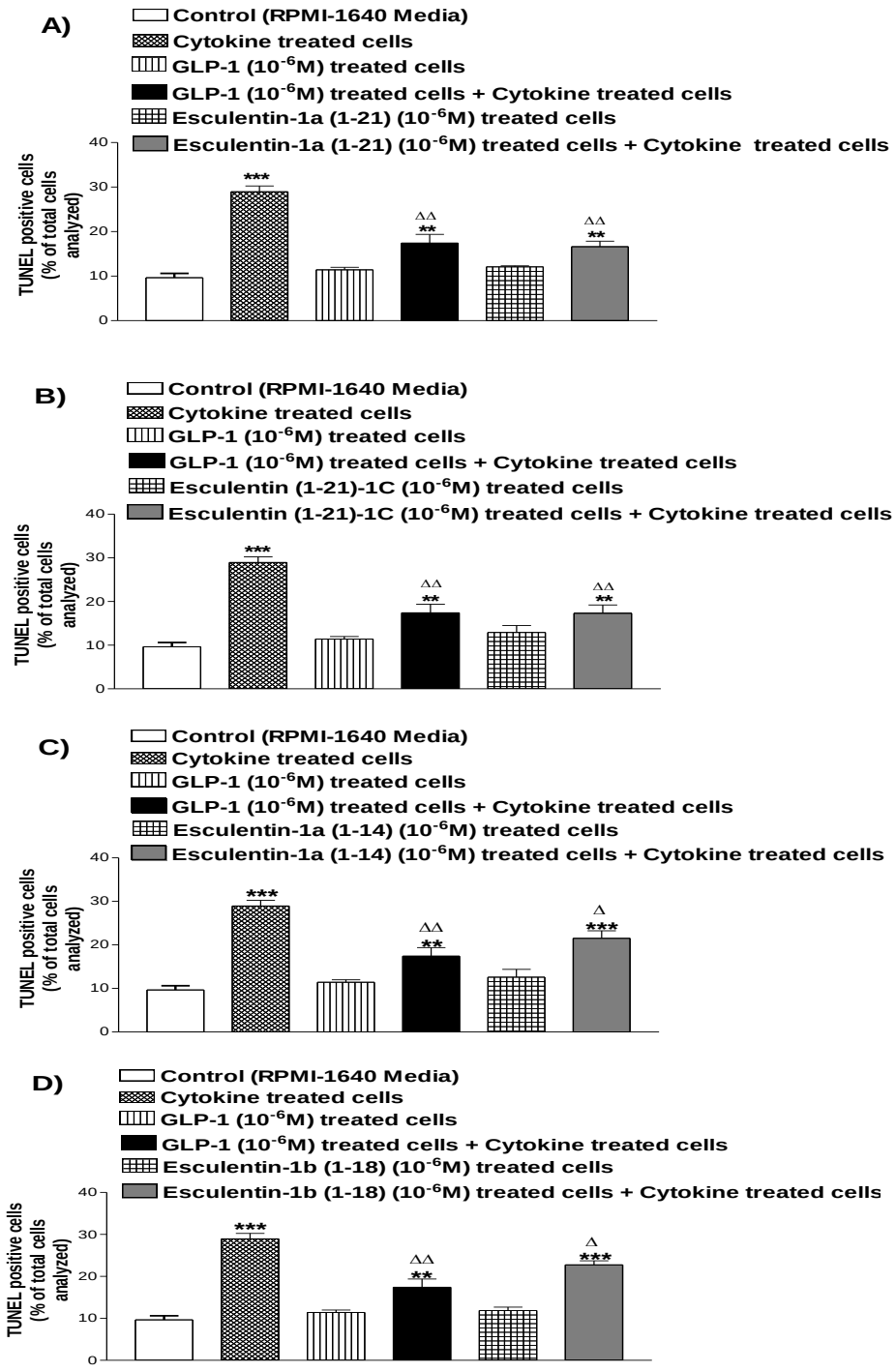

Effects of 1 µM A) Esculentin-1a (1-21), B) Esculentin (1-21)-1C, C) Esculentin-1a (1-14) and D) Esculentin-1b (1-18) on apoptosis in BRIN-BD11 cells compared with 1 µM GLP-1. Values are mean ± SEM for n=3. **P<0.01, ***P<0.001 compared with incubation in culture medium alone, $^{\Delta}$P<0.05, $^{\Delta\Delta}$P<0.01 compared with incubation in cytokine-containing medium.

Figure 3.24 Effect of esculentin-1 peptides on proliferation in BRIN-BD11 cells

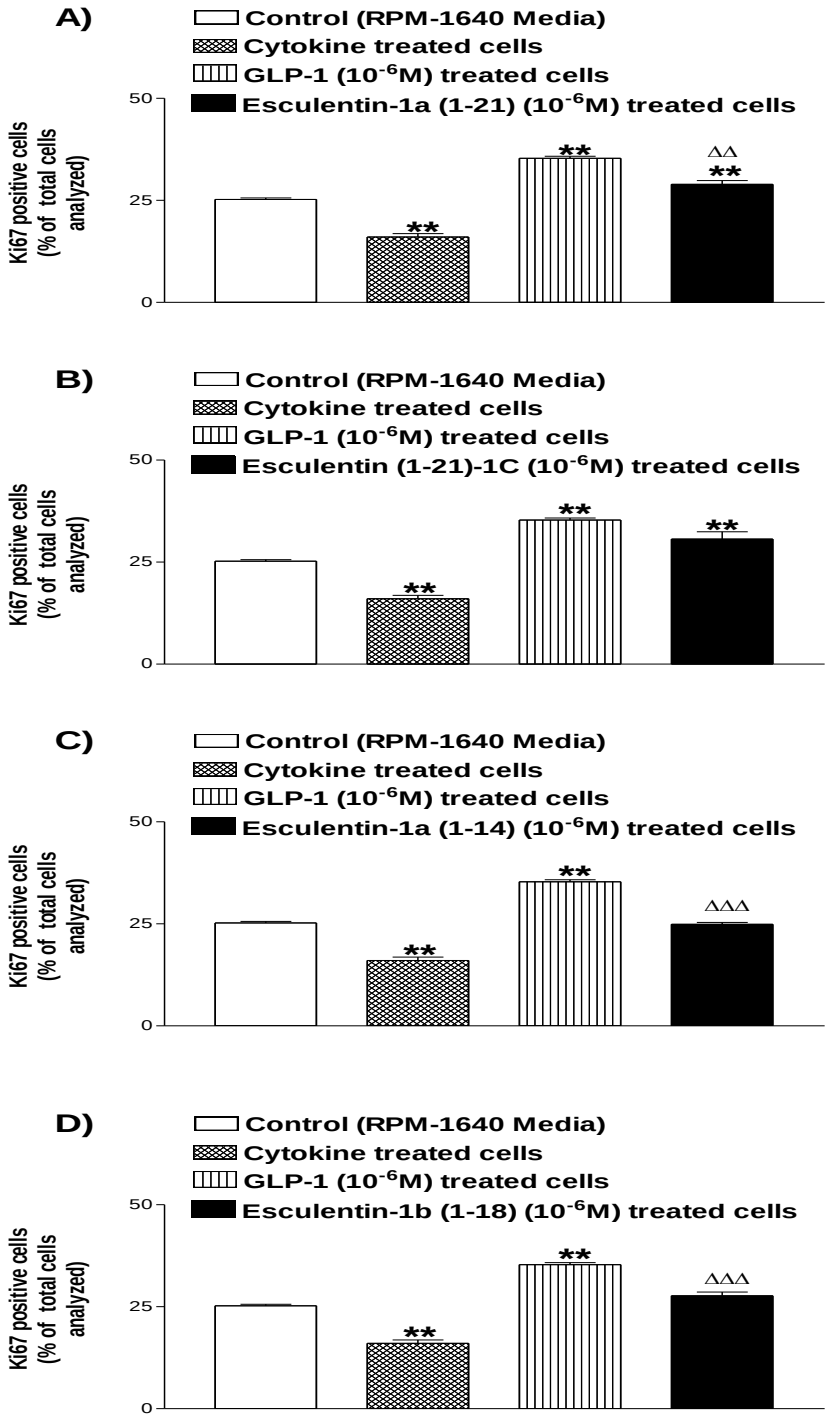

Effects of 1 µM A) Esculentin-1a (1-21), B) Esculentin (1-21)-1C, C) Esculentin-1a (1-14) and D) Esculentin-1b (1-18) on proliferation in BRIN-BD11 cells compared with 1 µM GLP-1. Values are mean ± SEM Values are mean ± SEM for n=3. **P<0.01 compared with incubation in culture medium alone, $^{\Delta\Delta}$P<0.01 and $^{\Delta\Delta\Delta}$P<0.001 compared to GLP-1 treated cells.

Figure 3.25 Effects of temporin G on glucose tolerance and insulin concentrations in mice

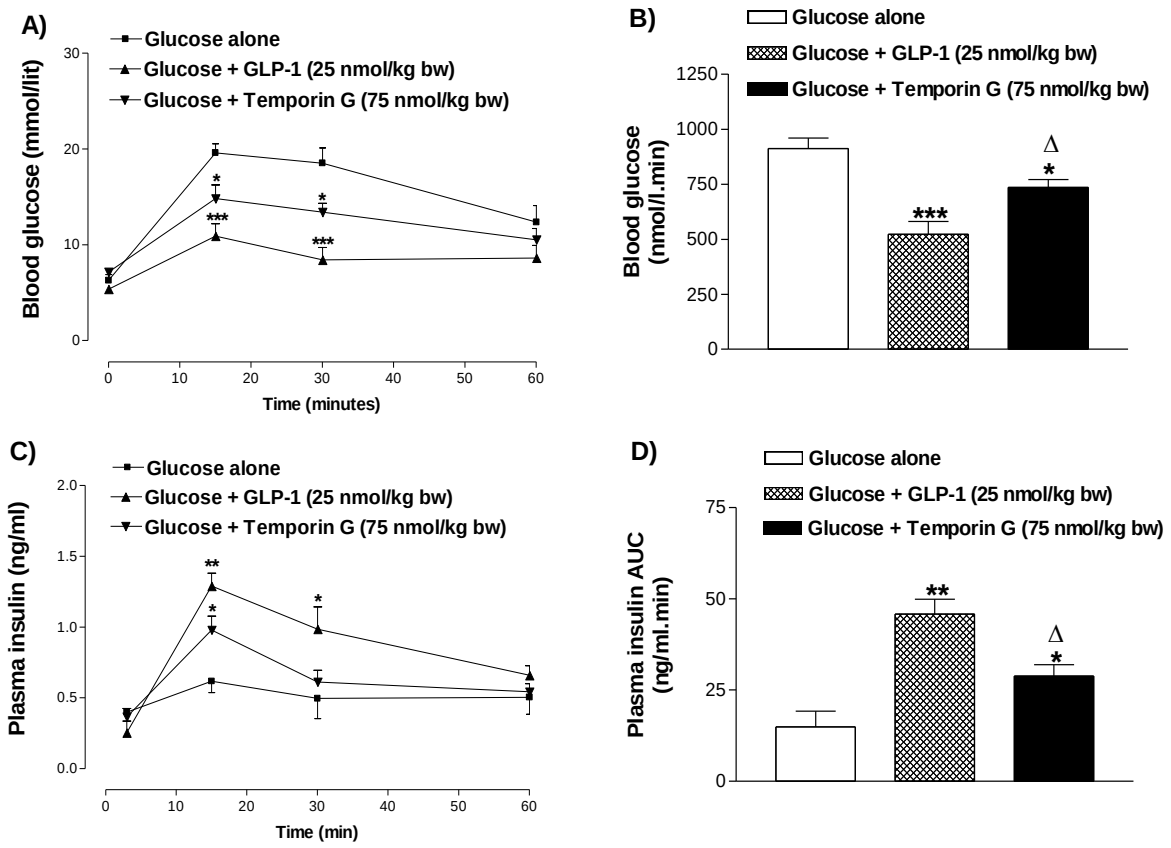

Effects of intraperitoneal administration of Temporin G Peptide (75 nmol/kg bw) and GLP-1 (25 nmol/kg bw) on blood glucose (panels A and B) and plasma insulin (panels C and D) concentrations in lean mice after co-injection of glucose (18 mmol/ kg bw). Values are mean ± SEM for n = 6). *P<0.05, **P<0.01 and ***P<0.001 compared with glucose alone, $^{\Delta}$P<0.05 compared with the effect of GLP-1.

Figure 3.26 Effects of temporin A and temporin F on glucose tolerance in mice

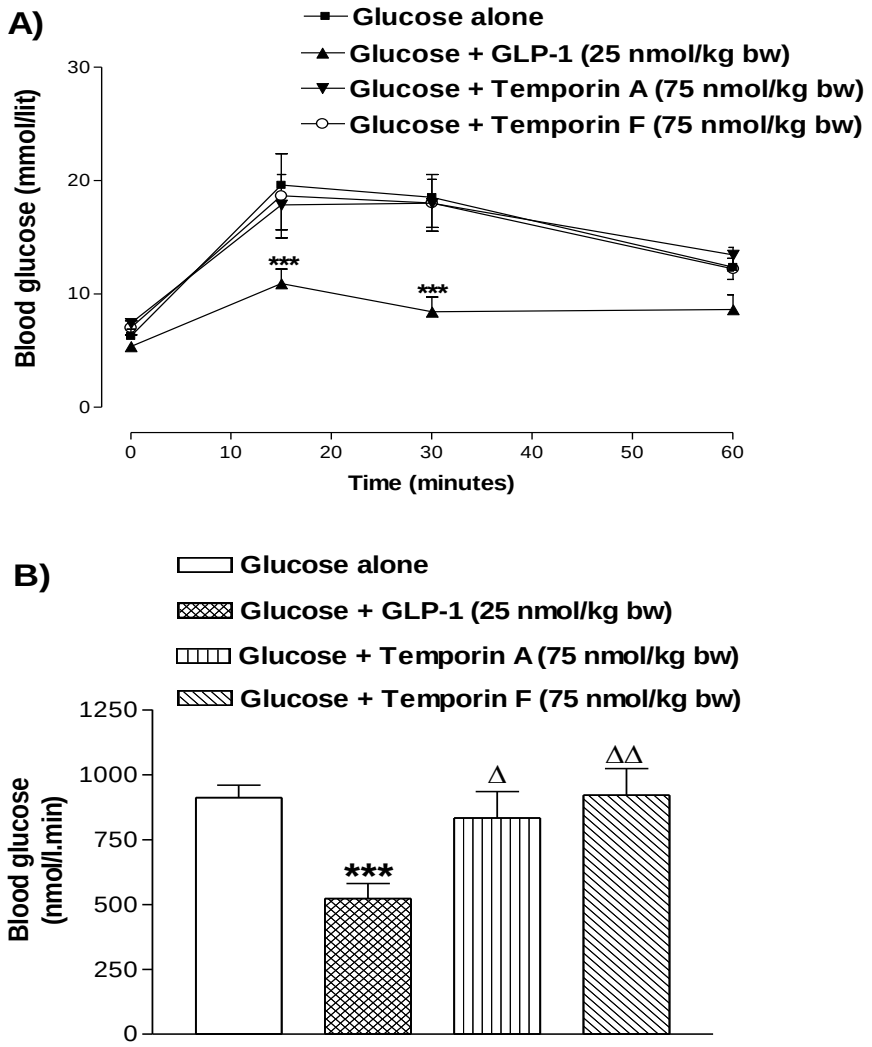

Effects of intraperitoneal administration of Temporin A, Temporin F (75 nmol/kg bw) and GLP-1 (25 nmol/kg bw) on blood glucose (panels A and B) in lean mice after co-injection of glucose (18 mmol/ kg bw). Values are mean ± SEM for n = 6). ***P<0.001 compared with glucose alone, $^{\Delta}$P<0.05 and $^{\Delta\Delta}$P<0.01 compared with the effect of GLP-1.

Figure 3.27 Effects of esculentin (1-21)-1C on glucose tolerance and insulin concentrations in mice

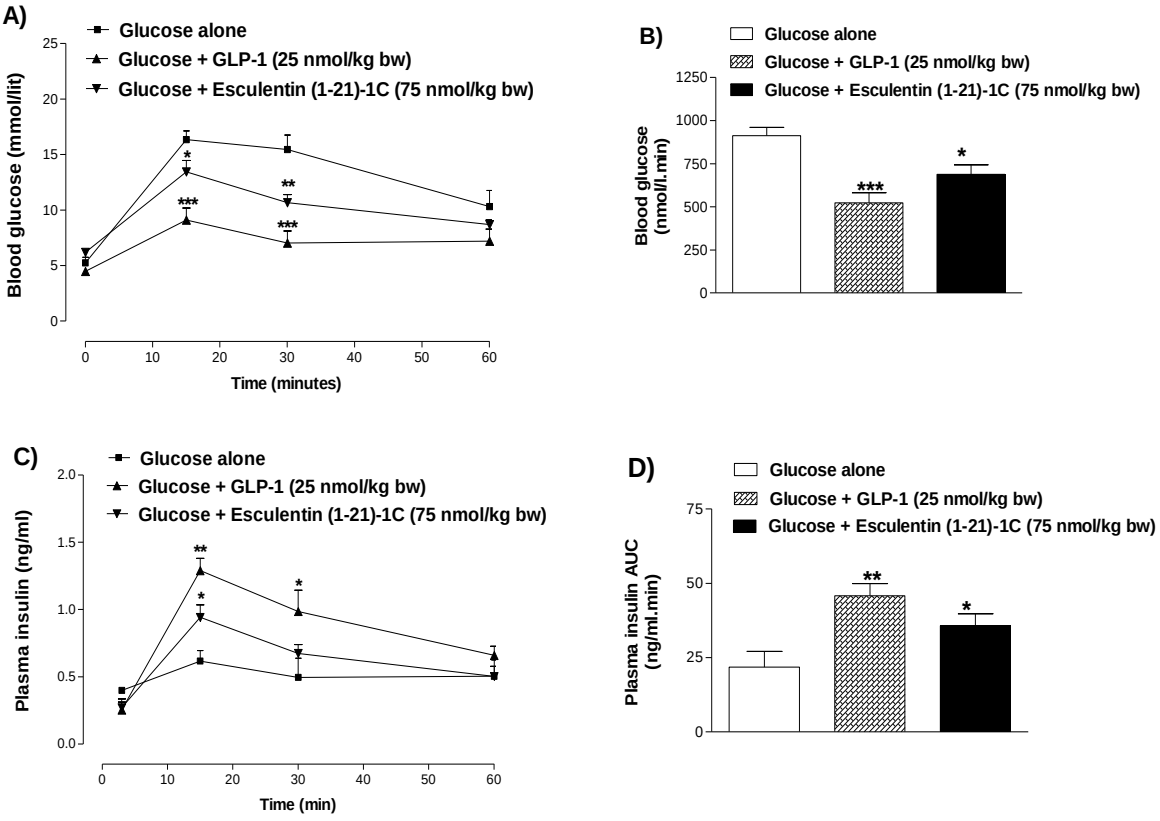

Effects of intraperitoneal administration of esculentin (1-21)-1C peptide (75 nmol/kg bw) and GLP-1 (25 nmol/kg bw) on blood glucose (panels A and B) and plasma insulin (panels C and D) concentrations in lean mice after co-injection of glucose (18 mmol/ kg bw). Values are mean ± SEM for n = 6. *P<0.05, **P<0.01 and ***P<0.001 compared with glucose alone.

Figure 3.28 Effects of esculentin-1a (1-21), esculentin-1a (1-14) and esculentin-1b (1-18) on glucose tolerance in mice

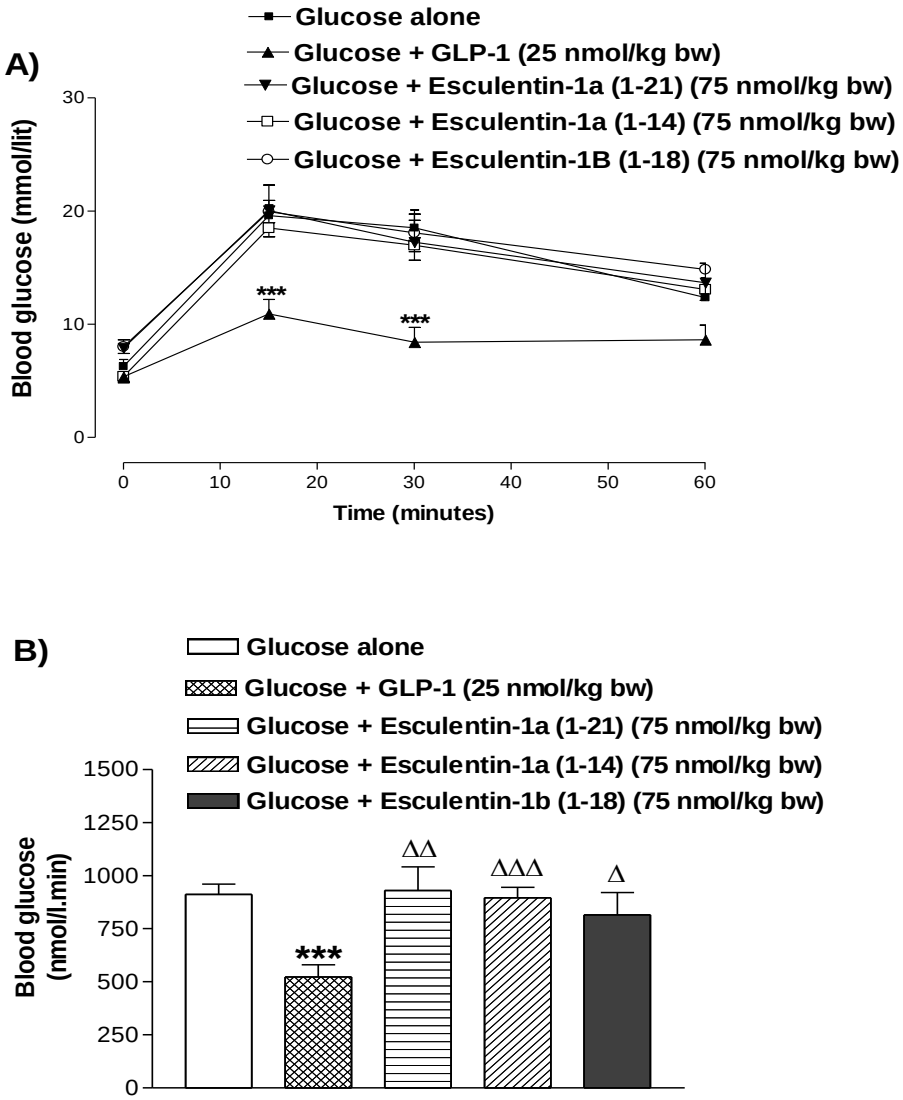

Effects of intraperitoneal administration of esculentin-1a (1-21), esculentin-1a (1-14) and esculentin-1b (1-18) peptide (75 nmol/kg bw) and GLP-1 (25 nmol/kg bw) on blood glucose (panels A & B) concentrations in lean mice after co-injection of glucose (18 mmol/ kg bw). Values are mean ± SEM for n = 6. ***P<0.001 compared with glucose alone, $^{\Delta}$P<0.05, $^{\Delta\Delta}$P<0.01, $^{\Delta\Delta\Delta}$P<0.001 compared with the effect of GLP-1.

Figure 3.29 A Schiffer-Edmundson helical wheel projection of the temporin B and temporin F structures

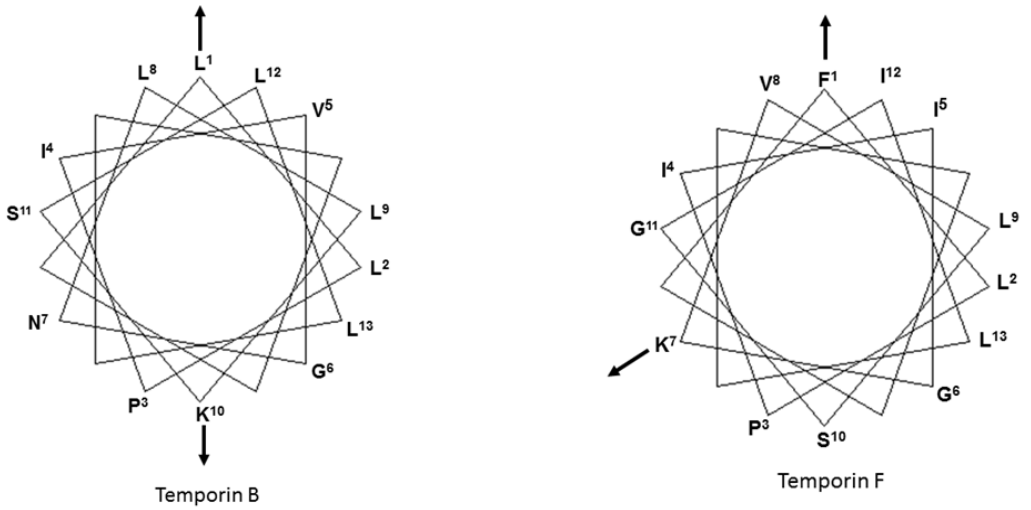

The arrows illustrate the angle (Φ) subtended by the positive charge on the α-amino group of the N-terminal residue and the positive charge on the ε-amino group of the lysine residue.

Chapter 4

In vitro and *in vivo* antidiabetic effects of Frenatin 2D peptide and its synthetic analogues

4.1 Summary

Four naturally occurring frenatin peptides [frenatin 2.1S (GLVGTLLGHIGKAILG.NH_2), frenatin 2.2S (GLVGTLLGHIGKAILS.NH_2) and frenatin 2.3S (GLVGTLLGHIGKAILG.COOH) from *Sphaenorhynchus lacteus* and frenatin 2D (DLLGTLGNLPLPFI.NH_2) from *Discoglossus sardus*] were tested for insulin-releasing effects from BRIN-BD11 rat clonal β-cells cells. Frenatin 2D was the most promising and effective in releasing insulin in a concentration-dependent manner without displaying cytotoxicity. The strategy to replace each amino acid residue in frenatin 2D by a bulky, hydrophobic tryptophan (W) did not lead to the design of analogues with increased insulinotropic activity, but the [D1W] and [G7W] analogues were as potent and effective as the native peptide. Also, deletion of the C-terminal α-amide group did not affect the activity. Frenatin 2D and its synthetic analogues [D1W] and [G7W] also stimulated insulin release from 1.1B4 human-derived clonal β-cells and isolated mouse islets. The insulinotropic activity of these peptides was not associated with membrane depolarization or an increase in intracellular [Ca^{2+}]. Frenatin 2D and its synthetic analogues [(D1W and (G7W)] maintained their activities in the presence of verapamil, diazoxide and 4,4-diisothiocyanostilbene-2,2-disulfonic acid (DIDS). Incubation of frenatin 2D and its synthetic analogues [(D1W and (G7W)] (1μM) with BRIN-BD11 cells produced a modest, but significant, increase in cAMP production. Stimulation of insulin release was abolished in protein kinase A-downregulated cells but maintained in protein kinase C-downregulated cells. Frenatin 2D and its synthetic analogues [(D1W and (G7W)] (1μM) also stimulated proliferation of BRIN-BD11 cells and provided significant protection to the cells against cytokine-induced apoptosis. Furthermore, [G7W] frenatin 2D, significantly suppressed appetite in overnight fasted mice (18 hr).

Acute *in vivo* administration of frenatin 2D and its synthetic analogues [(D1W and (G7W)] also improved glucose tolerance concomitant with increased circulating insulin concentrations in mice. However, [D1W] frenatin 2D was most effective, and hence it was chosen for further studies. We then assessed long-term treatment (28 days) of [D1W] frenatin 2D (75 nmol/kg bw) analogue in genetically obese-diabetic mice (*db/db*), in comparison to native peptide frenatin 2D (75 nmol/kg bw) and exenatide (25 nmol/kg bw). Blood glucose, HbA1c, glycaemic response to intraperitoneal glucose challenge and insulin sensitivity were improved significantly in all treated groups. Plasma insulin level remained unchanged in [D1W] frenatin 2D treatment but improved significantly in frenatin 2D and exenatide-treated groups. Liver and kidney functions were improved in all treated groups. Plasma triglycerides and low-density lipoprotein level were decreased with both frenatin 2D and [D1W] frenatin 2D treatment, but not to the same extent as in exenatide treatment. Amylase activity was unaltered by frenatin 2D and [D1W] frenatin 2D treatment. However, it was increased significantly by exenatide treatment group. Frenatin 2D and [D1W] frenatin 2D treatment exhibited a beneficial effect on islet morphology by preventing a loss of large and medium-size islet in *db/db* mice. Furthermore, all peptides tested exerted a positive effects on expression of genes involved in glucose homeostasis both in muscle and islets. Taken together, these data suggest that frenatin 2D peptides exert beneficial metabolic effects in genetically obese-diabetic mice (*db/db*).

4.2 Introduction

The dramatic global increase in the incidence of T2DM in the past decade has necessitated the search for new naturally occurring therapeutic agents that regulate glucose concentrations and prevent the complications associated with the disease. The

discovery of exendin-4 in the venom of a reptile, the Gila monster *Heloderma suspectum* (Eng *et al.,* 1992) highlights the importance of non-mammalian sources in the search for new antidiabetic peptides. Exendin-4 is an agonist at the glucagon-like peptide-1 (GLP-1) receptor (GLP1R) that stimulates glucose-dependent insulin release and improves pancreatic β-cell function (Fehse *et al.,* 2005). Exendin-4 is more potent and longer-acting *in vivo* than GLP-1 and is used in routine clinical practice in T2DM therapy (Bunck *et al.,* 2011). The skin secretions of many frog species contain bioactive peptides that play an important contributory role in protecting the host from invasion by a pathogenic microorganism in the environment and ingestion by predators (Raaymakers *et al.,* 2017). These peptides are multifunctional and may possess antimicrobial, antifungal, antiviral, anticancer and immunomodulatory activities (reviewed in (Conlon *et al.,* 2014a, Xu & Lai *et al.,* 2015)]. Additionally, several host defence peptides that were first identified on the basis of their antimicrobial properties have been shown to stimulate insulin release from clonal β-cells and isolated pancreatic islets and improve glucose tolerance following intraperitoneal administration in mice and so represent agents with therapeutic potential for treatment of patients with T2DM [reviewed in (Conlon *et al.,* 2018)].

The frenatins are a family of structurally related small peptides that were first identified in skin secretions of the Australian treefrog *Litoria infrafrenata* (reclassified as *Nyctimystes infrafrenatus*) (Pelodryadidae) (Raftery *et al.,* 1996) Subsequently, frenatin 2D [DLLGTLGNLPLPFI.NH_2] was isolated from skin secretions of the Tyrrhenian painted frog *Discoglossus sardus* (Alytidae) (Conlon *et al.,* 2013) and frenatin 2.1S [GLVGTLLGHIGKAILG.NH_2], frenatin 2.2S [GLVGTLLGHIGKAILS.NH_2] and frenatin 2.3S [GLVGTLLGHIGKAILG] from the Orinoco lime frog *Sphaenorhynchus lacteus* (Hylidae) (Conlon *et al.,* 2014b).

Frenatin 2D lacked antimicrobial activity but stimulated the production of the proinflammatory cytokines TNF-α, and IL-1β by mouse peritoneal macrophages suggesting that the peptide may act on macrophages in frog skin to produce a cytokine-mediated stimulation of the adaptive immune system in response to invasion by microorganisms (Conlon *et al.,* 2013). In contrast, frenatin 2.1S and 2.2S show potent antimicrobial activity against Gram-negative bacteria and are cytotoxic to non-small cell lung adenocarcinoma A549 cells (Conlon *et al.,* 2014b). Frenatin 2.1S also stimulates the production of pro-inflammatory cytokines by mouse peritoneal macrophages and downregulates production of the anti-inflammatory cytokine IL-10 by lipopolysaccharide-stimulated cells. A single injection of frenatin 2.1S (100 μg) in BALB/c mice enhances the activation state and homing capacity of Th1 type lymphocytes (Pantic *et al.,* 2015) and led to a marked increase in the number and tumoricidal capacity of activated peritoneal natural killer (NK) cells (Pantic *et al.,* 2017a) in the peritoneal cavity suggesting that the peptide should be regarded as a candidate for antitumor immunotherapy. Activity against yellow fever virus has also been reported for the frenatin 2 peptides present in *S. lacteus* skin secretions (Muñoz-Camargo *et al.,* 2016).

Certain frog skin peptides, such as esculentin-2cha (1-30) from Chiricahua leopard frog *Lithobates chiricahuensis* (Vasu *et al.,* 2017), tigerinin-1R from *Haplobatrachus rugulosus* (Ojo *et al.,* 2015b), CPF-SE1 from *Silurana epitropicalis* (Srinivasan *et al.,* 2015), Magainin related peptides from *Xenopus amieti* (Ojo *et al.,* 2015a) have shown to improve glycaemic control, glucose tolerance, insulin sensitivity and pancreatic beta cell function in animal model of T2DM. The present study aimed to investigate the therapeutic potential of frenatin 2D, 2.1S. 2.2S, and 2.3S (Table 4.1 for the structure of peptides) for development into agents for the treatment of patients with

T2DM. Their ability to stimulate insulin release *in vitro* was evaluated using BRIN-BD11 rat clonal β-cells (McClenaghan *et al.,* 1996), 1.1 B4 human clonal β-cells (McCluskey *et al.,* 2011) and isolated mouse islets. Their ability to lower blood glucose concentration and stimulate insulin release *in vivo* was determined in overnight-fasted, male NIH Swiss TO mice. Also, the effects of frenatin 2D on β- cell proliferation and its ability to inhibit cytokine-induced apoptosis was studied in BRIN-BD11 cells. The antidiabetic effects of frenatin 2D peptides were also studied in *db/db* mice, in comparison to the established antidiabetic agent, exenatide.

4.3 Materials and Methods

4.3.1 Reagents

All the chemical reagents used in the experiments were of analytical grade and listed in Chapter 2, Section 2.1. Synthetic frenatin peptides were purchased from SynPeptide (China) and GL Biochem Ltd (Shanghai, China). Cytotoxicity Assay kit (Catalogue number: G1780) was supplied by Promega (Southampton, UK). Intracellular calcium assay kit (Catalogue number: R8041) and membrane potential assay kit (Catalogue number: R8042) were purchased from Molecular Device (Berkshire, UK). Apoptosis and proliferation experiments were performed using IN SITU Cell Death Fluorescein kit (Sigma-Aldrich, Catalogue number: 11684795910) and Rabbit polyclonal to Ki67 (Abcam, Catalogue number: ab15580) respectively. Masterclear Cap Strips and real-time PCR TubeStrips (Catalogue number: 0030132890) purchased from Mason Technology Ltd (Dublin, Ireland).

4.3.2 Peptide synthesis and purification

Frenatin 2D and its tryptophan-containing analogues, as well as non-amidated frenatin 2D and its tryptophan-containing analogues (listed in Table 4.1), were supplied in crude form by SynPeptide Ltd (Shanghai, China). Frenatin 2.1S, 2.2S, and 2.3S were supplied in crude form by GL Biochem Ltd (Shanghai, China). The peptides were purified to near homogeneity (>98 % purity) by reversed-phase HPLC as previously described in Chapter 2, Section 2.2.1.1. The identity of all peptides was confirmed by MALDI-TOF mass spectrometry (Chapter 2, Section 2.2.2) using a Voyager DE-PRO instrument (Applied Biosystems, Foster City, USA).

4.3.3 Insulin release studies using clonal beta cells

The culture of BRIN-BD11 rat clonal β-cells and 1.1B4 human-derived pancreatic β-cells and the method for measuring the effects of peptides on the release of insulin has been described in Chapter 2, Section 2.3.1 and 2.4.1.1, respectively. Incubations with the frenatin peptides (3×10^{-6} - 10^{-12} M; n = 8) were carried out for 20 min at 37°C in Krebs-Ringer bicarbonate (KRB) buffer, pH 7.4 supplemented with 5.6 mM glucose. Control incubations were carried out in the presence of GLP-1 (10 nM), exendin-4 (10 nM) and alanine (10 mM). After incubation, aliquots of cell supernatant were removed for measurement of insulin by radioimmunoassay as outlined in Chapter 2, Section 2.4.4. In order to determine cytotoxicity, the effects of the frenatin peptides (10^{-12} M - 3×10^{-6} M; n = 4) on the rate of lactate dehydrogenase (LDH) release from BRIN-BD11 cells were measured using a CytoTox 96 non-radioactive cytotoxicity assay kit (Promega, Southampton, UK) according to the manufacturer's instructions Chapter 2, Section 2.5.

In the second series of experiments designed to investigate mechanisms of action, incubations of BRIN-BD11 cells with frenatin 2D and its analogues (1 µM) were

carried out in the presence of known modulators of insulin release (Chapter 2, Section 2.4.1.2): the K^+ channel activator diazoxide (300 µM), the L-type voltage-dependent Ca^{2+} channel blocker verapamil (50 µM), depolarizing stimulus KCl (30 mM) and a and chloride channel blocker 4,4-diisothiocyanostilbene-2,2-disulfonic acid (0.66 mM). To determine the role of extracellular calcium in mediating the insulinotropic activity of the peptide, cells were pre-incubated in calcium-free KRB buffer (pH 7.4) supplemented with 1.1 mM glucose and 1 mM EGTA for 1 hr at 37°C (Chapter 2, Section 2.4.1.3). After pre-incubation, cells were incubated for 20 min at 37°C with frenatin 2D (1 µM) in calcium-free KRB buffer containing 5.6 mM glucose.

4.3.4 Insulin release studies using isolated mouse islets

The preparation of isolated pancreatic islets from an adult, male National Institutes of Health NIH Swiss mice (Harlan Ltd, Bicester, UK) and the procedure for determining the effects of peptides on the rate of insulin release have been described in Chapter 2, Section 2.4.2.2. The islets were incubated for 1 hr at 37°C with synthetic peptides (10^{-8} and 10^{-6} M) in KRB buffer supplemented with 16.7 mM glucose. Supernatants were removed for determination of insulin by radioimmunoassay (Chapter 2, Section 2.4.4). The islet cells were retrieved and extracted with acid-ethanol to determine total insulin content as previously described in Chapter 2, Section 2.4.2.4.

4.3.5 Effects of peptides on membrane potential and intracellular Ca^{2+} concentrations

Changes in membrane potential and intracellular Ca^{2+} concentrations in response to incubation with either frenatin 2D or its analogue (1 µM) were determined fluorimetrically with monolayers of BRIN-BD11 cells using a FLIPR Membrane

Potential Assay Kit and a FLIPR Calcium 5 Assay Kit (Molecular Devices, Sunnyvale, CA, USA) according to the manufacturer's recommended protocols as described in Chapter 2, Section 2.6 and 2.7. Cells were incubated in 5.6 mM glucose with peptide at 37°C for 5 min and data were acquired using a Flex Station scanning fluorimeter with integrated fluid transfer workstation (Molecular Devices). Control incubations with 5.6 mM glucose alone, 5.6 mM glucose plus 30 mM KCl, and 5.6 mM glucose plus 10 mM alanine) were also carried out.

4.3.6 Effects of peptides on cyclic AMP production

The procedure for determining the effects of frenatin 2D and its analogues (1 µM) on the production of cAMP by BRIN-BD11 cells has been described in Chapter 2, Section 2.8. Incubations were carried out for 20 min in KRB buffer supplemented with 5.6 mM glucose and the phosphodiesterase inhibitor, 3-isobutyl-1-methylxanthine (IBMX; 200µM). cAMP concentrations in the cell lysate were measured using a Parameter kit (R & D Systems, Abingdon, UK) following the manufacturer's recommended protocol. Control incubations in the presence of 5.6 mM glucose alone and GLP-1 (10 nM) were also carried out.

4.3.7 Effects of down-regulation of the PKA and PKC pathways on insulin release

In order to investigate further the mechanism of insulinotropic action of frenatin 2D and its analogues, BRIN-BD11 cells were incubated for 18 hr at 37°C in an atmosphere of 5 % CO_2 and 95 % air with 25 µM forskolin (Sigma-Aldrich, UK) to downregulate the PKA pathway or with 10 nM phorbol 12-myristate 13-acetate (PMA; Sigma-Aldrich, UK) to downregulate the PKC pathway or with 25 µM forskolin plus 10 nM PMA to downregulate both pathways. Details of the experimental procedure have been

described in Chapter 2, Section 2.9. Cells were preincubated for 40 min at 37°C with KRB buffer, pH 7.4 supplemented with 1.1 mM glucose and 0.1 % bovine serum albumin followed by a 20 min incubation with (a) either frenatin 2D or its analogue (1 µM), (b) GLP-1 (10 nM) and (c) CCK-8 (10 nM) in KRB buffer supplemented with 5. 6 mM glucose. Control incubations with forskolin alone (25 µM), PMA (10 nM) alone and forskolin (25 µM) + PMA (10 nM) alone were also carried out. Aliquots of the cell supernatants were removed for measurement of insulin by radioimmunoassay (Chapter 2, Section Section 2.4.4).

4.3.8 Effects of the peptides on cytokine-induced apoptosis and proliferation

The ability of frenatin 2D and its analogues to protect against cytokine-induced DNA damage was analysed by incubating BRIN-BD11 cells, seeded at a density of 5 x 10^4 cells per well, for 18 hr at 37°C with a cytokine mixture (200 U/ml tumour-necrosis factor-a, 20 U/ml interferon-γ and 100 U/ml interleukin-1β), in the presence and absence of either frenatin 2D (1 µM) or its analogues (1 µM) or GLP-1 (1 µM). The details of the experimental procedure have been described in Chapter 2, Section 2.10. To study effects on β-cell proliferation, BRIN-BD11 cells were incubated with either frenatin 2D (1 µM) or its analogues (1 µM) or GLP-1 (1 µM) for 18 hr at 37°C as described in Chapter 2, Section 2.10.

4.3.9 Assessments of plasma degradation of the frenatin 2D peptide.

The metabolic stability of frenatin 2D was evaluated by incubating peptide with murine plasma. The experimental procedure is described in Section 2.12.

4.3.10 Effects of peptides on glucose uptake in C2C12 cells

The procedure for determining the effects of peptides on the glucose uptake in C2C12 cells is described in Chapter 2, Section 2.11.

4.3.11 Acute *in vivo* effects of peptides on food intake

After i.p injection of saline and test peptide, food intake was measured in overnight (21 hr) fasted mice as described in Chapter 2, Section 2.13.4.

4.3.12 Acute *in vivo* insulin release studies

All animal experiments were carried out by the UK Animals (Scientific Procedures) Act 1986 and EU Directive 2010/63EU for animal experiments and approved by Ulster University Animal Ethics Review Committee. All necessary steps were taken to prevent any potential animal suffering. Eight-week-old male NIH Swiss TO mice (Harlan Ltd, Bicester, UK), were housed separately and maintained in an air-conditioned room (22 ± 2 °C) with a 12-hr light: 12-hr dark cycle. The procedure for determining the effects of intraperitoneal administration glucose alone (18 mmol/kg bw) and in combination with frenatin 2D or its analogues (75 nmol/kg bw) or GLP-1 (25 nmol/kg bw) has been described in Chapter 2, Section 2.13.2. Blood samples were collected and measured for glucose concentrations using an Ascencia Contour Blood Glucose Meter and plasma insulin by radioimmunoassay (Chapter 2, Section 2.13.5). In another set of experiments, in overnight (21 hr) fasted mice, food intake was measured after i.p injection of saline and test peptides as described in Chapter 2, Section 2.13.4.

4.3.13 Effects of twice daily administration of frenatin 2D and its synthetic analogue [D1W] frenatin 2D in *db/db* mice

Before the initiation of treatment with peptides, *db/db* mice were injected twice daily with saline (0.9 % w/v) for 3 days to adapt mice to handling and injection stress. During this period mice were monitored for body weight, energy intake, glucose and insulin. Mice (*db/db*) received twice daily i.p. injections of either saline (0.9 % w/v) or frenatin 2D (75 nmol/kg bw) or [D1W] frenatin 2D (75 nmol/kg bw) or exenatide (25 nmol/kg bw) for 28 consecutive days. Every 72 hr during the study, body weight, energy intake, non-fasted blood glucose and plasma insulin were assessed. After the end of treatment period, terminal studies were performed which included measurement of the HbA1c (Chapter 2, Section 2.13.9), glucose tolerance test using an intraperitoneal or oral glucose load (Chapter 2, Section 2.13.2), and insulin sensitivity (Section 2.13.3). Fasting (18 hr) blood was collected and measured for insulin and glucose to determine insulin resistance using homeostatic model assessment (HOMA) formula: HOMA-IR = fasting glucose (mmol/l) x fasting insulin (mU/l)/22.5. After collecting terminal blood, animals were subjected to DEXA scan (PIXImus densitometer, USA) (Chapter 2, Section 2.13.8) to measure body fat composition and bone mineral content/density. Dissected tissues from animals were processed for histology studies (Chapter 2, Section 2.14), hormonal content (Chapter 2, Section 2.13.11) and expression of key genes involved in glucose homeostasis (Chapter 2, Section 2.15). Islets were isolated from the pancreas (Chapter 2, Section 2.4.2.1) and examined for insulin secretory response to glucose and established insulin secretagogues as described in Chapter 2, Section 2.4.2.3.

4.3.14 Biochemical tests

Plasma was retrieved from blood and used for various biochemical tests. The procedures for measuring blood/plasma glucose and plasma insulin are described in

Chapter 2, Section 2.13.5. Additional tests included lipid profile, liver and kidney function test and amylase activity (Chapter 2, Section 2.13.12).

4.3.15 Effects of twice daily administration of frenatin 2D and its synthetic analogue [D1W] frenatin 2D on islet morphology

The pancreatic tissues were embedded in paraffin wax after processing on tissue processor. Using microtome, sections of 7 µM thickness were made and placed on a slide. Sections were allowed to dry overnight on a hotplate and then stained for insulin and glucagon as described in Chapter 2, Section 2.14.1.

4.3.16 Effects of twice daily administration of frenatin 2D and its synthetic analogue [D1W] frenatin 2D on gene expression

RNA was extracted from skeletal muscle tissue and islet cells (Chapter 2, Section 2.15.1), and examined for the expression of genes involved in glucose homeostasis (Chapter 2, Section 2.15.2 and 2.15.3).

4.3.17 Statistical Analysis

Experimental data analysed using GraphPad PRISM (Version 3) were expressed as means ± SEM and data were compared using the unpaired student *t*-test (nonparametric, with two-tailed P values and 95% confidence interval) and one-way ANOVA with Bonferroni post-hoc test. Group of datasets were considered to be significantly different if $P<0.05$.

4.4 Results

4.4.1 Characterization of peptides

The purity of all frenatin peptides was confirmed using reverse phase HPLC (Figure 4.1-4.5). The molecular weight of peptides confirmed by MALDI- TOF (Figure 4.6-4.10) was closely related to the theoretical molecular weight (Table 4.2).

4.4.2 Effects of frenatin peptides on insulin release from BRIN BD11 rat clonal β-cells

The rate of insulin release from BRIN-BD11 cells in the presence of 5.6 mM glucose alone was 1.01 ± 0.04 ng/10^6 cells/20 min. Incubation with the established insulin secretagogue alanine (10 mM) increased insulin release to 5.42 ± 0.30 ng/10^6 cells/20 min and to 3.08 ± 0.10 ng/10^6 cells/20 min with GLP-1 (10 nM). The effects of increasing concentrations of frenatin 2D, 2.1S, 2.2S and 2.3S are shown in Figure 4.11(A-D). Frenatin 2D was the most potent peptide with a threshold concentration (the concentration producing a significant increase in the rate of insulin release compared with the rate in the presence of 5.6 mM glucose alone) of 0.1 nM and the greater stimulator of insulin release (a 2.3-fold increase at 3 µM). At concentrations up to 3 µM, no significant increase in the rate of release of the cytosolic enzyme LDH from the BRIN-BD11 cells was observed for any of the frenatin peptides indicating that the integrity of plasma membrane remained intact (Figure 4.12).

Substitution of the Thr^5, Asn^8, Pro^{10}, and Ile^{14} residues in frenatin 2D by Trp (W) and interchange of Pro^{12} and Phe^{13} led to the loss of insulinotropic activity. [L2W], [L3W], [G4W], [L6W], [L9W] and [L11W] analogue displayed weak insulin-releasing activity (Table 4.3), but the [D1W] and [G7W] analogues were as potent and effective as the native peptide (Figure 4.13A-C). The insulinotropic activity of frenatin 2D and its [D1W] and [G7W] analogues were unaffected by the removal of the amidated group and was equally effective to their amidated counterpart (Table 4.3).

4.4.3 Effects of frenatin 2D and its synthetic analogues ([D1W] frenatin 2D and [G7W] frenatin 2D) on insulin release from 1.1B4 human clonal β-cells and isolated mouse islets

The stimulatory effect of frenatin 2D and its synthetic analogues ([D1W] frenatin 2D and [G7W] frenatin 2D) on insulin release was replicated in the glucose-responsive 1.1B4 human-derived cell line at both 5.6 mM and 16.7 mM glucose. The native peptide and analogues produced a significant ($P<0.05$) increase in insulin release at a 0.1 nM in the presence of 5.6 mM glucose (Figure 4.15A-C) and 1 nM in the presence of 16.7 mM glucose (Figure 4.16A-C), with an approximate 2-fold increase at 3 µM concentration. The magnitude of the response to 3 µM frenatin 2D was less than the response to 10 nM GLP-1. Incubation of frenatin 2D with isolated mouse islets also produced a significant increase of insulin release at 10 nM ($P<0.05$) and at 1 µM ($P<0.01$) compared with the rate in the presence of 16.7 mM glucose only (Figure 4.17). Similar stimulatory effects were observed with islets incubated with either [D1W] or [G7W] frenatin 2D. Again, the magnitudes of insulin responses of frenatin 2D peptides were significantly less than the responses to GLP-1 at the same concentration.

4.4.4 Effects of frenatin 2D and its synthetic analogues ([D1W] frenatin 2D and [G7W] frenatin 2D) on membrane depolarization and intracellular calcium ($[Ca^{2+}]i$)

Incubation of BRIN-BD11 cells with 30 mM KCl produced an immediate and sustained increase in membrane potential. In contrast, incubation with frenatin 2D peptides (1 µM) had no significant effect on membrane depolarization (Figure 4.18). Similarly, incubation of BRIN-BD11 cells with 10 mM alanine produced an

immediate and sustained increase in $[Ca^{2+}]i$, whereas incubation with frenatin 2D peptides (1 µM) had no significant effect on this parameter (Figure 4.19).

4.4.5 Effects of established modulators of insulin release and chloride channel blocker on the insulinotropic activity of frenatin 2D and its synthetic analogues ([D1W] frenatin 2D and [G7W] frenatin 2D)

The effects of known insulin release modulators, Ca^{2+} free buffer and chloride channel blocker on the insulinotropic activity of frenatin 2D peptides are shown in Figure 4.20, 4.21 and 4.22 respectively. The ability of the peptides to stimulate insulin release from BRIN-BD11 cells was unaffected in the presence of diazoxide (300 µM), the K^+ channel activator, verapamil (50 µM), the L-type voltage-dependent and Ca^{2+} channels blocker (Figure 4.20), Ca^{2+} free buffer (Figure 4.21) and 4,4-diisothiocyanostilbene-2,2-disulfonic acid (0.66 mM), the chloride channel blocker (Figure 4.22). The depolarizing stimulus 30 mM KCl produced a marked (3-fold) increase in insulin release, and the rate was significantly ($P<0.01$) augmented when the 30 mM KCl solution was supplemented with frenatin 2D peptides (1 µM). In the presence of IBMX (200 µM) frenatin 2D peptides produced a minor but still significant ($P<0.05$) increase in insulin release.

4.4.6 Effects of frenatin 2D and its synthetic analogues ([D1W] frenatin 2D and [G7W] frenatin 2D) on cyclic AMP in BRIN-BD11 rat clonal β-cells

Incubation of BRIN-BD11 cells with GLP-1 (10 nM) in the presence of IBMX resulted in a 215% increase ($P<0.001$) in cAMP compared with cells incubated with 5.6 mM glucose plus IBMX alone. Incubation with frenatin 2D peptides (1 µM) produced a smaller but still significant ($P<0.01$) increase in cAMP, which was associated with

enhanced in insulin release, suggesting an involvement of the PKA pathway (Figure 4.23A-B). In the second series of experiments, the insulinotropic activity of frenatin 2D peptides was examined after down-regulation of the PKA and PKC pathways by overnight culture of BRIN-BD11 cells with forskolin and PMA respectively (Figure 4.24A-C). When the activators were not present, the rates of insulin release produced by frenatin 2D peptides, GLP-1, and CCK-8 were significantly ($P<0.001$) greater than that produced by 5.6 mM glucose alone. The insulin stimulatory activities of frenatin 2D peptides and GLP-1, but not CCK-8, were significantly reduced when the PKA pathway was down-regulated with 25µM forskolin. In contrast, down-regulation of the PKC pathway with 10 nM PMA was without significant effect on the stimulatory activity of frenatin 2D and GLP-1, but the effect of CCK-8 was abolished. Down-regulation of both the PKA and PKC pathways by preincubation with forskolin plus PMA abolished the stimulatory responses of all peptides tested.

4.4.7 Effects of frenatin 2D and its synthetic analogues ([D1W] frenatin 2D and [G7W] frenatin 2D) on proliferation and cytokine-induced apoptosis in BRIN-BD11 β-cells

Incubation of BRIN-BD11 cells with frenatin 2D peptides (1 µM) or with GLP-1 (1 µM) did not affect the number of cells exhibiting DNA damage, as measured by TUNEL assay. Incubation of the cells with a mixture of proinflammatory cytokines resulted in a 272% increase ($P<0.001$) in the number of cells displaying apoptosis. The number of the apoptotic cells was reduced by 48% ($P<0.001$) when the BRIN-BD11 cells were co-incubated with GLP-1 (1µM) and the cytokine mixture. A comparable (38%-42%, $P<0.05$) reduction in the number of apoptotic cells was observed when the cells were co-incubated with frenatin 2D peptides (1µM) and the cytokine mixture

(Figure 4.25A-C). Incubation of BRIN-BD11 cells with frenatin 2D, [D1W] frenatin 2D and [G7W] frenatin 2D (1 µM) significantly ($P<0.05$) increased proliferation by 18%, 21% and 17% respectively, compared with incubations in the presence of culture medium alone (Figure 4.26). This degree of proliferative stimulation was less than that provided by incubation with 1 µM GLP-1 (48% increase).

4.4.8 Stability of frenatin 2D in murine plasma

Metabolic stability of frenatin 2D was evaluated by incubating peptide with murine plasma. HPLC profile reveals that frenatin 2D was resistant to the proteolytic enzyme in plasma for at least 4 hrs. The identity of the frenatin 2D peptide in the collected fraction was further confirmed by MALDI-TOF MS (Figure 4.27-4.28)

4.4.9 Effects of frenatin 2D and its synthetic analogues ([D1W] frenatin 2D and [G7W] frenatin 2D) on glucose uptake in C2C12 cells

As shown in Figure 4.29-4.30, insulin (1 µM) stimulated a significant increase ($P<0.05$) in glucose uptake in C2C12 cells. On the other hand, treatment of frenatin 2D peptides (1 µM) showed no positive effect on glucose uptake. However, a modest increase in glucose uptake was observed in the presence of insulin, but not significant.

4.4.10 Acute effects of frenatin 2D and its synthetic analogues ([D1W] frenatin 2D and [G7W] frenatin 2D) on food intake in mice

As shown in Figure 4.31, GLP-1 significantly ($P<0.05$) suppressed appetite from 60 min up to 180 min post-injection in mice. Administration of frenatin 2D did not affect food intake. However, a noticeable decrease in food intake was observed in [D1W]

frenatin 2D injected mice. [G7W] frenatin 2D, significantly ($P<0.05$) inhibited food intake from 120 min up to 180 min post-injection.

4.4.11 Effects of frenatin 2D and its synthetic analogues ([D1W] frenatin 2D and [G7W] frenatin 2D) on glucose tolerance and insulin concentrations in mice

Blood glucose concentrations in lean male NIH swiss TO mice receiving intraperitoneal glucose plus frenatin 2D (75 nmol/kg bw) or [G7W] frenatin 2D (75 nmol/kg bw) were significantly ($P<0.05$) lower at 15 min and 30 min after administration compared with animals receiving glucose only (Figure 4.32A). [D1W] frenatin 2D (75 nmol/kg bw) displayed a significant reduction in glucose at 30 and 60 min. The integrated responses of blood glucose (area under the curve) after frenatin 2D or [G7W] frenatin 2D or [D1W] frenatin 2D were significantly ($P<0.05$, $P<0.01$) less after administration of vehicle only (Figure 4.32B). Plasma insulin concentrations were significantly ($P<0.001$) higher at 15 min after glucose administration in animals receiving frenatin 2D peptides (Figure 4.32C) and the integrated response (total amount of insulin released over 60 min) was significantly ($P<0.05$, $P<0.01$) greater compared with animals receiving glucose alone (Figure 4.32D). However, the magnitude of the effects on blood glucose concentrations and insulin release produced by administration of 75 nmol/kg bw of [D1W] frenatin 2D peptide was comparable to the effects produced by administration of 25 nmol/kg bw of GLP-1 (Figure 4.32A-D).

4.4.12 Effects of frenatin 2D and its synthetic analogues ([D1W] frenatin 2D and [G7W] frenatin 2D) on glucose tolerance, 2 hrs and 4 hrs after peptide administration in mice

In another set of experiments overnight fasted male NIH swiss TO mice were injected with either saline or peptides [frenatin 2D, [D1W] frenatin 2D, [G7W] frenatin 2D (all at 75 nmol/kg bw) and GLP-1 (25 nmol/kg bw)] two or four hr prior to glucose administration (18 mmol/kg bw) (Figure 4.33 & 4.34). Frenatin 2D peptide significantly decreases blood glucose at 15 min, when administered 2 hr prior to glucose challenge. Under the same experimental conditions [D1W] frenatin 2D decreased blood glucose at 15 and 30 min. The integrated responses of blood glucose in mice receiving either frenatin 2D or [D1W] frenatin 2D (area under the curve) were comparable to mice receiving GLP-1. [G7W] frenatin 2D, however, failed to produce a beneficial effect on blood glucose (Figure 4.33A-B). Only [D1W] frenatin 2D, exhibited a glucose-lowering effect ($P<0.05$) when administered 4 hr prior to glucose challenge (Figure 4.34A-B).

4.4.13 Effects of different doses of frenatin 2D and its synthetic analogues [D1W] frenatin 2D on glucose tolerance in mice

Mice administered with frenatin 2D at 50 nmol/kg body weight did not produce any significant changes in plasma glucose concentrations compared with mice administered with glucose alone (Figure 4.35 A, B). In contrast, [D1W] frenatin 2D produced a smaller but significant ($P<0.05$) decrease in plasma glucose concentration (Figure 4.35 C, D). However, at 25 nmol/kg body weight, [D1W] frenatin 2D did not show any effects on plasma glucose concentration. Mice when administered with either 75 nmol/kg body weight or 150 nmol/kg body weight of frenatin 2D or [D1W] frenatin 2D, produced comparable glucose-lowering effects. No statistical difference in glucose concentrations were observed between the groups treated with 75 and 150 nmol/kg body weight of either frenatin 2D or [D1W] frenatin 2D.

4.4.14 Effects of twice daily administration of frenatin 2D and its synthetic analogue [D1W] frenatin 2D on body weight, energy intake, fluid intake, non-fasting blood glucose and plasma insulin in *db/db* mice

All *db/db* mice exhibited significant (P<0.001) increase in body weight, energy intake, water, non-fasting blood glucose and plasma insulin compared to lean controls (Figure 4.36 and 4.37). Twice daily intraperitoneal administration of frenatin 2D and [D1W] frenatin 2D for 28 days had no effects on body weight and energy intake in *db/db* mice (Figure 4.36A-D). As expected, energy intake was significantly (P<0.001) decreased with exenatide treatment, however, no difference in body weight was observed compared to *db/db* controls. In *db/db* mice, blood glucose concentration was significantly (P<0.05) decreased by both frenatin 2D and [D1W] frenatin 2D, but not to the same extent as exenatide (Figure 4.37A, B). Frenatin 2D and exenatide but not [D1W] frenatin 2D significantly (P<0.05, P<0.001) increased overall plasma insulin compared to *db/db* controls (Figure 4.37D). As shown in Figure 4.36E, significant (P<0.05, P<0.01) decrease in fluid intake was observed from 24th days onwards, in both frenatin 2D and [D1W] frenatin 2D treatment group compared to *db/db* control. However, no statistical difference was observed in the overall fluid intake (Figure 4.36F). With exenatide treatment, fluid intake was decreased significantly (P<0.001) by 42% compared to *db/db* control.

4.4.15 Effects of twice daily administration of frenatin 2D and its synthetic analogue [D1W] frenatin 2D on glycated haemoglobin (HbA1c) in *db/db* mice

Glycated haemoglobin (HbA1c) level reflects the average blood glucose level to a period of 2-3 month. As expected, all *db/db* mice, exhibited significantly higher HbA1c level (P<0.05 - P<0.001) than the lean control. As shown in Figure 4.38, twice

daily injection of frenatin 2D and [D1W] frenatin 2D resulted significant ($P<0.05$) decrease in blood HbA1c level by 34% and 27% respectively compared to *db/db* control. Treatment with exenatide induced 52% decrease in HbA1c level.

4.4.16 Effects of twice daily administration of frenatin 2D and its synthetic analogue [D1W] frenatin 2D on glucose tolerance in *db/db* mice following intraperitoneal and oral glucose load

As expected, saline-treated *db/db* mice exhibited impaired glucose tolerance after a glucose load (18 mmol/kg bw), resulting in a higher area under the glucose curve compared to lean littermates. After 28 days of treatment, intraperitoneal glucose tolerance was significantly ($P<0.05$) improved in both frenatin 2D and [D1W] frenatin 2D treated mice (Figure 4.39A-D). Blood glucose concentration was significantly ($P <0.05$) lowered at 15 min in both frenatin 2D and [D1W] frenatin 2D treated mice compared to saline-treated *db/db* mice (Figure 4.39A). This improvement was associated with significant ($P<0.05$) increase in insulin response (93% to 95% increase, $P<0.05$, Figure 4.39D). However, the magnitude of the decrease in blood glucose and an increase in insulin response in both frenatin 2D and [D1W] frenatin 2D treated *db/db* mice were less than exenatide-treated *db/db* mice.

In another set of experiments, the glycaemic response to an oral glucose load (OGTT) was investigated (Figure 4.40A-D). In [D1W] frenatin 2D treated group, blood glucose was significantly ($P<0.05$) less at 15 and 30 min compared to *db/db* control group (Figure 4.40A). This was associated with significant ($P<0.05$) increase in insulin release at 30 min (Figure 4.40C). However, no statistical difference was observed in overall insulin response (Figure 4.40D). Frenatin 2D treated mice showed a tendency to lower blood glucose and improve insulin level, but no significant difference was

observed compared to *db/db* control. On the other hand, blood glucose and insulin after oral glucose challenge were significantly (P<0.05) improved in exenatide-treated mice.

4.4.17 Effects of twice daily administration of frenatin 2D and its synthetic analogue [D1W] frenatin 2D on insulin sensitivity in *db/db* mice

Following 28 days treatment, a significant (P<0.05, Figure 4.41A-B) improvement in the hypoglycaemic effect of insulin was observed in both frenatin 2D and [D1W] frenatin 2D treated mice compared to saline-treated *db/db* mice. The alleviation of insulin resistance was further confirmed by HOMA-IR calculations derived using fasted blood glucose and plasma insulin concentrations. Both frenatin 2D and [D1W] frenatin 2D exhibited lower HOMA-IR index although it was not significant compared to *db/db* control. In exenatide-treated mice, the HOMA-IR index was reduced by 53% (P<0.05, Figure 4.41C).

4.4.18 Effects of twice daily administration of frenatin 2D and its synthetic analogue [D1W] frenatin 2D on bone mineral density, bone mineral content and fat composition in *db/db* mice

Figure 4.42A-G shows the results of a DEXA scan of the various groups of mice. At the end of treatment period, bone mineral density (BMD), bone mineral content (BMC), bone area, lean body mass, body fat and body fat (expressed a percentage of total body mass) were similar in all *db/db* groups. In comparison to lean control, lean body mass was decreased (P<0.001) significantly in frenatin 2D and [D1W] frenatin 2D treatment group. Whereas, body fat in [D1W] frenatin 2D treatment group was found similar to lean control.

4.4.19 Effects of twice daily administration of frenatin 2D and its synthetic analogue [D1W] frenatin 2D on pancreatic weight and insulin content

All *db/db* mice exhibited similar pancreatic weights (Figure 4.43A). However, when compared to lean mice, we observed a significant ($P<0.05$, $P<0.01$) increase in pancreatic weight in exenatide and frenatin 2D treated *db/db* mice. The pancreatic insulin content in saline-treated *db/db* mice was significantly ($P<0.01$) decreased by 68% compared to lean control (Figure 4.43B). The exenatide and frenatin 2D treated group showed significant ($P<0.05$, $P<0.01$) increase in pancreatic insulin content compared to *db/db* control. On the other hand, [D1W] frenatin 2D treated group had had similar pancreatic insulin content as *db/db* control.

4.4.20 Effects of twice daily administration of frenatin 2D and its synthetic analogue [D1W] frenatin 2D on insulin secretory responses of islets of *db/db* mice

At the end of the treatment period, insulin secretory responses of islets isolated from treated and untreated mice were examined. As expected, islets from saline-treated *db/db* mice displayed impaired insulin secretory response to glucose (1.4 mM, 5.6 mM, 16.7 mM) and known modulators of insulin release including alanine, GIP, GLP-1, KCl and arginine (Figure 4.43C, D). Under the same experimental conditions, islets from frenatin 2D treated mice demonstrated significant improvements in insulin release (Figure 4.43C), but not to the same extent as that observed following exenatide-treatment *db/db* mice. On the other hand, islets from [D1W] frenatin 2D treated *db/db* mice, displayed marginal improvement in insulin secretory response (Figure 4.43D).

4.4.21 Effects of twice daily administration of frenatin 2D and its synthetic analogue [D1W] frenatin 2D on lipid profile in *db/db* mice

Plasma lipid levels were examined in all experimental groups after 28 days treatment period. As shown in Figure 4.44A, C, cholesterol and high-density lipoprotein (HDL) were unaffected by peptide treatments in *db/db* mice. However, triglycerides and low-density lipoprotein (LDL) were decreased by both frenatin 2D and [D1W] frenatin 2D treatment, but not to the same extent as in exenatide-treated mice (Figure 4.44B, D).

4.4.22 Effects of twice daily administration of frenatin 2D and its synthetic analogue [D1W] frenatin 2D on liver and kidney functions in *db/db* mice

The biomarkers for a liver function such as ALT, AST and ALP levels were examined after the end of treatment period. As shown in Figure 4.45A-C, these liver parameters were significantly ($P<0.001$) increased by 76%, 246% and 105% respectively in saline-treated *db/db* mice compared to lean control. In the exenatide treatment group, these elevated parameters were decreased markedly ($P<0.05$ - $P<0.001$) by 1.2 – 2.0 folds. Interestingly, we observed a similar decrease in these parameters in both frenatin 2D and [D1W] frenatin 2D treatment group. Also, elevated creatinine level in *db/db* was reduced significantly ($P<0.05$, $P<0.01$) by frenatin 2D and [D1W] frenatin 2D treatment, but not to the same as exenatide (Figure 4.45D).

4.4.23 Effects of twice daily administration of frenatin 2D and its synthetic analogue [D1W] frenatin 2D on plasma amylase concentration in *db/db* mice

As shown in figure 4.46, amylase activity was unaltered in both frenatin 2D and [D1W] frenatin 2D treated *db/db* mice. However, in exenatide treatment, significant

(P<0.001) increase in amylase activity was observed compared to *db/db* and lean control.

4.4.24 Effects of twice daily administration of frenatin 2D and its synthetic analogue [D1W] frenatin 2D on islet number, islet area, beta cell areas, alpha cell area and islet size distribution

At the end of the treatment period, effects of peptides on islet morphology were evaluated. (Figure 4.47A-F). Figure 4.47A presents images of pancreatic islets of lean control and both untreated and treated *db/db* mice, showing alpha cells in red and beta cells in green. The number of islets per mm^2 was significantly (P<0.05, P<0.01) decreased in all *db/db* mice compared to lean controls. However, within *db/db* groups, no significant difference in islet number was observed (Figure 4.47 B). Lean control, *db/db* control, frenatin 2D and [D1W] frenatin 2D treatment groups exhibited no significant differences in islet area. Exenatide-treated group displayed significantly (P<0.05) increased islet area compared to *db/db* control (Figure 4.47C). As expected, the beta cell area was decreased (P<0.05) and alpha cell area was increased (P<0.01) in *db/db* controls compared to lean littermates. Frenatin 2D and [D1W] frenatin 2D induced no significant changes in beta cell area (Figure 4.47D). A noticeable decrease in the alpha cell was observed compared to *db/db* controls, this was not significant (Figure 4.47E). On the other hand, exenatide treatment significantly improved overall islet morphology, showing positive effects on islet, beta cell, and alpha cell area comparable to lean controls. The number of large and medium-size islet were increased (P<0.05 - P<0.001) and small size islet were decreased (P<0.05, P<0.01) in all treatment groups compared to *db/db* controls (Figure 4.47F).

4.4.25 Effects of twice daily administration of frenatin 2D and its synthetic analogue [D1W] frenatin 2D on gene expression in skeletal muscle

Effects of frenatin 2D and [D1W] frenatin 2D on the expression of skeletal muscle insulin signalling genes were examined after the treatment period (Figure 4.48A-G). We observed elevated mRNA expression of glucose transporter 4 (*Slc2a4*), insulin receptor (*Insr*), insulin receptor substrate 1 (*Irs1*), phosphatidylinositol 3-kinase, catalytic, alpha polypeptide (*Pik3ca*), protein kinase B alpha (*Akt1*) and protein phosphatase 1B (*Ptb1*) genes in untreated *db/db* mice compared to the lean controls (Figure 4.48A-C & E-G). The expression of these genes was downregulated by both frenatin 2D and [D1W] frenatin 2D treatment. Interestingly, effects produced by the frenatin 2D peptides were not different from exenatide treatment. No statistical differences in expression of 3-phosphoinositide-dependent protein kinase 1 (*Pdk1*) gene were observed in the various groups of mice (Figure 4.48D).

4.4.26 Effects of twice daily administration of frenatin 2D and its synthetic analogue [D1W] frenatin 2D on gene expression in islets

In *db/db* mice, expression of islet genes involved in insulin secretion including Mus musculus insulin 1 (*Ins1*), ATP-binding cassette, sub-family C (CFTR/MRP), member 8 (*Abcc8*), potassium inwardly-rectifying channel, subfamily J, member 11 (Transcript variant 1) (*Kcnj11*), glucose transporter 2 (*Slc2a2*), calcium channel, voltage-dependent, L type, alpha 1C subunit (*Cacna1c*) and glucokinase, transcript variant 1 (*Gck*) were investigated following 28 days treatment (Figure 4.49A-F). In saline-treated *db/db* mice, expression of these genes was significantly ($P<0.001$) downregulated compared to lean littermate mice. Frenatin 2D prevented down-regulation of these genes ($P<0.01$, $P<0.001$), but not to the same extent as observed in

exenatide-treated *db/db* mice. On the other hand, [D1W] frenatin 2D countered downregulation of *Ins1, Abcc8, Slc2a2* and *Gck* genes in *db/db* treated mice.

Downregulation of mRNA expression of gastric inhibitory polypeptide receptor (*Gipr*), glucagon-1 like peptide receptor (*Glp1r*), glucagon (*Gcg*) and pancreatic islets of homeobox 1 (*Pdx1*) genes in *db/db* mice was countered ($P<0.05$ - $P<0.001$) by exenatide and frenatin 2D treatments (Figure 4.50A-D). Signal transducer and activator of transcription 1 (*Stat1*) that were significantly upregulated in *db/db* mice were less highly expressed after treatment with exenatide and frenatin 2D (Figure 4.50E). [D1W] frenatin 2D treatment had no significant effects on *Gipr, Glp1r, Gcg, Pdx1* and *Stat1* genes' expressions.

4.5 Discussion

The bioactive peptides in frog skin secretions with antimicrobial activity are regarded as an essential component in the animal's system of host-defence. The initial enthusiasm of the discovery that these peptides to kill antibiotic-resistant microorganisms that had become resistant to conventional antibiotics has dwindled thus no frog skin peptide is currently in clinical practice as an antimicrobial agent. More promising potential clinical applications of amphibian host-defence peptides might lie in their use as immunomodulatory agents (Pantic *et al.,* 2017b), promoters of wound healing [reviewed in (Mangoni *et al.,* 2016)] and as templates for the design of drugs to treat patients with T2DM (Conlon *et al.,* 2018).

The present study has shown that naturally occurring frenatin peptides (frenatin 2D from *Discoglossus sardus* and frenatin 2.1S, 2.2S & 2.3S from *Sphaenorhynchus lacteus*) demonstrate dose-dependent insulin-releasing activity from clonal β-cells (BRIN-BD11 cells) at concentrations that are not cytotoxic to the cells. Frenatin 2D

was the most potent peptide producing a significant increase in insulin release from BRIN-BD11 cells at a concentration of 100 pM with an impressive 2.3-fold increase at a concentration of 3 µM. The stimulatory effects of frenatin 2D were also replicated in human 1.1B4 cells as well as isolated mouse islet cells. Consequently, frenatin 2D was chosen for further studies aimed at designing analogues with increased insulinotropic activity and to elucidate the mechanism of action of the frenatins.

The relative antimicrobial and cytotoxic activities of naturally occurring peptides are determined by complex interactions between molecular charge, conformation, hydrophobicity and, in the case of α-helical peptides, amphipathicity (Mojsoska & Jenssen, 2015). Studies with a wide range of such peptides have shown that increasing cationicity, while maintaining amphipathicity, generally by substitution of appropriate neutral or acidic amino acids by L-lysine, results in increased antimicrobial activity by promoting interaction with the negatively charged cell membrane of prokaryotes (Kumar *et al.*, 2018). In the present study, each amino acid in frenatin 2D was replaced by a bulky, hydrophobic tryptophan (W) residue in an attempt to promote interaction with the zwitterionic plasma membrane of BRIN-BD11 cells. The strategy did not lead to the design of an analogue with increased insulinotropic activity, but the study demonstrated that the frenatin 2D molecule was very sensitive to changes in amino acid composition. Replacement of Thr^{5}, Asn^{8}, Pro^{10}, and Ile^{14} by Trp (W) led to the loss of insulinotropic activity at concentrations up to and including 3 µM. Substitutions at Leu^{2}, Leu^{3}, Gly^{4}, Leu^{6}, Leu^{9}, Leu^{11}, Phe^{12} and Phe^{13} also led to marked decreases in insulinotropic activity (Table 4.3). In contrast, replacements at Asp^{1} and Gly^{7} and deletion of the C-terminal α-amide group did not affect activity. The stimulatory effects of [D1W], [G7W] analogues was also replicated in human 1.1B4 cells and isolated moue islet cells.

Insulin release from pancreatic β-cells is regulated by K_{ATP} channel-dependent and K_{ATP} channel-independent pathways (Henquin, 2000, 2004). In the former pathway, an increase in intracellular ATP generated from glucose metabolism results in closure of ATP-sensitive potassium channels, activation of chloride channels and an influx of Ca^{2+} through the opening of voltage-dependent Ca^{2+} channels, leading to exocytosis. The insulinotropic frog skin peptides CPF-SE1 (Srinivasan *et al.,* 2013), tigerinin-1R (Ojo *et al.,* 2016), and PGLa-AM1 (Owolabi *et al.,* 2017) depolarise BRIN-BD11 cells and increase $[Ca^{2+}]_i$ suggesting that they operate via the K_{ATP} channel-dependent pathway. In contrast, pseudin-2 (Abdel-Wahab *et al.,* 2008a), hymenochirin 1B (Owolabi *et al.,* 2016), and temporins A, F, and G (chapter 6) stimulate insulin release without significant effects on membrane depolarization or $[Ca^{2+}]_i$. Similar to the second group of peptides, incubation of BRIN-BD11 cells with either frenatin 2D or its analogues ([D1W] and [G7W] frenatin 2D) did not affect membrane potential or $[Ca^{2+}]_i$ suggesting an involvement of the K_{ATP} channel-independent pathway. Consistent with this hypothesis, the insulinotropic activity of frenatin 2D peptide and its analogues was preserved in calcium-free medium and in the presence of diazoxide, an agent that inhibits the secretion of insulin by opening ATP-sensitive potassium channels in β-cells, and verapamil, an agent that inhibits insulin release by blocking voltage-dependent Ca^{2+} channels. Although less well studied, activation of the chloride channel in pancreatic beta cells causes comparatively modest membrane depolarization and to release of insulin (Kinard *et al.,* 2001). The insulin-releasing activity of peptide was unaffected even after blocking chloride channel by using DIDS. In K_{ATP} channel-independent pathway, activation of adenylate cyclase by an agonist such as GLP-1 results in the generation of cAMP which in turn activates PKA to promote insulin release (Green *et al.,* 2004a, 2005). Incubation of BRIN-BD11 cells

with either frenatin 2D or its analogues produced a modest but significant increase of cAMP. Consistent with this observation, the stimulatory effect of frenatin 2D and its analogues on insulin release was abolished in PKA-downregulated BRIN-BD11 cells, whereas in PKC downregulated cells the stimulatory effect of peptides was unaffected. It is suggested, therefore, that the insulin-releasing activity of frenatin 2D in these cells is mediated predominantly, if not exclusively, by the K_{ATP} channel-independent pathway.

The progression of T2DM is associated with a decrease in the ability of the pancreatic β-cell to release insulin due to a decline in β-cell number and function. It has also been shown also that the GLP-1 stimulates proliferation of β-cells and protect the cells against apoptosis stimulated by cytokines, glucose and fatty acids (Cornu *et al.*, 2009, Lee *et al.*, 2014). Overnight incubation of BRIN-BD11 cells with either frenatin 2D or its analogue, also stimulated β-cell proliferation but the effect was significantly less than the effects of an equimolar concentration of GLP-1. Similarly, frenatin 2D provided significant protection of cells against cytokine-induced apoptosis and, in this case, the effect was comparable to that provided by GLP-1.

The frenatin 2D peptide was also active *in vivo* when administered to mice together with a glucose load, resulting in lower blood glucose and higher circulating insulin concentrations. Also, both analogues ([D1W] and [G7W] frenatin 2D) improved glucose tolerance by increasing insulin release following intraperitoneal administration with glucose in normal NIH TO mice. Moreover, we observed that glucose lowering effect of [D1W] frenatin 2D was sustained when administered 4 hr before glucose load, suggesting enhanced peptide stability. On the other hand, frenatin 2D and [G7W] frenatin 2D failed to retain its activity when pre-administered *in vivo*.

Glucose tolerance tests conducted with coadministration of different doses of peptide revealed that doses of frenatin 2D or [G7W] frenatin 2D peptide below 75 nmol/kg body, failed to retain its glucose-lowering effects. In contrast, the [D1W] frenatin 2D analogue induced a modest decrease in blood glucose level. When tested at a higher dose of 150 nmol/kg, no additional glucose lowering effect was observed with frenatin 2D and [D1W] frenatin 2D peptide. Hence, the peptide dose of 75 nmol/kg bw was selected for further studies.

Based on these findings, we further investigated long-term (28 days) effects of twice daily administration of frenatin 2D and [D1W] frenatin 2D, in comparison with antidiabetic agent exenatide, in genetically obese-diabetic mice (*db/db*). In line with previous reports (Wang *et al.*, 2002, Breyer *et al.*, 2005), *db/db* mice used for the present study displayed hyperglycaemia, hyperinsulinemia, insulin resistance, hyperlipidaemia and impaired blood glucose control.

With the progress of the study, a steady decrease of plasma insulin and an increase in blood glucose level were observed in *db/db* mice receiving saline only. These observations in *db/db* mice are in line with previous reports and indicate a degenerative form of diabetes (Coleman, 1978, Dalbøge *et al.*, 2013). In frenatin 2D treated *db/db* mice, progressive loss of insulin was delayed significantly. Blood glucose in both frenatin 2D and [D1W] Frenatin 2D treated *db/db* mice was delayed significantly. The intraperitoneal glucose tolerance and blood HbA1c level were also improved significantly. These beneficial effects of frenatin 2D and [D1W] Frenatin 2D peptide were independent of any changes in body weight or fat content of *db/db* mice. In agreement with acute *in vivo* feeding studies, no effect of the frenatin 2D and [D1W] frenatin 2D peptide was observed on energy intake. Both, frenatin 2D and [D1W] frenatin 2D also exhibited a tendency to improve glycaemic response to an oral

glucose load. Furthermore, a decrease in water intake was observed in both frenatin 2D and [D1W] frenatin 2D treated *db/db* mice from day 24 onwards, which correlates with improved glycaemic control. However, the magnitude of the beneficial effects of frenatin 2D and [D1W] frenatin 2D on blood glucose, insulin, glucose tolerance, HbA1c and water intake were less impressive than exenatide. With exenatide treatment, we observed a decrease in energy intake, which corresponds well to the previous studies (Gedulin *et al.*, 2005, Schlögl *et al.*, 2015), but body weight remained unaltered.

The hypoglycemic action of exogenous insulin was significantly improved in both frenatin 2D and [D1W] frenatin 2D treated *db/db* mice, which correlated with improved HOMA-IR index. To further evaluate the mechanisms by which the peptides improved insulin resistance, mRNA expression of insulin signalling genes was studied. We observed elevated expression of *Glut4, Insr, Irs1, Akt1, Pik3ca* and *Ptb1* in saline-treated *db/db* mice compared to their littermates. These observations are in harmony with previous studies where an increase in the activity of PI 3-kinase and Akt/PKB were observed in the liver and kidney of *db/db* mice (Feliers *et al.*, 2001). Similarly, an increase in the activity of proximal insulin signalling cascade was observed in the animal model of liver cirrhosis, (Jessen *et al.*, 2006). In L6 myotubules after chronic exposure to glucose or insulin, an increase in GLUT4 activity was also observed (Huang *et al.*, 2001). In both frenatin 2D and [D1W] frenatin 2D treatment mice, expression of *SlC2a4*, *Insr*, *Irs1, Akt1, Pik3ca* and *Ptb1* genes were downregulated. Interestingly, the magnitude of these effects was comparable to exenatide treatment.

In agreement with other studies (Son *et al.*, 2015, Lee *et al.*, 2014), lipid metabolism was impaired in *db/db* mice. Elevated plasma triglycerides and LDL levels of *db/db*

mice were reversed by frenatin 2D and [D1W] frenatin 2D treatment, but the effect was significantly less than the exenatide. Plasma cholesterol and HDL remain unaffected in all peptide-treated mice. The *db/db* mice are also used as a model of non-alcoholic fatty liver disease (NAFLD), which is characterised by elevated liver enzymes such as ALT, AST and ALP (Biden *et al.,* 2014, Parikh *et al.,* 2014, Lau *et al.,* 2016). In agreement, these liver biomarkers were significantly elevated in control *db/db* mice and decreased significantly by both frenatin 2D and [D1W] frenatin 2D treatment. The creatinine level in *db/db* mice was also lowered by these peptides, indicating that liver and kidney function were improved by peptide treatment. Furthermore, amylase activity was unaffected by frenatin 2D and [D1W] frenatin 2D treatment. These observations suggest that frenatin 2D peptides could be safe for the treatment of diabetes. Importantly, no adverse effects were observed in treated *db/db* mice which correlated well with *in vitro* toxicity studies. Nevertheless, we did observe an increase in amylase activity in exenatide-treated mice. In several clinical studies, enhanced amylase activity has been observed in type 2 diabetes and linked to possible incidence of pancreatitis (Nauck, 2013).

In harmony with others (Ishida *et al.,* 2004, Do *et al.,* 2014), islets from saline-treated *db/db* mice showed impaired insulin secretory responses to glucose and known insulin secretagogues. In the present study, frenatin 2D treatment significantly improved insulin secretory responses of *db/db* mouse islets. This was associated with a significant increase in pancreatic insulin content, suggesting the beneficial effects of the peptide on pancreatic beta cell function. However, the beneficial effects of [D1W] frenatin 2D treatment on islet insulin secretory response and pancreatic insulin content was not to the same as the native peptide. As expected, insulin secretory defect was reversed and the pancreatic insulin content was significantly increased in exenatide-

treated mice. The beneficial effects of peptides on the pancreatic beta cell was further evaluated by gene expression studies and immunohistochemical analysis. The positive effects of frenatin 2D on beta cell function corresponded with an improved expression of insulin secretory genes (*Ins1*, *Pdx1*, *Glp1R*, *Gipr*, *Abcc8*, *Kcnj11*, *Gck*, *Cacna1c*, *SlC2a2* and *Gcg*). In addition, upregulation of apoptosis *Stat1* gene was prevented by frenatin 2D treatment. Although frenatin 2D and [D1W] frenatin 2D treatment did not alter islet area/beta cell area, a noticeable decrease in alpha cell area was observed. Furthermore, a substantial decrease in large and medium-size islets and an increase in small size islets of *db/db* mice were prevented by all peptide treatments. Overall the beneficial effects of frenatin 2D and [D1W] frenatin 2D on islet architecture were similar but not as prominent as with exenatide.

In conclusion, the present Chapter has demonstrated the antidiabetic potential of frenatin 2D peptides. In *db/db* mice, frenatin 2D treatment significantly delayed the demise of beta cell function and insulin concentration, improved glycemic control and enhanced insulin sensitivity. The abnormal expression of the genes involved in glucose homeostasis in muscle and islets of *db/db* mice were reversed by frenatin 2D treatment. However, [D1W] frenatin 2D was not as effective as frenatin 2D in *db/db* mice.

Table 4.1 Amino acid sequence of frenatin peptides

Sr. No	Peptide	Sequence
1	Frenatin 2D	DLLGTLGNLPLPFI.NH_2
2	Frenatin 2.1S	GLVGTLLGHIGKAILG.NH_2
3	Frenatin 2.2S	GLVGTLLGHIGKAILS.NH_2
4	Frenatin 2.3S	GLVGTLLGHIGKAILG.COOH
5	[D1W] Frenatin 2D	WLLGTLGNLPLPFI.NH_2
6	[L2W] Frenatin 2D	DWLGTLGNLPLPFI.NH_2
7	[L3W] Frenatin 2D	DLWGTLGNLPLPFI.NH_2
8	[G4W] Frenatin 2D	DLLWTLGNLPLPFI.NH_2
9	[T5W] Frenatin 2D	DLLGWLGNLPLPFI.NH_2
10	[L6W] Frenatin 2D	DLLGTWGNLPLPFI.NH_2
11	[G7W] Frenatin 2D	DLLGTLWNLPLPFI.NH_2
12	[N8W] Frenatin 2D	DLLGTLGWLPLPFI.NH_2
13	[L9W] Frenatin 2D	DLLGTLGNWPLPFI.NH_2
14	[P10W] Frenatin2D	DLLGTLGNLWLPFI.NH_2
15	[L11W] Frenatin 2D	DLLGTLGNLPWPFI.NH_2
16	[P12W] Frenatin 2D	DLLGTLGNLPLWFI.NH_2
17	[F13W] Frenatin 2D	DLLGTLGNLPLPWI.NH_2
18	[I14W] Frenatin 2D	DLLGTLGNLPLPFW.NH_2
19	Frenatin 2D (Non-amidated)	DLLGTLGNLPLPFI
20	[D1W] Frenatin 2D (Non-amidated)	WLLGTLGNLPLPFI
21	[G7W] Frenatin 2D (Non-amidated)	DLLGTLWNLPLPFI

Table 4.2 Reverse phase HPLC, retention time and molecular weight

Sr. No	Peptide	Molecular weight Da (Theoretical)	Molecular weight Da (Experimental)	Retention time (min)
1	Frenatin 2D	1481.78	1481.90	25
2	Frenatin 2.1S	1518.89	1517.03	30
3	Frenatin 2.2S	1571.92	1572.54	33
4	Frenatin 2.3S	1519.88	1519.91	31
5	[D1W] Frenatin 2D	1552.9	1552.65	26
6	[L2W] Frenatin 2D	1554.83	1554.65	25
7	[L3W] Frenatin 2D	1554.83	1555.64	26
8	[G4W] Frenatin 2D	1610.93	1611.83	26
9	[T5W] Frenatin 2D	1566.68	1567.55	28
10	[L6W] Frenatin 2D	1554.83	1555.09	25
11	[G7W] Frenatin 2D	1610.93	1611.11	26
12	[N8W] Frenatin 2D	1553.88	1553.48	26
13	[L9W] Frenatin 2D	1554.83	1554.83	26
14	[P10W] Frenatin2D	1570.87	1571.62	26
15	[L11W] Frenatin 2D	1554.83	1555.75	25
16	[P12W] Frenatin 2D	1570.87	1571.61	26
17	[F13W] Frenatin 2D	1520.81	1521.04	25
18	[I14W] Frenatin 2D	1554.83	1555.47	27
19	Frenatin 2D (Non-amidated)	1482.78	1483.06	25
20	[D1W] Frenatin 2D (Non-amidated)	1553.9	1554.7	26
21	[G7W] Frenatin 2D (Non-amidated)	1611.94	1611.72	27

Purity and molecular mass of peptides were confirmed using RP-HPLC and MALDI-TOF respectively. The retention time was verified using ChromQuest software.

Table 4.3 Effects of analogues and non-amidated frenatin 2D peptide on insulin release from BRIN-BD11 rat clonal β-cells

Conditions	Threshold Concentration (nM)	Insulin release at 3 μM ($ng/10^6$ cells/20 min)
5.6 mM Glucose		1.01 ± 0.04
Frenatin 2D	0.1	2.30 ± 0.03 ***
[D1W] Frenatin 2D	0.1	2.61 ± 0.25 ***
[L2W] Frenatin 2D	10	1.81 ± 0.11 ***
[L3W] Frenatin 2D	3000	1.21 ± 0.04 **
[G4W] Frenatin 2D	3000	1.26 ± 0.07 **
[T5W] Frenatin 2D	>3000	1.17 ± 0.15
[L6W] Frenatin 2D	1000	1.59 ± 0.05 ***
[G7W] Frenatin 2D	0.1	2.57 ± 0.12 ***
[N8W] Frenatin 2D	>3000	1.09 ± 0.04
[L9W] Frenatin 2D	100	1.63 ± 0.01 ***
[P10W] Frenatin 2D	>3000	1.10 ± 0.06
[L11W] Frenatin 2D	100	1.30 ± 0.02 ***
[P12W] Frenatin 2D	1000	1.30 ± 0.05 ***
[F13W] Frenatin 2D	3000	1.44 ± 0.02 ***
[114W] Frenatin 2D	>3000	1.10 ± 0.04
Frenatin 2D non-amidated	0.1	2.14 ± 0.12***
[D1W] Non-amidated	0.1	2.00 ± 0.24***
[G7W] Non-amidated	0.1	2.01 ± 0.11***
[P12F, F13P] Frenatin 2D	>3000	1.00 ± 0.03

Values are mean ± SEM for n = 8. **P<0.01 and ***P<0.001 compared to 5.6 mM glucose alone.

Figure 4.1 Representative reverse-phase HPLC profile of frenatin peptides.

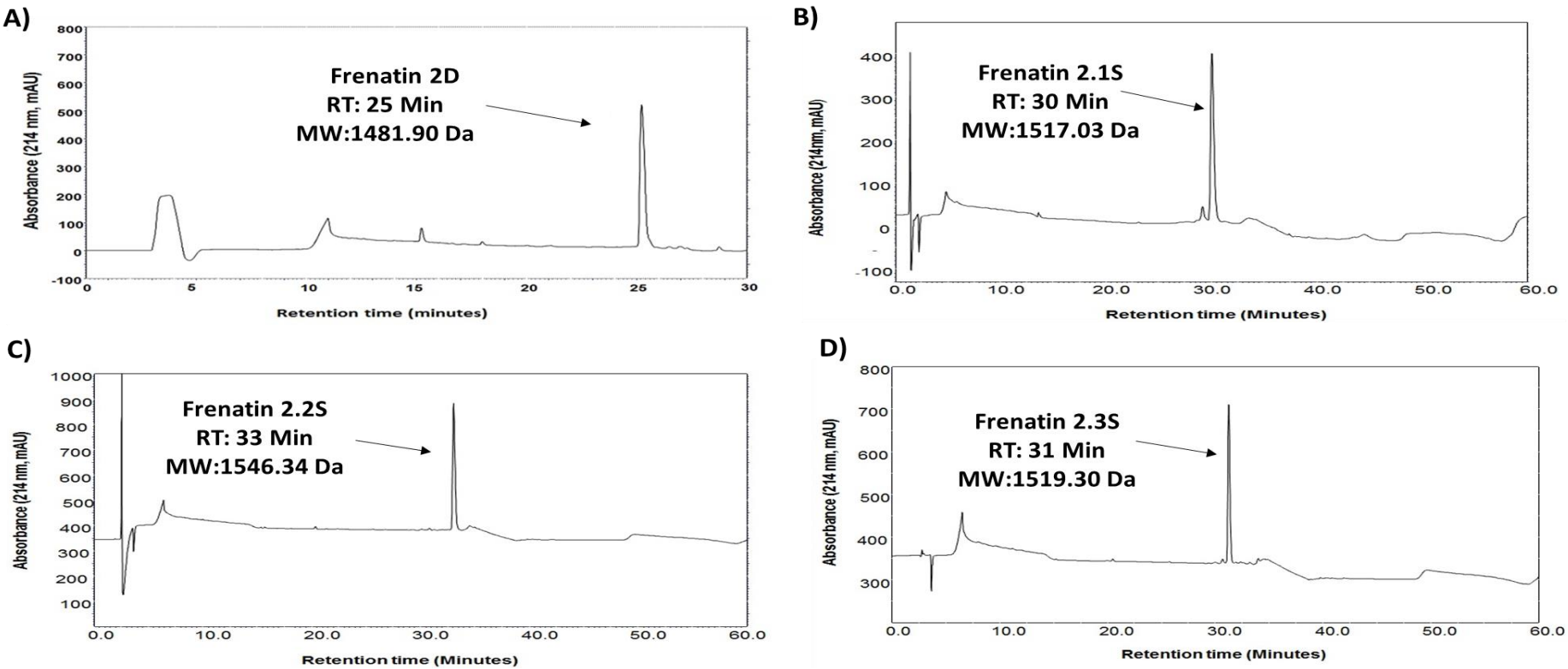

C-8 analytical column was used to obtain profile using a gradient from 0 to 100 % acetonitrile over 28 min for frenatin 2D and gradient from 0 to 40% of acetonitrile over 10 minutes, to 60% over 20 minutes and from 60% to 100% over 5 minutes for frenatin 2.1S, 2.2S and 2.3S

Figure 4.2 Representative reverse-phase HPLC profile of frenatin 2D peptides

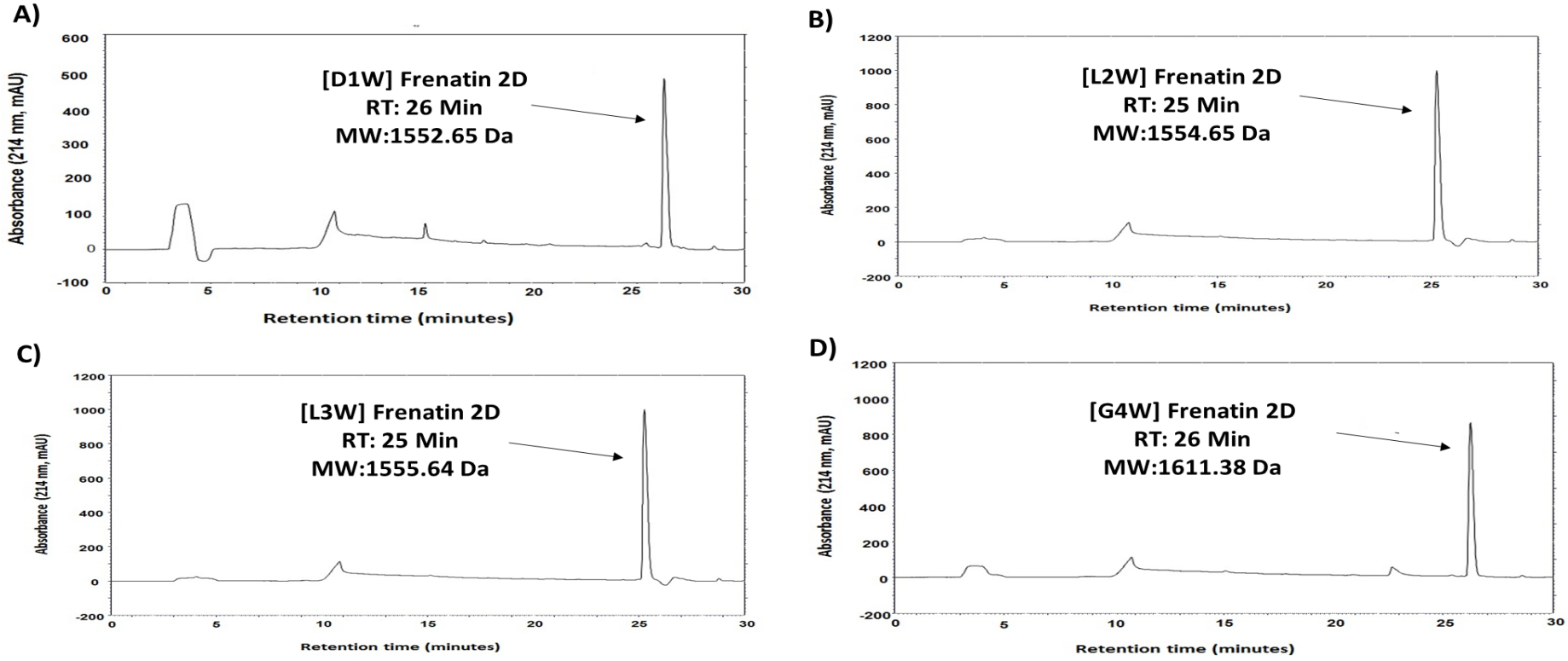

C-8 analytical column was used to obtain a profile using a gradient from 0 to 100 % acetonitrile over 28 min.

Figure 4.3 Representative reverse-phase HPLC profile of frenatin 2D peptides

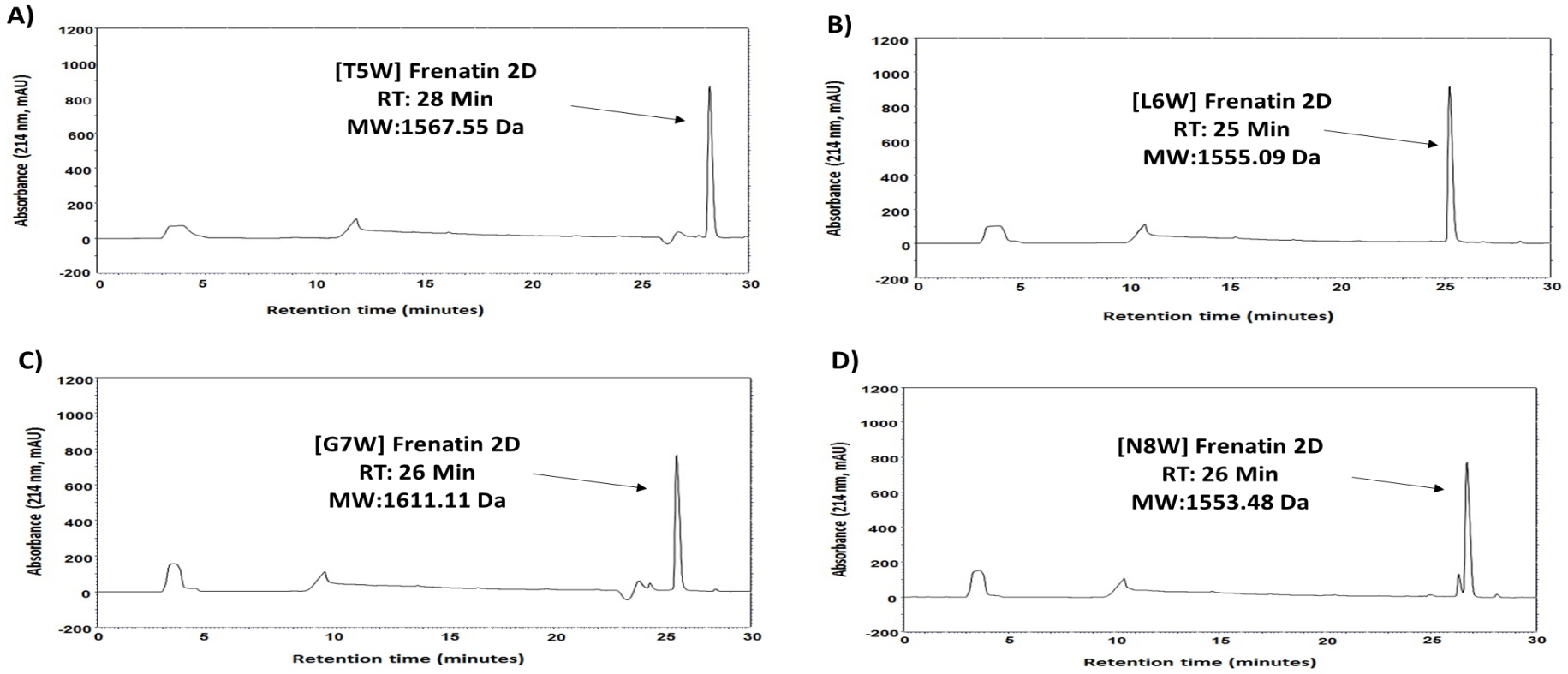

C-8 analytical column was used to obtain a profile using a gradient from 0 to 100 % acetonitrile over 28 min.

Figure 4.4 Representative reverse-phase HPLC profile of frenatin 2D peptides

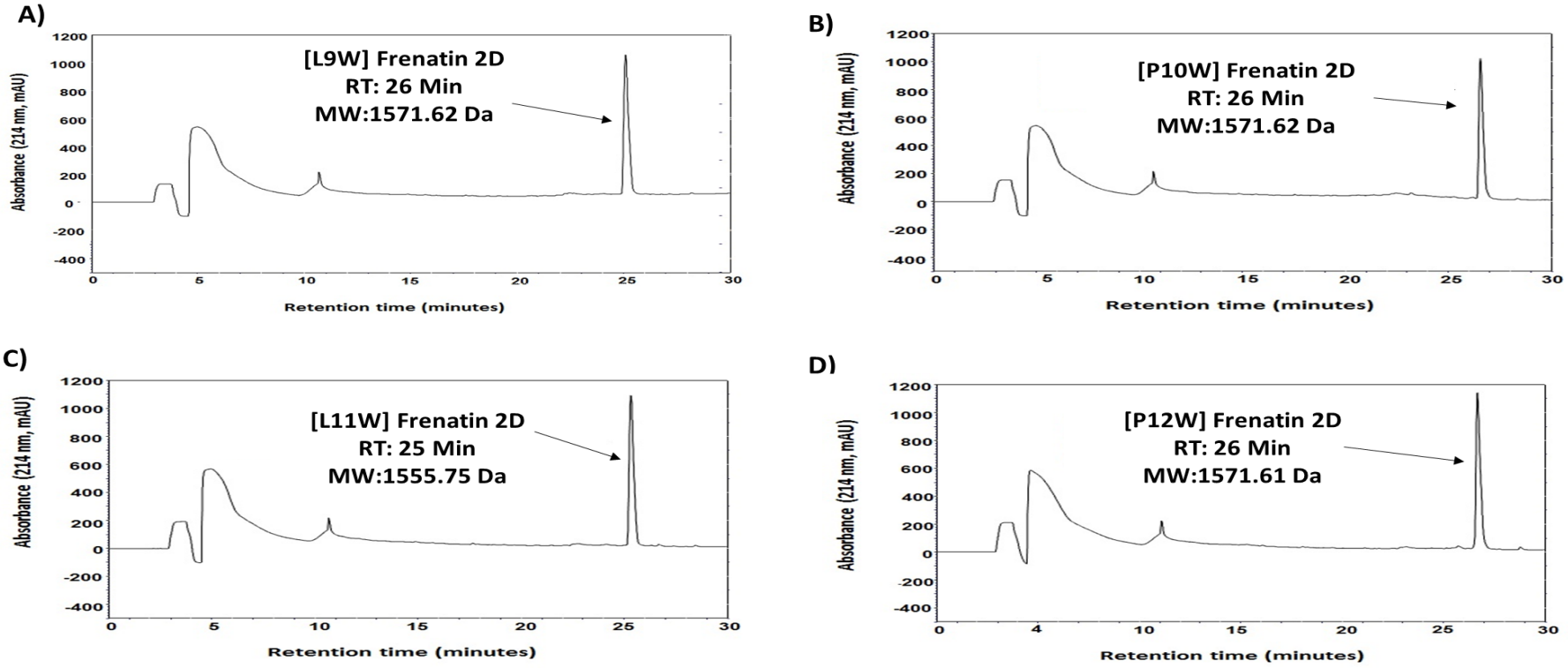

C-8 analytical column was used to obtain a profile using a gradient from 0 to 100 % acetonitrile over 28 min.

Figure 4.5 Representative reverse-phase HPLC profile of frenatin 2D peptides

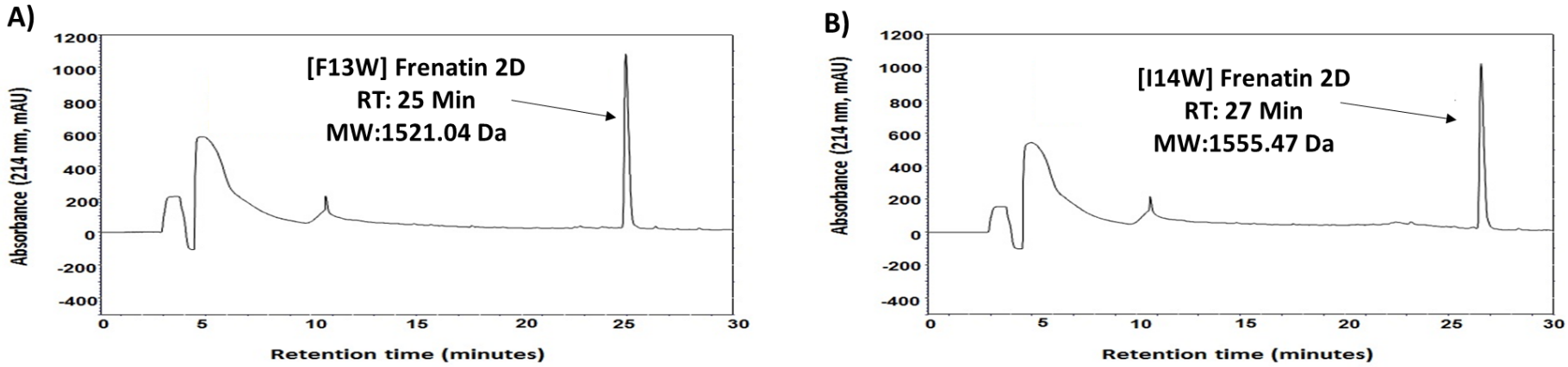

C-8 analytical column was used to obtain a profile using a gradient from 0 to 100 % acetonitrile over 28 min.

Figure 4.6 Representative MALDI-TOF spectra of frenatin peptides

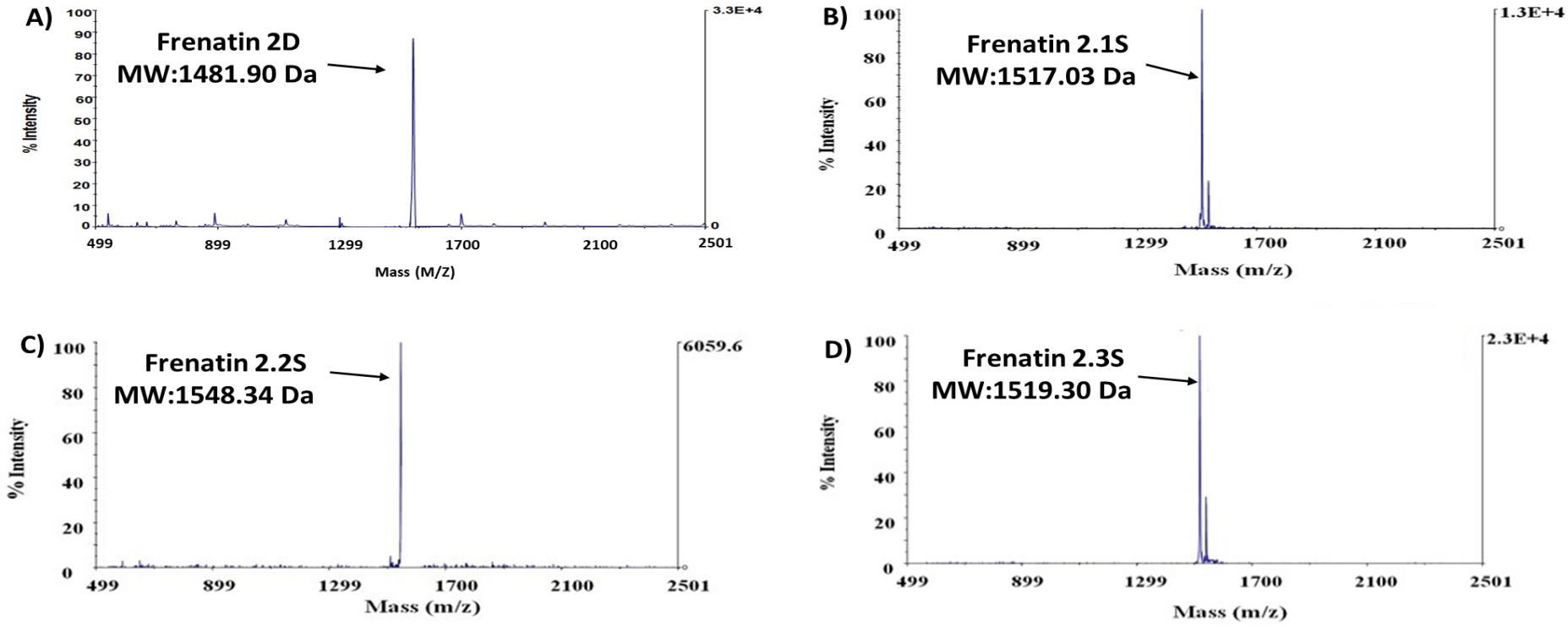

Matrix α-cyano cinnamic acid (1.5 µl) was mixed with purified peptide (1.5 µl) and left to dry on the MALDI plate. After drying, MALDI plate was applied to Voyager DE Bio spectrometry workstation. The mass-to-charge ratio versus peak intensity was recorded.

Figure 4.7 Representative MALDI-TOF spectra of frenatin 2D peptides

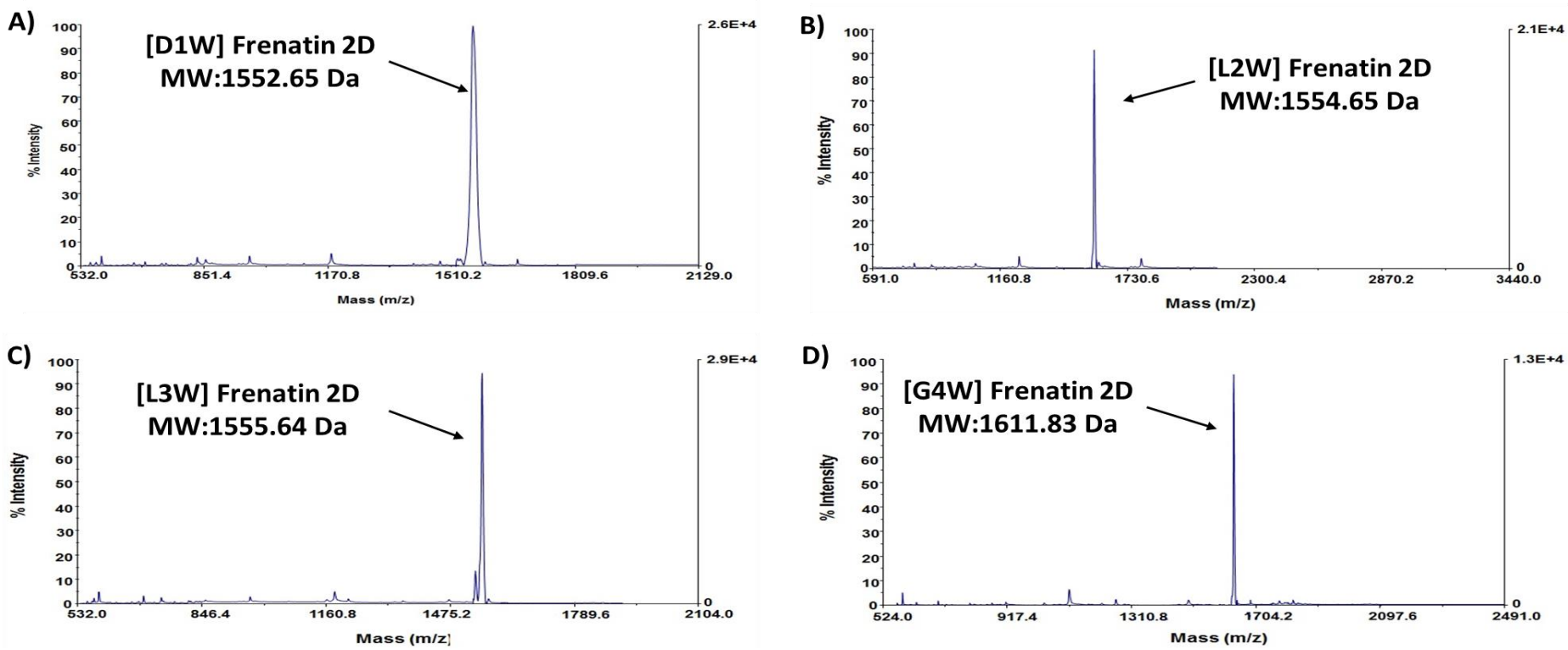

Matrix α-cyano cinnamic acid (1.5 µl) was mixed with purified peptide (1.5 µl) and left to dry on the MALDI plate. After drying, MALDI plate was applied to Voyager DE Bio spectrometry workstation. The mass-to-charge ratio versus peak intensity was recorded.

Figure 4.8 Representative MALDI-TOF spectra of frenatin 2D peptides

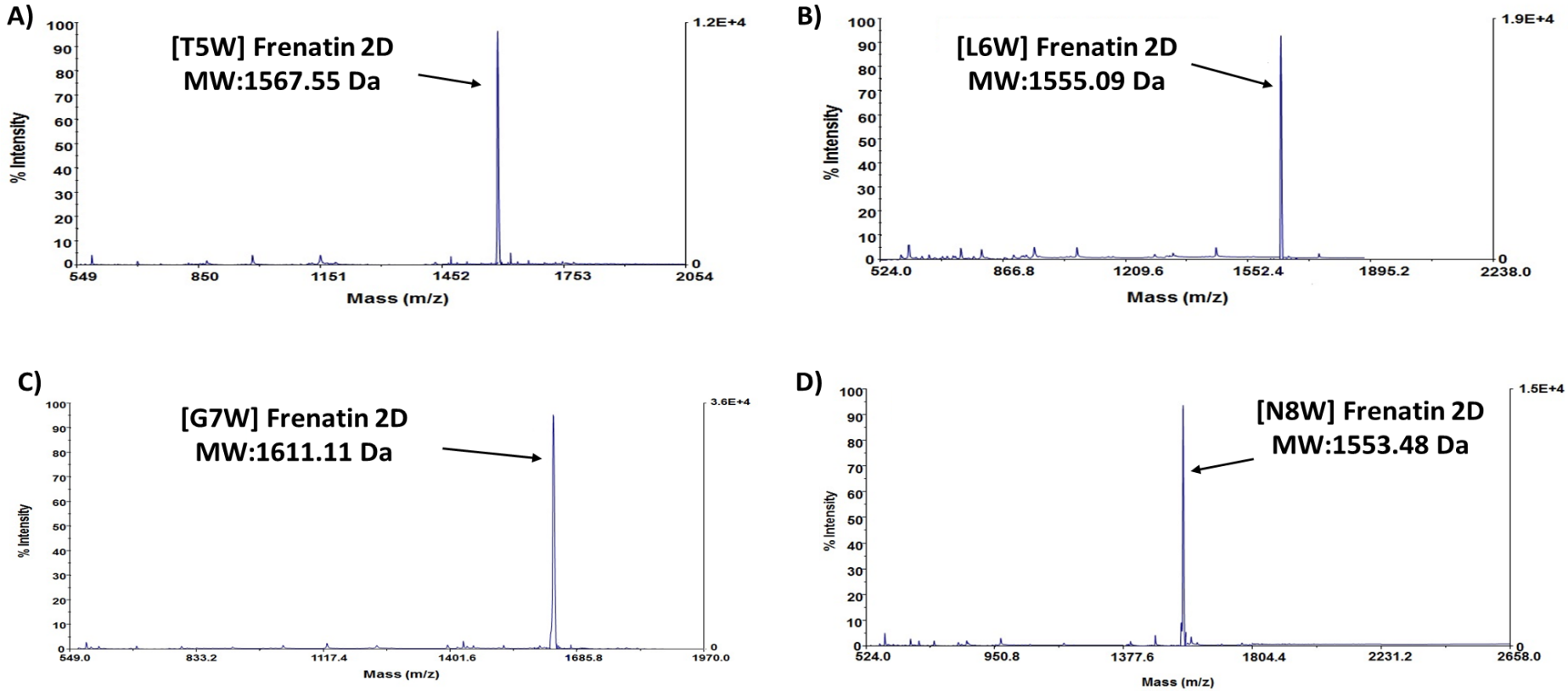

Matrix α-cyano cinnamic acid (1.5 µl) was mixed with purified peptide (1.5 µl) and left to dry on the MALDI plate. After drying, MALDI plate was applied to Voyager DE Bio spectrometry workstation. The mass-to-charge ratio versus peak intensity was recorded.

Figure 4.9 Representative MALDI-TOF spectra of frenatin 2D peptides

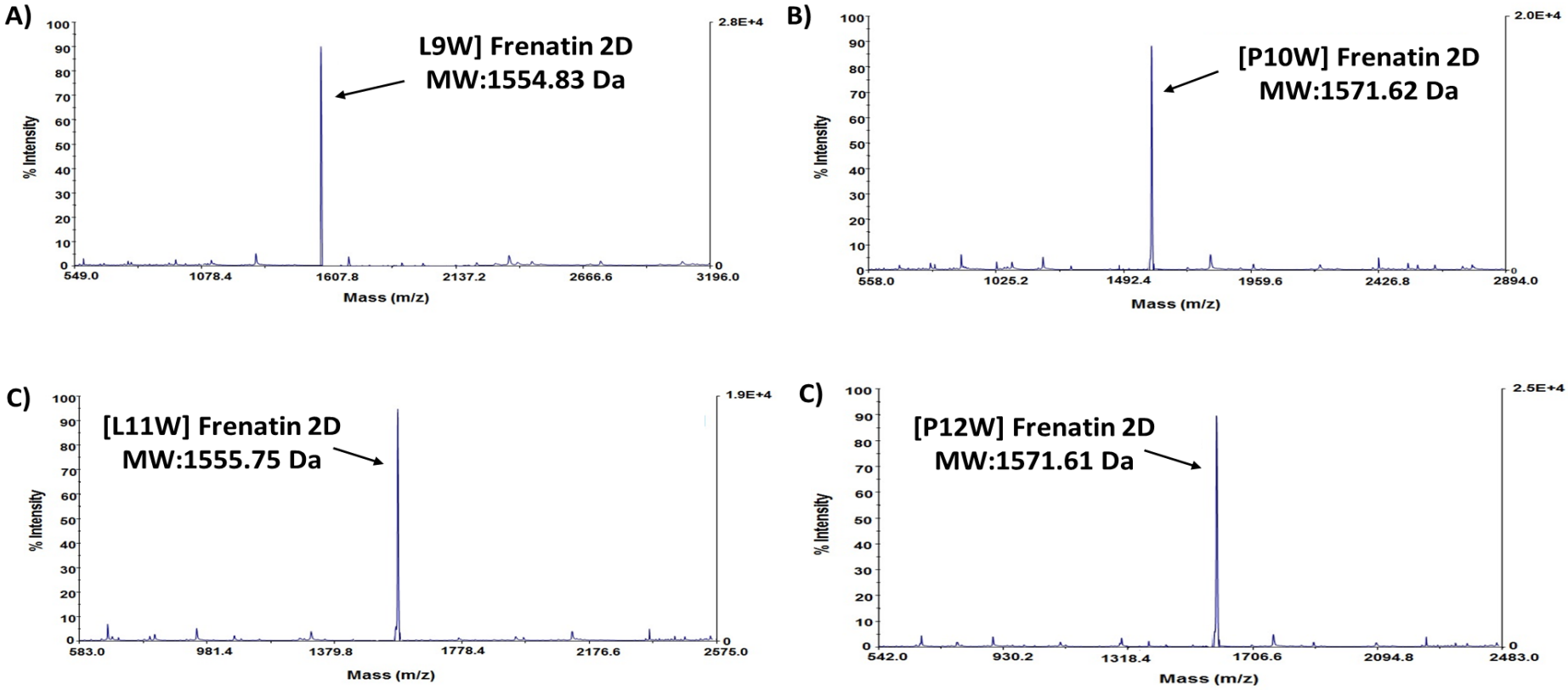

Matrix α-cyano cinnamic acid (1.5 µl) was mixed with purified peptide (1.5 µl) and left to dry on the MALDI plate. After drying, MALDI plate was applied to Voyager DE Bio spectrometry workstation. The mass-to-charge ratio versus peak intensity was recorded.

Figure 4.10 Representative MALDI-TOF spectra of frenatin 2D peptides

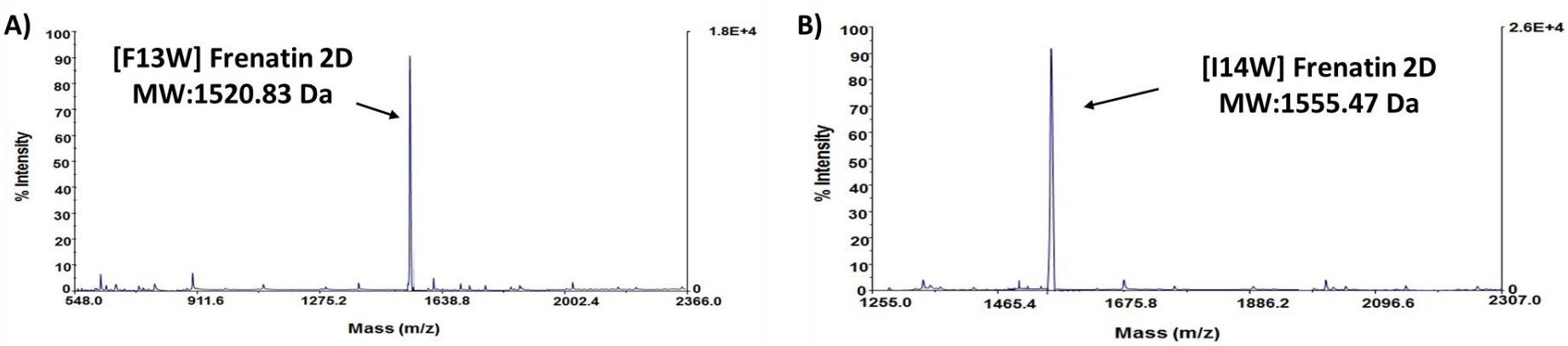

Matrix α-cyano cinnamic acid (1.5 µl) was mixed with purified peptide (1.5 µl) and left to dry on the MALDI plate. After drying, MALDI plate was applied to Voyager DE Bio spectrometry workstation. The mass-to-charge ratio versus peak intensity was recorded.

Figure 4.11 Effects of frenatin peptides on insulin release from BRIN-BD11 rat clonal β-cells

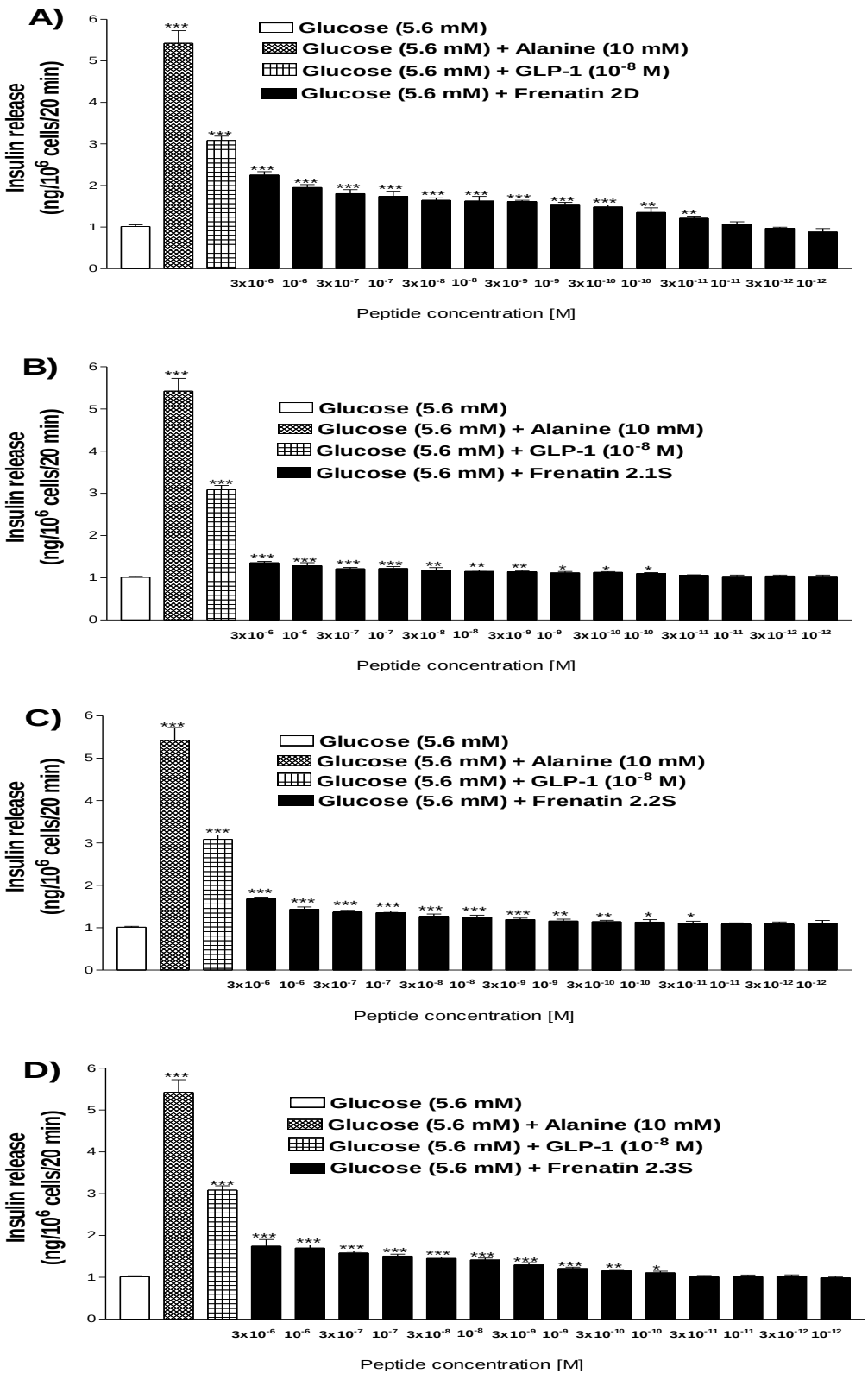

Effects of (A) frenatin 2D, (B) frenatin 2.1S, (C) frenatin 2.2S and (D) frenatin 2.3S on insulin release from BRIN-BD11 rat clonal β-cells. Values are mean ± SEM for n = 8. *P < 0.05, **P<0.01, and ***P<0.001 compared to 5.6 mM glucose alone.

Figure 4.12 Effects of frenatin peptides on LDH release from BRIN-BD11 rat clonal β-cells

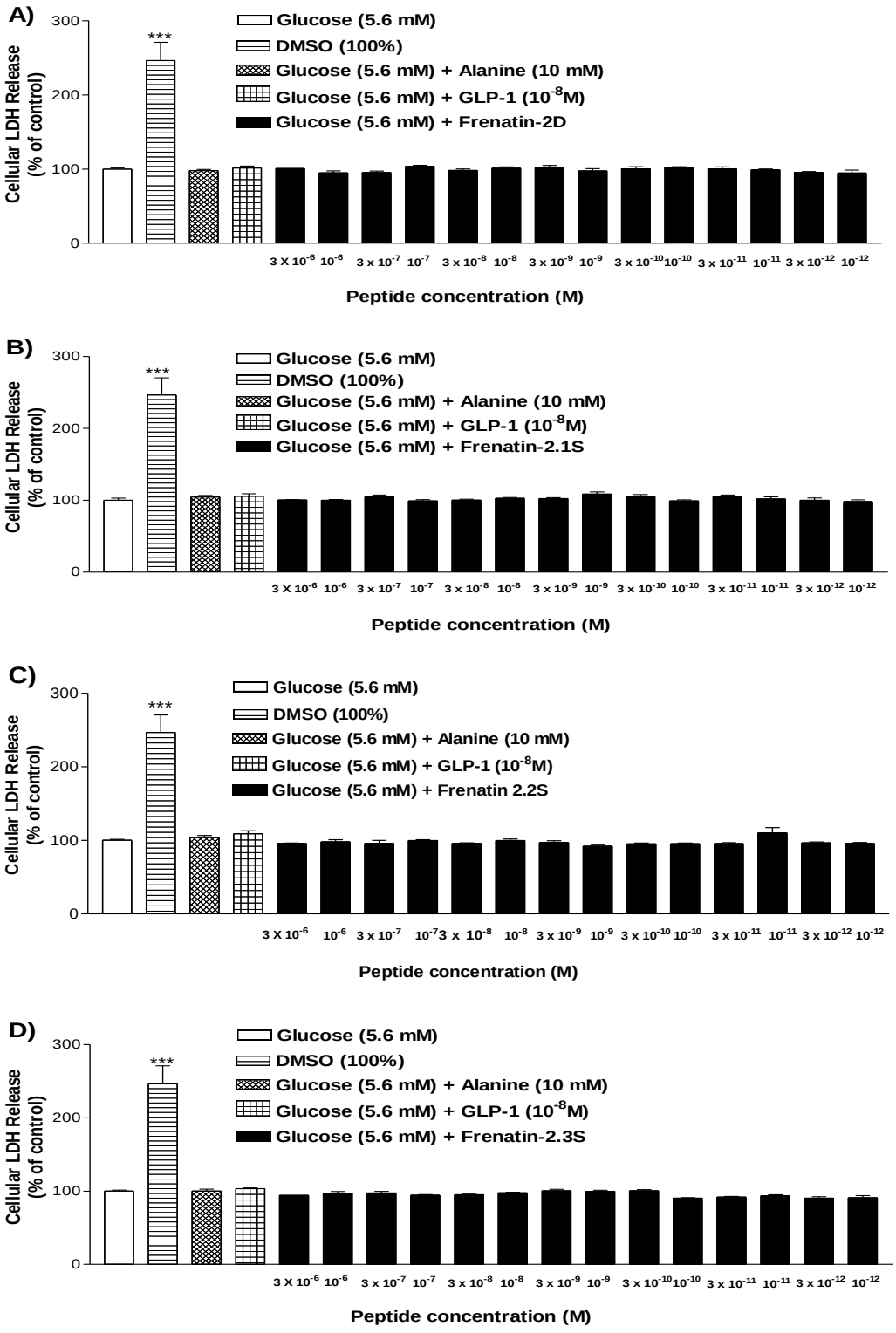

Values are Mean ± SEM with n=4 for LDH. DMSO (100%) was used as positive control. ***P<0.001 compared to 5.6 mM glucose alone.

Figure 4.13 Effects of frenatin 2D and its synthetic analogues ([D1W] frenatin 2D and [G7W] frenatin 2D) on insulin release from BRIN-BD11 rat clonal β-cells

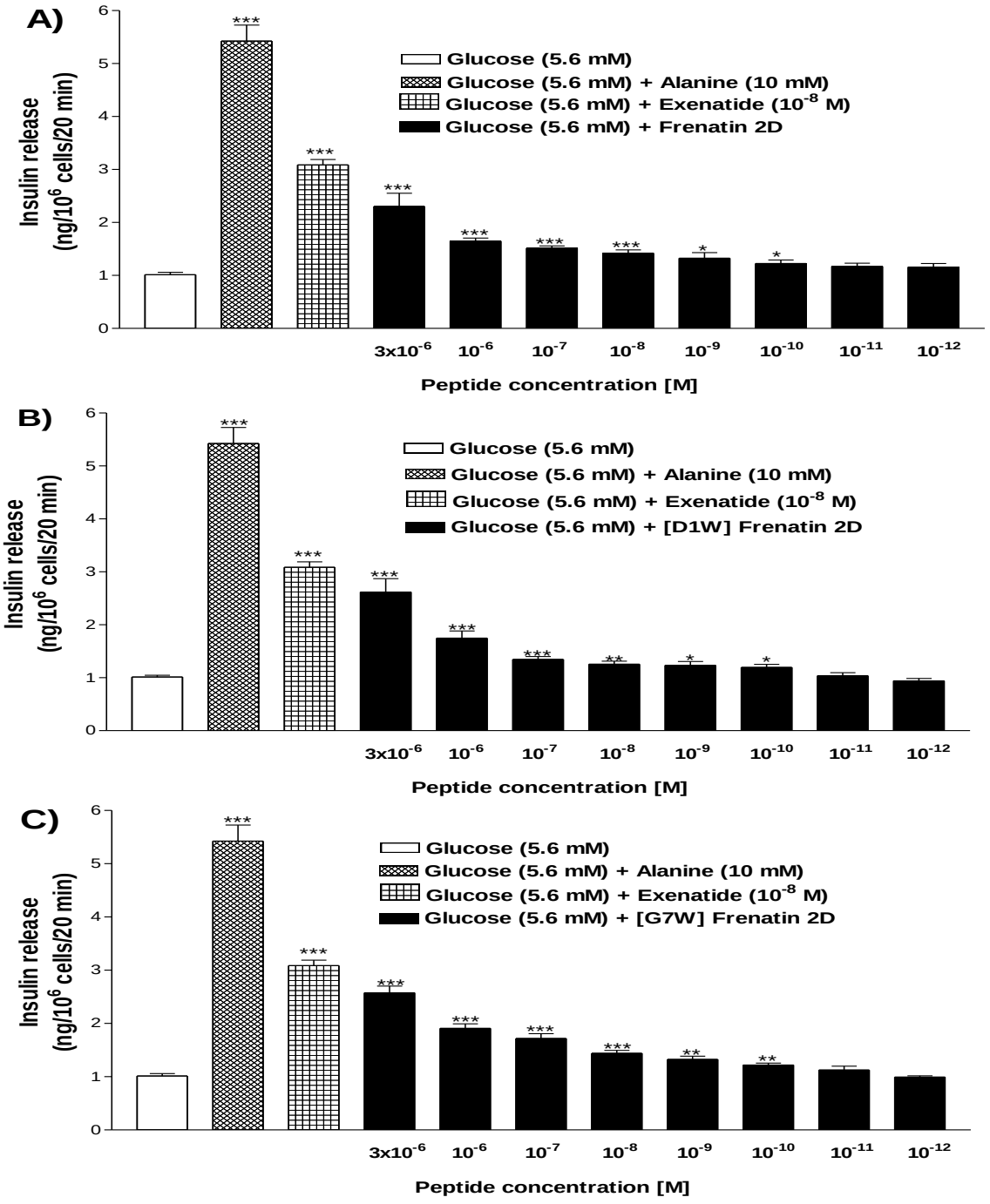

Comparison of the effects of A) Frenatin 2D, B) [D1W] frenatin 2D, and C) [G7W] frenatin 2D on insulin release from BRIN-BD11 rat clonal β-cells. Values are mean ± SEM for n = 8. *P<0.05, **P<0.01, and ***P<0.001 compared to 5.6 mM glucose alone.

Figure 4.14 Effects of [D1W] frenatin 2D and [G7W] frenatin 2D on LDH release from BRIN-BD11 rat clonal β-cells

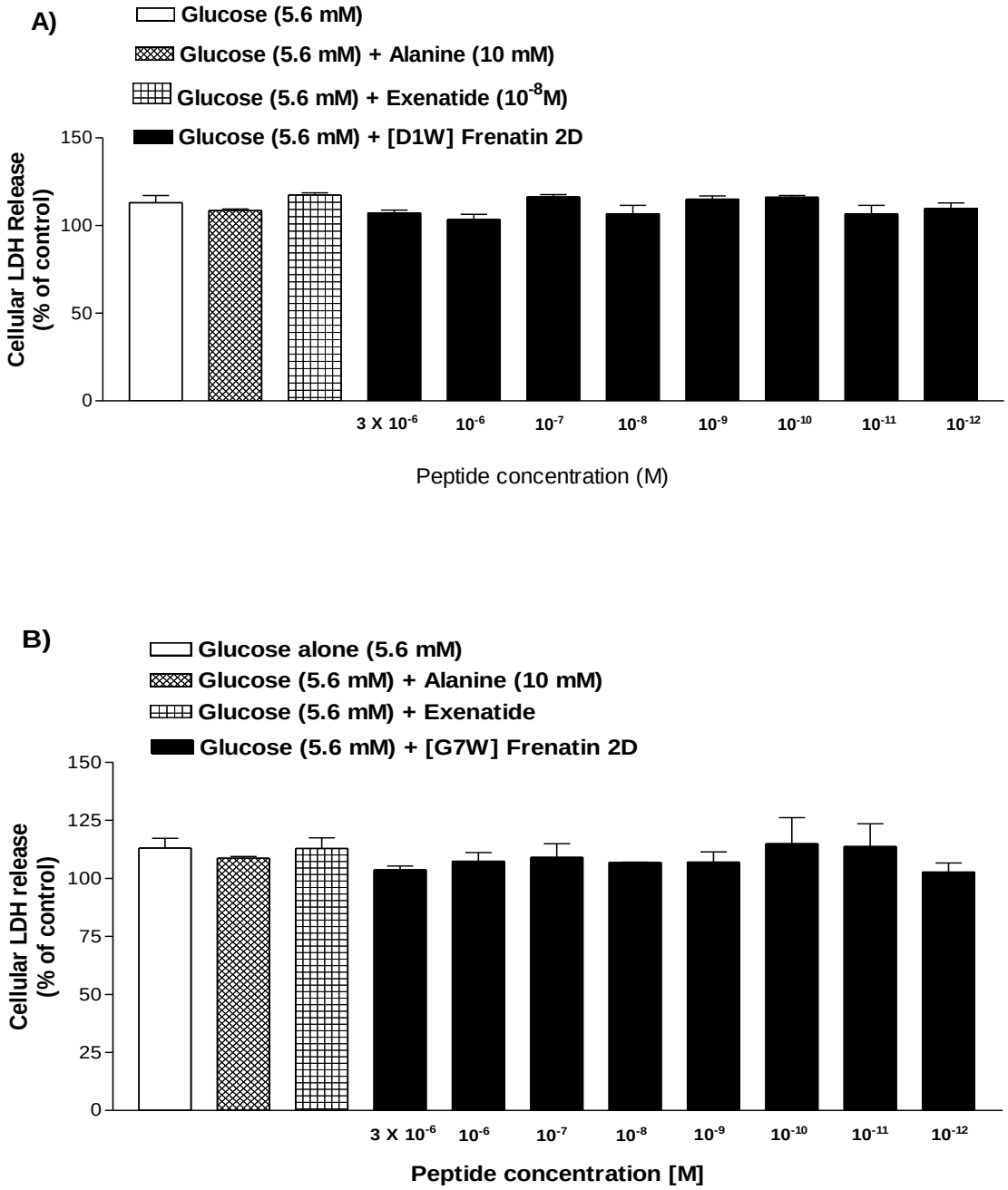

Values are Mean ± SEM with n=4 for LDH.

Figure 4.15 Effects of frenatin 2D and its synthetic analogues ([D1W] frenatin 2D and [G7W] frenatin 2D) on insulin release from 1.1B4 human clonal β-cells

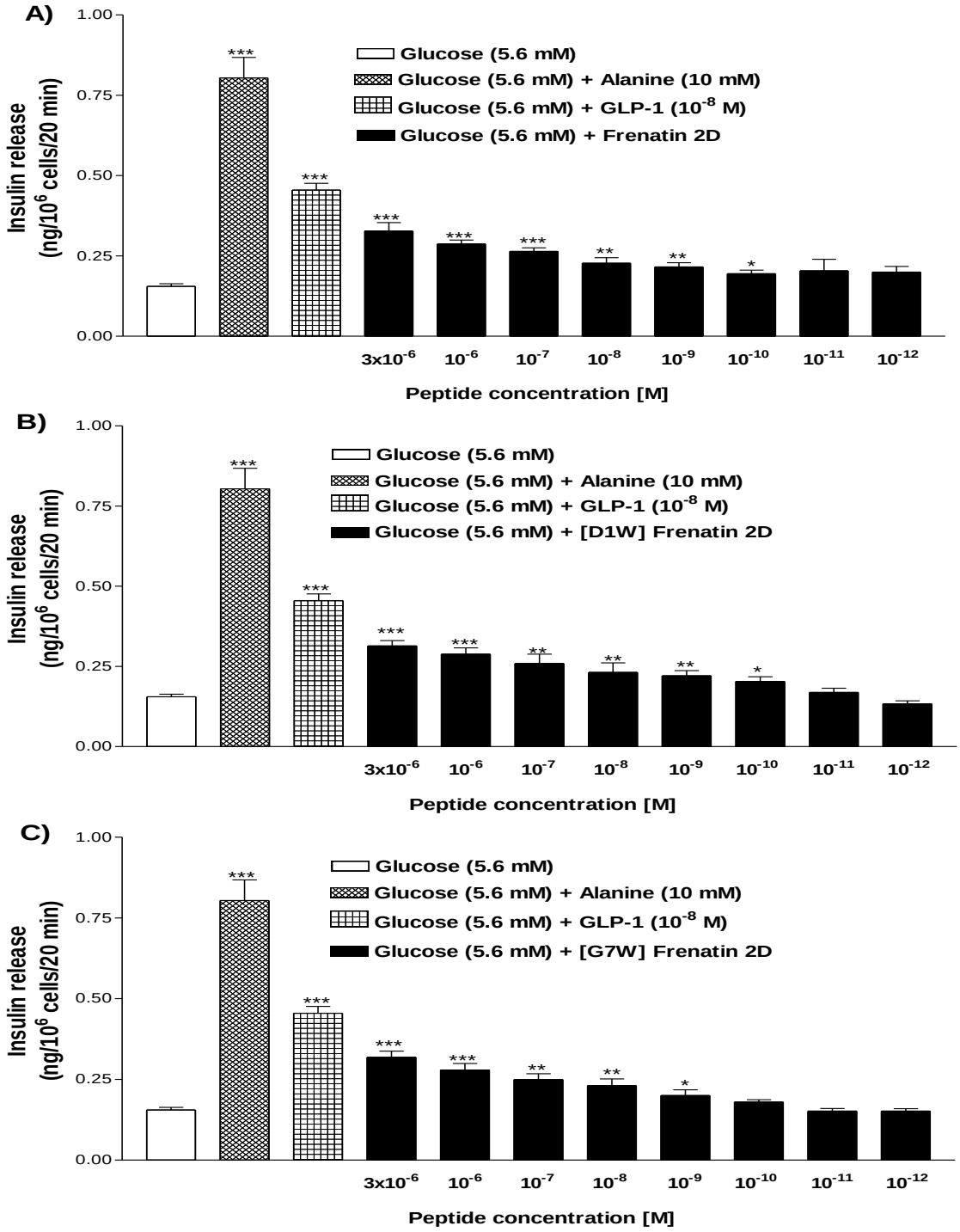

Effects of A) Frenatin 2D, B) [D1W] frenatin 2D, and C) [G7W] frenatin 2D on insulin release from 1.1B4 human clonal β-cells. Values are mean ± SEM for n = 8. *P<0.05, **P<0.01 and ***P<0.001 compared to 5.6 mM glucose alone.

Figure 4.16 Effects of frenatin 2D and its synthetic analogues ([D1W] frenatin 2D and [G7W] frenatin 2D) on insulin release from 1.1B4 human clonal β-cells

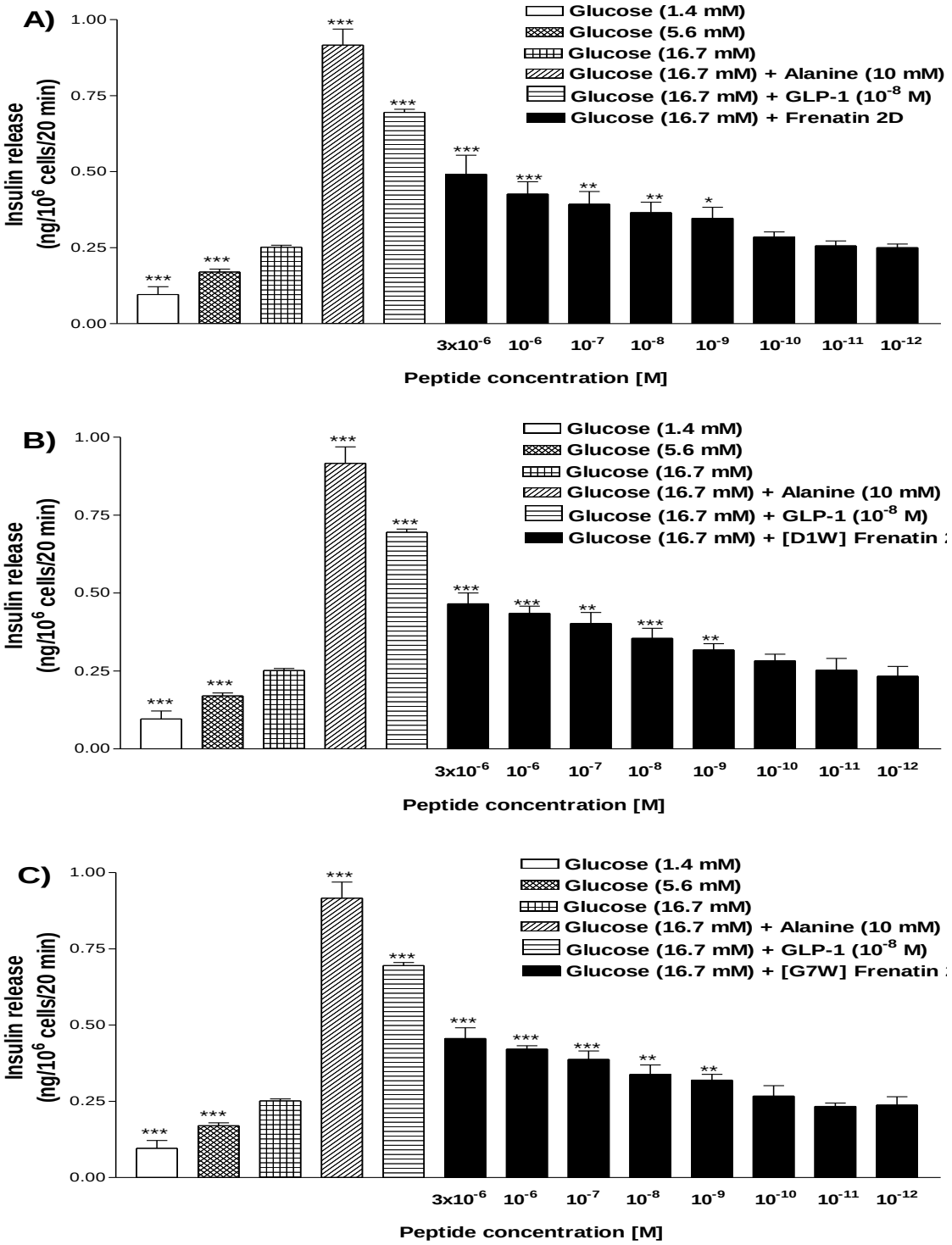

Effects of A) Frenatin 2D, B) [D1W] Frenatin 2D, and C) [G7W] Frenatin 2D on insulin release from 1.1B4 human clonal β-cells. Values are mean ± SEM for n = 8. *P<0.05, **P<0.01 and ***P<0.001 compared to 16.7 mM glucose alone.

Figure 4.17 Effects of frenatin 2D and its synthetic analogues ([D1W] frenatin 2D and [G7W] frenatin 2D) on insulin release from isolated mouse islets

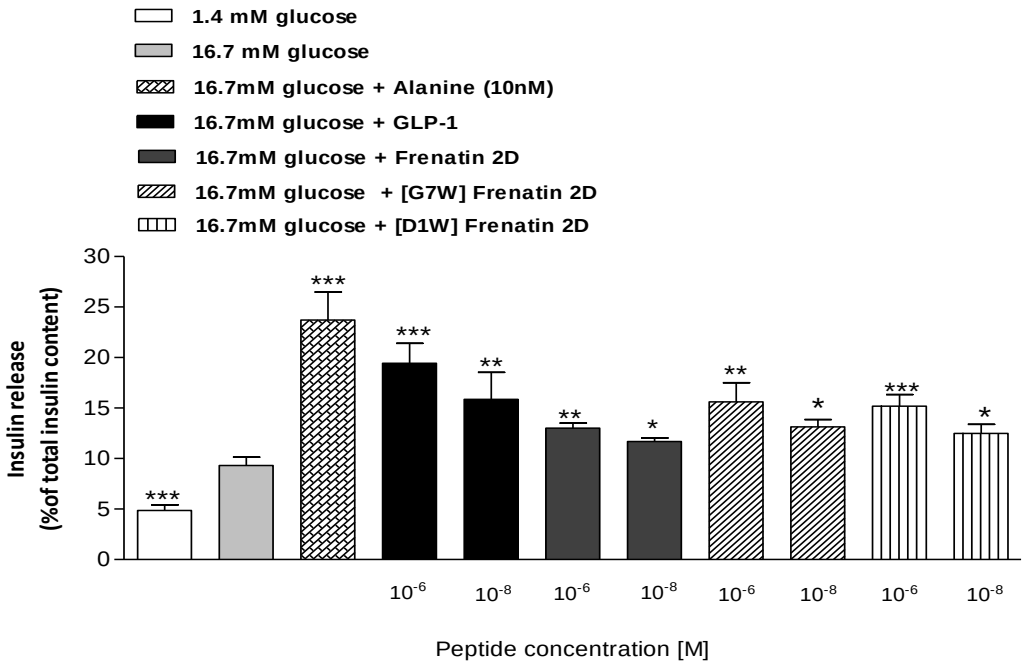

Effects of frenatin 2D, [D1W] and [G7W] Frenatin 2D on insulin release from isolated mouse islets. Values are Mean ± SEM (n=4). *P<0.05, **P<0.01 and ***P<0.001 compared to 16.7 mM glucose.

Figure 4.18 Effects of frenatin 2D and its synthetic analogues ([D1W] frenatin 2D and [G7W] frenatin 2D) on membrane potential in BRIN-BD11 rat clonal β-cells expressed as line graph (A, C, E) and area under the curve (B, D, F)

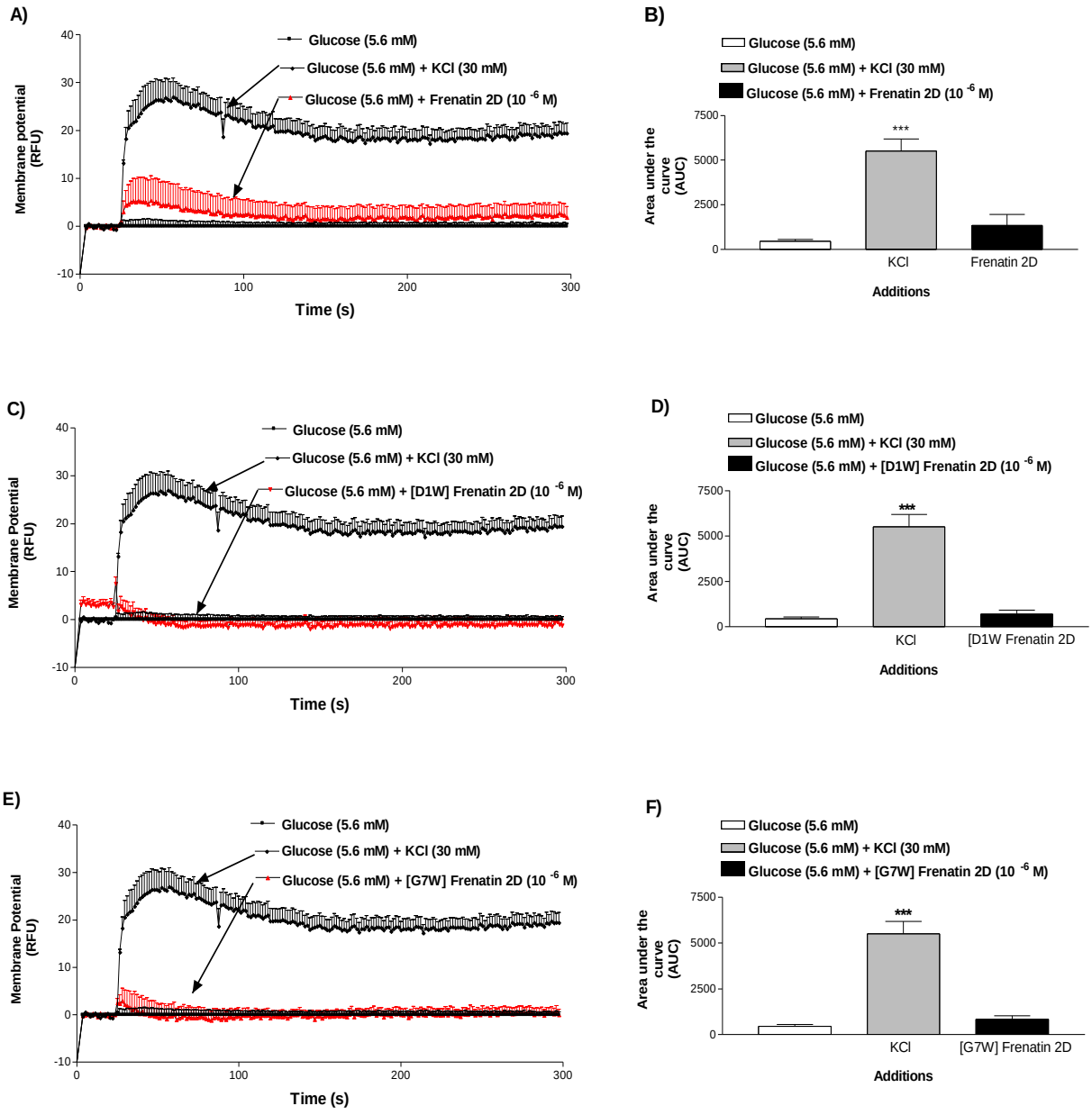

Effects of frenatin 2D (A), [D1W] frenatin 2D (C), [G7W] frenatin 2D (E) on membrane potential in BRIN-BD11 cells expressed as relative fluorescence units, RFU as a function of time and (B), (D) and (F) the integrated response (area under the curve) for respective peptide. Peptides were added 20 sec after start of data acquisition at a rate of ~62 µl/sec. Values are mean ± SEM (n = 6). ***P < 0.001 compared with 5.6 mM glucose alone.

Figure 4.19 Effects of frenatin 2D and its synthetic analogues ([D1W] frenatin 2D and [G7W] frenatin 2D) on intracellular calcium in BRIN-BD11 rat clonal β-cells expressed as line graph (A, C, E) and area under the curve (B, D, F)

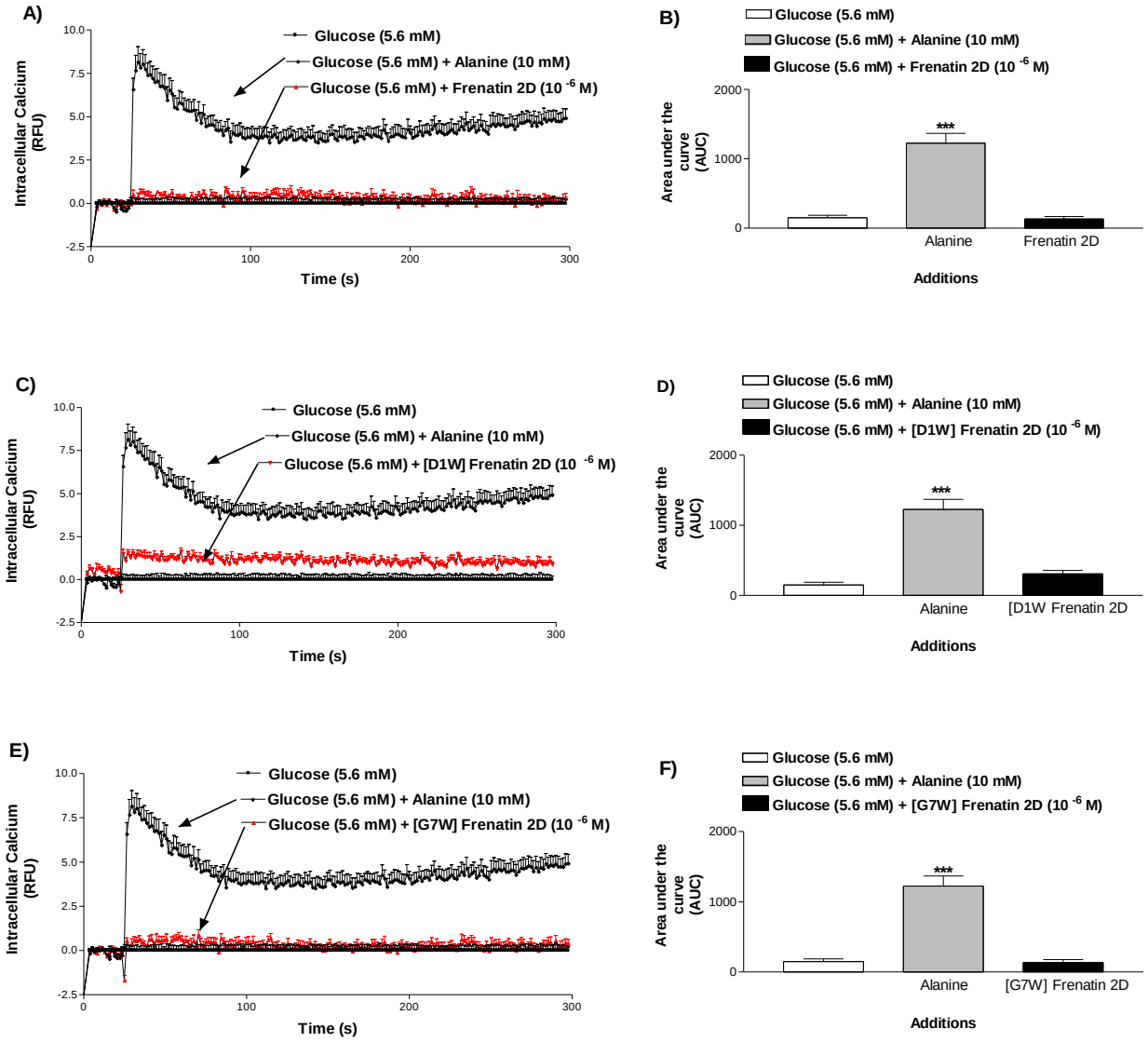

Effects of frenatin 2D (A), [D1W] frenatin 2D (C), [G7W] frenatin 2D (E) on intracellular calcium ion concentration $[Ca^{2+}]_i$ in BRIN-BD11 cells expressed as relative fluorescence units, RFU as a function of time and (B), (D) and (F) the integrated response (area under the curve) for respective peptide. Peptides were added 20 sec after start of data acquisition at a rate of ~62 µl/sec. Values are mean ± SEM for n = 6. ***P<0.001 compared with 5.6 mM glucose alone.

Figure 4.20 Effects of frenatin 2D and its synthetic analogues ([D1W] frenatin 2D and [G7W] frenatin 2D) on insulin release from BRIN-BD11 rat clonal β-cells in the presence of known modulators of insulin release

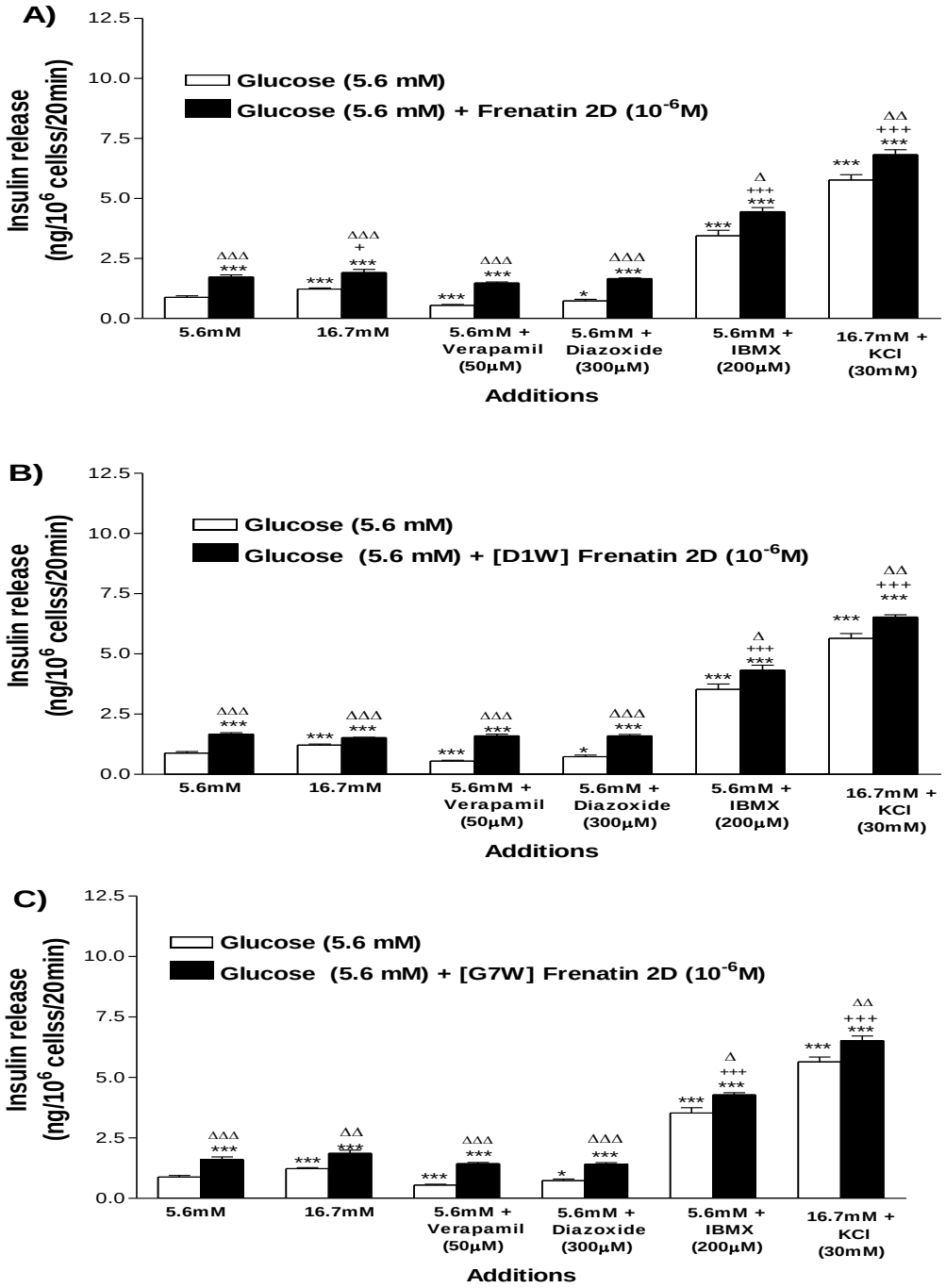

Values are Mean ± SEM (n=8). *P<0.05, ***P<0.001 compared to 5.6 mM glucose alone. $^{+++}$P<0.001 compared to 5.6 mM glucose in the presence of the peptide. $^{\Delta}$P<0.05, $^{\Delta\Delta}$P<0.01, $^{\Delta\Delta\Delta}$P<0.001 compared to respective incubation in the absence of the peptide.

Figure 4.21 Effects of frenatin 2D and its synthetic analogues ([D1W] frenatin 2D and [G7W] frenatin 2D) on insulin release from BRIN-BD11 rat clonal β-cells in the presence or absence of extracellular calcium

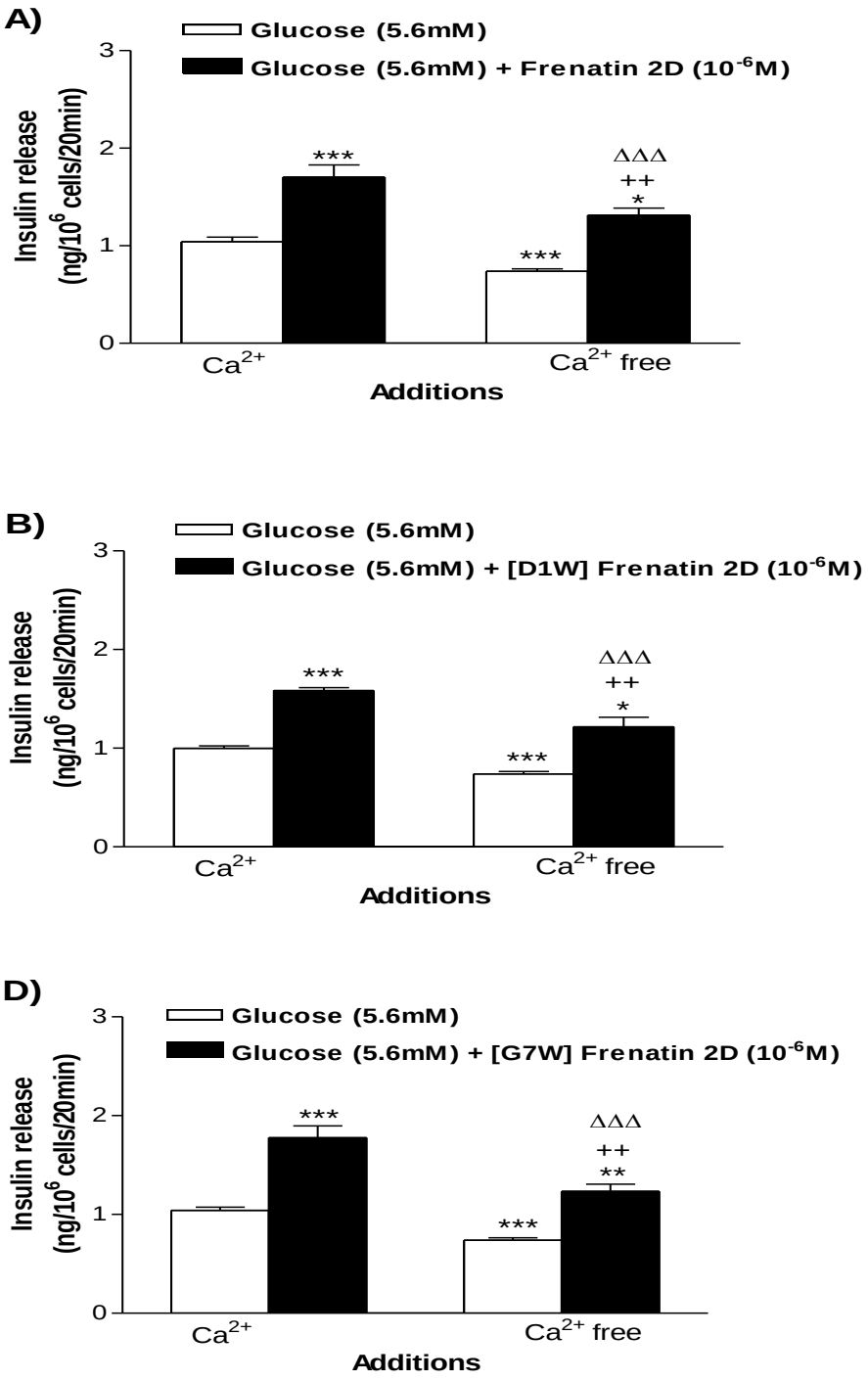

Values are Mean ± SEM (n=8). *P<0.05, **P<0.01, ***P<0.001 compared to 5.6 mM glucose alone. $^{++}$P<0.01 compared to 5.6 mM glucose in the presence of the peptide. $^{\Delta\Delta\Delta}$P<0.001 compared to respective incubation in the absence of the peptide.

Figure 4.22 Effects of frenatin 2D on insulin release in the presence of chloride channel blocker DIDS from BRIN-BD11 rat clonal β-cells

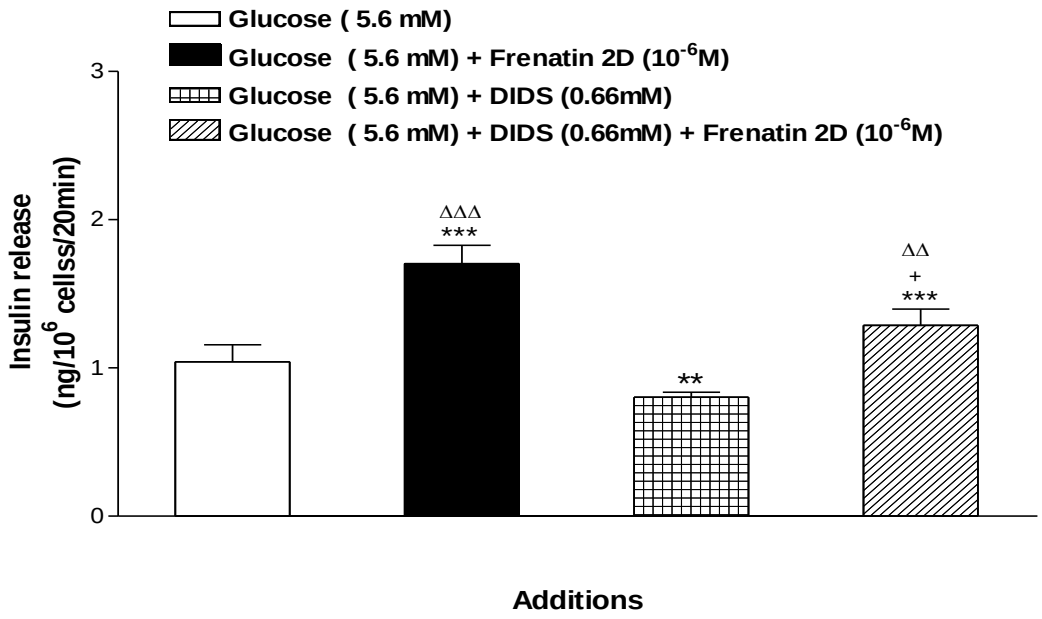

Values are mean ± SEM (n=8). **P<0.01, ***P<0.001 compared to 5.6 mM glucose alone. $^{+}$P<0.05 compared to 5.6 mM glucose in the presence of the peptide. $^{\Delta\Delta}$P<0.01, $^{\Delta\Delta\Delta}$P<0.001 compared to respective incubation in the absence of the peptide.

Figure 4.23 Effects of frenatin 2D and its synthetic analogues ([D1W] frenatin 2D and [G7W] frenatin 2D) on cyclic AMP in BRIN-BD11 rat clonal β-cells

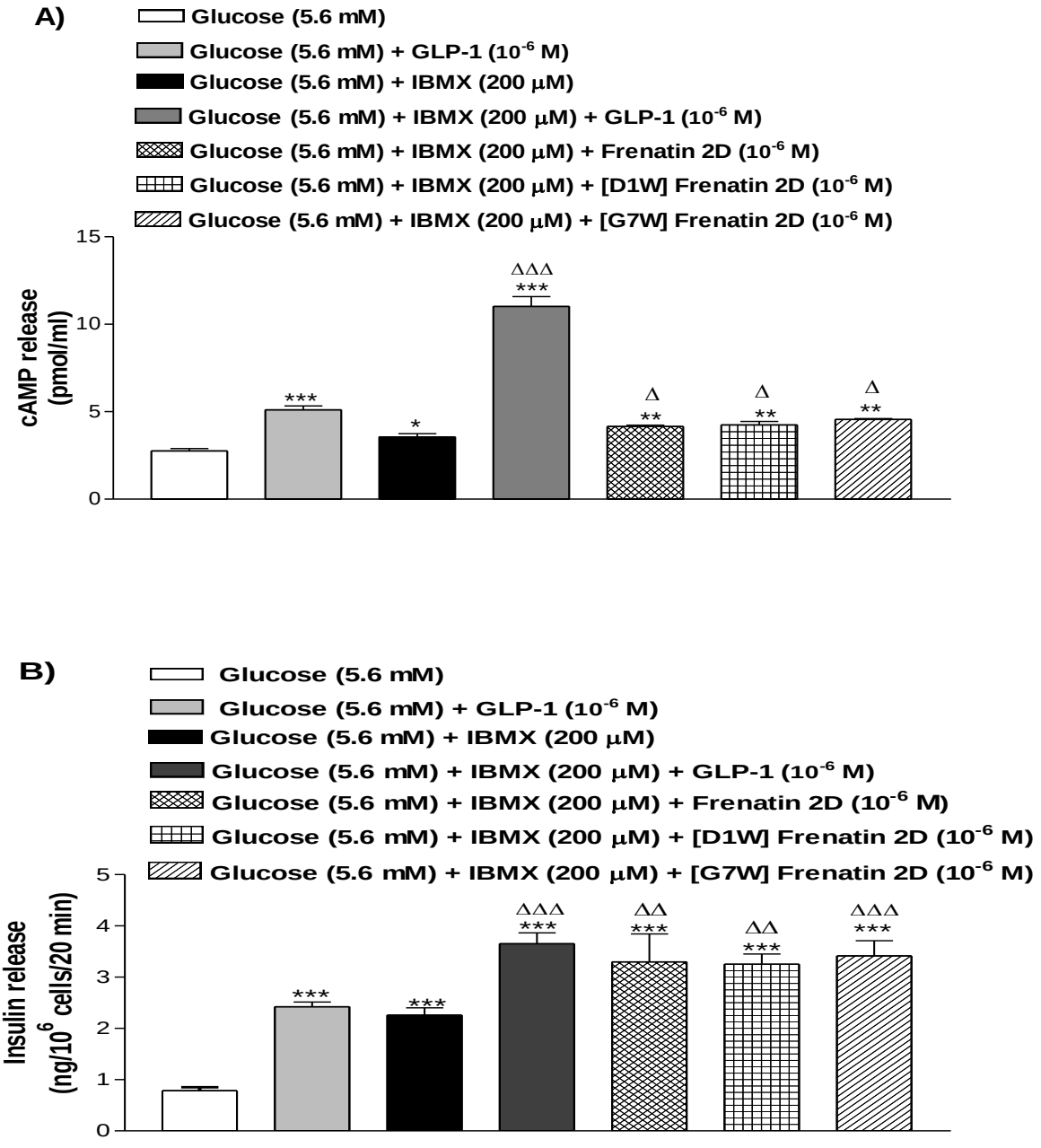

Effects of frenatin 2D peptides on A) cAMP production and B) Insulin release in BRIN-BD11 cells. Values are Mean ± SEM with n=3 for cAMP and n=4 for insulin release. *P<0.05, **P<0.01, ***P<0.001 compared to 5.6mM glucose alone. $^{\Delta}$P<0.05, $^{\Delta\Delta}$P<0.01, $^{\Delta\Delta\Delta}$P<0.001 compared to 5.6mM glucose + IBMX.

Figure 4.24 Effects of frenatin 2D and its synthetic analogues ([D1W] frenatin 2D and [G7W] frenatin 2D) on down-regulation of the PKA and PKC pathways in BRIN-BD11 rat clonal β-cells

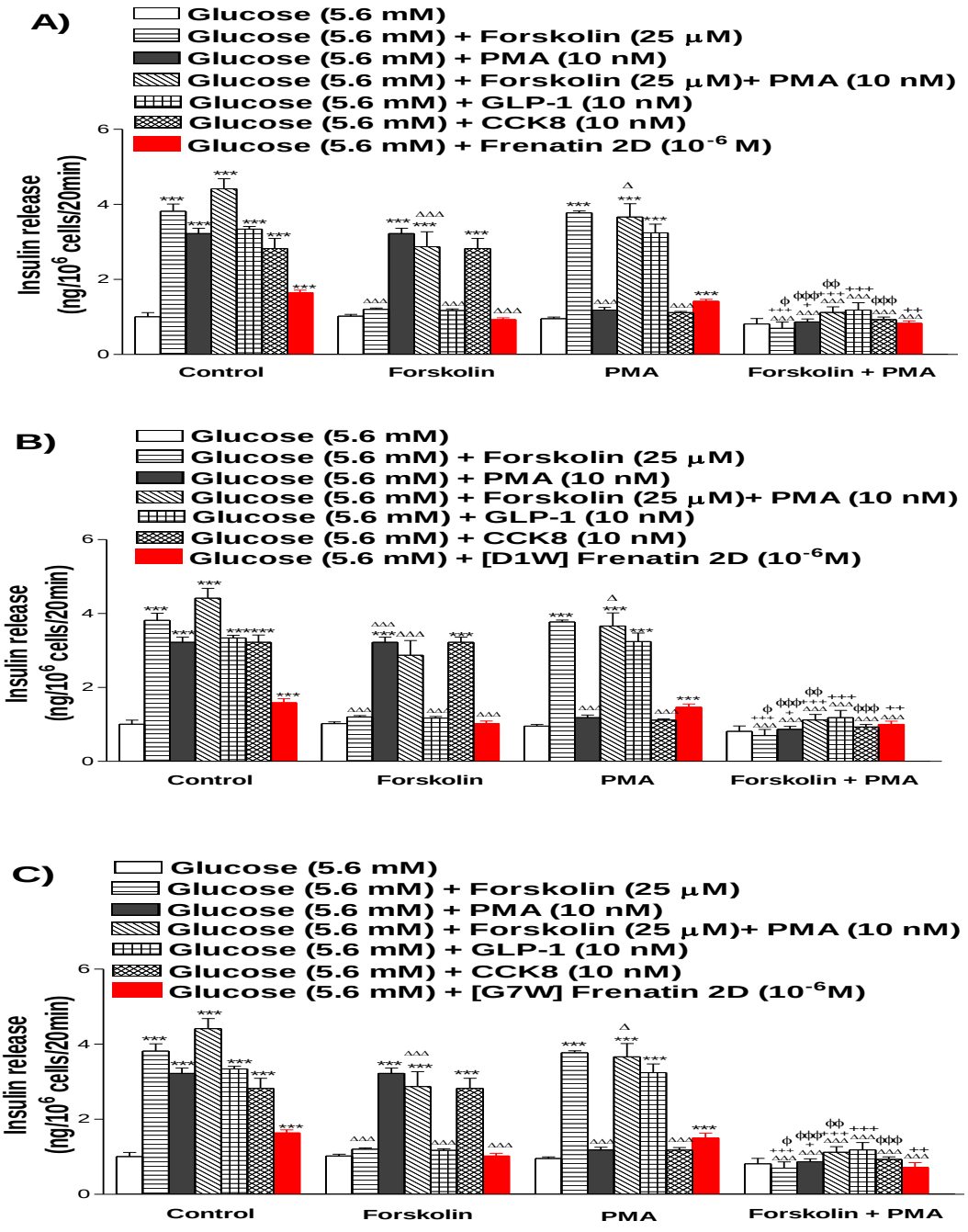

Values are mean ± SEM for n = 8. ***P<0.001 compared with 5.6 mM glucose, $^{\Delta\Delta\Delta}$P<0.001, $^{\Delta}$P<0.05 compared to standard culture conditions, $^{+++}$P<0.001, $^{++}$P<0.01, $^{+}$P<0.05 compared to culture with PMA, $^{\varphi\varphi\varphi}$P<0.001, $^{\varphi\varphi}$P<0.01, $^{\varphi}$P<0.05 compared with culture with forskolin.

Figure 4.25 Effect of frenatin 2D and its synthetic analogues ([D1W] frenatin 2D and [G7W] frenatin 2D) on cytokine-induced apoptosis in BRIN-BD11 rat clonal β-cells

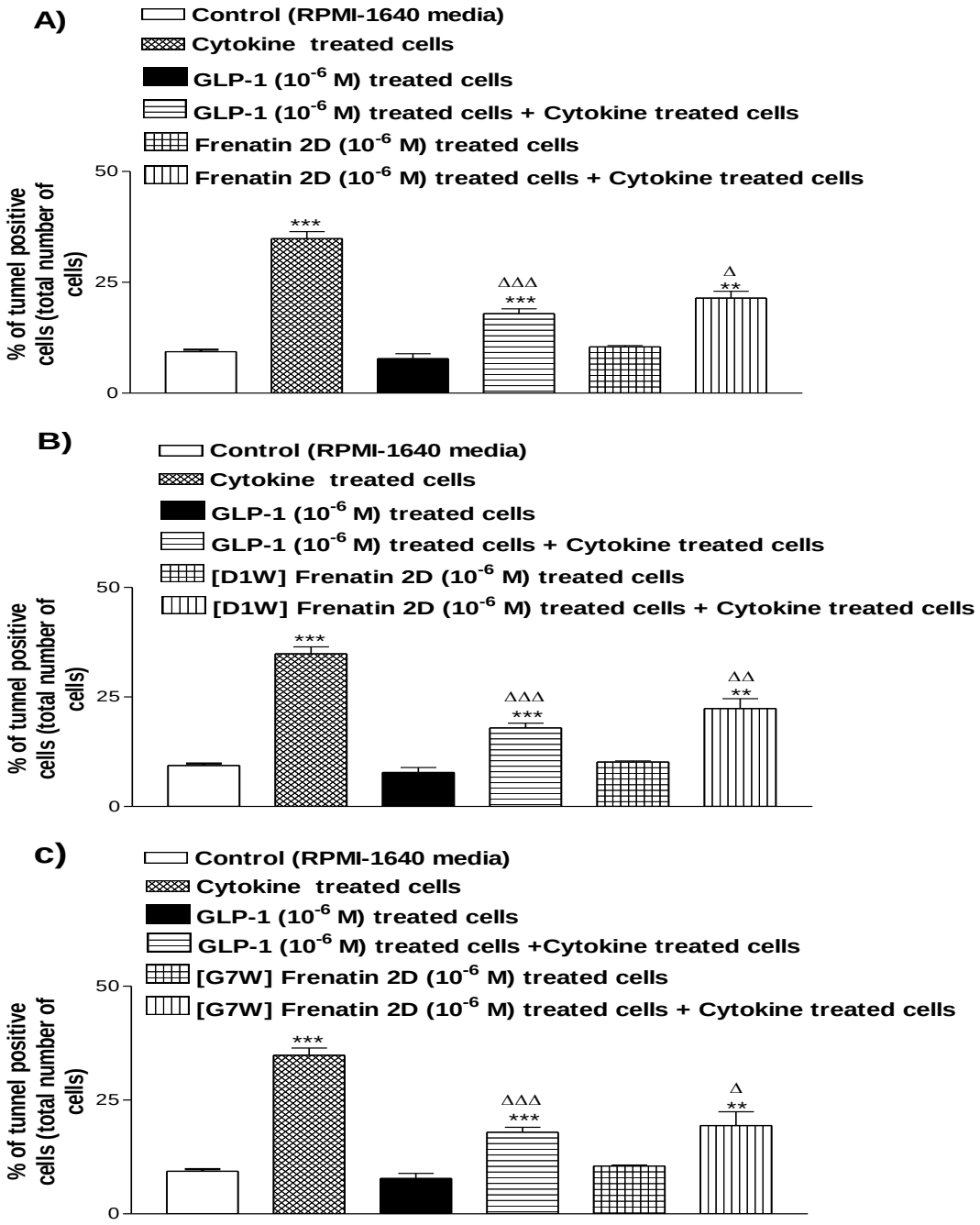

Effects of 1 µM A) frenatin 2D, B) [D1W] and C) [G7W] frenatin 2D on apoptosis in BRIN-BD11 cells compared with 1 µM GLP-1. Values are mean ± SEM for n=3. **P<0.01, ***P<0.001 compared with incubation in culture medium alone, $^{\Delta}$P<0.05, $^{\Delta\Delta}$P<0.01 and $^{\Delta\Delta\Delta}$P<0.001 compared with incubation in cytokine-containing medium.

Figure 4.26 Effect of frenatin 2D and its synthetic analogues ([D1W] frenatin 2D and [G7W] frenatin 2D) on proliferation in BRIN-BD11 rat clonal β-cells

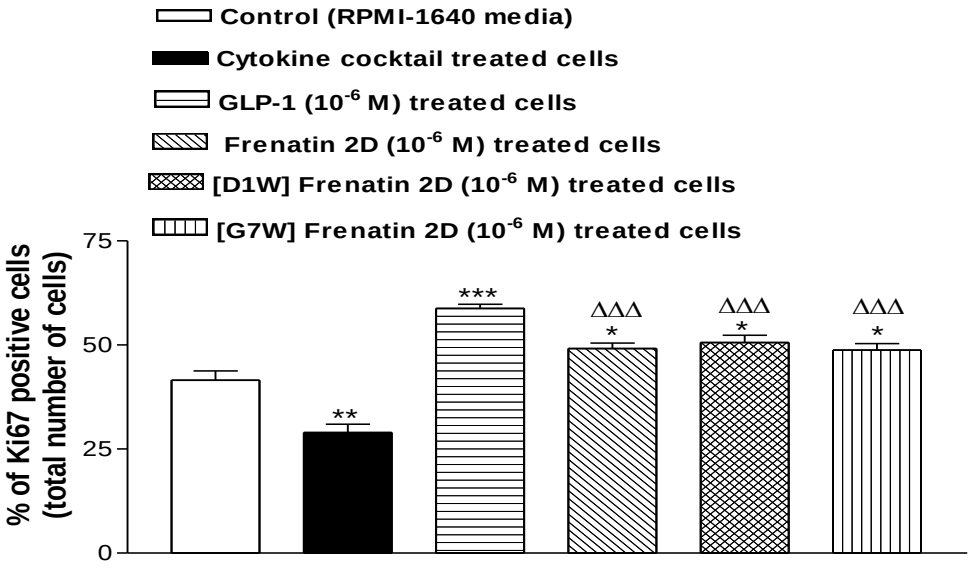

Effects of 1 µM Frenatin 2D and [D1W], [G7W] analogues on proliferation in BRIN-BD11 cells compared with 1 µM GLP-1. Values are mean ± SEM Values are mean ± SEM for n=3. *P<0.05, **P<0.01, ***P<0.001 compared with incubation in culture medium alone, $^{\Delta\Delta\Delta}$P<0.001 compared to GLP-1 treated cells.

Figure 4.27 HPLC profile of Plasma degradation of frenatin 2D at 0 hrs (A) and 4 hrs (B)

A)

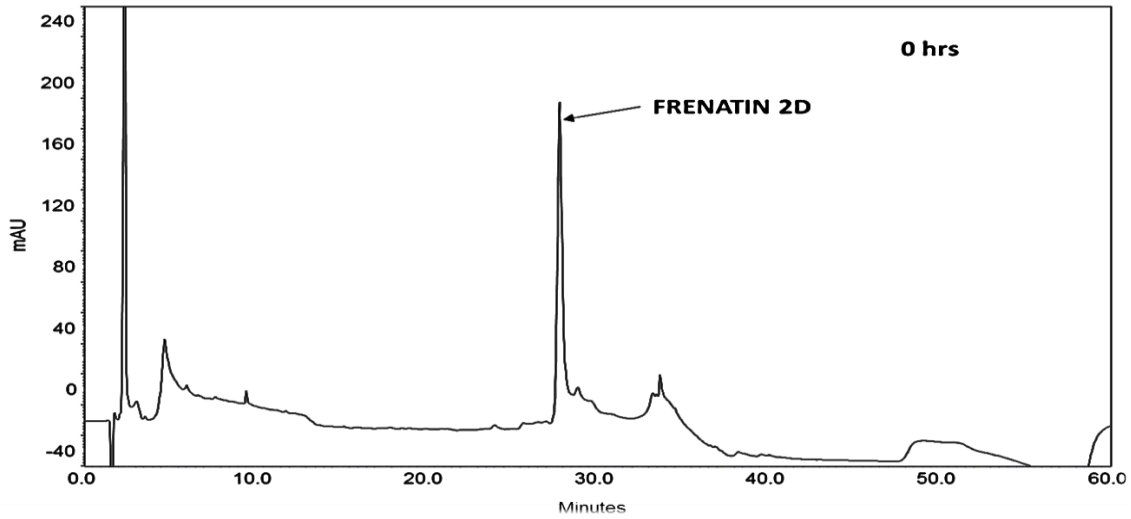

B)

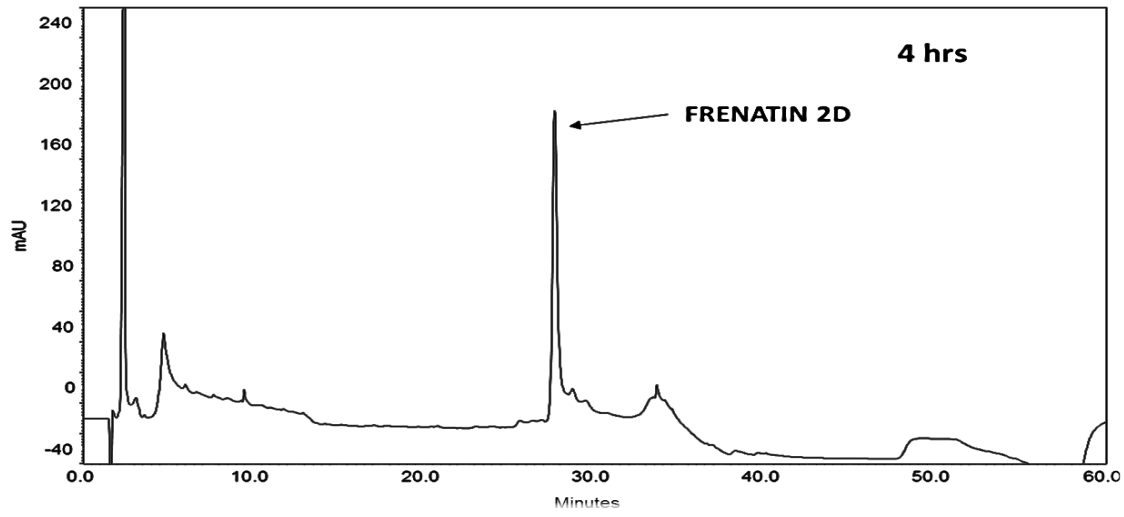

HPLC profile of frenatin 2D following incubation with Swiss lean mice plasma for 0 and 4 hrs. The fraction was separated with a C8 column using a gradient from 0 to 40% acetonitrile from 0 to 10 min, to 60% over 30 min.

Figure 4.28 MALDI-TOF spectra of plasma degradation of frenatin 2D fraction collected at 4 hrs

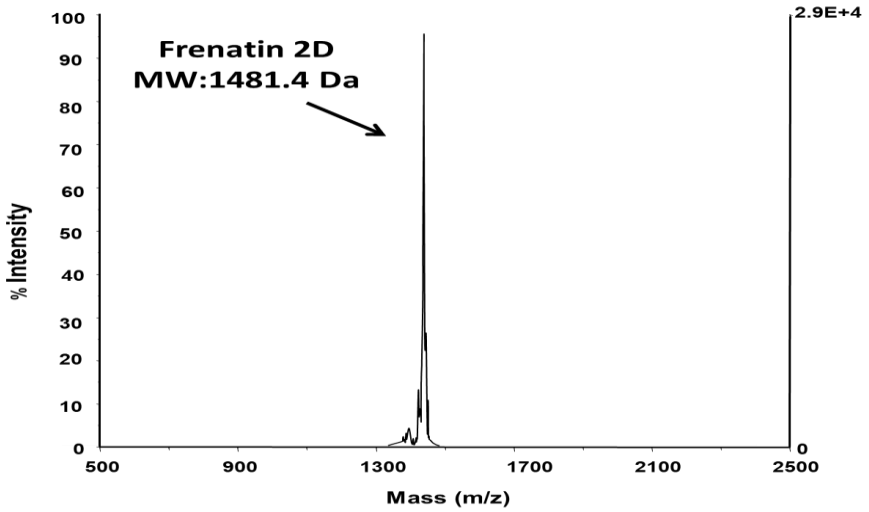

Peptide samples (1.5 µl) were mixed with matrix α-cyanocinnamic acid (1.5 µl) on a 100 well MALDI plate and left to dry. After complete drying, samples were applied to a Voyager DE Biospectrometry workstation. The mass-to-charge ratio (m/z) versus peak intensity was recorded**.**

Figure 4.29 Effect of insulin on glucose uptake in differentiated C2C12 cells

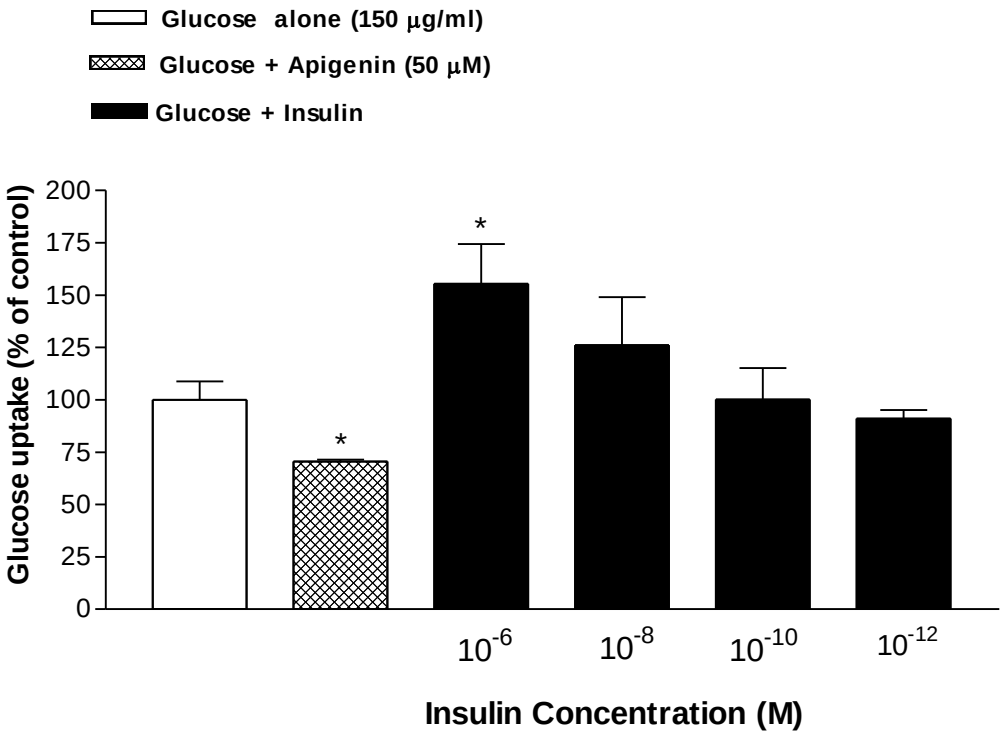

Glucose uptake was expressed as % of control (glucose). Apigenin was used as negative control for glucose uptake. Values are Mean ± SEM with n=3. *P<0.05 compared with glucose alone.

Figure 4.30 Effect of frenatin 2D and its synthetic analogues ([D1W] frenatin 2D and [G7W] frenatin 2D) on glucose uptake in differentiated C2C12 cells

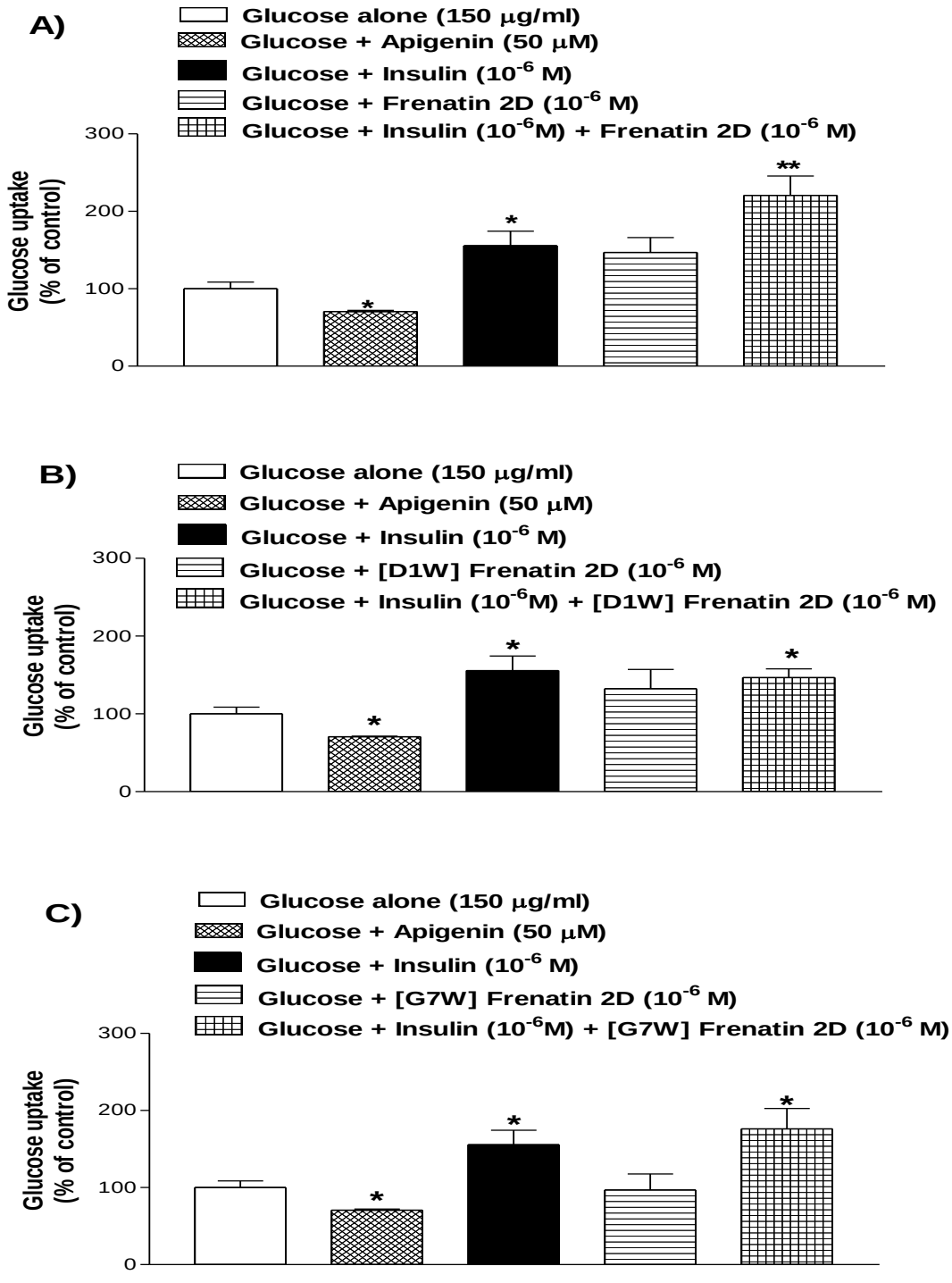

Glucose uptake was expressed as % of control (glucose). Apigenin was used as negative control for glucose uptake. Values are Mean ± SEM with n=3. *P<0.05, **P<0.01 compared with glucose alone.

Figure 4.31 Acute effect of frenatin 2D and its synthetic analogues ([D1W] frenatin 2D and [G7W] frenatin 2D) on cumulative food intake in 21 hr fasted lean NIH Swiss TO mice

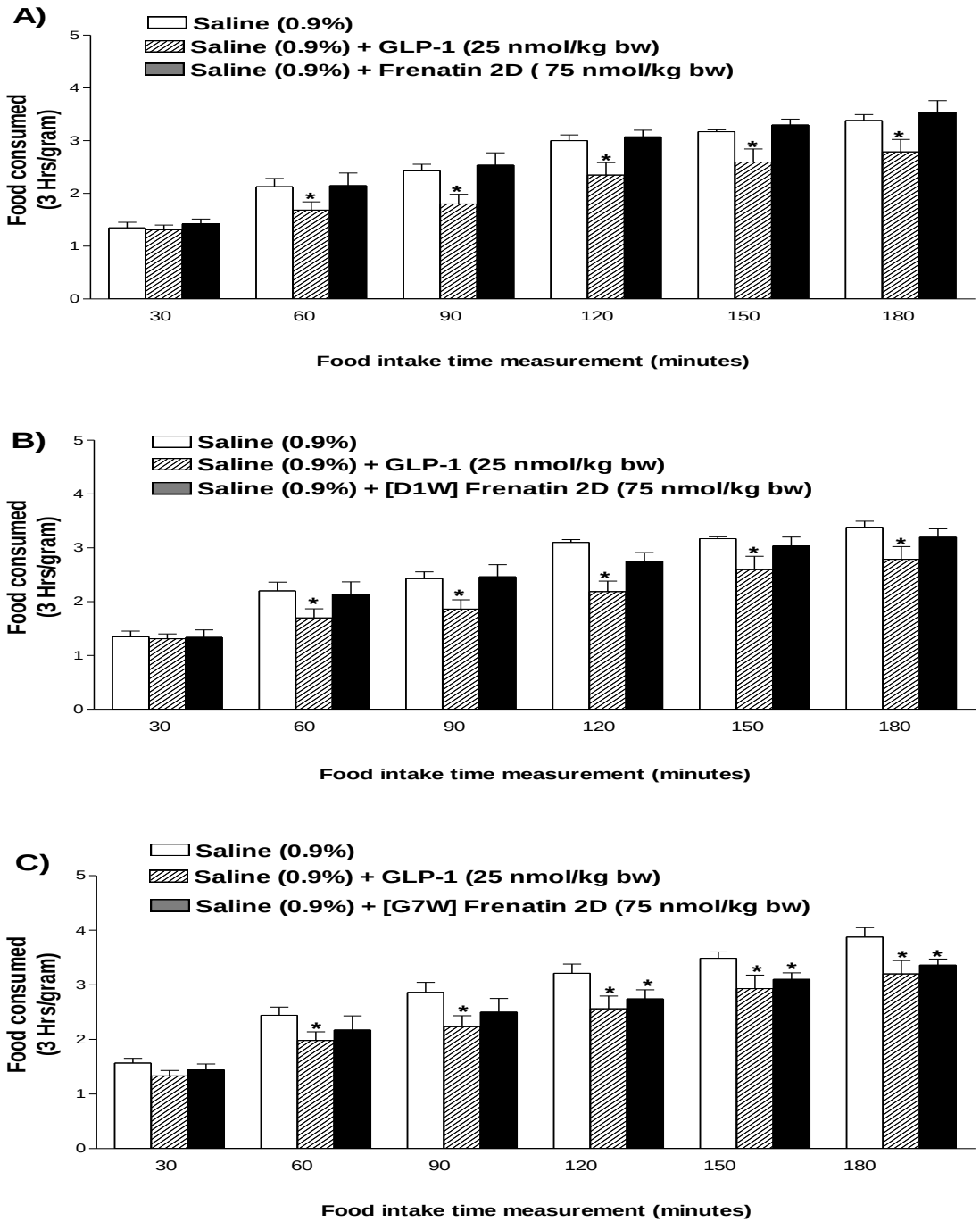

Cumulative food intake was measured before at 0 min and after i.p. injection of saline vehicle (0.9% w/v NaCl) or GLP-1 (25 nmol/kg bw) or test peptides (75 nmol/kg bw) at time point 30, 60, 90, 120, 150, 180 min in overnight (21 hr) fasted mice. Values represent mean ± SEM (n=8). *P<0.05 compared to saline control.

Figure 4.32 Effects of frenatin 2D and its synthetic analogues ([D1W] frenatin 2D and [G7W] frenatin 2D) on glucose tolerance and insulin concentrations in mice

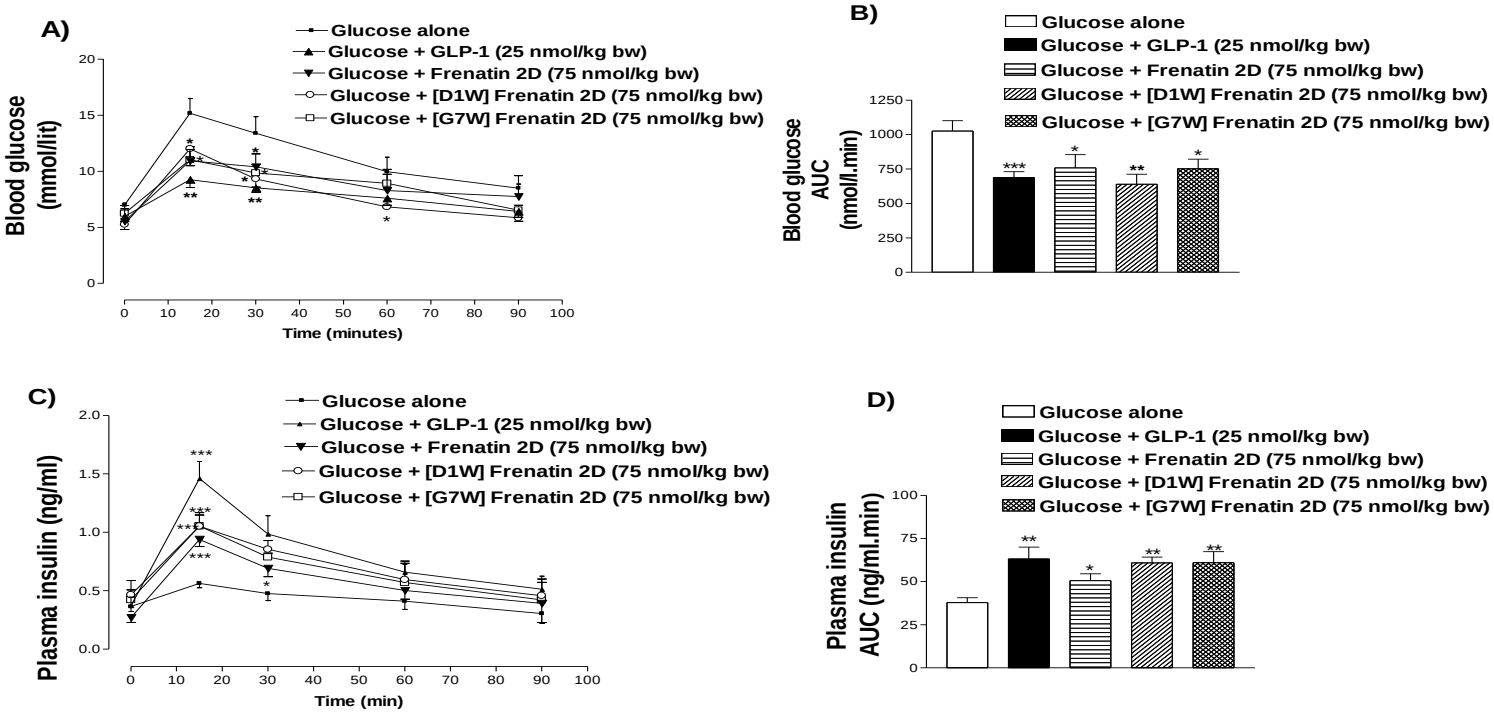

A comparison of the effects of intraperitoneal administration of frenatin 2D peptides (75 nmol/kg body weight) and GLP-1 (25 nmol/kg body weight) on blood glucose (panels A and B) and plasma insulin (panels C and D) concentrations in lean mice after co-injection of glucose (18 mmol/ kg body weight). Values are mean ± SEM (n = 6). *P<0.05, **P<0.01 and ***P<0.001 compared with glucose alone.

Figure 4.33 Effects of 2 hours pre-treatment with frenatin 2D and its synthetic analogues ([D1W] frenatin 2D and [G7W] frenatin 2D) on blood glucose levels expressed as line graph (A) and area under the curve (B) in lean NIH Swiss TO mice

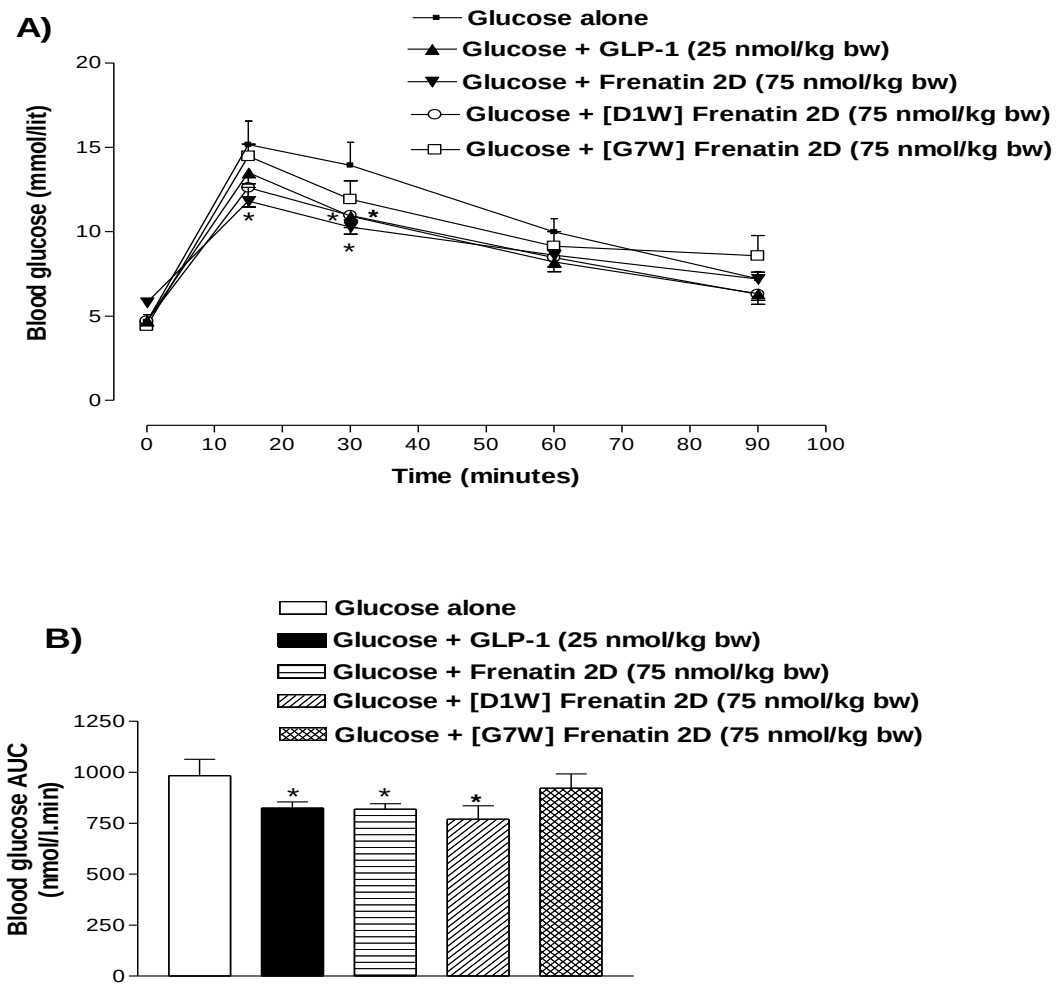

Blood glucose was measured before and after intraperitoneal injection of glucose (18 mmol/kg bw, control) in lean NIH Swiss TO mice treated with saline or GLP-1 (25 nmol/kg bw) or frenatin 2D peptides (75 nmol/kg bw) 2 hr prior to experiment. Values are mean ± SEM (n=6). *P<0.05 compared to control.

Figure 4.34 Effects of 4 hours pre-treatment with frenatin 2D and its synthetic analogues ([D1W] frenatin 2D and [G7W] frenatin 2D) on blood glucose levels expressed as line graph (A) and area under the curve (B) in lean NIH Swiss TO mice

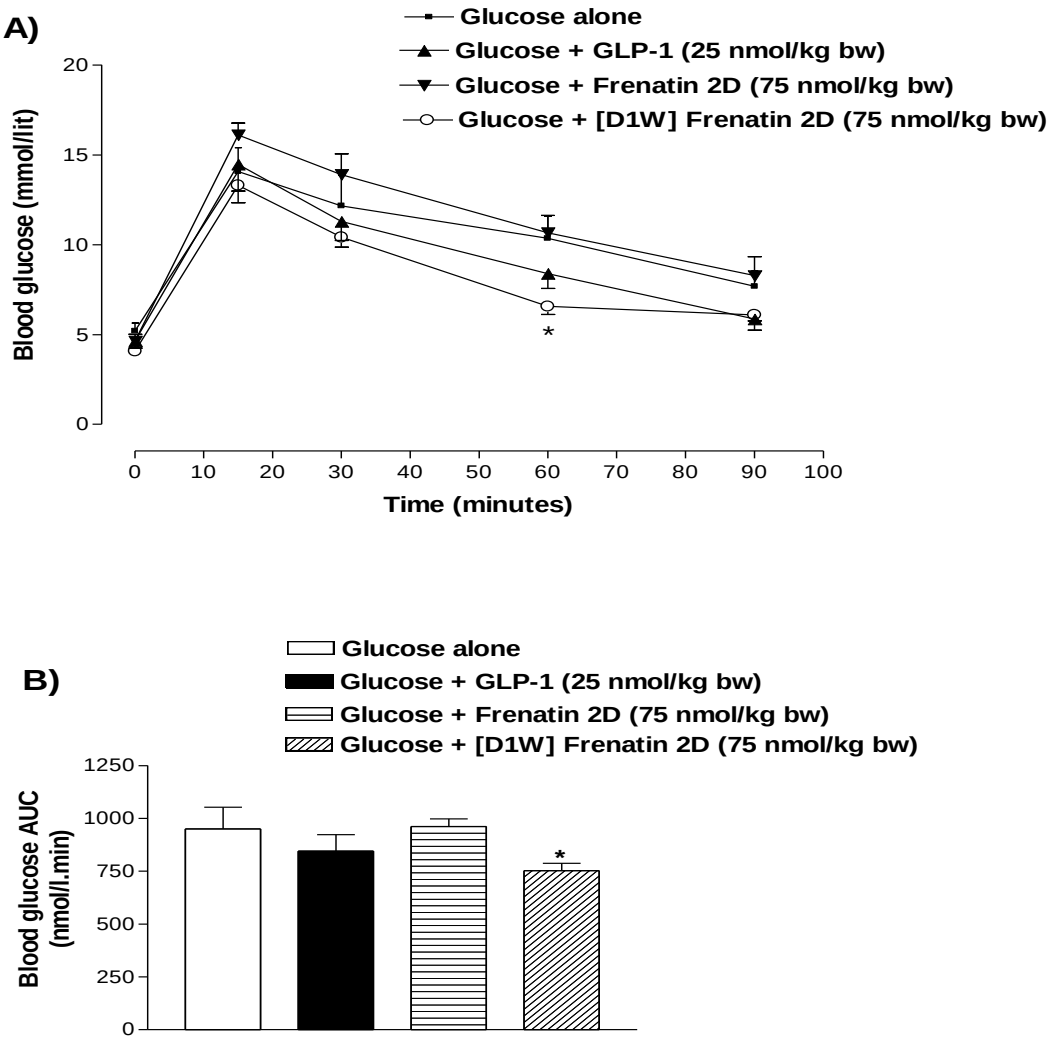

Blood glucose was measured before and after intraperitoneal injection of glucose (18 mmol/kg bw, control) in lean NIH Swiss TO mice treated with saline or GLP-1 (25 nmol/kg bw) or frenatin 2D peptides (75 nmol/kg bw) 4 hr prior to experiment. Values are mean ± SEM (n=6). *P<0.05 compared to control.

Figure 4.35 Acute effects of frenatin 2D and its synthetic analogues ([D1W] frenatin 2D and [G7W] frenatin 2D) on blood glucose levels expressed as line graph (A, C) and area under the curve (B, D) in lean NIH Swiss TO mice

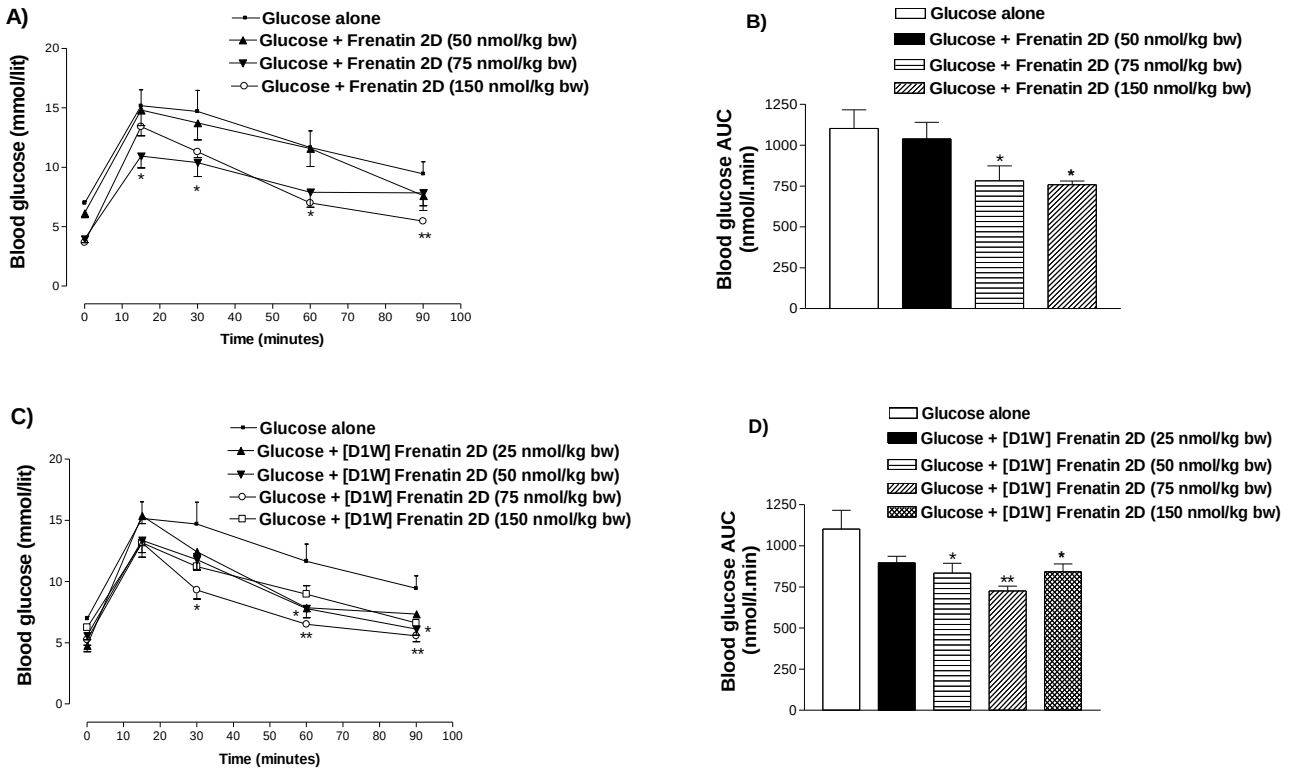

Blood glucose was measured before and after intraperitoneal administration of glucose (18 mmol) or in combination with frenatin 2D (50/75/150 nmol/kg body weight) or [D1W] Frenatin 2D (25/50/75/150 nmol/kg body weight) in NIH Swiss TO mice. Values are mean ± SEM (n=6). *P<0.05, **P<0.01 compared to glucose alone mice.

Figure 4.36 Effects of 28-day treatment with frenatin 2D and its synthetic analogue [D1W] frenatin 2D on body weight (A, B), energy intake (C, D) and water Intake (E, F) in *db/db* mice

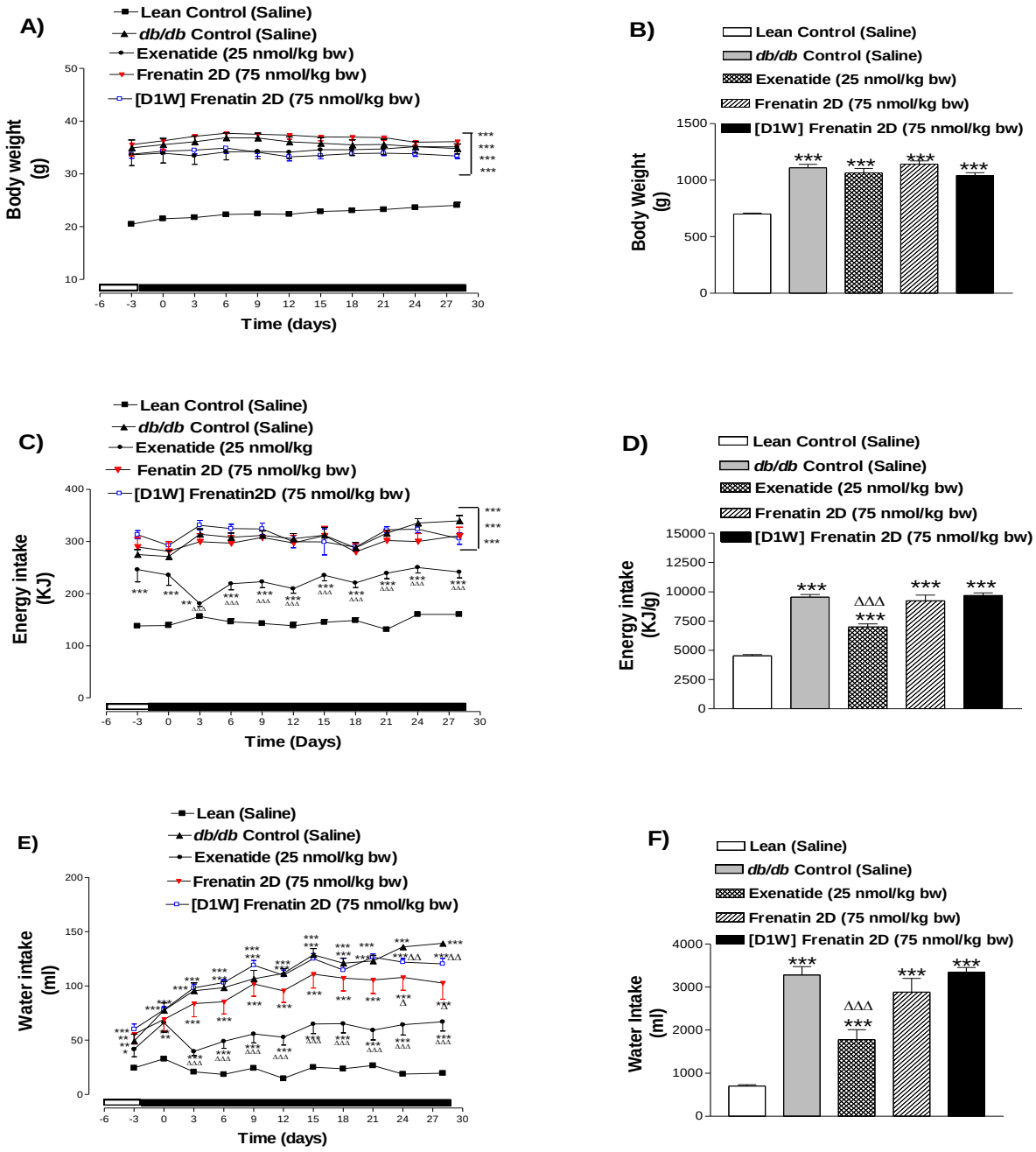

Body weight, energy intake and water intake were measured 3 days prior to, and every 72 hours during treatment with saline or exenatide (25 nmol/kg bw) or peptide (75 nmol/kg bw) for 28 days. Values are mean ±SEM for 8 mice. *P<0.05, **P<0.01 ***P<0.001 compared to lean mice and $^{\Delta}$P<0.05, $^{\Delta\Delta}$P<0.01, $^{\Delta\Delta\Delta}$P<0.001compared to control *db/db* mice.

Figure 4.37 Effects of 28-day treatment with frenatin 2D and its synthetic analogue [D1W] frenatin 2D on non-fasting blood glucose (A, B) and plasma insulin (C, D) in *db/db* mice

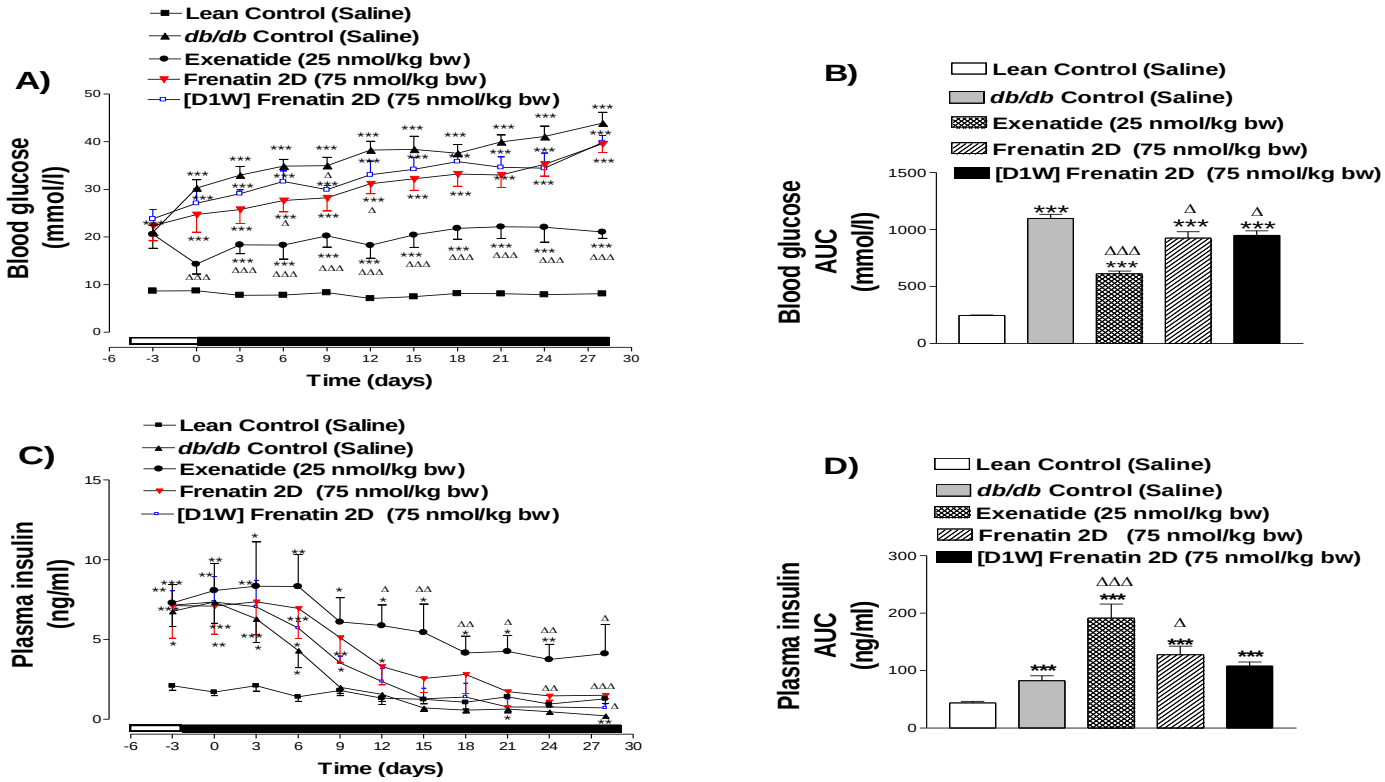

Parameters were measured 3 days prior to, and every 72 hours during treatment (indicated with black bar) with saline or exenatide (25 nmol/kg bw) or peptide (75 nmol/kg bw) for 28 days. Values are mean ±SEM for 8 mice. *P<0.05, **P<0.01 ***P<0.001 compared to lean mice and $^{\Delta}$P<0.05, $^{\Delta\Delta}$P<0.01, $^{\Delta\Delta\Delta}$P<0.001 compared to control *db/db* mice.

Figure 4.38 Effects of frenatin 2D and its synthetic analogue [D1W] frenatin 2D on HbA1c in *db/db* mice

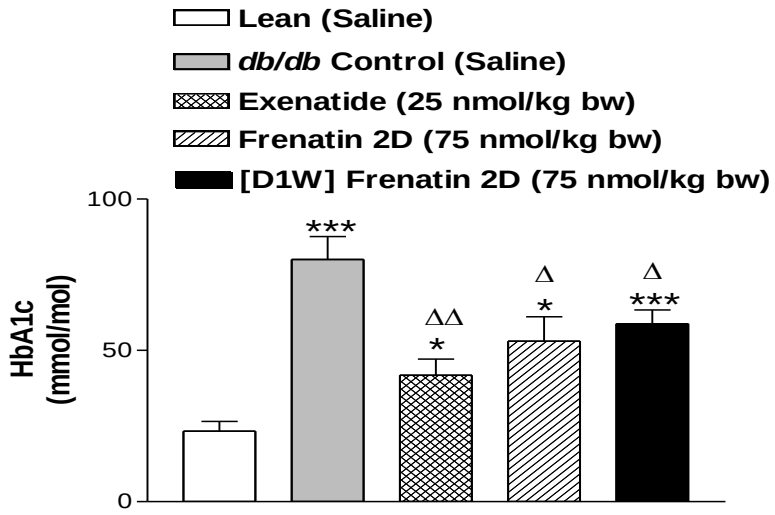

HbA1c level was measured after long term treatment with twice-daily injections of either saline or exenatide (25 nmol/kg bw) or peptide (75 nmol/kg bw) for 28 days. Values are mean ± SEM for 4 mice. ***P<0.001, **P<0.01, *P<0.05 compared with lean mice and $^{\Delta}$P<0.05, $^{\Delta\Delta}$P<0.01compare with *db/db* control mice.

Figure 4.39 Long-term effects of frenatin 2D and its synthetic analogue [D1W] frenatin 2D on plasma glucose (A, B) and insulin (C, D) concentrations following intraperitoneal glucose administration to *db/db* mice

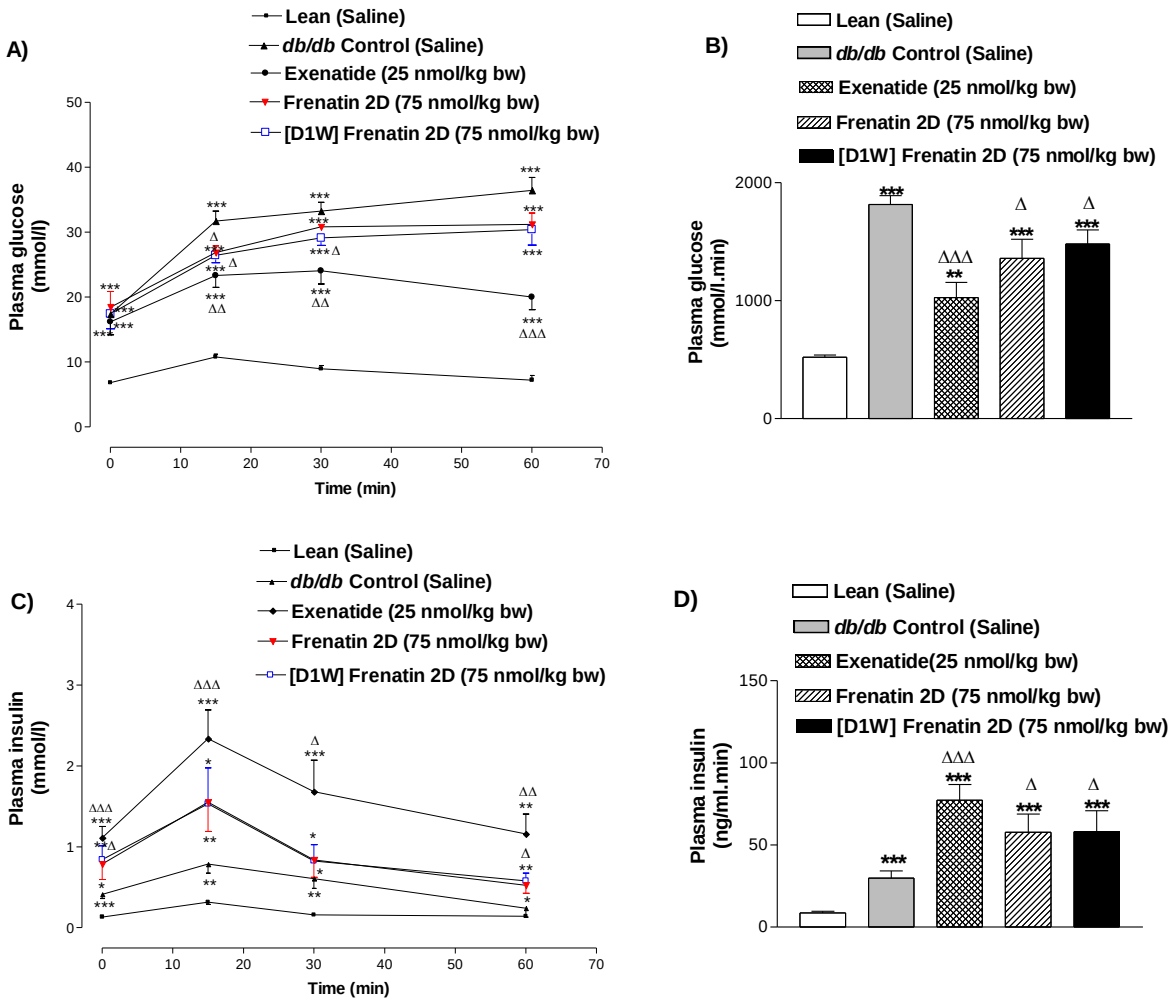

Plasma glucose and insulin concentrations were measured prior to and after intraperitoneal administration of glucose (18 mmol/kg bw) to *db/db* mice pre-treated with twice-daily injections of either saline or exenatide (25 nmol/kg bw) or peptide (75 nmol/kg bw) for 28 days. Values are mean ± SEM for 8 mice. *P<0.05, **P<0.01 ***P<0.001 compared to lean mice and $^{\Delta}$P<0.05, $^{\Delta\Delta}$P<0.01, $^{\Delta\Delta\Delta}$P<0.001compared to control *db/db* mice.

Figure 4.40 Long-term effects of frenatin 2D and its synthetic analogue [D1W] frenatin 2D on plasma glucose (A, B) and insulin (C, D) concentrations following oral glucose administration to *db/db* mice

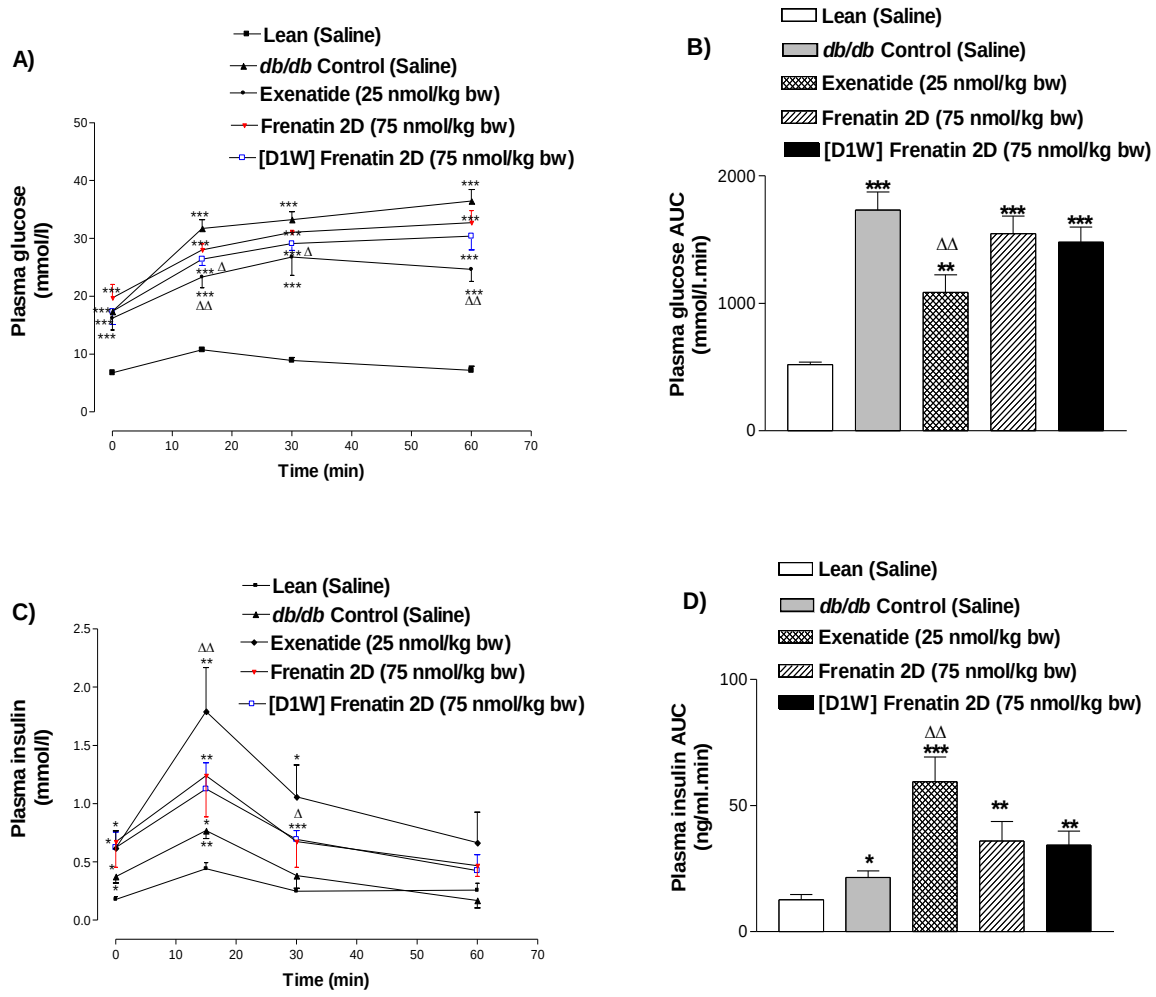

Plasma glucose and insulin concentrations were measured prior to and after oral administration of glucose (18 mmol/kg bw) to *db/db* mice pre-treated with twice-daily injections of either saline or exenatide (25 nmol/kg bw) or peptide (75 nmol/kg bw) for 28 days. Values are mean ± SEM for 8 mice. *P<0.05, **P<0.01 ***P<0.001 compared to lean mice and $^{\Delta}$P<0.05, $^{\Delta\Delta}$P<0.01 compared to control *db/db* mice.

Figure 4.41 Long-term effects of frenatin 2D and its synthetic analogue [D1W] frenatin 2D on insulin sensitivity in *db/db* mice

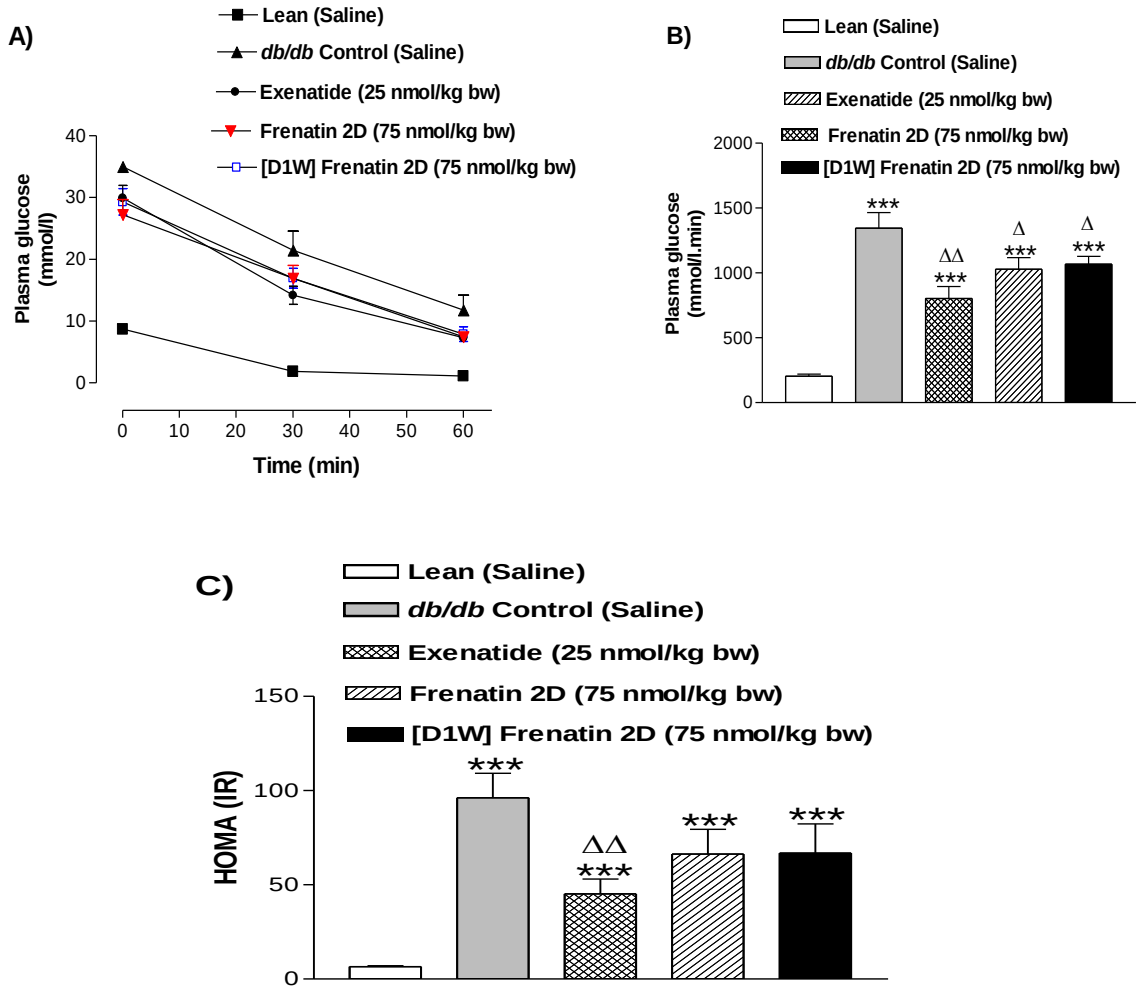

Plasma glucose was measured prior to and after intraperitoneal injection of insulin (50 U/kg bw) in *db/db* mice pre-treated with twice-daily injections of either saline or exenatide (25 nmol/kg bw) or peptide (75 nmol/kg bw) for 28 days. Values are mean ± SEM for 8 mice. ***P<0.001 compared with lean mice and $^{\Delta}$P<0.05, $^{\Delta\Delta}$P<0.01 compare with *db/db* control mice.

Figure 4.42 Effects of frenatin 2D and its synthetic analogue [D1W] frenatin 2D on body composition in *db/db* mice

A)

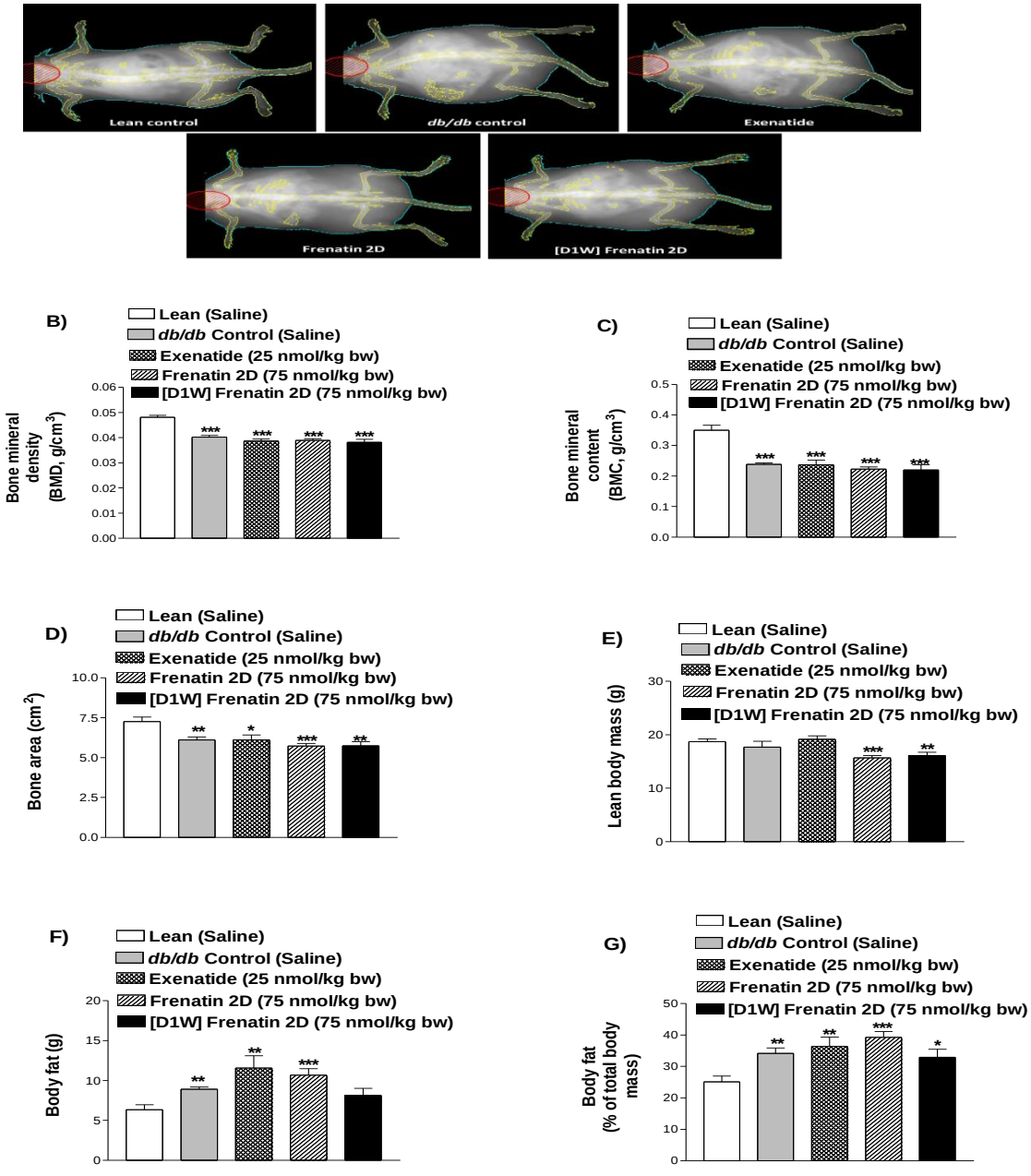

Effects of frenatin 2D and [D1W] frenatin 2D on body composition in lean and *db/db* mice. Animals were injected with either saline or peptide (25/75 nmol/kg bw) for 28 days. The figure shows (A) representative DEXA scans, (B) bone mineral density, (C) bone mineral content, (D) bone area. (E) lean body mass, (F) body fat and (G) body fat expressed a percentage of total body mass. Values are mean ± SEM for 8 mice. *P<0.05, **P<0.01, ***P<0.001 compared with saline-treated lean mice.

Figure 4.43 Effects of frenatin 2D and its synthetic analogue [D1W] frenatin 2D on pancreatic weight (A), total insulin content (B), and insulin secretory response of isolated islets (C&D) from lean, and *db/db* mice treated

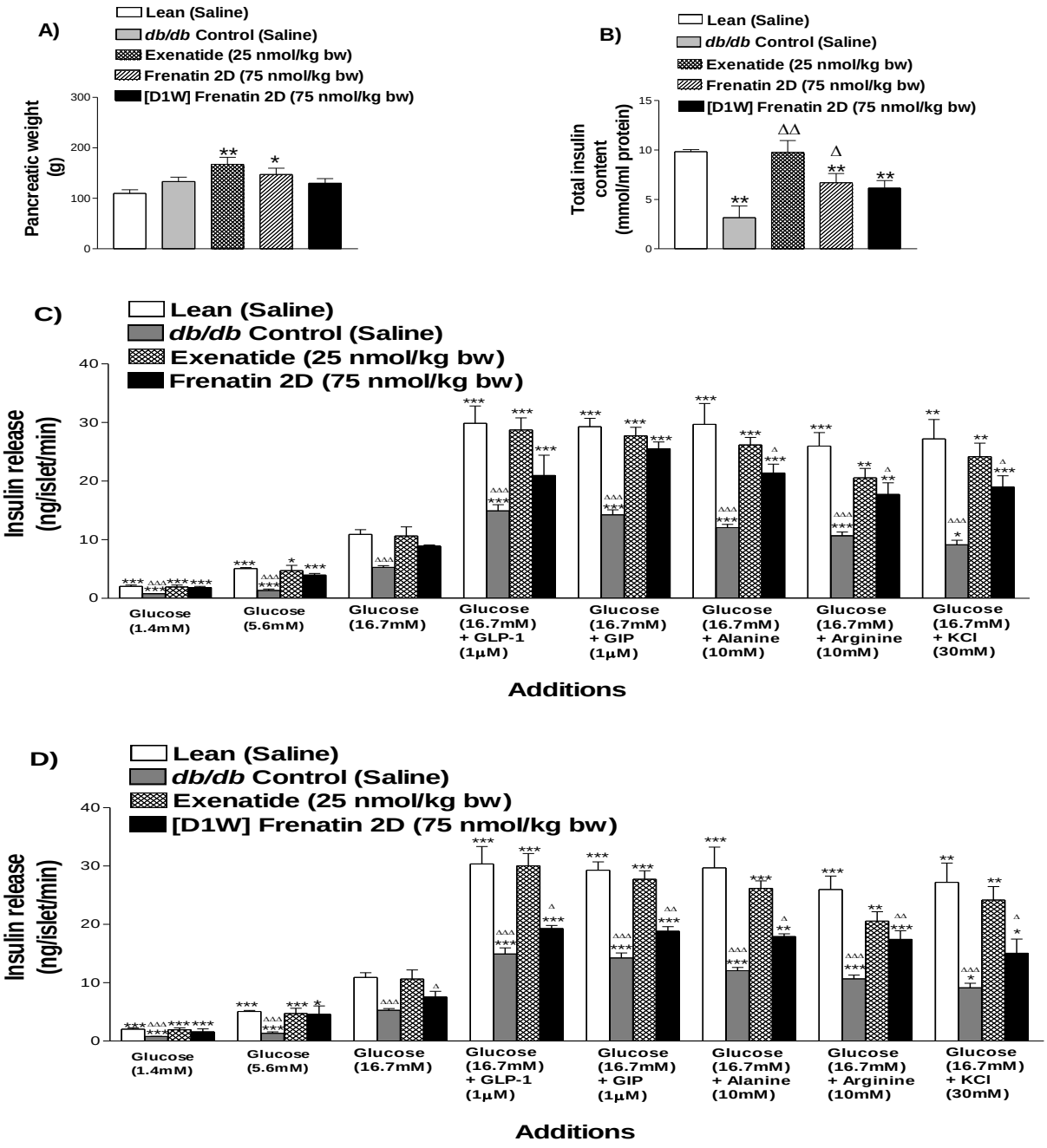

Mice were treated with saline or exenatide (25 nmol/kg bw) or peptide (75 nmol/kg bw) for 28 days prior to the experiment. Values are mean ± SEM with n=4. *P<0.05, **P<0.01, ***P<0.001 compared with the response of islets isolated from each group of mice at 16.7 mM glucose; $^{\Delta}$P<0.05, $^{\Delta\Delta}$P<0.01, $^{\Delta\Delta\Delta}$P<0.001 compared with the response of islets isolated from lean mice (saline treated) to each secretagogue or glucose concentration.

Figure 4.44 Effects of long-term treatment with frenatin 2D and its synthetic analogue [D1W] frenatin 2D on total cholesterol (A), Triglycerides (B), HDL (C) and LDL (D) in *db/db* mice

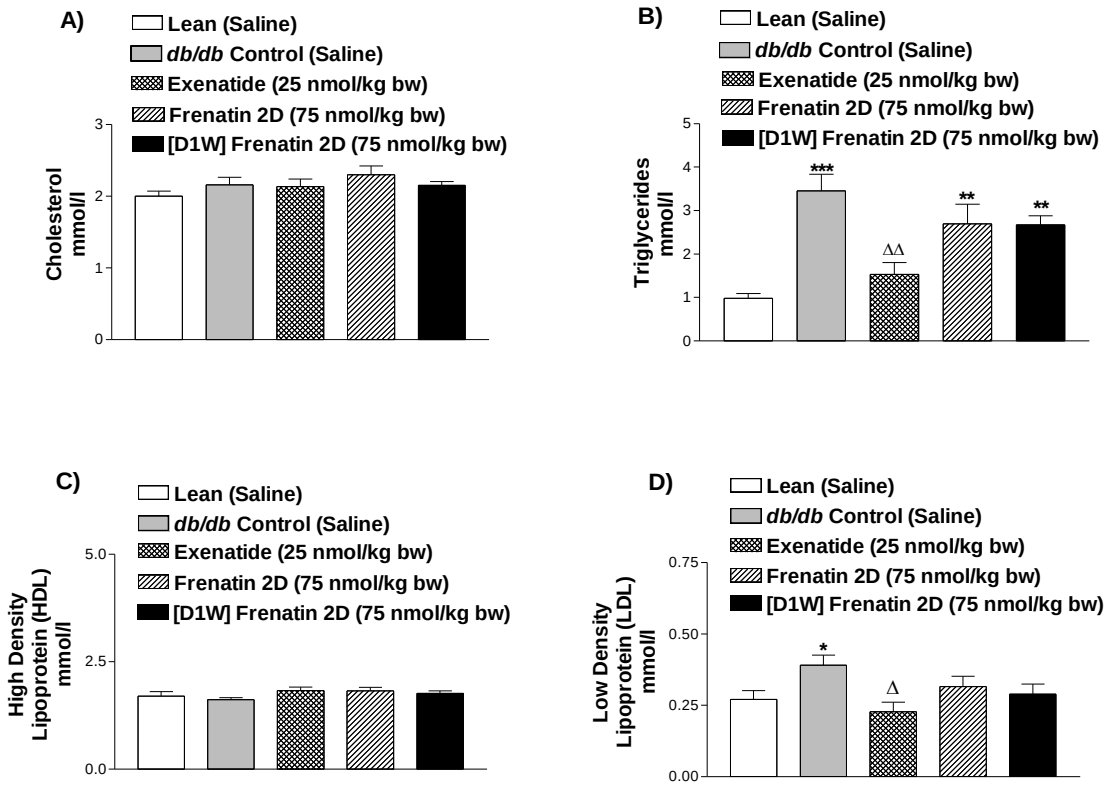

Plasma sample was collected after 28 days treatment with either saline (control) or exenatide or peptide. Values are mean ± SEM for 6 mice. *P<0.05, *P<0.05, ***P<0.001 compared to lean mice. $^{\Delta}$P<0.05, $^{\Delta\Delta}$P<0.01 compared to *db/db* control mice.

Figure 4.45 Effects of long-term treatment with frenatin 2D and its synthetic analogue [D1W] frenatin 2D on plasma AST (A) ALT (B) ALP (C) and creatinine (D) levels in *db/db* mice

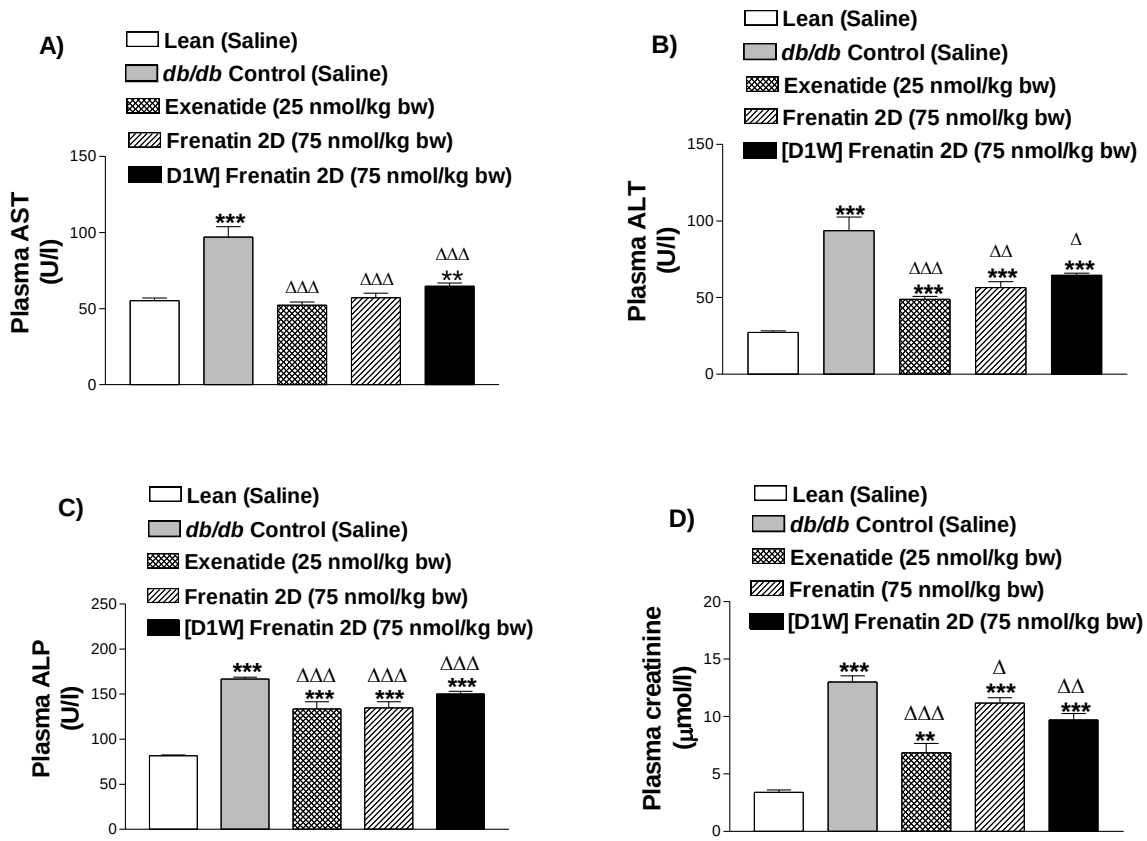

Following 28 days injection with either saline (control) or exenatide or peptide, a plasma sample was collected and measured for ALT, AST, ALP and creatinine levels. Values are mean ± SEM for 6 mice. **P<0.01, ***P<0.001 compared to lean control. $^{\Delta}$P<0.05, $^{\Delta\Delta}$P<0.01, $^{\Delta\Delta\Delta}$P<0.001 compared to *db/db* control.

Figure 4.46 Effects of long-term treatment with frenatin 2D and its synthetic analogue [D1W] frenatin 2D on amylase activity in diabetic mice (*db/db*)

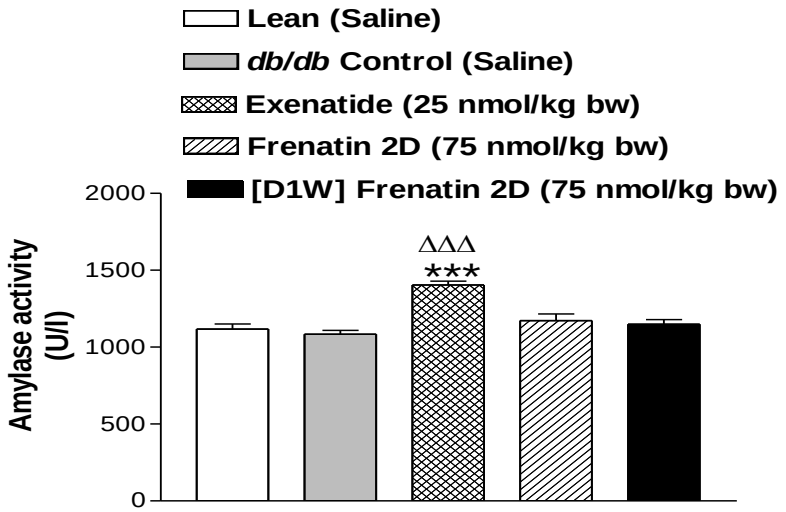

Following 28 days injection with either saline (control) or exenatide or peptide, a plasma sample was collected and measured for amylase activity. Values are mean ± SEM for n=6 mice. ***P<0.001 compared to lean control. $^{\Delta\Delta\Delta}$P<0.001 compared to *db/db* control.

Figure 4.47 Effects of frenatin 2D & its synthetic analogue [D1W] frenatin 2D treatment on islet morphology in *db/db* mice

A)

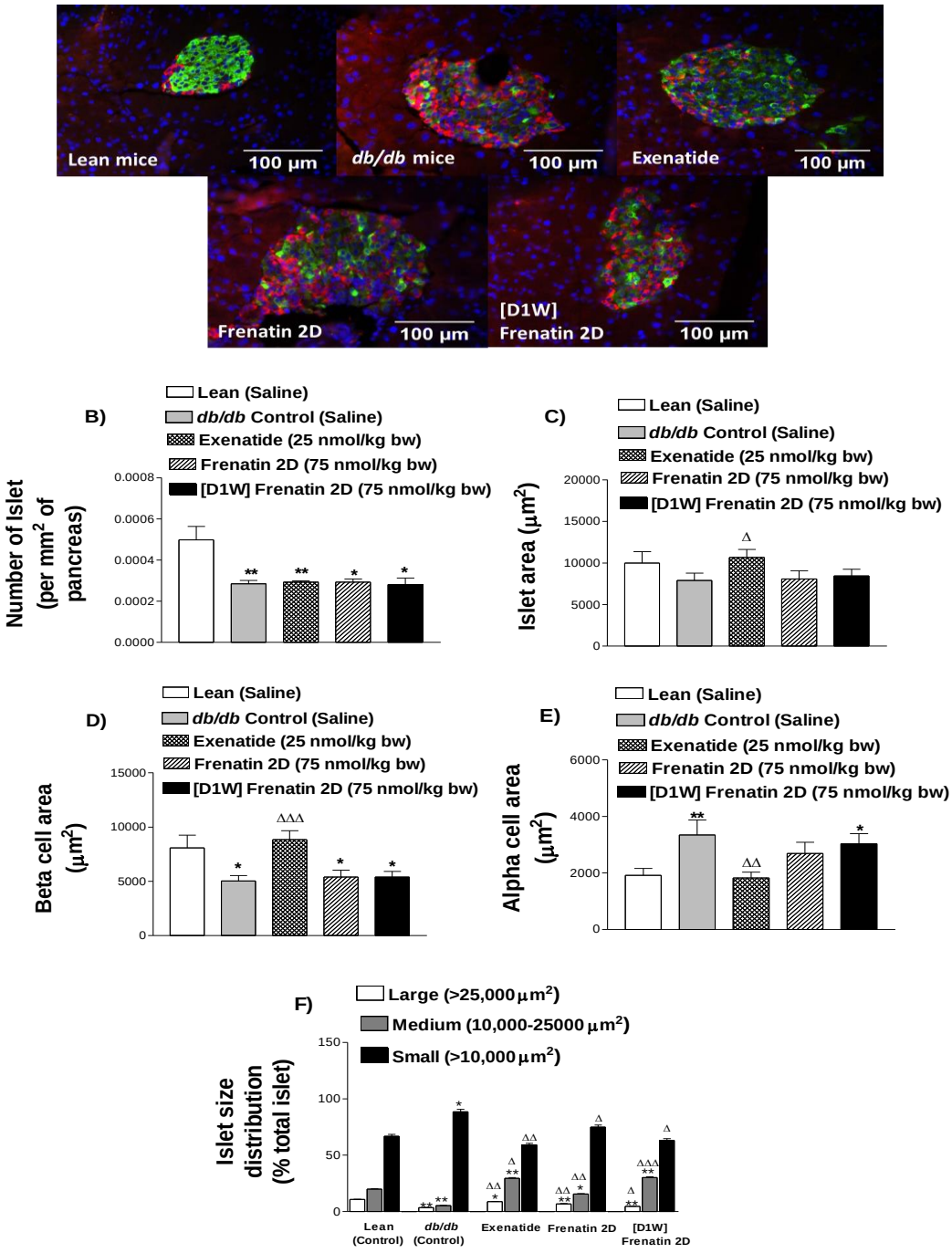

Representative images (A) showing insulin (green) and glucagon (red) immunoreactivity from lean, *db/db* control, frenatin 2D and [D1W] frenatin 2D treated mice. B, C, D, E and F shows islet number, islet area, beta cell area, alpha cell area and islet size distribution respectively. Values are mean ± SEM for 6 mice (~80 islets per group). *P<0.05, **P<0.01 compared to normal saline control. $^{\Delta}$P<0.05, $^{\Delta\Delta}$P<0.01, $^{\Delta\Delta\Delta}$P<0.001 compared to *db/db* control.

Figure 4.48 Effects of frenatin 2D & its synthetic analogue [D1W] frenatin 2D treatment on expression of genes involved in insulin action in skeletal muscle

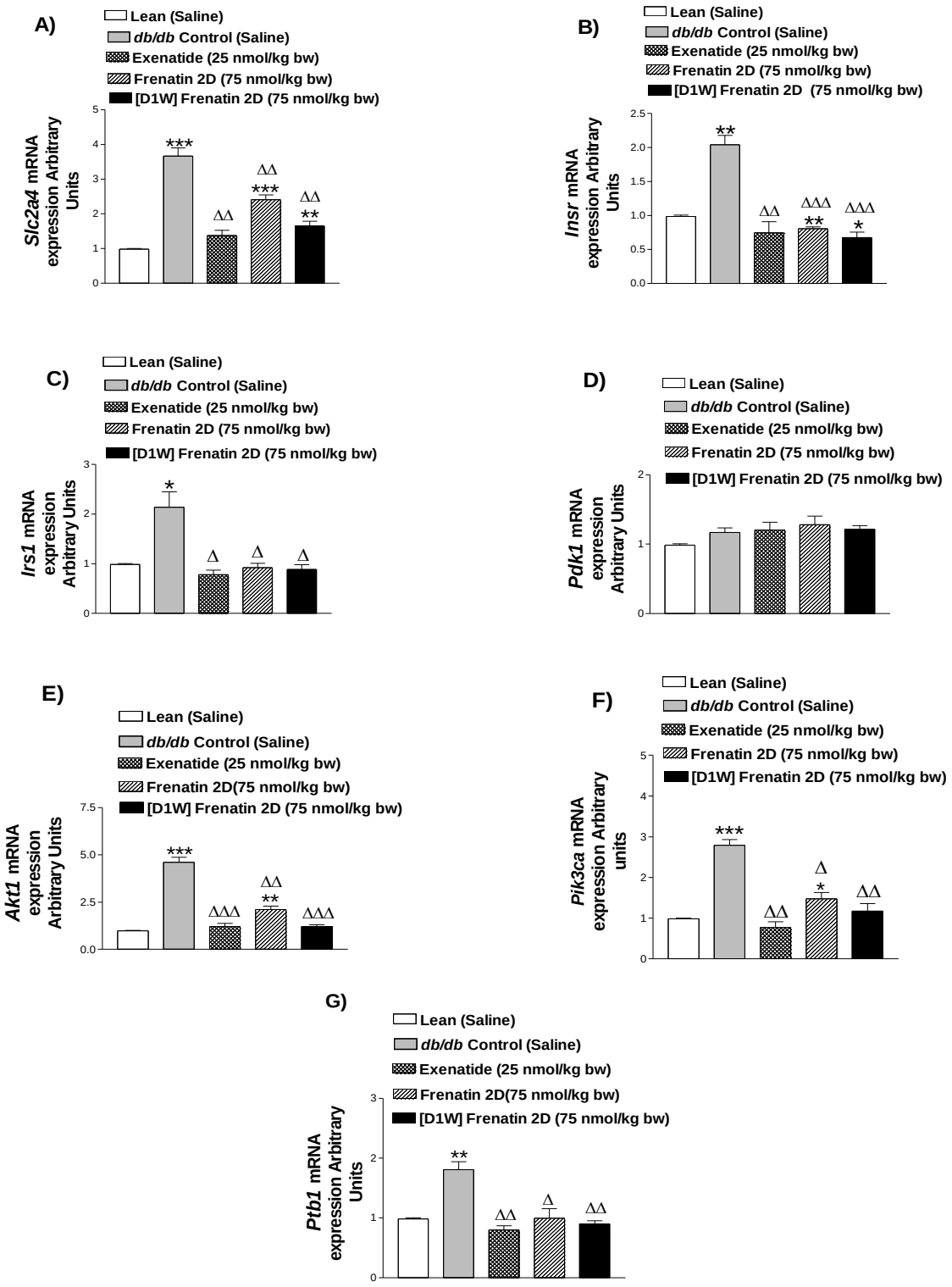

3µg of mRNA was used for cDNA synthesis. Expression values were normalised to Actb. Values are mean ± SEM for n=4. *P<0.05, **P<0.01, ***P<0.001 compared to normal control. $^{\Delta}$P<0.05, $^{\Delta\Delta}$P<0.01, $^{\Delta\Delta\Delta}$P<0.001 compared to *db/db* control.

Figure 4.49 Effects of frenatin 2D and its synthetic analogue [D1W] Frenatin 2D treatment on expression of genes involved in insulin secretion from mouse islets

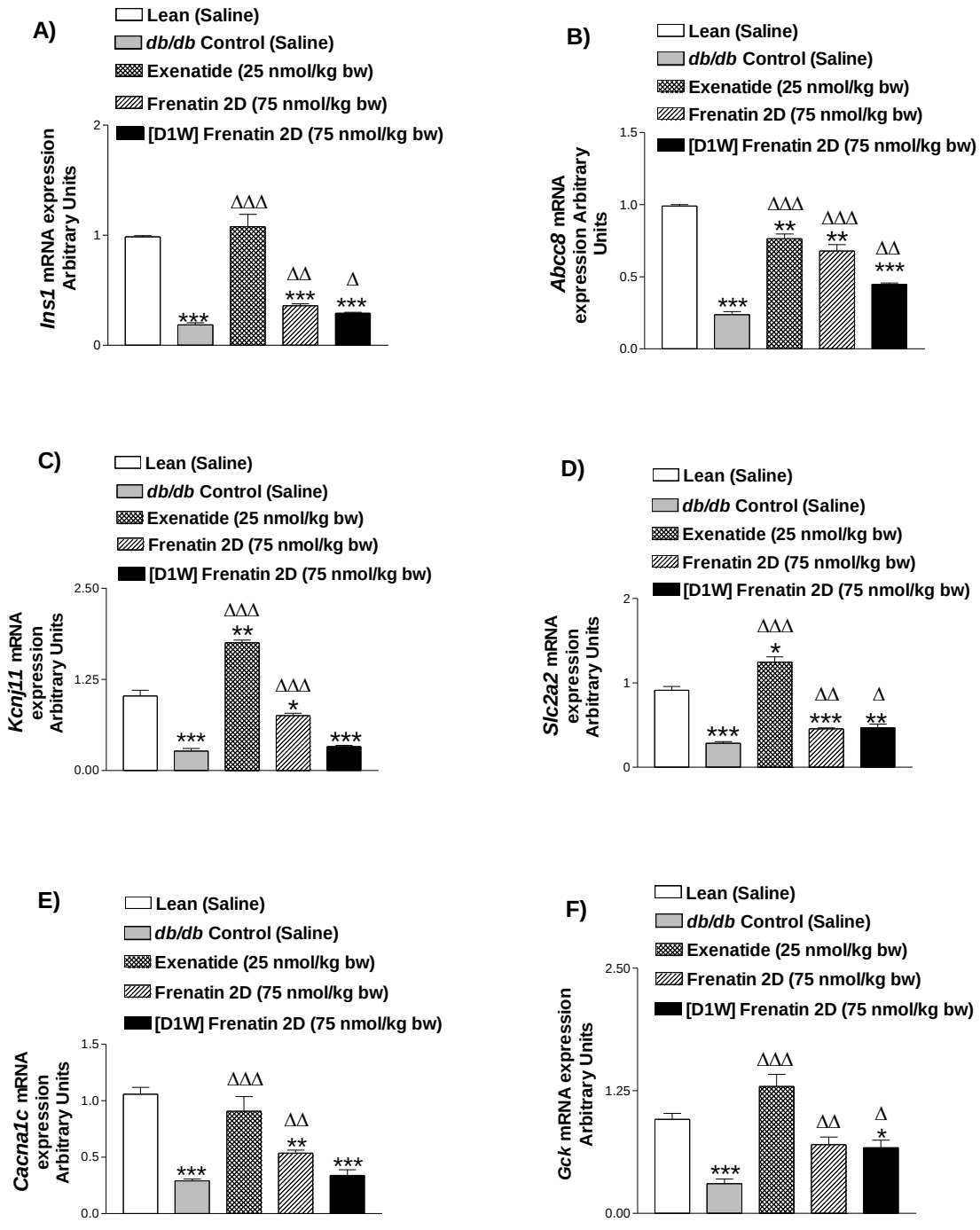

3µg of mRNA was used for cDNA synthesis. Expression values were normalised to Actb. Values are mean ± SEM for n=4. *P<0.05, **P<0.01, ***P<0.001 compared to normal control. $^{\Delta}$P<0.05, $^{\Delta\Delta}$P<0.01, $^{\Delta\Delta\Delta}$P<0.001 compared to *db/db* control.

Figure 4.50 Effects of frenatin 2D and its synthetic analogue [D1W] frenatin 2D treatment on expression of genes involved in insulin secretion (A-C), beta cell proliferation (D) and beta cell apoptosis (E) in mouse islets

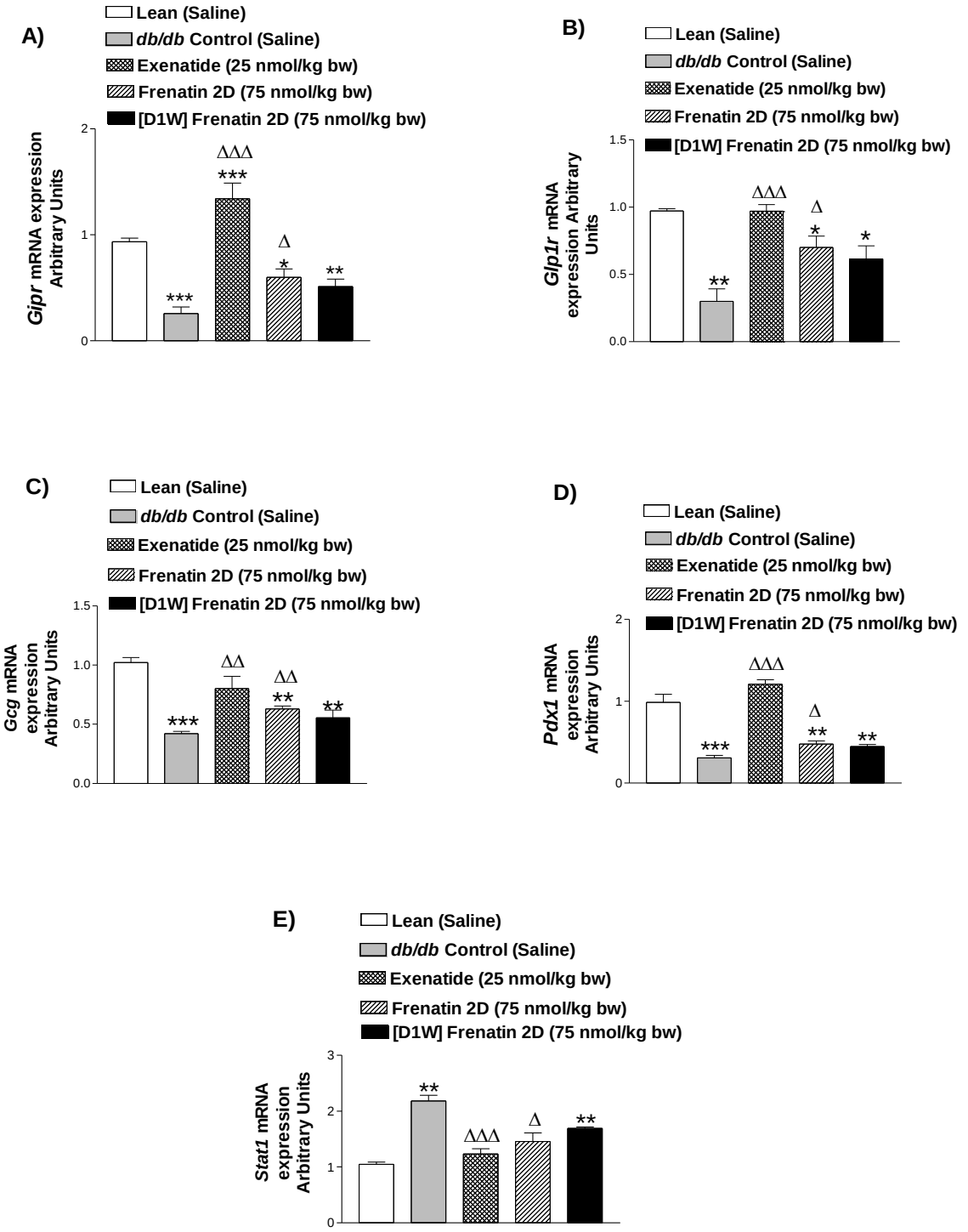

3µg of mRNA was used for cDNA synthesis. Expression values were normalised to Actb. Values are mean ± SEM for n=4. *P<0.05, **P<0.01, ***P<0.001 compared to normal control. $^{\Delta}$P<0.05, $^{\Delta\Delta}$P<0.01, $^{\Delta\Delta\Delta}$P<0.001 compared to *db/db* control mice.

Chapter 5

In vitro and *in vivo* antidiabetic effects of a structurally modified analogue of peptide glycine leucine amide-AM1 (PGLa-AM1) isolated from frog *Xenopus amieti*

5.1 Summary

The present Chapter investigated the antidiabetic potential of [A14K] PGLa-AM1 (GMASKAGSVLGKVKKVALKAAL.NH_2), an analogue of native PGLa-AM1 (GMASKAGSVLGKVAKVALKAAL.NH_2) with increased cationicity. Like the native peptide, [A14K] PGLa-AM1 displayed dose-dependent stimulatory nontoxic effects on insulin release from BRIN-BD11 as well as from human-derived pancreatic 1.1B4 beta cells. [A14K] PGLa-AM1 also provided protection against cytokine-induced apoptosis and stimulated proliferation in BRIN-BD11 cells. Twice daily administration of [A14K] PGLa-AM1 (75 nmol/kg bw) or exenatide (25 nmol/kg bw) to *db/db* mice for 28 days, markedly delayed gradual decline of insulin and improved HbA1c, hyperglycaemia, glucose tolerance and insulin sensitivity. In contrast, native PGLa-AM1 (75 nmol/kg bw) produced no significant changes in these parameters. Energy intake and fluid intake were unaffected in PGLa-AM1 and [A14K] PGLa-AM1 but decreased significantly by exenatide. Elevated levels of triglycerides and LDL were reversed by [A14K] PGLa-AM1 and exenatide but not by PGLa-AM1. The cholesterol level was decreased significantly by [A14K] PGLa-AM1. Plasma AST, ALT, ALP and creatinine were decreased markedly by [A14K] PGLa-AM1 and exenatide. Except for ALP, these biomarkers were also significantly decreased by PGLa-AM1. Amylase activity was elevated in all treatment groups. Pancreatic insulin was significantly increased by [A14K] PGLa-AM1and exenatide. No significant changes were observed in the islet, beta cell and alpha cell area in the treated groups except for exenatide. However, the loss of large and medium-size islet in *db/db* mice was significantly countered in all peptide treated groups. Islets isolated from peptide-treated *db/db* mice showed improved insulin secretory responses to glucose and known insulin modulators. In un-treated *db/db* mice, the expression of insulin

signalling genes was upregulated, and that of insulin secretory genes was down-regulated. These changes were reversed by [A14K] PGLa-AM1 and exenatide treatment. In transgenic GluCre-ROSA26EYFP mice, receiving [A14K] PGLa-AM1, the numbers of Ins^+/GFP^+ cells, GFP^+ cells and Ins^+/Glu^+ were increased significantly, indicating that the analogue could have positive effects on transdifferentiation of glucagon-expressing alpha to insulin-expressing beta cells.

5.2 Introduction

The granular glands present in the frog skin has proven to contain biologically active peptides having a wide range of pharmacological activities that may have medicinal importance (Conlon, 2017). These peptides play an important role in host defence against pathogenic microorganisms such as bacteria, fungi, protozoa and viruses. Hence, they were called host defence peptides and classified based on antimicrobial activities. Additionally, these peptides have displayed tumoricidal activity and cytokine-mediated immunomodulatory properties (Xu and Lai *et al.,* 2015, Conlon *et al.*, 2014a). Interestingly, few peptides in frog skin secretions were structurally related to mammalian peptides such as cholecystokinin and tachykinins (Marenah *et al.,* 2004a).

Many host defence peptides with multifunctional activities have also shown insulin-releasing activity *in vitro* using rat clonal pancreatic beta cell line (BRIN-BD11 cell line), human-derived pancreatic beta cells (1.1B4 cell line) and mouse pancreatic islets, without affecting the architecture of plasma membrane (Conlon *et al.,* 2017). Additionally, these peptides have been shown to improve glycemic response both in lean and high fat-induced insulin resistance diabetic mice when administered together with glucose (Srinivasan *et al.,* 2015, Owolabi *et al.,* 2016, Vasu *et al.,* 2017).

Furthermore, some of these peptides stimulated the release of GLP-1, an incretin peptide which plays an essential role in maintaining pancreatic beta cell mass and function, from GLUTag murine enteroendocrine cell line (Ojo *et al.*, 2013a).

Based on structure-activity analysis of frog skin insulinotropic peptides, previous studies have revealed the key determinants that influence the insulin-releasing activity of frog skin peptides (Abdel Wahab *et al.*, 2008a, Ojo *et al.*, 2013b, Srinivasan *et al.*, 2016). Analogues containing lysine (K) or tryptophan (W) substitution have shown greater insulinotropic potency than the parent peptide. Synthetic analogues of the brevinine 2-related -peptide (B2RP) (Abdel Wahab *et al.*, 2010), tigerinin-1R (Srinivasan *et al.*, 2016), hymenochirin–1B (Owolabi *et al.*, 2016), esculentin-2Cha (Vasu *et al.*, 2017) exhibited potent insulinotropic activity both *in vitro* and *in vivo*.

Peptide glycine-leucine-amide (PGLa) is well-known for its broad-spectrum antibacterial and antifungal activities (Gibson *et al.*, 1986). It was first isolated from skin secretions of the South African frog *Xenopus laevis* (Glattard *et al.*, 2016). PGLa-AM1 (GMASKAGSVLGKVAKVALKAAL.NH_2) is a paralogue of PGLa, found in skin secretions of the octoploid frog *Xenopus amieti* (Conlon *et al.*, 2010). It demonstrated a dose-dependent release of GLP-1 and insulin from GLUTag and BRIN-BD11 cells respectively, without compromising architecture of plasma membrane (Ojo *et al.*, 2013a, Owolabi *et al.*, 2017). In the recent study, the synthetic analogue [A14K] PGLa-AM1, generated by substituting alanine at position 14 by lysine in the parent peptide, produced the stronger insulin secretory response from BRIN-BD11 cells and mouse islets (Abdel-Wahab *et al.*, 2010, Manzo *et al.*, 2015, Owolabi *et al.*, 2017). Furthermore, acute administration of [A14K] PGLa-AM1 (75 nmol/ kg bw) both in lean and high fat-fed mice, resulted in a significant increase of plasma insulin and improved blood glucose.

Based on these promising preliminary results, the insulinotropic activity of [A14K] PGLa-AM1 was further investigated in 1.1B4 human-derived pancreatic β-cells. Additionally, the beneficial effects of [A14K] PGLa-AM1 on beta cell proliferation and its ability to protect cytokine-induced DNA damage was examined in BRIN-BD11 cells. Furthermore, longer-term *in vivo* antidiabetic effects of [A14K] PGLa-AM1 were examined in genetically obese-diabetic mice (*db/db*), in comparison to its parent peptide (PGLa-AM1) and an antidiabetic agent, exenatide. An additional *in vivo* study was performed using transgenic GluCre-ROSA26EYFP mice, to investigate beneficial effects of [A14K] PGLa-AM1 on transdifferentiation of glucagon-producing alpha cells to insulin-producing beta cells. These *in vivo* studies were carried out in parallel with the evaluation of frenatin 2D as presented in Chapter 4.

5.3 Materials and Methods

5.3.1 Reagents

All the reagents used in the experiments were of analytical grade and listed in Chapter 2, Section 2.1. Synthetic peptide (PGLa-AM1 and [A14K] PGLa-AM1) used in this Chapter were supplied by SynPeptide (China). CytoTox 96 Non-Radioactive Cytotoxicity Assay kit (Catalogue number: G1780) purchased from Promega (Southampton, UK). FLIPR Calcium Assay Kit (Catalogue number: R8041) and Membrane potential blue (Catalogue number: R8042) were purchased from Molecular Devices (Berkshire, UK). Apoptosis and proliferation experiments were performed using IN SITU Cell Death Fluorescein kit (Sigma-Aldrich, Catalogue number: 11684795910) and Rabbit polyclonal to Ki67 (Abcam, Catalogue number: ab15580) respectively. Masterclear Cap Strips and real-time PCR TubeStrips (Catalogue number: 0030132890) purchased from Mason Technology Ltd (Dublin, Ireland).

5.3.2 Peptide synthesis and purification

Synthetic peptide [A14K] PGLa-AM1 was purified to near homogeneity (>98% purity) by reverse phase HPLC using a Vydac (C-18) column as described in Chapter 2, Section 2.2.1.1. The molecular mass of the collected peak was characterised using MALDI-TOF MS (Chapter 2, Section 2.2.2). Peptide PGLa-AM1 used in this Chapter was supplied in pure form by SynPeptide (China). (See Figure 5.1 for peptides structure)

5.3.3 Effects of [A14K] PGLa-AM1 on insulin release from BRIN-BD11 and 1.1B4 cells

The dose-dependent insulin secretory studies of peptide [A14K] PGLa-AM1 was performed using BRIN-BD11 (passage 15-30) and 1.1B4 cells (passage 25-28). The procedure for studying the insulin-releasing activity of peptide has been described in Chapter 2, Section 2.4.1.1. [A14K] PGLa-AM1 ($3x10^{-6}$ - 10^{-12} M, n=8) was incubated for 20 min at 37 °C using Krebs-Ringer bicarbonate (KRB) buffer supplemented with 5.6 mM glucose. After incubation, the cell supernatant was aliquoted and stored at -20 °C for insulin radioimmunoassay as outlined in Chapter 2, Section 2.4.4.

5.3.4 Cytotoxicity studies

LDH release from [A14K] PGLa-AM1 treated cells was determined using CytoTox 96 non-radioactive cytotoxicity assay kit, as described in Chapter 2, Section 2.5.

5.3.5 Effects of [A14K] PGLa-AM1 on apoptosis and proliferation in BRIN-BD11 cells

The ability of [A14K] PGLa-AM1 to protect against cytokine-induced DNA damage was investigated in BRIN-BD11 cells. Cells were seeded at a density of 5 $x10^4$ cells per well in 12 well plate and exposed to a cytokine mixture (200 U/ml tumour-necrosis factor-α, 20 U/ml interferon-γ and 100 U/ml interleukin-1β), in the presence or absence of [A14K] PGLa-AM1 (10^{-6} M) for 18 hr at 37 °C. GLP-1 (10^{-6} M) was used as a positive control in the experiment. The detailed procedure is described in Chapter 2, Section 2.10.

The positive effect of [A14K] PGLa-AM1 (10^{-6} M) or GLP-1 (10^{-6} M) on the proliferation of BRIN-BD11 cells is described in Chapter 2, Section 2.10. After fixing of BRIN-BD11 cells using 0.1 M sodium citrate buffer (pH 6.0) and treatment with 300 µl of 1.1% BSA, cells were stained with rabbit anti-Ki-67 primary antibody and subsequently with Alexa Fluor 594 secondary antibody (Abcam. Cambridge, UK).

5.3.6 Effects of the peptide on glucose uptake in C2C12 cells

The procedure for determining the effects of peptides on the glucose uptake in C2C12 cells is described in Chapter 2, Section 2.11.

5.3.7 Acute *in vivo* effects of the peptide on food intake

Food intake was measured in overnight (21 hr) fasted mice after i.p injection of saline and test peptides as described in Chapter 2, Section 2.13.4.

5.3.8 Effects of twice daily administration of PGLa-AM1 and [A14K] PGLa-AM1 in *db/db* mice

Twice daily i.p. injections of saline (control) or peptide (75 nmol/kg bw) or Exenatide 4 (75 nmol/kg bw) were administered for 28 days in *db/db* male mice. The various

control groups were the same mice as reported in chapter 4. Before the start of the treatment, all mice were injected twice daily with saline for 3 days and body weight, energy intake and blood glucose were observed. After initiation of treatment at every 3 days interval body weight, energy intake, non-fasted blood glucose and plasma insulin were assessed. Glucose in blood and plasma were measured by Ascencia counter blood glucose meter (Bayer, UK) and GOD-PAP reagent, respectively (Chapter 2, Section 2.13.5). Plasma insulin was measured by radioimmunoassay, as outlined in Chapter 2, Section 2.13.5. At the end of treatment, terminal studies were performed to measure HbA1c (Chapter 2, Section 2.13.9), glycaemic response to an intraperitoneal and oral glucose load (Chapter 2, Section 2.13.2) and insulin sensitivity test (Section 2.13.3). Fasting (18 hr) blood glucose and plasma were measured and used to assess insulin resistance using homeostatic model assessment (HOMA) formula: HOMA-IR = fasting glucose (mmol/l) x fasting insulin (mU/l)/22.5. After collecting terminal blood, animals were sacrificed, and terminal analysis was performed which include measurement of body fat composition and bone mineral density using DEXA scanning (PIXImus densitometer, USA) (Chapter 2, Section 2.13.8). Terminal plasma was used for lipid profile, assessment of liver and kidney function and amylase activity (Chapter 2, Section 2.13.12). Tissues dissected from sacrificed animals were processed for immunohistochemistry (Chapter 2, Section 2.14), measurement of pancreatic insulin (Chapter 2, Section 2.13.11) and expression of key genes involved in glucose haemostasis (Chapter 2, Section 2.15). Islets were isolated from the pancreas (Chapter 2, Section 2.4.2.1) and used to evaluate insulin secretory responses to established insulin secretagogues as described in Chapter 2, Section 2.4.2.3.

5.3.9 Biochemical analysis

Pancreatic tissues were homogenised in acid ethanol to measure insulin content by radioimmunoassay as described in Chapter 2, Section 2.13.11. The HbA1c level in saline and peptide-treated mice was measured using A1cNow^{+} kits (PTS diagnostics, IN, USA) (Chapter 2, Section 2.13.9). Effect of peptide treatment on renal and liver function test was performed by measuring creatinine, alanine transaminase (ALT), aspartate transaminase (AST), alkaline phosphatase (ALP) level (Chapter 2, Section 2.13.12).

5.3.10 Effects of twice daily administration of PGLa-AM1 and [A14K] PGLa-AM1 on islet morphology

Pancreatic tissue was excised from saline and peptide-treated mice and fixed in 4% paraformaldehyde. Tissue was processed in an automated tissue processor (Leica TP1020, Leica Microsystems, Nussloch, Germany) as outlined in Chapter 2, Section 2.14. After processing, tissues were embedded in paraffin and sectioned (7 μm thickness) using microtome. Sections were placed on a slide and stained for insulin and glucagon as described in Chapter 2, Section 2.14.1.

5.3.11 Effects of twice daily administration of PGLa-AM1 and [A14K] PGLa-AM1 on gene expression

Tissues dissected from saline and peptide treated *db/db* mice were used to study the expression of key genes involved in glucose homeostasis. Islet cells were isolated from pancreatic tissue by collagenase digestion methods (Chapter 2, Section 2.4.2.1) on the same day after culling of mice and stored at -70 °C to study the expression of insulin secretory genes. RNA was extracted from muscle tissue and islet cells using TriPure

reagent as outlined in Chapter 2, Section 2.15.1, followed by synthesis of cDNA (Chapter 2, Section 2.15.2). Genes involved in glucose homeostasis were examined using SYBR Green real-time PCR (Chapter 2, Section 2.15.3).

5.3.12 Effects of twice daily administration of [A14K] PGLa-AM1 in GluCre-ROSA26EYFP mice

Streptozotocin pre-treated GluCre-ROSA26EYFP mice received twice daily intraperitoneal injections of saline or test peptide (75 nmol/kg bw) for 11 days (Chapter 2 Section 2.13.1.3). Every 3 days interval non-fasting blood glucose, body weight, food intake and water intake were measured. Blood samples were collected prior to strep treatment, before initiation of peptide treatment and after peptide treatment, and analysed for insulin concentration using RIA (Chapter 2, Section 2.13.6). Animals were sacrificed, and pancreatic tissues were excised and processed for histological staining as described in Chapter 2, Section 2.14 and 2.14.1.

5.3.13 Statistical Analysis

Experimental data were analysed using GraphPad PRISM (Version 3). Results were expressed as means ± SEM and data compared using unpaired student's t-test (nonparametric, with two-tailed P values and 95% confidence interval) and one-way ANOVA with Bonferroni post-hoc test wherever applicable. Group of datasets were considered to be significantly different if $P<0.05$.

5.4 Results

5.4.1 Purification and characterisation of [A14K] PGLa-AM1

[A14K] PGLa-AM1 was purified and characterised by reverse-phase HPLC and MALDI-TOF respectively, as described in Chapter 2, Section 2.2.1.1 and Section 2.2.2 (Figure 5.2).

5.4.2 Effects of [A14K] PGLa-AM1 on insulin release from BRIN-BD11 and 1.1B4 cells

The insulin-releasing activity of [A14K] PGLa-AM1 was investigated in glucose-responsive BRIN-BD11 and 1.1B4 cell line. As shown in Figure 5.3A, [A14K] PGLa-AM1 (3×10^{-6} M – 10^{-12} M) treated BRIN-BD11 cells exhibited a significant dose-dependent insulin release ($P<0.05$) up to a concentration of 30 pM. The stimulatory response observed at 3 µM was 3.6-fold greater than basal (0.74 ng/10^6 cells/20 min). [A14K] PGLa-AM1 at concentrations up to and including 3 µM, did not affect the release of LDH from the cells indicating that the integrity of the plasma membrane was not compromised (Figure 5.3B). As shown in Figure 5.4 A, B incubation of 1.1B4 cells with [A14K] PGLa-AM1 in 5.6 mM and 16.7 glucose evoked approximately 2.5-fold increase in insulin response at 3 µM. The peptide exhibited a significant ($P<0.05$) increase in the rate of insulin release at concentrations ≥ 30 pM.

5.4.3 Effects of [A14K] PGLa-AM1 on apoptosis and proliferation in BRIN-BD11 cells

[A14K] PGLa-AM1 (1 µM) treated BRIN-BD11 cells were subject to TUNEL assay and rabbit anti-Ki-67 primary antibody to evaluate the effects on beta cells apoptosis and proliferation. GLP-1(1 µM) used as positive control in the experiment. As shown in Figure 5.5A, neither [A14K] PGLa-AM1 nor GLP-1 alone had any effects on apoptosis. On the other hand, in cytokine-treated BRIN-BD11 cells, the number of

cells undergoing apoptosis was increased 3.7-fold. When the BRIN-BD11 cells were incubated with [A14K] PGLa-AM1 and the cytokine mixture, the number of the apoptotic cells reduced significantly ($P<0.001$) by 49%. The degree of protection provided by [A14K] PGLa-AM1 was comparable to that provided by GLP-1 (48 % reduction). As shown in the Figure 5.5B, [A14K] PGLa-AM1 (1 µM) treatment for 18 hrs significantly ($P<0.001$) increased proliferation (42% increase) of BRIN-BD11, that was comparable to that produced by 1 µM GLP-1 (43 % increase). On the other hand, the proliferation of cytokine-treated BRIN-BD11 cells decreased significantly ($P<0.01$) by 30%.

5.4.4 Effects of [A14K] PGLa-AM1 on glucose uptake in C2C12 cells

As shown in Figure 5.6, [A14K] PGLa-AM1 (1 µM) treatment had no significant effect on glucose uptake. However, in the presence of insulin, peptide showed a noticeable increase in glucose uptake. In the presence of negative control (Apigenin 50µM), glucose uptake was significantly decreased by 30% ($P<0.05$).

5.4.5 Acute effects of [A14K] PGLa-AM1 peptides on food intake in mice

As shown in Figure 5.7, GLP-1 significantly ($P<0.05$) decreased food intake from 60 min up to 180 min post-injection in mice. [A14K] PGLa-AM1 showed no effect on food intake.

5.4.6 Effects of twice daily administration of PGLa-AM1 and [A14K] PGLa-AM1 on body weight, energy intake, non-fasting blood glucose and plasma insulin in *db/db* mice

Effects of twice daily administration of PGLa-AM (75 nmol/kg bw) and [A14K] PGLa-AM1 (75 nmol/kg bw) on body weight, energy intake, water intake, non-fasting blood glucose and plasma insulin were investigated in diabetic male mice (*db/db*, BKS.Cg-+Leprdb/+Leprdb/OlaHsd). As discussed in Chapter 4, Exenatide was used as positive control (25 nmol/kg bw). As expected, these parameters were significantly increased ($P<0.001$) in all *db/db* mice compared to their littermates (Figure 5.8 & 5.9). After 28 days of treatment, no significant change in body weight, energy intake and fluid intake was observed in PGLa-AM1 and [A14K] PGLa-AM1 treated groups in comparison to *db/db* control group (Figure 5.8A-F). Elevated blood glucose and decreased plasma insulin in saline-treated *db/db* mice was reversed by treatment with exenatide and [A14K] PGLa-AM1 (Figure 5.9A-D). Whereas in PGLa-AM1 treated *db/db* mice, these parameters were not significantly different from saline-treated *db/db* mice.

5.4.7 Effects of twice daily administration of PGLa-AM1 and [A14K] PGLa-AM1 on Glycated haemoglobin (HbA1c) in *db/db* mice

Treatment with 25 nmol/kg bw exenatide and 75 nmol/kg bw [A14K] PGLa-AM resulted in significant decrease in HbA1c by 48% ($P<0.05$) and 30% ($P<0.01$) respectively compared to saline-treated *db/db* mice. On the other hand, there was no significant decrease in blood HbA1c level in PGLa-AM1 treated *db/db* mice (Figure 5.10).

5.4.8 Effects of twice daily administration of PGLa-AM1 and [A14K] PGLa-AM1 on glucose tolerance in *db/db* mice following intraperitoneal and oral glucose load

Following intraperitoneal glucose load (18 mmol/kg bw), a significant reduction ($P<0.01$, $P<0.001$) in individual glucose was observed at all time point (15, 30 and 60 min) in exenatide and [A14K] PGLa-AM1 treated groups compared to saline-treated *db/db* mice (Figure 5.11A). This resulted in a decrease ($P<0.05$, $P<0.001$) in an overall glycaemic excursion in these mice (Figure 5.11B). Correspondingly, insulin concentration was significantly ($P<0.05$ - $P<0.001$) increased at all time points with exenatide, and at 15 and 30 min after [A14K] PGLa-AM1 (Figure 5.11C). The overall insulin concentration was also increased ($P<0.05$, $P<0.001$) significantly in these mice compared to *db/db* controls (Figure 5.11D). PGLa-AM1 treated group also showed a tendency to improve blood glucose and insulin concentration.

In another set of experiments, the glycaemic response to an oral glucose challenge was investigated in treated and untreated mice (Figure 5.12A-D). Post oral glucose administration, blood glucose concentrations were significantly ($P<0.01$, $P<0.001$) decreased at all time points in [A14K] PGLa-AM1 treated group compared to *db/db* control mice. In the exenatide-treated group, blood glucose was decreased at 15 and 30 min resulting in significant ($P<0.01$, $P<0.001$) reduction in overall blood glucose AUC values compared to *db/db* control mice (Figure 5.12A, B). Similarly, plasma insulin concentrations were increased ($P<0.05$, $P<0.01$) at 15 and 60 min in exenatide and [A14K] PGLa-AM1 treated groups respectively (Figure 5.12C). Furthermore, the overall insulin concentration was increased ($P<0.05$, $P<0.01$) significantly in these groups (Figure 5.12D). The PGLa-AM1 treated group showed a similar pattern of glucose and insulin response to those observed after intraperitoneal glucose load.

5.4.9 Effects of twice daily administration of PGLa-AM1 and [A14K] PGLa-AM1 on insulin sensitivity in *db/db* mice

Following intraperitoneal administration of insulin (50 U/kg bw), circulating blood glucose levels were substantially decreased in [A14K] PGLa-AM1 and exenatide-treated *db/db* mice compared to saline-treated *db/db* mice (Figure 5.13A, B). There was no significant decrease in blood glucose in PGLa-AM1 treated *db/db* mice. The improvement in insulin sensitivity in [A14K] PGLa-AM1 treated mice was further confirmed by HOMA-IR calculation. [A14K] PGLa-AM1 and exenatide decreased ($P<0.05$, $P<0.01$) HOMA-IR by 45% and 54% respectively compared to *db/db* controls (Figure 5.13C). Whereas in PGLa-AM1 treated mice, there was no significant decrease in HOMA-IR index.

5.4.10 Effects of twice daily administration of PGLa-AM1 and [A14K] PGLa-AM1 on bone mineral density, bone mineral content and fat composition in *db/db* mice

Figure 5.14 illustrates a DEXA scan of all groups of mice (lean control, *db/db* control, Exenatide, PGLa-AM1 and [A14K] PGLa-AM1 treated group). After 28 days of treatment, no significant changes in bone mineral density (BMD), bone mineral content (BMC), bone area, body fat and body fat (expressed a percentage of total body mass) were observed in the *db/db* mouse groups. Interestingly, lean body mass was significantly less than lean control in both PGLa-AM1 and [A14K] PGLa-AM1 treated groups (Figure 5.14E).

5.4.11 Effects of twice daily administration of PGLa-AM1 and [A14K] PGLa-AM1 on pancreatic weight and insulin content

As shown in Figure 5.15A, pancreatic weight remained unchanged in all treatment groups compared to *db/db* control mice. However, in comparison to lean control, the

pancreatic weight was significantly ($P<0.05$, $P<0.01$) higher. Exenatide and [A14K] PGLa-AM1 treatment resulted significant ($P<0.05$, $P<0.01$) increase in pancreatic insulin content compared to *db/db* controls (Figure 5.15B). Whereas in PGLa-AM1 treated group pancreatic insulin content remained unchanged.

5.4.12 Effects of twice daily administration of PGLa-AM1 and [A14K] PGLa-AM1 on insulin secretory responses of islets in *db/db* mice

As expected, islets from saline-treated *db/db* mice exhibited impaired insulin secretory response to exogenous glucose (1.4 mM, 5.6 mM, 16.7 mM) and insulin secretagogues (like alanine, GIP, GLP-1, KCl and arginine) compared to lean control. Treatment with exenatide and [A14K] PGLa-AM1 resulted in significant improvements in insulin secretory responses compared to untreated *db/db* control (Figure 5.15C). Under the same experimental conditions, islets from PGLa-AM1 treated mice also showed improved insulin secretory responses, but not to the same extent as [A14K] PGLa-AM1 (Figure 5.15D).

5.4.13 Effects of twice daily administration of PGLa-AM1 and [A14K] PGLa-AM1 on lipid profile in *db/db* mice

Treatment with exenatide and [A14K] PGLa-AM1 significantly ($P<0.05$, $P<0.01$) lowered triglycerides and LDL level compared with *db/db* control (Figure 5.16B, D). Whereas, in a PGLa-AM1 treated group no significant change was observed. Interestingly, significant ($P<0.05$) reduction in cholesterol was observed in [A14K] PGLa-AM1 treated mice compared with saline-treated *db/db* mice and lean controls (Figure 5.16A). HDL was similar in all groups of mice (Figure 5.16C).

5.4.14 Effects of twice daily administration of PGLa-AM1 and [A14K] PGLa-AM1 on liver and kidney function in *db/db* mice

Plasma aspartate transaminase (AST), alanine transaminase (ALT), alkaline phosphatase (ALP) and creatinine were increased ($P<0.001$) in saline-treated *db/db* mice (Figure 5.17). Exenatide and [A14K] PGLa-AM1 significantly decreased AST (1.5-2.0-fold, $P<0.001$), ALT (1.3-1.9-fold, $P<0.05$, $P<0.001$) ALP (1-1.25-fold, $P<0.05$, $P<0.001$) and creatinine (1.3-1.9-fold, $P<0.001$) compared to control *db/db* mice. These biomarkers were significantly ($P<0.05$ - $P<0.001$) decreased with PGLa-AM1 except ALP.

5.4.15 Effects of twice daily administration of PGLa-AM1 and [A14K] PGLa-AM1 on plasma amylase concentration in *db/db* mice

Amylase activity was significantly ($P<0.01$, $P<0.001$) increased in peptide treated groups compared with saline-treated *db/db* mice and lean controls (Figure 5.18).

5.4.16 Effects of twice daily administration of PGLa-AM1 and [A14K] PGLa-AM1 on islet number, islet area, beta cell areas, alpha cell area and islet size distribution

Figure 5.19A, represent images of pancreatic islets, showing alpha cells in red and beta cells in green. The number of islets (per mm^2 of the pancreas) was significantly ($P<0.05$, $P<0.01$) decreased in all *db/db* mice. In all peptide treated *db/db* groups, there was no significant difference in the number of islets (Figure 5.19B). Lean control, *db/db* control, PGLa-AM1 and [A14K] PGLa-AM1treated groups showed no differences in islet area (Figure 5.19C). On the other hand, islet area was significantly ($P<0.05$) increased after exenatide treatment. Beta cell area was decreased ($P<0.05$)

and alpha cell area was increased (P<0.01) in *db/db* mice compared to their littermates (Figure 5.19D,E). Except for exenatide, no significant improvement in beta cell and the alpha area was observed in peptide treated *db/db* mice. Interestingly, in all treated groups, the number of large (>25,000 μm^2) and medium (10,000-25,000 μm^2) size islet were increased (P<0.05 - P<0.001) and the number of small size (<10,000 μm^2) islet was decreased (P<0.01) compared to *db/db* control (Figure 5.19F).

5.4.17 Effects of twice daily administration of PGLa-AM1 and [A14K] PGLa-AM1 on gene expression in skeletal muscle

Insulin signalling genes were significantly (P<0.05 - P<0.001) upregulated in *db/db* mice. The increased expression of *Slc2a4* gene in *db/db* mice was reversed by exenatide and [A14K] PGLa-AM1 (Figure 5.20A). Similarly, upregulated *Insr*, *Irs1*, *Pik3ca, Akt1* and *Ptb1* genes were reversed (Figure 5.20B-C & 5.20E-G). No significant changes in the expression of *Irs1, Pik3ca* and *Ptb1* were observed after PGLa-AM1 treatment. However, the enhanced expression of *Slc2a4, Insr* and *Akt1* genes was countered. In all groups, no significant differences in the expression of *Pdk1* gene were observed (Figure 5.20D).

5.4.18 Effects of twice daily administration of PGLa-AM1 and [A14K] PGLa-AM1 on gene expression in islets

Expression of genes involved in insulin secretion including *Ins1, Abcc8, Kcnj11, Slc2a2, Cacna1c* and *Gck* were investigated after 4 week treatment of *db/db* mice (Figure 5.21A-F). These genes were significantly (P<0.001) downregulated in saline-treated *db/db* mice compared with lean mice. In PGLa-AM1 and [A14K] PGLa-AM1 treated mice, expression of diabetes downregulated *Ins1, Abcc8, Kcnj11, Slc2a2* and

Gck genes were significantly (P<0.01, P<0.001) upregulated. However, mRNA expression of *Cacna1c* remained downregulated in PGLa-AM1 and [A14K] PGLa-AM1 treated mice. All genes were significantly (P<0.001) upregulated in the exenatide-treated group.

Diabetes-induced down-regulation of *Gipr*, *Glp1r*, *Gcg* and *Pdx1* genes were reversed (P<0.05 - P<0.001) by treatment with exenatide, PGLa-AM1 and [A14K] PGLa-AM1 (Figure 5.22A-D). The upregulation of *Stat1* gene was reversed by exenatide and [A14K] PGLa-AM1. However, expression of *Stat1* gene was comparable to *db/db* controls in PGLa-AM1 treated mice (Figure 5.22E).

5.4.19 Effects of twice daily administration of [A14K] PGLa-AM1 on body weight change, food intake and water intake in GluCre-ROSA26EYFP mice

Following streptozotocin (STZ) treatment, a significant increase (P<0.01, P<0.001) in water intake and energy intake was observed in GluCre mice compared to the lean controls (5.23C,D). A decrease in body weight was also observed (5.23A). In [A14K] PGLa-AM1 (75 nmol/kg bw) treated group, no significant changes were observed compared to STZ mice.

5.4.20 Effects of twice daily administration of [A14K] PGLa-AM1 on blood glucose and plasma insulin in GluCre-ROSA26EYFP mice

Treatment with streptozotocin (STZ) resulted in significant (P<0.001) increase in blood glucose compared to lean controls (5.24A). Following 11 days of treatment, significant (P<0.001) decrease in plasma insulin concentrations were observed in STZ control mice (Figure 5.24B). This was associated with significant (P<0.001) increase in blood glucose. [A14K] PGLa-AM1 treatment at the close showed a tendency to

improve blood glucose and plasma insulin, but no statistical significance was observed compared to STZ controls.

5.4.21 Effects of twice daily administration of [A14K] PGLa-AM1 on pancreatic insulin content in GluCre-ROSA26EYFP mice

Insulin content in all regions of the pancreas was significantly ($P<0.05$, $P<0.01$, $P<0.001$) decreased in GluCre mice following streptozotocin (STZ) treatment compared to untreated controls (Figure 5.25). Administration of [A14K] PGLa-AM1 significantly ($P<0.05$, $P<0.01$) improved insulin content, particularly in the tail region of pancreas compared to STZ controls.

5.4.22 Effects of twice daily administration of [A14K] PGLa-AM1 on islet number, islet area, beta cell areas, alpha cell area and islet size distribution in GluCre-ROSA26EYFP mice

At the end of the treatment period, pancreatic islet morphology was evaluated in all groups. Figure 5.26A represents images of pancreatic islets, showing alpha cell in green and beta cell in red colour. As shown in Figure 5.26B, no statistical significances were observed in the number of islets per mm^2 in the whole pancreas. However, in the pancreatic head region, the number of islets per mm^2 was significantly ($P<0.01$) decreased in both STZ and peptide-treated groups compared to lean controls. Interestingly, in the tail region, the opposite pattern was observed. In STZ controls, islet area was significantly decreased ($P<0.01$, $P<0.001$) in the whole pancreas specifically in the tail region which was reversed by peptide treatment (Figure 5.26C). Insulin-expressing beta cells were markedly reduced ($P<0.001$) by STZ treatment particularly in the tail region compared to lean controls (Figure 5.26D). However, in

peptide-treated mice, beta cell area was significantly increased in both head (1.6-fold, $P<0.05$) and tail regions (1.7-fold, $P<0.01$) of the pancreas compared to STZ control. Glucagon expressing alpha cells were substantially increased by STZ treatment, particularly in the head region of pancreas compared to lean controls (Figure 5.26E). However, in peptide treated groups no significant differences were noticed compared to STZ control. Islet size distribution was also significantly altered by streptozotocin treatment (Figure 5.26F). The number of smaller size islet were significantly increased in the whole pancreas, whereas large and medium-size islet were reduced particularly in the pancreatic tail region in saline-treated STZ mice compared to lean control group. The peptide-treated groups exhibited 20% ($P<0.05$) decrease in smaller sized islets and 49% ($P<0.05$) and 65% ($P<0.001$) increase in medium and large-sized islets compared to STZ control.

5.4.23 Effects of twice daily administration of [A14K] PGLA-AM1 on pancreatic islets in GluCre-ROSA26EYFP mice

The immunofluorescent staining revealed that GFP was significantly expressed in glucagon-producing alpha cells in all mice groups (Figure 5.27A). The number GFP positive cells expressing insulin (Ins^+/GFP^+) was significantly ($P<0.05$, $P<0.001$) increased in streptozotocin-treated mice compared to lean controls (Figure 5.27B). However, in [A14K] PGLa-AM1 treated mice, the number of Ins^+/GFP^+ cells was increased ($P<0.05$) compared to STZ controls. Interestingly, in [A14K] PGLa-AM1 treated mice, the percentage of cells expressing only GFP was significantly increased in the head region of the pancreas (Figure 5.27D). However, in the whole pancreas, no significant difference was observed. On the other hand, the number of cells co-

expressing both insulin and glucagon was increased ($P<0.05$) significantly in the whole pancreas compared to both lean and STZ control mice (5.27E).

5.5 Discussion

Type 2 diabetes is one of the severe health problems in modern society (World Health Organization, 2016). In the last few decades, the exponential growth in the diabetes population has triggered the search for alternative treatment options that can achieve good glycaemic control and prevent the complications associated with the disease. The discovery of Exendin-4 from the venom of the Gila monster lizard, which showed glucose-dependent insulin release and improved pancreatic beta cell function (Fehse *et al.,* 2005; Bunk *et al.,* 2011), has intensified the search for the potential antidiabetic peptides from animal sources.

Bioactive peptides found in skin secretions of frogs, whose primary function is to protect the host from microorganisms, has also shown anti-tumour and immunomodulatory activities (Jackway *et al.,* 2011, Conlon *et al.,* 2014a, Xu *et al.,* 2015). Interestingly, some of these peptides have been shown to stimulate insulin release from rat clonal pancreatic beta cell line (BRIN-BD11) and primary islet cells in a dose-dependent manner without affecting the integrity of plasma membrane (Conlon *et al.,* 2017). Additionally, these peptides have been shown to improve blood glucose and plasma insulin concentration when administered together with glucose in lean and high-fat fed mice. PGLa-AM1 is one such peptide isolated from *Xenopus amieti*, its [A14K] analogue, synthesised by substituting alanine at position 14 by lysine, displayed appreciably greater insulinotropic activity than the parent peptide. The [A14K] analogue significantly increased membrane potential and intracellular calcium, but no direct effect on K_{ATP} channels was observed. Additionally, [A14K]

produced a significant increase in cellular cAMP and its insulin-releasing activity was abolished in protein kinase A downregulated cells. Furthermore, the [A14K] analogue exhibited improved glycaemic response both in lean and high-fat diet mice following intraperitoneal administration with glucose (Owolabi *et al.*, 2017). Based on these evidences, the [A14K] PGLa-AM1 analogue was selected for further studies.

Reassuringly, this analogue displayed potent insulinotropic activity both in BRIN-BD11 and 1.1B4 cells without affecting the architecture of plasma membrane up to 3 µM concentrations. This observation is line with previous studies where analogues carrying lysine substitution have displayed potent insulinotropic activity, with no cytotoxic action (Abdel-Wahab *et al.*, 2008b, Ojo *et al.*, 2013b, Owolabi *et al.*, 2015). The detrimental effects of proinflammatory cytokines in islet dysfunction are well documented (Morris *et al.*, 2015). When tested in BRIN-BD11 cells, [A14K] PGLa-AM1 displayed beta-cell proliferative activity comparable to that of GLP-1 and was also equally effective in protecting the cells against cytokine-induced apoptosis. Similarly, Esculentin (1-21)1c, Temporin A and Temporin F peptides have also shown these positive effects (Musale *et al.*, 2018a, b). However further studies are required to delineate the mechanism by which these peptides exhibit proliferative and protective effects. Taken together these results provided a strong base to study long-term *in vivo* effects of [A14K] PGLa-AM1 in an animal model of diabetes.

In the present study, the antidiabetic potential of [A14K] PGLa-AM1 was examined in *db/db* mouse model of obesity-diabetes in comparison with native peptide PGLa-AM1 and a well-known antidiabetic agent, exenatide. The *db/db* mouse is leptin receptor-deficient, having characteristics similar to human type 2 diabetes. Hence, it is widely used to study diseases pathogenesis and development of therapeutic agents for type 2 diabetes (Bogdanov *et al.*, 2014, Cat *et al.*, 2018, Simon and Taylor, 2001,

Kim *et al.,* 2008). In general, *db/db* mice are hyperinsulinemia, with age plasma insulin level decreases and eventually, *db/db* mice develop insulinopia, which resembles late stage of T2DM (Fujiwara *et al.,* 1991, Dalbøge *et al.,* 2013). Consistent with this observation, in saline-treated *db/db* mice plasma insulin level was gradually decreased to the level close to their littermates. Interestingly, in [A14K] PGLa-AM1 treatment mice, a gradual decrease in plasma insulin was markedly delayed. This observation points towards a beneficial effect of analogue on pancreatic beta cell function. In agreement with previous studies (Wang *et al.,* 2002, Park *et al.,* 2007), exenatide, which was used as positive control in the study attenuated the age-related decline of insulin in *db/db* mice. The increase of blood glucose in *db/db* mice was suppressed by treatment with [A14K] PGLa-AM1 and exenatide. The native peptide PGLa-AM1, however, failed to produce the same effect as analogue.

Glycated haemoglobin (HbA1c) reflects the average blood glucose levels up to 3-month period (American Diabetes Association, 2011). In the recent study, esculentin-2CHa and its analogue have shown to improve blood HbA1c in insulin resistance high-fat fed mice (Vasu *et al.,* 2017). In the present study, the HbA1c was significantly decreased in [A14K] PGLa-AM1 and exenatide-treated group compared to saline-treated *db/db* mice. However, in PGLa-AM1 treated mice, no significant change in blood HbA1c was observed. This finding suggests, [A14K] PGLa-AM1 improves glucose concentration in *db/db* mice, along with exenatide.

At the end of the chronic treatment period, the glycaemic response was significantly improved in [A14K] PGLa-AM1 and exenatide-treated groups compared to *db/db* controls. This include improvement of insulin sensitivity and lowered HOMA-IR index. Body weight and fat content were not affected, ruling out the possibility that improvement in insulin sensitivity was simply due to the reduction of adipose tissue

in these mice. However, in PGLa-AM1 treated mice, no significant change in glucose tolerance and insulin sensitivity were noticed. Also, no significant changes in energy intake were observed in PGLa-AM1 and [A14K] PGLa-AM1 treated mice, which correlated with results of acute *in vivo* feeding studies. In agreement with others (Gedulin *et al.,* 2005, Schlögl *et al.,* 2013), energy intake was reduced significantly by exenatide treatment. However, body weight was unaffected. Bone mineral density/ content and lean body mass were similar in all groups of *db/db* mice.

We observed elevated mRNA expression of insulin signalling gene in *db/db* mice. As shown in Figure 5.18, of mRNA expression of *Slc2a2*, *Insr*, *Irs1, Akt1, Pik3ca* and *Ptb1* was upregulated significantly compared with littermates. Such observation could be due to a defect in GLUT4 translocation. A study conducted by Jassen *et al.,* 2006 also observed an increase in the activity of proximal insulin signalling cascade, in the animal model of liver cirrhosis. In fact, insulin resistance in liver cirrhosis patient is well documented (Moscatiello *et al.,* 2007, Garcia-Compean *et al.,* 2009, Goral & Kucukoner, 2010) An increase in GLUT4 activity was observed in L6 myotubules on chronic exposure to glucose and inulin (Huang *et al.,* 2001). Interestingly, in [A14K] PGLa-AM1 and exenatide treatment groups, the expression of these genes was reversed. Therefore, it is essential to explore the factors responsible for these changes to understand the mechanism of insulin resistance.

It is evident that hyperlipidaemia is a major risk factor in the progression of diabetes (Zang *et al.,* 2008, Chen *et al.,* 2015). In type 2 diabetes patients with non-alcoholic fatty liver diseases (NAFLD), triglycerides (TG), total cholesterol (TC), Low-density lipoprotein (LDL) are increased significantly, whereas high-density lipoprotein (HDL) is decreased (Biden *et al.,* 2014, Parikh *et al.,* 2014). Biden *et al.,* 2014, reported adverse effects of hyperlipidaemia on glucose homeostasis. Therefore, controlling the

level of TG, TC, LDL and HDL levels could have a positive effect on glucose homeostasis. Several other synthetic analogues of amphibian host defence peptides have shown to improved blood lipid profile in high fat fed mice (Srinivasan *et al.,* 2015, Ojo *et al.,* 2015c, Owolabi *et al.,*2016). In the present study, plasma TG and LDL level were decreased significantly in [A14K] PGLa-AM1 and exenatide-treated mice. Also, in the PGLa-AM1 treated group, these parameters were decreased but not significantly. Interestingly, TC was decreased significantly only in [A14K] PGLa-AM1 treated *db/db* mice, indicating that peptide could have a role in the prevention of cardiovascular events associated with type 2 diabetes. Plasma HDL level remained unaffected in all *db/db* mice compared to their littermates.

In diabetes, the normal function of the liver is compromised by the accumulation of lipid, which induces hypertrophic changes in hepatocytes, as indicated by the elevated level of ALT, AST and ALP (Son *et al.,*2015). In the present study, elevated liver enzymes of control *db/db* mice were reversed by [A14K] PGLa-AM1 and exenatide treatment. Interestingly, the positive effect of these peptides on the lipid profile in *db/db* mice was corroborated with improved liver function test. Except for ALP, other liver parameters were also reduced significantly in PGLa-AM1 treated mice. Furthermore, the creatinine level was markedly decreased in all treatment groups. These observations suggest that native peptide and its synthetic analogue have positive effects on liver and kidney function, and therefore could be safely used for the treatment.

Serum amylase is a commonly used biomarker of acute pancreatitis (Pieper-Bigelow *et al.,* 1990). In the present study, an increase in amylase activity was observed in all peptide-treated mice, suggesting the potential risk of pancreatitis. In several studies, incretin-based drugs have been linked to pancreatitis and pancreatic cancer (Filippatos

et al., 2014, Egan *et al.,* 2014). However, the study by Steinberg *et al.,* 2017, reports that elevated amylase activity in liraglutide-treated patients was not related to the development of acute pancreatitis.

Impaired insulin secretion is one of the significant hallmarks of type 2 diabetes (Kahn *et al.,* 2006). In agreement with others (Do *et al.,* 2014), islet isolated from *db/db* mice exhibited impaired insulin release in response to the different concentration of exogenous glucose and insulin secretagogues. However, in [A14K] PGLa-AM1 and exenatide-treated group, insulin secretion was improved significantly. On the other hand, PGLa-AM1 also showed a tendency to enhance insulin secretory response but failed to produces the same effect as its analogue. Furthermore, pancreatic insulin content was significantly higher in [A14K] PGLa-AM1 and exenatide but not in PGLa-AM1 treated group compared to saline-treated *db/db* mice.

To further evaluate the positive effects of peptides on pancreatic beta cell function, gene expression was studied. Consistent with other studies (Wang & Thurmond, 2012, Poitout, 2013, Shimoda *et al.,* 2011), in *db/db* mice insulin secretory genes including *Ins1, Pdx1, Glp1r, Gipr, Abcc8, Kcnj11, Gck, Cacna1c* and *Gcg* were significantly downregulated, and the gene for apoptosis *Stat1* was significantly upregulated compared to lean littermates. These diabetes-induced changes were attenuated by [A14K] and exenatide treatment. The parent peptide also showed a tendency to improve the expression of these genes except for *Stat1* gene. Immunohistochemical analysis of pancreatic sections revealed that all peptides prevented a substantial decline of the large and medium-size islet in *db/db* mice. In PGLa-M1 treated group no significant changes in the islet area, beta-cell area and alpha-cell area were observed compared to saline treatment *db/db* mice. However, [A14K] PGLa-AM1

treatment showed a tendency to improve this islet morphology. As expected, islet morphology was significantly enhanced in the exenatide-treated group.

An additional study was performed using the transgenic mouse bearing the transgenes GluCre (tamoxifen inducible tagger) and ROSA26-YFP (reporter), to investigate the effects of [A14K] PGLa-AM1 on transdifferentiation of glucagon-expressing alpha cells to insulin-expressing beta cells. Alpha cells whose primary function is to produce glucagon hormone have also shown the ability to transdifferentiate into insulin-producing beta cells under conditions of extreme beta cell loss (Thorel *et al.*, 2010). In agreement with this, in our study, we observed a significant increase in the number of beta cells which were transdifferentiated from alpha cells (i.e. Ins^+ GFP^+) as well as cells expressing both insulin and glucagon (i.e. Ins^+ Glu^+) were increased in streptozotocin-treated mice compared to lean control. However, in peptide-treated mice, these cells were increased significantly compared to STZ control mice. Furthermore, peptide treatment resulted in significant increases of islet area and beta cell area compared to STZ control. Additionally, large and medium-sized islets increased, and smaller sized islet decreased significantly in the peptide-treated mice. Taken together, these results indicate that the [A14K] PGLa-AM1 could have an important role in the regeneration of beta cells by transdifferentiation of alpha to beta cells.

In conclusion, the present study has demonstrated the insulinotropic activity of [A14K] PGLa-AM1 in BRIN-BD11 and 1.1B4 cells. Furthermore, [A14K] PGLa-AM1 triggered proliferation and protected BRIN-BD11 cells against cytokine-induced apoptosis. The *in vivo* studies suggest that [A14K] PGLa-AM1 was more impressive than parent peptide PGLa-AM1, showing positive effects on the HbA1c, glycaemic responses, insulin secretion, hyperlipidaemia and insulin resistance in *db/db* mice.

Liver and kidney function was significantly improved in all treatment groups. [A14K] PGLa-AM1 treatment attenuated diabetes-induced expression of islet genes in *db/db* mice. Importantly, analogue has the potential to delay the progression of diabetes. Furthermore, data from the GluCre study suggest that [A14K] PGLa-AM1 could have an important role in the transdifferentiation of glucagon-expressing alpha cells to insulin-expressing beta cells. These observations are encouraging for the development of frog skin peptide analogues for the treatment of type 2 diabetes.

Figure 5.1 Schematic diagrams of the amino acid sequence of A) PGLa-AM1 and B) [A14K] PGLA-AM1

A)

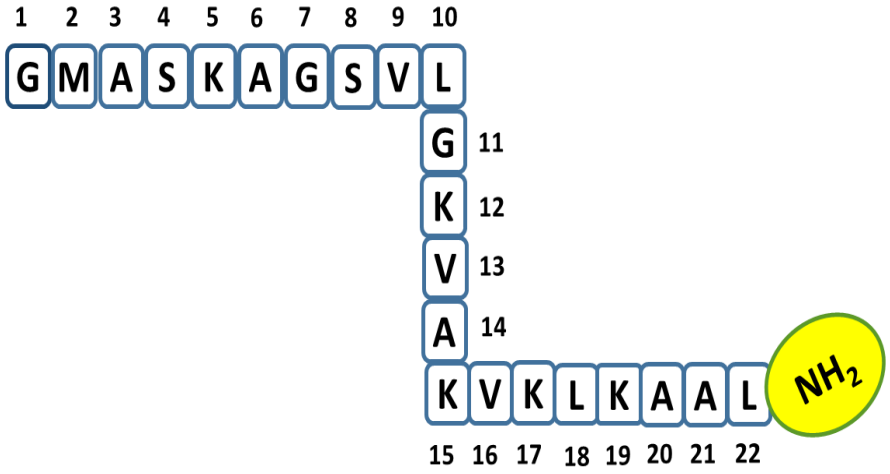

B)

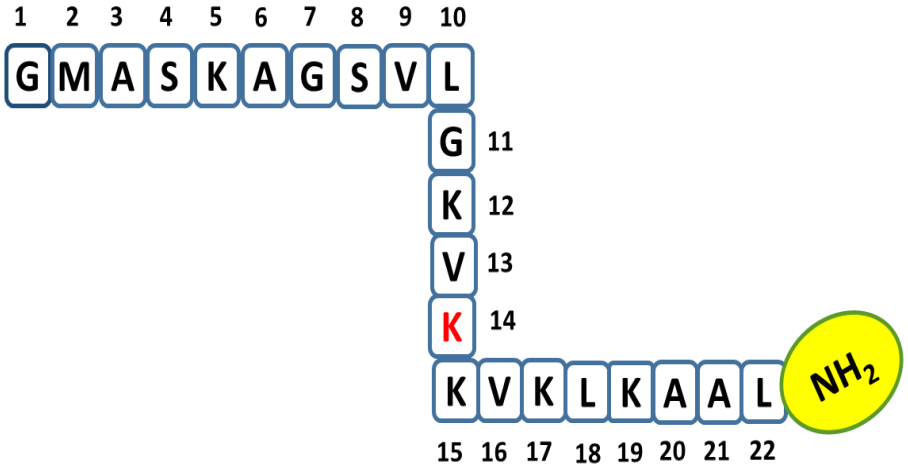

G=Glycine (Gly), M= Mthionine (Met), A= Alanine (Ala), S= Serine (Ser), K= Lysine (Lys). V= Valine (Val), L=Leucine (Leu).

Figure 5.2 Representation of Reverse-Phase HPLC (A) and MALDI-TOF profile (B) of [A14K] PGLA-AM1

A)

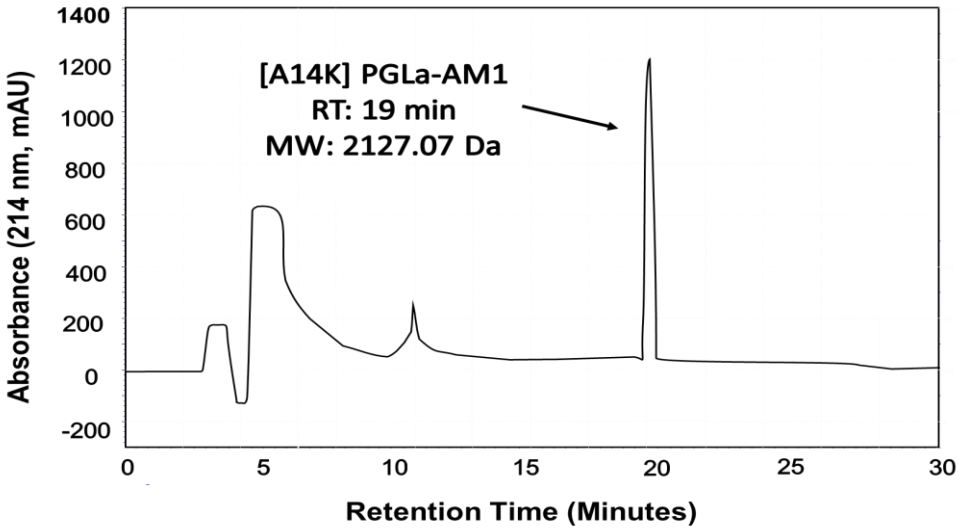

B)

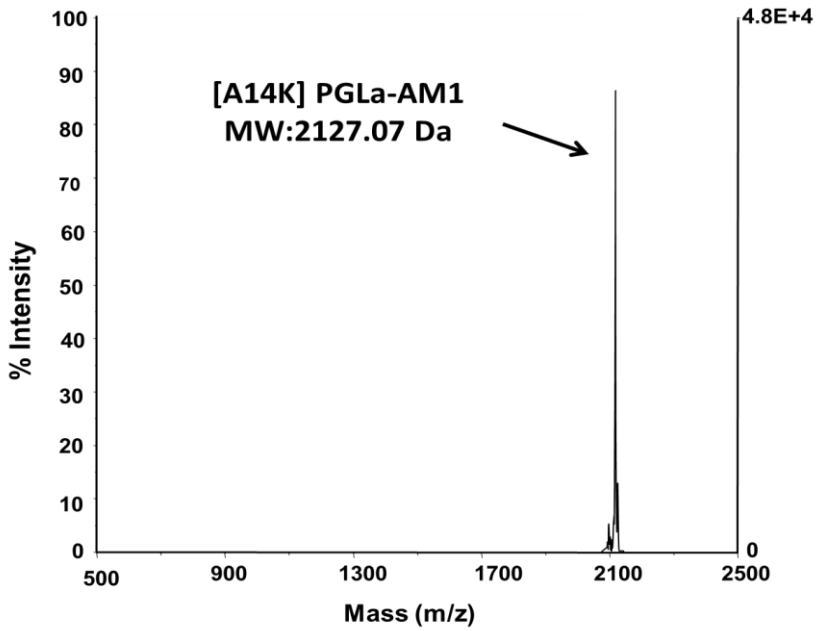

Purity and molecular mass of peptide were confirmed using RP-HPLC and MALDI-TOF respectively. The retention time was verified using ChromQuest software.

Figure 5.3 Dose-dependent effects of [A14K] PGLa-AM1 on Insulin (A) and LDH (B) release from BRIN-BD11 cells.

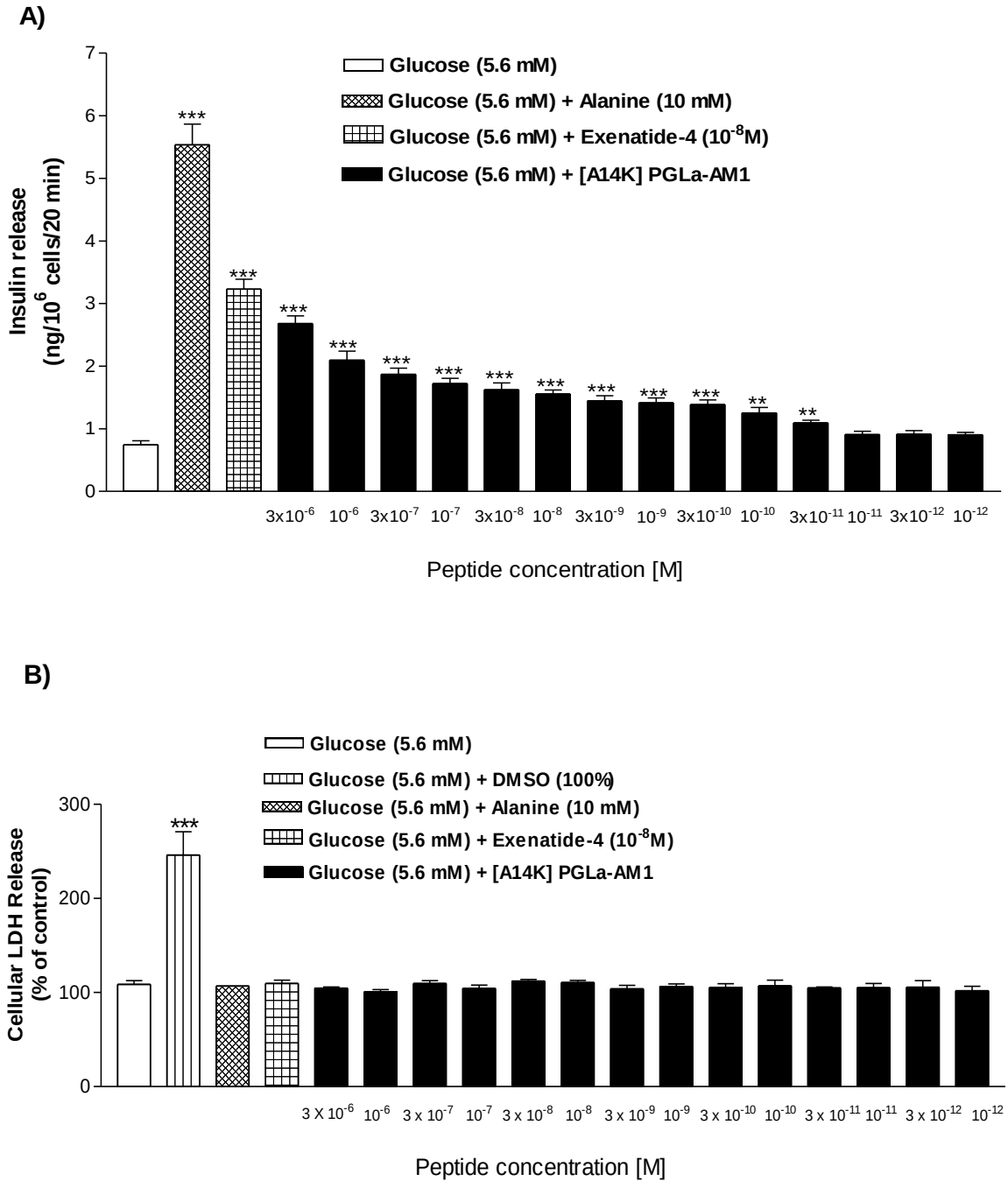

Values are Mean ± SEM with n=8 for insulin release and n=4 for LDH. Alanine (10 mM) and Exenatide-4 (10^{-8} M) were used as positive control for insulin secretion studies. DMSO (100%) was used as positive control for LDH assay. *P<0.05, **P<0.01, ***P<0.001 compared to 5.6mM glucose alone.

Figure 5.4 Dose-dependent effects of [A14K] PGLa-AM1 on Insulin release from 1.1B4 cells in (A) 5.6 and (B)16.7 mM glucose

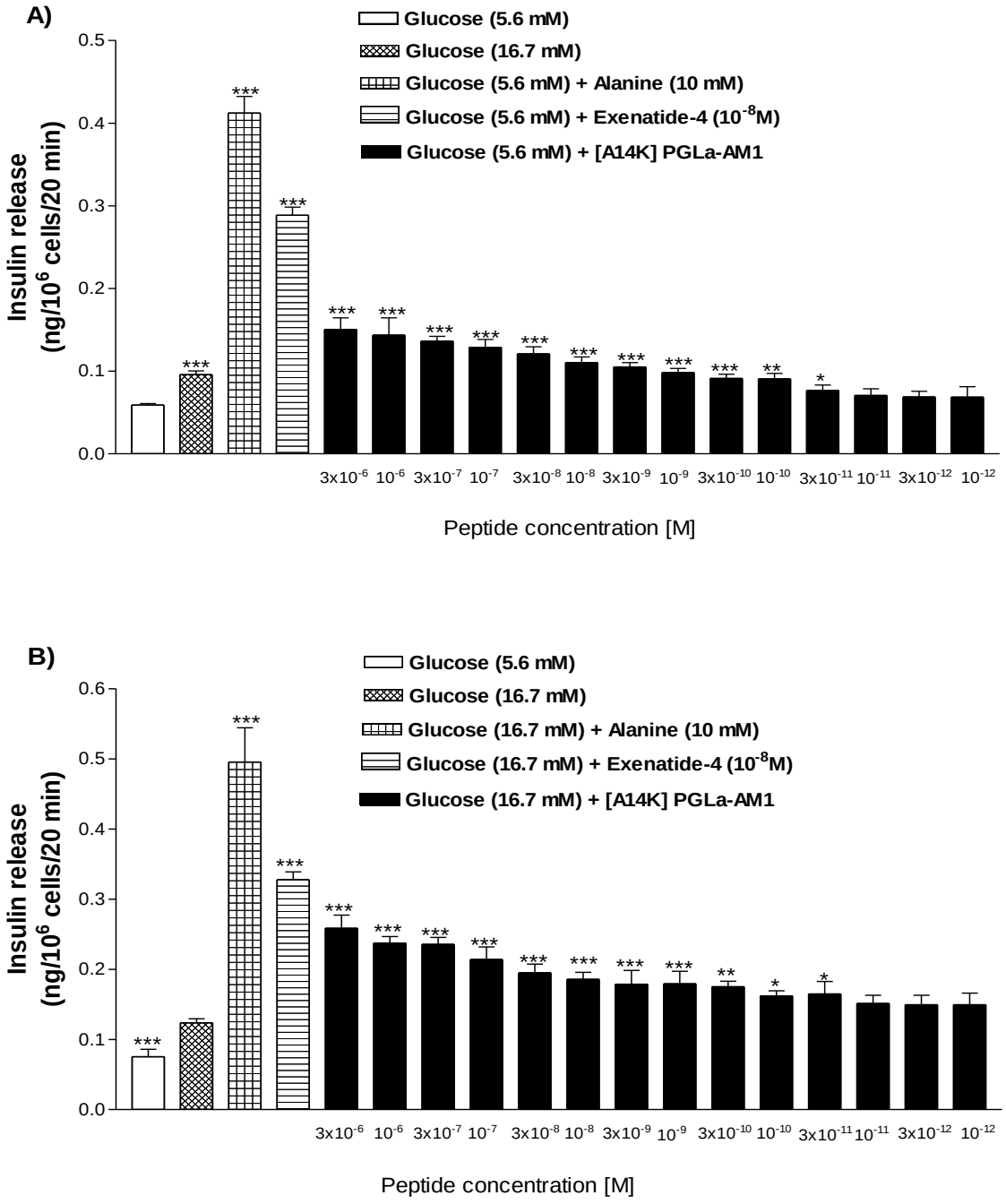

Values are Mean ± SEM with n=8 for insulin release. Alanine (10 mM) and Exenatide-4 (10^{-8} M) were used as positive control for insulin secretion studies. *P<0.05, **P<0.01, ***P<0.001 compared to 5.6 mM glucose (A) and *P<0.05, **P<0.01, ***P<0.001 compared to 16.7 mM glucose (B).

Figure 5.5 Effects of [A14K] PGLa-AM1 on apoptosis (A) and cell proliferation (B) in BRIN-BD11 cells

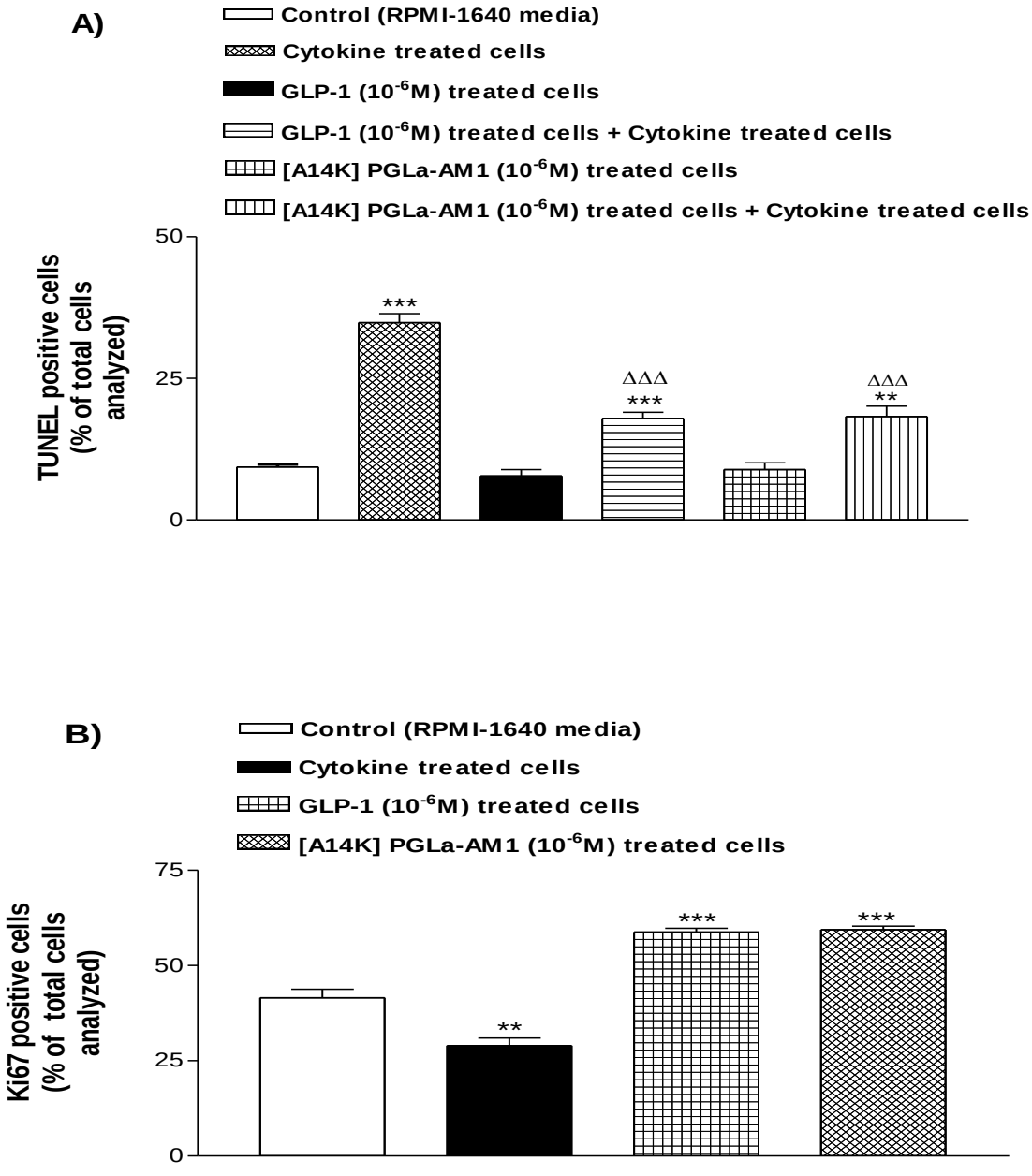

(A) Comparison of the effects of [A14K] PGLa-AM1 (1 µM) and GLP-1 (1 µM) on protection against cytokine-induced apoptosis in BRIN-BD11 cells. **P<0.01, ***P < 0.001 compared to incubation in culture medium alone, $^{\Delta\Delta\Delta}$P < 0.001 compared to incubation in cytokine-containing medium. (B) Comparison of the effects of [A14K] PGLa-AM1 (1 µM) and GLP-1 (1 µM) on proliferation of BRIN-BD11 cells. **P<0.01, ***P < 0.001 compared to incubation in culture medium alone

Figure 5.6 Effects of [A14K] PGLa-AM1 on glucose uptake in differentiated C2C12 cells

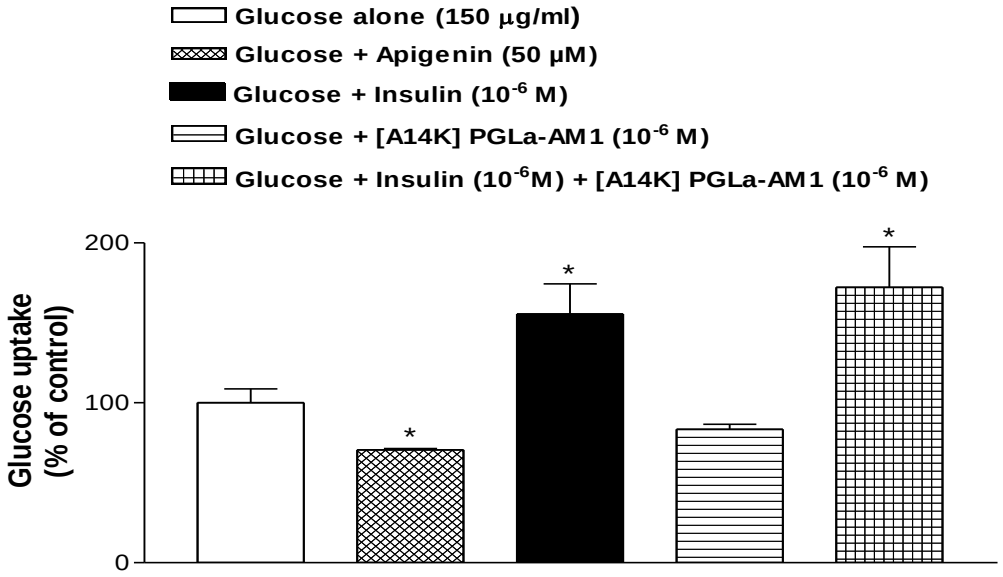

Glucose uptake was expressed as % of control (glucose). Apigenin was used as negative control for glucose uptake. Values are mean ± SEM with n=3. *P<0.05 compared with glucose alone.

Figure 5.7 Acute effects of [A14K] PGLa-AM1 peptide on cumulative food intake in 21 hr fasted lean NIH Swiss TO mice

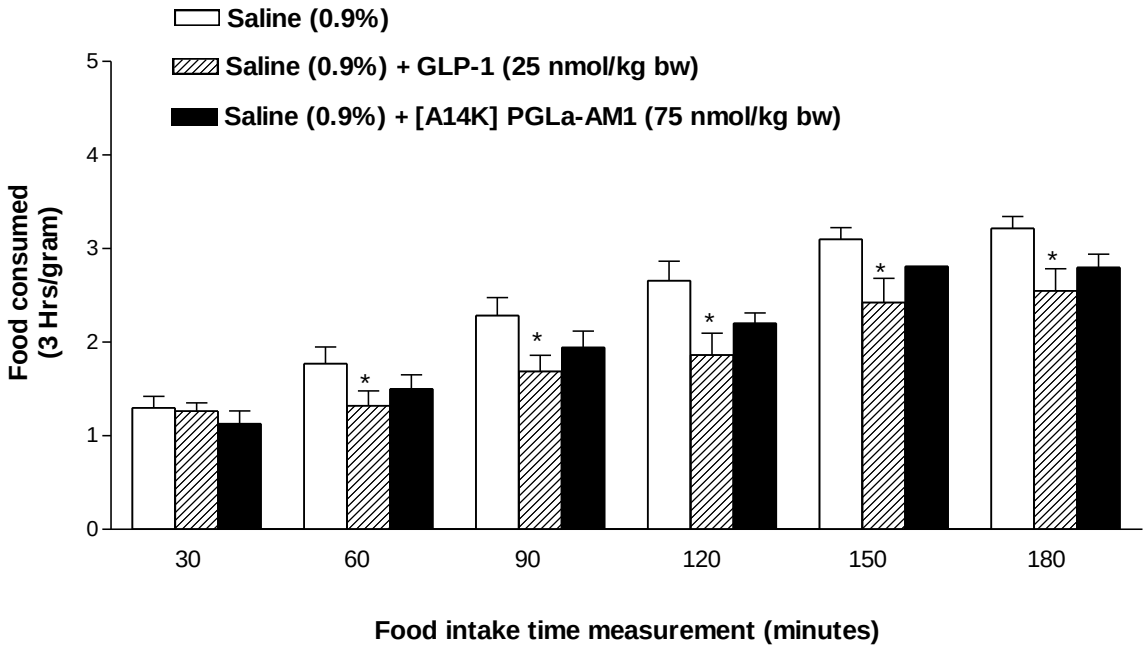

Cumulative food intake was measured prior to and after after i.p. injection of saline vehicle (0.9% w/v NaCl) or GLP-1 (25 nmol/kg bw) or test peptides (75 nmol/kg bw) at time point 30, 60, 90, 120, 150, 180 min in overnight (21 hr) fasted mice. Values represent mean ± SEM (n=8). *P<0.05 compared to saline control.

Figure 5.8 Effects of 28-day treatment with PGLa-AM1 and [A14K] PGLa-AM1 on body weight (A, B), energy intake (C, D) and water intake (E, F) in *db/db* mice

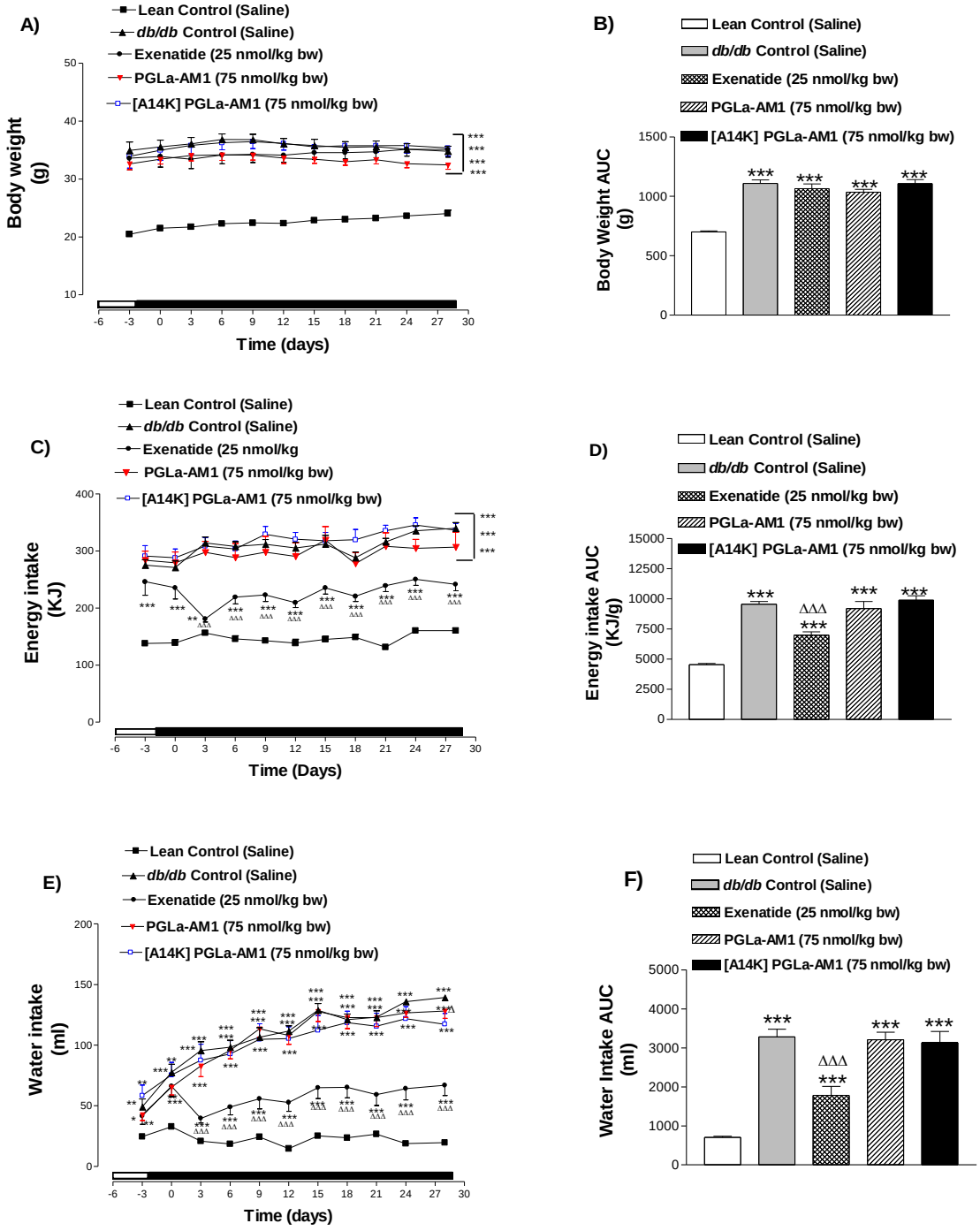

Body weight, energy intake and water intake were measured 3 days prior to, and every 72 hours during treatment with saline or exenatide (25 nmol/kg bw) or peptide (75 nmol/kg bw) for 28 days. Values are mean ±SEM for 8 mice. *P<0.05, **P<0.01 ***P<0.001 compared to lean mice and $^{\Delta}$P<0.05, $^{\Delta\Delta}$P<0.01, $^{\Delta\Delta\Delta}$P<0.001compared to control *db/db* mice

Figure 5.9 Effects of 28-day treatment with PGLa-AM1 and [A14K] PGLa-AM1 on non-fasting blood glucose (A, B) and plasma insulin (C, D) in *db/db* mice

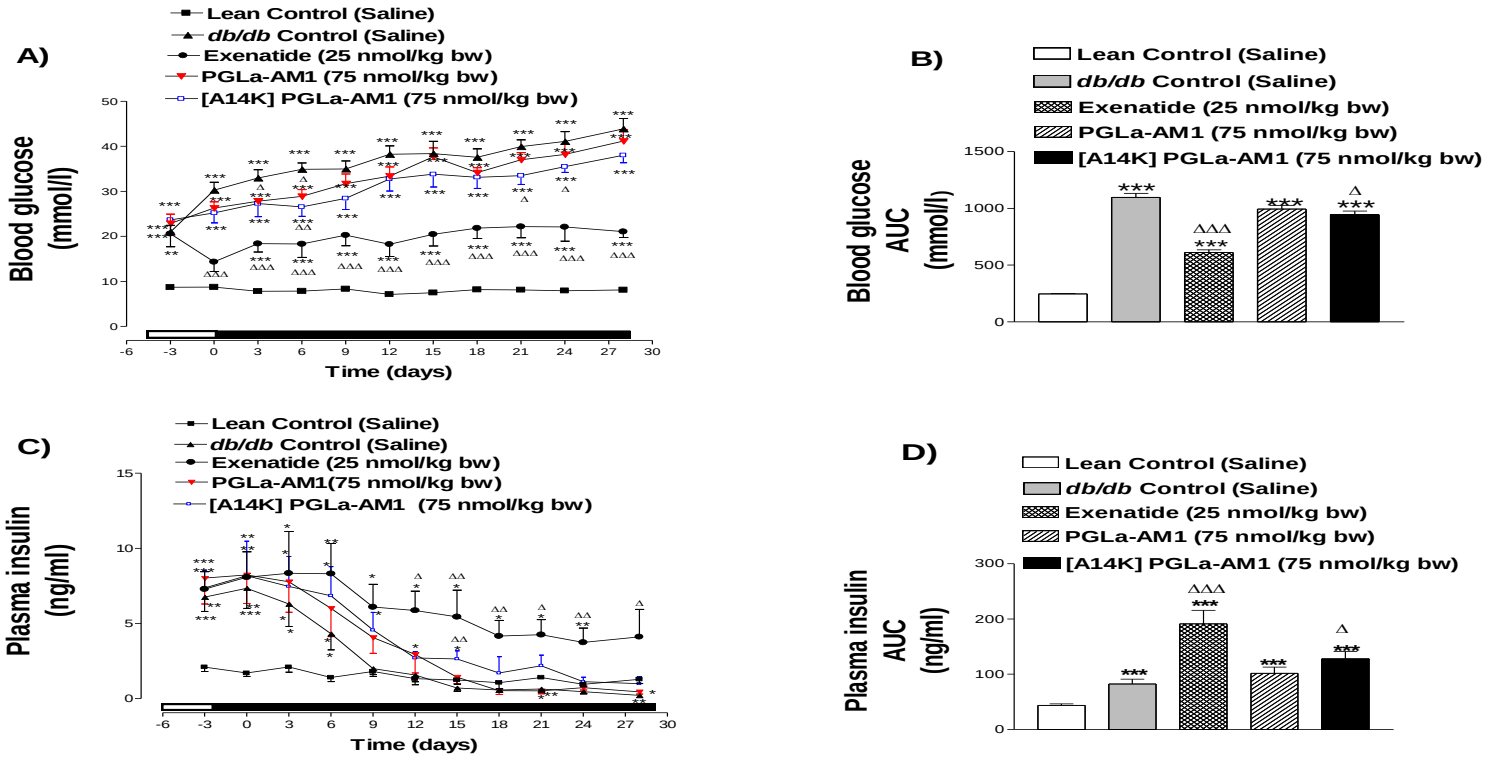

Parameters were measured 3 days prior to, and every 72 hours during treatment (indicated with black bar) with saline or exenatide (25 nmol/kg bw) or peptide (75 nmol/kg bw) for 28 days. Values are mean ±SEM for 8 mice. *P<0.05, **P<0.01 ***P<0.001 compared to lean mice and $^{\Delta}$P<0.05, $^{\Delta\Delta}$P<0.01, $^{\Delta\Delta\Delta}$P<0.001 compared to control *db/db* mice

Figure 5.10 Long-term effects of PGLa-AM1 and [A14K] PGLa-AM1 on HbA1c in *db/db* mice

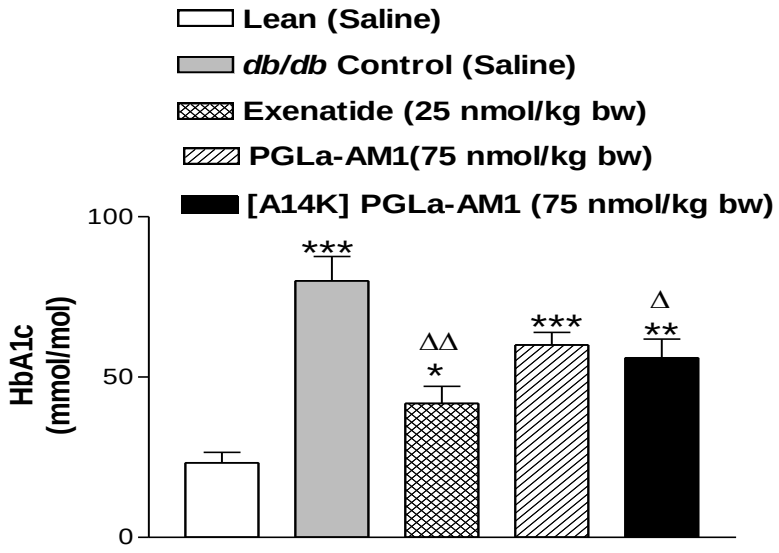

HbA1c level was measured after long term treatment with twice-daily injections of either saline or peptide (75nmol/kg bw) for 28 days. Values are Mean ± SEM for 4 mice. *P<0.05, **P<0.01, ***P<0.001 compared with lean mice and $^{\Delta}$P<0.05, $^{\Delta\Delta}$P<0.01 compare with *db/db* control mice.

Figure 5.11 Long-term effects of PGLa-AM1 and [A14K] PGLa-AM1 on plasma glucose (A, B) and insulin (C, D) concentrations following intraperitoneal glucose administration to *db/db* mice

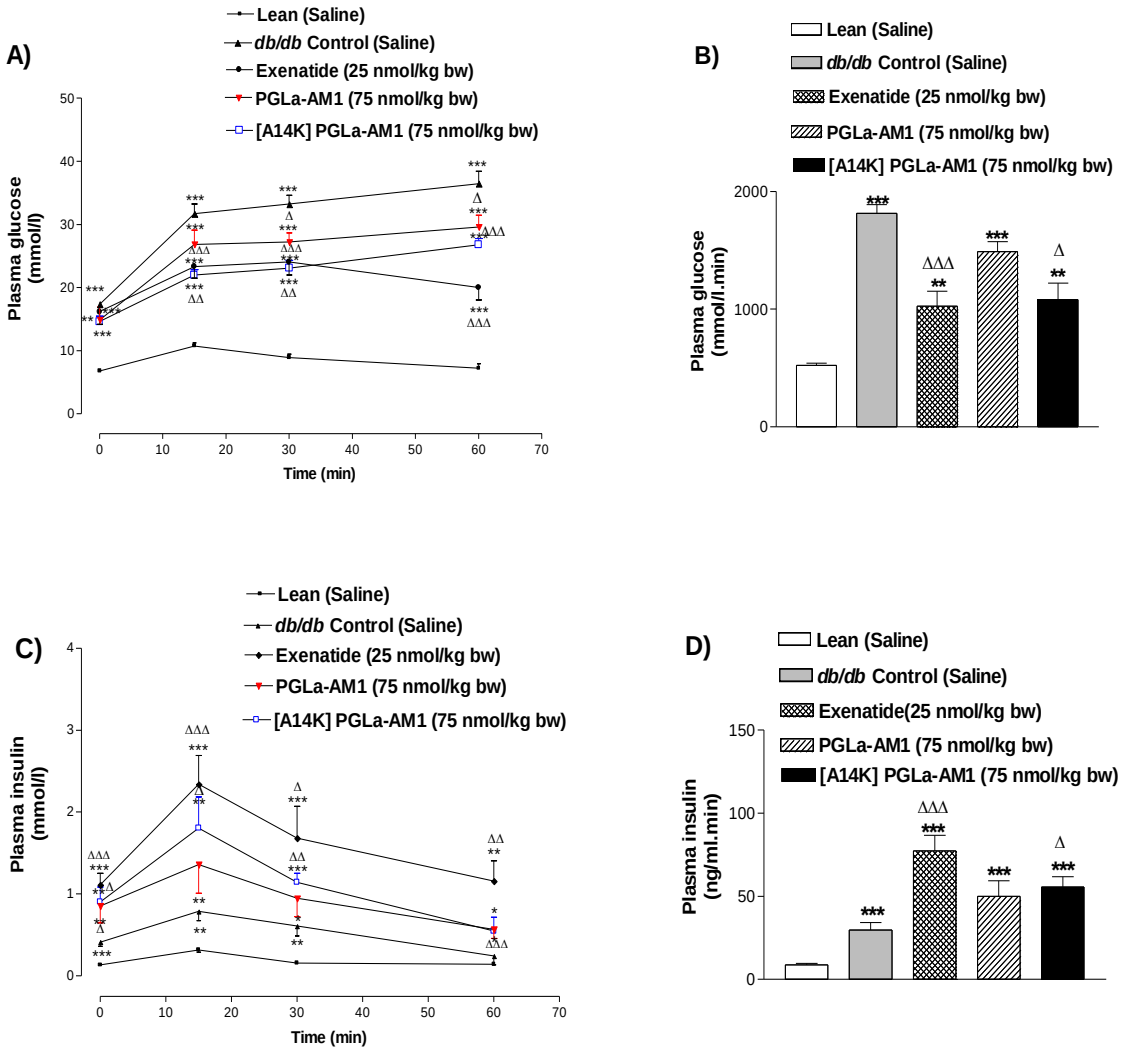

Plasma glucose and insulin concentrations were measured prior to and after intraperitoneal administration of glucose (18 mmol/kg bw) to *db/db* fed mice pre-treated with twice-daily injections of either saline or peptide (75nmol/kg bw) for 28 days. Values are Mean ± SEM for 8 mice. *P<0.05, **P<0.01 ***P<0.001 compared to lean mice and $^{\Delta}$P<0.05, $^{\Delta\Delta}$P<0.01, $^{\Delta\Delta\Delta}$P<0.001compared to control *db/db* mice.

Figure 5.12 Long-term effects of PGLa-AM1 and [A14K] PGLa-AM1 on plasma glucose (A, B) and insulin (C, D) concentrations following oral glucose administration to *db/db* mice

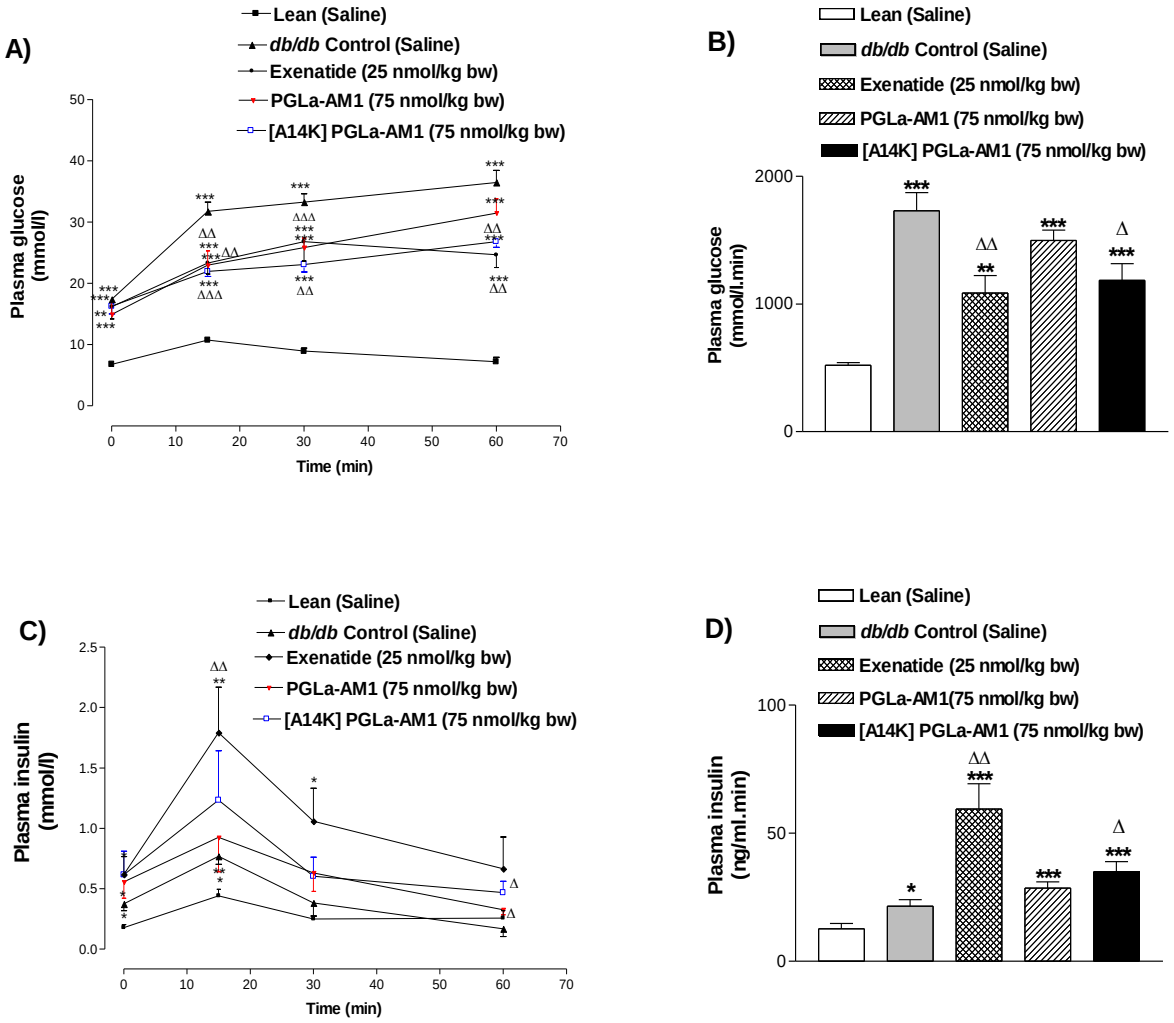

Plasma glucose and insulin concentrations were measured prior to and after oral administration of glucose (18 mmol/kg bw) to *db/db* mice pre-treated with twice-daily injections of either saline or peptide (75nmol/kg bw) for 28 days. Values are Mean ± SEM for 8 mice. *P<0.05, **P<0.01 ***P<0.001 compared to lean mice and $^{\Delta}$P<0.05, $^{\Delta\Delta}$P<0.01, $^{\Delta\Delta\Delta}$P<0.001compared to control *db/db* mice.

Figure 5.13 Long-term effects of PGLa-AM1 and [A14K] PGLa-AM1 on insulin sensitivity in *db/db* mice

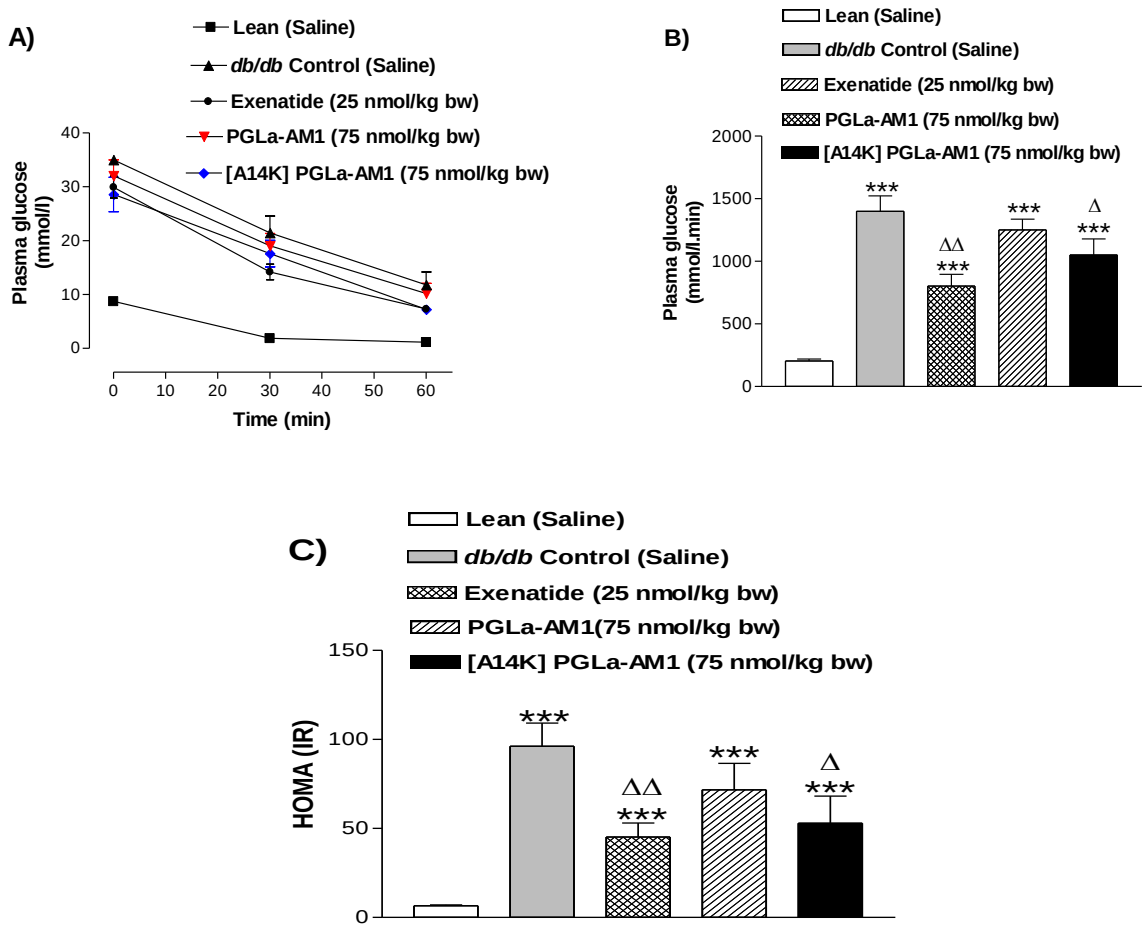

Plasma glucose were measured prior to and after intraperitoneal injection of insulin (50 U/kg bw) in *db/db* mice pre-treated with twice-daily injections of either saline or peptide (75nmol/kg bw) for 28 days. Values are Mean ± SEM for 8 mice. $^{***}P<0.001$ compared with to lean mice and $^{\Delta\Delta}P<0.05$, $^{\Delta\Delta}P<0.01$ compare with *db/db* control mice.

Figure 5.14 Effects of PGLa-AM1 and [A14K] PGLa-AM1 on body composition in *db/db* mice

A)

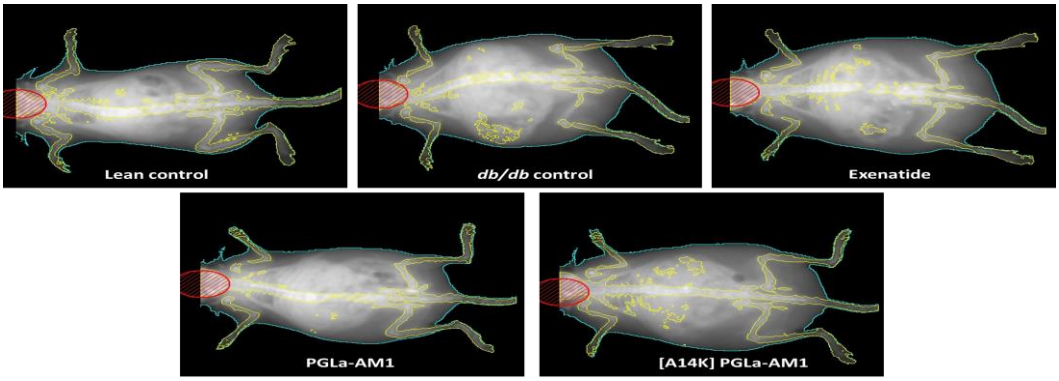

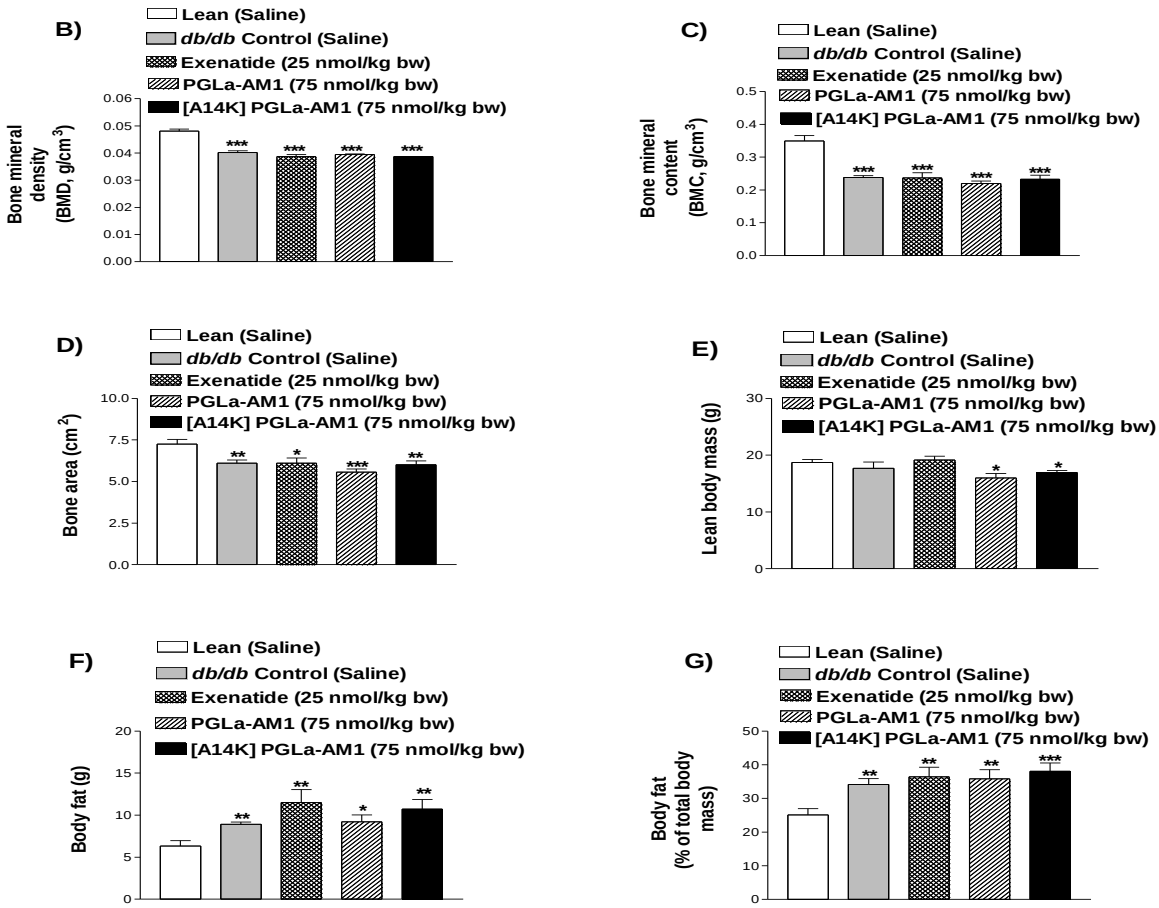

Effects of PGLa-AM1 and [A14K] PGLa-AM1 on body composition in lean and *db/db* mice. Animals were injected with either saline or peptide (75 nmol/kg body weight per day) for 28 days. The figure shows (A) representative DEXA scans, (B) bone mineral density, (C) bone mineral content, (D) bone area. (E) lean body mass, (F) body fat and (G) body fat expressed and percentage of total body mass. Values are means ± SEM for 8 mice. *P<0.05, **P<0.01, ***P<0.001 compared with saline-treated lean mice.

Figure 5.15 Effects of PGLa-AM1 and [A14K] PGLa-AM1 on pancreatic weight (A), total insulin content (B), and insulin secretory response of isolated islets (C&D) from lean and *db/db* mice to glucose and insulin secretagogues

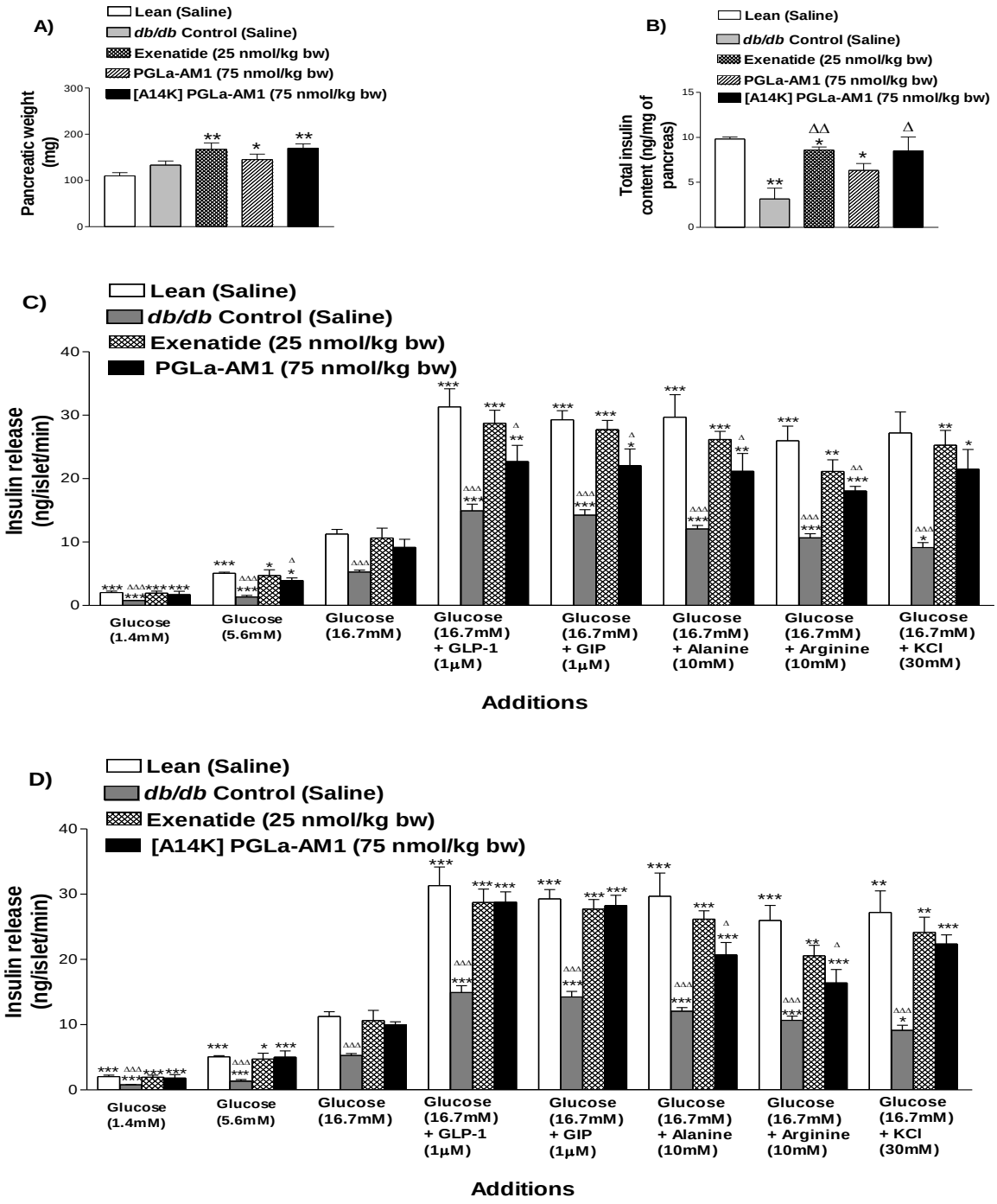

Mice were treated with saline or peptide (75nmol/kg bw) for 28 days prior to experiment. Values are means ± SEM with n=4. *P<0.05, **P<0.01, ***P<0.001 compared with the response of islets isolated from each group of mice at 16.7mM glucose; $^{\Delta}$P<0.05, $^{\Delta\Delta}$P<0.01, $^{\Delta\Delta\Delta}$P<0.001 compared with the response of islets isolated from lean mice (saline treated) to each secretagogue or glucose concentration.

Figure 5.16 Effects of long-term treatment with PGLa-AM1 and [A14K] PGLa-AM1 on total cholesterol (A), triglycerides (B), HDL (C) and LDL (D) in *db/db* mice

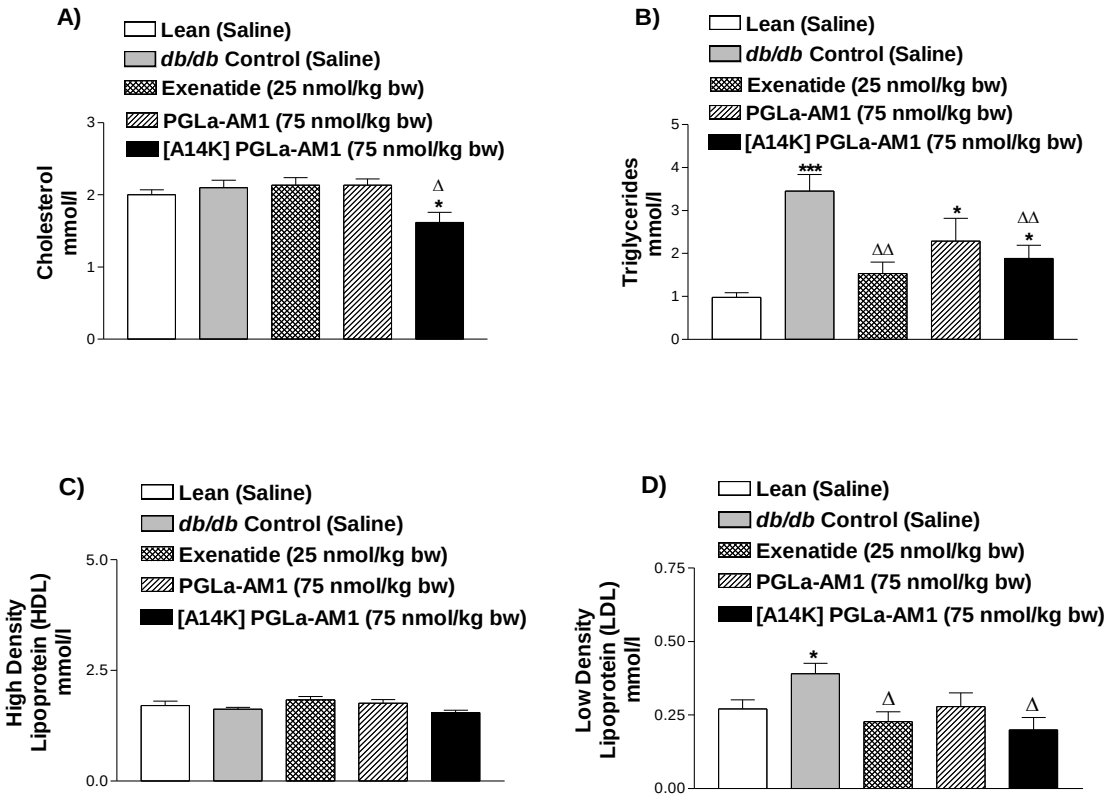

Plasma sample was collected after 28 days treatment with either saline (control) or peptide. Values are Mean ± SEM for 6 mice. *P<0.05, ***P<0.001 compared to lean mice. $^{\Delta}$P<0.05, $^{\Delta\Delta}$P<0.01 compared to *db/db* control mice.

Figure 5.17 Effects of long-term treatment with PGLa-AM1 and [A14K] PGLa-AM1 on plasma AST (A) ALT (B) ALP (C) and creatinine (D) levels in *db/db* mice

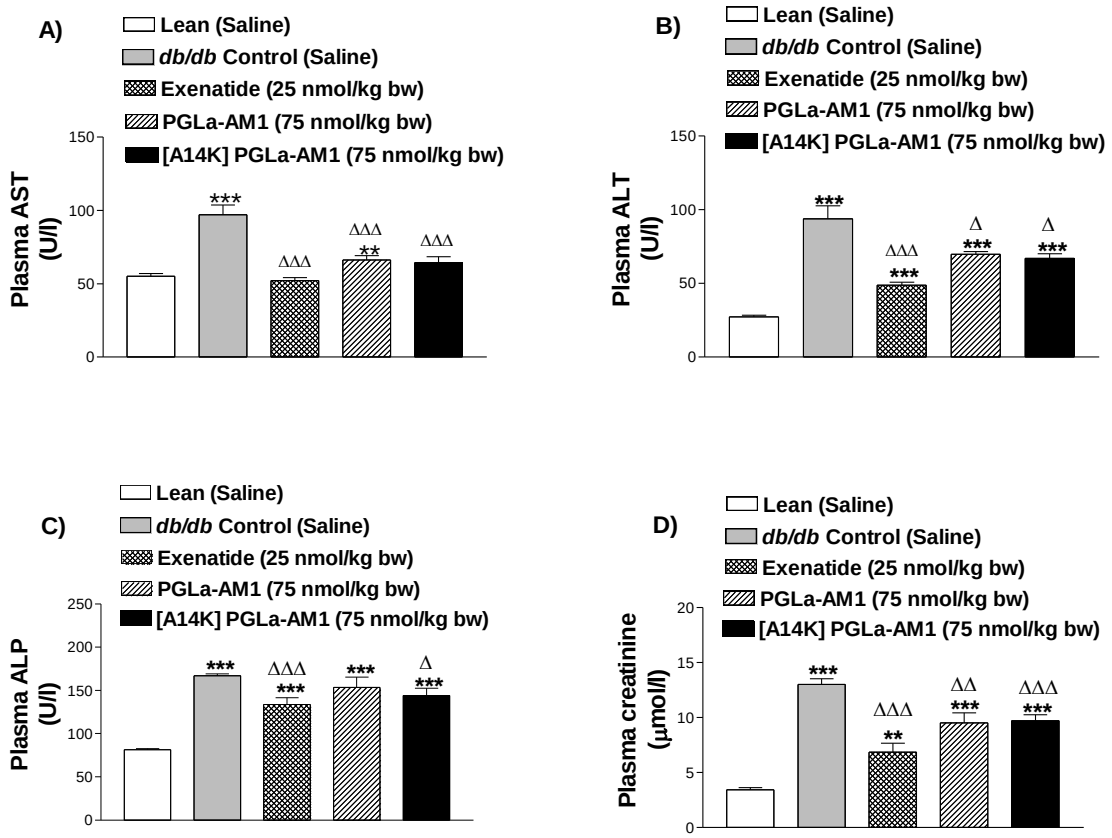

Following 28 days injection with either saline (control) or peptide, plasma sample was collected and measured for ALT, AST, ALP and creatinine levels. Values are Mean ± SEM for 6 mice. **P<0.01, ***P<0.001 compared to lean control. $^{\Delta}$P<0.05, $^{\Delta\Delta}$P<0.01, $^{\Delta\Delta\Delta}$P<0.001 compared to *db/db* control.

Figure 5.18 Effects of long-term treatment with PGLa-AM1 and [A14K] PGLa-AM1 on amylase activity in diabetic mice (*db/db*)

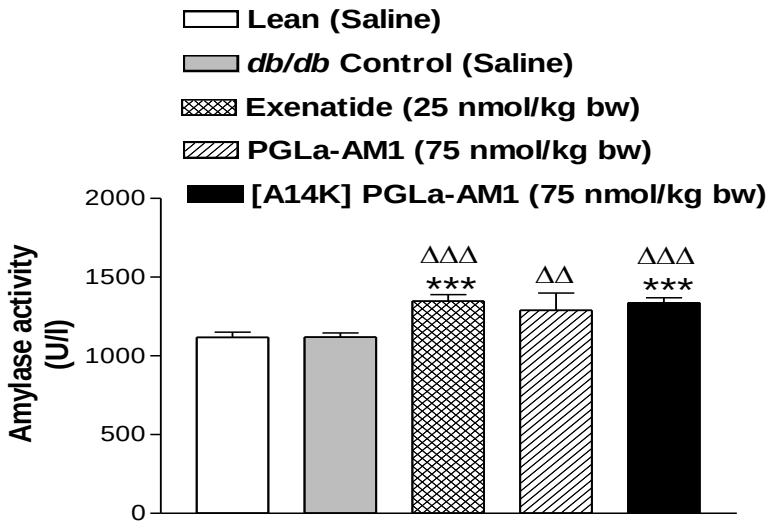

Plasma samples were collected after 28 days injection of [A14K] PGLa-AM1 and amylase activity was measured. Values are Mean ± SEM for n=6 mice. ***P<0.001 compared to lean control, $^{\Delta\Delta}$P<0.01, $^{\Delta\Delta\Delta}$P<0.001 compared to *db/db* control.

Figure 5.19 Effects of PGLa-AM1 & [A14K] PGLa-AM1 treatment on islet morphology in *db/db* mice

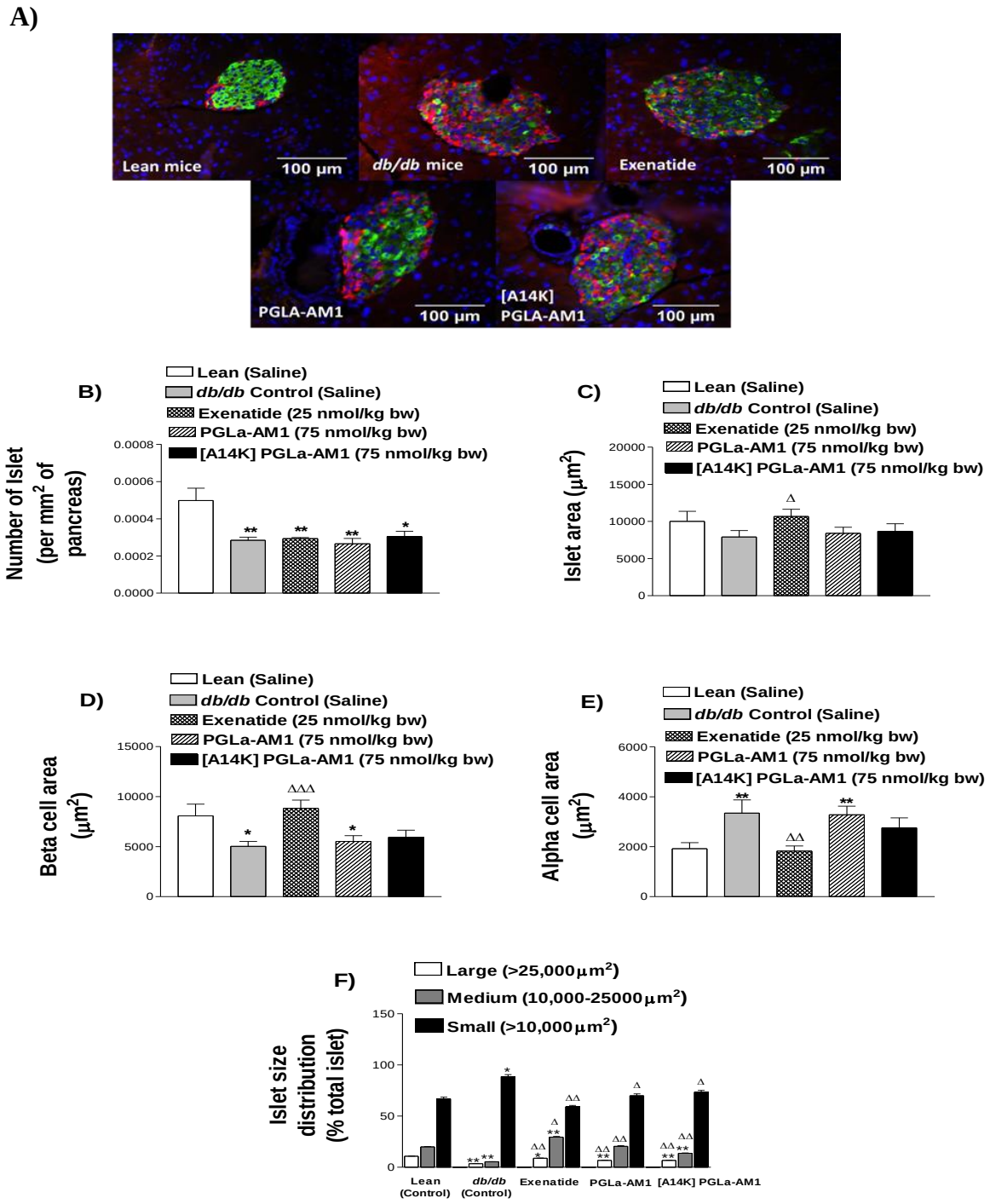

Representative islets (A) showing insulin (green) and glucagon (red) immunoreactivity from lean, *db/db* control, Exenatide, PGLa-AM1 and [A14K] PGLa-AM1 treated mice. B, C, D, E, and F shows islet number, islet area, beta cell area, alpha cell area and islet size distribution respectively. Mean ± SEM for 6 mice (~80 islets per group). *P<0.05, **P<0.01 compared to normal saline control, $^{\Delta}$P<0.05, $^{\Delta\Delta}$P<0.01, $^{\Delta\Delta\Delta}$P<0.001 compared to *db/db* control.

Figure 5.20 Effects of PGLa-AM1 & [A14K] PGLa-AM1 treatment on expression of genes involved in insulin action in skeletal muscle

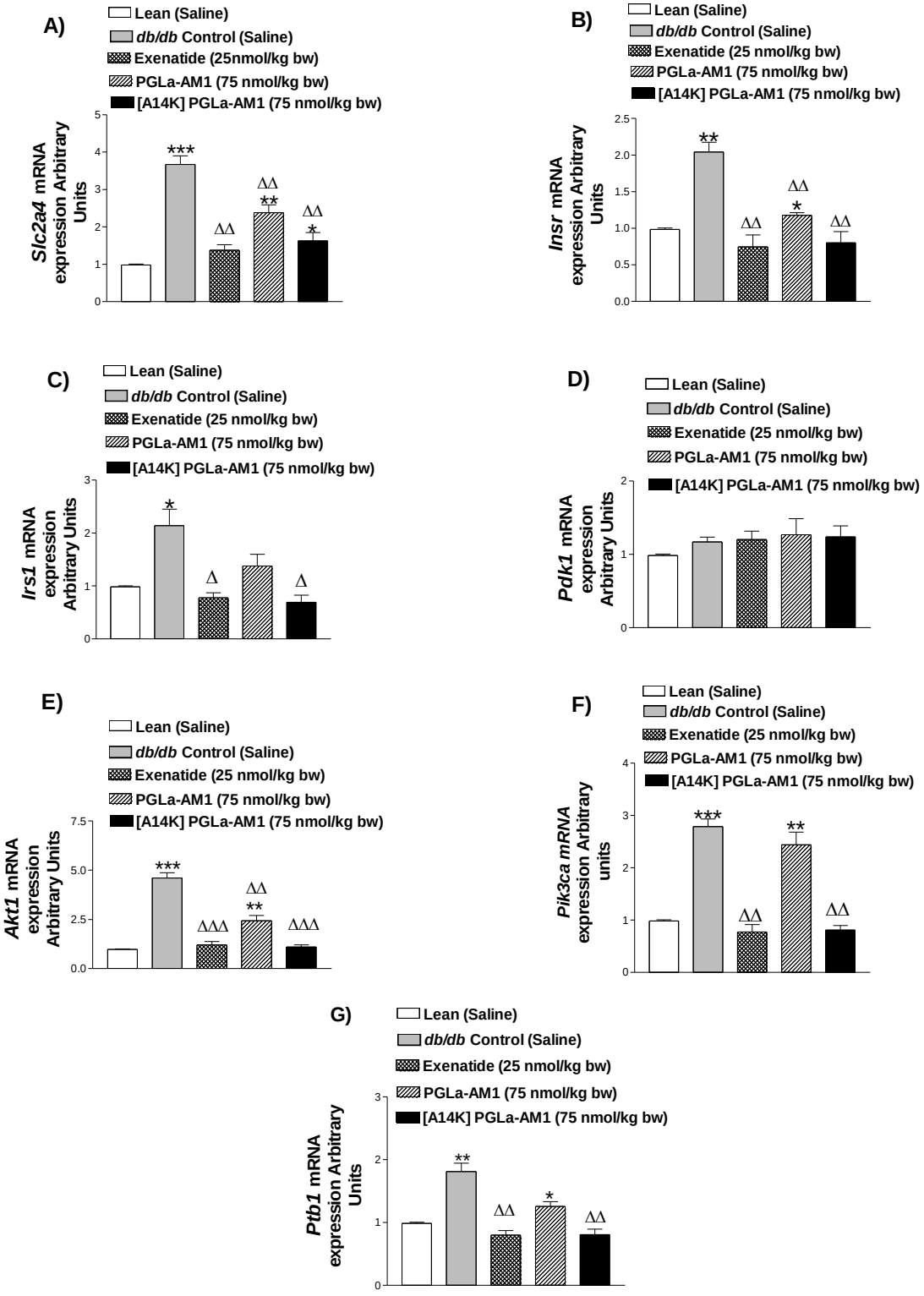

3µg of mRNA was used for cDNA synthesis. Expression values were normalised to Actb. Values are mean ± SEM for n=4. *P<0.05, **P<0.01, ***P<0.001 compared to normal control, $^{\Delta}$P<0.05, $^{\Delta\Delta}$P<0.01, $^{\Delta\Delta\Delta}$P<0.001 compared to *db/db* control.

Figure 5.21 Effects of PGLa-AM1 and [A14K] PGLa-AM1 treatment on expression of genes involved in insulin secretion from islets

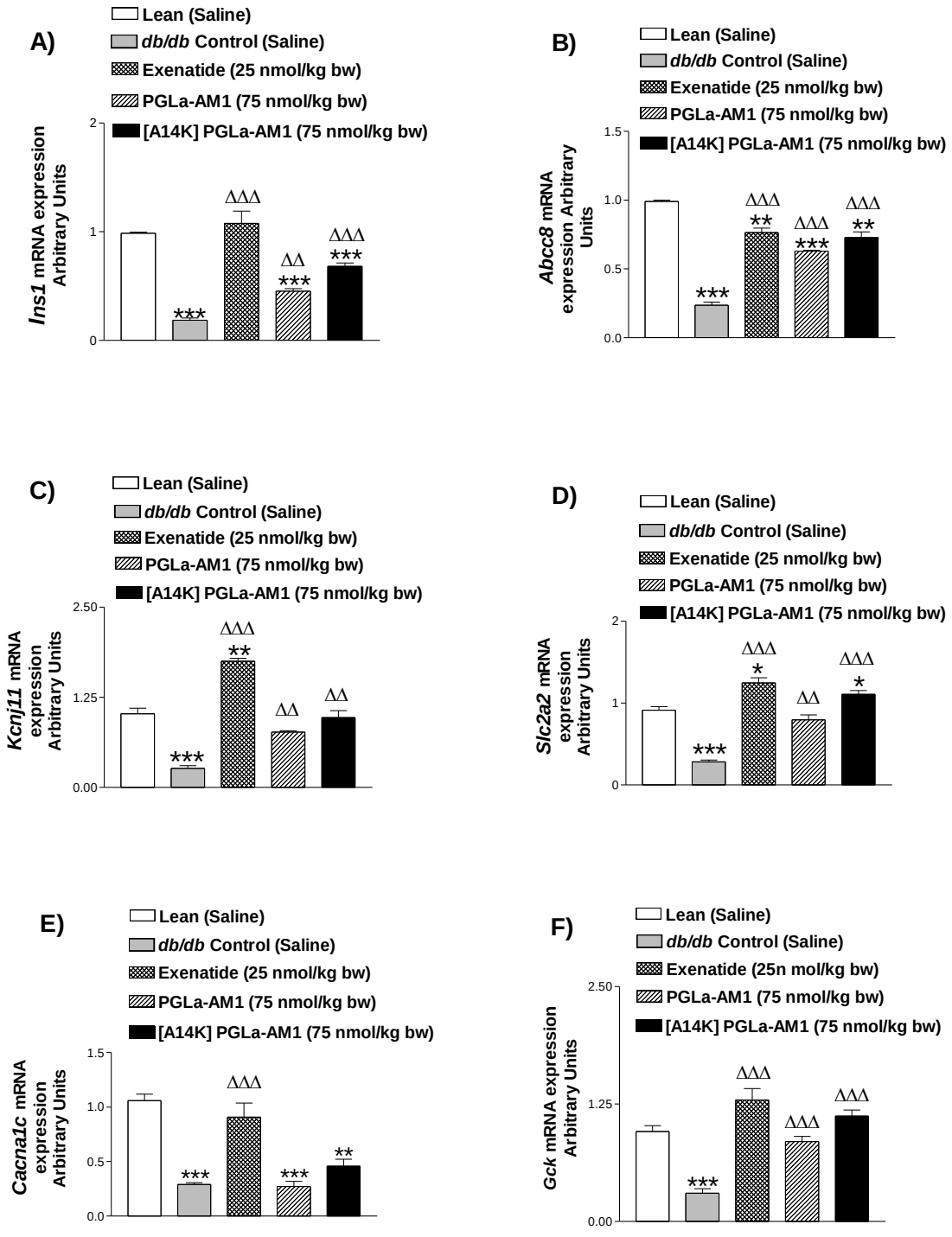

3 µg of mRNA was used for cDNA synthesis. Expression values were normalised to Actb. Values are mean ± SEM for n=4. *P<0.05, **P<0.01, ***P<0.001 compared to normal control, $^{\Delta\Delta}$P<0.01, $^{\Delta\Delta\Delta}$P<0.001 compared to *db/db* control mice.

Figure 5.22 Effects of PGLa-AM1 and [A14K] PGLa-AM1 treatment on expression of genes involved in insulin secretion (A- C), beta cell proliferation (D) and beta cell apoptosis (E) in islets

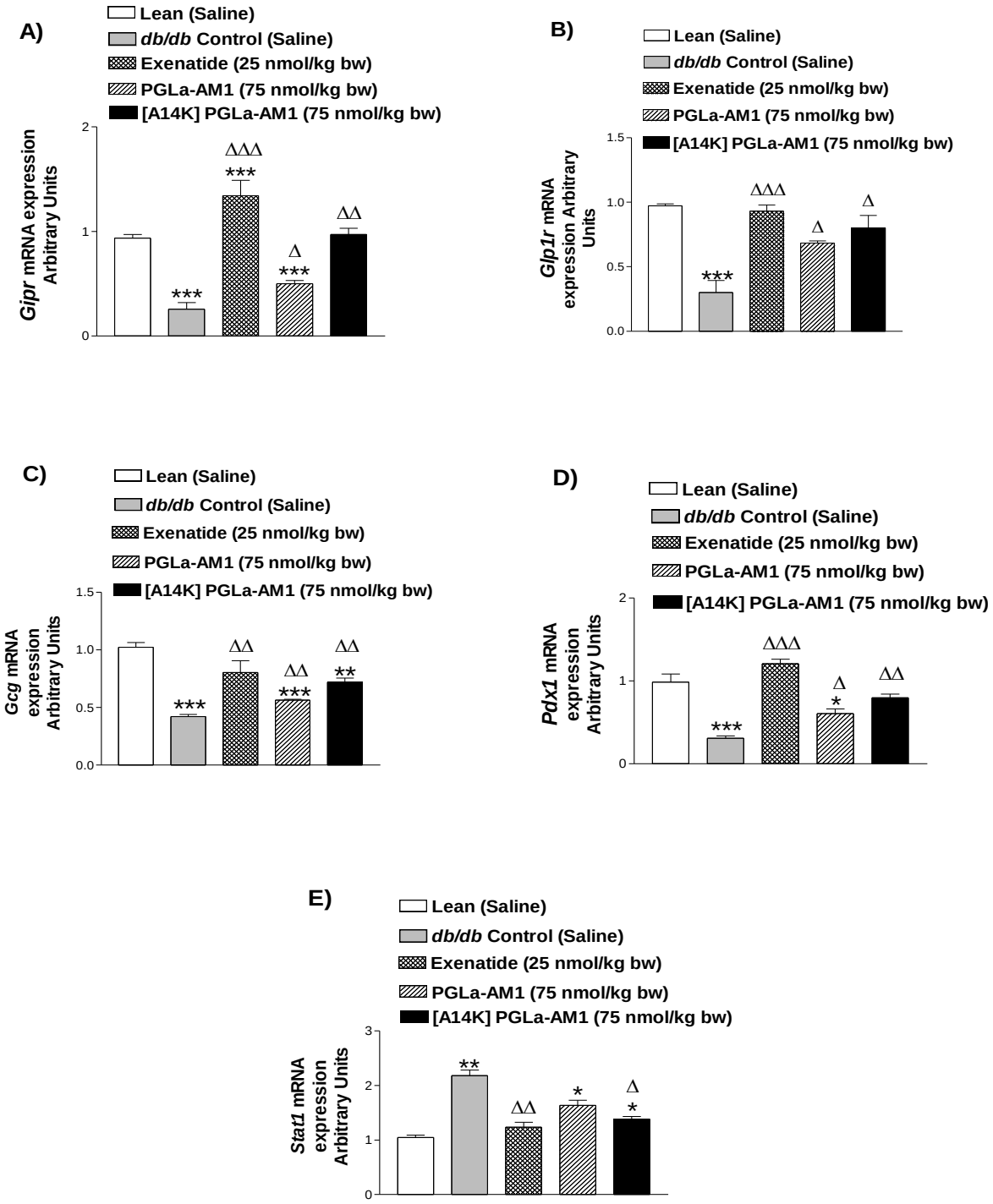

3 µg of mRNA was used for cDNA synthesis. Expression values were normalised to Actb. Values are mean ± SEM for n=4. *P<0.05, **P<0.01, ***P<0.001 compared to normal control, $^{\Delta}$P<0.05, $^{\Delta\Delta}$P<0.01, $^{\Delta\Delta\Delta}$P<0.001 compared to *db/db* control mice.

Figure 5.23 Effects of twice daily administration of [A14K] PGLa-AM1 on body weight change (A and B), food intake (C) and water intake (D) in GluCre-ROSA26EYFP mice

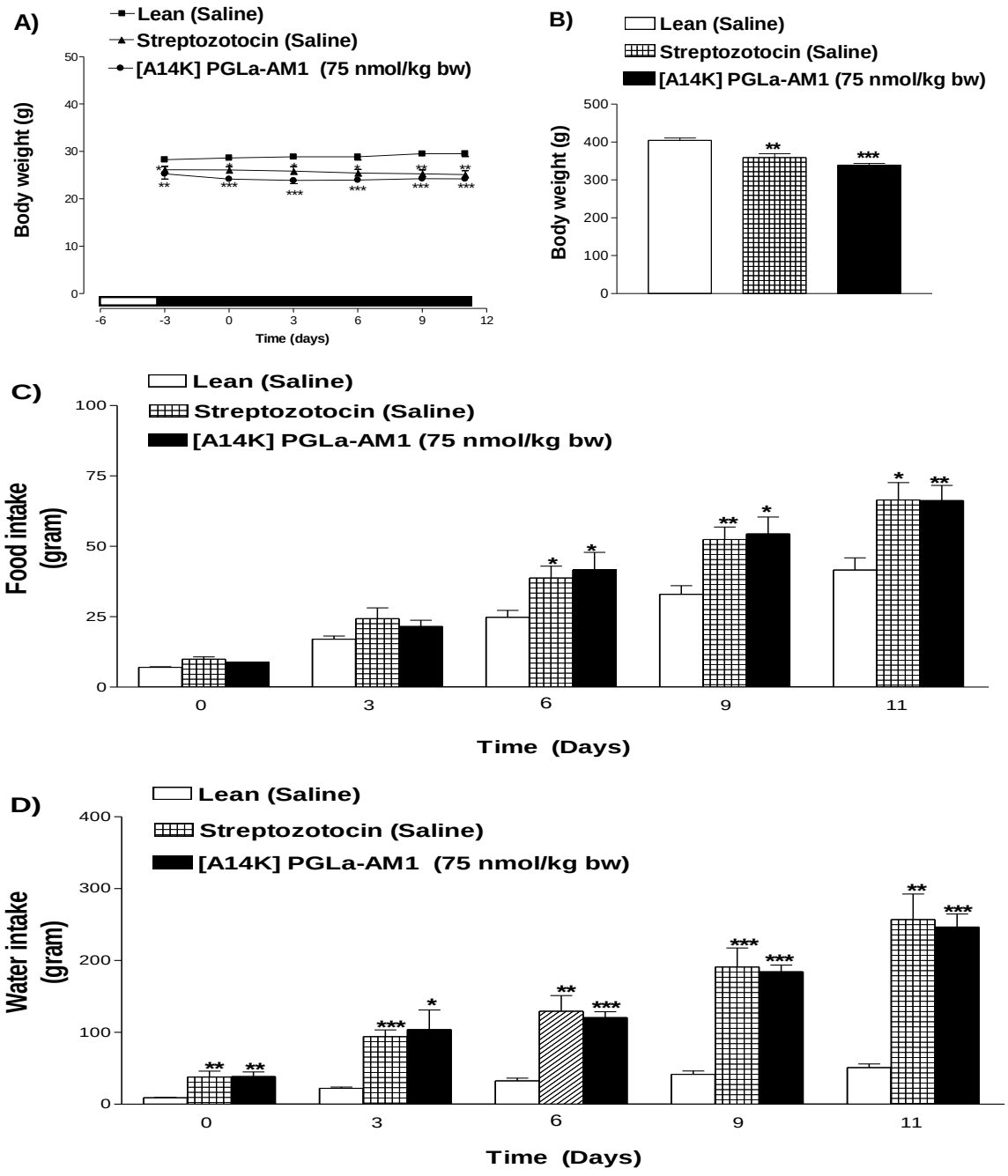

Streptozotocin (50mg/kg bw) induced diabetic mice were grouped prior to the peptide treatment. Body weight (A & B), food intake (C), water intake (D) were measured 3 days prior to, and every 72 hours during treatment with saline or [A14K] PGLa-AM1 (75 nmol/kg bw) for 11 days. Values are mean ±SEM for 5 mice. *P<0.05, **P<0.01 ***P<0.001 compared to lean mice.

Figure 5.24 Effects of twice daily administration of [A14K] PGLa-AM1 on blood glucose (A) and plasma insulin (B) in GluCre-ROSA26EYFP

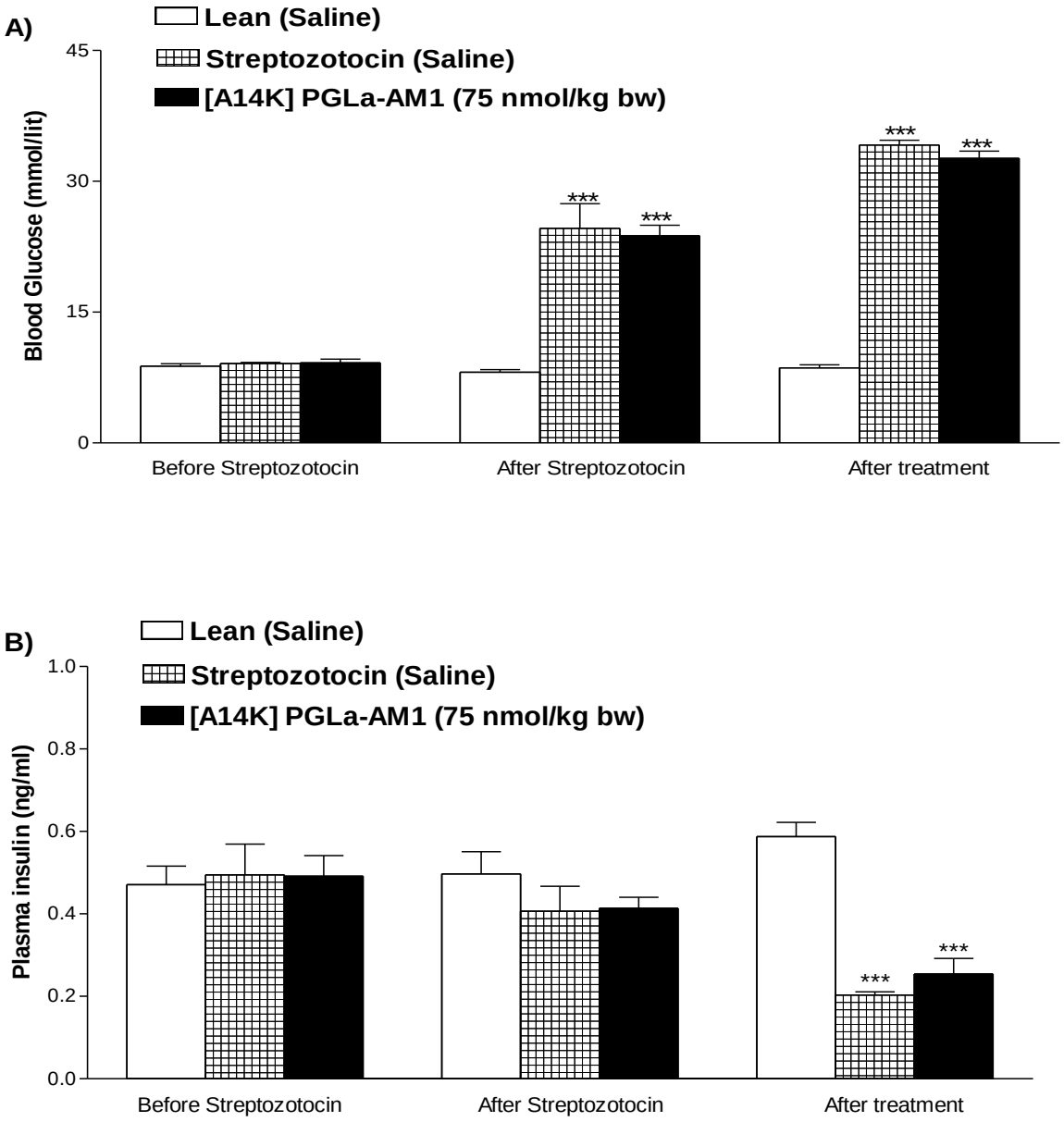

Blood glucose (A) and plasma insulin (B) were measured before and after streptozotocin, and after 11 days treatment with saline or [A14K] PGLa-AM1 (75 nmol/kg bw). Values are mean ±SEM for 5 mice. ***P<0.001 compared to lean mice.

Figure 5.25 Effects of twice daily administration of [A1K] PGLa-AM1 on pancreatic insulin content in GluCre-ROSA26EYFP mice

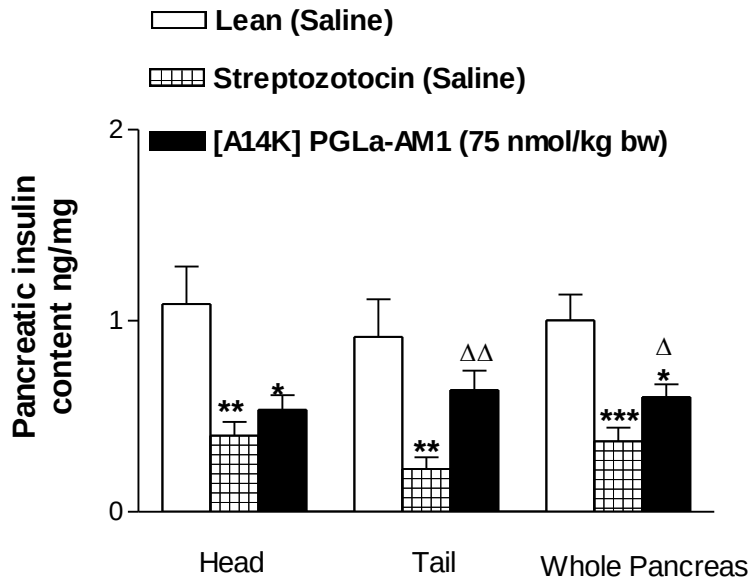

Pancreatic insulin content was measured after 11 days treatment with saline or [A14K] PGLa-AM1(75 nmol/kg bw). Values are mean ±SEM for 5 mice *P<0.05, **P<0.01, ***P<0.001 compared to normal saline control, $^{\Delta}$P<0.05, $^{\Delta\Delta}$P<0.01 compared to streptozotocin control.

Figure 5.26 Effects of [A14K] PGLa-AM1 treatment on islet morphology in GluCre-ROSA26EYFP mice

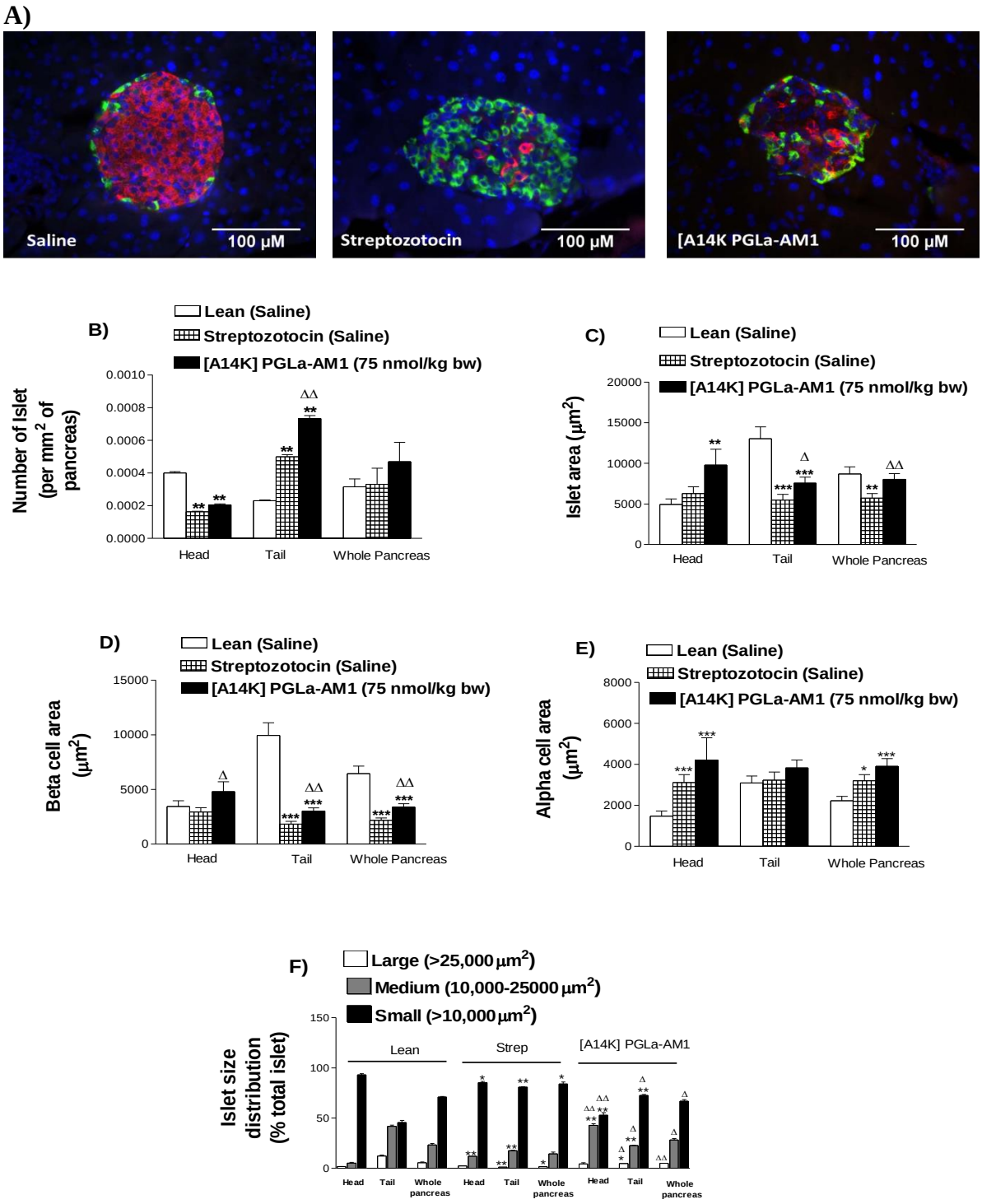

Representative islets (A) showing insulin (red) and glucagon (green) immunoreactivity from lean, streptozotocin and [A14K]-PGLa-AM1 treated mice. B, C, D, E, and F shows islet number, islet area, beta cell area, alpha cell area and islet size distribution respectively. Mean ± SEM for 5 mice (~50 Islets per group). *P<0.05, **P<0.01, ***P<0.001 compared to normal lean control, $^{\Delta}$P<0.05, $^{\Delta\Delta}$P<0.01 compared to streptozotocin control.

Figure 5.27 Effect of [A14K] PGLa-AM1 on pancreatic Islets in GluCre-ROSA26EYFP mice

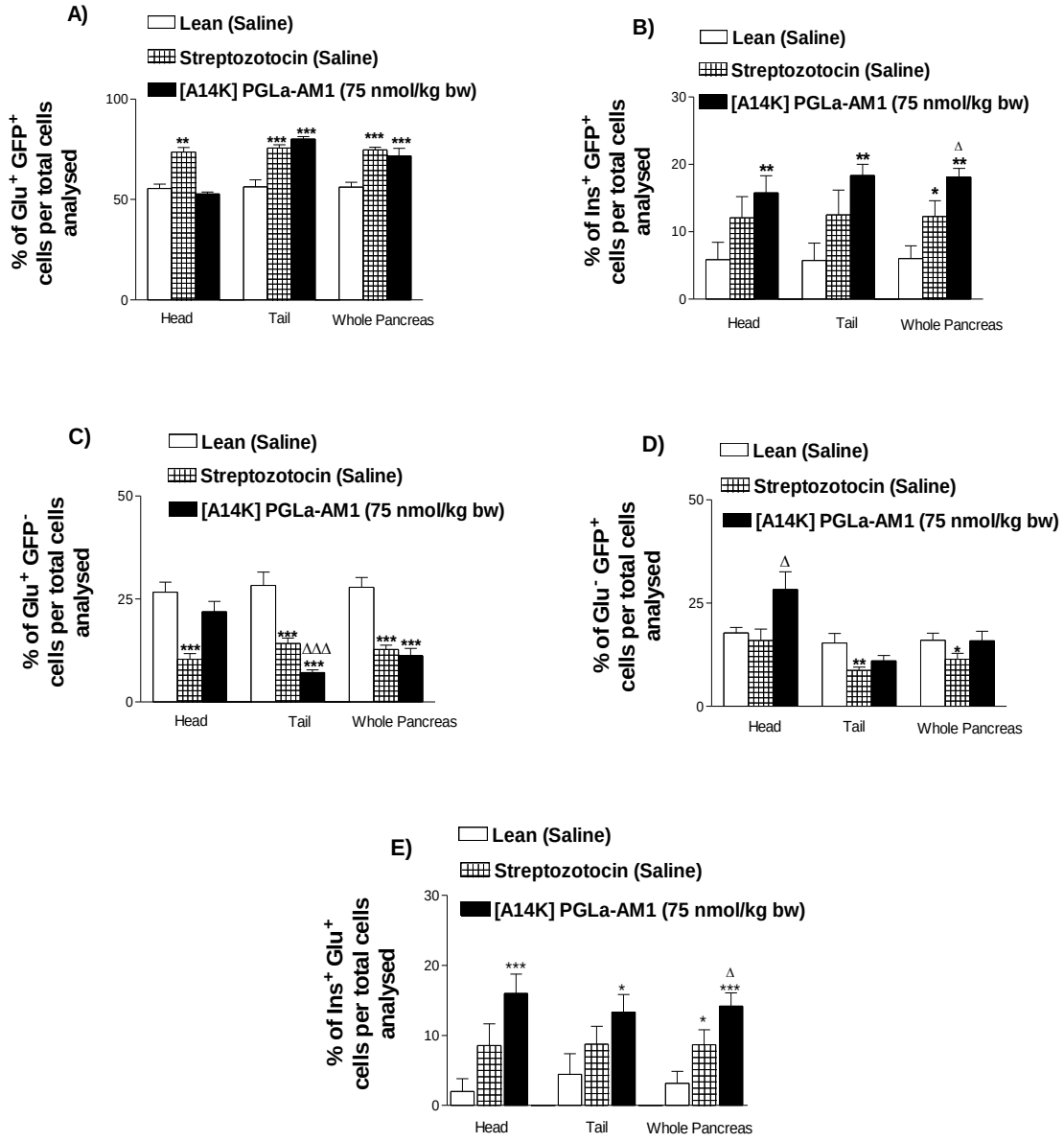

Quantification Of A) Glucagon-GFP positive cells, B), Insulin-GFP positive cells C) Glucagon positive cells and D) GFP positive cells per total islets (~50 Islets per group). *P<0.05, **P<0.01, **P<0.001 compared to normal saline control, $^{\Delta}$P<0.05, $^{\Delta\Delta\Delta}$P<0.001 compared to streptozotocin control.

Chapter 6

In vitro and *in vivo* antidiabetic effects of [Lys4] substituted analogue of CPF-AM1 from *Xenopus amieti*

6.1 Summary

We studied the pharmacological properties of [S4K] CPF-AM1 analogue, synthesised by substituting serine at position 4 by lysine in parent peptide CPF-AM1 isolated from frog *Xenopus amieti*. [S4K] CPF-AM1 exhibited dose-dependent insulin release in BRIN-BD11 and 1.1B4 cells without affecting the integrity of the plasma membrane. [S4K] CPF-AM1 also provided protection against cytokine-induced DNA damage, as well as stimulated proliferation of BRIN-BD11 cells. Chronic effects of [S4K] CPF-AM1 in *db/db* mice were studied in comparison with its parent peptide and antidiabetic agent exenatide. [S4K] CPF-AM1 treatment significantly delayed the progressive decline of insulin in *db/db* mice. This was associated with significant improvement in glycaemic control, HbA1c, glycaemic response to intraperitoneal glucose challenge and insulin sensitivity. However, these effects were less pronounced than with exenatide. The parent CPF-AM1 (75 nmol/kg bw) treatment also significantly improved glycaemic control and insulin sensitivity. Body weight remained unchanged in all peptide-treated groups, whereas energy intake and water intakes were decreased considerably by exenatide treatment. Biomarkers of liver and kidney function were improved significantly in all treated groups, indicating the non-toxic nature of the peptides. The triglyceride levels were significantly decreased in the CPF-AM1 treated group. In all peptide-treated groups, amylase activity was increased. Bone mineral density/content, body fat mass was not affected by peptide treatment. Islets from all treated groups displayed improved insulin secretory responses to glucose and insulin secretagogues. Pancreatic insulin was significantly increased in [S4K] CPF-AM1 and exenatide but not in CPF-AM1 treated group. Except for exenatide, no significant changes were observed in the islet, beta cell and alpha cell area. However, the loss of large and medium-size islets was significantly prevented by all peptide treatment. The

insulin signalling genes were upregulated, and secretory genes were downregulated by exenatide and [S4K] CPF-AM1. In [S4K] CPF-AM1 treated transgenic mice, the number of Ins^+/GFP^+ cells, GFP^+ cells and Ins^+/Glu^+ were increased significantly, indicating that peptide has a significant role in the conversion of glucagon-expressing alpha to insulin-expressing beta cells.

6.2 Introduction

Type 2 diabetes is becoming one of the significant health challenges particularly in developing countries, due to increasingly sedentary lifestyles, urbanisation and obesity (Hu, 2011, Animaw & Seyoum, 2017). Currently available antidiabetic drugs fail to achieve long-term glycaemic control and secondary complications associated with diabetes (Parkes *et al.,* 2013, Kahn *et al.,* 2014). Hence, there is a constant need to develop alternative therapies that can overcome these challenges. The discovery of exendin-4 from the venom of the Gila monster lizard (*Heloderma suspectum*), which share similar properties with GLP-1 (Conlon *et al.,* 2006, Parkes *et al.,* 2013), has intensified the search for the antidiabetic peptide from an animal source.

Skin secretion of frog has proven to contain a rich source of peptides with therapeutic potential (Conlon *et al.,* 2014a, Xu and Lai, 2015). Isolation and characterisation of these peptides have become a useful strategy to identify their therapeutic potential. Peptides, particularly from *Pipidae, Hylidae, Ranidae* family, which were isolated based on its antimicrobial activity, have subsequently been shown to demonstrated anti-viral, anti-cancer and immunomodulatory activity (Conlon *et al.,* 2014). In our lab, some of these peptides [e.g. brevinin-2-related peptide, tigerinin-1R, hymenochirin 1B, esculentin-2Cha (1-30)] have shown to stimulate insulin release *in vitro* in BRIN-BD11 cell and mouse pancreatic islet cells, as well as improved

glycaemic response both in lean and high fat fed mice (Abdel-Wahab *et al.,* 2010, Ojo *et al.,* 2011, Owolabi *et al.,* 2015, Vasu *et al.,* 2017).

In a recent study, Conlon *et al.,* 2012a designed alyteserin-2a-derived cationic analogue containing D-lysin substitution at position 7 and 11, which resulted in a superior antimicrobial potency than the parent peptide. Interestingly, the analogue showed lower haemolytic activity, suggesting that such modification of peptide could be safe for treatment. Similarly, hymenochirin-1B derived analogues carrying D-lysin or L-lysin substitution showed potent anti-tumour activity with lower haemolytic activity (Attoub *et al.,* 2013a). Based on this knowledge, synthetic analogues of frog skin insulinotropic peptides including brevinin-2-related peptide, tigerinin-1R, hymenochirin 1B, esculentin-2Cha (1-30) with enhanced cationicity were designed which exhibited potent insulinotropic activity *in vitro* and also improved blood glucose by upregulating expression of crucial genes involved in glucose homeostasis in an animal model of type 2 diabetes (Abdel-Wahab *et al.,* 2010, Ojo *et al.,* 2016, Owolabi *et al.,* 2016, Vasu *et al.,* 2017).

A previous study has reported broad-spectrum antimicrobial activity of CPF-AM1 (GLGSVLGKALKIGANLL.NH_2), derived from skin secretion of frog *Xenopus amieti* (Conlon *et al.,* 2010, 2012b). CPF-AM1 is orthologous to Caerulein precursor fragment (CPF) and caerulein precursor fragment (CPF) related peptides which have shown insulin-releasing activity in BRIN-BD11 cells with no cytotoxic effects (Srinivasan *e al.,* 2013). In recent studies, like CPF and CPF related peptides, CPF-AM1 also exhibited concentration-dependent insulin-releasing activity in BRIN-BD11 cells (Ojo *et al.,* 2012). Additionally, CPF-AM1 induced the release of GLP-1 in a dose dependent-manner from GLUtag cells (Ojo *et al.,* 2013a). Furthermore, its L-lysine substituted analogue (GLGKVLGKALKIGANLL.NH_2) which was

synthesised by substituting serine at 4th position by lysine displayed superior insulin-releasing activity than parent peptide in BRIN-BD11 cells and improved glycaemic responses both in lean and high-fat diet induced diabetic mice in response to glucose challenge (unpublished data).

Based on these promising results, in the present study the insulin-releasing activity of [S4K] CPF-AM1 was verified in BRIN-BD11 cells and 1.1B4 cells. Also, the effects of the analogue on proliferation and apoptosis were investigated. We then examined the effects of twice-daily administration of [S4K] CPF-AM1 (75 nmol/kg bw) for 28 days on glycemic control, insulin level, islet morphology and expression of key genes in muscles and islets involved in glucose homeostasis in genetically obese-diabetic mice (*db/db*) in comparison with native peptide CPF-AM1 (75 nmol/kg bw) and antidiabetic agent exenatide (25 nmol/kg bw). An additional study was also performed, to investigate beneficial effects of [S4K] CPF-AM1 on reprogramming of alpha to beta cells using GluCre-ROSA26EYFP mice.

6.3 Materials and Methods

6.3.1 Reagents

In this Chapter, all the reagents used for the experiments were of analytical grade listed in Chapter 2, Section 2.1. Membrane potential (Catalogue number: R8042) and Intracellular calcium assay kit (Catalogue number: R8041) were purchased from Molecular Devices (Berkshire, UK). IN SITU Cell Death Fluorescein kit (Catalogue number: 11684795910) were purchased from Sigma-Aldrich and Rabbit polyclonal to Ki67 (Catalogue number: ab15580) from Abcam for apoptosis and proliferation experiment, respectively. [S4K] CPF-AM1 was supplied in crude form by GL Biochem Ltd (Shanghai, China) and native peptide CPF-AM1 was purchased in pure

form by SynPeptide (China). LightCycler 480 Sybr Green (Catalogue number: 04707516001) was purchased from Roche Diagnostics Limited, UK. Masterclear Cap Strips and real-time PCR TubeStrips for gene expression studies (Catalogue number: 0030132890) were supplied by Mason Technology Ltd (Dublin, Ireland).

6.3.2 Peptide synthesis and purification

Using Reverse phase HPLC, crude peptide [S4K] CPF-AM1 was purified to near homogeneity (>98% purity) using a Vydac (C-18) column as described in Chapter 2, Section 2.2.1.1. The molecular mass of the collected peak was confirmed by MALDI-TOF MS (Chapter 2, Section 2.2.2). Parent peptide CPF-AM1 used in this Chapter was supplied in pure form by SynPeptide (China) (See Figure 6.1 for peptides structure).

6.3.3 Effects of [S4K] CPF-AM1 on insulin release from BRIN-BD11 and 1.1B4 cells

Insulinotropic activity of [S4K] CPF-AM1 ($3x10^{-6}$ - 10^{-12} M, n=8) was verified in BRIN-BD11 (passage 15-30) and 1.1B4 cells (passage 25-28). The experimental procedure outlined in Chapter 2, Section 2.4.1.1. After 20 min incubation with different dilutions of peptide made in 5.6 mM glucose Krebs-Ringer bicarbonate (KRB) buffer, the supernatants were aliquoted and measured for insulin using radioimmunoassay as outlined in Chapter 2, Section 2.4.4.

6.3.4 Cell viability assay

Lactate dehydrogenase (LDH) assay was performed to determine the cytotoxic effect of the peptide, using a CytoTox 96 non-radioactive cytotoxicity assay kit (Promega), as described in Chapter 2, Section 2.5.

6.3.5 Effects of [S4K] CPF-AM1 on apoptosis and proliferation in BRIN-BD11 cells

The protective effects of [S4K] CPF-AM1 against cytokine-induced DNA damage was studied in BRIN-BD11 cells, as outlined in Chapter 2, Section 2.10. Cells were incubated with [S4K] CPF-AM1 or GLP-1 (10^{-6}M) for 18 hr at 37°C in the presence or absence of cytokine mixture (200 U/ml tumour-necrosis factor-α, 20 U/ml interferon-γ and 100 U/ml interleukin-1β). After incubation, cells were fixed and permeabilised using 4 % paraformaldehyde and 0.1 M sodium citrate buffer (pH 6.0) respectively and subsequently stained using TUNEL reaction mixture. The proliferative effect of [S4K] CPF-AM1 (10^{-6} M) was investigate in BRIN-BD11 cells using anti-Ki-67 primary antibody (Chapter 2, Section 2.10). GLP-1 (10^{-6} M) was used as a positive control in the experiment.

6.3.6 Effects of the peptides on glucose uptake in C2C12 cells

The procedure for determining the effects of peptides on the glucose uptake in C2C12 cells is described in Chapter 2, Section 2.11.

6.3.7 Acute *in vivo* effect of the peptide on food intake

In overnight (21 hr) fasted mice, food intake was measured after i.p injection of saline and test peptides as described in Chapter 2, Section 2.13.4.

6.3.8 Effects of twice daily administration of CPF-AM1 and [S4K] CPF-AM1 in *db/db* mice

Before initiation of treatment all mice were injected twice daily with saline for 3 days to adapt mice to handling and injection stress. Genetically obese-diabetic mice *(db/db)* were administered for 28 days with a twice-daily dose of exenatide 4 (25 nmol/kg bw) or CPF-AM1 (75 nmol/kg bw) or [S4K] CPF-AM1(75 nmol/kg bw). Various parameters like body weight, food intake, water intake, blood glucose and plasma insulin were monitored at 3 day intervals. After 28 days treatment period intraperitoneal and oral glucose tolerance test (Chapter 2, Section 2.13.2), HbA1c test (Chapter 2, Section 2.13.9) and insulin sensitivity (Chapter 2, Section 2.13.3) were performed. Insulin resistance was determined using the homeostatic model assessment (HOMA) formula: HOMA-IR = fasting glucose (mmol/l) x fasting insulin (mU/l)/22.5.

After performing the above tests, mice were sacrificed by cervical dislocation and measured for body fat composition and bone mineral density using DEXA scanning (PIXImus densitometer, USA) (Chapter 2, Section 2.13.8). Islets were isolated from pancreases by collagenase digestion method (Chapter, Section 2.4.2.1) and investigated for insulin secretory responses (Chapter 2, Section 2.4.2.3) and expression of insulin secretory genes (Chapter 2, Section 2.15). Pancreatic tissues were processed for immunohistochemistry. Tissues including pancreases and skeletal muscle were snap frozen in liquid nitrogen and stored at -80 °C to perform further studies.

6.3.9 Biochemical analysis

Blood glucose and plasma/pancreatic insulin content were measured as outlined in Chapter 2, section 2.13.5 and 2.13.11. Various biochemical test such as lipid profile test, liver and kidney function test and amylase activity (Chapter 2, Section 2.13.12) were performed.

6.3.10 Effects of twice daily administration of CPF-AM1 and [S4K] CPF-AM1 on islet morphology

After processing, pancreatic tissues were embedded in paraffin wax, and sections of 7 µM thickness were made using microtome. Sections were placed on a slide and allowed to dry overnight on a hotplate. Sections were then stained for insulin and glucagon as described in Chapter 2, Section 2.14.1.

6.3.11 Effects of twice daily administration of CPF-AM1 and [S4K] CPF-AM1 on gene expression

The expression of genes in muscles and islets involved in glucose homeostasis was investigated in *db/db* mice after chronic treatment with peptides. RNA was extracted from muscle tissue and islet cells using TriPure reagent (Chapter 2, Section 2.15.1). cDNA was synthesised from extracted RNA by following the procedure described in Chapter 2, Section 2.15.2. The reaction mix was prepared, and PCR condition was set as outlined in Chapter 2, Section 2.15.3.

6.3.12 Effects of twice daily administration of [S4K] CPF-AM1 in GluCre-ROSA26EYFP mice

GluCre-ROSA26EYFP mice were treated with streptozotocin (STZ) and grouped as previously described in Chapter 2 Section 2.13.1.3. Grouped GluCre mice than

received twice daily intraperitoneal injections of saline or test peptide (75 nmol/kg bw) for 11 consecutive days. Parameters such as non-fasting blood glucose, body weight, food intake and water intake were monitored every 3 days interval during the treatment period. Additionally, blood samples were collected 3 times: prior to STZ treatment, before peptide treatment and after peptide treatment, and analysed for insulin concentration using RIA, as described previously in Chapter 2, Section 2.13.6. After the end of the treatment, animals were sacrificed by cervical dislocation, and pancreatic tissues were excised and processed for histological staining as described in Chapter 2, Section 2.14 and 2.14.1.

6.3.13 Statistical Analysis

Experimental data were analysed using GraphPad PRISM (Version 3). Results were expressed as means ± SEM and data compared using unpaired student's t-test (nonparametric, with two-tailed P values and 95% confidence interval) and one-way ANOVA with Bonferroni post-hoc test wherever applicable. Group of datasets were considered to be significantly different if $P<0.05$.

6.4 Results

6.4.1 Purification and characterisation of [S4K] CPF-AM1

[S4K] CPF-AM1 was purified and characterised by reverse-phase HPLC and MALDI-TOF respectively, as described in Chapter 2, Section 2.2.1.1 and Section 2.2.2 (Figure 6.2).

6.4.2 Effects of [S4K] CPF-AM1 on insulin release from BRIN-BD11 and 1.1B4 cells

The insulinotropic activity of analogue [S4K] CPF-AM1 was studied from concentration 3 µM to 1 pm in BRIN-BD11 cells and 1.1B4 cells. As shown in Figure 6.3A, [S4K] CPF-AM1 treated BRIN-BD11 cells displayed dose-dependent insulin release with significant ($P<0.05$) stimulatory effects up to a concentration of 0.1 nM. At 3 µM, [S4K] CPF-AM1 produced approximately 2.6-fold increase in insulin release compared to the basal rate (0.98 ± 0.02 ng/10^6 cells/20 min). Leakage of the lactate dehydrogenase enzyme was not detected from peptide-treated BRIN-BD11 cells (Figure 6.3B), suggesting that the integrity of the plasma membrane remained intact. As shown in Figure 6.4A, treatment of 1.1B4 cells with [S4K] CPF-AM1 (3×10^{-6} M - 10^{-12} M) in 5.6 mM glucose produced dose-dependent insulin release with approximately 3-fold increase at 3 µM. The peptide demonstrated significant ($P<0.05$) insulin release up to concentrations of 0.1 nM. A similar stimulatory effect was observed when the 1.1B4 cells were incubated with peptide in 16.7 mM glucose (Figure 6.4B). As expected, alanine and exenatide demonstrated maximum stimulatory response compared to basal rate both in BRIN-BD11 and 1.1B4 cells.

6.4.3 Effects of [S4K] CPF-AM1 on apoptosis and proliferation in BRIN-BD11 cells

[S4K] CPF-AM1 (1 µM), treatment had no effects on apoptosis of BRIN-BD11 cells. On the other hand, in cytokine-treated BRIN-BD11 cells, the number of cells undergoing apoptosis was increased by 272%. When the BRIN-BD11 cells were co-incubated with [S4K] CPF-AM1 and the cytokine mixture, the number of tunnel positive cells were reduced to 115%. This degree of protection was comparable to that provided by GLP-1 (1 µM) (Figure 6.5A). As shown in Figure 6.5B, [S4K] CPF-AM1 (1 µM) treatment for 18 hr resulted in a significant ($P<0.001$) increase in proliferation

(33% increase) of BRIN-BD11, that was comparable to that produced by 1 µM GLP-1 (43% increase). BRIN-BD11 cells Co-cultured with cytokine cocktail resulted in a decrease in proliferation by 30% compared to control cultures (P<0.001).

6.4.4 Effects of [S4K] CPF-AM1 peptides on glucose uptake in C2C12 cells

[S4K] CPF-AM1 peptides (1 µM) had no significant effect on glucose uptake in C2C12 cells compared to control (Figure 6.6). However, in the presence of insulin, a noticeable increase in glucose uptake was observed. As expected, insulin (1 µM) showed a significant increase (P < 0.05) in glucose uptake in C2C12 cells compared to control. In the presence of negative control (Apigenin 50µM), glucose uptake was decreased significantly by 30% (P<0.05).

6.4.5 Acute effect of [S4K] CPF-AM1 peptides on food intake in lean mice

As expected, in overnight fasted lean mice, GLP-1 significantly (P<0.05) suppressed appetite from 60 min up to 180 min. [S4K] CPF-AM1 did not affect food intake (Figure 6.7).

6.4.6 Effects of twice daily administration of CPF-AM1 and [S4K] CPF-AM1 on body weight, energy intake, fluid intake, non-fasting blood glucose and plasma insulin in *db/db* mice

As excepted, body weight, energy intake, fluid intake, non-fasting blood glucose and plasma insulin were significantly increased (P<0.001) in all groups of *db/db* mice (BKS.Cg-+Leprdb/+Leprdb/OlaHsd) mice compared to their littermates (Figure 6.8 & 6.9). After 28 days of treatment, no significant differences in body weight were observed in all four *db/db* groups [*db/db* control, CPF-AM1 (75 nmol/kg bw), [S4K]

CPF-AM1 (75 nmol/kg bw), Exenatide (25 nmol/kg bw)] (Figure 6.8A, B). Also, energy intake and fluid intake in CPF-AM1 and [S4K] CPF-AM1 treated groups showed no difference compared to *db/db* controls. However, these parameters were decreased significantly (P<0.001) in the exenatide-treated group (Figure 6.8 C-F). As shown in Figure 6.9A-D, [S4K] CPF-AM1 significantly (P<0.05, P<0.01) lowered blood glucose and delayed the progressive decline of circulating insulin in *db/db* mice, but not to the same extent as exenatide. The native peptide lowered (P<0.05) blood glucose in *db/db* mice but failed to produce any positive effects on plasma insulin.

6.4.7 Effects of twice daily administration of CPF-AM1 and [S4K] CPF-AM1 on Glycated haemoglobin (HbA1c) in *db/db* mice

As shown in Figure 6.10, [S4K] CPF-AM1 and exenatide treatment significantly (P<0.05, P<0.01) decreased blood HbA1c by 29% and 52% respectively, compared to *db/db* controls. CPF-AM1 treatment also decreased blood HbA1c level in *db/db* mice, but not significantly.

6.4.8 Effects of twice daily administration of CPF-AM1 and [S4K] CPF-AM1 on glucose tolerance in *db/db* mice following intraperitoneal and oral glucose load

[S4K] CPF-AM1 and exenatide-treated *db/db* mice exhibited significant improvement in glycaemic response following intraperitoneal glucose load (18 mmol/kg bw) (Figure 6.11A, B). The blood glucose was significantly (P <0.05 - P<0.001) lowered at 15, 30 and 60 min in [S4K] CPF-AM1 and exenatide-treated mice compared to *db/db* control. The integrated blood glucose response was also significantly (P<0.01, P<0.001) less than *db/db* controls. Correspondingly, significantly (P<0.01, P<0.001) increased insulin response was observed at 15 min in [S4K] CPF-AM1 and exenatide-

treated *db/db* mice after glucose load. The overall AUC insulin was increased significantly (P <0.05, P<0.001) in these mice compared to saline-treated *db/db* mice. CPF-AM1 treated group, also exhibited lowered (P<0.05, P<0.01) blood glucose at 15 and 30 min (see table below), but no significant difference in overall AUC glucose and insulin were observed compared to *db/db* controls (Figure 6.11C, D).

In another set of experiments, both [S4K] CPF-AM1 and CPF-AM1 treated *db/db* mice showed a tendency to lower blood glucose and improve insulin response following an oral glucose load. However, a significant difference in overall AUC glucose and insulin compared to *db/db* controls was not observed. AUC blood glucose and insulin were significantly (P<0.01) improved in exenatide-treated mice after oral glucose challenge (Figure 6.12A-D).

6.4.9 Effects of twice daily administration of CPF-AM1 and [S4K] CPF-AM1 on insulin sensitivity in *db/db* mice

As shown in Figure 6.13A-B, CPF-AM1**,** [S4K] CPF-AM1 and exenatide treatment significantly improved insulin sensitivity in *db/db* mice. After intraperitoneal administration of insulin (50 U/kg bw), a decrease in blood glucose level was observed in all peptide treated groups compared to *db/db* control. When the data presented in the form of the area under the curve, the overall blood glucose level in CPF-AM1, [S4K] CPF-AM1 and the exenatide treatment group were reduced significantly (P<0.05, P<0.01) by 23%, 25% and 40% respectively, compared to *db/db* controls. This observation was further supported by HOMA-IR calculations, revealing improved insulin resistance in [S4K] CPF-AM1 and the exenatide-treated mice compared to *db/db* control. Whereas in CPF-AM1 treated group a noticeable decrease in HOMA-IR index was observed (Figure 6.13C).

6.4.10 Effects of twice daily administration of CPF-AM1 and [S4K] CPF-AM1 on bone mineral density, bone mineral content and fat composition in *db/db* mice

Figure 6.14 illustrates a DEXA scan of all groups of mice. After 28 days of treatment, no significant differences were found in bone mineral density (BMD), bone mineral content (BMC), body fat and body fat (expressed a percentage of total body mass) in any of the *db/db* groups**.** Interestingly, the bone area in CPF-AM1 treated mice was similar to lean controls.

6.4.11 Effects of twice daily administration of CPF-AM1 and [S4K] CPF-AM1 on pancreatic weight and insulin content

After 28 days of treatment, no significant changes in pancreatic weight were observed in peptide treated *db/db* mice compared to *db/db* controls (Figure 6.15A). In comparison to lean mice, the pancreatic weights of [S4K] CPF-AM1 and exenatide-treated groups were significantly ($P<0.05$, $P<0.01$) higher. Both [S4K] CPF-AM1 and exenatide-treated groups also considerably increased (1.7-2.4-fold, $P<0.05$, $P<0.01$) pancreatic insulin compared to *db/db* controls. In CPF-AM1 treated group, pancreatic insulin remained unaltered Figure 6.15B).

6.4.12 Effects of twice daily administration of CPF-AM1 and [S4K] CPF-AM1 on insulin secretory response of islet in *db/db* mice

Islets from treated and untreated mice were examined for insulin secretory responses to glucose (1.4 mM, 5.6 mM, 16.7 mM) and other established insulin secretagogues (Figure 6.15C & D). Islets from *db/db* mice exhibited impaired insulin secretory responses, were reversed by treatment with exenatide and [S4K] CPF-AM1. Less pronounced effects were observed with CPF-AM1.

6.4.13 Effects of twice daily administration of CPF-AM1 and [S4K] CPF-AM1 on lipid profile in *db/db* mice

Plasma TC (total cholesterol), triglycerides, LDL (low-density lipoprotein) and HDL (high-density lipoprotein) levels were analysed after the treatment period (Figure 6.16). As shown in figure (Figure 6.16A, C), cholesterol and high-density lipoprotein (HDL) were not significantly different in all mice groups. In *db/db* mice elevated triglycerides and LDL levels were reversed ($P<0.05$, $P<0.01$) by exenatide treatment (Figure 6.16B, D). Treatment with [S4K] CPF-AM1 significantly lowered triglyceride but not LDL compared to *db/db* controls. CPF-AM1 treatment showed a tendency to reduce triglyceride and LDL in *db/db* mice.

6.4.14 Effects of twice daily administration of CPF-AM1 and [S4K] CPF-AM1 on liver and kidney function in *db/db* mice

As shown in Figure 6.17A-C, the basal levels of ALT, AST and ALP were significantly ($P<0.001$) elevated in saline-treated *db/db* mice by 76%, 246% and 105% respectively compared to their littermates. Treatment with exenatide, CPF-AM1 and [S4K] CPF-AM1 significantly ($P<0.05$, $P<0.001$) lowered these biochemical parameters compared to *db/db* controls. Interestingly, both CPF-AM1 and [S4K] CPF-AM1 was equally effective as exenatide in lowering ALT and ALP level. Additionally, all peptide treatment resulted significant ($P<0.05$, $P<0.01$) reduction in creatinine compared to *db/db* controls (Figure 6.17D).

6.4.15 Effects of twice daily administration of CPF-AM1 and [S4K] CPF-AM1 on plasma amylase concentration in *db/db* mice

All *db/db* mice subjected to peptide treatment displayed significantly ($P<0.05$ - $P<0.001$) increased amylase activity relative to *db/db* mice and lean controls (Figure 6.18).

6.4.16 Effects of twice daily administration of CPF-AM1 and [S4K] CPF-AM1 on islet number, islet area, beta cell areas, alpha cell area and islet size distribution

Following 28 days, islet morphology was examined in both treated and untreated mice. Figure 6.19A represents images of pancreatic islets of mice, showing alpha cells in red and beta cells in green. In all *db/db* mice, no significant differences in a number of islets per mm^2 were observed (Figure 6.19B). Lean control, *db/db* control and CPF-AM1 treated groups showed no differences in islet area. [S4K] CPF-AM1 treated group showed a tendency to improve islet area, but no statistical difference was observed compared to *db/db* controls (Figure 6.19C). In contrast, islet area was significantly ($P<0.05$) increased in the exenatide-treated group. In the *db/db* control group, pancreatic beta cell population were decreased, and alpha cell population were increased significantly compared to their littermates (Figure 6.19D-E). Both CPF-AM1 and [S4K] CPF-AM1 treatment had no effects on beta cell and alpha cell area. Exenatide treatment significantly increased ($P<0.05$) beta cell area and decreased ($P<0.01$) alpha cell area compared to *db/db* controls. In all peptide treated groups, the number of large and medium-size islets were increased ($P<0.01$, $P<0.001$) and small size islets were decreased ($P<0.01$) significantly compared to *db/db* controls (Figure 6.19F).

6.4.17 Effects of twice daily administration of CPF-AM1 and [S4K] CPF-AM1 on gene expression in skeletal muscle

After the treatment period, the expression of insulin signalling genes in skeletal muscle tissue of treated and untreated mice was examined. (Figure 6.20). Muscles from *db/db* mice showed significant ($P<0.05$ - $P<0.001$) increase in mRNA expression of *Slc2a4, Insr, Irs1, Pik3ca, Akt1* and *Ptb1* genes compared to lean littermates (Figure 6.20A-C & 6.20E-G). Expression of these genes was reversed in [S4K] CPF-AM1 and exenatide-treated mice. After CPF-AM1, the expression of these genes was diminished but the effect was not to the same extent as analogue. No significant differences in expression of *Pdk1* gene were observed in any of the groups (Figure 6.20D).

6.4.18 Effects of twice daily administration of CPF-AM1 and [S4K] CPF-AM1 on gene expression in islets

Expression of essential genes involved in the insulin secretion including *Ins1, Abcc8, Kcnj11, Slc2a2, Cacna1c* as well as *Gck* were investigated in the islet cells isolated from pancreatic tissue from treated and untreated mice (Figure 6.21A-F). In saline-treated *db/db* mice, expression of these genes was significantly ($P<0.001$) downregulated, which was reversed by treatment with exenatide and [S4K] CPF-AM1. The native peptide CPF-AM1 also upregulated these genes, except for *Kcnj11*. Exenatide and [S4K] CPF-AM1 treatment also prevented downregulation of *Gipr, Glp1r, Gcg* and *Pdx1* genes in the islets of *db/db* mice (Figure 6.22A-D). *Stat1* gene which was significantly upregulated in *db/db* mice was reversed by treatment with exenatide and [S4K] CPF-AM1. CPF-AM1 treatment had no effects on these genes, except for *Glp1r* and *Gcg* which was upregulated ($P<0.05$) compared with *db/db* controls (Figure 6.22E).

6.4.19 Effects of twice daily administration of [S4K] CPF-AM1 on body weight change, food intake and water intake in GluCre-ROSA26EYFP mice

Treatment with streptozotocin (STZ) resulted in a significant ($P<0.01$) decrease in body weight and an increase ($P<0.01$, $P<0.001$) in water intake and energy intake in GluCre mice compared to the lean controls (Figure 6.23A-C). [S4K] CPF-AM1 had no significant effects on body weight, water intake and energy intake in GluCre mice.

6.4.20 Effects of twice daily administration of [S4K] CPF-AM1 on blood glucose and plasma insulin in GluCre-ROSA26EYFP mice

Blood glucose was significantly ($P<0.001$) increased in streptozotocin (STZ) control mice compared to lean controls (Figure 6.24A). This was associated with significant ($P<0.001$) decrease in plasma insulin (Figure 6.24B). [S4K] CPF-AM1 treatment showed a tendency to improve blood glucose and plasma insulin, but no statistical significance was observed compared to compared to STZ controls.

6.4.21 Effects of twice daily administration of [S4K] CPF-AM1 on pancreatic insulin content in GluCre-ROSA26EYFP mice

As expected, treatment with streptozotocin (STZ) resulted in a significant ($P<0.01$, $P<0.001$) decrease of insulin content in all regions of the pancreas in GluCre mice compared to untreated controls (Figure 6.25). [S4K] CPF-AM1, significantly ($P<0.05$, $P<0.01$) improved insulin content, particularly in the tail region of pancreas compared to STZ controls.

6.4.22 Effects of twice daily administration of [S4K] CPF-AM1 on islet number, islet area, beta cell area, alpha cell area and islet size distribution in GluCre-ROSA26EYFP mice

Pancreatic islet morphology was evaluated after the treatment period. Figure 6.26A represents images of pancreatic islets, showing alpha cells in green and beta cells in red colour. As shown in Figure 6.26B, no significant changes in the number of islets per mm^2 were observed in the whole pancreas. However, in [S4K] CPF-AM1 treated mice, the number of islets per mm^2 was significantly ($P<0.01$) increased in the pancreatic head region. In the tail region, the opposite pattern was observed. A noticeable increase in islet area was seen in the whole pancreas, particularly in the tail region, of peptide-treated mice compared to STZ controls (Figure 6.26C). As expected, a significant ($P<0.001$) beta cell loss was observed in STZ control mice, particularly in the tail region of the pancreas which was prevented ($P<0.001$) by the [S4K] CPF-AM1 treatment (Figure 6.26D). Also, a noticeable decrease in alpha cell area was observed in the head region of the pancreas of peptide-treated mice (Figure 6.26E). The islet size distribution was altered by streptozotocin treatment. The number of smaller size islets were significantly increased in the whole pancreas in STZ controls compared to lean controls. Additionally, large and medium-size islet were reduced particularly in the pancreatic tail region. The peptide treatment resulted in significant ($P<0.05$) increase in the number of large size islets in the whole pancreas and significant ($P<0.05$) increase in medium size islets particularly in the tail region of pancreas compared to STZ controls (Figure 6.26F).

6.4.23 Effect of [S4K] CPF-AM1 on pancreatic islets in GluCre-ROSA26EYFP mice

The immunofluorescent staining of pancreatic section confirmed that in all mice groups GFP was significantly expressed in glucagon expressing alpha cells (Figure 6.27A). The number GFP positive cells expressing insulin were significantly ($P<0.05$, $P<0.001$) increased in STZ controls compared to lean controls. In [S4K] CPF-AM1 treated mice, Ins^{+}/GFP^{+} cells were increased significantly (65%, $P<0.05$) compared to STZ controls (Figure 6.27B). Interestingly, the percentage of cells expressing only GFP as well as cells co-expressing both insulin and glucagon (bihormonal cells) were increased ($P<0.05$ - $P<0.001$) significantly in the peptide-treated mice compared to both STZ and lean controls (Figure 6.27D, E).

6.5 Discussion

The pharmaceutical industry has shown immense interest in peptide drug development after the discovery of insulin therapy. To date, more than 60 peptide drugs are approved for clinical use, and over 150 are currently evaluated in human clinical studies (Lau and Dunn, 2018). The major obstacles faced by peptide drug candidates are 1) rapid degradation by a proteolytic enzyme, 2) toxicity, and 3) rapid clearance from circulation (Green *et al.,* 2004b, Fosgerau & Hoffmann, 2014). As a result, researchers have begun to use peptide chemistry techniques to develop peptide analogues by substituting amino acid or by modifying C or N terminal or by covalently linking fatty acid moiety to enhance pharmaceutical properties of peptides (Heard *et al.,* 2013, Conlon *et al.,* 2007a). Using similar approaches several host defence peptides with antidiabetic properties were transformed to analogues, which demonstrated potent *in vitro* and *in vivo* antidiabetic activities (Abdel-Wahab *et al.,* 2008a, Srinivasan *et al.,* 2015).

Previous studies conducted in our laboratory have shown the insulin-releasing activity of Caerulein-precursor fragment (CPF-AM1) peptide isolated from frog skin secretion of *Xenopus amieti.* Additionally, CPF-AM1 has been shown to induce the release of GLP-1 from GLUtag cells (Ojo *et al.,* 2012, 2013a). The [S4K] analogue of CPF-AM1, which was synthesised by substituting serine (S) at 4th position by lysine, displayed appreciably greater insulinotropic activity in rat clonal BRIN-BD11 cells than native peptide, as well as, improved glycaemic response both in lean and high-fat diet induced diabetic mice in response to glucose challenge (Unpublished data). Based on these promising results, [S4K] CPF-AM1 analogue was selected for further studies. Reassuringly, in the present study [S4K] CPF-AM1 analogue displayed potent insulinotropic activity in BRIN-BD11, as well as, in 1.1B4 pancreatic β-cells without affecting the architecture of the plasma membrane. The improved insulinotropic activity of [S4K] CPF-AM1 analogue is in harmony with previous studies, where analogues of PGLa-AM1, hymenochirine-1B with lysine substitution displayed potent insulinotropic activity (Owolabi *et al.,* 2016, 2017). The role of cytokines in beta cell dysfunction is well documented, which is characterised by impaired glucose-stimulated insulin release (Donath *et al.,* 2009, Vasu *et al.,* 2014, Barlow *et al.,* 2018). Interestingly, [S4K] CPF-AM1 analogue was effective in protecting BRIN-BD11 cells against cytokine-induced apoptosis. Additionally, analogue also displayed beta-cell proliferative activity comparable to that of GLP-1. A similar effect was also shown by peptide [A14K] PGLa-A1M, esculentin (1-21)1c, temporin A and temporin F (Owolabi *et al.,* 2017, Musale *et al.,* 2018). Although, more detail studies are required to investigate the mechanism by which these peptides induce protective and proliferative effects. Based on these findings long-term *in vivo* studies was conducted

to evaluate the beneficial effects of [S4K] CPF-AM1 analogue in an animal model of type 2 diabetes.

In T2DM, with time insulin biosynthesis and secretion decline progressively, which results in a decrease in insulin and an increase in glucose level (Butler *et al.*, 2003). After initiation of treatment the progressive loss of non fasting insulin was delayed significantly in *db/db* mice receiving [S4K] CPF-AM1 treatment, suggesting positive effects of analogues on pancreatic beta cell function. When the results for insulin was presented in the form of the area under the curve, the insulin level was significantly higher than *db/db* controls. On the other hand, native peptide also showed a tendency to delay loss of insulin, but the effect was not to the same extent as analogue. The reason for the beneficial effects of analogue on plasma insulin over parent peptide could be due to the improved enzymatic stability.

In T2DM, maintaining strict glycaemic control is one of the key factors to prevent microvascular complications (UK Prospective Diabetes Study (UKPDS) Group, 1998). In the present study, [S4K] CPF-AM1 treatment significantly improved blood glycaemic control as well as decreased HbA1c in *db/db* mice. The reduction of blood glucose was correlated with improvement in polydipsia, which is commonly observed in the severe diabetic state (Zimmermann *et al.*, 2012, Grosbellet *et al.*, 2016). On the other hand, native peptide also significantly lowered blood glucose in *db/db* mice, however, an only a small decrease in HbA1c was observed. The improvement in blood glucose in CPF-AM1 and [S4K] CPF-AM1 treated groups was not associated with any change in body weight or energy intake. However, in the exenatide-treated group, energy intake was reduced significantly in *db/db* mice, which corresponds well to the previous studies (Gedulin *et al.*, 2005, Schlögl *et al.*, 2015). Body weight remained

unaffected suggesting that increased energy expenditure might explain the reason for no change in body weight.

Genetically obese-diabetic mice (*db/db*) as early as 6 weeks of age show impaired glycaemic response to a glucose load, and this impairment deteriorates with age (Wang *et al.,* 2002). There have been previous reports of several frog skin peptides and their analogues showing improved glucose tolerance in insulin resistance high-fat fed mice (Vasu *et al.,* 2017, Ojo *et al.,* 2015b, Owolabi *et al.,* 2016, Srinivasan *et al.,* 2015). In the present study, untreated *db/db* mice showed an impaired glycaemic response to both intraperitoneal and oral glucose load. After chronic treatment with [S4K] CPF-AM1 for 28 days, the glycaemic response was improved substantially to intraperitoneal glucose challenge but failed to produce the same effect to oral glucose challenge. On the other hand, CPF- AM1 treated mice, under the same experimental condition, also showed a tendency to improve glycaemic response. Whereas, exenatide-treated *db/db* mice, displayed a positive effect on both intraperitoneal and oral glucose challenge. This improvement in glycaemic response correlated with improved insulin sensitivity in [S4K] CPF-AM1 and exenatide-treated group, which was further confirmed by HOMA-IR calculation.

It is evident that hyperlipidaemia, exacerbate insulin resistance in type 2 diabetes (Kraegen *et al.,* 2001). Hyperlipidaemia is one of the significant factors in the development of diabetic nephropathy (Yang *et al.,* 2017), therefore, improving lipid metabolism may have beneficial effects in a diabetes patient. In agreement with others (Son *et al.,* 2015, Kim *et al.,* 2013), impaired lipid metabolism was observed in *db/db* mice. Plasma triglycerides and LDL levels were elevated significantly in *db/db* control compared to their littermates. In the present study, [S4K] CPF-AM1 treatment showed a tendency to restore elevated triglycerides and LDL levels; however, there was no

significant difference compared to *db/db* controls. Interestingly, triglycerides were significantly decreased with CPF-AM1 treatment, which was comparable to exenatide. This observation is in agreement with previous studies where CPF-SE1 peptide which is orthologues to CPF-AM1 have been shown to reduce triglycerides levels in high fat fed mice (Srinivasan *et al.,* 2015). Plasma HDL level remained unaffected in all *db/db* mice and was comparable to lean littermates. However, a small decrease in cholesterol level was observed in both [S4K] CPF-AM1 and CPF-AM1 treatment, but this was not significant. The improvement in plasma lipids could be the reason for improved insulin sensitivity in CPF-AM1 treated *db/db* mice. Bone mineral density/ content, lean body mass and body fat were unaffected by all peptide treatment in *db/db* mice.

In clinical practice, liver parameters such as ALT, AST and ALP levels are tested to monitor the progression of diseases and toxicity of drugs. T2D patient suffering from liver dysfunction have elevated levels ALT, AST and ALP (Bora *et al.,* 2016). According to the results of the present study, these liver parameters were significantly decreased in both [S4K] CPF-AM1 and CPF-AM1 treated *db/db* mice. The magnitude of these effects was comparable to exenatide treatment. The creatinine in *db/db* mice was also attenuated by [S4K] CPF-AM1 and CPF-AM1. These observations show that liver and kidney function were improved by peptide treatment suggesting that peptides could be safe for the treatment of type 2 diabetes. A significant increase in amylase activity was observed in all peptide treated *db/db* mice compared to *db/db* controls, suggesting a potential issue with pancreatitis. This has previously been reported for GLP-1 mimetics, but it is not considered to be clinically significance (Nauck, 2013).

Insulin resistance in type 2 diabetes has been proposed due to impairment of insulin signalling in the muscle tissue (Björnholm *et al.,* 1997, Goodyear *et al.,* 1995,

Defronzo and Tripathi, 2009). In the present study, an increase in mRNA expression of insulin signalling genes was observed in the muscles of *db/db* mice. The expression of *GLU4, Insr, Irs1, Akt1, Pik3ca* and *Ptb1* was upregulated significantly compared to lean controls. These observations are in harmony with previous findings, where an increase in the activity of proximal insulin signalling cascade was observed in the animal model of liver cirrhosis, (Jessen *et al.*, 2006). Similarly, an increase in the activity of PI 3-kinase and Akt/PKB was observed in the liver and kidney of *db/db* mice (Feliers *et al.*, 2001). The increase in insulin signalling activity could be to compensate GLUT4 translocation defect from intracellular membrane to cell surface, which is observed in diabetes (Huang *et al.*, 2002, DeFronzo & Tripathy, 2009). Interestingly, in [S4K] CPF-AM1 and exenatide treatment, expression of these genes was reversed in *db/db* mice. A similar finding was also observed in a native peptide-treated group. However, the effect was comparatively less than analogue.

In the present study, immunohistochemical analysis of pancreatic tissue revealed that the number of islets per mm^2 was unaffected by the treatment and was comparable to *db/db* controls. However, a substantial decline in a large and medium-size islet in *db/db* mice were prevented by all peptide treatments. The loss of islets and beta cell area and an increase in alpha cell area in *db/db* mice were attenuated by [S4K] CPF-AM1 treatment, but not significantly. This observation correlated with an increase in pancreatic insulin content and improved insulin secretory response to glucose and insulin secretagogues after [S4K] CPF-AM1 treatment. On the other hand, the native peptide also displayed these beneficial effects but not to the same extent as the analogue. To further evaluate the positive effects of both [S4K] CPF-AM1 and CPF-AM1 on pancreatic beta cell function, gene expression studies were performed. In *db/db* mice insulin secretory genes *Ins1, Pdx1, Glp1r, Gipr, Abcc8, Kcnj11, Gck,*

Cacna1c and *Gcg* were significantly downregulated, and the apoptosis gene *Stat1* was significantly upregulated compared to littermates. The high blood glucose and lipid levels could be the reason for these changes in gene expression in *db/db* mice (Piro *et al.*, 2002, Wang & Thurmond, 2012, Poitout, 2013, Shimoda *et al.*, 2011). In [S4K] CPF-AM1 treatment, upregulation of insulin secretory genes and downregulation of apoptosis gene could explain its beneficial effect on beta cell function. On the other hand, parent peptide also showed a tendency to improve the expression of these genes, but the effect was not to the same extent as the analogue.

An additional study was performed using the transgenic mouse (GluCre-ROSA26EYFP mice) bearing the transgenes GluCre (tamoxifen inducible tagger) and ROSA26-YFP (reporter), to investigate chronic effects (11 days) of [S4K] CPF-AM1 on reprogramming of alpha to beta cells. Immunohistochemical analysis of pancreatic section revealed that the number of beta cells which were transdifferentiated from alpha cells (Ins^+/GFP^+ cells), as well as cells co-expressing both insulin and glucagon (Ins^+/Glu^+), were increased significantly in STZ group compared to lean control, indicating that glucagon expressing alpha cells started expressing insulin. These observations are consistent with the previous study, where transdifferentiate of glucagon-producing alpha cells into insulin-producing beta cells were observed under conditions of extreme beta cell loss (Thorel *et al.*, 2010). [S4K] CPF-AM1 treatment, substantially increased the number of Ins^+/GFP^+ and Ins^+/Glu^+ cells compared to both lean and STZ control. This observation correlates with increased beta cell area and insulin content in [S4K] CPF-AM treated mice. Also, cells expressing only GFP was increased significantly. Furthermore, an increase in large size islets in peptide-treated mice also shows the sign of beta cell regeneration. Taken together, these results

indicate that [S4K] CPF-AM1 treatment could influence the conversion of the glucagon-expressing alpha cell to insulin-producing beta cells.

In conclusion, L -lysine substituted analogue of CPF-AM1 showed superior beneficial metabolic effects in *db/db* mice than the parent peptide. [S4K] CPF-AM1 treatment improved circulating plasma insulin concentration, glucose haemostasis, glucose tolerance, insulin resistance, insulin secretory response and liver and kidney function, in *db/db* mice. Also, the expression of genes involved in insulin secretion and insulin signalling were enhanced. Data from the GluCre study suggested that [S4K] CPF-AM1 treatment could also influence the transdifferentiation of alpha to beta cells. These observations encourage further investigation to identify the specific receptor through which [S4K] CPF-AM1 exerts its beneficial effects.

Figure 6.1 Schematic diagrams of the amino acid sequence of A) CPF-AM1 and B] [S4K]-CPF-AM1

A) CPF-AM1

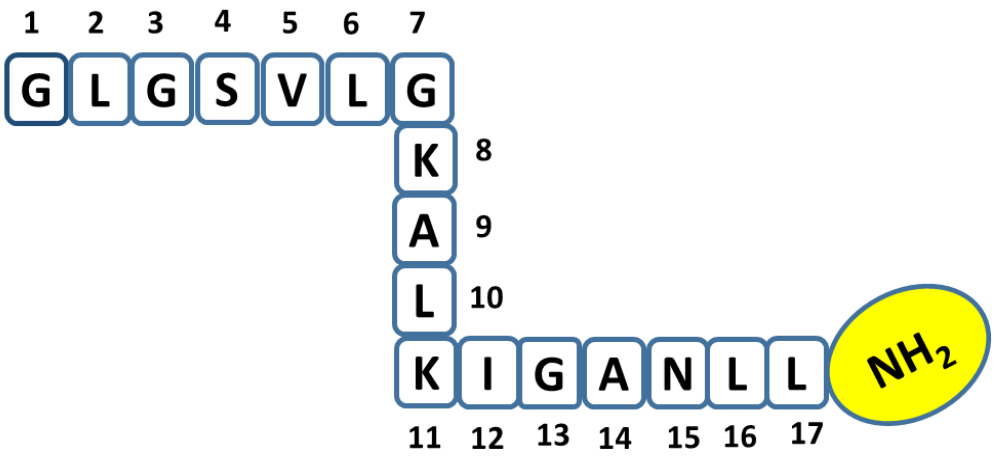

B) [S4K] CPF-AM1

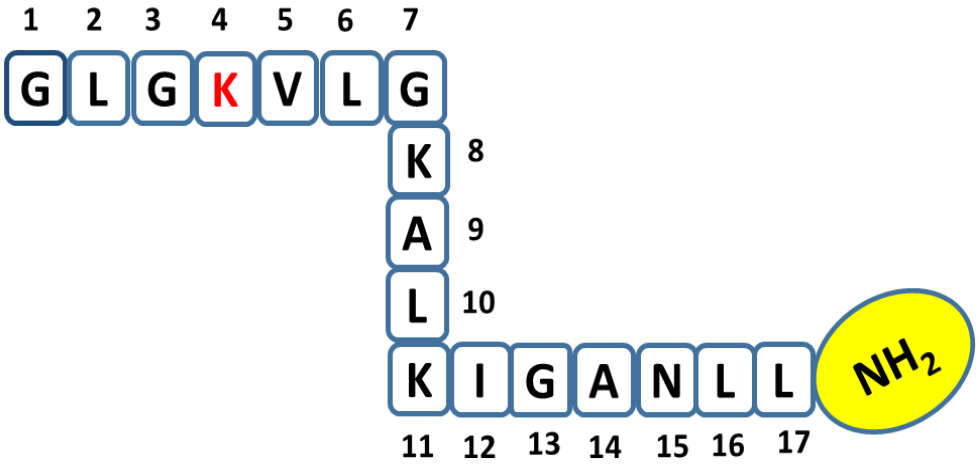

I=Isoleucin (Ile), K=Lysine (Lys), L=Leucine (Leu), N= Asparagine (Asn), V=Valine (Val), G=Glycine (Gly), A=Alanine (Ala).

Figure 6.2 Representation of reverse-phase HPLC profile (A) and MALDI-TOF spectra (B) of [S4K] CPFA-M1

A)

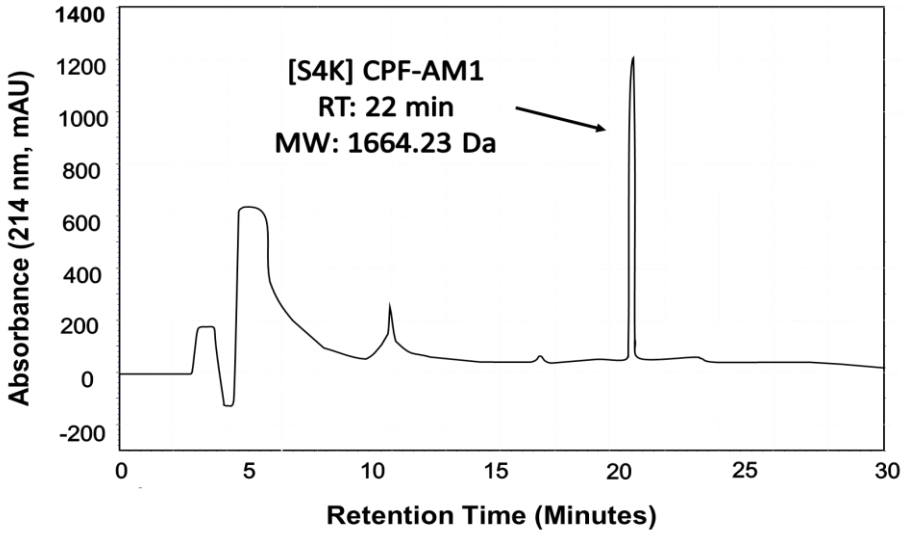

B)

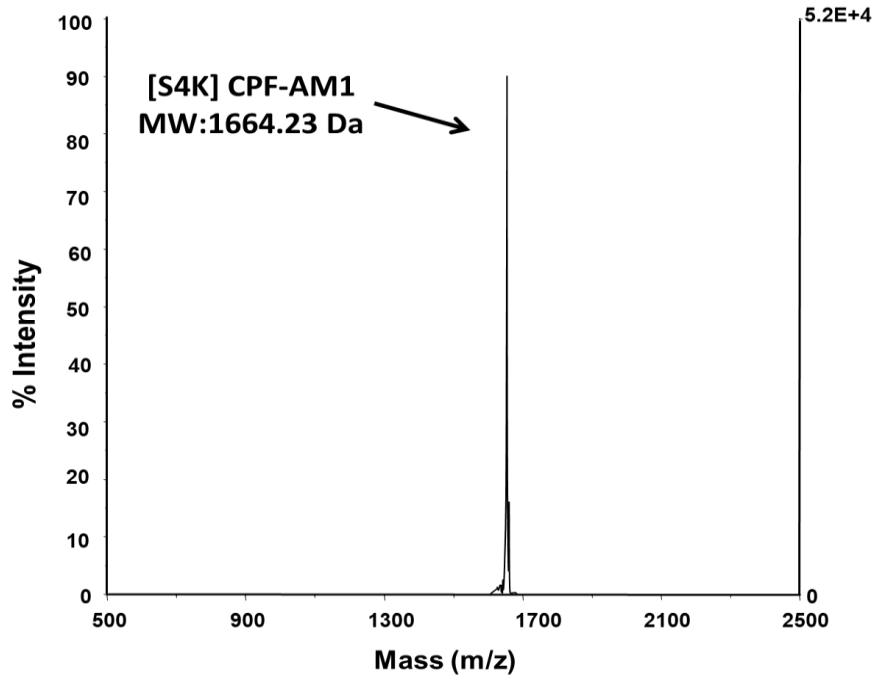

Purity and molecular mass of peptide were confirmed using RP-HPLC and MALDI-TOF respectively. The retention time was verified using ChromQuest software.

Figure 6.3 Dose-dependent effects of [S4K] CPF-AM1 on insulin release from BRIN-BD11 cells

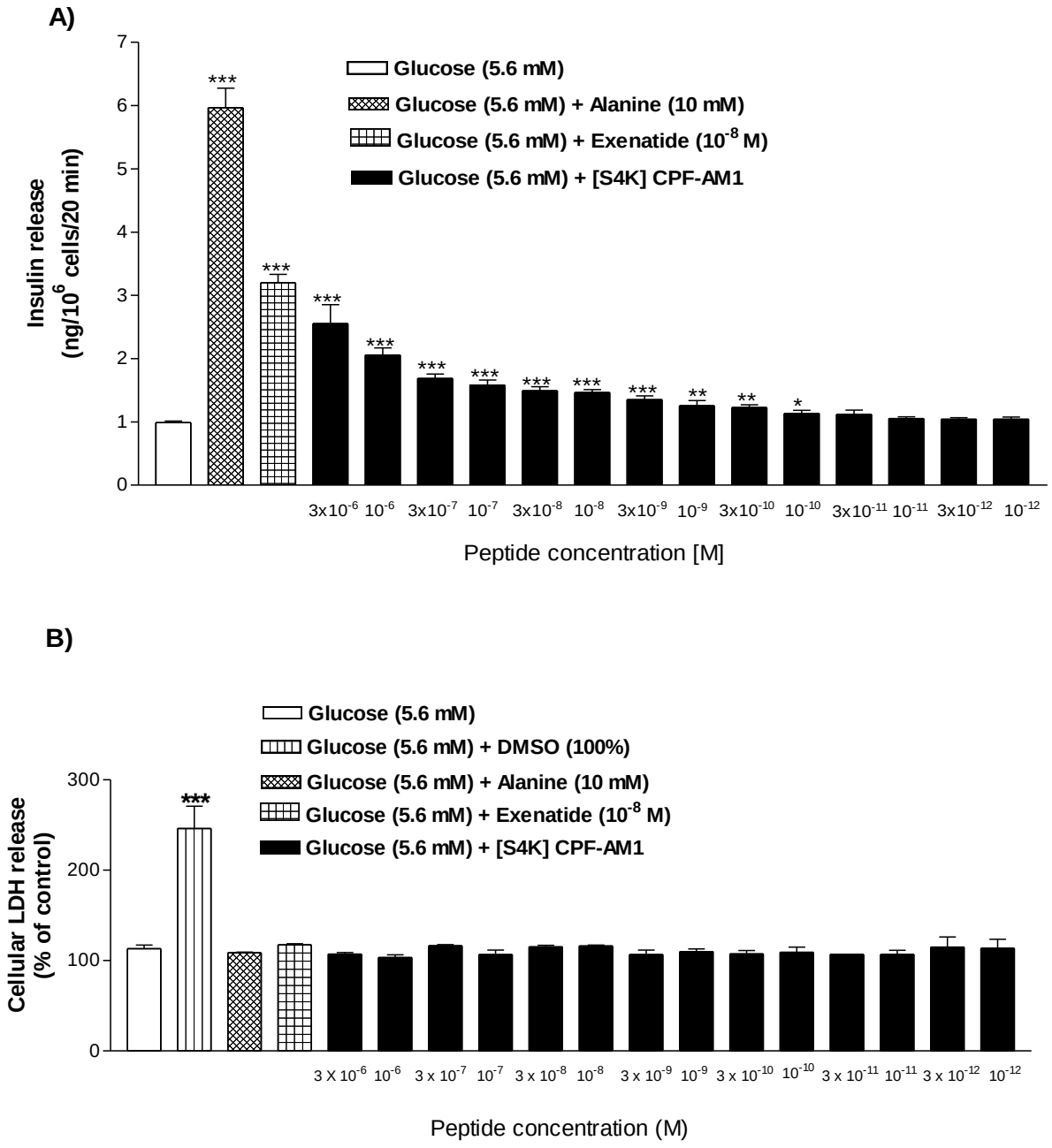

Values are mean ± SEM with n=8 for insulin release and n=4 for LDH. Alanine (10 mM) and Exenatide (10^{-8} M) were used as positive control for insulin secretion studies. DMSO (100%) was used as positive control for LDH assay. *P<0.05, **P<0.01, ***P<0.001 compared to 5.6 mM glucose alone.

Figure 6.4 Dose-dependent effects of [S4K] CPF-AM1 on insulin release from 1.1B4 cells in (A) 5.6 and (B) 16.7 mM glucose

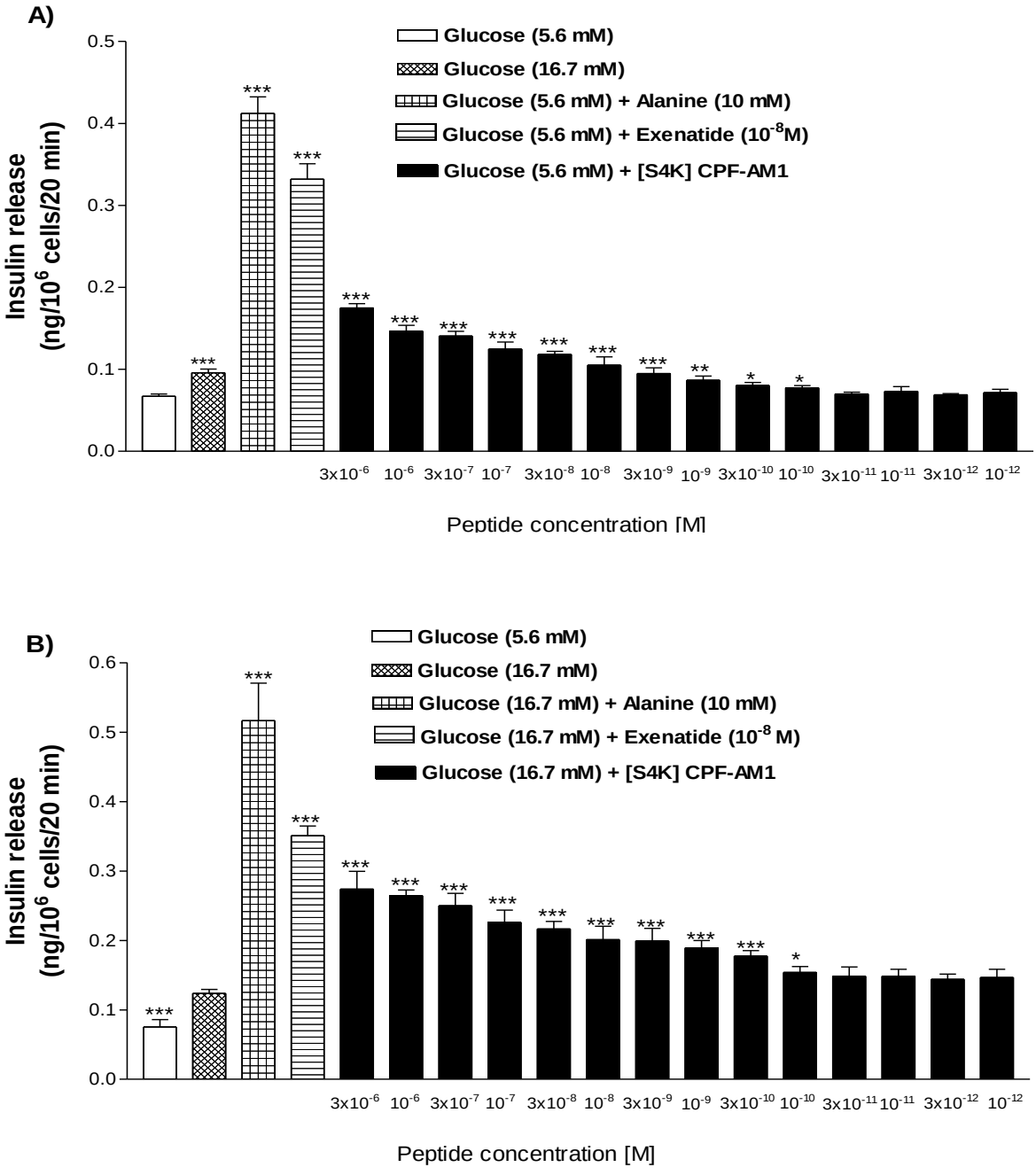

Values are mean ± SEM with n=8 for insulin release. Alanine (10 Mm) and Exenatide (10^{-8} M) were used as positive control for insulin secretion studies. *P<0.05, **P<0.01, ***P<0.001 compared to 5.6 mM glucose (A) and *P<0.05, ***P<0.001 compared to 16.7 mM glucose (B).

Figure 6.5 Effects of [S4K] CPF-AM1 on apoptosis (A) and cell proliferation (B) in BRIN-BD11 cells

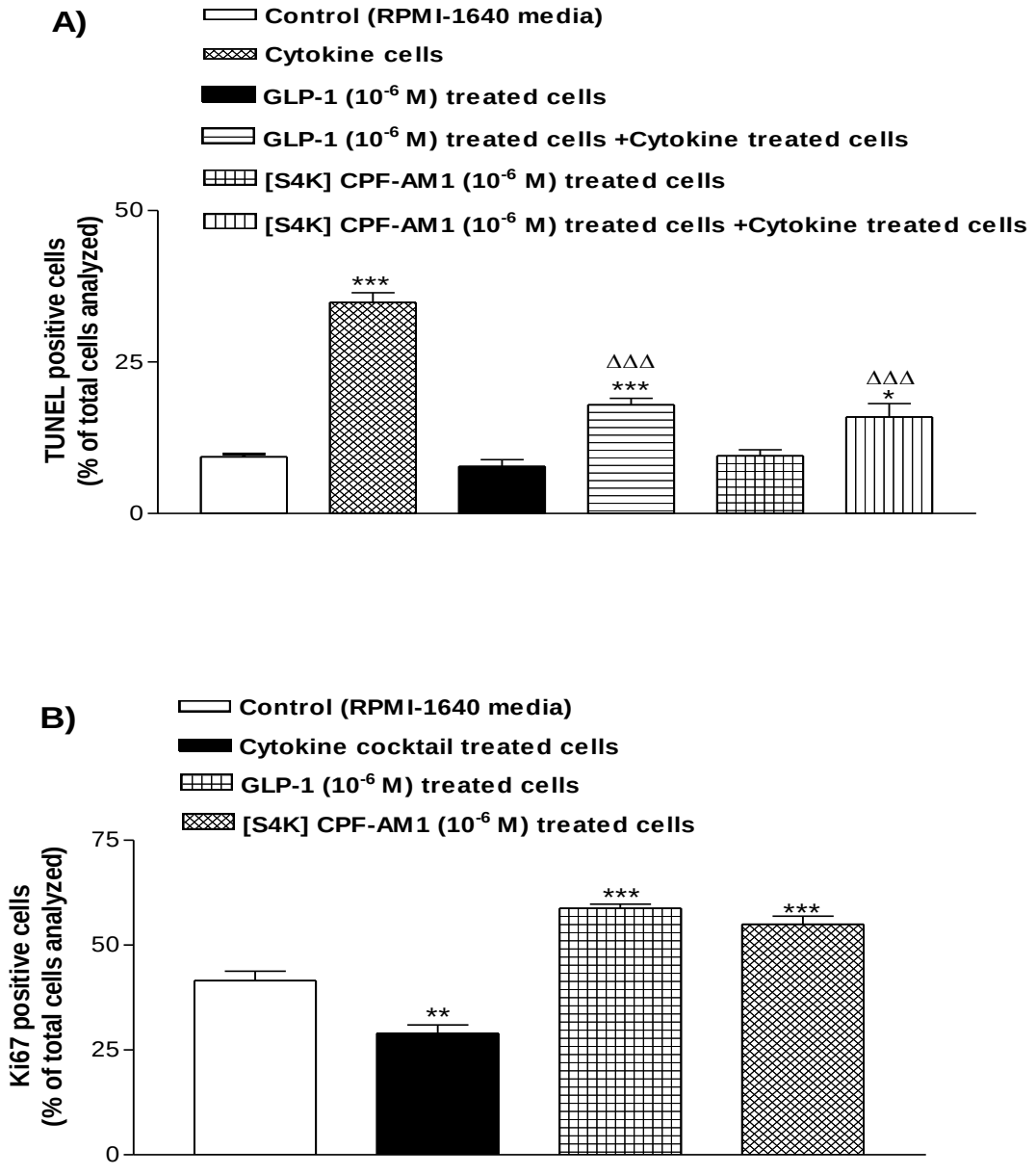

Comparison of the effects of [S4K] CPF-AM1 (1 µM) and GLP-1 (1 µM) on protection against cytokine-induced apoptosis in BRIN-BD11 cells. *P<0.05, ***P<0.001 compared to incubation in culture medium alone. $^{\Delta\Delta\Delta}$P<0.001 compared to incubation in cytokine-containing medium. (B) Ccomparison of the effects of [S4K] CPF-AM1 (1 µM) and GLP-1 (1 µM) on proliferation of BRIN-BD11 cells. **P<0.01, ***P<0.001 compared to incubation in culture medium alone

Figure 6.6 Effect of [S4K] CPF-AM1 on glucose uptake in differentiated C2C12 cells

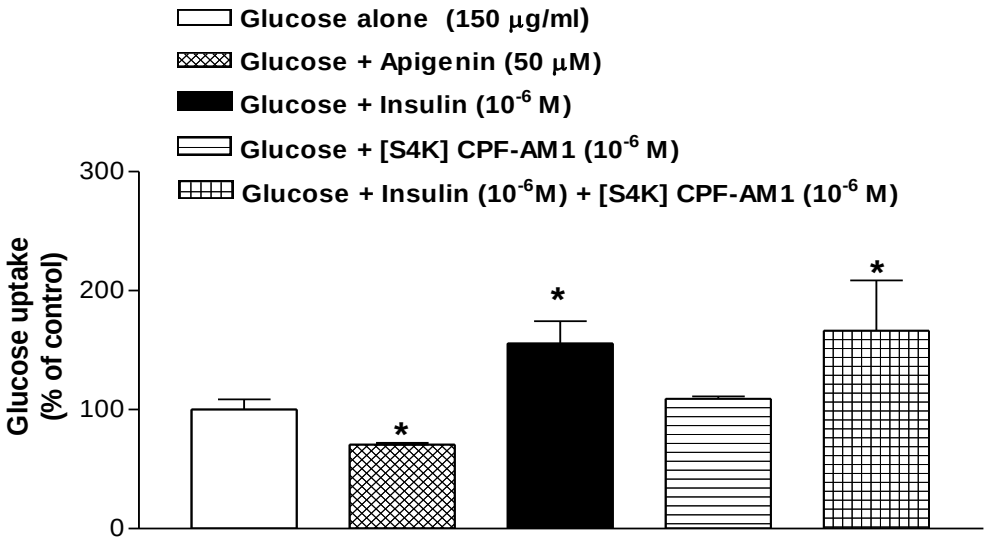

Glucose uptake was expressed as % of control (glucose). Apigenin was used as negative control for glucose uptake. Values are mean ± SEM with n=3. *P<0.05 compared with glucose alone.

Figure 6.7 Effect of peptide [S4K] CPF-AM1 on food intake in intake in 21 hr fasted lean NIH Swiss TO mice

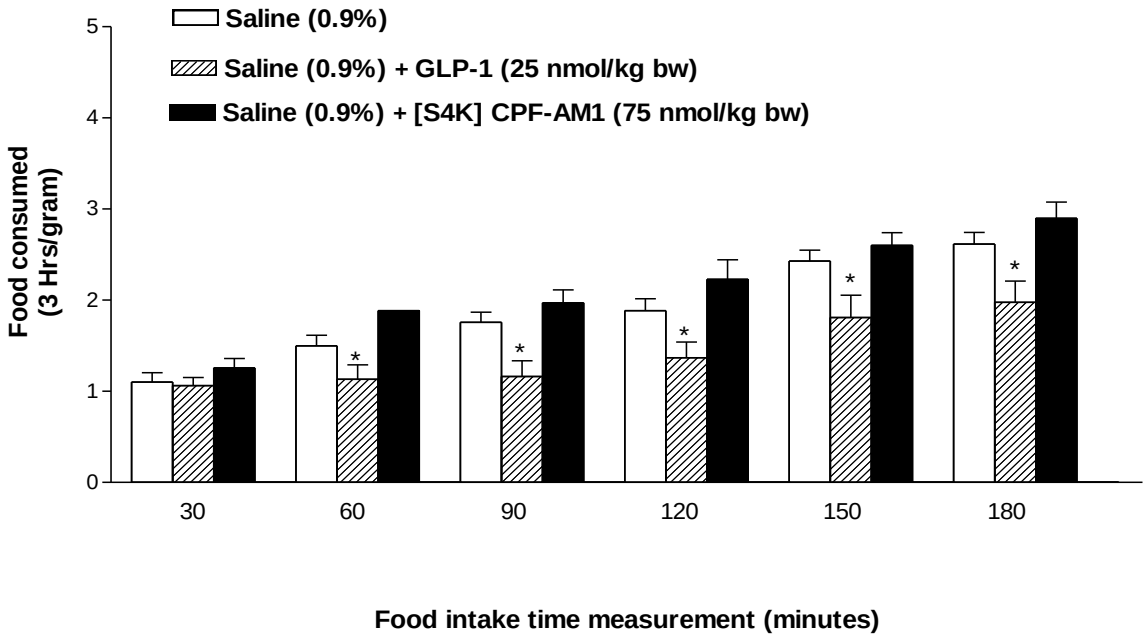

Cumulative food intake was measured prior to and after after i.p. injection of saline vehicle (0.9% w/v NaCl) or GLP-1 (25 nmol/kg bw) or test peptides (75 nmol/kg bw) at time point 30, 60, 90, 120, 150, 180 min in overnight (21 hr) fasted mice. Values represent mean ± SEM (n=8). *P<0.05 compared to saline control.

Figure 6.8 Effects of 28-day treatment with CPF-AM1 and [S4K] CPF-AM1 on body weight (A, B), energy intake (C, D) and water Intake (E, F) in *db/db* mice

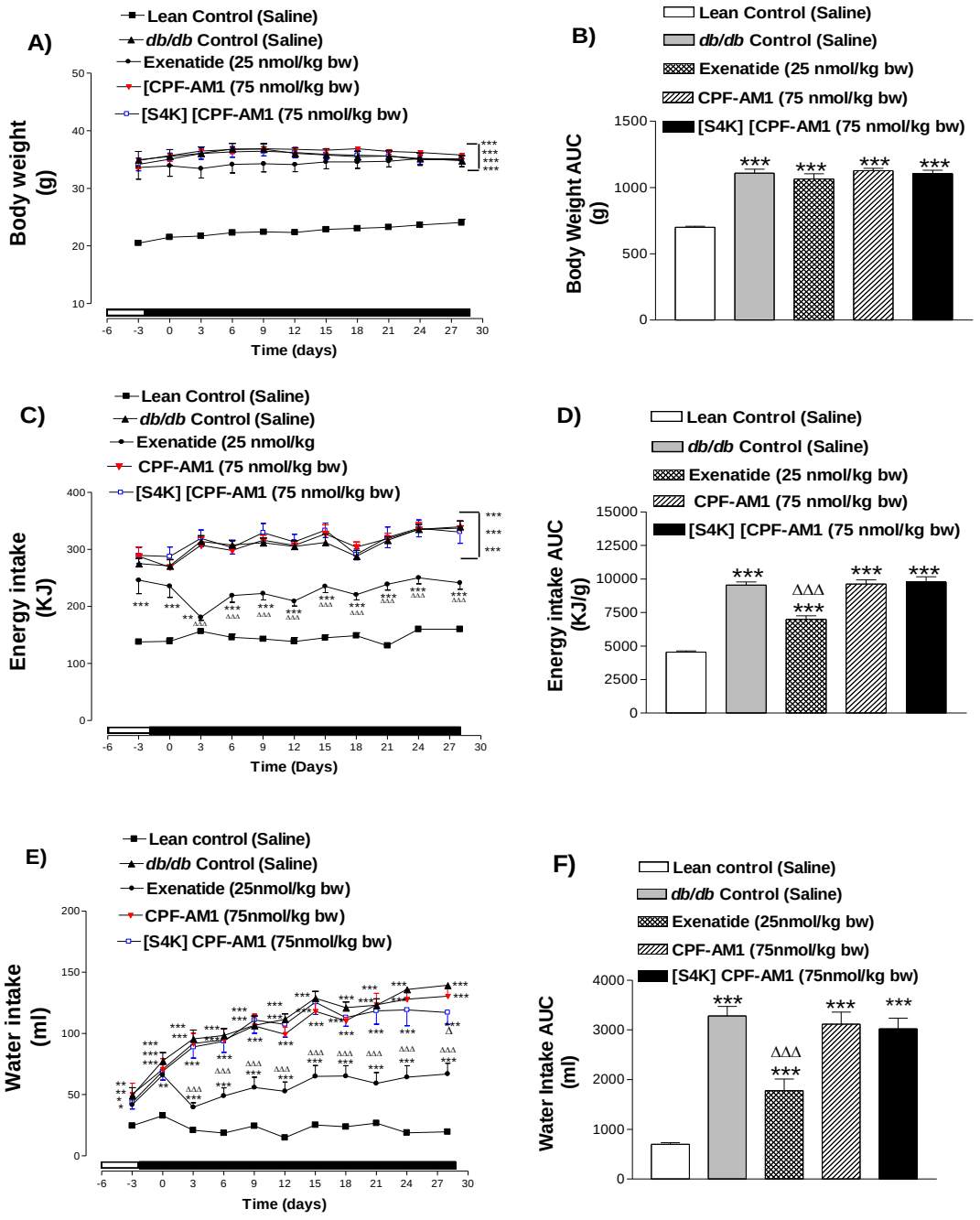

Body weight, energy intake and water intake were measured 3 days prior to, and every 72 hours during treatment with saline or exenatide (25 nmol/kg bw) or peptide (75 nmol/kg bw) for 28 days. Values are mean ±SEM for 8 mice. *P<0.05, **P<0.01 ***P<0.001 compared to lean mice and $^{\Delta}$P<0.05, $^{\Delta\Delta}$P<0.01, $^{\Delta\Delta\Delta}$P<0.001compared to control *db/db* mice

Figure 6.9 Effects of 28-day treatment with CPF-AM1 and [S4K] CPF-AM1 on non-fasting blood glucose (A, B) and plasma insulin (C, D) in *db/db* mice

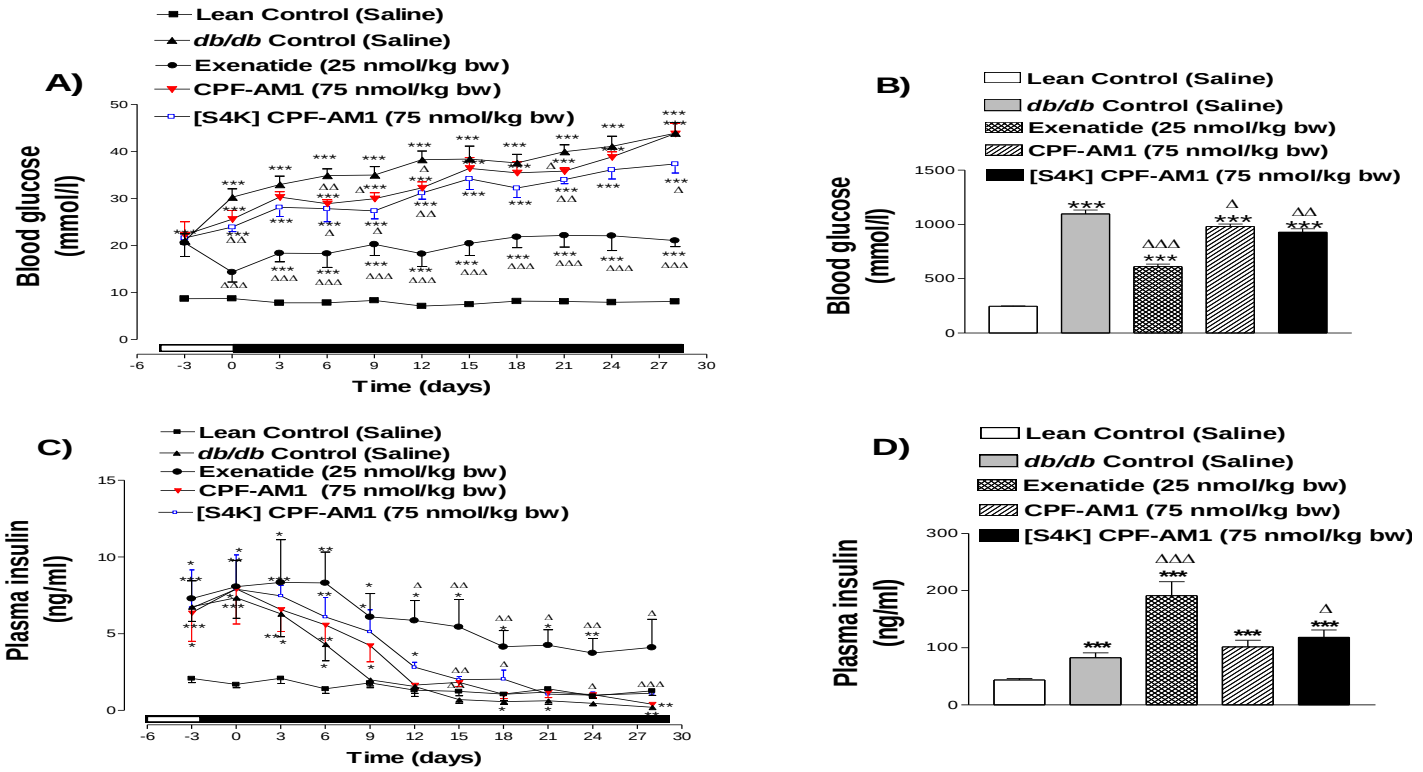

Parameters were measured 3 days prior to, and every 72 hours during treatment (indicated with black bar) with saline or exenatide (25 nmol/kg bw) or peptide (75 nmol/kg bw) for 28 days. Values are mean ±SEM for 8 mice. *P<0.05, **P<0.01 ***P<0.001 compared to lean mice and $^{\Delta}$P<0.05, $^{\Delta\Delta}$P<0.01, $^{\Delta\Delta\Delta}$P<0.001 compared to control *db/db* mice.

Figure 6.10 Effects of CPF-AM1 and [S4K] CPF-AM1 on HbA1c in *db/db* mice

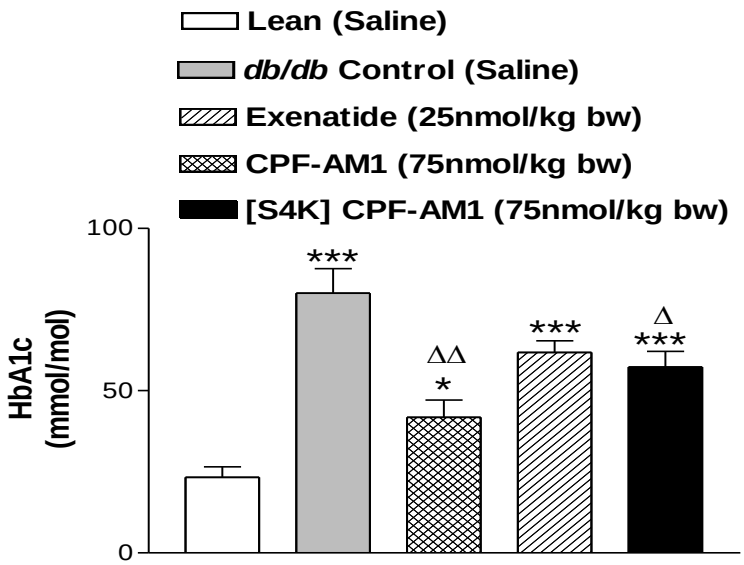

HbA1c level was measured after long term treatment with twice-daily injections of either saline or exenatide (25 nmol/kg bw) or peptide (75 nmol/kg bw) for 28 days. Values are mean ± SEM for 4 mice. *P<0.05, ***P<0.001 compared with lean mice and $^{\Delta}$P<0.05, $^{\Delta\Delta}$P<0.01compare with *db/db* control mice.

Figure 6.11 Long-term effects of CPF-AM1 and [S4K] CPF-AM1 on plasma glucose (A, B) and insulin (C, D) concentrations following intraperitoneal glucose administration to *db/db* mice

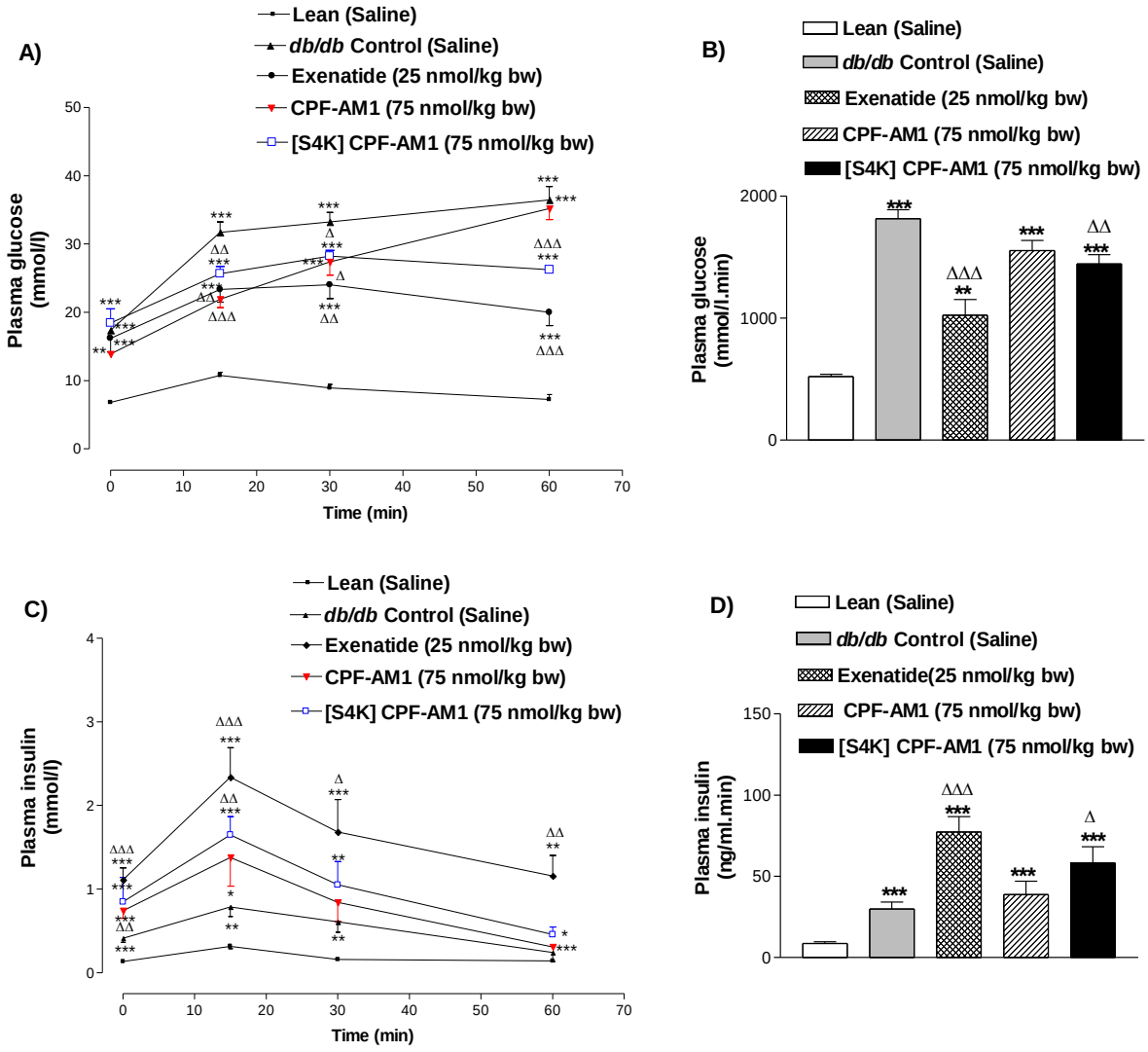

Plasma glucose and insulin concentrations were measured prior to and after intraperitoneal administration of glucose (18 mmol/kg bw) to *db/db* mice pre-treated with twice-daily injections of either with saline or exenatide (25 nmol/kg bw) or peptide (75 nmol/kg bw) for 28 days. Values are mean ± SEM for 8 mice. *P<0.05, **P<0.01, ***P<0.001 compared with lean mice (normal, saline). $^{\Delta}$P<0.05, $^{\Delta\Delta}$P<0.01, $^{\Delta\Delta\Delta}$P<0.001 compared to *db/db* control mice.

Figure 6.12 Long-term effects of CPF-AM1 and [S4K] CPF-AM1 on plasma glucose (A, B) and insulin (C, D) concentrations following oral glucose administration to *db/db* mice

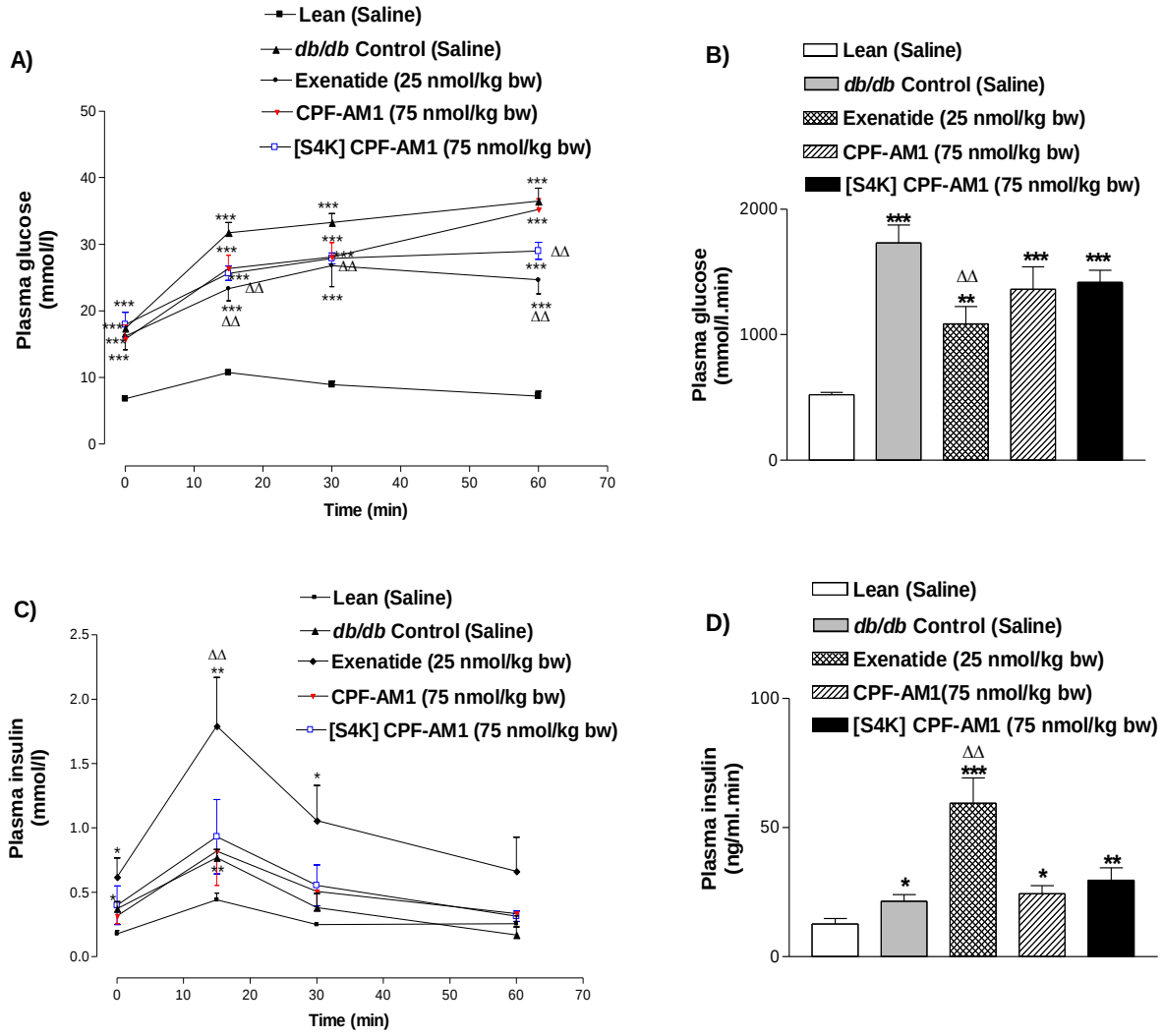

Plasma glucose and insulin concentrations were measured prior to and after oral administration of glucose (18 mmol/kg bw) to *db/db* mice pre-treated with twice-daily injections of either saline or exenatide (25 nmol/kg bw) or peptide (75 nmol/kg bw) for 28 days. Values are Mean ± SEM for 8 mice. *P<0.05, **P<0.01, ***P<0.001 compared with lean mice (normal, saline). $^{\Delta\Delta}$P<0.01 compared to *db/db* control.

Figure 6.13 Long-term effects of CPF-AM1 and [S4K] CPF-AM1 on insulin sensitivity in *db/db* mice

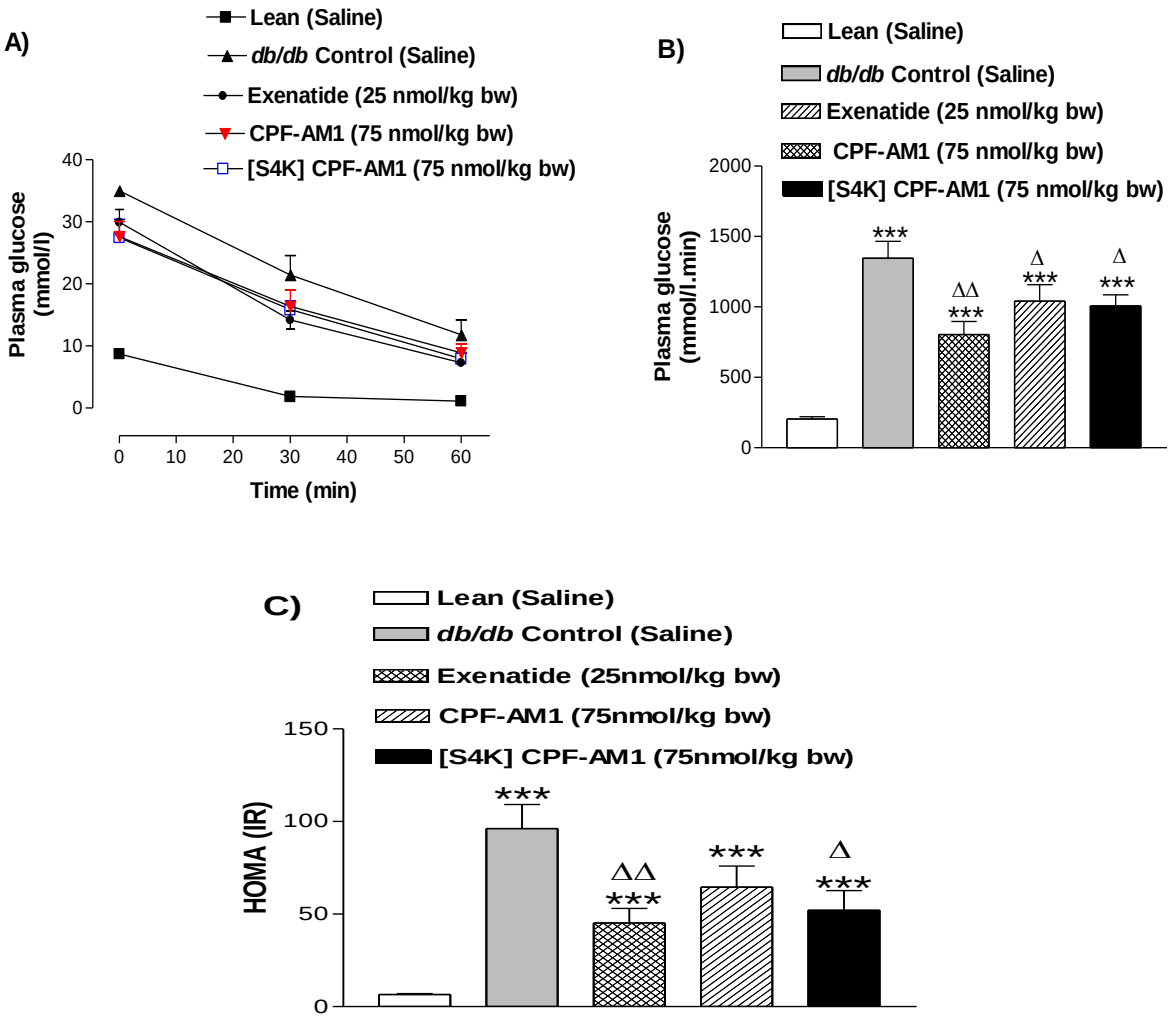

Plasma glucose were measured prior to and after intraperitoneal injection of insulin (50 U/kg bw) in *db/db* mice pre-treated with twice-daily injections of either saline or exenatide (25 nmol/kg bw) or peptide (75 nmol/kg bw) for 28 days. Values are mean ± SEM for 8 mice. ***P<0.001 compared with to lean mice and $^{\Delta}$P<0.05, $^{\Delta\Delta}$P<0.01 compare with *db/db* control mice.

Figure 6.14 Effects of CPF-AM1 and [S4K] CPF-AM1 on body composition in *db/db* mice.

(A)

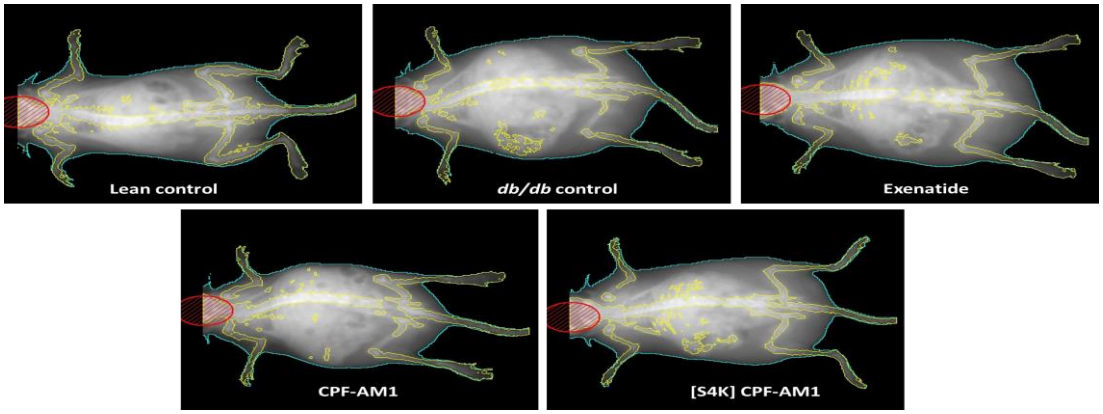

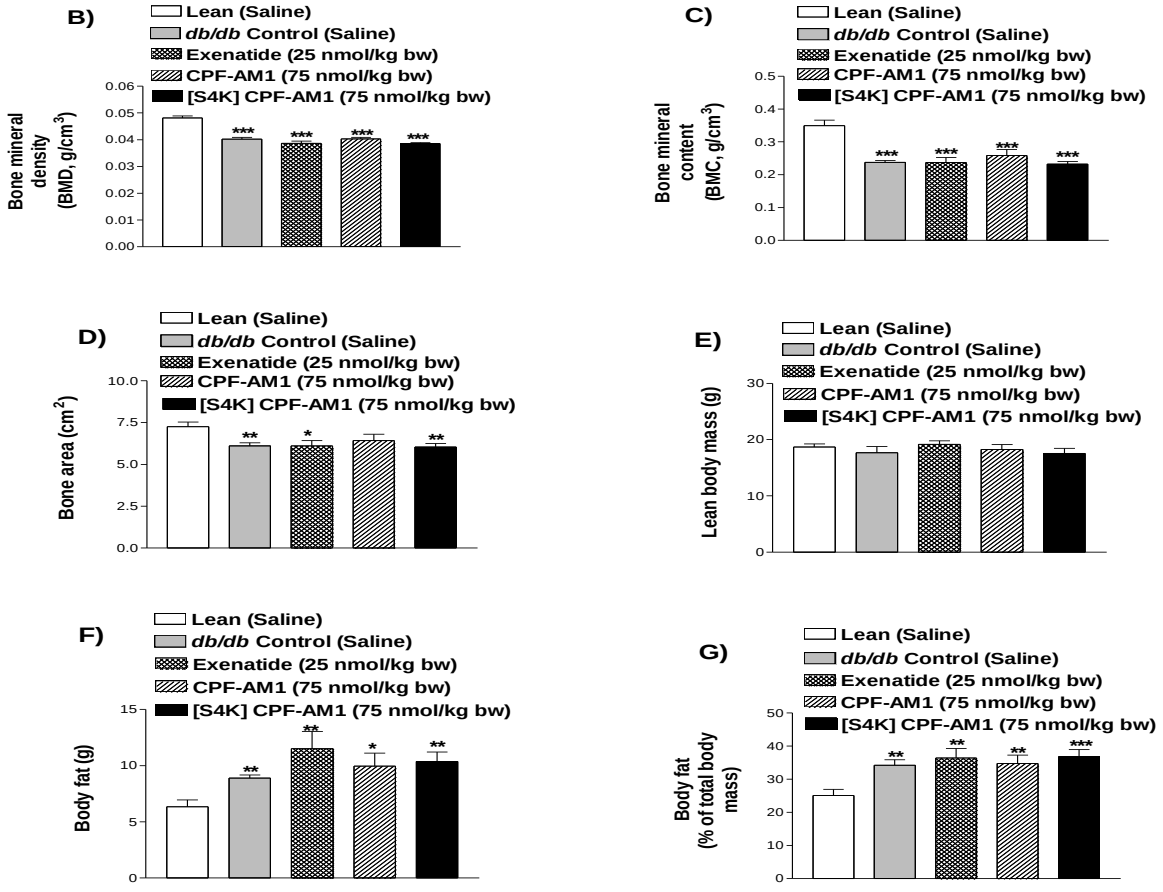

Effects of CPF-AM1 and [S4K] CPF-AM1 on body composition in lean and *db/db* mice. Animals were injected with either saline or exenatide (25 nmol/kg bw) or peptide (75 nmol/kg bw) for 28 days. The figure shows (A) representative DEXA scans, (B) bone mineral density, (C) bone mineral content, (D) bone area. (E) lean body mass, (F) body fat and (G) body fat expressed a percentage of total body mass. Values are means ± SEM for 8 mice. *P<0.05, **P<0.01, ***P<0.001 compared with saline-treated lean mice.

Figure 6.15 Effects of [S4K] CPF-AM1 on pancreatic weight (A), total insulin content (B), and insulin secretory response of isolated islets (C&D) from lean, and *db/db* mice treated

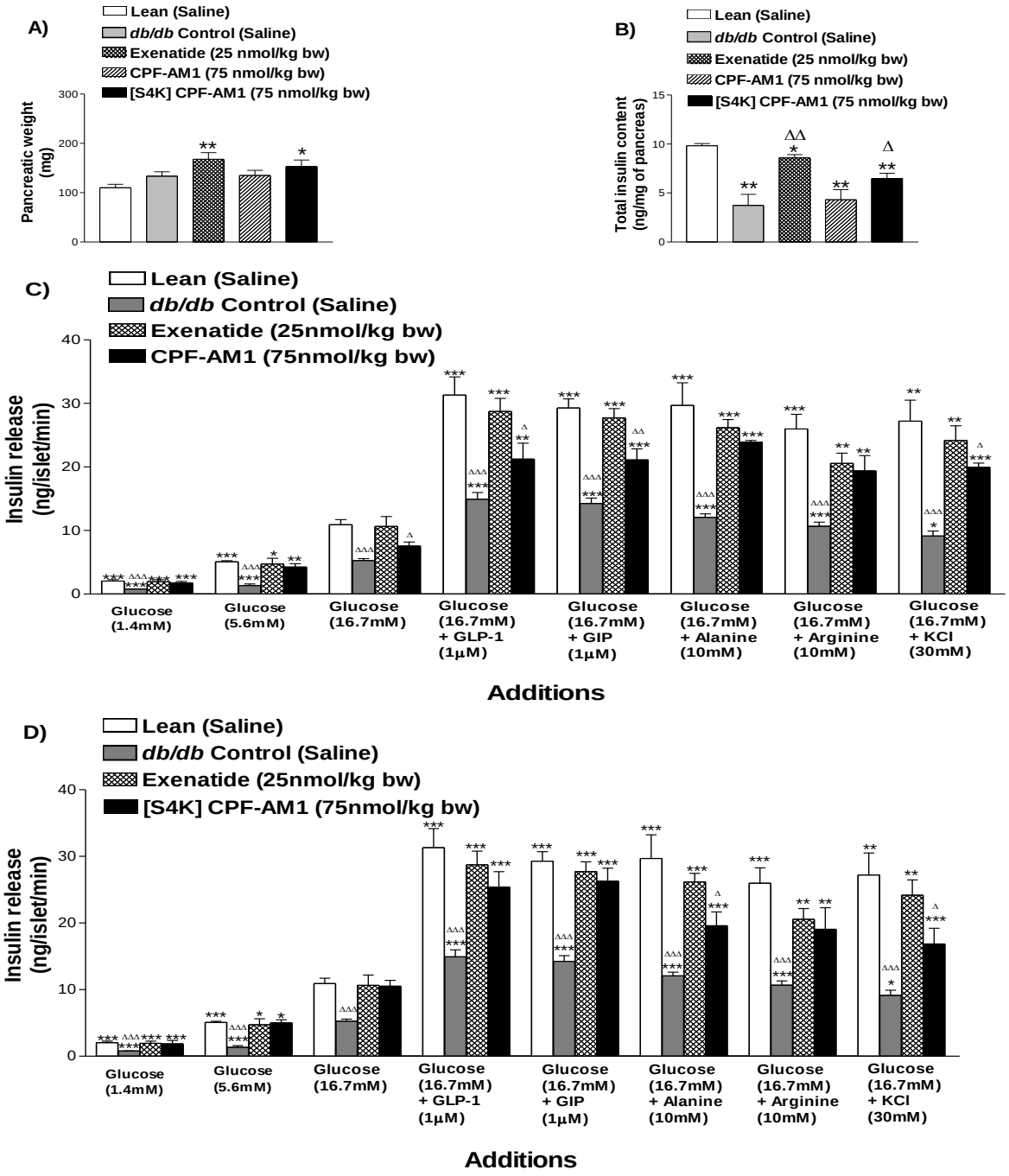

Mice were treated with saline or exenatide (25 nmol/kg bw) or peptide (75 nmol/kg bw) for 28 days prior to experiment. Values are means ± SEM with n=4. *P<0.05, **P<0.01, ***P<0.001 compared with the response of islets isolated from each group of mice at 16.7 mM glucose. $^{\Delta}$P<0.05, $^{\Delta\Delta}$P<0.01, $^{\Delta\Delta\Delta}$P<0.001 compared with the response of islets isolated from lean mice (saline treated) to each secretagogue or glucose concentration.

Figure 6.16 Effects of long-term treatment with CPF-AM1 and [S4K] CPF-AM1 on total cholesterol (A), Triglycerides (B), HDL (C) and LDL (D) in *db/db* mice

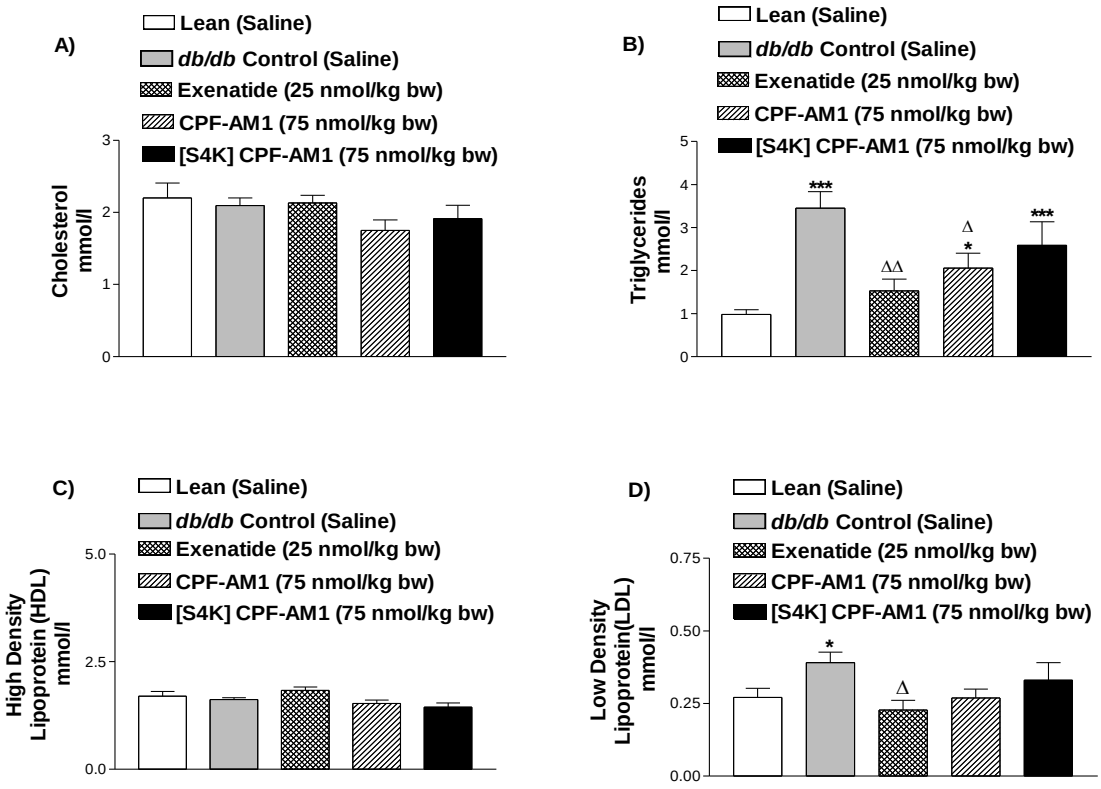

Plasma sample was collected after 28 days treatment with either saline or exenatide (25 nmol/kg bw) or peptide (75 nmol/kg bw). Values are mean ± SEM for 6 mice. *P<0.05, ***P<0.001 compared to lean mice. $^{\Delta}$P<0.05, $^{\Delta\Delta}$P<0.01 compared to *db/db* control mice.

Figure 6.17 Effects of long-term treatment with CPF-AM1 and [S4K] CPF-AM1 on plasma AST (A) ALT (B) ALP (C) and creatinine (D) levels in *db/db* mice

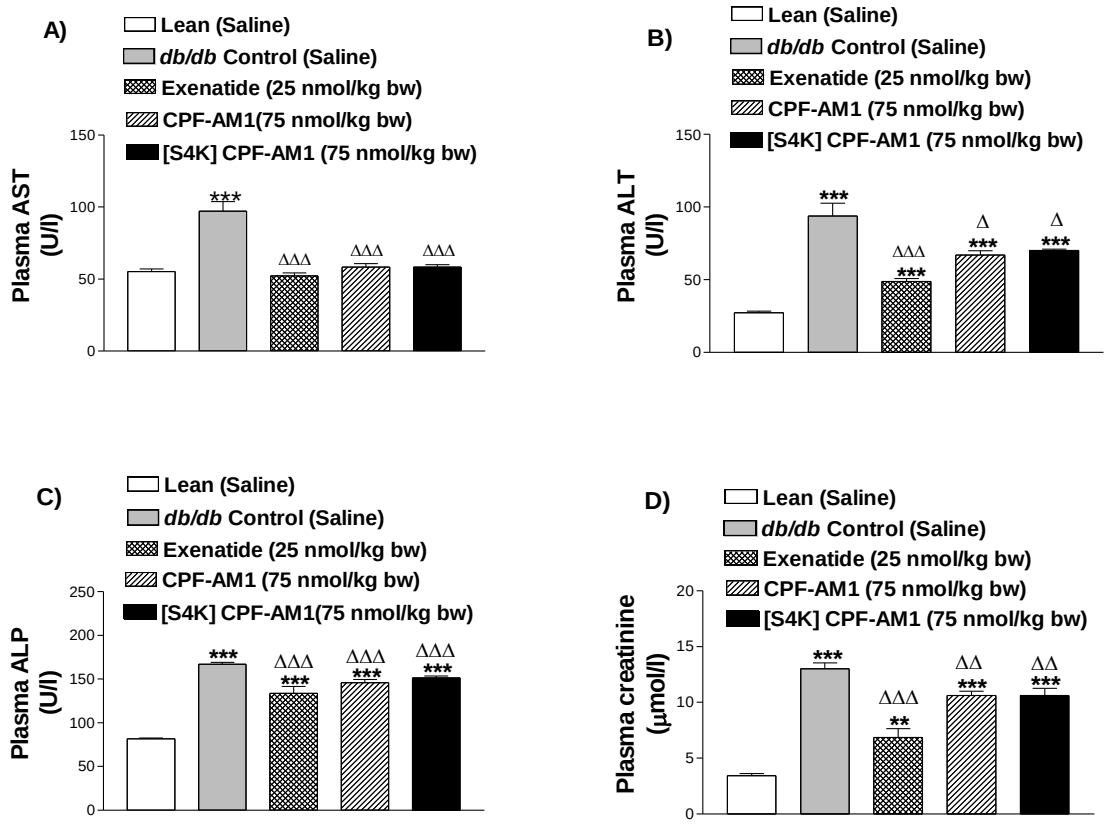

Following 28 days injection with either saline or exenatide (25 nmol/kg bw) or peptide (75 nmol/kg bw), plasma sample was collected and measured for ALT, AST, ALP and creatinine levels. Values are mean ± SEM for 6 mice. **P<0.01, ***P<0.001 compared to lean control. $^{\Delta}$P<0.05, $^{\Delta\Delta}$P<0.01, $^{\Delta\Delta\Delta}$P<0.001 compared to *db/db* control.

Figure 6.18 Effects of long-term treatment with [S4K] CPF-AM1 on amylase activity in *db/db* mice.

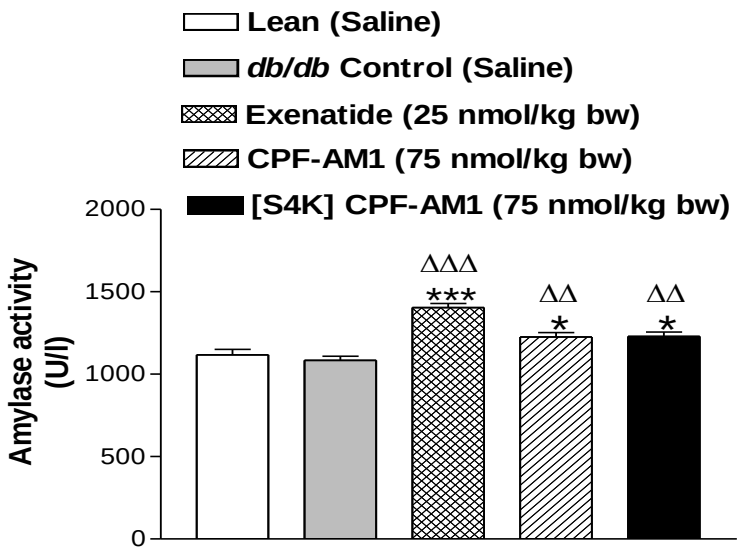

Following 28 days injection with either saline (control) or exenatide or peptide, plasma sample was collected, and amylase activity was measured. Values are mean ± SEM for n=6 mice. *P<0.05, ***P<0.001 compared to normal control, $^{\Delta\Delta}$P<0.01, $^{\Delta\Delta\Delta}$P<0.001 compared to *db/db* control.

Figure 6.19 Effects of CPF-AM1 & [S4K] CPF-AM1 treatment on islet morphology in *db/db* mice.

A)

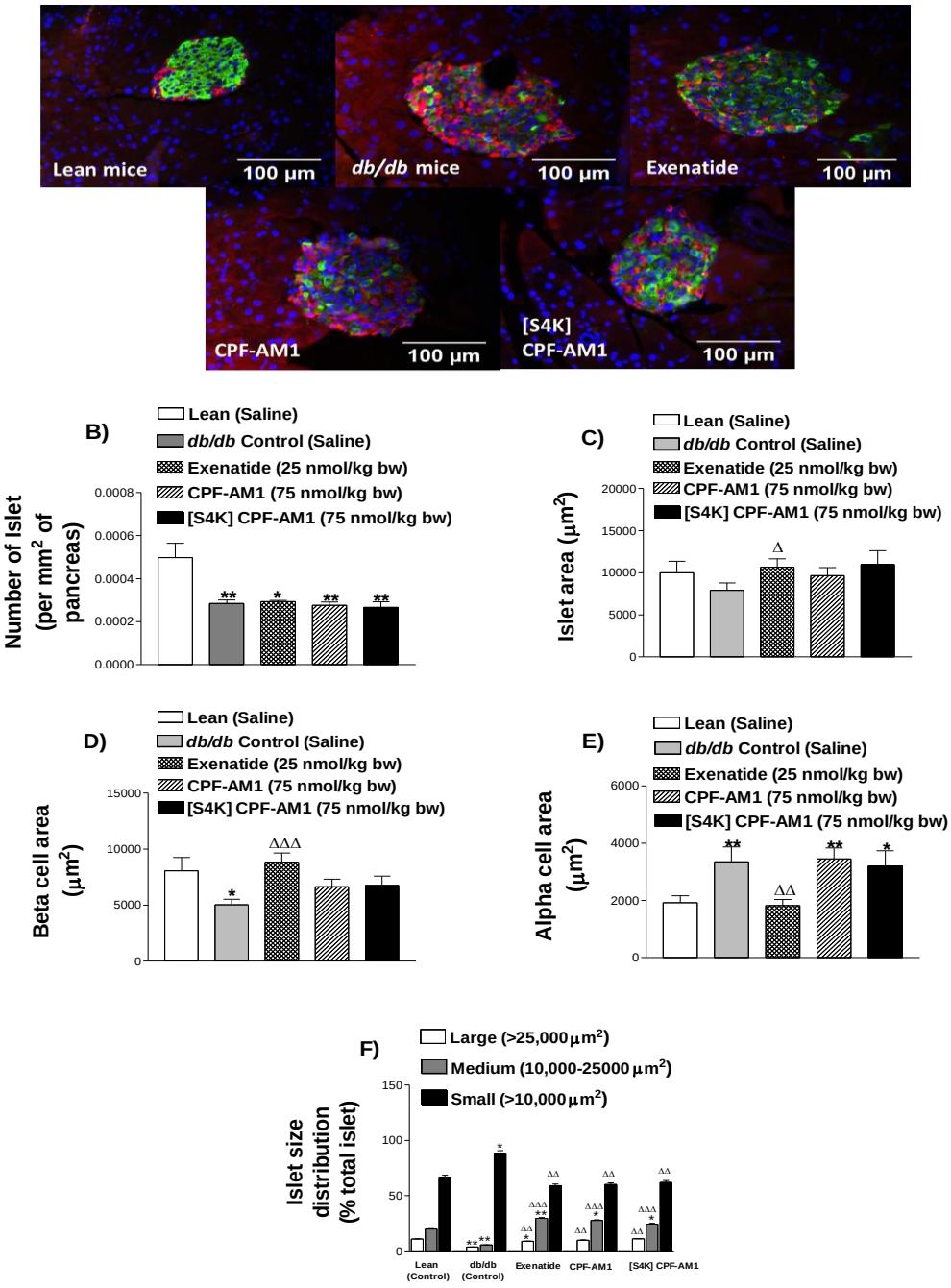

Representative image (A) showing insulin (green) and glucagon (red) immunoreactivity from lean, *db/db* control, CPF-AM1 and [S4K] CPF-AM1 treated mice. B, C, D, E and F shows islet number, islet area, beta cell area, alpha cell area, and islet size distribution respectively. Mean ± SEM for 6 mice (~80 islets per group). *P<0.05, **P<0.01 compared to normal saline control, $^{\Delta\Delta}$P<0.05, $^{\Delta\Delta}$P<0.01, $^{\Delta\Delta\Delta}$P<0.001 compared to *db/db* control.

Figure 6.20 Effects of CPF-AM1 & [S4K] CPF-AM1 treatment on expression of genes involved in insulin action in skeletal muscle

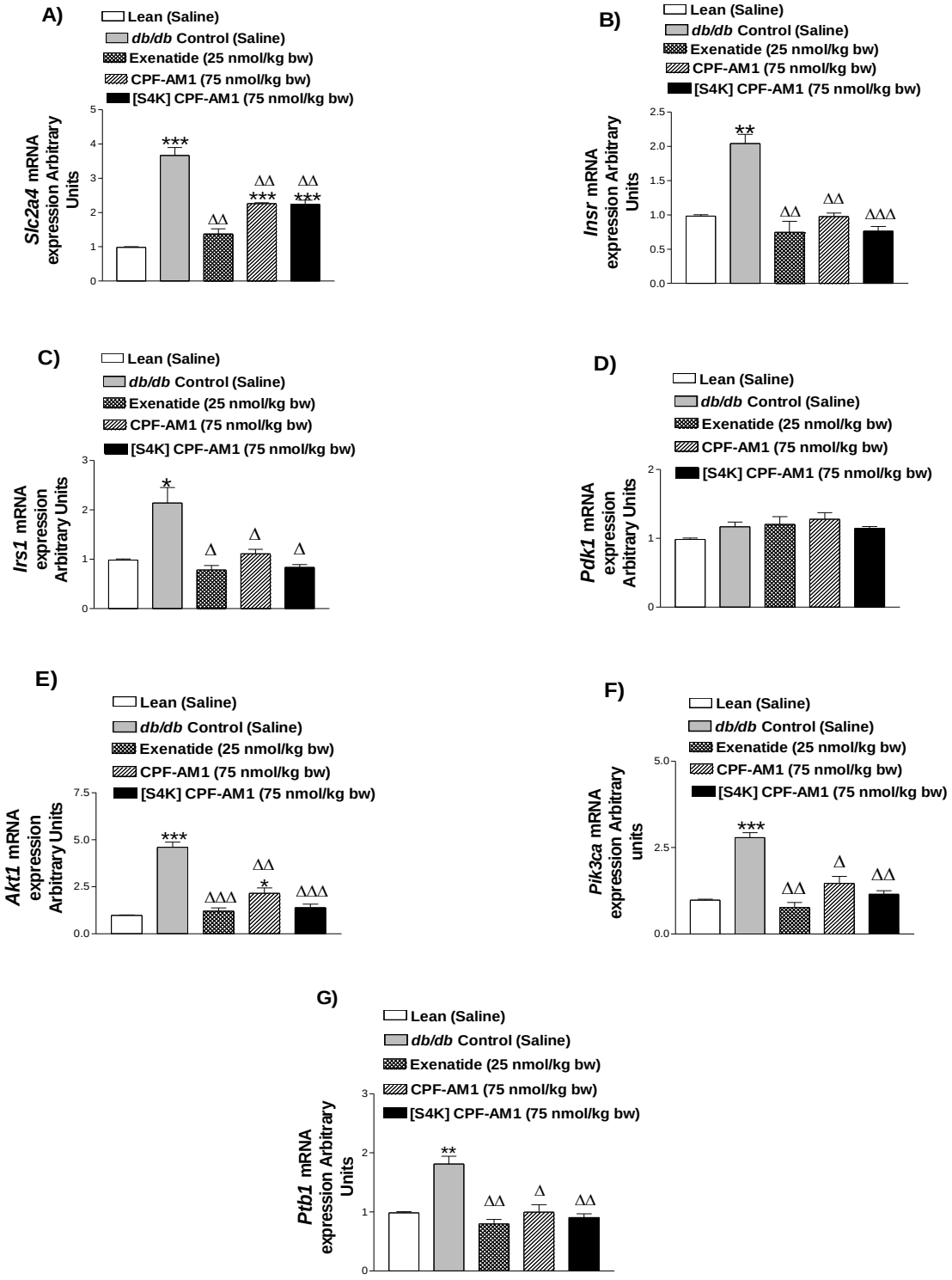

3 µg of mRNA was used for cDNA synthesis. Expression values were normalised to Actb. Values are mean ± SEM for n=4. *P<0.05, **P<0.01, ***P<0.001 compared to normal control. $^{\Delta}$P<0.05, $^{\Delta\Delta}$P<0.01, $^{\Delta\Delta\Delta}$P<0.001 compared to *db/db* control.

Figure 6.21 Effects of [S4K] CPF-AM1 treatment on expression of genes involved in insulin secretion from islets

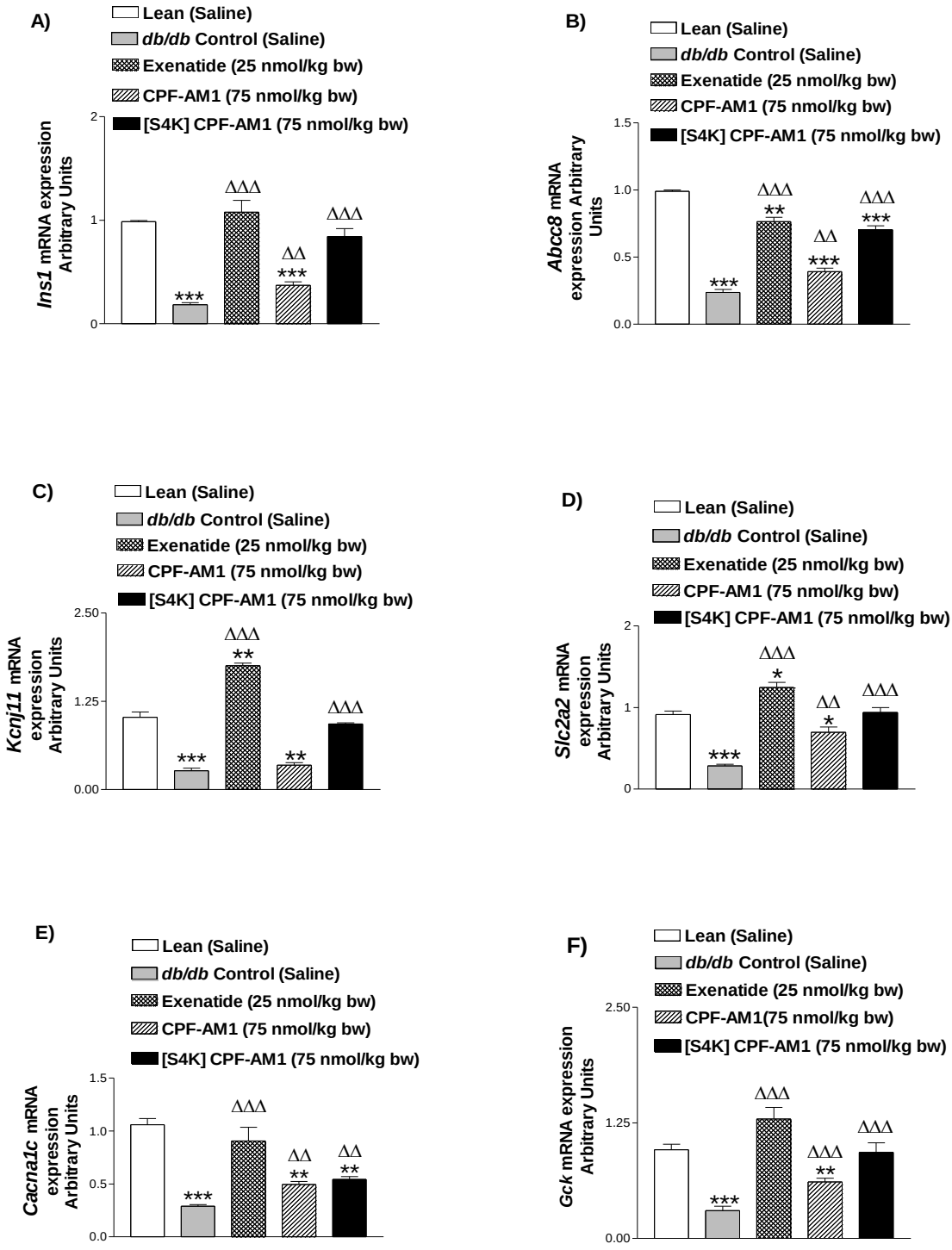

3 µg of mRNA was used for cDNA synthesis. Expression values were normalised to Actb. Values are mean ± SEM for n=4. *P<0.05, **P<0.01, ***P<0.001 compared to normal control, $^{\Delta\Delta}$P<0.01, $^{\Delta\Delta\Delta}$P<0.001 compared to *db/db* control mice.

Figure 6.22 Effects of [S4K] CPF-AM1 treatment on expression of genes involved in insulin secretion (A- C), beta cell proliferation (D) and beta cell apoptosis (E) in islets

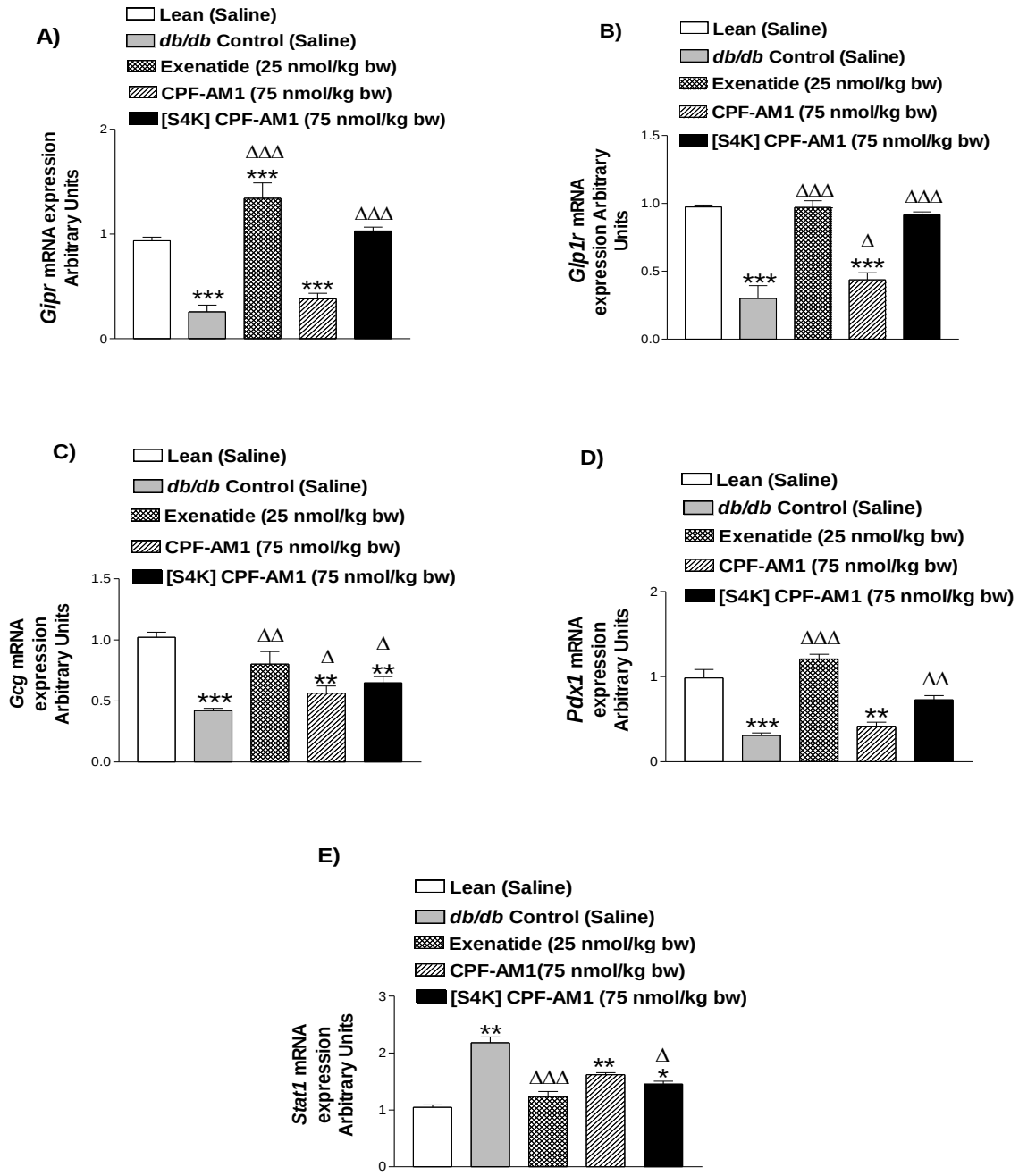

3 µg of mRNA was used for cDNA synthesis. Expression values were normalised to Actb. Values are mean ± SEM for n=4. *P<0.05, **P<0.01, ***P<0.001 compared to normal control, $^{\Delta}$P<0.05, $^{\Delta\Delta}$P<0.01, $^{\Delta\Delta\Delta}$P<0.001 compared to *db/db* control mice.

Figure 6.23 Effects of twice daily administration of [S4K] CPF-AM1 on body weight change (A and B), food intake (C) and water intake (D) in GluCre-ROSA26EYFP mice

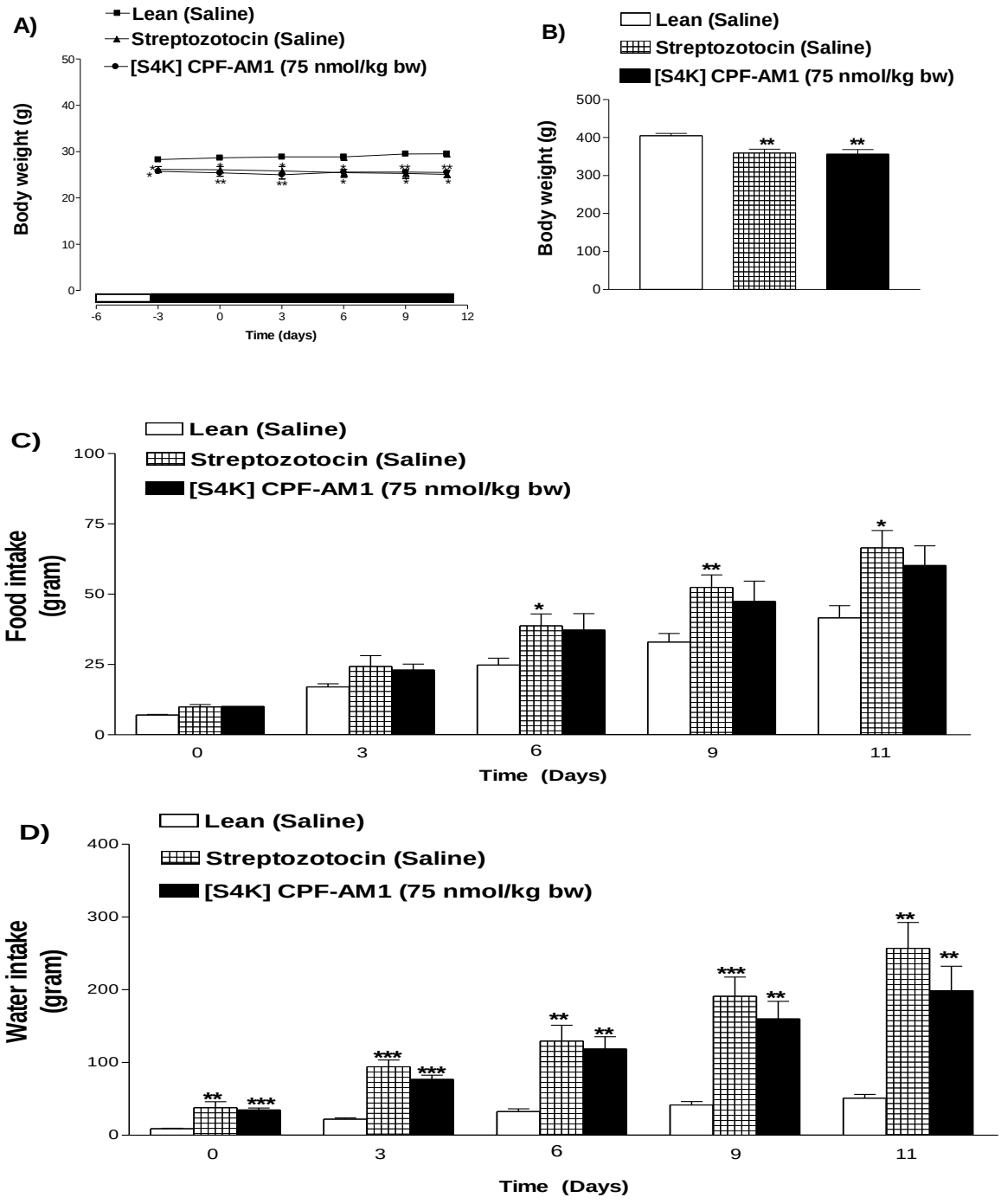

Streptozotocin (50mg/kg bw) induced diabetic mice were grouped prior to the peptide treatment. Body weight (A & B), food intake (C), water intake (D) were measured 3 days prior to, and every 72 hours during treatment with saline or [S4K] CPF-AM1 (75 nmol/kg bw) for 11 days. Values are mean ±SEM for 5 mice. *P<0.05, **P<0.01 ***P<0.001 compared to lean mice.

Figure 6.24 Effects of twice daily administration of [S4K] CPF-AM1 on blood glucose (A) and plasma insulin (B) in GluCre-ROSA26EYFP mice

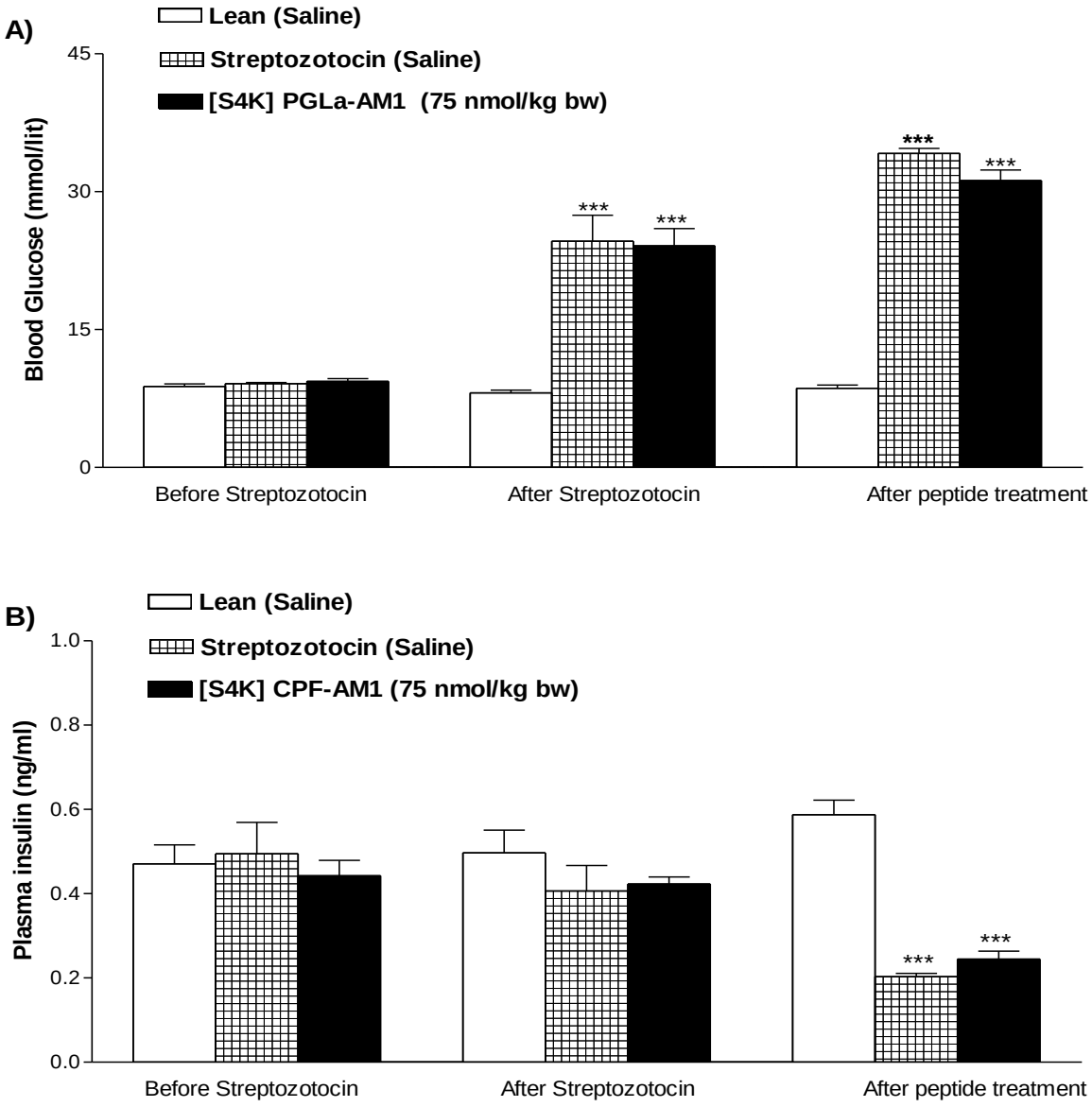

Blood glucose (A) and plasma insulin (B) were measured before and after streptozotocin, and after 11 days treatment with saline or [S4K] CPF-AM1(75 nmol/kg bw). Values are mean ±SEM for 5 mice. ***P<0.001 compared to lean mice.

Figure 6.25 Effects of twice daily administration of [S4K] CPF-AM1 on pancreatic insulin content in GluCre-ROSA26EYFP mice

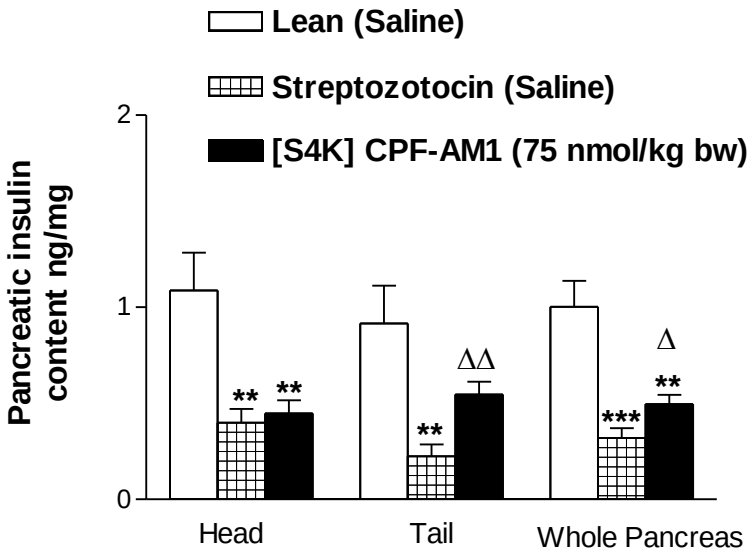

Pancreatic insulin content was measured after 11 days treatment with saline or [S4K] CPF-AM1(75 nmol/kg bw). Values are mean ±SEM for 5 mice **P<0.01, ***P<0.001 compared to normal saline control, $^{\Delta}$P<0.05, $^{\Delta\Delta}$P<0.01 compared to streptozotocin control.

Figure 6.26 Effects of [S4K] CPF-AM1 treatment on islet morphology in GluCre-ROSA26EYFP mice

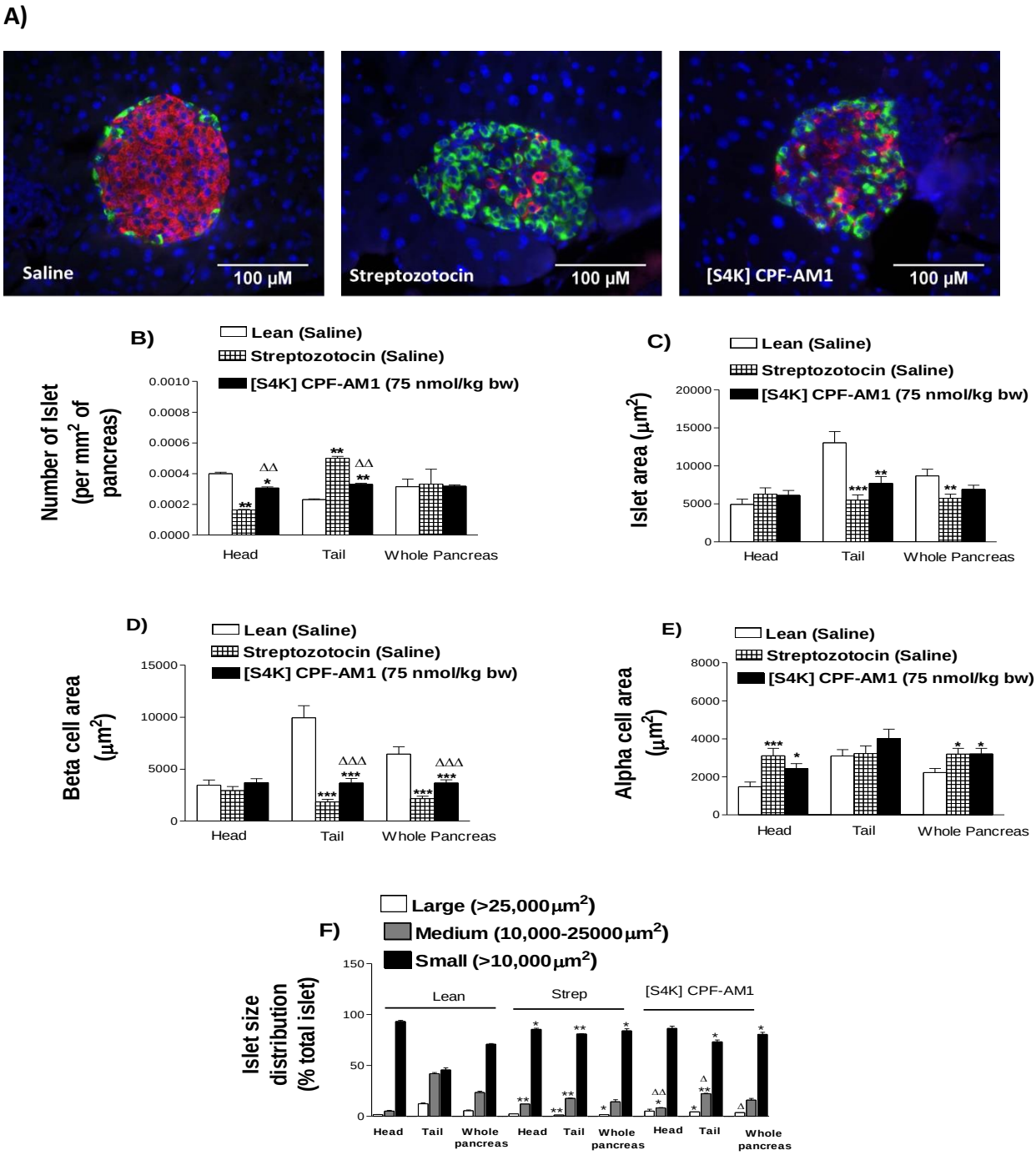

Representative islets (A) showing insulin (red) and glucagon (green) immunoreactivity from lean, streptozotocin and [S4K] PGLa-AM1 treated mice. B, C, D, E, and F shows islet number, islet area, beta cell area, alpha cell area, and islet size distribution respectively. Mean ± SEM for 5 mice (~50 Islets per group). *P<0.05, **P<0.01, ***P<0.001 compared to normal saline control, $^{\Delta}$P<0.05, $^{\Delta\Delta}$P<0.01, $^{\Delta\Delta\Delta}$P<0.001 compared to streptozotocin control.

Figure 6.27 Effect of [S4K] PGLa-AM1 on pancreatic Islets in GluCre-ROSA26EYFP mice

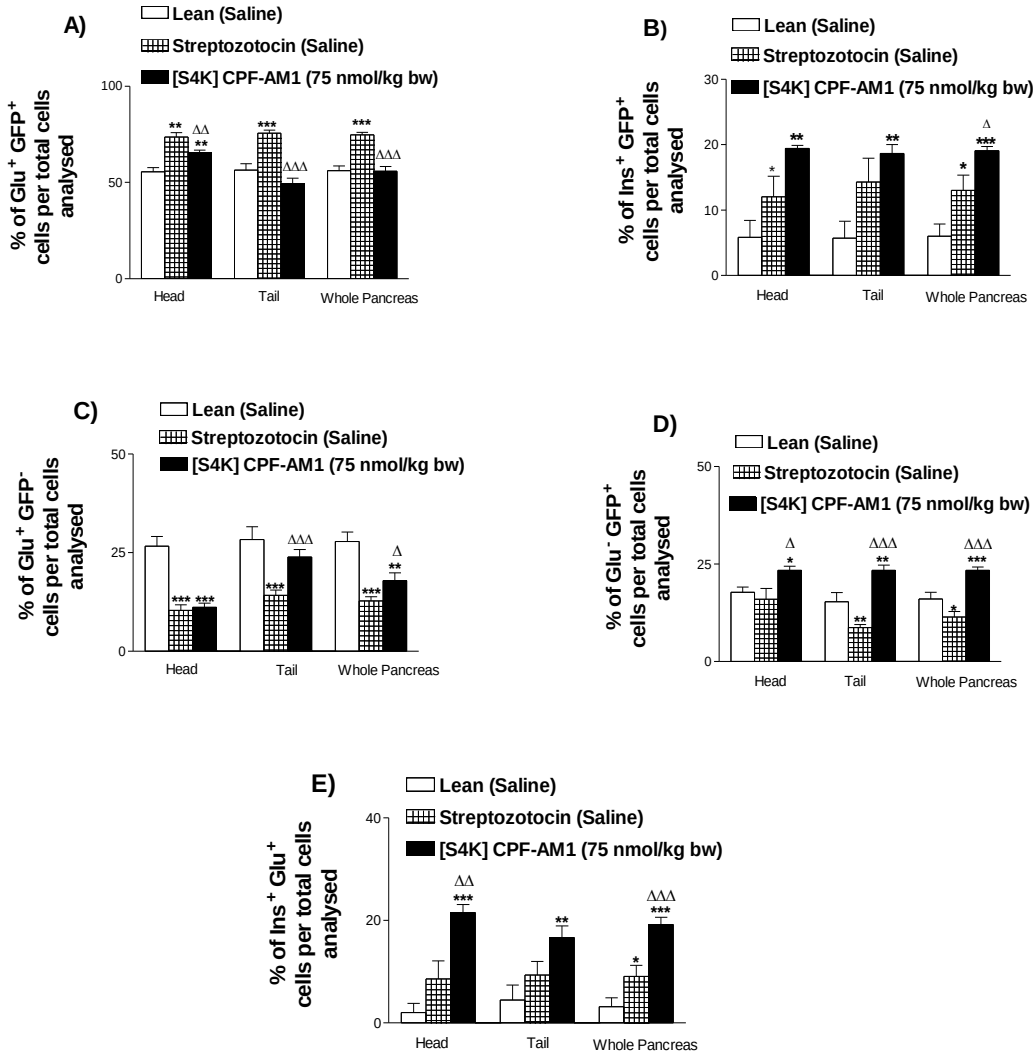

Quantification Of A) Glucagon-GFP positive cells, B) Insulin-GFP positive cells, C) Glucagon positive cells, D) GFP positive cells per total islets and E) Insulin-Glucagon positive cells (~50 Islets per group). *P<0.05, **P<0.01, **P<0.001 compared to normal saline control, $^{\Delta}$P<0.05, $^{\Delta\Delta}$P<0.01, $^{\Delta\Delta\Delta}$P<0.001 compared to streptozotocin control.

Chapter 7

General Discussion

7.1 Type 2 diabetes- The growing epidemic

Type 2 diabetes, which is a complex metabolic disorder characterised by pancreatic beta cells dysfunction and insulin resistance, is currently one of the major healthcare problem globally. More prevalent in adults, type 2 diabetes is also seen in children and young adults due to an increasingly sedentary lifestyle (Basu *et al.,* 2013). It accounts for 91% of the global diabetes population, out of which 80% resides particularly in developing nations like India and China. According to data published by the International Diabetes Federation (IDF), more than 400 million people were reported with type 2 diabetes in 2015. If no appropriate actions are taken, this figure is predicted to rise to 629 million by 2045.

Type 2 diabetes can be controlled and managed by living a healthy lifestyle; however, due to the progressive nature of diseases, it becomes necessary to rely on antidiabetic drugs. Several antidiabetic drugs are in clinical use to tackle type 2 diabetes which include metformin, sulphonylureas, thiazolidinediones, acarbose, GLP-1 agonists, DPP-4 inhibitors, SGLT2 inhibitors and insulin. However, none of these drugs is successful in achieving long-term glycaemic control and preventing secondary complications associated with diabetes. Several studies have reported the close association of these drugs with hypoglycaemia, weight gain, inflammation of the pancreas, heart failure and hepatotoxicity (Bolen *et al.,* 2007, Kelly *et al.,* 2009, Ray *et al.,* 2009, Tahrani *et al.,* 2011). Moreover, these antidiabetics drugs are recommended in combination, which make patients more prone to the side effect associated with drugs. Also, the cost associated with treatment, which has reached USD 727 billion, is expected to rise due to increasing diabetes population. Hence required new alternative therapies that are cost-effective and can overcome the limitations of existing drugs.

7.2 Exploiting Natural antidiabetic agents

7.2.1 Antidiabetic agents from plants

Since ancient times native plants and their active ingredients have been used in Ayurvedic medicine for the treatment of wide range a of diseases including diabetes (Shakya, 2016). The main active ingredients found in the plants displaying antidiabetic activities are being used as lead molecules for the synthesis of new drugs. It is estimated that one in four currently prescribed drugs are developed from active ingredients of plants (Ye & Stanley, 2013). Antidiabetic drug metformin, developed from parent compound guanide found in the plant *Galega officinalis,* is currently in clinical use and recommended as the first line of drug for type 2 diabetes treatment (Koehn & Carter, 2003).

More than 1200 plants have been reported with antidiabetic activities, and these plants majorly belong to the family of Fabaceae, Asteraceae & Lamiaceae (Marles and Farnsworth, 1995, Trojan-Rodrigues *et al.,* 2012). Permender *et al*., 2010 presented an overview of the most effective antidiabetic activities of 54 plants of the Fabaceae family. Few examples of these plants are *Abrus precatorius*, *Acacia arabica, Acacia catechu, Albizia lebbek, Arachis hypogaea* and *Bauhinia forficate. Cinnamomum tamala* which belongs to the family of Lamiaceae demonstrated antidiabetic and antidyslipidemic effects in streptozotocin-induced diabetic rats (Bisht & Sisodia, 2011). In 2013, Sidhu and Sharma from Punjab University (India), created a database of antidiabetic plants which belong to family Asteraceae, Euphorbiaceae, Fabaceae, Lamiaceae and Moraceae. Studies conducted in the Diabetes Research Laboratory at Ulster University have also revealed the antidiabetic activity of plants which include *Medicago sativa* (Gray & Flatt 1997), *Agrimony eupatoria* (Gray & Flatt 1998), *Agaricus bisporus* (Swanston-Flatt *et al.,* 1989), *Coriandrum sativum* (Gray & Flatt

1999), *Sambucus nigra* **(**Gray *et al.,* 2000) and *Terminalis berllirica* (Kasabri *et al.,* 2010)

7.2.2 Antidiabetic agents from animals' source

Many animals' species have developed specialised organs during evolution that produces venom to protect from predator and to capture prey (Casewell *et al.,* 2013). These animal venoms are rich in biologically active molecules such as peptides and proteins. In the past, whole animal venom was used in Chinese traditional and Indian Ayurvedic medicine for the treatment of wide range of diseases which include arthritis, asthma, cancer, gastrointestinal alignment and rheumatism and pain (Ried, 2007, King, 2011). The advancement in bioanalytical technologies and progress in the area of genomics and transcriptomics have accelerated the development of the drugs from the animal venom. The presence of disulphide bonds in most of the venom-derived peptides provide stability and resistance to proteolytic enzyme thus making them unique biomolecules for the development of therapeutic agents. Several of these venoms derived peptides produce a response by binding with a receptor present on the mammalian cell surface.

Both peptides and proteins found in the venom of animals such as snakes, scorpions, spiders, jellyfishes, anemones and cone snails are the most well-known and studied biomolecules. The majority of these molecules either act directly on the cardiovascular or nervous system of the prey and predators (Utkin *et al.,* 2015). Captopril, an angiotensin-converting enzyme (ACE) inhibitor, isolated from Brazilian viper *Bothrops jararaca,* is the first venom-derived drug approved by FDA for treatment of cardiovascular diseases (Ferreira *et al.,* 1970). Eptifibatide and tirofiban from Pygmy rattlesnake and Saw-scaled viper respectively are available for the treatment of acute

coronary syndromes. Exendin-4, a GLP-1 analogue, is the first venom bioactive molecule, approved for the metabolic treatment (Eng *et al.,* 1990). Exendin-4, isolated from the venom of Gila monster *Heloderma suspectum*, is available in the market by name Byetta from the treatment of type 2 diabetes. (Eng *et al.,* 1992).

Exendin-4 is 39 amino acid peptide which shares 53% structural homology with native GLP-1 (Furman, 2012). In comparison to native GLP-1, exendin-4 displayed longer *in vivo* half-life of around 160 min (20-30 fold higher) and potent (5500-fold greater) glucose lowering effects (Parkes *et al.,* 2001; Young *et al.,* 1999). After the discovery of exendin-4, several other venom peptides have been identified with potent glucose-lowering effects. Recently, new GLP-1 peptide analogues were identified in the venom and intestine of platypus and echidna, which were resistant to DPP-4 degradation and displayed potent insulinotropic activities in cultured rodent islets (Tsend-Ayush *et al.,* 2016). Safavi-Hemamiet *al.,* 2015, found insulin analogue peptide in the venom of con snail (*Conus geographus*). Cone snail captures its prey by inducing hypoglycemic shock. *C. geographus* insulin (Con-Ins G1) was found similar to fish insulin and has shown to activate insulin signalling pathway by binding to the insulin receptor (Menting *et al.,* 2016). Unlike human insulin, Con-Ins G1 lacks the region of B chain responsible for dimerisation. This makes Con-Ins G1 as an ideal candidate for the development of fast-acting insulin formulation for the treatment of diabetes.

Delayed rectifier KV channels and BK channels are important for repolarisation of beta cells following insulin secretion (Smith *et al.,*1990). Peptide hanatoxin (k-theraphotoxin-Gr1a), found in the venom of the tarantula *Grammostola rosea,* has been shown to stimulate insulin release from mouse and human beta cells in a glucose-dependent manner by blocking delayed rectifier KV2.1 channel (Swartz &

MacKinnon, 1995). Guangxitoxin-1, another KV2.1 channel blocker, isolated from Chinese earth tiger tarantula, also demonstrated insulin release in a glucose-dependent manner by increasing intracellular calcium concentrations (Herrington *et al.,* 2006). Iberiotoxin (bTx), found in the venom of red scorpion *Buthus tamulus,* enhanced insulin secretion in human beta cells by blocking BK channels (Galvez *et al.,* 1990, Braun *et al.,* 2008).

Several studies have reported the presence of insulinotropic bioactive compounds in the snake venom (Toyama *et al.,* 2000, 2005, Nogueira *et al.,* 2005, Hernandez *et al.,* 2008, Nguyen *et al.,* 2012). The venom of *Crotalus adamanteus, Crotalus vegrandis, Bitisnas icornis, Pseudechis australis* and *Pseudechis butleri* snakes were studied in our laboratory for insulin-releasing activity in BRIN-BD11 cells. In this study, insulinotropic compounds which belong to the family of phospholipases A2 (PLA2), serine proteinases and disintegrins were identified in snake venom (Moore *et al.,* 2015a, Moore *et al.,* 2015). The discovery of drugs with therapeutic utility in the venoms of the snake, lizards, scorpion, cone snail and other animals has created curiosity to investigate amphibian skin secretions for antidiabetic peptides.

7.3 Insulinotropic, glucose-lowering, and beta-cell anti-apoptotic actions of temporin and Esculentin-1 peptides

Temporin and esculentin-1 peptides were identified in frogs belonging to the extensive family Ranidae of both Eurasian and N. American (Conlon *et al.,* 2009, Xu & Lai, 2015). Temporins were obtained from *Rana temporaria*, and esculentin-1 from *Rana esculenta* [(*Pelophylax lessonae* (Pool frog) x *Pelophylax ridibundus* (marsh frog)]. These peptides are well known for their antimicrobial activity (Ponti *et al.,* 1999, Mangoni *et al.,* 2016). Chapter 3, reports antidiabetic effects of these peptides.

Acute *in vitro* insulin release studies revealed that Temporin A, B and G exhibited potent insulin release studies in BRIN-BD11 cells with no cytotoxic effects. Esculentin-1a (1-21).NH_2, esculentin-1b (1-18).NH_2 and esculentin-1a (1-14).NH_2 which are N terminal derived peptides of esculentin-1a and -1b also exhibited similar effects. In addition, analogue [D-Lys^{14}, D-Ser^{17}] esculentin-1a (1-21).NH_2 (Esc(1-21)-1c) also produced insulinotropic activity. The insulin inducing ability of these peptides were also replicated in human clonal β-cells and isolated mouse islets. The study also revealed that that cationicity, hydrophobicity and angle subtended by charged residue are an important factor for the insulin-releasing activity of temporin peptides, whereas helicity plays a key role in the insulinotropic activity of the esculentin-1 peptide.

Esculentin-1 peptides produced a significant increase in membrane potential and intracellular calcium concentration in BRIN-BD11 cells. On the other hand, temporins peptide had no significant effects on these parameters. This preliminary observation suggests that esculentin-1a could exhibit its effects by the K_{ATP} channel-dependent pathway and temporin peptides by the K_{ATP} channel-independent pathway.

In T2DM, insulin concentration declines with age due to loss of beta cell mass and function (Cantley & Ashcroft, 2015, Arden, 2018). Therefore, treatment strategies towards restoring beta cell mass and beta cell function would be beneficial in tackling T2DM. Temporin A, temporin F, esculentin-1a (1-21) NH_2 and esculentin (1-21)-1c but not temporin G (1 μM) protected BRIN-BD11 cells against cytokine-induced apoptosis as well as the augmented proliferation of cells. On the other hand, esculentin-1b (1-18).NH_2 and esculentin-1a (1-14).NH_2 also showed a tendency to protect beta cells against cytokine-induced apoptosis and enhanced proliferation of the cells. Further acute *in vivo* studies revealed that temporin G and esculentin (1-21)-1c improved glycemic response in lean mice after intraperitoneal injection with glucose.

On the other hand, temporin A, temporin F, esculentin-1a (1-21).NH_2, esculentin-1b (1-18).NH_2 and esculentin-1a (1-14) failed to improve glucose tolerance (See Table 7.1 and 7.2: For the summary of acute *in vitro* and *in vivo* studies of temporin and esculentin-1a peptides).

In conclusion, Chapter 3 highlighted the insulin-releasing activity of temporin and esculentin-1 peptides and analogue esculentin (1-21)-1c. Also, the study revealed positive effects of these peptides on beta cell proliferation and protection against cytokines induced DNA damage. These peptides can be used as a templet to develop long-acting analogues with improved antidiabetic activities.

7.4 Insulinotropic activities of frenatin 2D and its synthetic analogues

Amphibian skin peptides have been reported with a wide range of biological activities (Conlon *et al.,* 2014, Xu & Lai *et al.,* 2015). This include antimicrobial, antifungal, antiviral, anticancer and immunomodulatory activities. Interestingly, some of these peptides have shown to evoke insulin release from BRIN-BD11 cells and primary islet cells and improve glycaemic response both in lean and high fat fed mice following intraperitoneal administration (Conlon *et al.,* 2018). The norepinephrine-stimulated skin secretions of *Discoglossus sardus* and *Sphaenorhynchus lacteus* were reported with a high concentration of peptides that showed structural similarity to frenatin 2 peptides found in the Australian frog *Litoria infrafrenata*. Hence these peptides were named as frenatins. Frenatin 2D from *Discoglossus sardus* was the most potent of four naturally occurring frenatin peptides tested for insulin-releasing activity in BRIN-BD11 cells. Frenatin 2D, evoked dose-dependent insulin release from rat clonal beta cells without producing cytotoxic effects. In this study, 14 analogues of frenatin 2D were designed by replacing each amino acid by hydrophobic tryptophan (W) residue.

This strategy did not lead to design analogues with potent insulinotropic activity. However, the insulinotropic action of frenatin 2D was unaffected by substitution at Asp^1 and Gly^7. Interestingly, the activity of peptide was retained after deletion of the C-terminal α-amide group. Furthermore, the insulinotropic activity of [D1W] and [G7W] was replicated in human-derived pancreatic beta cells (1.1B4 cells) and isolated mouse islet cells.

Frenatin 2D peptides did not produce any significant change in membrane potential and intracellular calcium. In agreement with this, the insulin-releasing ability of peptides was not completely diminished in the presence of verapamil, diazoxide and DIDS as well as in the absence of extracellular calcium. The similar observation was reported with pseudin-2 and hymenochirin 1B (Abdel-Wahab *et al.*, 2008, Owolabi *et al.*,2016). However, frenatin 2D peptides produced a significant increase in cAMP. In line with this, the stimulatory effects of frenatin 2D peptides were abolished in PKA-downregulated BRIN-BD11. These data indicate that frenatin 2D peptides may exhibit its action by the K_{ATP} channel-independent pathway. The role of GLP-1 in beta cell survival and proliferation is well documented (Cornu *et al.*, 2009, Lee *et al.*, 2014). Interestingly, frenatin 2D protected beta cells against cytokine-induced apoptosis as well as improved proliferation of BRIN-BD11 cells. Furthermore, acute *in vivo* glucose tolerance studies revealed that [D1W] Frenatin 2D was effective than other frenatin 2D peptides (See Table 7.3: For the summary of acute *in vitro* studies, and Table 7.4: For the summary of acute *in vivo* studies).

Based on these results, we further investigated the long-term metabolic effects of [D1W] and parent peptide frenatin 2D in diabetic mice (*db/db* mice). In all treatment groups, blood glucose concentration was significantly decreased. This was associated with improved blood HbA1C and glucose tolerance. Furthermore, the overexpression

of insulin signalling genes in *db/db* mice was reversed by peptide treatment which could explain the augmentation of insulin sensitivity. Antidiabetic drugs lowering body fat and energy intake would be beneficial in preventing the occurrence of type 2 diabetes. Unfortunately, frenatin 2D and [D1W] frenatin 2D had no significant effects on body fat and energy intake.

In frenatin 2D and exenatide-treated mice, the improvement in glycaemic control was associated with augmentation of plasma insulin. The genes involved in insulin secretion were markedly increased, which might explain augmentation of beta cell function, secretion and pancreatic insulin content in these mice (Li *et al.,* 2005, Bae *et al.,* 2010). On the other hand, in [D1W] frenatin 2D treated mice, these changes were not equally effective as parent peptide. Except for exenatide, no significant changes in beta and alpha cells population were observed. However, loss of large and medium-size islets was significantly prevented in all treated mice. With both frenatin 2D and [D1W] frenatin 2D treatment, no significant changes in lipid profile were observed. The biomarkers for liver and kidney function were improved significantly. Furthermore, amylase activity remained unaffected suggesting that peptide does not exert any toxic effects on the pancreas (See Table 7.5: For the summary of long-term *in vivo* studies).

In conclusion, Chapter 4 highlighted the antidiabetic effects of frenatin 2D peptides both *in vitro* and *in vivo*. The amino acids substitution in frenatin 2D did not produce analogue with greater insulinotropic potency, suggesting that the peptide is sensitive to any change in its primary structure.

7.5 Antidiabetic effects of a structurally modified analogue of peptide glycine leucine amide-AM1 (PGLa-AM1)

PGLa-AM is a 22 amino acids peptide, which was initially isolated from *Xenopus amieti* based on antimicrobial activity, interestingly have also shown to induce insulin release from BRIN-BD11 cells (Conlon *et al.,* 2010, Owolabi *et al.,* 2017). Additionally, peptide also stimulated the dose-dependent release of GLP-1 from GLUTag cell line (Ojo *et al.,* 2013). Several frog skin peptide analogues containing L lysine substitution showed substantially greater insulinotropic activity than the parent peptide (Abdel-Wahab *et al.,* 2008, Owolabi *et al.,* 2016). Its more cationic analogue, [A14K] showed greater insulin-releasing activity in BRIN-BD11 cells than the parent peptide. Interestingly, in primary islet cells, the insulinotropic activity of [A14K] was comparable to that of GLP-1 at 1µM concentration. Furthermore, a decrease in blood glucose and an increase in plasma insulin concentration was noticed in both lean and high fat fed mice when injected together with glucose (Owolabi *et al.,* 2017). Based on these promising findings, [A14K] analogue was chosen to investigate its long-term metabolic effects.

In agreement, [A14K] analogue exhibited greater insulinotropic activity in glucose-responsive rat clonal pancreatic beta-cell line with no cytotoxic effects. The insulin-releasing activity of analogue was also replicated in the human-derived pancreatic beta cell line (1.1B4 cells), at 5.6 and 16.7 mM glucose concentration. This suggests that analogue not only exhibit insulinotropic activity at physiological glucose level but also retain its activity at a higher glucose level. Moreover, analogue was equally effective as GLP-1, in protecting BRIN-BD11 cells against cytokine-induced apoptosis. An increase in beta cell proliferation was also observed. Further studies of the expression of protein kinase B (PKB), which plays a key role in beta-cell growth and survival, will help to delineate the mechanism by which the analogue produced protective and proliferative effects (Li *et al.,* 2005).

Based on these results, a long-term (28 days) study was conducted in *db/db* mice to investigate antidiabetic effects of [A14K] PGLa-AM1 in comparison with its parent peptide PGLa-AM1 and FDA approved antidiabetic agent exenatide. In *db/db* mice, a gradual decline in plasma insulin was significantly delayed by [A14K] PGLa-AM1 and exenatide treatments. This was associated with improved expression of insulin secretory genes in these mice. For example, a *Pdx-1* gene which is an important transcription factor for insulin gene was increased in these mice (Kimura *et al.*, 2014). The expression of GLUT2 and glucokinase genes were also elevated, which could explain the increase in pancreatic insulin content and the augmentation of glucose-stimulated insulin secretion in these mice (Li *et al.*, 2005, Bae *et al.*, 2010). On the other hand, PGLa-AM1 had little beneficial effects on plasma insulin and insulin content, but not significant.

In *db/db* mice, an increase in blood glucose was countered by [A14K] PGLa-AM1 and exenatide treatment. This was corroborated with improved HbA1c in these mice. In the hyperglycemic state, expression of the GLP-1 receptor was significantly downregulated in beta cells (Kaneto and Matsuoka, 2013). Upregulation of this gene could also explain improved blood glucose in [A14K] PGLa-AM1 and exenatide-treated mice. PGLa-AM1 also showed a tendency to improve blood glucose and HbA1c, but no statistical significance was observed. Glycaemic response to oral and intraperitoneal glucose challenge was significantly improved by treatment with [A14K] PGLa-AM1 and exenatide. Irrespective of any change in body weight, insulin sensitivity was significantly improved by [A14K] PGLa-AM1 and exenatide. This was corroborated with lower HOMA-IR index and improved insulin signalling genes in skeletal muscle of these mice.

The risk of cardiovascular diseases in type 2 diabetes patient can be reduced by improving lipid metabolism (Chehade *et al.*, 2013). Elevated triglycerides and LDL in *db/db* mice were reversed by treatment with [A14K] PGLa-AM1 and exenatide. Interestingly, cholesterol level in *db/db* mice was decreased only by [A14K] PGLa-AM1 treatment. Liver and kidney functions were significantly improved by all peptide treatments. However, the increase in amylase activity was observed in all treated mice. Except for islet size distribution, no significant changes in islet morphology were observed in both PGLa-AM1 and [A14K] PGLa-AM1 treated mice. The large and medium islets were increased in these mice. As expected, islet morphology was significantly improved by treatment with exenatide (See Table 7.6: For the summary of long-term *in vivo* studies). In transgenic mice (GluCre-ROSA26EYFP mice), the number of Ins^{+}/GFP^{+} and Ins^{+}/Glu^{+} cells were increased by [A14K] PGLa-AM1 treatment. In line with this, the increase in the beta cell area and, large and medium-size islet were observed, indicating that [A14K] PGLa-AM1 could have an important role in transdifferentiation of alpha to beta cells.

In conclusion, Chapter 5 reported the beneficial effects of [A14K] PGLa-AM1 on plasma insulin, blood HbA1c, glucose tolerance, lipid profile and insulin resistance. *In vivo* studies in transgenic mice showed that [A14K] PGLa-AM1 has an important role in the generation of new beta cells from glucagon-producing alpha cells. These results are encouraging to further develop frog skin peptide analogues for the treatment of T2DM.

7.6 Therapeutic potential of [Lys4] substituted analogue of CPF-AM1

Several frog skin host defence peptide with insulin releasing activity were transformed to analogues showing superior antidiabetic activity both *in vitro* and *in vivo* (Ojo *et*

al., 2013, Srinivasan *et al.*, 2015, Owolabi *et al.*, 2015, Vasu *et al.*, 2017). CPF-AM1 peptide found in the skin secretion of frog *Xenopus amieti* demonstrated concentration-dependent insulinotropic activity in rat clonal pancreatic beta cells (BRIN-BD11 cells). Additionally, peptide also showed to induce GLP-1 release from GLUTag cell line. Its more cationic [S4K] analogue, developed by substitution of L lysine at position 4, displayed potent insulinotropic activity than the parent peptide. Furthermore, analogue also showed the ability to decrease blood glucose and improve plasma insulin concentration in lean and high fat fed mice when injected together with glucose.

In agreement, [S4K] analogue displayed potent insulin-releasing activity in BRIN-BD11 cells. Its insulinotropic activity was also replicated in human-derived pancreatic beta cells (1.1B4 cells). Interestingly, [S4K] analogue when co-incubated with cytokine mixture, the number of tunnel positive cells were decreased significantly. Additionally, analogue improved beta-cell proliferative activity similar to that of glucagon-like peptide-1 (GLP-1). Based on these results and previous studies, [S4K] analogue was selected for long-term studies in *db/db* and GluCre-ROSA26EYFP mice.

In T2DM, with the time, plasma insulin level decline due to beta cell loss (Buttler *et al.*, 2003). Therefore, antidiabetic agent preventing beta cell loss would be beneficial. [S4K] CPF-AM1analogue and exenatide significantly delayed a gradual decline of plasma insulin levels in *db/db* mice. These findings correlated with improved pancreatic insulin content by [S4K] CPF-AM1 and exenatide treatment. CPF-AM1 also showed a tendency to delay a gradual decline of plasma insulin levels, but no statistical significance was observed compared to *db/db* controls.

The onset of secondary complications in type 2 diabetes can be prevented by maintaining strict glycaemic control (UK Prospective Diabetes Study (UKPDS) Group, 1998). In all treated groups, blood glucose was significantly decreased. In both [S4K] CPF-AM1 and CPF-AM1 treated mice, a decrease in blood glucose was not associated with any significant change in either body weight or energy intake. Whereas in the exenatide-treated group, energy intake was reduced significantly. Blood HbA1c, which reflects average blood glucose levels up to a 3-month period, was lowered by [S4K] CPF-AM1 and exenatide treatment. CPF-AM1 also lowered blood HbA1c but not statistically significant compared to *db/db* controls. Treatment with [S4K] CPF-AM1 and exenatide, significantly improved glycaemic response to intraperitoneal glucose challenge. This was associated with an improvement in insulin sensitivity in these mice. In agreement with this, elevated expression of insulin singling genes in *db/db* mice was reversed by [S4K] CPF-AM1 and exenatide treatment. On the other hand, in CPF-AM1 treatment, no significant changes in glucose tolerance and insulin sensitivity were observed.

In *db/db* mice elevated triglycerides and LDL levels were decreased by [S4K] CPF-AM1, but not significantly. Interestingly, the triglyceride level was significantly decreased by CPF-AM1, suggesting that peptide could also play an essential role in the prevention of cardiovascular diseases. Elevated liver and kidney biomarkers in *db/db* mice, were reversed in all treated groups indicating that peptides are safe for the treatment. In all peptide treated groups, increase in amylase activity was observed, suggesting a potential issue with pancreatitis.

Islets from [S4K] CPF-AM1 treated mice showed improved insulin secretory response. These observations correlate with enhanced expression of insulin secretory genes. The expression of *Glp1r, Gipr, Pdx1* and other secretory genes were

significantly upregulated. CPF-AM1 also showed a tendency to improve insulin secretory responses and expression of genes. No significant change was noticed in the islet area, beta-cell area and alpha cell area in both CPF-AM1 and [S4K] CPF-AM1 treated groups. However, the loss of large and medium-size islet was prevented. As expected, insulin secretory responses, beta cell function and islet morphology were significantly improved by exenatide (See Table 7.7: For the summary of long-term *in vivo* studies). Furthermore, immunohistochemical analysis of pancreata from transgenic mice (GluCre-ROSA26EYFP mice) treated with [S4K] CPF-AM1 showed increase in Ins^+/GFP^+, Ins^+/Glu^+ and GFP^+ cells. This result correlated with increased beta cell population, indicating that peptide could influence the conversion of alpha to beta cells.

In conclusion, Chapter 6 reported that more cationic L -lysine substituted analogue of CPF-AM1 demonstrated potent antidiabetic activity than the parent peptide and could have an essential role in transdifferentiation of alpha to beta cells. These observations encourage further studies to find the specific receptor through which [S4K] CPF-AM1 exerts its beneficial metabolic effects.

7.7 Future studies

This thesis demonstrated *in vitro* and *in vivo* antidiabetic potency of frog skin peptides and their synthetic analogue belonging to the family of *Alytidae, Hylidae, Pipidae* and *Ranidae*. Both, [A14K] PGLa-AM1 and [S4K] CPF-AM1 analogue exhibited positive effects on blood glucose and plasma insulin concentration in *db/db* mice. Also, the genes involved in insulin secretions and insulin signalling were significantly improved by the treatment. Positive effects of these peptide was also observed in transdifferentiation of glucagon producing alpha to insulin producing beta cells in

streptozotocin induced diabetic mice. Interestingly, [A14K] PGLa-AM1, significantly lowered cholesterol level in *db/db* mice. These promising data, will hopefully leds to further development these peptides into therapeutic agents. [D1W] frenatin 2D relatively showed weak antidiabetic activity in *db/db* mice compared to parent peptide. Further structure-activity relationship studies of frenatin 2D, as well as of temporin and esculentin-1 peptides are required to develop analogues with improved metabolic stability and insulinotropic activities.

However, further studies are necessary to understand the precise mechanism of biological actions of these peptides. Understanding structural changes of these peptides upon interaction with membranes will help to improve the biological activities. The membrane interaction studies would be beneficial to identify the receptor through which peptides exert insulin-releasing activity followed by *in vivo* studies in receptor knockout mice. Studying the effects of the peptide on GLP-1 release *in vivo* would be interesting. Investigation the expression of signalling protein [e.g. phospho-protein kinase B (PKB/AKT)] and transcription factor [phospho-Forkhead box protein O1 (FOXO1) and pancreas duodenum homeobox-1 (PDX-1)] would help to delineate the mechanism through which peptide induce proliferation and protect the beta cell from cytokine-induced DNA damage. Additional studies to investigate the expression of insulin signalling genes in liver and adipose tissue would provide a better understanding of the biological action of these peptides. Esculentin-1 peptides stimulated insulin release by K_{ATP} channel-dependent pathway. Further performing patch-clamp experiments will help to better understand the electrophysiological effects of the peptide on K_{ATP} and L-type calcium channels in beta cells. To examine the molecular mechanism through which peptide influence reprogramming of glucagon-expressing alpha to insulin-expressing beta cells. It would

be interesting to further investigate the effects of the peptide on the generation of new beta cells from non-beta cells using transgenic InsCre-ROSA26EYFP mice. The data in the present thesis and studies outlined above can form a strong base to develop frog skin peptides into antidiabetic agents.

Table 7.1 Summary of *in vitro* and acute *in vivo* results of temporin peptides

Peptides	Insulin release from BRIN-BD11 cells		Insulin release from 1.1 B4 cells		Insulin release from islet at 1 µM (% of total insulin content)	LHD assay	Intracellular calcium	Membrane potential	Effects on apoptosis in BRIN-BD11		Effects on proliferation in BRIN-BD11	Acute effects of peptides on glucose tolerance *in vivo*	
	% of basal insulin release at 3 µM	Threshold concentration (nM)	% of basal insulin release at 3 µM	Threshold concentration (nM)					Without cytokine	With cytokine		Plasma Glucose	Plasma Insulin
Temporin A	262.6 ± 27.81	10^{-9}	190.4 ± 10.98	10^{-9}	10.60 ± 0.43	NS	NS	NS	NS	↓	↑	NS	NS
Temporin B	170.2 ± 10.16	10^{-9}	NT	NT	NT	NS	NT	NT	NT	NT	NT	NT	NT
Temporin C	135.2 ± 7.284	10^{-7}	NT	NT	NT	NS	NT	NT	NT	NT	NT	NT	NT
Temporin E	135.0 ± 4.173	10^{-7}	NT	NT	NT	NS	NT	NT	NT	NT	NT	NT	NT
Temporin F	251.9 ± 28.37	10^{-9}	176.1 ± 10.72	10^{-9}	12.64 ± 1.612	NS	NS	NS	NS	↓	↑	NS	NS
Temporin G	235.8 ± 24.44	10^{-9}	219.1 ± 14.41	10^{-9}	12.24 ± 1.067	NS	NS	NS	↑	↑	NS	↓	↑
Temporin H	NS	NA	NT	NA	NT	NT	NT	NT	NT	NT	NT	NT	NT
Temporin K	NS	NA	NT	NA	NT	NT	NT	NT	NT	NT	NT	NT	NT

NA: Not applicable, NS: No Significant, NT: Not tested, (↑) increase significantly, (↓) decrease significantly

Table 7.2 Summary of *in vitro* and acute *in vivo* results of esculentin-1 peptides

Peptides	Insulin release from BRIN-BD11 cells		Insulin release from 1.1 B4 cells		Insulin release from islet at 1 µM (% of total insulin content)	LDH assay	Memb-rane potential	Intracel-lular calcium	Effects on apoptosis in BRIN-BD11		Effects on proliferation BRIN-BD11	Acute effects of peptides on glucose tolerance *in vivo*	
	% of basal insulin release at 3 µM	Thres-hold concent-ration (nM)	% of basal insulin release at 3 µM	Threshold concent-ration (nM)					Without cytokine	With cytokine		Plasma Glucose	Plasma Insulin
Esculentin -1a (1-21)	196.0 ± 4.24	10^{-9}	224.2 ± 15.21	10^{-10}	12.76 ± 0.52	NS	↑	↑	NS	↓	↑	NS	NS
Esculentin - (1-21)-1C	189.7 ± 15.25	10^{-8}	175.2 ± 10.86	10^{-0}	13.79 ± 1.025	NS	NS	NS	NS	↓	↑	↓	↑
Esculentin -1a(1-14)	206.5 ± 2.380	10^{-9}	180.2 ± 23.02	10^{-10}	13.68 ± 0.63	NS	↑	↑	NS	↓	NS	NS	NS
Esculentin -1a(9-21)	NS	NA	NT	NA	NT	NS	NT	NT	NT	NT	NT	NT	NT
Esculentin -1b(1-18)	218.0 ± 6.419	10^{-9}	176.2 ± 11.14	10^{-9}	13.51 ± 0.97	NS	↑	↑	NS	↓	NS	NS	NS

NA: Not applicable, NS: No Significant, NT: Not tested, (↑) increase significantly, (↓) decrease significantly

Table 7.3 Acute *invitro* studies of frenatin 2D, [D1W] frenatin 2D & [G7W] frenatin 2D

Tests		Peptides		
		Frenatin 2D	**[D1W] frenatin 2D**	**[G7W] frenatin 2D**
Insulin release from BRIN-BD11 cells	%Basal insulin release at 3µM concentration	227.3 ± 24.54	258.5 ± 24.95	254.2 ± 12.45
	Threshold concentration (nM)	0.01	0.01	0.01
Insulin release from 1.1B4 cells	% Basal insulin release at 3µM concentration	215.7 ± 17.68	200.9 ± 12.04	164.6 ± 11.85
	Threshold concentration (nM)	0.1	0.1	1
Insulin release from islet at 1 µM (% of total insulin content)		13.01 ± 0.52	15.62 ± 1.90	15.20 ± 1.13
LDH assay		NS	NS	NS
Membrane potential		NS	NS	NS
Intracellular calcium		NS	NS	NS
Insulin release in presence of modulators	Verapamil	↑	↑	↑
	Diazoxide	↑	↑	↑
	IBMX	NS	NS	NS
	KCl	↑	↑	↑
Insulin release in the absence extracellular calcium		↑	↑	↑
Insulin release in presence of chloride channel blocker DIDS		↑	NT	NT
cAMP production		↑	↑	↑
Insulin release in PKA and PKC downregulated cells	PKA downregulated	↑	↑	↑
	PKC downregulated	NS	NS	NS
	PKA & PKC downregulated	NS	NS	NS
Effects on apoptosis in BRIN-BD11	Without cytokine	NS	NS	NS
	With cytokine	↓	↓	↓
Effects on Proliferation in BRIN-BD11		↑	↑	↑
Glucose uptake in C2C12 cells	Without insulin	NS	NS	NS
	With insulin	NS	NS	NS

NS: No Significant, NT: Not tested, (↑) increased significantly, (↓) decreased significantly

Table 7.4 Acute *in vivo* studies of frenatin 2D [D1W] frenatin 2D & [G7W] frenatin 2D

Acute *in vivo* studies			**Peptides**		
			Frenatin 2D	**[D1W] frenatin 2D**	**[G7W] frenatin 2D**
Acute effect of peptide (75 nmol/kg/bw) on food intake			**NS**	**NS**	↓
Acute effect of peptide (75 nmol/kg/bw) on glucose tolerance		Glucose	↓	↓	↓
		Insulin	↑	↑	↑
Persistent effect of peptide on glucose tolerance	2 hr	Glucose	↓	↓	NS
	4 hr	Glucose	NS	↓	NT
Acute effect of different dose of peptide on glucose tolerance	150 nmol/kg/bw	Glucose	↓	↓	↓
	50 nmol/kg/bw	Glucose	NS	↓	NT
	25 nmol/kg/bw	Glucose	NT	NS	NT

NS: No Significant, NT: Not tested, (↑) increased significantly, (↓) decreased significantly

Table 7.5 Metabolic effects of 28 days administration of frenatin 2D and [D1W] frenatin 2D in *db/db* mice

Parameters		Peptides		
		Frenatin 2D	**[D1W] frenatin 2D**	**Exenatide**
Non-fasting glucose		↓	↓	↓
Non-fasting insulin		↑	**NS**	↑
Body weight		**NS**	**NS**	**NS**
Energy Intake		**NS**	**NS**	↓
Water Intake		**NS**	**NS**	↓
IPGTT	Blood Glucose	↓	↓	↓
	Plasma Insulin	↑	↑	↑
OGTT	Blood Glucose	**NS**	**NS**	↓
	Plasma Insulin	**NS**	**NS**	↑
Insulin sensitivity		↑	↑	↑
Blood HBA1c		↓	↓	↓
Lipid profile	Cholesterol	**NS**	**NS**	**NS**
	Triglycerides	**NS**	**NS**	↓
	HDL	**NS**	**NS**	**NS**
	LDL	**NS**	**NS**	↓
Liver and kidney function	AST	↓	↓	↓
	ALT	↓	↓	↓
	ALP	↓	↓	↓
	Creatinine	↓	↓	↓
Amylase activity		**NS**	**NS**	↑
Islet morphology	Islet area	**NS**	**NS**	↑
	Beta Cell area	**NS**	**NS**	↑
	Alpha cell area	**NS**	**NS**	↓

NS: No Significant, NT: Not tested, (↑) increased significantly, (↓) decreased significantly

Table 7.6 Metabolic effects of 28 days administration of PGLa-AM1 and [A14K] PGLa-AM1 in *db/db* mice

Parameters		Peptides		
		PGLa-AM1	**[A14K] PGLa-AM1**	**Exenatide**
Non-fasting glucose		**NS**	↓	↓
Non-fasting insulin		**NS**	↑	↑
Body weight		**NS**	**NS**	**NS**
Energy Intake		**NS**	**NS**	↓
Water Intake		**NS**	**NS**	↓
IPGTT	Blood Glucose	**NS**	↓	↓
	Plasma Insulin	**NS**	↑	↑
OGTT	Blood Glucose	**NS**	↓	↓
	Plasma Insulin	**NS**	↑	↑
Insulin sensitivity		**NS**	↑	↑
Blood HBA1c		**NS**	↓	↓
Lipid profile	Cholesterol	**NS**	↓	**NS**
	Triglycerides	**NS**	↓	↓
	HDL	**NS**	**NS**	**NS**
	LDL	**NS**	↓	↓
Liver and kidney function	AST	↓	↓	↓
	ALT	↓	↓	↓
	ALP	**NS**	↓	↓
	Creatinine	↓	↓	↓
Amylase activity		↑	↑	↑
Islet morphology	Islet area	**NS**	**NS**	↑
	Beta Cell area	**NS**	**NS**	↑
	Alpha cell area	**NS**	**NS**	↓

NS: No Significant, NT: Not tested, (↑) increased significantly, (↓) decreased significantly

Table 7.7 Metabolic effects of 28 days administration of CPF-AM1 and [S4K] CPF-AM1 in *db/db* mice

Parameters		Peptides		
		CPF-AM1	**[S4K] CPF-AM1**	**Exenatide**
Non-fasting glucose		↓	↓	↓
Non-fasting insulin		**NS**	↑	↑
Body weight		**NS**	**NS**	**NS**
Energy Intake		**NS**	**NS**	↓
Water Intake		**NS**	**NS**	↓
IPGTT	Blood Glucose	**NS**	↓	↓
	Plasma Insulin	**NS**	↑	↑
OGTT	Blood Glucose	**NS**	**NS**	↓
	Plasma Insulin	**NS**	**NS**	↑
Insulin sensitivity		↑	↑	↑
Blood HBA1c		**NS**	↓	↓
Lipid profile	Cholesterol	**NS**	**NS**	**NS**
	Triglycerides	↓	**NS**	↓
	HDL	**NS**	**NS**	**NS**
	LDL	**NS**	**NS**	↓
Liver and kidney function	AST	↓	↓	↓
	ALT	↓	↓	↓
	ALP	↓	↓	↓
	Creatinine	↓	↓	↓
Amylase activity		↑	↑	↑
Islet morphology	Islet area	**NS**	**NS**	↑
	Beta Cell area	**NS**	**NS**	↑
	Alpha cell area	**NS**	**NS**	↓

NS: No Significant, NT: Not tested, (↑) increased significantly, (↓) decreased significantly

Chapter 8

References

Abdeen, G. and Le Roux, C. (2016) Mechanism underlying the weight loss and complications of Roux-en-Y gastric bypass. Review. *Obesity Surgery,* 26(2), 410-421

Abdel-Wahab, Y.H., Marenah, L., Flatt, P.R. and Conlon, J.M. (2007) Insulin releasing properties of the temporin family of antimicrobial peptides. *Protein and Peptide Letters,* 14(7), 702-707.

Abdel-Wahab, Y.H., Marenah, L., Orr, D.F., Shaw, C. and Flatt, P.R. (2005) Isolation and structural characterisation of a novel 13-amino acid insulin-releasing peptide from the skin secretion of *Agalychnis calcarifer*. *Biological Chemistry,* 386(6), 581-587.

Abdel-Wahab, Y.H., Power, G.J., Ng, M.T., Flatt, P.R. and Conlon, J.M. (2008a) Insulin-releasing properties of the frog skin peptide pseudin-2 and its [Lys18]-substituted analogue. *Biological Chemistry,* 389(2), 143-148.

Abdel-Wahab, Y.H., Power, G.J., Flatt, P.R., Woodhams, D.C., Rollins-Smith, L.A. and Conlon, J.M. (2008b) A peptide of the phylloseptin family from the skin of the frog *Hylomantis lemur* (Phyllomedusinae) with potent *in vitro* and *in vivo* insulin-releasing activity. *Peptides,* 29(12), 2136-2143.

Abdel-Wahab, Y., Patterson, S., Flatt, P. and Conlon, J.M. (2010) Brevinin-2-related peptide and its [D4K] analogue stimulate insulin release *in vitro* and improve glucose tolerance in mice fed a high fat diet. *Hormone and Metabolic Research,* 42(09), 652-656.

Adriaenssens, A.E., Svendsen, B., Lam, B.Y., Yeo, G.S., Holst, J.J., Reimann, F. and Gribble, F.M. (2016) Transcriptomic profiling of pancreatic alpha, beta and delta cell populations identifies delta cells as a principal target for ghrelin in mouse islets. *Diabetologia,* 59(10), 2156-2165.

Ahmed, A.M. (2002) History of diabetes mellitus. *Saudi Medical Journal,* 23(4), 373-378.

Akter, R., Cao, P., Noor, H., Ridgway, Z., Tu, L., Wang, H., Wong, A.G., Zhang, X., Abedini, A. and Schmidt, A.M. (2016) Islet amyloid polypeptide: structure, function, and pathophysiology. *Journal of Diabetes Research,* 2016

American Diabetes Association. (2011) Executive summary: standards of medical care in diabetes--2011. *Diabetes Care,* 34 Suppl 1, S4-10.

Amori, R.E., Lau, J. and Pittas, A.G. (2007) Efficacy and safety of incretin therapy in type 2 diabetes: systematic review and meta-analysis. *Jama,* 298(2), 194-206.

Andrade, E. (2015) Amphibians: why preserve. *Entomol.Ornithol.Herpetol,* 5(1)

Andralojc, K., Mercalli, A., Nowak, K., Albarello, L., Calcagno, R., Luzi, L., Bonifacio, E., Doglioni, C. and Piemonti, L. (2009) Ghrelin-producing epsilon cells in the developing and adult human pancreas. *Diabetologia,* 52(3), 486-493.

Animaw, W. and Seyoum, Y. (2017) Increasing prevalence of diabetes mellitus in a developing country and its related factors. *PloS One,* 12(11), e0187670.

Arden, C. (2018) A role for glucagon-like peptide-1 in the regulation of β-cell autophagy. *Peptides,* 100, 85-93.

Aschner, P., Kipnes, M.S., Lunceford, J.K., Sanchez, M., Mickel, C., Williams-Herman, D.E. and Sitagliptin Study 021 Group. (2006) Effect of the dipeptidyl peptidase-4 inhibitor sitagliptin as monotherapy on glycemic control in patients with type 2 diabetes. *Diabetes Care,* 29(12), 2632-2637.

Atkinson, M.A. and Eisenbarth, G.S. (2001) Type 1 diabetes: new perspectives on disease pathogenesis and treatment. *The Lancet,* 358(9277), 221-229.

Atkinson, B.J., Griesel, B.A., King, C.D., Josey, M.A. and Olson, A.L. (2013) Moderate GLUT4 overexpression improves insulin sensitivity and fasting triglyceridemia in high-fat diet-fed transgenic mice. *Diabetes,* 62(7), 2249-2258.

Atlas, D. (2017) International diabetes federation. *IDF Diabetes Atlas, 8th edn: Brussels Belgium: International Diabetes Federation.*

Attoub, S., Arafat, H., Mechkarska, M. and Conlon, J.M. (2013a) Anti-tumor activities of the host-defense peptide hymenochirin-1B. *Regulatory Peptides,* 187, 51-56.

Attoub, S., Mechkarska, M., Sonnevend, A., Radosavljevic, G., Jovanovic, I., Lukic, M.L. and Conlon, J.M. (2013b) Esculentin-2CHa: a host-defense peptide with differential cytotoxicity against bacteria, erythrocytes and tumor cells. *Peptides,* 39, 95-102.

Bae, J., Kim, T., Kim, M., Park, J. and Ahn, Y. (2010) Transcriptional regulation of glucose sensors in pancreatic β-Cells and liver: an update. *Sensors,* 10(5), 5031-5053.

Balasubramanian, R., Robaye, B., Boeynaems, J. and Jacobson, K.A. (2014) Enhancement of glucose uptake in mouse skeletal muscle cells and adipocytes by P2Y6 receptor agonists. *PloS One,* 9(12), e116203.

Barlow, J., Solomon, T.P. and Affourtit, C. (2018) Pro-inflammatory cytokines attenuate glucose-stimulated insulin secretion from INS-1E insulinoma cells by restricting mitochondrial pyruvate oxidation capacity–Novel mechanistic insight from real-time analysis of oxidative phosphorylation. *PloS One,* 13(6), e0199505.

Baron, A.D. (1998) Postprandial hyperglycaemia and α-glucosidase inhibitors. *Diabetes Research and Clinical Practice,* 40, S51-S55.

Basu, S., Yoffe, P., Hills, N. and Lustig, R.H. (2013) The relationship of sugar to population-level diabetes prevalence: an econometric analysis of repeated cross-sectional data. *PloS One,* 8(2), e57873.

Belaid, A., Aouni, M., Khelifa, R., Trabelsi, A., Jemmali, M. and Hani, K. (2002) In vitro antiviral activity of dermaseptins against herpes simplex virus type 1. *Journal of Medical Virology,* 66(2), 229-234.

Belgi, A., Akhter Hossain, M., W Tregear, G. and D Wade, J. (2011) The chemical synthesis of insulin: from the past to the present. *Immunology, Endocrine & Metabolic Agents in Medicinal Chemistry (Formerly Current Medicinal Chemistry-Immunology, Endocrine and Metabolic Agents),* 11(1), 40-47.

Bergaoui, I., Zairi, A., Tangy, F., Aouni, M., Selmi, B. and Hani, K. (2013) In vitro antiviral activity of dermaseptin S4 and derivatives from amphibian skin against herpes simplex virus type 2. *Journal of Medical Virology,* 85(2), 272-281.

Berridge, M.J., Bootman, M.D. and Roderick, H.L. (2003) Calcium: calcium signalling: dynamics, homeostasis and remodelling. *Nature Reviews Molecular Cell Biology,* 4(7), 517.

Bettge, K., Kahle, M., Abd El Aziz, Mirna S, Meier, J.J. and Nauck, M.A. (2017) Occurrence of nausea, vomiting and diarrhoea reported as adverse events in clinical trials studying glucagon-like peptide-1 receptor agonists: A systematic analysis of published clinical trials. *Diabetes, Obesity and Metabolism,* 19(3), 336-347.

Bhuiyan, M.B.A., Fant, M.E. and Dasgupta, A. (2003) Study on mechanism of action of Chinese medicine Chan Su: dose-dependent biphasic production of nitric oxide in trophoblastic BeWo cells. *Clinica Chimica Acta,* 330(1-2), 179-184.

Biden, T.J., Boslem, E., Chu, K.Y. and Sue, N. (2014) Lipotoxic endoplasmic reticulum stress, β cell failure, and type 2 diabetes mellitus. *Trends in Endocrinology & Metabolism,* 25(8), 389-398.

Bisht, S. and Sisodia, S.S. (2011) Assessment of antidiabetic potential of Cinnamomum tamala leaves extract in streptozotocin induced diabetic rats. *Indian Journal of Pharmacology,* 43(5), 582-585.

Bjornholm, M., Kawano, Y., Lehtihet, M. and Zierath, J.R. (1997) Insulin receptor substrate-1 phosphorylation and phosphatidylinositol 3-kinase activity in skeletal muscle from NIDDM subjects after *in vivo* insulin stimulation. *Diabetes,* 46(3), 524-527.

Blind, E., Janssen, H., Dunder, K. and de Graeff, P.A. (2018) The European Medicines Agency's Approval of New Medicines for Type 2 Diabetes. *Diabetes, Obesity and Metabolism*

Bogan, J.S. (2012) Regulation of glucose transporter translocation in health and diabetes. *Annual Review of Biochemistry,* 81, 507-532.

Bogdanov, P., Corraliza, L., Villena, J.A., Carvalho, A.R., Garcia-Arumí, J., Ramos, D., Ruberte, J., Simó, R. and Hernández, C. (2014) The *db/db* mouse: a useful model for the study of diabetic retinal neurodegeneration. *PLOS One,* 9(5), e97302.

Bora, K., Borah, M., Chutia, H., Nath, C.K., Das, D. and Ruram, A.A. (2016) Presence of Concurrent Derangements of Liver Function Tests in Type 2 Diabetes and Their Relationship with Glycemic Status: A Retrospective Observational Study from Meghalaya. *Journal of Laboratory Physicians,* 8(1), 30-35.

Boucher-Berry, C., Parton, E.A. and Alemzadeh, R. (2016) Excess weight gain during insulin pump therapy is associated with higher basal insulin doses. *Journal of Diabetes & Metabolic Disorders,* 15(1), 47.

Bouskila, M., Hirshman, M.F., Jensen, J., Goodyear, L.J. and Sakamoto, K. (2008) Insulin promotes glycogen synthesis in the absence of GSK3 phosphorylation in skeletal muscle. *American Journal of Physiology-Endocrinology and Metabolism,* 294(1), E28-E35.

Braun, M., Ramracheya, R., Bengtsson, M., Zhang, Q., Karanauskaite, J., Partridge, C., Johnson, P.R. and Rorsman, P. (2008) Voltage-gated ion channels in human pancreatic beta-cells: electrophysiological characterization and role in insulin secretion. *Diabetes,* 57(6), 1618-1628.

Brereton, M.F., Vergari, E., Zhang, Q. and Clark, A. (2015) Alpha-, delta-and PP-cells: are they the architectural cornerstones of islet structure and co-ordination? *Journal of Histochemistry & Cytochemistry,* 63(8), 575-591.

Breyer, M.D., Bottinger, E., Brosius, F.C.,3rd, Coffman, T.M., Harris, R.C., Heilig, C.W., Sharma, K. and AMDCC. (2005) Mouse models of diabetic nephropathy. *Journal of the American Society of Nephrology: JASN,* 16(1), 27-45.

Briant, L., Salehi, A., Vergari, E., Zhang, Q. and Rorsman, P. (2016) Glucagon secretion from pancreatic α-cells. *Upsala Journal of Medical Sciences,* 121(2), 113-119.

Broglio, F., Gottero, C., Benso, A., Prodam, F., Destefanis, S., Gauna, C., Maccario, M., Deghenghi, R., van der Lely, A. and Ghigo, E. (2003) Effects of ghrelin on the insulin and glycemic responses to glucose, arginine, or free fatty acids load in humans. *The Journal of Clinical Endocrinology & Metabolism,* 88(9), 4268-4272.

Buchanan, T.A., Metzger, B.E., Freinkel, N. and Bergman, R.N. (1990) Insulin sensitivity and B-cell responsiveness to glucose during late pregnancy in lean and moderately obese women with normal glucose tolerance or mild gestational diabetes. *American Journal of Obstetrics & Gynecology,* 162(4), 1008-1014.

Bunck, M.C., Corner, A., Eliasson, B., Heine, R.J., Shaginian, R.M., Taskinen, M.R., Smith, U., Yki-Jarvinen, H. and Diamant, M. (2011) Effects of exenatide on measures of beta-cell function after 3 years in metformin-treated patients with type 2 diabetes. *Diabetes Care,* 34(9), 2041-2047.

Butler, A.E., Janson, J., Soeller, W.C. and Butler, P.C. (2003) Increased beta-cell apoptosis prevents adaptive increase in beta-cell mass in mouse model of type 2

diabetes: evidence for role of islet amyloid formation rather than direct action of amyloid. *Diabetes,* 52(9), 2304-2314.

Cantley, J. and Ashcroft, F.M. (2015) Q&A: insulin secretion and type 2 diabetes: why do β-cells fail? *BMC Biology,* 13(1), 33.

Capparelli, R., Romanelli, A., Iannaccone, M., Nocerino, N., Ripa, R., Pensato, S., Pedone, C. and Iannelli, D. (2009) Synergistic antibacterial and anti-inflammatory activity of temporin A and modified temporin B in vivo. *PLoS One,* 4(9), e7191.

Cappiello, F., Di Grazia, A., Segev-Zarko, L.A., Scali, S., Ferrera, L., Galietta, L., Pini, A., Shai, Y., Di, Y.P. and Mangoni, M.L. (2016) Esculentin-1a-Derived Peptides Promote Clearance of Pseudomonas aeruginosa Internalized in Bronchial Cells of Cystic Fibrosis Patients and Lung Cell Migration: Biochemical Properties and a Plausible Mode of Action. *Antimicrobial Agents and Chemotherapy,* 60(12), 7252-7262.

Casewell, N.R., Wüster, W., Vonk, F.J., Harrison, R.A. and Fry, B.G. (2013) Complex cocktails: the evolutionary novelty of venoms. *Trends in Ecology & Evolution,* 28(4), 219-229.

Cat, A.N.D., Callera, G.E., Friederich-Persson, M., Sanchez, A., Dulak-Lis, M.G., Tsiropoulou, S., Montezano, A.C., He, Y., Briones, A.M. and Jaisser, F. (2018) Vascular dysfunction in obese diabetic db/db mice involves the interplay between aldosterone/mineralocorticoid receptor and Rho kinase signaling. *Scientific Reports,* 8(1), 2952.

Cernea, S. and Dobreanu, M. (2013) Diabetes and beta cell function: from mechanisms to evaluation and clinical implications. *Biochemia Medica: Biochemia Medica,* 23(3), 266-280.

Chang, S., Choi, K., Jang, S. and Shin, H. (2003) Role of disulfide bonds in the structure and activity of human insulin. *Molecules & Cells (Springer Science & Business Media BV),* 16(3)

Chang, T.W. and Goldberg, A.L. (1978) The metabolic fates of amino acids and the formation of glutamine in skeletal muscle. *The Journal of Biological Chemistry,* 253(10), 3685-3693.

Chehade, J.M., Gladysz, M. and Mooradian, A.D. (2013) Dyslipidemia in type 2 diabetes: prevalence, pathophysiology, and management. *Drugs,* 73(4), 327-339.

Chen, G., Li, L., Dai, F., Li, X., Xu, X. and Fan, J. (2015) Prevalence of and risk factors for type 2 diabetes mellitus in hyperlipidemia in China. *Medical Science Monitor: International Medical Journal of Experimental and Clinical Research,* 21, 2476.

Chen, Q., Wade, D., Kurosaka, K., Wang, Z.Y., Oppenheim, J.J. and Yang, D. (2004) Temporin A and related frog antimicrobial peptides use formyl peptide receptor-like 1

as a receptor to chemoattract phagocytes. *Journal of Immunology (Baltimore, Md.: 1950)*, 173(4), 2652-2659.

Chon, S. and Gautier, J. (2016) An update on the effect of incretin-based therapies on β-cell function and mass. *Diabetes & Metabolism Journal*, 40(2), 99-114.

Chong, S., Ding, D., Byun, R., Comino, E., Bauman, A. and Jalaludin, B. (2017) Lifestyle changes after a diagnosis of type 2 diabetes. *Diabetes Spectrum*, 30(1), 43-50.

Clarke, B.T. (1997) The natural history of amphibian skin secretions, their normal functioning and potential medical applications. *Biological Reviews*, 72(3), 365-379.

Coleman, D.L. (1978) Obese and diabetes: two mutant genes causing diabetes-obesity syndromes in mice. *Diabetologia*, 14(3), 141-148.

Conlon, J.M. (2008) Reflections on a systematic nomenclature for antimicrobial peptides from the skins of frogs of the family Ranidae. *Peptides*, 29(10), 1815-1819.

Conlon, J.M., Al-Ghaferi, N., Abraham, B. and Leprince, J. (2007a) Strategies for transformation of naturally-occurring amphibian antimicrobial peptides into therapeutically valuable anti-infective agents. *Methods*, 42(4), 349-357.

Conlon, J.M., Al-Ghaferi, N., Ahmed, E., Meetani, M.A., Leprince, J. and Nielsen, P.F. (2010) Orthologs of magainin, PGLa, procaerulein-derived, and proxenopsin-derived peptides from skin secretions of the octoploid frog *Xenopus amieti* (Pipidae). *Peptides*, 31(6), 989-994.

Conlon, J.M., Kolodziejek, J. and Nowotny, N. (2009) Antimicrobial peptides from the skins of North American frogs. *Biochimica Et Biophysica Acta (BBA)-Biomembranes*, 1788(8), 1556-1563.

Conlon, J.M. and Mechkarska, M. (2014) Host-defense peptides with therapeutic potential from skin secretions of frogs from the family pipidae. *Pharmaceuticals*, 7(1), 58-77.

Conlon, J.M., Mechkarska, M., Abdel-Wahab, Y.H. and Flatt, P.R. (2018) Peptides from frog skin with potential for development into agents for Type 2 diabetes therapy. *Peptides*, 100, 275-281.

Conlon, J.M., Mechkarska, M., Arafat, K., Attoub, S. and Sonnevend, A. (2012a) Analogues of the frog skin peptide alyteserin-2a with enhanced antimicrobial activities against Gram-negative bacteria. *Journal of Peptide Science*, 18(4), 270-275.

Conlon, J.M., Mechkarska, M. and King, J.D. (2012b) Host-defense peptides in skin secretions of African clawed frogs (Xenopodinae, Pipidae). *General and Comparative Endocrinology*, 176(3), 513-518.

Conlon, J.M., Mechkarska, M., Lukic, M.L. and Flatt, P.R. (2014a) Potential therapeutic applications of multifunctional host-defense peptides from frog skin as anti-cancer, anti-viral, immunomodulatory, and anti-diabetic agents. *Peptides,* 57, 67-77.

Conlon, J.M., Mechkarska, M., Pantic, J.M., Lukic, M.L., Coquet, L., Leprince, J., Nielsen, P.F. and Rinaldi, A.C. (2013) An immunomodulatory peptide related to frenatin 2 from skin secretions of the Tyrrhenian painted frog *Discoglossus sardus* (Alytidae). *Peptides,* 40, 65-71.

Conlon, J.M., Mechkarska, M., Radosavljevic, G., Attoub, S., King, J.D., Lukic, M.L. and McClean, S. (2014b) A family of antimicrobial and immunomodulatory peptides related to the frenatins from skin secretions of the Orinoco lime frog *Sphaenorhynchus lacteus* (Hylidae). *Peptides,* 56, 132-140.

Conlon, J.M., Patterson, S. and Flatt, P.R. (2006) Major contributions of comparative endocrinology to the development and exploitation of the incretin concept. *Journal of Experimental Zoology Part A: Comparative Experimental Biology,* 305(9), 781-786.

Conlon, J.M. and Sonnevend, A. (2011) Clinical applications of amphibian antimicrobial peptides. *J.Med.Sci,* 4(2), 62-72.

Conlon, J.M., Woodhams, D.C., Raza, H., Coquet, L., Leprince, J., Jouenne, T., Vaudry, H. and Rollins-Smith, L.A. (2007b) Peptides with differential cytolytic activity from skin secretions of the lemur leaf frog *Hylomantis lemur* (Hylidae: Phyllomedusinae). *Toxicon,* 50(4), 498-506.

Cornu, M., Poussin, C., Yang, J., Widmann, C. and Thorens, B. (2008) Glucagon-like peptide-1 protects beta-cells against apoptosis by increasing the activity of an IGF-2/IGF-1 receptor autocrine loop. *Diabetes,* 58(8):1816-25.

Cruciani, R.A., Barker, J.L., Zasloff, M., Chen, H.C. and Colamonici, O. (1991) Antibiotic magainins exert cytolytic activity against transformed cell lines through channel formation. *Proceedings of the National Academy of Sciences of the United States of America,* 88(9), 3792-3796.

Cuervo, J.H., Rodriguez, B. and Houghten, R.A. (1988) The Magainins: sequence factors relevant to increased antimicrobial activity and decreased hemolytic activity. *Peptide Research,* 1(2), 81-86.

Cummings, D.E. and Cohen, R.V. (2016) Bariatric/Metabolic Surgery to Treat Type 2 Diabetes in Patients with a BMI <35 kg/m2. *Diabetes Care,* 39(6), 924-933.

Da Silva Xavier, G. (2018) The cells of the islets of langerhans. *Journal of Clinical Medicine,* 7(3), 54.

Dalbøge, L.S., Almholt, D.L., Neerup, T.S., Vassiliadis, E., Vrang, N., Pedersen, L., Fosgerau, K. and Jelsing, J. (2013) Characterisation of age-dependent beta cell dynamics in the male db/db mice. *PloS One,* 8(12), e82813.

Dandona, P., Freedman, D.B., Foo, Y., Perkins, J., Katrak, A., Mikhailidis, D.P., Rosalki, S.B. and Beckett, A.G. (1984) Exocrine pancreatic function in diabetes mellitus. *Journal of Clinical Pathology,* 37(3), 302-306.

Daneman, D. (2006) Type 1 diabetes. *The Lancet,* 367(9513), 847-858.

Das, A.K. and Shah, S. (2011) History of diabetes: from ants to analogs. *The Journal of the Association of Physicians of India,* 59 Suppl, 6-7.

Daskin, J.H. and Alford, R.A. (2012) Context-dependent symbioses and their potential roles in wildlife diseases. *Proceedings.Biological Sciences,* 279(1733), 1457-1465.

Dathe, M., Wieprecht, T., Nikolenko, H., Handel, L., Maloy, W.L., MacDonald, D.L., Beyermann, M. and Bienert, M. (1997) Hydrophobicity, hydrophobic moment and angle subtended by charged residues modulate antibacterial and haemolytic activity of amphipathic helical peptides. *FEBS Letters,* 403(2), 208-212.

Davidson, H.W. (2004) (Pro) Insulin processing. *Cell Biochemistry and Biophysics,* 40(3), 143-157.

De Meyts, P., Sajid, W., Palsgaard, J., Theede, A., Gauguin, L., Aladdin, H. and Whittaker, J. (2007) Insulin and IGF-I receptor structure and binding mechanism. *In:* Anon.*Mechanisms of Insulin Action.* Springer, 1-32.

DeFronzo, R.A. (2004) Pathogenesis of type 2 diabetes mellitus. *Medical Clinics,* 88(4), 787-835.

DeFronzo, R., Fleming, G.A., Chen, K. and Bicsak, T.A. (2016) Metformin-associated lactic acidosis: current perspectives on causes and risk. *Metabolism,* 65(2), 20-29.

DeFronzo, R.A. and Tripathy, D. (2009) Skeletal muscle insulin resistance is the primary defect in type 2 diabetes. *Diabetes Care,* 32 Suppl 2, S157-63.

Di Grazia, A., Cappiello, F., Cohen, H., Casciaro, B., Luca, V., Pini, A., Di, Y.P., Shai, Y. and Mangoni, M.L. (2015) D-Amino acids incorporation in the frog skin-derived peptide esculentin-1a (1-21) NH 2 is beneficial for its multiple functions. *Amino Acids,* 47(12), 2505-2519.

Di Grazia, A., Luca, V., Segev-Zarko, L.A., Shai, Y. and Mangoni, M.L. (2014) Temporins A and B stimulate migration of HaCaT keratinocytes and kill intracellular Staphylococcus aureus. *Antimicrobial Agents and Chemotherapy,* 58(5), 2520-2527.

Dicker, D. (2011) DPP-4 inhibitors: impact on glycemic control and cardiovascular risk factors. *Diabetes Care,* 34 Suppl 2, S276-8.

Dimitriadis, G., Mitrou, P., Lambadiari, V., Maratou, E. and Raptis, S.A. (2011) Insulin effects in muscle and adipose tissue. *Diabetes Research and Clinical Practice,* 93 Suppl 1, S52-9.

Dixon, G., Nolan, J., McClenaghan, N., Flatt, P.R. and Newsholme, P. (2003) A comparative study of amino acid consumption by rat islet cells and the clonal beta-cell line BRIN-BD11 - the functional significance of L-alanine. *The Journal of Endocrinology,* 179(3), 447-454.

Do, O.H., Low, J.T., Gaisano, H.Y. and Thorn, P. (2014) The secretory deficit in islets from db/db mice is mainly due to a loss of responding beta cells. *Diabetologia,* 57(7), 1400-1409.

Donath, M.Y., Böni-Schnetzler, M., Ellingsgaard, H. and Ehses, J.A. (2009) Islet inflammation impairs the pancreatic β-cell in type 2 diabetes. *Physiology,* 24(6), 325-331.

Drummond, M.J., Glynn, E.L., Fry, C.S., Timmerman, K.L., Volpi, E. and Rasmussen, B.B. (2010) An increase in essential amino acid availability upregulates amino acid transporter expression in human skeletal muscle. *American Journal of Physiology-Endocrinology and Metabolism,* 298(5), E1011-E1018.

Egan, A.G., Blind, E., Dunder, K., De Graeff, P.A., Hummer, B.T., Bourcier, T. and Rosebraugh, C. (2014) Pancreatic safety of incretin-based drugs—FDA and EMA assessment. *New England Journal of Medicine,* 370(9), 794-797.

Eng, J., Andrews, P.C., Kleinman, W.A., Singh, L. and Raufman, J.P. (1990) Purification and structure of exendin-3, a new pancreatic secretagogue isolated from Heloderma horridum venom. *The Journal of Biological Chemistry,* 265(33), 20259-20262.

Eng, J., Kleinman, W.A., Singh, L., Singh, G. and Raufman, J.P. (1992) Isolation and characterization of exendin-4, an exendin-3 analogue, from Heloderma suspectum venom. Further evidence for an exendin receptor on dispersed acini from guinea pig pancreas. *The Journal of Biological Chemistry,* 267(11), 7402-7405.

Erspamer, V. (1971) Biogenic amines and active polypeptides of the amphibian skin. *Annual Review of Pharmacology,* 11(1), 327-350.

Fadini, G.P., Bonora, B.M. and Avogaro, A. (2017) SGLT2 inhibitors and diabetic ketoacidosis: data from the FDA Adverse Event Reporting System. *Diabetologia,* 60(8), 1385-1389.

Fehse, F., Trautmann, M., Holst, J.J., Halseth, A.E., Nanayakkara, N., Nielsen, L.L., Fineman, M.S., Kim, D.D. and Nauck, M.A. (2005) Exenatide augments first-and second-phase insulin secretion in response to intravenous glucose in subjects with type 2 diabetes. *The Journal of Clinical Endocrinology & Metabolism,* 90(11), 5991-5997.

Feliers, D., Duraisamy, S., Faulkner, J.L., Duch, J., Lee, A.V., Abboud, H.E., Choudhury, G.G. and Kasinath, B.S. (2001) Activation of renal signaling pathways in db/db mice with type 2 diabetes. *Kidney International,* 60(2), 495-504.

Ferreira, S., Greene, L., Alabaster, V.A., Bakhle, Y. and Vane, J. (1970) Activity of various fractions of bradykinin potentiating factor against angiotensin I converting enzyme. *Nature,* 225(5230), 379.

Filippatos, T.D., Panagiotopoulou, T.V. and Elisaf, M.S. (2014) Adverse Effects of GLP-1 Receptor Agonists. *The Review of Diabetic Studies: RDS,* 11(3-4), 202-230.

Flatt, P. and Bailey, C. (1981) Abnormal plasma glucose and insulin responses in heterozygous lean (ob/+) mice. *Diabetologia,* 20(5), 573-577.

Forouzanfar, M.H., Afshin, A., Alexander, L.T., Anderson, H.R., Bhutta, Z.A., Biryukov, S., Brauer, M., Burnett, R., Cercy, K. and Charlson, F.J. (2016) Global, regional, and national comparative risk assessment of 79 behavioural, environmental and occupational, and metabolic risks or clusters of risks, 1990–2015: a systematic analysis for the Global Burden of Disease Study 2015. *The Lancet,* 388(10053), 1659-1724.

Fosgerau, K. and Hoffmann, T. (2015) Peptide therapeutics: current status and future directions. *Drug Discovery Today,* 20(1), 122-128.

Fraker, P.J. and Speck Jr, J.C. (1978) Protein and cell membrane iodinations with a sparingly soluble chloroamide, 1, 3, 4, 6-tetrachloro-3a, 6a-diphenylglycoluril. *Biochemical and Biophysical Research Communications,* 80(4), 849-857.

Frese, T. and Sandholzer, H. (2013) The epidemiology of type 1 diabetes mellitus. *In:* Anon.*Type 1 Diabetes.* InTech,

Frost, D. (2015) *Amphibian Species of the World: An Online Reference.Version 6.0. Electronic Database.American Museum of Natural History, New York, USA,*

Fujiwara, T., Wada, M., Fukuda, K., Fukami, M., Yoshioka, S., Yoshioka, T. and Horikoshi, H. (1991) Characterization of CS-045, a new oral antidiabetic agent, II. Effects on glycemic control and pancreatic islet structure at a late stage of the diabetic syndrome in C57BLKsJ-dbdb mice. *Metabolism,* 40(11), 1213-1218.

Fukao, T., Lopaschuk, G.D. and Mitchell, G.A. (2004) Pathways and control of ketone body metabolism: on the fringe of lipid biochemistry. *Prostaglandins, Leukotrienes and Essential Fatty Acids,* 70(3), 243-251.

Furman, B.L. (2012) The development of Byetta (exenatide) from the venom of the Gila monster as an anti-diabetic agent. *Toxicon,* 59(4), 464-471.

Galvez, A., Gimenez-Gallego, G., Reuben, J.P., Roy-Contancin, L., Feigenbaum, P., Kaczorowski, G.J. and Garcia, M.L. (1990) Purification and characterization of a unique, potent, peptidyl probe for the high conductance calcium-activated potassium channel from venom of the scorpion Buthus tamulus. *The Journal of Biological Chemistry,* 265(19), 11083-11090.

Garcia-Compean, D., Jaquez-Quintana, J.O., Gonzalez-Gonzalez, J.A. and Maldonado-Garza, H. (2009) Liver cirrhosis and diabetes: risk factors, pathophysiology, clinical implications and management. *World Journal of Gastroenterology: WJG,* 15(3), 280.

Gedulin, B.R., Nikoulina, S.E., Smith, P.A., Gedulin, G., Nielsen, L.L., Baron, A.D., Parkes, D.G. and Young, A.A. (2005) Exenatide (exendin-4) improves insulin sensitivity and β-cell mass in insulin-resistant obese fa/fa Zucker rats independent of glycemia and body weight. *Endocrinology,* 146(4), 2069-2076.

Geerlings, S., Fonseca, V., Castro-Diaz, D., List, J. and Parikh, S. (2014) Genital and urinary tract infections in diabetes: impact of pharmacologically-induced glucosuria. *Diabetes Research and Clinical Practice,* 103(3), 373-381.

Ghosh, A., Bera, S., Shai, Y., Mangoni, M.L. and Bhunia, A. (2016) NMR structure and binding of esculentin-1a (1–21) NH 2 and its diastereomer to lipopolysaccharide: Correlation with biological functions. *Biochimica Et Biophysica Acta (BBA)-Biomembranes,* 1858(4), 800-812.

Gibson, B.W., Poulter, L., Williams, D.H. and Maggio, J.E. (1986) Novel peptide fragments originating from PGLa and the caerulein and xenopsin precursors from Xenopus laevis. *The Journal of Biological Chemistry,* 261(12), 5341-5349.

Glattard, E., Salnikov, E.S., Aisenbrey, C. and Bechinger, B. (2016) Investigations of the synergistic enhancement of antimicrobial activity in mixtures of magainin 2 and PGLa. *Biophysical Chemistry,* 210, 35-44.

Gomes, A., Giri, B., Saha, A., Mishra, R., Dasgupta, S.C., Debnath, A. and Gomes, A. (2007) Bioactive molecules from amphibian skin: their biological activities with reference to therapeutic potentials for possible drug development. *Indian J Exp Biol,* 45(7):579-93.

Goodyear, L.J., Giorgino, F., Sherman, L.A., Carey, J., Smith, R.J. and Dohm, G.L. (1995) Insulin receptor phosphorylation, insulin receptor substrate-1 phosphorylation, and phosphatidylinositol 3-kinase activity are decreased in intact skeletal muscle strips from obese subjects. *The Journal of Clinical Investigation,* 95(5), 2195-2204.

Goral, V., Atalay, R. and Kucukoner, M. (2010) Insulin resistance in liver cirrhosis. *Hepato-Gastroenterology,* 57(98), 309-315.

Grant, S.F., Thorleifsson, G., Reynisdottir, I., Benediktsson, R., Manolescu, A., Sainz, J., Helgason, A., Stefansson, H., Emilsson, V. and Helgadottir, A. (2006) Variant of transcription factor 7-like 2 (TCF7L2) gene confers risk of type 2 diabetes. *Nature Genetics,* 38(3), 320.

Grarup, N., Sandholt, C.H., Hansen, T. and Pedersen, O. (2014) Genetic susceptibility to type 2 diabetes and obesity: from genome-wide association studies to rare variants and beyond. *Diabetologia,* 57(8), 1528-1541.

Gray, A.M., Abdel-Wahab, Y.H. and Flatt, P.R. (2000) The traditional plant treatment, *Sambucus nigra* (elder), exhibits insulin-like and insulin-releasing actions in vitro. *The Journal of Nutrition,* 130(1), 15-20.

Gray, A.M. and Flatt, P.R. (1997) Pancreatic and extra-pancreatic effects of the traditional anti-diabetic plant, *Medicago sativa* (lucerne). *British Journal of Nutrition,* 78(2), 325-334.

Gray, A.M. and Flatt, P.R. (1998) Actions of the traditional anti-diabetic plant, Agrimony eupatoria (agrimony): effects on hyperglycaemia, cellular glucose metabolism and insulin secretion. *British Journal of Nutrition,* 80(1), 109-114.

Gray, A.M. and Flatt, P.R. (1999) Insulin-releasing and insulin-like activity of the traditional anti-diabetic plant *Coriandrum sativum* (coriander). *British Journal of Nutrition,* 81(3), 203-209.

Green, B., Gault, V., Flatt, P., Harriott, P., Greer, B. and O'Harte, F. (2004a) Comparative effects of GLP-1 and GIP on cAMP production, insulin secretion, and *in vivo* antidiabetic actions following substitution of Ala8/Ala2 with 2-aminobutyric acid. *Archives of Biochemistry and Biophysics,* 428(2), 136-143.

Green, B., Gault, V., O'harte, F. and Flatt, P. (2005) A comparison of the cellular and biological properties of DPP-IV-resistant N-glucitol analogues of glucagon-like peptide-1 and glucose-dependent insulinotropic polypeptide. *Diabetes, Obesity and Metabolism,* 7(5), 595-604.

Green, B.D., Gault, V.A., Mooney, M.H., Irwin, N., Harriott, P., Greer, B., Bailey, C.J., O'harte, F.P. and Flatt, P.R. (2004b) Degradation, receptor binding, insulin secreting and antihyperglycaemic actions of palmitate-derivatised native and Ala8-substituted GLP-1 analogues. *Biological Chemistry,* 385(2), 169-177.

Grieco, P., Luca, V., Auriemma, L., Carotenuto, A., Saviello, M.R., Campiglia, P., Barra, D., Novellino, E. and Mangoni, M.L. (2011) Alanine scanning analysis and structure–function relationships of the frog-skin antimicrobial peptide temporin-1Ta. *Journal of Peptide Science,* 17(5), 358-365.

Grosbellet, E., Dumont, S., Schuster-Klein, C., Guardiola-Lemaitre, B., Pevet, P., Criscuolo, F. and Challet, E. (2016) Circadian phenotyping of obese and diabetic db/db mice. *Biochimie,* 124, 198-206.

Guo, S., Dai, C., Guo, M., Taylor, B., Harmon, J.S., Sander, M., Robertson, R.P., Powers, A.C. and Stein, R. (2013) Inactivation of specific β cell transcription factors in type 2 diabetes. *The Journal of Clinical Investigation,* 123(8), 3305-3316.

Haataja, L., Snapp, E., Wright, J., Liu, M., Hardy, A.B., Wheeler, M.B., Markwardt, M.L., Rizzo, M. and Arvan, P. (2013) Proinsulin intermolecular interactions during secretory trafficking in pancreatic beta cells. *The Journal of Biological Chemistry,* 288(3), 1896-1906.

Hall, R.K., Wang, X.L., George, L., Koch, S.R. and Granner, D.K. (2007) Insulin represses phosphoenolpyruvate carboxykinase gene transcription by causing the rapid disruption of an active transcription complex: a potential epigenetic effect. *Molecular Endocrinology,* 21(2), 550-563.

Hanefeld, M. and Schaper, F. (2008) Acarbose: oral antidiabetes drug with additional cardiovascular benefits. *Expert Review of Cardiovascular Therapy,* 6(2), 153-163.

He, K., Shi, J.C. and Mao, X.M. (2014) Safety and efficacy of acarbose in the treatment of diabetes in Chinese patients. *Therapeutics and Clinical Risk Management,* 10, 505-511.

Heard, K.R., Wu, W., Li, Y., Zhao, P., Woznica, I., Lai, J.H., Beinborn, M., Sanford, D.G., Dimare, M.T. and Chiluwal, A.K. (2013) A general method for making peptide therapeutics resistant to serine protease degradation: application to dipeptidyl peptidase IV substrates. *Journal of Medicinal Chemistry,* 56(21), 8339-8351.

Helmerhorst, E.J., Reijnders, I.M., van't Hof, W., Simoons-Smit, I., Veerman, E.C. and Amerongen, A.V. (1999) Amphotericin B- and fluconazole-resistant Candida spp., Aspergillus fumigatus, and other newly emerging pathogenic fungi are susceptible to basic antifungal peptides. *Antimicrobial Agents and Chemotherapy,* 43(3), 702-704.

Henquin, J.C. (2000) Triggering and amplifying pathways of regulation of insulin secretion by glucose. *Diabetes,* 49(11), 1751-1760.

Henquin, J.C. (2004) Pathways in beta-cell stimulus-secretion coupling as targets for therapeutic insulin secretagogues. *Diabetes,* 53 Suppl 3, S48-58.

Hernandez Cruz, A., Garcia-Jimenez, S., Zucatelli Mendonca, R. and Petricevich, V.L. (2008) Pro- and anti-inflammatory cytokines release in mice injected with Crotalus durissus terrificus venom. *Mediators of Inflammation,* 2008, 874962.

Herrington, J., Zhou, Y.P., Bugianesi, R.M., Dulski, P.M., Feng, Y., Warren, V.A., Smith, M.M., Kohler, M.G., Garsky, V.M., Sanchez, M., Wagner, M., Raphaelli, K., Banerjee, P., Ahaghotu, C., Wunderler, D., Priest, B.T., Mehl, J.T., Garcia, M.L., McManus, O.B., Kaczorowski, G.J. and Slaughter, R.S. (2006) Blockers of the delayed-rectifier potassium current in pancreatic beta-cells enhance glucose-dependent insulin secretion. *Diabetes,* 55(4), 1034-1042.

Hirschhorn, J.N. (2003) Genetic epidemiology of type 1 diabetes. *Pediatric Diabetes,* 4(2), 87-100.

Holman, R.R., Paul, S.K., Bethel, M.A., Matthews, D.R. and Neil, H.A.W. (2008) 10-year follow-up of intensive glucose control in type 2 diabetes. *New England Journal of Medicine,* 359(15), 1577-1589.

Home, P., Riddle, M., Cefalu, W.T., Bailey, C.J., Bretzel, R.G., Del Prato, S., Leroith, D., Schernthaner, G., van Gaal, L. and Raz, I. (2014) Insulin therapy in people with type 2 diabetes: opportunities and challenges? *Diabetes Care,* 37(6), 1499-1508.

Hoogwerf, B.J., Doshi, K.B. and Diab, D. (2008) Pramlintide, the synthetic analogue of amylin: physiology, pathophysiology, and effects on glycemic control, body weight, and selected biomarkers of vascular risk. *Vascular Health and Risk Management,* 4(2), 355-362.

Hsia, D.S., Grove, O. and Cefalu, W.T. (2017) An update on sodium-glucose co-transporter-2 inhibitors for the treatment of diabetes mellitus. *Current Opinion in Endocrinology & Diabetes and Obesity,* 24(1), 73-79.

Hu, F.B. (2011) Globalization of diabetes: the role of diet, lifestyle, and genes. *Diabetes Care,* 34(6), 1249-1257.

Huang, C., Somwar, R., Patel, N., Niu, W., Török, D. and Klip, A. (2002) Sustained exposure of L6 myotubes to high glucose and insulin decreases insulin-stimulated GLUT4 translocation but upregulates GLUT4 activity. *Diabetes,* 51(7), 2090-2098.

Huang, S. and Czech, M.P. (2007) The GLUT4 glucose transporter. *Cell Metabolism,* 5(4), 237-252.

Huang, C., Somwar, R., Patel, N., Niu, W., Torok, D. and Klip, A. (2002) Sustained exposure of L6 myotubes to high glucose and insulin decreases insulin-stimulated GLUT4 translocation but upregulates GLUT4 activity. *Diabetes,* 51(7), 2090-2098.

Hummel, C.S., Lu, C., Loo, D.D., Hirayama, B.A., Voss, A.A. and Wright, E.M. (2011) Glucose transport by human renal Na+/D-glucose cotransporters SGLT1 and SGLT2. *American Journal of Physiology.Cell Physiology,* 300(1), C14-21.

Hummel, K.P., Dickie, M.M. and Coleman, D.L. (1966) Diabetes, a new mutation in the mouse. *Science (New York, N.Y.),* 153(3740), 1127-1128

Hyde, R., Peyrollier, K. and Hundal, H.S. (2002) Insulin promotes the cell surface recruitment of the SAT2/ATA2 system A amino acid transporter from an endosomal compartment in skeletal muscle cells. *Journal of Biological Chemistry,*

Iepsen, E., Lundgren, J., Dirksen, C., Jensen, J., Pedersen, O., Hansen, T., Madsbad, S., Holst, J.J. and Torekov, S.S. (2015) Treatment with a GLP-1 receptor agonist diminishes the decrease in free plasma leptin during maintenance of weight loss. *International Journal of Obesity,* 39(5), 834.

Imura, Y., Choda, N. and Matsuzaki, K. (2008) Magainin 2 in action: distinct modes of membrane permeabilization in living bacterial and mammalian cells. *Biophysical Journal,* 95(12), 5757-5765.

Ionescu-Tirgoviste, C., Gagniuc, P.A., Gubceac, E., Mardare, L., Popescu, I., Dima, S. and Militaru, M. (2015) A 3D map of the islet routes throughout the healthy human pancreas. *Scientific Reports,* 5, 14634.

Ishida, H., Takizawa, M., Ozawa, S., Nakamichi, Y., Yamaguchi, S., Katsuta, H., Tanaka, T., Maruyama, M., Katahira, H. and Yoshimoto, K. (2004) Pioglitazone

improves insulin secretory capacity and prevents the loss of β-cell mass in obese diabetic db/db mice: possible protection of β cells from oxidative stress. *Metabolism,* 53(4), 488-494.

Islas-Rodrìguez, A.E., Marcellini, L., Orioni, B., Barra, D., Stella, L. and Mangoni, M.L. (2009) Esculentin 1–21: a linear antimicrobial peptide from frog skin with inhibitory effect on bovine mastitis-causing bacteria. *Journal of Peptide Science: An Official Publication of the European Peptide Society,* 15(9), 607-614.

Jackway, R.J., Pukala, T.L., Donnellan, S.C., Sherman, P.J., Tyler, M.J. and Bowie, J.H. (2011) Skin peptide and cDNA profiling of Australian anurans: genus and species identification and evolutionary trends. *Peptides,* 32(1), 161-172.

Jessen, N., Buhl, E.S., Schmitz, O. and Lund, S. (2006) Impaired insulin action despite upregulation of proximal insulin signaling: novel insights into skeletal muscle insulin resistance in liver cirrhosis. *Journal of Hepatology,* 45(6), 797-804.

Kahn, S.E., Cooper, M.E. and Del Prato, S. (2014) Pathophysiology and treatment of type 2 diabetes: perspectives on the past, present, and future. *The Lancet,* 383(9922), 1068-1083.

Kahn, S.E., Hull, R.L. and Utzschneider, K.M. (2006) Mechanisms linking obesity to insulin resistance and type 2 diabetes. *Nature,* 444(7121), 840.

Kailey, B., van de Bunt, M., Cheley, S., Johnson, P.R., MacDonald, P.E., Gloyn, A.L., Rorsman, P. and Braun, M. (2012) SSTR2 is the functionally dominant somatostatin receptor in human pancreatic β-and α-cells. *American Journal of Physiology-Endocrinology and Metabolism,* 303(9), E1107-E1116.

Kalantar-Zadeh, K., Uppot, R.N. and Lewandrowski, K.B. (2013) Case 23-2013: a 54-year-old woman with abdominal pain, vomiting, and confusion. *New England Journal of Medicine,* 369(4), 374-382.

Kalra, S., Aamir, A., Raza, A., Das, A., Azad Khan, A., Shrestha, D., Qureshi, M.F., Md, F., Pathan, M.F. and Jawad, F. (2015) Place of sulfonylureas in the management of type 2 diabetes mellitus in South Asia: A consensus statement. *Indian J Endocrinol Metab,* 19(5), 577-596.

Kalra, S., Baruah, M.P. and Sahay, R. (2014) Medication counselling with sodium glucose transporter 2 inhibitor therapy. *Indian Journal of Endocrinology and Metabolism,* 18(5), 597-599.

Kaneto, H. and Matsuoka, T.A. (2013) Down-regulation of pancreatic transcription factors and incretin receptors in type 2 diabetes. *World Journal of Diabetes,* 4(6), 263-269.

Kasabri, V., Flatt, P.R. and Abdel-Wahab, Y.H. (2010) Terminalia bellirica stimulates the secretion and action of insulin and inhibits starch digestion and protein glycation in vitro. *British Journal of Nutrition,* 103(2), 212-217.

Kashi, Z., Mahrooz, A., Kianmehr, A. and Alizadeh, A. (2016) The role of metformin response in lipid metabolism in patients with recent-onset type 2 diabetes: HbA1c level as a criterion for designating patients as responders or nonresponders to metformin. *PloS One,* 11(3), e0151543.

Kassem, M.A.M., Durda, M.A., Stoicea, N., Cavus, O., Sahin, L. and Rogers, B. (2017) The impact of bariatric surgery on type 2 diabetes mellitus and the management of hypoglycemic events. *Frontiers in Endocrinology,* 8, 37

Kastin, A. (2013) *Handbook of biologically active peptides.* Academic press.

Keller, U., Gerber, P.P. and Stauffacher, W. (1988) Fatty acid-independent inhibition of hepatic ketone body production by insulin in humans. *The American Journal of Physiology,* 254(6 Pt 1), E694-9.

Kendall, D.M. (2006) Thiazolidinediones: the case for early use. *Diabetes Care,* 29(1), 154-157.

Kido, Y., Nakae, J. and Accili, D. (2001) The insulin receptor and its cellular targets. *The Journal of Clinical Endocrinology & Metabolism,* 86(3), 972-979.

Kim, A., Miller, K., Jo, J., Kilimnik, G., Wojcik, P. and Hara, M. (2009) Islet architecture: A comparative study. *Islets,* 1(2), 129-136.

Kim, D., Jeong, Y., Kwon, J., Moon, K., Kim, H., Jeon, S., Lee, M., Park, Y.B. and Choi, M. (2008) Beneficial effect of chungkukjang on regulating blood glucose and pancreatic β-cell functions in C75BL/KsJ-*db/db* mice. *Journal of Medicinal Food,* 11(2), 215-223.

Kim, J.E., Lee, M.H., Nam, D.H., Song, H.K., Kang, Y.S., Lee, J.E., Kim, H.W., Cha, J.J., Hyun, Y.Y. and Han, S.Y. (2013) Celastrol, an NF-κB inhibitor, improves insulin resistance and attenuates renal injury in *db/db* mice. *PloS One,* 8(4), e62068.

Kinard, T.A., Goforth, P.B., Tao, Q., Abood, M.E., Teague, J. and Satin, L.S. (2001) Chloride channels regulate HIT cell volume but cannot fully account for swelling-induced insulin secretion. *Diabetes,* 50(5), 992-1003.

King, G. (2013) Venoms to drugs: translating venom peptides into therapeutics. *Australian Biochemist,* 44(3), 931-939.

King, G.F. (2011) Venoms as a platform for human drugs: translating toxins into therapeutics. *Expert Opinion on Biological Therapy,* 11(11), 1469-1484.

Knoch, K., Meisterfeld, R., Kersting, S., Bergert, H., Altkrüger, A., Wegbrod, C., Jäger, M., Saeger, H. and Solimena, M. (2006) cAMP-dependent phosphorylation of PTB1 promotes the expression of insulin secretory granule proteins in β cells. *Cell Metabolism,* 3(2), 123-134.

Knowler, W.C., Barrett-Connor, E., Fowler, S.E., Hamman, R.F., Lachin, J.M., Walker, E.A., Nathan, D.M. and Diabetes Prevention Program Research Group. (2002) Reduction in the incidence of type 2 diabetes with lifestyle intervention or metformin. *The New England Journal of Medicine,* 346(6), 393-403.

Ko, W.S., Park, T.Y., Park, C., Kim, Y.H., Yoon, H.J., Lee, S.Y., Hong, S.H., Choi, B.T., Lee, Y.T. and Choi, Y.H. (2005) Induction of apoptosis by Chan Su, a traditional Chinese medicine, in human bladder carcinoma T24 cells. *Oncology Reports,* 14(2), 475-480.

Kocer, D., Bayram, F. and Diri, H. (2014) The effects of metformin on endothelial dysfunction, lipid metabolism and oxidative stress in women with polycystic ovary syndrome. *Gynecological Endocrinology,* 30(5), 367-371.

Koehn, F.E. and Carter, G.T. (2005) The evolving role of natural products in drug discovery. *Nature Reviews Drug Discovery,* 4(3), 206.

Kraegen, E., Cooney, G., Ye, J. and Thompson, A. (2001) Triglycerides, fatty acids and insulin resistance-hyperinsulinemia. *Experimental and Clinical Endocrinology & Diabetes,* 109(04), 516-526.

Kumar, P., Kizhakkedathu, J. and Straus, S. (2018) Antimicrobial peptides: Diversity, mechanism of action and strategies to improve the activity and biocompatibility in vivo. *Biomolecules,* 8(1), 4.

Kyte, J. and Doolittle, R.F. (1982) A simple method for displaying the hydropathic character of a protein. *Journal of Molecular Biology,* 157(1), 105-132.

Lacy, P.E. and Kostianovsky, M. (1967) Method for the isolation of intact islets of Langerhans from the rat pancreas. *Diabetes,* 16(1), 35-39.

Lakhtakia, R. (2013) The history of diabetes mellitus. *Sultan Qaboos University Medical Journal,* 13(3), 368-370.

Lass, A., Zimmermann, R., Oberer, M. and Zechner, R. (2011) Lipolysis–a highly regulated multi-enzyme complex mediates the catabolism of cellular fat stores. *Progress in Lipid Research,* 50(1), 14-27.

Lau, J.K.C., Zhang, X. and Yu, J. (2017) Animal models of non-alcoholic fatty liver disease: current perspectives and recent advances. *The Journal of Pathology,* 241(1), 36-44.

Lau, J.L. and Dunn, M.K. (2018) Therapeutic peptides: Historical perspectives, current development trends, and future directions. *Bioorganic & Medicinal Chemistry,* 26(10), 2700-2707.

Lee, H., Kim, A. and Lee, J. (2014) Effects of ramie leaf extract on blood glucose and lipid metabolism in db/db mice. *Journal of the Korean Society for Applied Biological Chemistry,* 57(5), 639-645.

Lee, Y. and Han, H. (2007) Regulatory mechanisms of Na /glucose cotransporters in renal proximal tubule cells. *Kidney International,* 72, S27-S35.

Lee, Y. and Jun, H. (2014) Anti-diabetic actions of glucagon-like peptide-1 on pancreatic beta-cells. *Metabolism,* 63(1), 9-19.

Lehmann, J., Retz, M., Sidhu, S.S., Suttmann, H., Sell, M., Paulsen, F., Harder, J., Unteregger, G. and Stöckle, M. (2006) Antitumor activity of the antimicrobial peptide magainin II against bladder cancer cell lines. *European Urology,* 50(1), 141-147.

Li, L., El-Kholy, W., Rhodes, C. and Brubaker, P. (2005) Glucagon-like peptide-1 protects beta cells from cytokine-induced apoptosis and necrosis: role of protein kinase B. *Diabetologia,* 48(7), 1339-1349.

Li, Y., Cao, X., Li, L.X., Brubaker, P.L., Edlund, H. and Drucker, D.J. (2005) beta-Cell Pdx1 expression is essential for the glucoregulatory, proliferative, and cytoprotective actions of glucagon-like peptide-1. *Diabetes,* 54(2), 482-491.

Lin, W.W. and Karin, M. (2007) A cytokine-mediated link between innate immunity, inflammation, and cancer. *The Journal of Clinical Investigation,* 117(5), 1175-1183.

Liu, A.Y., Silvestre, M.P. and Poppitt, S.D. (2015) Prevention of type 2 diabetes through lifestyle modification: is there a role for higher-protein diets? *Advances in Nutrition,* 6(6), 665-673.

Liu, M., Wright, J., Guo, H., Xiong, Y. and Arvan, P. (2014) Proinsulin entry and transit through the endoplasmic reticulum in pancreatic beta cells. *In:* Anon.*Vitamins & Hormones.* Elsevier, 35-62.

Loffredo, M.R., Ghosh, A., Harmouche, N., Casciaro, B., Luca, V., Bortolotti, A., Cappiello, F., Stella, L., Bhunia, A. and Bechinger, B. (2017) Membrane perturbing activities and structural properties of the frog-skin derived peptide Esculentin-1a (1-21) NH2 and its Diastereomer Esc (1-21)-1c: Correlation with their antipseudomonal and cytotoxic activity. *Biochimica Et Biophysica Acta (BBA)-Biomembranes,* 1859(12), 2327-2339.

Longnecker, D.S. (2014) Anatomy and Histology of the Pancreas. *Pancreapedia: The Exocrine Pancreas Knowledge Base,*

Lu, Y., Long, M., Zhou, S., Xu, Z., Hu, F. and Li, M. (2014) Mibefradil reduces blood glucose concentration in db/db mice. *Clinics,* 69(1), 61-67.

Luca, V., Olivi, M., Di Grazia, A., Palleschi, C., Uccelletti, D. and Mangoni, M.L. (2014) Anti-Candida activity of 1–18 fragment of the frog skin peptide esculentin-1b: in vitro and in vivo studies in a Caenorhabditis elegans infection model. *Cellular and Molecular Life Sciences,* 71(13), 2535-2546.

Luca, V., Stringaro, A., Colone, M., Pini, A. and Mangoni, M.L. (2013) Esculentin (1-21), an amphibian skin membrane-active peptide with potent activity on both planktonic

and biofilm cells of the bacterial pathogen Pseudomonas aeruginosa. *Cellular and Molecular Life Sciences,* 70(15), 2773-2786.

Ludwig, G., Sinsch, U. and Pelster, B. (2015) Behavioural adaptations of Rana temporaria to cold climates. *Journal of Thermal Biology,* 49, 82-90.

Luisa Mangoni, M., Di Grazia, A., Cappiello, F., Casciaro, B. and Luca, V. (2016) Naturally occurring peptides from Rana temporaria: antimicrobial properties and more. *Current Topics in Medicinal Chemistry,* 16(1), 54-64.

Maahs, D.M., West, N.A., Lawrence, J.M. and Mayer-Davis, E.J. (2010) Epidemiology of type 1 diabetes. *Endocrinology and Metabolism Clinics of North America,* 39(3), 481-497.

Maechler, P. and Wollheim, C.B. (1999) Mitochondrial glutamate acts as a messenger in glucose-induced insulin exocytosis. *Nature,* 402(6762), 685.

Maedler, K., Carr, R.D., Bosco, D., Zuellig, R.A., Berney, T. and Donath, M.Y. (2005) Sulfonylurea induced β-cell apoptosis in cultured human islets. *The Journal of Clinical Endocrinology & Metabolism,* 90(1), 501-506.

Malmgren, S. and Ahrén, B. (2015) DPP-4 inhibition contributes to the prevention of hypoglycaemia through a GIP–glucagon counterregulatory axis in mice. *Diabetologia,* 58(5), 1091-1099.

Mangoni, M.L., Fiocco, D., Mignogna, G., Barra, D. and Simmaco, M. (2003) Functional characterisation of the 1–18 fragment of esculentin-1b, an antimicrobial peptide from Rana esculenta. *Peptides,* 24(11), 1771-1777.

Mangoni, M.L., Luca, V. and McDermott, A.M. (2015) Fighting microbial infections: a lesson from amphibian skin-derived esculentin-1 peptides. *Peptides,* 71, 286-295.

Mangoni, M.L., McDermott, A.M. and Zasloff, M. (2016) Antimicrobial peptides and wound healing: biological and therapeutic considerations. *Experimental Dermatology,* 25(3), 167-173.

Mangoni, M.L. and Shai, Y. (2009) Temporins and their synergism against Gram-negative bacteria and in lipopolysaccharide detoxification. *Biochimica Et Biophysica Acta (BBA)-Biomembranes,* 1788(8), 1610-1619.

Manzo, G., Sanna, R., Casu, M., Mignogna, G., Mangoni, M.L., Rinaldi, A.C. and Scorciapino, M.A. (2012) Toward an improved structural model of the frog-skin antimicrobial peptide esculentin-1b (1-18). *Biopolymers,* 97(11), 873-881.

Marcellini, L., Borro, M., Gentile, G., Rinaldi, A.C., Stella, L., Aimola, P., Barra, D. and Mangoni, M.L. (2009) Esculentin-1b (1–18)–a membrane-active antimicrobial peptide that synergizes with antibiotics and modifies the expression level of a limited number of proteins in *Escherichia coli*. *The FEBS Journal,* 276(19), 5647-5664.

Marenah, L., Flatt, P., Orr, D., Shaw, C. and Abdel-Wahab, Y.H. (2005) Characterization of naturally occurring peptides in the skin secretion of *Rana pipiens* frog reveal pipinin-1 as the novel insulin-releasing agent. *The Journal of Peptide Research,* 66(4), 204-210.

Marenah, L., Flatt, P.R., Orr, D.F., McClean, S., Shaw, C. and Abdel-Wahab, Y.H. (2004a) Skin secretion of the toad *Bombina variegata* contains multiple insulin-releasing peptides including bombesin and entirely novel insulinotropic structures. *Biological Chemistry,* 385(3-4), 315-321.

Marenah, L., Flatt, P.R., Orr, D.F., McClean, S., Shaw, C. and Abdel-Wahab, Y.H. (2004b) Brevinin-1 and multiple insulin-releasing peptides in the skin of the frog *Rana palustris*. *The Journal of Endocrinology,* 181(2), 347-354.

Marenah, L., Flatt, P.R., Orr, D.F., Shaw, C. and Abdel-Wahab, Y.H. (2006) Skin secretions of *Rana saharica* frogs reveal antimicrobial peptides esculentins-1 and -1B and brevinins-1E and -2EC with novel insulin releasing activity. *The Journal of Endocrinology,* 188(1), 1-9.

Marles, R.J. and Farnsworth, N.R. (1995) Antidiabetic plants and their active constituents. *Phytomedicine,* 2(2), 137-189.

Matanic, V.C.A. and Castilla, V. (2004) Antiviral activity of antimicrobial cationic peptides against Junin virus and herpes simplex virus. *International Journal of Antimicrobial Agents,* 23(4), 382-389.

Mathews, J.N., Flatt, P.R. and Abdel-Wahab, Y.H. (2006) *Asparagus adscendens* (Shweta musali) stimulates insulin secretion, insulin action and inhibits starch digestion. *British Journal of Nutrition,* 95(3), 576-581.

McCarthy, M.I. (2010) Genomics, type 2 diabetes, and obesity. *New England Journal of Medicine,* 363(24), 2339-2350.

McClenaghan, N.H., Barnett, C.R., Ah-Sing, E., Abdel-Wahab, Y.H., O'Harte, F.P., Yoon, T.W., Swanston-Flatt, S.K. and Flatt, P.R. (1996) Characterization of a novel glucose-responsive insulin-secreting cell line, BRIN-BD11, produced by electrofusion. *Diabetes,* 45(8), 1132-1140.

McCluskey, J.T., Hamid, M., Guo-Parke, H., McClenaghan, N.H., Gomis, R. and Flatt, P.R. (2011) Development and functional characterization of insulin-releasing human pancreatic beta cell lines produced by electrofusion. *The Journal of Biological Chemistry,* 286(25), 21982-21992.

Mechkarska, M., Ojo, O.O., Meetani, M.A., Coquet, L., Jouenne, T., Abdel-Wahab, Y.H., Flatt, P.R., King, J.D. and Conlon, J.M. (2011) Peptidomic analysis of skin secretions from the bullfrog Lithobates catesbeianus (Ranidae) identifies multiple peptides with potent insulin-releasing activity. *Peptides,* 32(2), 203-208.

Mechkarska, M., Prajeep, M., Radosavljevic, G.D., Jovanovic, I.P., Al Baloushi, A., Sonnevend, A., Lukic, M.L. and Conlon, J.M. (2013) An analog of the host-defense peptide hymenochirin-1B with potent broad-spectrum activity against multidrug-resistant bacteria and immunomodulatory properties. *Peptides,* 50, 153-159.

Menting, J.G., Gajewiak, J., MacRaild, C.A., Chou, D.H., Disotuar, M.M., Smith, N.A., Miller, C., Erchegyi, J., Rivier, J.E. and Olivera, B.M. (2016) A minimized human insulin-receptor-binding motif revealed in a Conus geographus venom insulin. *Nature Structural & Molecular Biology,* 23(10), 916.

Menting, J.G., Whittaker, J., Margetts, M.B., Whittaker, L.J., Kong, G.K., Smith, B.J., Watson, C.J., Žáková, L., Kletvíková, E. and Jiráček, J. (2013) How insulin engages its primary binding site on the insulin receptor. *Nature,* 493(7431), 241.

Michael Conlon, J., Galadari, S., Raza, H. and Condamine, E. (2008) Design of potent, non-toxic antimicrobial agents based upon the naturally occurring frog skin peptides, ascaphin-8 and peptide XT-7. *Chemical Biology & Drug Design,* 72(1), 58-64.

Miller, K.M., Beck, R.W., Bergenstal, R.M., Goland, R.S., Haller, M.J., McGill, J.B., Rodriguez, H., Simmons, J.H., Hirsch, I.B. and T1D Exchange Clinic Network. (2013) Evidence of a strong association between frequency of self-monitoring of blood glucose and hemoglobin A1c levels in T1D exchange clinic registry participants. *Diabetes Care,* 36(7), 2009-2014.

Mojsoska, B. and Jenssen, H. (2015) Peptides and peptidomimetics for antimicrobial drug design. *Pharmaceuticals,* 8(3), 366-415.

Moore, S.W., Bhat, V.K., Flatt, P.R., Gault, V.A. and McClean, S. (2015) Isolation and characterisation of insulin-releasing compounds from Crotalus adamanteus, Crotalus vegrandis and Bitis nasicornis venom. *Toxicon,* 101, 48-54.

Moore, S.W., Bhat, V.K., Flatt, P.R., Gault, V.A. and McClean, S. (2016) Isolation and Characterisation of Insulin-Releasing Compounds from Pseudechis australis and Pseudechis butleri Venom. *International Journal of Peptide Research and Therapeutics,* 22(2), 211-218.

Moreno-Indias, I., Cardona, F., Tinahones, F.J. and Queipo-Ortuño, M.I. (2014) Impact of the gut microbiota on the development of obesity and type 2 diabetes mellitus. *Frontiers in Microbiology,* 5, 190.

Morita, H., Deguchi, J., Motegi, Y., Sato, S., Aoyama, C., Takeo, J., Shiro, M. and Hirasawa, Y. (2010) Cyclic diarylheptanoids as Na -glucose cotransporter (SGLT) inhibitors from Acer nikoense. *Bioorganic & Medicinal Chemistry Letters,* 20(3), 1070-1074.

Morris, D.L. (2015) Minireview: emerging concepts in islet macrophage biology in type 2 diabetes. *Molecular Endocrinology,* 29(7), 946-962.

Moscatiello, S., Manini, R. and Marchesini, G. (2007) Diabetes and liver disease: an ominous association. *Nutrition, Metabolism and Cardiovascular Diseases,* 17(1), 63-70.

Muller, L., Gorter, K., Hak, E., Goudzwaard, W., Schellevis, F., Hoepelman, A. and Rutten, G. (2005) Increased risk of common infections in patients with type 1 and type 2 diabetes mellitus. *Clinical Infectious Diseases,* 41(3), 281-288.

Muñoz-Camargo, C., Méndez, M.C., Salazar, V., Moscoso, J., Narváez, D., Torres, M.M., Florez, F.K., Groot, H. and Mitrani, E. (2016) Frog skin cultures secrete anti-yellow fever compounds. *The Journal of Antibiotics,* 69(11), 783.

Musale, V., Abdel-Wahab, Y.H., Flatt, P.R., Conlon, J.M. and Mangoni, M.L. (2018a) Insulinotropic, glucose-lowering, and beta-cell anti-apoptotic actions of peptides related to esculentin-1a (1-21). NH 2. *Amino Acids,* 50(6), 723-734

Musale, V., Casciaro, B., Mangoni, M.L., Abdel-Wahab, Y.H., Flatt, P.R. and Conlon, J.M. (2018b) Assessment of the potential of temporin peptides from the frog Rana temporaria (Ranidae) as anti-diabetic agents. *Journal of Peptide Science,* 24(2), e3065

Nadal, A., Rovira, J.M., Laribi, O., Leon-quinto, T., Andreu, E., Ripoll, C. and Soria, B. (1998) Rapid insulinotropic effect of 17β-estradiol via a plasma membrane receptor. *The FASEB Journal,* 12(13), 1341-1348.

Nansel, T., Lipsky, L. and Iannotti, R. (2013) Cross-sectional and longitudinal relationships of body mass index with glycemic control in children and adolescents with type 1 diabetes mellitus. *Diabetes Research and Clinical Practice,* 100(1), 126-132.

Nathan, D.M., Buse, J.B., Davidson, M.B., Ferrannini, E., Holman, R.R., Sherwin, R., Zinman, B., American Diabetes Association and European Association for Study of Diabetes. (2009) Medical management of hyperglycemia in type 2 diabetes: a consensus algorithm for the initiation and adjustment of therapy: a consensus statement of the American Diabetes Association and the European Association for the Study of Diabetes. *Diabetes Care,* 32(1), 193-203.

Nauck, M.A. (2013) A critical analysis of the clinical use of incretin-based therapies: The benefits by far outweigh the potential risks. *Diabetes Care,* 36(7), 2126-2132.

Newsholme, P., Brennan, L., Rubi, B. and Maechler, P. (2005) New insights into amino acid metabolism, beta-cell function and diabetes. *Clinical Science (London, England: 1979),* 108(3), 185-194.

Newsholme, P. and Krause, M. (2012) Nutritional regulation of insulin secretion: implications for diabetes. *The Clinical Biochemist.Reviews,* 33(2), 35-47.

Nguyen, T.T.N., Folch, B., Létourneau, M., Vaudry, D., Truong, N.H., Doucet, N., Chatenet, D. and Fournier, A. (2012) Cardiotoxin-I: An Unexpectedly Potent Insulinotropic Agent. *Chembiochem,* 13(12), 1805-1812.

Nogid, A. and Pham, D.Q. (2006) Adjunctive therapy with pramlintide in patients with type 1 or type 2 diabetes mellitus. *Pharmacotherapy: The Journal of Human Pharmacology and Drug Therapy,* 26(11), 1626-1640.

Nogueira, T.C., Ferreira, F., Toyama, M.H., Stoppiglia, L.F., Marangoni, S., Boschero, A.C. and Carneiro, E.M. (2005) Characterization of the insulinotropic action of a phospholipase A2 isolated from Crotalus durissus collilineatus rattlesnake venom on rat pancreatic islets. *Toxicon,* 45(2), 243-248.

Ohki-Hamazaki, H., Iwabuchi, M. and Maekawa, F. (2003) Development and function of bombesin-like peptides and their receptors. *International Journal of Developmental Biology,* 49(2-3), 293-300.

Ohsaki, Y., Gazdar, A.F., Chen, H.C. and Johnson, B.E. (1992) Antitumor activity of magainin analogues against human lung cancer cell lines. *Cancer Research,* 52(13), 3534-3538.

Ojo, O., Conlon, J., Flatt, P. and Abdel-Wahab, Y. (2012) Caerulin precursor fragment (CPF-AM1): a novel insulinotropic peptide from the skin secretion of the clawed frog, Xenopus amieti. *In:* Caerulin precursor fragment (CPF-AM1): a novel insulinotropic peptide from the skin secretion of the clawed frog, Xenopus amieti. *15th International & 14th European Congress of Endocrinology.* BioScientifica

Ojo, O., Abdel-Wahab, Y., Flatt, P., Mechkarska, M. and Conlon, J. (2011) Tigerinin-1R: a potent, non-toxic insulin-releasing peptide isolated from the skin of the Asian frog, Hoplobatrachus rugulosus. *Diabetes, Obesity and Metabolism,* 13(12), 1114-1122.

Ojo, O., Conlon, J., Flatt, P. and Abdel-Wahab, Y. (2013a) Frog skin peptides (tigerinin-1R, magainin-AM1, -AM2, CPF-AM1, and PGla-AM1) stimulate secretion of glucagon-like peptide 1 (GLP-1) by GLUTag cells. *Biochemical and Biophysical Research Communications,* 431(1), 14-18.

Ojo, O.O., Abdel-Wahab, Y.H., Flatt, P.R. and Conlon, J.M. (2013b) Insulinotropic Actions of the Frog Skin Host-Defense Peptide Alyteserin-2a: A Structure–Activity Study. *Chemical Biology & Drug Design,* 82(2), 196-204.

Ojo, O.O., Srinivasan, D.K., Owolabi, B.O., Conlon, J.M., Flatt, P.R. and Abdel-Wahab, Y.H. (2015a) Magainin-AM2 improves glucose homeostasis and beta cell function in high-fat fed mice. *Biochimica Et Biophysica Acta (BBA)-General Subjects,* 1850(1), 80-87.

Ojo, O.O., Srinivasan, D.K., Owolabi, B.O., Flatt, P.R. and Abdel-Wahab, Y.H. (2015b) Beneficial effects of tigerinin-1R on glucose homeostasis and beta cell function in mice with diet-induced obesity-diabetes. *Biochimie,* 109, 18-26.

Ojo, O.O., Srinivasan, D.K., Owolabi, B.O., McGahon, M.K., Moffett, R.C., Curtis, T.M., Conlon, J.M., Flatt, P.R. and Abdel-Wahab, Y.H. (2016) Molecular mechanisms

mediating the beneficial metabolic effects of [Arg4] tigerinin-1R in mice with diet-induced obesity and insulin resistance. *Biological Chemistry*, 397(8), 753-764.

Ojo, O.O., Srinivasan, D.K., Owolabi, B.O., Vasu, S., Conlon, J.M., Flatt, P.R. and Abdel-Wahab, Y.H. (2015c) Esculentin-2CHa-related peptides modulate islet cell function and improve glucose tolerance in mice with diet-induced obesity and insulin resistance. *PloS One,* 10(10), e0141549.

Otani, K., Kulkarni, R.N., Baldwin, A.C., Krutzfeldt, J., Ueki, K., Stoffel, M., Kahn, C.R. and Polonsky, K.S. (2004) Reduced β-cell mass and altered glucose sensing impair insulin-secretory function in βIRKO mice. *American Journal of Physiology-Endocrinology and Metabolism,* 286(1), E41-E49.

Owolabi, B.O., Musale, V., Ojo, O.O., Moffett, R.C., McGahon, M.K., Curtis, T.M., Conlon, J.M., Flatt, P.R. and Abdel-Wahab, Y.H. (2017) Actions of PGLa-AM1 and its [A14K] and [A20K] analogues and their therapeutic potential as anti-diabetic agents. *Biochimie*, 138, 1-12.

Owolabi, B.O., Ojo, O.O., Srinivasan, D.K., Conlon, J.M., Flatt, P.R. and Abdel-Wahab, Y.H. (2016) Glucoregulatory, endocrine and morphological effects of [P5K] hymenochirin-1B in mice with diet-induced glucose intolerance and insulin resistance. *Naunyn-Schmiedeberg's Archives of Pharmacology*, 389(7), 769-781.

Owolabi, B.O., Ojo, O.O., Srinivasan, D.K., Conlon, J.M., Flatt, P.R. and Abdel-Wahab, Y.H. (2016) In vitro and in vivo insulinotropic properties of the multifunctional frog skin peptide hymenochirin-1B: a structure–activity study. *Amino Acids,* 48(2), 535-547.

Oyejide Ojo, O., Kumar Srinivasan, D., Olayinka Owolabi, B., Raymond Flatt, P. and Hassan Atef Abdel-Wahab, Y. (2015) Magainin-related peptides stimulate insulin-release and improve glucose tolerance in high fat fed mice. *Protein and Peptide Letters*, 22(3), 256-263.

Pantic, J.M., Jovanovic, I.P., Radosavljevic, G.D., Gajovic, N.M., Arsenijevic, N.N., Conlon, J.M. and Lukic, M.L. (2017a) The frog skin host-defense peptide frenatin 2.1 S enhances recruitment, activation and tumoricidal capacity of NK cells. *Peptides,* 93, 44-50.

Pantic, J.M., Radosavljevic, G.D., Jovanovic, I.P., Arsenijevic, N.N., Conlon, J.M. and Lukic, M.L. (2015) In vivo administration of the frog skin peptide frenatin 2.1 S induces immunostimulatory phenotypes of mouse mononuclear cells. *Peptides*, 71, 269-275.

Pantic, J., Jovanovic, I., Radosavljevic, G., Arsenijevic, N., Conlon, J. and Lukic, M. (2017b) The potential of frog skin-derived peptides for development into therapeutically-valuable immunomodulatory agents. *Molecules,* 22(12), 2071.

Parikh, N.H., Parikh, P.K. and Kothari, C. (2014) Indigenous plant medicines for health care: treatment of Diabetes mellitus and hyperlipidemia. *Chinese Journal of Natural Medicines*, 12(5), 335-344.

Park, C.W., Kim, H.W., Ko, S.H., Lim, J.H., Ryu, G.R., Chung, H.W., Han, S.W., Shin, S.J., Bang, B.K., Breyer, M.D. and Chang, Y.S. (2007) Long-term treatment of glucagon-like peptide-1 analog exendin-4 ameliorates diabetic nephropathy through improving metabolic anomalies in db/db mice. *Journal of the American Society of Nephrology: JASN*, 18(4), 1227-1238.

Parkes, D.G., Mace, K.F. and Trautmann, M.E. (2013) Discovery and development of exenatide: the first antidiabetic agent to leverage the multiple benefits of the incretin hormone, GLP-1. *Expert Opinion on Drug Discovery,* 8(2), 219-244.

Parkes, D., Jodka, C., Smith, P., Nayak, S., Rinehart, L., Gingerich, R., Chen, K. and Young, A. (2001) Pharmacokinetic actions of exendin-4 in the rat: comparison with glucagon-like peptide-1. *Drug Development Research*, 53(4), 260-267.

Patterson, C., Guariguata, L., Dahlquist, G., Soltész, G., Ogle, G. and Silink, M. (2014) Diabetes in the young–a global view and worldwide estimates of numbers of children with type 1 diabetes. *Diabetes Research and Clinical Practice,* 103(2), 161-175.

Pieper-Bigelow, C., Strocchi, A. and Levitt, M.D. (1990) Where does serum amylase come from and where does it go? *Gastroenterology Clinics of North America,* 19(4), 793-810.

Piro, S., Anello, M., Di Pietro, C., Lizzio, M.N., Patane, G., Rabuazzo, A.M., Vigneri, R., Purrello, M. and Purrello, F. (2002) Chronic exposure to free fatty acids or high glucose induces apoptosis in rat pancreatic islets: possible role of oxidative stress. *Metabolism: Clinical and Experimental,* 51(10), 1340-1347.

Poitout, V. (2013) Lipotoxicity impairs incretin signalling. *Diabetologia,* 56(2), 231-233.

Ponti, D., Mignogna, G., Mangoni, M.L., De Biase, D., Simmaco, M. and Barra, D. (1999) Expression and activity of cyclic and linear analogues of esculentin-1, an anti-microbial peptide from amphibian skin. *European Journal of Biochemistry,* 263(3), 921-927.

Poulsen, P., Kyvik, K.O., Vaag, A. and Beck-Nielsen, H. (1999) Heritability of type II (non-insulin-dependent) diabetes mellitus and abnormal glucose tolerance–a population-based twin study. *Diabetologia*, 42(2), 139-145.

Powers, A.C. and Stein, R.W. (2011) New insight of islet biology and the pathophysiology of type 2 diabetes. *Translational Endocrinology and Metabolism,* 2, 95-116.

Proud, C. (2006) Regulation of Protein Synthesis by Insulin, *Biochem Soc Trans, 34(Pt 2):213-6.*

Pukala, T.L., Bowie, J.H., Maselli, V.M., Musgrave, I.F. and Tyler, M.J. (2006) Host-defence peptides from the glandular secretions of amphibians: structure and activity. *Natural Product Reports,* 23(3), 368-393.

Puri, S., Akiyama, H. and Hebrok, M. (2013) VHL-mediated disruption of Sox9 activity compromises beta-cell identity and results in diabetes mellitus. *Genes & Development,* 27(23), 2563-2575.

Quoix, N., Cheng-Xue, R., Guiot, Y., Herrera, P.L., Henquin, J. and Gilon, P. (2007) The GluCre-ROSA26EYFP mouse: A new model for easy identification of living pancreatic α-cells. *FEBS Letters,* 581(22), 4235-4240.

Raaymakers, C., Verbrugghe, E., Hernot, S., Hellebuyck, T., Betti, C., Peleman, C., Claeys, M., Bert, W., Caveliers, V. and Ballet, S. (2017) Antimicrobial peptides in frog poisons constitute a molecular toxin delivery system against predators. *Nature Communications,* 8(1), 1495.

Raftery, M.J., Waugh, R.J., Bowie, J.H., Wallace, J.C. and Tyler, M.J. (1996) The structures of the frenatin peptides from the skin secretion of the giant tree frog Litoria infrafrenata. *Journal of Peptide Science: An Official Publication of the European Peptide Society,* 2(2), 117-124.

Ramesh, S., Govender, T., Kruger, H.G., de la Torre, Beatriz G and Albericio, F. (2016) Short AntiMicrobial Peptides (SAMPs) as a class of extraordinary promising therapeutic agents. *Journal of Peptide Science,* 22(7), 438-451.

Ramnanan, C.J., Edgerton, D.S., Rivera, N., Irimia-Dominguez, J., Farmer, B., Neal, D.W., Lautz, M., Donahue, E.P., Meyer, C.M., Roach, P.J. and Cherrington, A.D. (2010) Molecular characterization of insulin-mediated suppression of hepatic glucose production in vivo. *Diabetes,* 59(6), 1302-1311.

Randle, P., Garland, P., Hales, C. and Newsholme, E. (1963) The glucose fatty-acid cycle its role in insulin sensitivity and the metabolic disturbances of diabetes mellitus. *The Lancet,* 281(7285), 785-789.

Reid, P.F. (2007) PART II. Toxins as Therapeutic Agents Alpha-Cobratoxin as a Possible Therapy for Multiple Sclerosis: A Review of the Literature Leading to Its Development for This Application. *Critical Reviews™ in Immunology,* 27(4)

Rena, G., Hardie, D.G. and Pearson, E.R. (2017) The mechanisms of action of metformin. *Diabetologia,* 60(9), 1577-1585.

Richter, B., Bandeira-Echtler, E., Bergerhoff, K. and Lerch, C. (2008) Dipeptidyl peptidase-4 (DPP-4) inhibitors for type 2 diabetes mellitus. *Cochrane Database of Systematic Reviews,* (2)

Rimoin, D.L. (1969) Ethnic variability in glucose tolerance and insulin secretion. *Archives of Internal Medicine,* 124(6), 695-700.

Rinaldi, A.C. (2002) Antimicrobial peptides from amphibian skin: an expanding scenario: Commentary. *Current Opinion in Chemical Biology,* 6(6), 799-804.

Ríos, J.L., Francini, F. and Schinella, G.R. (2015) Natural products for the treatment of type 2 diabetes mellitus. *Planta Medica,* 81(12/13), 975-994.

Robertson, R.P. (2004) Chronic oxidative stress as a central mechanism for glucose toxicity in pancreatic islet beta cells in diabetes. *The Journal of Biological Chemistry,* 279(41), 42351-42354.

Roden, M., Price, T.B., Perseghin, G., Petersen, K.F., Rothman, D.L., Cline, G.W. and Shulman, G.I. (1996) Mechanism of free fatty acid-induced insulin resistance in humans. *The Journal of Clinical Investigation,* 97(12), 2859-2865.

Rojas, L.B.A. and Gomes, M.B. (2013) Metformin: an old but still the best treatment for type 2 diabetes. *Diabetology & Metabolic Syndrome,* 5(1), 6.

Rorsman, P. and Ashcroft, F.M. (2017) Pancreatic β-cell electrical activity and insulin secretion: of mice and men. *Physiological Reviews,* 98(1), 117-214.

Rothney, M.P., Brychta, R.J., Schaefer, E.V., Chen, K.Y. and Skarulis, M.C. (2009) Body composition measured by dual-energy X-ray absorptiometry half-body scans in obese adults. *Obesity,* 17(6), 1281-1286.

Rubino, F., Nathan, D.M., Eckel, R.H., Schauer, P.R., Alberti, K.G.M., Zimmet, P.Z., Del Prato, S., Ji, L., Sadikot, S.M. and Herman, W.H. (2016) Metabolic surgery in the treatment algorithm for type 2 diabetes: a joint statement by international diabetes organizations. *Surgery for Obesity and Related Diseases,* 12(6), 1144-1162.

Safavi-Hemami, H., Gajewiak, J., Karanth, S., Robinson, S.D., Ueberheide, B., Douglass, A.D., Schlegel, A., Imperial, J.S., Watkins, M. and Bandyopadhyay, P.K. (2015) Specialized insulin is used for chemical warfare by fish-hunting cone snails. *Proceedings of the National Academy of Sciences,* 112(6), 1743-1748.

Saltiel, A.R. and Kahn, C.R. (2001) Insulin signalling and the regulation of glucose and lipid metabolism. *Nature,* 414(6865), 799.

Samuel, V.T. and Shulman, G.I. (2012) Mechanisms for insulin resistance: common threads and missing links. *Cell,* 148(5), 852-871.

Schlogl, H., Kabisch, S., Horstmann, A., Lohmann, G., Muller, K., Lepsien, J., Busse-Voigt, F., Kratzsch, J., Pleger, B., Villringer, A. and Stumvoll, M. (2013) Exenatide-induced reduction in energy intake is associated with increase in hypothalamic connectivity. *Diabetes Care,* 36(7), 1933-1940.

Seino, S. (2012) Cell signalling in insulin secretion: the molecular targets of ATP, cAMP and sulfonylurea. *Diabetologia,* 55(8), 2096-2108.

Shakya, A.K. (2016) Medicinal plants: future source of new drugs. *International Journal of Herbal Medicine,* 4(4), 59-64.

Sharma, R.B. and Alonso, L.C. (2014) Lipotoxicity in the pancreatic beta cell: not just survival and function, but proliferation as well? *Current Diabetes Reports,* 14(6), 492.

Shimizu, Y., Inoue, E. and Ito, C. (2004) Effect of the water-soluble and non-dialyzable fraction isolated from Senso (Chan Su) on lymphocyte proliferation and natural killer activity in C3H mice. *Biological and Pharmaceutical Bulletin,* 27(2), 256-260.

Shimoda, M., Kanda, Y., Hamamoto, S., Tawaramoto, K., Hashiramoto, M., Matsuki, M. and Kaku, K. (2011) The human glucagon-like peptide-1 analogue liraglutide preserves pancreatic beta cells via regulation of cell kinetics and suppression of oxidative and endoplasmic reticulum stress in a mouse model of diabetes. *Diabetologia,* 54(5), 1098-1108.

Shulman, G.I. (2000) Cellular mechanisms of insulin resistance. *The Journal of Clinical Investigation,* 106(2), 171-176.

Sidhu, M. and Tanu, S. (2013) A database of antidiabetic plant species of family Asteraceae, Euphorbiaceae, Fabaceae, Lamiaceae and Moraceae. *International Journal of Herbal Medicine,* 1(2), 187-199.

Simmaco, M., Mignogna, G., Canofeni, S., Miele, R., Mangoni, M.L. and Barra, D. (1996) Temporins, antimicrobial peptides from the European red frog *Rana temporaria*. *European Journal of Biochemistry,* 242(3), 788-792.

Simmaco, M., Mignogna, G., Barra, D. and Bossa, F. (1994) Antimicrobial peptides from skin secretions of Rana esculenta. Molecular cloning of cDNAs encoding esculentin and brevinins and isolation of new active peptides. *The Journal of Biological Chemistry,* 269(16), 11956-11961.

Simon, S.F. and Taylor, C.G. (2001) Dietary zinc supplementation attenuates hyperglycemia in db/db mice. *Experimental Biology and Medicine,* 226(1), 43-51.

Skelin, M., Rupnik, M. and Cencič, A. (2010) Pancreatic beta cell lines and their applications in diabetes mellitus research. *ALTEX-Alternatives to Animal Experimentation,* 27(2), 105-113.

Smith, P.A., Bokvist, K., Arkhammar, P., Berggren, P.O. and Rorsman, P. (1990) Delayed rectifying and calcium-activated K+ channels and their significance for action potential repolarization in mouse pancreatic beta-cells. *The Journal of General Physiology,* 95(6), 1041-1059.

Sola, D., Rossi, L., Schianca, G.P., Maffioli, P., Bigliocca, M., Mella, R., Corliano, F., Fra, G.P., Bartoli, E. and Derosa, G. (2015) Sulfonylureas and their use in clinical practice. *Archives of Medical Science: AMS,* 11(4), 840-848.

Son, D.J., Hwang, S.Y., Kim, M., Park, U.K. and Kim, B.S. (2015) Anti-diabetic and hepato-renal protective effects of Ziyuglycoside II methyl ester in type 2 diabetic mice. *Nutrients,* 7(7), 5469-5483.

Sonagra, A.D., Biradar, S.M., K, D. and Murthy, D.S.J. (2014) Normal pregnancy- a state of insulin resistance. *Journal of Clinical and Diagnostic Research: JCDR,* 8(11), CC01-3.

Soravia, E., Martini, G. and Zasloff, M. (1988) Antimicrobial properties of peptides from Xenopus granular gland secretions. *FEBS Letters,* 228(2), 337-340.

Srinivasan, D.K., Ojo, O.O., Owolabi, B.O., Conlon, J.M., Flatt, P.R. and Abdel-Wahab, Y.H. (2016) [I10W] tigerinin-1R enhances both insulin sensitivity and pancreatic beta cell function and decreases adiposity and plasma triglycerides in high-fat mice. *Acta Diabetologica,* 53(2), 303-315.

Srinivasan, D., Mechkarska, M., Abdel-Wahab, Y.H., Flatt, P.R. and Conlon, J.M. (2013) Caerulein precursor fragment (CPF) peptides from the skin secretions of Xenopus laevis and Silurana epitropicalis are potent insulin-releasing agents. *Biochimie,* 95(2), 429-435.

Standl, E. and Schnell, O. (2012) Alpha-glucosidase inhibitors 2012–cardiovascular considerations and trial evaluation. *Diabetes and Vascular Disease Research,* 9(3), 163-169.

Stein, S.A., Lamos, E.M. and Davis, S.N. (2013) A review of the efficacy and safety of oral antidiabetic drugs. *Expert Opinion on Drug Safety,* 12(2), 153-175.

Steinberg, W.M., Buse, J.B., Ghorbani, M.L.M., Orsted, D.D., Nauck, M.A., LEADER Steering Committee and LEADER Trial Investigators. (2017) Amylase, Lipase, and Acute Pancreatitis in People with Type 2 Diabetes Treated With Liraglutide: Results From the LEADER Randomized Trial. *Diabetes Care,* 40(7), 966-972.

Steiner, D.J., Kim, A., Miller, K. and Hara, M. (2010) Pancreatic islet plasticity: interspecies comparison of islet architecture and composition. *Islets,* 2(3), 135-145.

Susan van, D., Beulens, J.W., Yvonne T. van der, Schouw, Grobbee, D.E. and Nealb, B. (2010) The global burden of diabetes and its complications: an emerging pandemic. *European Journal of Cardiovascular Prevention & Rehabilitation,* 17(1_suppl), s3-s8.

Swanston-Flatt, S.K., Day, C., Flatt, P.R., GoULD, B.J. and Bailey, C. (1989) Glycaemic effects of traditional European plant treatments for diabetes. Studies in normal and streptozotocin diabetic mice. *Diabetes Res,* 10(2), 69-73.

Swartz, K.J. and MacKinnon, R. (1995) An inhibitor of the Kv2. 1 potassium channel isolated from the venom of a Chilean tarantula. *Neuron,* 15(4), 941-949.

Talchai, C., Xuan, S., Lin, H.V., Sussel, L. and Accili, D. (2012) Pancreatic β cell dedifferentiation as a mechanism of diabetic β cell failure. *Cell,* 150(6), 1223-1234.

Tamba, Y., Ariyama, H., Levadny, V. and Yamazaki, M. (2010) Kinetic pathway of antimicrobial peptide magainin 2-induced pore formation in lipid membranes. *The Journal of Physical Chemistry B,* 114(37), 12018-12026.

Tan, C., Voss, U., Svensson, S., Erlinge, D. and Olde, B. (2013) High glucose and free fatty acids induce beta cell apoptosis via autocrine effects of ADP acting on the P2Y 13 receptor. *Purinergic Signalling,* 9(1), 67-79.

Tan, T. and Bloom, S. (2013) Gut hormones as therapeutic agents in treatment of diabetes and obesity. *Current Opinion in Pharmacology,* 13(6), 996-1001.

Tangvarasittichai, S. (2015) Oxidative stress, insulin resistance, dyslipidemia and type 2 diabetes mellitus. *World Journal of Diabetes,* 6(3), 456-480.

Tarantino, G. and Finelli, C. (2013) What about non-alcoholic fatty liver disease as a new criterion to define metabolic syndrome? *World Journal of Gastroenterology,* 19(22), 3375-3384.

Tasyurek, H.M., Altunbas, H.A., Balci, M.K. and Sanlioglu, S. (2014) Incretins: their physiology and application in the treatment of diabetes mellitus. *Diabetes/metabolism Research and Reviews,* 30(5), 354-371.

Taylor, B.L., Liu, F. and Sander, M. (2013) Nkx6. 1 is essential for maintaining the functional state of pancreatic beta cells. *Cell Reports,* 4(6), 1262-1275.

Taylor, A.I., Irwin, N., McKillop, A.M., Patterson, S., Flatt, P.R. and Gault, V.A. (2010) Evaluation of the degradation and metabolic effects of the gut peptide xenin on insulin secretion, glycaemic control and satiety. *The Journal of Endocrinology,* 207(1), 87-93.

Thorel, F., Népote, V., Avril, I., Kohno, K., Desgraz, R., Chera, S. and Herrera, P.L. (2012) Conversion of adult pancreatic α-cells to β-cells after extreme β-cell loss. *Nature,* 464(7292), 1149.

Thulé, P.M. and Umpierrez, G. (2014) Sulfonylureas: a new look at old therapy. *Current Diabetes Reports,* 14(4), 473.

Toyama, D.O., Boschero, A.C., Martins, M., Fonteles, M., Monteiro, H. and Toyama, M.H. (2005) Structure–function relationship of new crotamine isoform from the Crotalus durissus cascavella. *The Protein Journal,* 24(1), 9-19.

Toyama, M.H., Carneiro, E.M., Marangoni, S., Barbosa, R.L., Corso, G. and Boschero, A.C. (2000) Biochemical characterization of two crotamine isoforms isolated by a single step RP-HPLC from Crotalus durissus terrificus (South American rattlesnake) venom and their action on insulin secretion by pancreatic islets. *Biochimica Et Biophysica Acta (BBA)-General Subjects,* 1474(1), 56-60.

Trojan-Rodrigues, M., Alves, T., Soares, G. and Ritter, M. (2012) Plants used as antidiabetics in popular medicine in Rio Grande do Sul, southern Brazil. *Journal of Ethnopharmacology,* 139(1), 155-163.

Tsend-Ayush, E., He, C., Myers, M.A., Andrikopoulos, S., Wong, N., Sexton, P.M., Wootten, D., Forbes, B.E. and Grutzner, F. (2016) Monotreme glucagon-like peptide-1 in venom and gut: one gene–two very different functions. *Scientific Reports,* 6, 37744.

Tyler, M.J., Stone, D.J. and Bowie, J.H. (1992) A novel method for the release and collection of dermal, glandular secretions from the skin of frogs. *Journal of Pharmacological and Toxicological Methods,* 28(4), 199-200.

UK Prospective Diabetes Study (UKPDS) Group. (1998) Intensive blood-glucose control with sulphonylureas or insulin compared with conventional treatment and risk of complications in patients with type 2 diabetes (UKPDS 33). *The Lancet,* 352(9131), 837-853.

Utkin, Y.N. (2015) Animal venom studies: Current benefits and future developments. *World Journal of Biological Chemistry,* 6(2), 28-33.

van Dalem, J., Brouwers, M.C., Stehouwer, C.D., Krings, A., Leufkens, H.G., Driessen, J.H., de Vries, F. and Burden, A.M. (2016) Risk of hypoglycaemia in users of sulphonylureas compared with metformin in relation to renal function and sulphonylurea metabolite group: populationbased cohort study. *BMJ (Clinical Research Ed.),* 354, i3625.

van Lierop, B., Ong, S.C., Belgi, A., Delaine, C., Andrikopoulos, S., Haworth, N.L., Menting, J.G., Lawrence, M.C., Robinson, A.J. and Forbes, B.E. (2017) Insulin in motion: The A6-A11 disulfide bond allosterically modulates structural transitions required for insulin activity. *Scientific Reports,* 7(1), 17239.

van Zoggel, H., Hamma-Kourbali, Y., Galanth, C., Ladram, A., Nicolas, P., Courty, J., Amiche, M. and Delbé, J. (2012) Antitumor and angiostatic peptides from frog skin secretions. *Amino Acids,* 42(1), 385-395.

VanCompernolle, S.E., Taylor, R.J., Oswald-Richter, K., Jiang, J., Youree, B.E., Bowie, J.H., Tyler, M.J., Conlon, J.M., Wade, D., Aiken, C., Dermody, T.S., KewalRamani, V.N., Rollins-Smith, L.A. and Unutmaz, D. (2005) Antimicrobial peptides from amphibian skin potently inhibit human immunodeficiency virus infection and transfer of virus from dendritic cells to T cells. *Journal of Virology,* 79(18), 11598-11606.

Vasu, S., McClenaghan, N.H., McCluskey, J.T. and Flatt, P.R. (2014) Mechanisms of toxicity by proinflammatory cytokines in a novel human pancreatic beta cell line, 1.1 B4. *Biochimica Et Biophysica Acta (BBA)-General Subjects,* 1840(1), 136-145.

Vasu, S., Moffett, R.C., Thorens, B. and Flatt, P.R. (2014) Role of endogenous GLP-1 and GIP in beta cell compensatory responses to insulin resistance and cellular stress. *PLoS One,* 9(6), e101005.

Vasu, S., Ojo, O.O., Moffett, R.C., Conlon, J.M., Flatt, P.R. and Abdel-Wahab, Y.H. (2017) Anti-diabetic actions of esculentin-2CHa (1–30) and its stable analogues in a diet-induced model of obesity-diabetes. *Amino Acids,* 49(10), 1705-1717.

Vasu, S., McGahon, M.K., Moffett, R.C., Curtis, T.M., Conlon, J.M., Abdel-Wahab, Y.H. and Flatt, P.R. (2017) Esculentin-2CHa(1-30) and its analogues: stability and mechanisms of insulinotropic action. *The Journal of Endocrinology,* 232(3), 423-435.

Vecchio, I., Tornali, C., Bragazzi, N.L. and Martini, M. (2018) The Discovery of Insulin: an important Milestone in the History of Medicine. *Frontiers in Endocrinology,* 9, 613.

Vivier, E., Tomasello, E., Baratin, M., Walzer, T. and Ugolini, S. (2008) Functions of natural killer cells. *Nature Immunology,* 9(5), 503.

Wade, D., Silberring, J., Soliymani, R., Heikkinen, S., Kilpeläinen, I., Lankinen, H. and Kuusela, P. (2000) Antibacterial activities of temporin A analogs. *FEBS Letters,* 479(1-2), 6-9.

Waldhauer, I. and Steinle, A. (2008) NK cells and cancer immunosurveillance. *Oncogene,* 27(45), 5932.

Wang, C., Tian, L., Li, S., Li, H., Zhou, Y., Wang, H., Yang, Q., Ma, L. and Shang, D. (2013) Rapid cytotoxicity of antimicrobial peptide tempoprin-1CEa in breast cancer cells through membrane destruction and intracellular calcium mechanism. *PloS One,* 8(4), e60462.

Wang, G., Li, X. and Wang, Z. (2008) APD2: the updated antimicrobial peptide database and its application in peptide design. *Nucleic Acids Research,* 37(suppl_1), D933-D937.

Wang, Q. and Brubaker, P. (2002) Glucagon-like peptide-1 treatment delays the onset of diabetes in 8 week-old *db/db* mice. *Diabetologia,* 45(9), 1263-1273.

Wang, Z. and Thurmond, D.C. (2012) PAK1 limits the expression of the pro-apoptotic protein Bad in pancreatic islet β-cells. *FEBS Open Bio,* 2, 273-277.

Wang, Z., York, N.W., Nichols, C.G. and Remedi, M.S. (2014) Pancreatic β cell dedifferentiation in diabetes and redifferentiation following insulin therapy. *Cell Metabolism,* 19(5), 872-882.

Wells, K. (2007) The Ecology and Behaviour of Amphibians., (University of Chicago Press: Chicago.).

Wen, W., Cho, Y., Zheng, W., Dorajoo, R., Kato, N., Qi, L., Chen, C., Delahanty, R.J., Okada, Y. and Tabara, Y. (2012) Meta-analysis identifies common variants associated with body mass index in east Asians. *Nature Genetics,* 44(3), 307.

Wolin, S.L. and Walter, P. (1993) Discrete nascent chain lengths are required for the insertion of presecretory proteins into microsomal membranes. *The Journal of Cell Biology,* 121(6), 1211-1219.

World Health Organization. (2016) *Global Report on Diabetes: World Health Organization,*

Wu, P., Wu, V., Lin, C., Pan, C., Chen, C., Huang, T., Wu, C., Chen, L., Wu, C. and NRPB Kidney Consortium. (2017) Meglitinides increase the risk of hypoglycemia in

diabetic patients with advanced chronic kidney disease: a nationwide, population-based study. *Oncotarget*, 8(44), 78086.

Xu, X. and Lai, R. (2015) The chemistry and biological activities of peptides from amphibian skin secretions. *Chemical Reviews*, 115(4), 1760-1846.

Yabe, D. and Seino, Y. (2011) Two incretin hormones GLP-1 and GIP: comparison of their actions in insulin secretion and β cell preservation. *Progress in Biophysics and Molecular Biology*, 107(2), 248-256.

Yang, Q., Xu, Y., Xie, P., Cheng, H., Song, Q., Su, T., Yuan, S. and Liu, Q. (2015) Retinal neurodegeneration in db/db mice at the early period of diabetes. *Journal of Ophthalmology*, 2015

Yang, S., Liu, M., Chen, Y., Ma, C., Liu, L., Zhao, B., Wang, Y., Li, X., Zhu, Y. and Gao, X. (2018) NaoXinTong Capsules inhibit the development of diabetic nephropathy in db/db mice. *Scientific Reports*, 8(1), 9158.

Yazbeck, R., Howarth, G.S. and Abbott, C.A. (2009) Dipeptidyl peptidase inhibitors, an emerging drug class for inflammatory disease? *Trends in Pharmacological Sciences*, 30(11), 600-607.

Ye, J. and Stanley, M. (2013) Strategies for the discovery and development of anti-diabetic drugs from the natural products of traditional medicines. *Journal of Pharmacy & Pharmaceutical Sciences*, 16(2), 207-216.

You, W. and Henneberg, M. (2016) Type 1 diabetes prevalence increasing globally and regionally: the role of natural selection and life expectancy at birth. *BMJ Open Diabetes Research and Care*, 4(1), e000161.

Young, A.A., Gedulin, B.R., Bhavsar, S., Bodkin, N., Jodka, C., Hansen, B. and Denaro, M. (1999) Glucose-lowering and insulin-sensitizing actions of exendin-4: studies in obese diabetic (ob/ob, db/db) mice, diabetic fatty Zucker rats, and diabetic rhesus monkeys (Macaca mulatta). *Diabetes*, 48(5), 1026-1034.

Zahid, O.K., Mechkarska, M., Ojo, O.O., Abdel-Wahab, Y.H., Flatt, P.R., Meetani, M.A. and Conlon, J.M. (2011) Caerulein-and xenopsin-related peptides with insulin-releasing activities from skin secretions of the clawed frogs, Xenopus borealis and Xenopus amieti (Pipidae). *General and Comparative Endocrinology*, 172(2), 314-320.

Zasloff, M. (1987) Magainins, a class of antimicrobial peptides from Xenopus skin: isolation, characterization of two active forms, and partial cDNA sequence of a precursor. *Proceedings of the National Academy of Sciences*, 84(15), 5449-5453.

Zasloff, M., Martin, B. and Chen, H.C. (1988) Antimicrobial activity of synthetic magainin peptides and several analogues. *Proceedings of the National Academy of Sciences of the United States of America*, 85(3), 910-913.

Zhang, L., Qiao, Q., Tuomilehto, J., Hammar, N., Alberti, K., Eliasson, M., Heine, R., Stehouwer, C., Ruotolo, G. and DECODE Study Group. (2008) Blood lipid levels in relation to glucose status in European men and women without a prior history of diabetes: the DECODE Study. *Diabetes Research and Clinical Practice,* 82(3), 364-377.

Zierath, J., Livingston, J., Thörne, A., Bolinder, J., Reynisdottir, S., Lönnqvist, F. and Arner, P. (1998) Regional difference in insulin inhibition of non-esterified fatty acid release from human adipocytes: relation to insulin receptor phosphorylation and intracellular signalling through the insulin receptor substrate-1 pathway. *Diabetologia,* 41(11), 1343-1354.

Zimmermann, C., Cederroth, C.R., Bourgoin, L., Foti, M. and Nef, S. (2012) Prevention of diabetes in db/db mice by dietary soy is independent of isoflavone levels. *Endocrinology,* 153(11), 5200-5211.

Zimmermann, R., Lass, A., Haemmerle, G. and Zechner, R. (2009) Fate of fat: the role of adipose triglyceride lipase in lipolysis. *Biochimica Et Biophysica Acta (BBA)-Molecular and Cell Biology of Lipids,* 1791(6), 494-500.

APPENDICES

Materials:

Sr No	Materials	Suppliers
1	Sodium hydroxide (NaOH)	BDH Chemicals Ltd
2	Calcium chloride dihydrate ($CaCl_2.2H_2O$)	BDH Chemicals Ltd
3	D-glucose	BDH Chemicals Ltd
4	Disodium hydrogen orthophosphate (Na_2HPO_4)	BDH Chemicals Ltd
5	Dichloromethane (CH_2Cl_2)	BDH Chemicals Ltd
6	Dimethyl sulphoxide (DMSO)	BDH Chemicals Ltd
7	Potassium chloride (KCl)	BDH Chemicals Ltd
8	Sodium chloride (NaCl)	BDH Chemicals Ltd
9	Hydrochloric acid (HCl)	BDH Chemicals Ltd
10	Sodium bicarbonate ($NaHCO_3$)	BDH Chemicals Ltd
11	Magnesium sulphate ($MgSO_4$)	BDH Chemicals Ltd
12	Ethylenediaminetetraacetic acid (EDTA)	Sigma-Aldrich (Poole, UK)
13	Bovine serum albumin (BSA)	Sigma-Aldrich (Poole, UK)
14	Dextran T-70	Sigma-Aldrich (Poole, UK)
15	Bovine insulin	Sigma-Aldrich (Poole, UK)
16	Collagenase-V, Clostridium histolyticum	Sigma-Aldrich (Poole, UK)
17	Forskolin	Sigma-Aldrich (Poole, UK)
18	L-Alanine	Sigma-Aldrich (Poole, UK)
19	Trifluoroacetic acid (TFA)	Sigma-Aldrich (Poole, UK)
20	Diazoxide	Sigma-Aldrich (Poole, UK)
21	Verapamil	Sigma-Aldrich (Poole, UK)
22	Probenecid	Sigma-Aldrich (Poole, UK)

Sr No	Materials	Suppliers
23	Ethylene glycol-bis-N, N, N', N'-tetraacetic acid (EGTA)	Sigma-Aldrich (Poole, UK)
24	Phorbol 12-myristate 13-acetate (PMA)	Sigma-Aldrich (Poole, UK)
25	Thimerosal	Sigma-Aldrich (Poole, UK)
26	Tolbutamide	Sigma-Aldrich (Poole, UK)
27	Trypan blue stain	Sigma-Aldrich (Poole, UK)
28	Activated charcoal	Sigma-Aldrich (Poole, UK)
29	HPLC grade acetonitrile	Sigma-Aldrich (Poole, UK)
30	Trifluoroacetic acid (TFA)	Sigma-Aldrich (Poole, UK)
31	HPLC grade ethanol	Sigma-Aldrich (Poole, UK)
32	α-Cyano-4-hydroxycinnamic acid (CHCA)	Sigma-Aldrich (Poole, UK)
33	Roswell Park Memorial Institute medium (RPMI 1640) tissue culture medium	Gibco Life Technologies Ltd (Paisley, Strathclyde, UK)
34	Hanks Buffered Saline Solution (HBSS)	Gibco Life Technologies Ltd (Paisley, Strathclyde, UK)
35	Trypsin/ Disodium ethylenediaminetetraacetate (EDTA)	Gibco Life Technologies Ltd (Paisley, Strathclyde, UK)
36	Foetal bovine serum (FBS)	Gibco Life Technologies Ltd (Paisley, Strathclyde, UK)
37	Penicillin and streptomycin	Gibco Life Technologies Ltd (Paisley, Strathclyde, UK)
38	FLIPR Calcium Assay Kit	Molecular device
39	FLIPR membrane potential blue	Molecular device
40	CytoTox 96® non-radioactive cytotoxicity kit	Promega (UK)
41	Radiolabelled sodium iodide (Na125I)	Perkin Elmer (UK)
42	Rabbit polyclonal to Ki67	Abcam (Cambridge, UK)

Sr no	Materials	Suppliers
43	Enzyme-linked immunosorbent assay (ELISA) kits for cAMP	Millipore (Millipore, Watford, UK).
44	In situ Cell Death Detection Kit	Roche Diagnostics (Burgess Hill, UK)
45	Lipid profile: Triglyceride, total cholesterol and HDL kit	Instrumentation Laboratory
46	Amylase assay kit	Instrumentation Laboratory
47	Liver and Kidney function test	Instrumentation Laboratory
48	Cholecystokinin-8 (CCK-8)	Sunnyvale (USA)
49	Rat insulin	Novo Industrial (Denmark)
50	Synthetic Peptides	SynPeptide (China)
51	GLP-1, exenatide	SynPeptide (China)
52	Lipid profile: Triglyceride, total cholesterol and HDL kit	Instrumentation Laboratory
53	Glucose uptake Cell-Based assay kit.	Cayman Chemicals, UK

Purified water (18.2 MΩ-cm purity) used in the experiments was obtained from an Elga PURELAB Ultra system (Elga, Celbridge, Ireland).